



Studies on Enantioselective Nickel-Catalyzed Hydrocyanation and Chromane Natural Products

Inaugural-Dissertation

zur Erlangung des Doktorgrades
der Mathematisch-Naturwissenschaftlichen Fakultät
der Universität zu Köln

Vorgelegt von

Joss Pepe Strache

aus Herdecke, Deutschland

-Köln 2023-

The present thesis was conducted under the scientific direction of *Prof. Dr. Hans-Günther Schmalz* at the Institute of Organic Chemistry of the University of Cologne. The experimental work was performed between April 2019 and August 2022.

First referee: Prof. Dr. Hans-Günther Schmalz

Second referee: Prof. Dr. Axel Griesbeck

Day of oral exam: 28th April 2023

Abstract

Hydrocyanation describes an atom-economic, C-C bond-forming reaction leading to nitriles, which are of high importance as target structures and synthetic intermediates. However, hydrocyanation of non-activated alkenes is less developed than other transition metal-catalyzed transformations, although it opens up valuable opportunities for (asymmetric) organic synthesis. In this work, enantioselective nickel-catalyzed hydrocyanation using TADDOL-derived chiral phosphine-phosphite ligands was investigated in terms of potential improvements, substrate scope and limitations. As a highly attractive substrate class, 1,3-diarylpropenes (homostilbenes) were hydrocyanated for the first time. For this purpose, a library of various substituted homostilbenes was initially synthesized and their hydrocyanation was investigated with respect to chemo-, regio- and enantioselectivity. Notably, high levels of regio-retention (and enantioselectivity) were observed despite the risk of chain-walking. The utility of the developed methodology was demonstrated in the synthesis of a new colchinol. In a separate project, an enantioselective iridium-catalyzed cyclobutanol fragmentation was employed in studies towards the synthesis of an antiplasmodial chromane natural product, and coupling strategies for the introduction of a terpene-derived side chain were investigated.

Kurzbeschreibung

Die Hydrocyanierung beschreibt eine atomökonomische, C-C bindungsknüpfende Reaktion zur Synthese von Nitrilen, die als Zielstrukturen und Syntheseintermediate von großer Bedeutung sind. Vor allem die Hydrocyanierung unaktivierter Alkene ist im Vergleich zu anderen Übergangsmetall-katalysierten Transformationen weniger entwickelt, obwohl sie wertvolle Möglichkeiten für die (asymmetrische) organische Synthese öffnet. In dieser Arbeit wurde die enantioselective Nickel-katalysierte Hydrocyanierung (unter dem Verwendung von TADDOL-abgeleiteten chiralen Phosphin-Phosphit Liganden) eingehender in Hinblick auf Verbesserungsmöglichkeiten, Substratspektrum und Limitierungen untersucht. Im Rahmen dieser Studien wurden erstmals auch 1,3-Diarylpropene (Homostilbene) als besonders attraktive Substrate hydrocyaniert. Hierfür wurde zunächst eine Bibliothek verschieden substituierter Homostilbene synthetisiert und deren Hydrocyanierung in Hinblick auf Chemo-, Regio- und Enantioselectivität untersucht. Dabei konnten trotz der Isomerisierungsgefahr durch Doppelbindungsmigration ein hohes Maß an Regio retention sowie gute Enantioselectivitäten erhalten werden. Den Nutzen der entwickelten Methodik wurde in der Synthese eines neuen Colchinols demonstriert. In einem separaten Teilprojekt wurde in Studien zur Synthese eines antiplasmodialen Chromannaturstoffes eine enantioselective Iridium-katalysierte Cyclobutanofragmentierung angewendet und Kupplungsstrategien zur Einführung einer Terpen-abgeleiteten Seitenkette untersucht.

Danksagung

Besonders herzlichst bedanken möchte ich mich bei Prof. Dr. Hans-Günther Schmalz für die Aufnahme in seine Forschungsgruppe, die im Rahmen der Forschungsprojekte gegebene Freiheit sowie die stetige Unterstützung bei Anliegen jeglicher Art.

Prof. Dr. Axel Georg Griesbeck danke ich in hohem Maß für die Zweitbetreuung während meiner Promotion, die sehr produktive Zusammenarbeit mit dem JCF als GDCh-Ortsvorstand sowie die Übernahme des Zweitgutachtens. Prof. Dr. Uwe Ruschewitz möchte ich für die Übernahme des Prüfungsvorsitzes danken.

Bei Dr. Jörg-Martin Neudörfl möchte ich mich für die gute Zusammenarbeit in allen Praktikumsangelegenheiten und ebenso für die Messungen der Kristallstrukturen bedanken. Mein außerordentlicher Dank gilt auch Priv. Doz. Dr. Dirk Blunk für die Übernahme der Schriftführung sowie die im Rahmen der Projekte durchgeführten Rechnungen.

Anja Bitners möchte ganz herzlichst für die Sprachkorrektur dieser Arbeit, ihre Menschlichkeit und Organisation rund um das Institut danken.

Mein Dank gilt außerdem Dietmar Rutsch, Andreas Wallraf und dem Team der Werkstatt als gute Seelen des Hauses und ihre stetige Hilfsbereitschaft. Ein Dankesgruß geht vor allem auch an das Chemikalienmanagement mit Sylvia Rakovac, Nihad El Ghachtoun und Ingo Müller. Ich danke Frau Dr. Henneken und Prof. Dr. Jan Riemer für die Zusammenarbeit und Unterstützung im Rahmen der CGSC.

Darüber hinaus danke ich herzlichst den Abteilungen der NMR-Analytik und Massenspektrometrie, insbesondere Kathrin König, Daniela Naumann, Prof. Dr. Mathias Schäfer, Michael Neihns sowie Frau Astrid Baum. Nicht zuletzt ein großes Dankeschön an Dipl. Chem. Andreas Adler für die Enantiomerenanalytik und schöne Gespräche.

Einen außerordentlichen Dank möchte ich gegenüber den ehemaligen und gegenwärtigen Mitgliedern des Arbeitskreises aussprechen, welche zu einer produktiven und fröhlichen Atmosphäre beitrugen und bei jeder Angelegenheit keine Mühen scheuten. Hierbei sind besonders Dr. Julian Baars, Dr. Friederike Ratsch, Dr. Andreas Maßen, Pascal Engelhardt, Isabelle Grimm, Dr. Judith Bruns, Felix Blüm, Dr. Ömer Taşpınar, Dr. Hanna Sebode, Dr. Christian Schumacher, Dr. Bernhard Krause, Dr. Daniel Schunkert, Dr. Dominik Albat, Lars Hemmersbach, Dr. Slim Chiha, Dr. Martin Reiher, Dr. Anna Falk, Dr. Dennis Zeh, Tobias Wilczek, Lukas Münzer, Marvin Schwamborn, Alicia Köcher, Mira Scheithe und Bei Gan hervorzuheben und alle nicht genannten, die zum Erfolg der Arbeitsgruppe beigetragen haben.

Eva-Maria Gatzka und Lukas Münzer danke ich für die eifrige und freudige Arbeit im Rahmen des JCFs Köln und darüber hinaus allen JCFlern, die für diese schöne Gemeinschaft quer durchs Land sorgten. Ich danke dem MNF Doctoral Representatives Council und dem MNF-Promotionsausschuss für spannende Einblicke und Diskussionen.

Ich danke allen lieben Doktoranden, Organisatoren, Professoren und Industrievertretern, welche SusChemSys 2.0 zu einer großartigen, familiären Community über den rein wissenschaftlichen Aspekt hinaus gemacht haben.

Für das fachliche Korrekturlesen dieser Arbeit danke ich Dr. Friederike Ratsch, Alicia Köcher, Dr. Bernhard Krause, Lukas Münzer, Dominik Albat, Marvin Schwamborn, Tobias Wilczek, Felix Blüm und Isabelle Grimm.

Für fleißige Unterstützung im Labor im Rahmen von Bachelorarbeiten oder Forschungspraktika danke ich Sara Lucio, Daniel Streup, Leonie Wilczek, Laura Plein, André Colliard-Granero, Felix Blüm, Mingsen Kuang, Ervin Aljic und Nicolaus Sondermann.

Was wäre die Chemie ohne ein wundervolles Leben, dass durch diese ermöglicht wird? Ich danke allen Menschen um mich herum, alten und neuen Freunden. Niemals zu vergessen sind die vielen Erlebnisse rund um das Centro Franco Allemand Guidel, Band und Musik, Gettworkout, Gruppentreffen 2.0, die drei Muskeltiere und Clays Clique.

Doris, Konradin, Martina, Michael, Leah, Nino, Helge, Melanie, Lambert, Julian, Philipp und Hannah. Ihr seid eine Familie, die so allgegenwärtig und liebevoll ist, wie das Leben in seinen schönsten Momenten. Ich bin in tiefster Dankbarkeit für eure bedingungslose Liebe und Unterstützung.

I am focused on what I am after. The key to the next open chapter. Cause I found a way to steal the sun from the sky. Long live that day that I decided to fly from the inside.

(Brent Stephen Smith)

Table of Contents

| | |
|---------------------------------------------------------------------------------------------|----|
| Part I: Studies on Enantioselective Ni-catalyzed Hydrocyanation | 1 |
| 1. Introduction | 1 |
| 2. State of Knowledge | 3 |
| 2.1. Nitriles and hydrogen cyanide | 3 |
| 2.2. Hydrocyanation | 6 |
| 2.2.1. General concept of hydrocyanation | 6 |
| 2.2.2. Industrial hydrocyanation: Adiponitrile process..... | 6 |
| 2.2.3. Selectivities and mechanistic principles..... | 8 |
| 2.2.4. Non-asymmetric (transfer) hydrocyanation..... | 10 |
| 2.2.5. Enantioselective hydrocyanation: Initial studies..... | 15 |
| 2.2.6. Enantioselective hydrocyanation: Phosphine-phosphite ligands by <i>Schmalz</i> ...18 | |
| 2.2.7. Enantioselective hydrocyanation: Current strategies and tactics | 24 |
| 2.2.8. Migratory hydrocyanation <i>via</i> nickel-catalyzed chain-walking | 29 |
| 2.3. Motifs and synthetic access to homostilbenes (1,3-diarylpropenes) | 33 |
| 3. Concept and Task | 37 |
| 4. Results and Discussion | 39 |
| 4.1. Notes on the hydrocyanation protocol, reproducibility and ligand synthesis..... | 39 |
| 4.2. Synthesis of new phosphine-phosphite ligands for hydrocyanation | 41 |
| 4.2.1. Derivatizing the TADDOL backbone: new phosphine-phosphite ligands..... | 41 |
| 4.2.2. New phosphine-phosphite ligands in enantioselective hydrocyanation..... | 42 |
| 4.3. Prospects of the substrate scope using phosphine-phosphite ligands | 46 |
| 4.3.1. 1,1-Disubstituted vinylarenes | 46 |
| 4.3.2. Range and limitations of the substrate spectrum | 47 |
| 4.4. Enantioselective nickel-catalyzed migratory hydrocyanation | 50 |
| 4.4.1. Aspects of chain-walking employing phosphine-phosphite ligands | 50 |
| 4.4.2. Migratory hydrocyanation of phenylalkenes..... | 51 |
| 4.5. Enantioselective hydrocyanation of homostilbenes | 53 |
| 4.5.1. General concept & initial studies | 53 |

| | | |
|--------|------------------------------------------------------------------------------|-----|
| 4.5.1. | Preparation of a homostilbene library | 56 |
| 4.5.2. | Hydrocyanation results..... | 59 |
| 4.6. | Studies towards new colchicinoids from a hydrocyanated homostilbene | 63 |
| 5. | Summary and Outlook..... | 67 |
| 5.1. | Summary..... | 67 |
| 5.2. | Outlook..... | 69 |
| | Part II: Studies on Chromane Natural Products | 71 |
| 6. | Introduction and State of Knowledge | 73 |
| 6.1. | Chromane natural products | 73 |
| 6.1.1. | (Toco)chromanols in the aspect of function and biosynthesis..... | 73 |
| 6.1.2. | New isolated chromanes | 75 |
| 6.2. | Enantioselective iridium-catalyzed cyclobutanol cleavage..... | 77 |
| 6.2.1. | C-C bond activation..... | 77 |
| 6.2.2. | Metal-catalyzed cyclobutanol cleavage | 78 |
| 6.2.3. | Application in the total synthesis of α -tocopherol methyl ether..... | 79 |
| 6.2.4. | Mechanistic aspects and scope..... | 80 |
| 6.3. | Synthetic studies towards chromanes of <i>Koeberlinia spinosa</i> | 83 |
| 7. | Concept and Task | 85 |
| 8. | Results and Discussion | 87 |
| 8.1. | Studies on the linear route towards chromanone 404..... | 87 |
| 8.2. | Side chain coupling attempts..... | 90 |
| 8.2.1. | Olefination coupling approaches | 90 |
| 8.2.2. | Enyne metathesis approach | 96 |
| 8.2.3. | <i>Grignard</i> -type coupling approach | 99 |
| 8.3. | Prospects of enantioselective Iridium-catalyzed cyclobutanol cleavage..... | 104 |
| 9. | Summary and Outlook..... | 107 |
| 9.1. | Summary..... | 107 |
| 9.2. | Outlook..... | 109 |
| 10. | Experimental Part | 111 |

| | | |
|---------|------------------------------------------------------------------------------------------------------------------------------|-----|
| 10.1. | General information | 111 |
| 10.2. | Experimental procedures towards the enantioselective Ni-catalyzed hydrocyanation employing phosphine-phosphite ligands | 114 |
| 10.2.1. | Synthesis of phosphine-phosphite ligands | 114 |
| 10.2.2. | Synthesis of homostilbenes (1,3-diarylpropenes)..... | 141 |
| 10.2.3. | Enantioselective Ni-catalyzed hydrocyanation | 164 |
| 10.3. | Experimental procedures towards chromane natural products by Ir-catalyzed asymmetric desymmetrization..... | 190 |
| 10.3.1. | Synthetic studies towards chromane natural products | 190 |
| 11. | List of References..... | 213 |
| 12. | Appendix..... | 223 |
| 12.1. | List of abbreviations..... | 223 |
| 12.2. | NMR spectra of selected compounds | 227 |
| 12.3. | X-ray crystallography | 268 |
| 12.3.1. | Crystal data of compound 245e | 268 |
| 12.3.2. | Crystal data of compound <i>cis</i> -438..... | 269 |
| 12.3.3. | Crystal data of compound <i>trans</i> -474 | 270 |
| 12.4. | Stereochemical analysis by ECD | 272 |
| 12.5. | Stereochemical analysis by chromatography | 274 |
| 12.5.1. | Gas chromatography on chiral stationary phase | 274 |
| 12.5.2. | High performance liquid chromatography on chiral stationary phase | 279 |
| 12.6. | Statutory Declaration | 282 |

Part I: Studies on Enantioselective Ni-catalyzed Hydrocyanation

1. Introduction

Our life is based on carbon compounds. All living things consist of similar carbon-rich molecules, which, functionalized with the incorporation of hydrogen, nitrogen, oxygen, phosphorus and sulfur, form the basis of all organic substances.^[1] An important property is the catenation of hydrocarbons, which allows the formation of longer open-chain structures or ring assemblies.^[2] The elucidation of carbon compounds with respect to their function and formation as well as the synthesis of new ones is essential for technological as well as human progress and the coexistence of a constantly growing world population. This necessity is not restricted to life sciences such as medical,^[3] nutritional and agrochemical research,^[4] plastics and technology development,^[5] but it is also present in all areas, from daily life to tackling the climate crisis.^[6]

New carbon compounds can be created either by derivatization of already existing complex structures or by building them from simple organic molecules. The diversity of possible reactions is crucial for this. In particular C-C bond forming reactions are among the most important transformations in organic chemistry. Without such reactions, no larger, functional molecules could be produced. For this reason, researchers have always tried to understand reaction sequences using examples from nature or simply through experimentation, and to develop new reactions.^[7] Asymmetric C-C bond forming reactions for the selective synthesis of chiral compounds is one of the most important modern challenges.^[8] Countless examples demonstrate the inevitability of obtaining enantiopure substances for the use in biochemical processes.^[9] Figure 1 shows the tuberculosis drug (*S,S*)-(+)-ethambutol (**1**). Its enantiomer (*R,R*)-(+)-ethambutol (*ent*-**1**) is not effective and causes blindness.^[10]

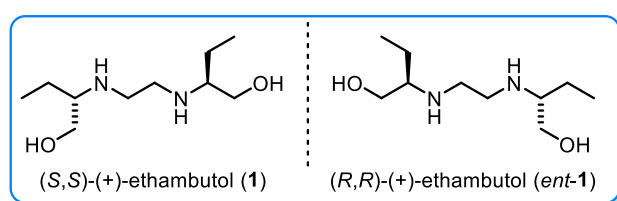


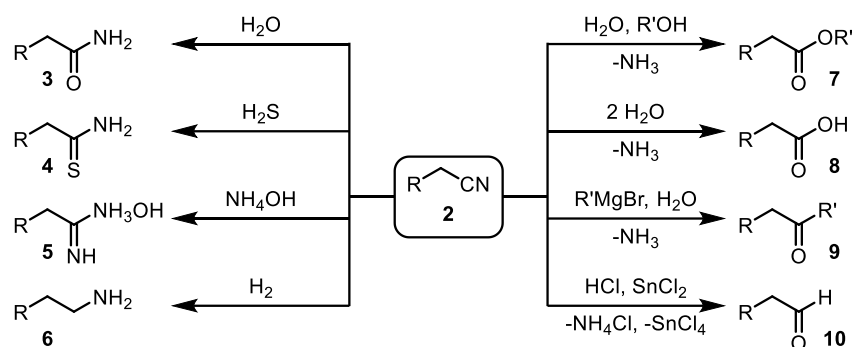
Figure 1: The enantiomeric pair of ethambutol.

Besides the options of racemic resolution, chiral pool synthesis or the use of chiral auxiliaries, enantioselective catalysis is by far the most elegant approach. Apart from biocatalysis using enzymes which are highly substrate specific^[11] and the promising field of organocatalysis,^[12] enantioselective transition metal catalysis is one of the most established approaches, since the use and development of chiral ligands allows the chemo-, regio- and enantioselectivities to be controlled in a very thorough manner.^[8, 13] At the same time, this leads to the challenge of developing suitable ligands and appropriate methodologies with the aim of achieving high selectivities.

2. State of Knowledge

2.1. Nitriles and hydrogen cyanide

Nitriles are versatile substances. The nitrile group is present in many natural products as well as in compounds used in pharmaceuticals, agrochemicals and functional materials/textiles.^[14] In addition, nitriles offer a large synthesis platform as they can be converted into a variety of functional groups by mostly simple, well-established transformations (Scheme 1).^[15]



Scheme 1: Exemplary synthetic transformations of nitriles into a variety of other functional groups.^[16]

The products include esters **7**, carboxylic acids **8**, ketones **9**, aldehydes **10**, amides **3**, and amines **6**. But also, the thioamides **4** and amidoxime salts **5**, which occur in a number of active pharmaceutical ingredients and prodrugs,^[17] can be easily derived from nitriles.

Prominent examples of pharmaceutical nitriles include the arylalkylamine (*S*)-verapamil (**11**), a calcium channel inhibitor for the treatment of hypertension and cardiovascular diseases in which direct coordination of the cyano group to calcium ions plays a critical role,^[18] or the nucleoside analogue drug remdesivir (**12**) (Figure 2).

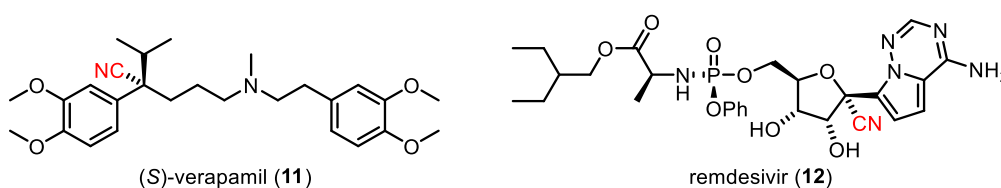


Figure 2: Structures of selected pharmaceutical nitriles.

The latter broad-spectrum antiviral medication was originally used to treat hepatitis C, and later also for cases of Ebola virus disease and Marburg virus infections.^[19] Since 2020, this biopharmaceutical has additionally been approved in many countries worldwide for the treatment of COVID-19 as it showed convincing results in clinical trials.^[20] The active metabolite of remdesivir (**12**) competes with endogenous nucleotides within virus RNA synthesis. Structure relationship analysis showed that the nitrile moiety provides higher antiviral activity through interaction with residues on the active site of the enzymes involved.^[21]

Cyanogenic glycosides are by far the most abundant naturally occurring nitriles.^[22] These β -glycosides belong to the class of cyanohydrins and therefore release hydrogen cyanide (HCN) under chemical or enzymatic hydrolysis. Primarily in plants, but in some animals as well, they contribute to the defense mechanism and are a natural source of reduced nitrogen.^[23] Structurally, there are only minor differences, since they them derive from common glycosides and only a few amino acids.^[14a] Well-known representatives are prunasin (**13a**), linamarin (**13b**) and heterodendrin (**13c**) (Figure 3).

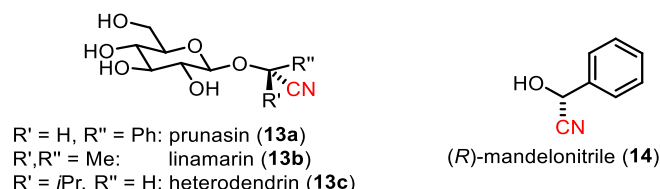
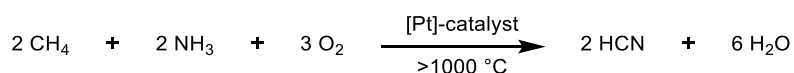


Figure 3: Structures of naturally occurring cyanogenic glycosides **13a-13c** and (*R*)-mandelonitrile (**14**).

In particular, structures binding mandelonitrile (**14**) such as prunasin and derivatives (including amygdalin) are frequently found in the seeds of plants.^[14a] They are often responsible for the bitter almond aroma. The naturally predominant (*R*)-mandelonitrile (**14**) itself is hydrolyzed enzymatically by mandelonitrile lyase to release HCN.^[24] Humans and animals can consume small amounts of cyanogenic plants without problems.^[25]

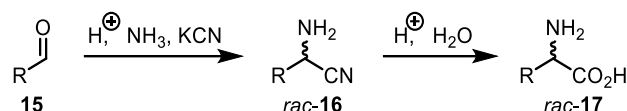
HCN as a pure substance is a colorless, water-soluble liquid with a low boiling point of 25.6 °C and with a pK_a value of 9.3, it is one of the weak acids.^[26] However, HCN is highly toxic and causes death within one hour at a concentration of 100 ppm.^[27] The cyanide irreversibly binds to the central iron(III) atom of the heme-a₃ cofactor in cytochrome c oxidase in mitochondria. Oxygen can still be transported in the blood but can no longer be taken up by the mitochondria, which interrupts ATP production and thus aerobic metabolism.^[28] As a synthesis building block, however, it is extremely useful. HCN, historically referred to as prussic acid, was first synthesized from the deep blue pigment iron hexacyanoferrate (Prussian blue).^[29] Nowadays, it can be obtained on a laboratory scale from the corresponding cyanides such as NaCN or KCN.^[30] Industrially, it is obtained by the *Andrussow* process from methane and ammonia by platinum-catalyzed oxidation at high temperatures (Scheme 2).^[31] Among similar large-scale processes, this highly exothermic procedure is the most important one.^[32]



Scheme 2: Reaction scheme of large-scale synthesis of HCN by the *Andrussow* process.

HCN is directly applied in the preparation of KCN, NaCN as well as in the adiponitrile process (see Section 2.2.2.).^[33] The cyanides are mainly used in mining for the extraction of precious metals such as gold cyanidation^[34] and in electroplating.^[35] In addition, KCN is used in the

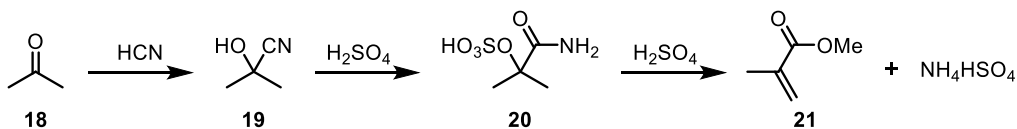
Strecker process to produce racemic α -aminonitriles and acids (Scheme 3). Since the reaction proceeds without asymmetric induction, other processes have become established in the commercial production of α -amino acids.^[36] Nevertheless, the *Strecker* synthesis is often used and many stereoselective variants employing cyanide addition to chiral imines or a catalytic enantioselective cyanation of imines have been developed.^[37]



Scheme 3: Use of the *Strecker* reaction for the preparation of racemic amino acids.

A condensation reaction of aldehydes **15** with ammonia in the presence of KCN leads to the α -aminonitrile *rac-16*. Acidic hydrolysis subsequently releases the α -amino acid *rac-17*. Both substituted amines and ketones can be used in the reaction.^[37b] Commercially, the process is used for the racemic synthesis of methionine from methional.^[36b]

The monomer of the widely used engineering plastic poly(methyl methacrylate) (PMMA, acrylic glass) is methyl methacrylate.^[38] The most common synthesis method is *via* the acetone cyanohydrin route (Scheme 4).^[39]



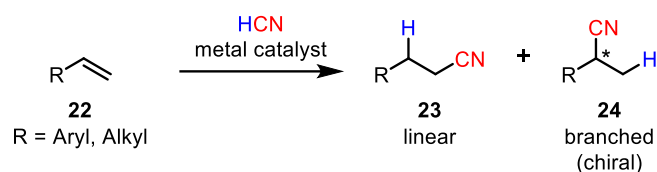
Scheme 4: Synthesis pathway to methyl methacrylate *via* the acetone cyanohydrin route.

Condensation of HCN with acetone (**18**) leads to acetone cyanohydrin (**19**), which reacts under hydrolysis with sulfuric acid to form sulfate ester **20**. Subsequent methanolysis affords methyl methacrylate (**21**) as the product and ammonium bisulfate. The large field of application of hydrocyanation of unsaturated hydrocarbon compounds is discussed in detail in the next section.

2.2. Hydrocyanation

2.2.1. General concept of hydrocyanation

Hydrocyanation describes the addition of hydrogen cyanide (HCN) to a carbon-carbon unsaturated bond (hydrofunctionalization), which usually occurs in a transition metal-catalyzed manner. It is mainly used for the conversion of alkenes of type **22** into nitriles, where linear (*anti-Markovnikov*) or branched (*Markovnikov*) products **23** or **24** are formed (Scheme 5).^[40] For the reaction, HCN can be used directly or formed *in situ* from HCN surrogates such as acetone cyanohydrin (**19**)^[41] or trimethylsilyl cyanide.^[42] The hydrocyanation of alkynes and allenes, which is in most parts analogous to that of alkenes, is becoming increasingly important in modern synthetic chemistry (see attached review articles).^[43] This introductory overview focuses on the well-studied hydrocyanation of alkenes.



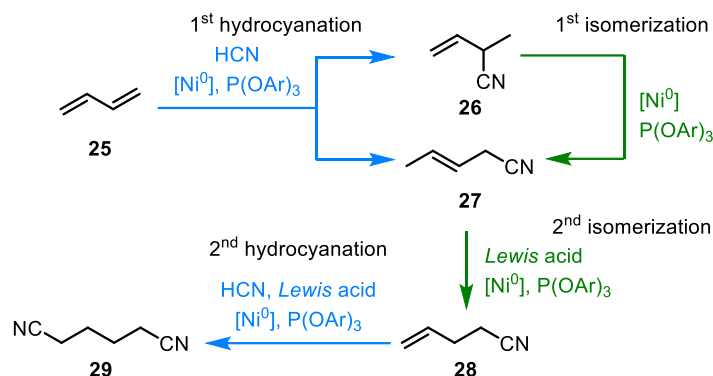
Scheme 5: Hydrocyanation of an alkene.

Due to the electron-rich properties of the cyanide ion, addition to strongly polarized double bonds of, for example, aldehydes, ketones or imines, as well as to electron-poorer alkenes and alkynes, is significantly more activated than to nonpolar systems.^[44] Therefore, the presence of a suitable transition metal catalyst is crucial for non-activated systems. In principle, nickel, palladium or cobalt complexes are suitable for this purpose, with nickel catalysis predominating due to its higher chemo-, regio- and enantioselectivities.^[16] Unfortunately, the ligand metal complexes used in hydrocyanation are very prone to form stable cyanide complexes (especially $\text{Ni}(\text{CN})_2$ species),^[16, 45] leading to deactivation of the catalytic system. Overall, this results in the hydrocyanation of non-activated alkenes lagging behind other transformations. Since hydrocyanation provides direct and atom-economical synthetic access to nitriles, its further development is particularly valuable. While the *Markovnikov* addition to terminal alkenes or the use of internal olefins lead to chiral products, enantioselective hydrocyanation in particular is being investigated by several research groups worldwide.^[16, 44, 46]

2.2.2. Industrial hydrocyanation: Adiponitrile process

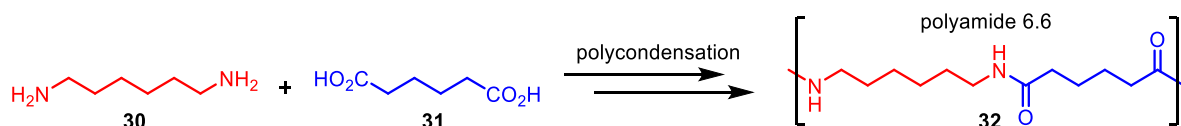
On an industrial scale, the hydrocyanation reaction is used in the production of adiponitrile, in which 1,3-butadiene (**25**) is converted by means of double hydrocyanation (Scheme 6). This process, developed by *DuPont* in 1971,^[47] has been used for decades for the large-scale

production of polyamide 6.6.^[48] The fact that the annual production of adiponitrile exceeds one million tons highlights the importance of the process.^[49]



Scheme 6: Simplified reaction scheme of industrial *DuPont* adiponitrile (**29**) production.^[48]

Starting from an initial hydrocyanation of 1,3-butadiene (**25**) using a triarylphosphite nickel complex as catalyst, the desired linear product 3-pentenenitrile (**27**) and the branched byproduct 2-methyl-3-butenenitrile (**26**) are formed in varying ratios. The latter can be separated by distillation during the process and isomerized to the desired linear nitrile product **27** using the same catalyst system.^[16] In the further course, employing a *Lewis* acid as co-catalyst, 3-pentenenitrile (**27**) is isomerized to 4-pentenenitrile (**28**), which is converted to adiponitrile (**29**) under a second addition of HCN. In this step, the *Lewis* acid provides regioselectivity control (see Section 2.2.3.). In the subsequent process, adiponitrile (**29**) is reduced to hexamethylenediamine (**30**) and polymerized with adipic acid (**31**) representing the second building block (Scheme 7). The latter, however, is not obtained by hydrolysis of the adiponitrile (**29**), but by double oxidation from cyclohexane.^[50]



Scheme 7: Synthesis of polyamide 6.6.

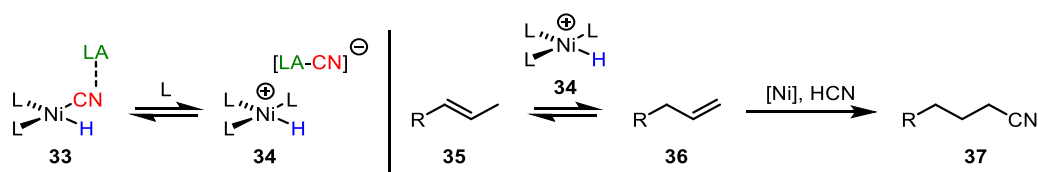
Polyamide 6.6 (*Nylon* 6.6, **32**) is an easily processable and extremely resistant raw material, which is mainly applied in the production of mechanical components as well as in the textile and clothing industry. In addition, polyamide 6.6 often provides mechanically more favorable properties than its related polyamide 6 (which is obtained from ϵ -caprolactam by ring-opening polymerization) due to the higher number of possible hydrogen bonds.^[51]

To date, the adiponitrile process remains the largest application of homogeneously catalyzed hydrocyanation. Due to the fact that in the adiponitrile process selectivity problems can occur, such as isomerization and uncontrolled addition of HCN without prior isomerization,^[52] the hydrocyanation of non-aryl-conjugated systems has been extensively studied. In general, the

triaryl phosphite nickel complexes $\text{Ni}[\text{P}(\text{OAr})_3]_n$ ($n = 3-4$; $\text{Ar} = \text{Ph}$, tolyl) are suitable for this purpose.^[40, 53] In addition, process development contributed to the deeper understanding of contemporary organometallic chemistry and led, among other things, to further elaboration of the 16 and 18 electron rule, the catalytic cycle concept, the influence of steric and electronic effects of ligands, and the ligand cone angle.^[47a, 54] The corresponding *Tolman* cone angle Θ , as a common example for the analysis of the steric claim of tertiary ligands in transition metal complexes,^[55] was named after the leading development chemist in the *DuPont* adiponitrile process at that time, *Chadwick A. Tolman*. He originally used the method for phosphine ligands in nickel complexes using accurate physical models.^[56]

2.2.3. Selectivities and mechanistic principles

The first foundations for the mechanistic understanding of hydrocyanation were laid by the extensive work of *Bäckvall et al.*^[57] and *McKinney et al.*^[58] on the nickel-catalyzed hydrocyanation of ethene, 1-3-dienes, and other olefins in the 1980s. In contrast to the first (cobalt-catalyzed) hydrocyanation examples published by *Arthur et al.* in 1954,^[59] nickel catalysis of alkenes that are non-aryl-conjugated leads predominantly to linear nitriles. This effect can be enhanced by the addition of *Lewis* acids. The cyanide anion of the oxidated nickel complex **33** is abstracted by these acids and cationic nickel-hydride **34** is formed (Scheme 8). This complex causes the isomerization of internal olefins such as **35** to terminal olefins **36** by chain-walking. The latter are converted much faster in the hydrocyanation.^[60] Furthermore, the use of *Lewis* acids usually increases the reaction rate by promoting the reductive elimination step.^[61]

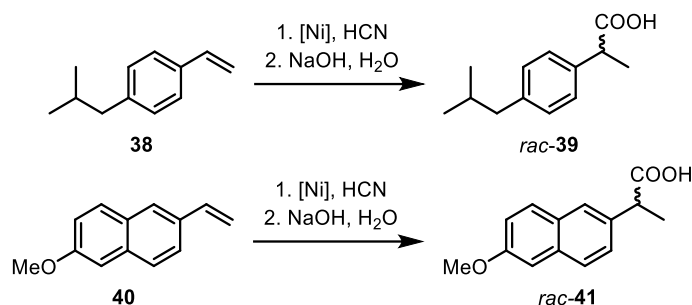


Scheme 8: Formation of nickel hydride **34** (left). Isomerization of internal olefins followed by hydrocyanation (right).

In addition, *Lewis* acids can coordinate to the nitrogen lone pair of the corresponding catalytic species and thus prevent the formation of indicated nickel-alkyl structures, which in turn favors the formation of linear products. The addition of *Lewis* acids can as well influence the hydrocyanation of aryl-conjugated alkenes.

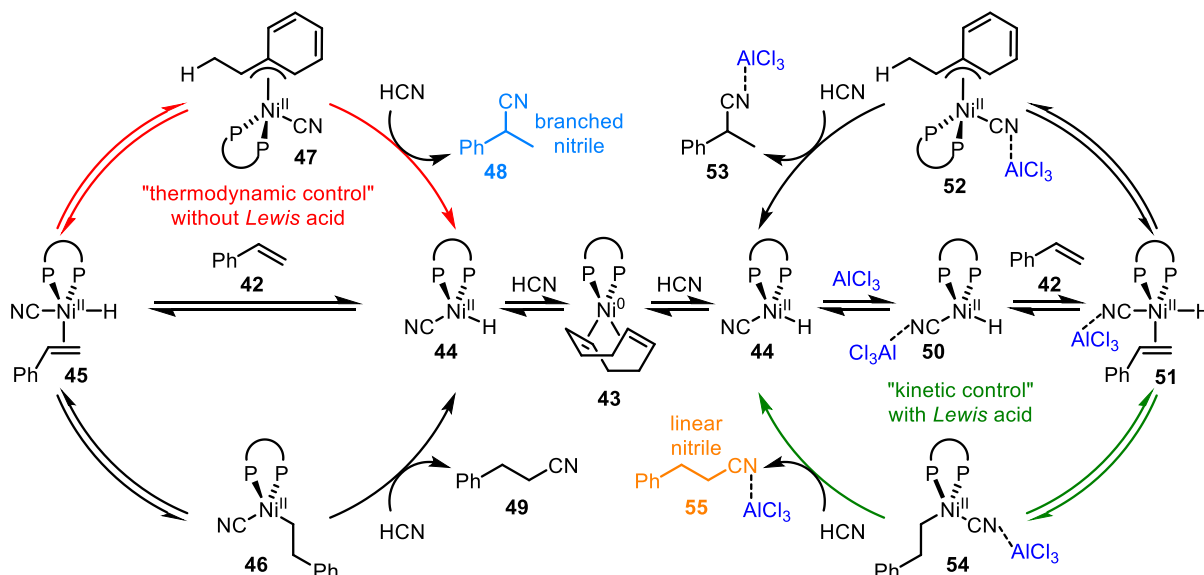
The phenomena described were first investigated with regard to the significant adiponitrile process, since these have a decisive influence on the product selectivities (see Section 2.2.2.). Through the investigation of ligand structures with respect to sterics and electronics, a change from monodentate to bidentate ligands has evolved since the 1990s, as these led to better

activities and selectivities.^[62] An early example of the hydrocyanation of styrene derivatives was achieved by the *McKinney* group in the racemic synthesis of the anti-inflammatories *Ibuprofen* (*rac*-**39**) and *Naproxen* (*rac*-**41**) (Scheme 9).^[63] Using a $\text{Ni}[\text{P}(\text{OpTol})_3]_4$ catalyst, the corresponding precursors **38** and **40** were reacted with HCN and subsequently subjected to basic hydrolysis.



Scheme 9: Hydrocyanation of styrene derivatives **38** and **40** in the synthesis of anti-inflammatories.^[63]

When vinylarenes are used, the regioselectivity changes in favor of the branched anti-*Markovnikov* products. This was impressively demonstrated by *Vogt* and coworkers, who investigated the hydrocyanation of styrene (**42**) with regard to the mechanism in the absence or presence of *Lewis* acids by means of deuterium labelling experiments, NMR studies and DFT calculations (Scheme 10).^[64] In their experiments, they used bidentate xantphos (**56**)-derived *P,P*-ligands.



Scheme 10: Hydrocyanation of styrene (**42**) in absence (left catalytic cycle) and presence (right catalytic cycle) of a *Lewis* acid reported by *Vogt* and coworkers.^[64]

The selectivity towards branched nitriles can be explained by the feasible intermediates in the left catalytic cycle. The precomplexed catalyst **43** is first subjected to an oxidative addition of HCN. Starting from the emerging species **44**, the π -complex **45** is formed by coordination. From this, either σ -alkyl intermediate **46** or η^3 -benzyl complex **47** can be formed by hydrogen

insertion. Since the latter is thermodynamically more stable and thus dominates at equilibrium, reductive elimination occurs mainly from **47** to the branched nitrile **48**. Similar to how the addition of *Lewis* acids to non-aryl-conjugated compounds increases selectivity toward linear products,^[61b] the *Vogt* group was able to show that for vinylarenes the high selectivity towards branched products could even be reversed. In the hydrocyanation of styrene **42**, the addition of AlCl_3 shifted the selectivity from 90% branched product to 90% linear product (right catalytic cycle). In the DFT calculations, it was shown that the η^3 -benzyl intermediate **52** is so strongly stabilized by the *Lewis* acid coordination leading to a “steady state” situation for this complex that reductive elimination hardly occurs from **52**.^[64] As a result, the reaction proceeds in a kinetically controlled manner *via* the less stable σ -alkyl complex **54**. Reductive elimination subsequently releases the linear product **55**.

The advantage of bidentate phosphorus ligands could be attributed by the groups led by *Vogt* and *Leeuwen* to the fact that ligands favoring a tetrahedral geometry of η^3 -benzyl complexes support reductive elimination, thereby accelerating the reaction.^[65] In particular, ligands with a bite angle of 106° were most suitable.^[65a] Diphosphine ligands such as xantphos **56** or thixantphos **57** showed superior results against monodentate phosphorus ligands (Figure 4).

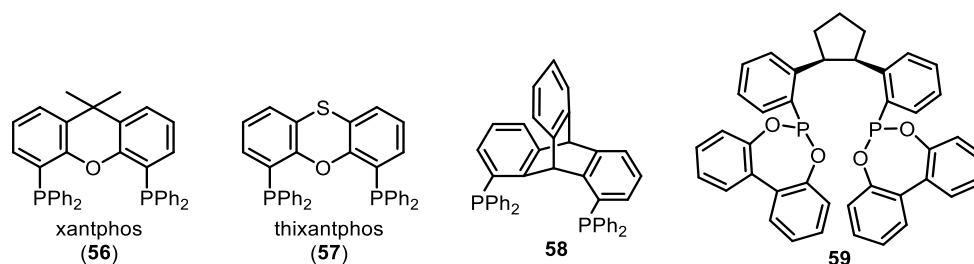


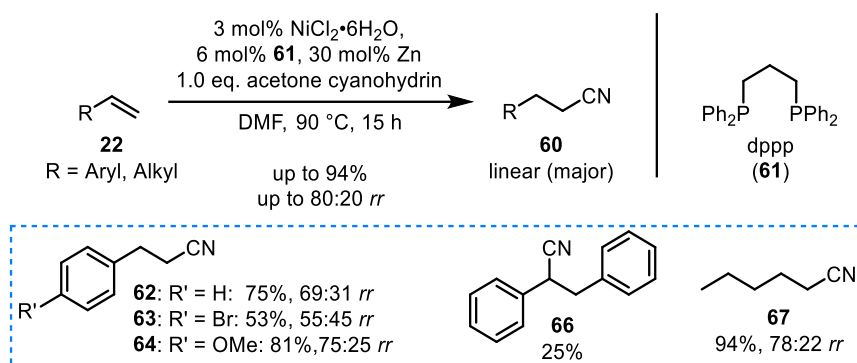
Figure 4. Examples of bidentate phosphorus ligands in achiral hydrocyanation.

Modification of these xantphos-type ligands with electron withdrawing groups led to higher activity.^[66] Triptycene-based diphosphine ligands of type **58** have shown to lead to a high selectivity towards the linear product, for example, in the hydrocyanation of 1,3-butadienes (compare Section 2.2.2.).^[67] Electron-deficient bidentate phosphonite ligands of type **59** were successfully used by the *Hofmann* group in the hydrocyanation of styrene.^[68]

2.2.4. Non-symmetric (transfer) hydrocyanation

In this section, modern achiral methods for the hydrocyanation of alkenes are presented based on the selectivities, ligands and catalysts development studies presented previously. In achiral synthesis, a switch from reduced nickel(0) precursors to nickel(II) salts as well as the use of nitriles as HCN substitutes can be observed (the latter called transfer hydrocyanation).^[46] The historical development and modern methods of enantioselective hydrocyanation are discussed in Sections 2.2.5.-2.2.7.

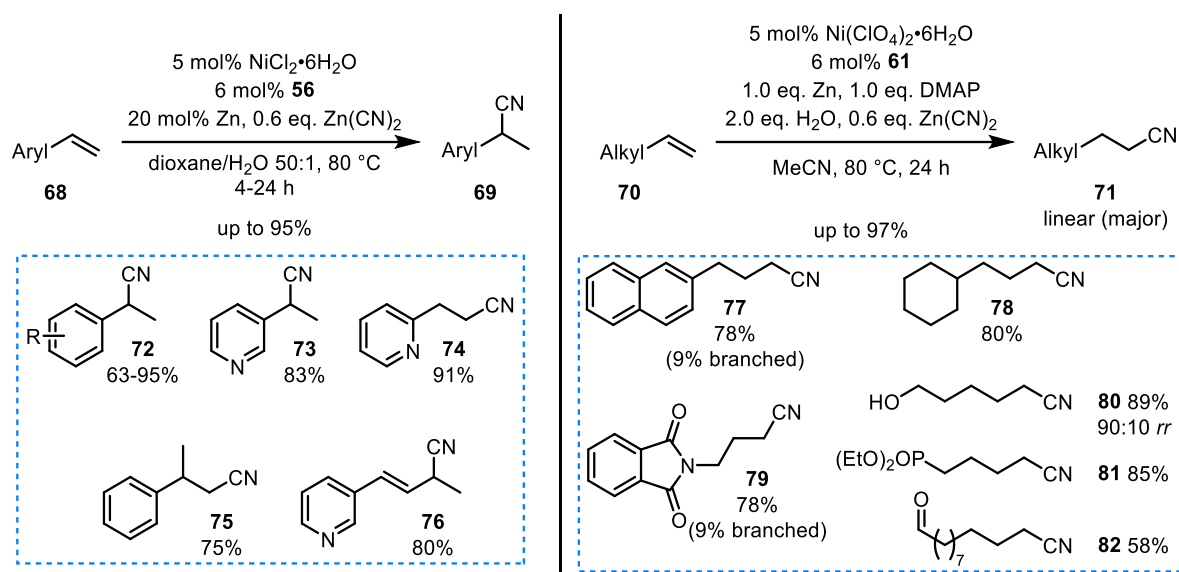
In 2016, *Nemoto et al.* presented their research on the hydrocyanation of some aliphatic olefins and vinylarenes of type **22** employing acetone cyanohydrin as HCN source (Scheme 11).^[69] In this work, an *in situ* catalyst system consisting of the nickel(II) salt $\text{NiCl}_2 \cdot 6\text{H}_2\text{O}$, the bidentate diphosphine ligand dppp (**61**), and zinc powder as a reductant was used. The regioselectivities ranged from 80:20 to 50:50 *rr* of linear to branched product.



Scheme 11: Hydrocyanation by *Nemoto et al.* starting from nickel salts as precatalyst and selected products.^[69]

Among the several substrates studied, (*E*)-stilbene (**65**) as 1,2-disubstituted substrate could be converted for the first time in low yield to 2,3-diphenylpropionitrile (**66**), or aliphatic systems such as 1-pentenene to 1-hexanenitrile (**67**) in excellent yield.

Recently, *Liu* and coworkers developed a more general protocol for a variety of aromatic and aliphatic systems starting from nickel(II) salts and zinc as reductant (Scheme 12).^[70] They used $\text{Zn}(\text{CN})_2$ and H_2O as the HCN source. For the vinylarene substrates **68** employed, xantphos (**56**) was a suitable ligand, and for non-aryl-conjugated olefins **70**, as in the work of *Nemoto et al.*, dppp ligand (**61**). This differentiation allowed the substrates to be obtained in a very regioselective manner. For linear product formation of type **71**, upon screening DMAP was shown to be crucial as a nickel co-ligand. It was suggested that increasing the steric bulkiness of the nickel complex favored the formation of linear products.

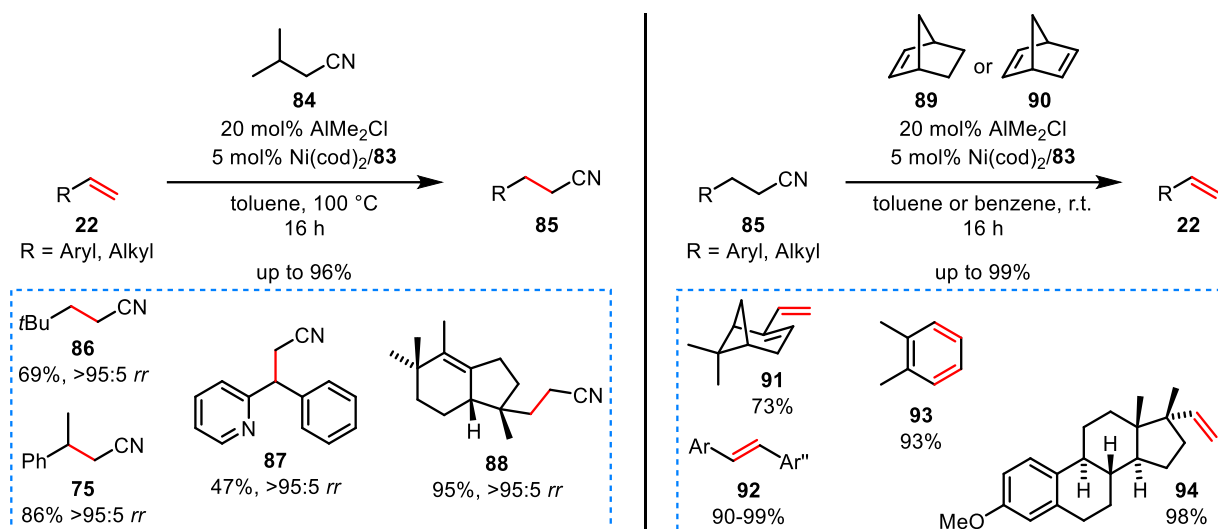


Scheme 12: General protocol of *Liu* and coworkers for the regioselective hydrocyanation of terminal olefins.^[70]

Moreover, heterocycles were investigated. Here, using 2-vinylpyridine, the linear product **74**, which is atypical for aryl-conjugated substrates, was obtained regioselectively in high yield. It is reasonable to assume that the coordinating pyridyl nitrogen leads to the formation of a five-membered metal chelate ring, thereby stabilizing the σ -alkyl complex (compare Scheme 10).^[71] In the case of α -methylstyrene as a 1,1-disubstituted example of a vinylarene, with the additional use of a reaction promoting Lewis acid ZnI_2 , product **75** could be derived in good yield.^[16, 72] The hydrocyanation conditions for aliphatic systems showed high tolerance to functional groups such as alcohols **80**, phosphonates **81** and aldehydes **82**.

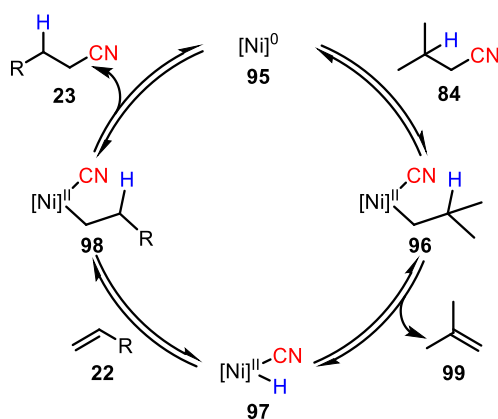
Many other research groups were looking for alternative sources of HCN. Among others, the *Yang* group was able to provide controlled HCN release using formamides that dehydrate Lewis acid-mediated and effectively hydrocyanate a range of terminal and internal alkenes using a xantphos **56**/nickel catalyst.^[73]

Although there are a number of less hazardous and easy-to-use HCN laboratory equivalents, however, most of these still release free HCN in solution and therefore are highly toxic. In 2016, *Morandi* and coworkers published a new methodology in which free HCN is not even generated during the reaction, but is abstracted from a nitrile (forming a corresponding alkene) and transferred to another alkene (HCN acceptor) using a nickel catalyst/DPEphos (**83**).^[74] Using isovaleronitrile (**84**) as the HCN donor, a wide variety of mostly terminal alkenes **22** (and alkynes) could be hydrocyanated efficiently to afford linear nitriles. Both 1,1-disubstituted alkenes could be converted to products such as **75** or **87** and late-stage natural product derivatives, like **88** derived from a cedrene analogue (Scheme 13).



Scheme 13: Invented transfer hydrocyanation (left) and transfer retro-hydrocyanation by Morandi and coworkers (right).^[74a]

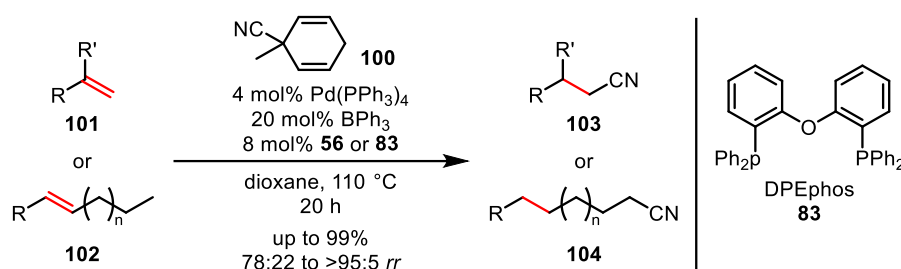
Since all steps of transfer hydrocyanation are reversible, the reaction process is thermodynamically controlled by the selection of HCN donor nitrile and HCN acceptor alkene. Thus, using norbornene (**89**) and norbornadiene (**90**) as HCN acceptors, many nitriles **85** (including secondary and tertiary nitriles) were converted *via* retro-hydrocyanation to the corresponding alkenes **22**. Moreover, late-stage transformations were exemplarily shown on terpene **91** or steroid derivative **94**. In addition, aromatic polyene derivatives like **92** or *ortho*-xylene (**93**) were synthesized by double HCN elimination. The *Lewis* acid-assisted catalyst system (ligand structure **83** is shown in Scheme 15) allows the elimination of HCN from the employed substrates, while the norbornene derivative (**89** or **90**) accepts HCN from the nickel catalyst under reduction of its ring strain. The proposed catalytic cycle is shown in Scheme 14 with isovaleronitrile (**84**) as the HCN donor nitrile. Starting from the catalytically active Nickel complex **95**, oxidative addition occurs into the C-CN bond of isovaleronitrile **84** to obtain **96**. This step is additionally supported by the *Lewis* acid as it is known to weaken the C-CN bond by coordination.^[60, 75]



Scheme 14: Proposed catalytic cycle of transfer hydrocyanation.^[74a]

From the metal-cyano compound **96**, H[Ni]CN complex **97** is formed by β -H elimination. This step generates isobutylene **99** as a byproduct derived from the HCN donor isovaleronitrile **84**. The intermediate **97** now acts as an HCN shuttle and transfers the nitrile group after coordination to the substrate **22** stepwise by β -H insertion (intermediate **98**) followed by reductive elimination. The latter releases both, the nitrile product **23** and the catalyst **95**. This proposed mechanism, based on deuterium-labeling and controlling experiments,^[74a] was independently confirmed by computational studies by the *Dang* group on the transfer hydrocyanation of simple olefins.^[76] *Morandi* and coworkers were furthermore able to fuse their retro-hydrocyanation approach with nickel-catalyzed cross-coupling in a dual catalytic cycle reaction cascade.^[77] Recently, they presented a highly kinetically controlled variant of their reversible transfer hydrocyanation approach, which overcame earlier selectivity problems and extended the substrate range.^[78] They additionally developed an operationally simplified, scalable procedure starting from nickel(II) salts.^[79]

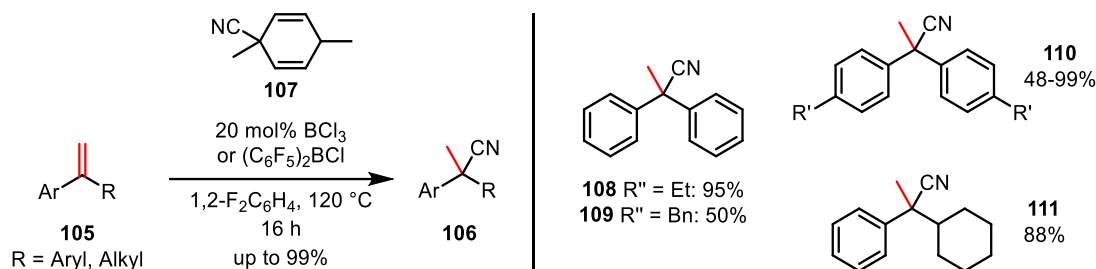
The *Studer* group developed the cyclohexadiene reagent **100**, which is highly suitable for transfer hydrocyanation and prepared from benzonitrile by reductive *Birch* methylation. In their *Lewis* acid-assisted palladium-catalyzed protocol, they produced an extensive range of nitriles **103** (>50 examples) from both aliphatic and aromatic alkenes **101** (Scheme 15).^[80]



Scheme 15: Palladium-catalyzed transfer hydrocyanation reported by the *Studer* group.^[80]

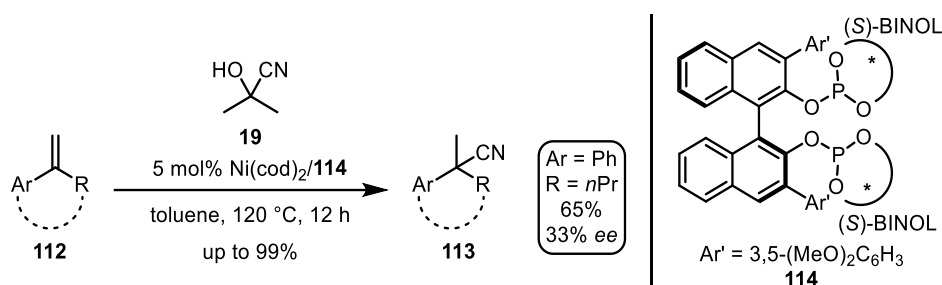
With their comprehensive catalysis protocol, linear nitriles **104** was obtained for the first time in reasonably good regioselectivity from internal olefins **102** by migratory hydrocyanation (see Section 2.2.8.). In order to access branched nitriles synthetically *via Markovnikov* transfer hydrocyanation, a nickel-catalyzed variant was developed in the absence of a *Lewis* acid using an HCN donor analogous to **100** (see Section 2.2.3., absence/presence of *Lewis* acids).^[81]

At about the same time, the *Oestreich* group developed a metal-free *Markovnikov* transfer hydrocyanation employing boron *Lewis* acid BCl₃ or (C₆F₅)₂BCl (Scheme 16).^[82] Under fair to excellent yields, tertiary nitriles **106** was obtained for the first time from aryl-conjugated alkenes **105** *via* hydrocyanation.



Scheme 16: Metal-free *Lewis* acid-catalyzed transfer hydrocyanation yielding tertiary nitriles.^[82]

Mechanistic studies revealed that in the first step, a *Wheland* σ -complex is formed from **107** by *Lewis* acid-catalyzed cyanide abstraction, which protonates the alkene **105** upon rearomatization (*para*-xylene as a byproduct) forming a tertiary benzyl cation, explaining the *Markovnikov* selectivity. The cyanide ion is subsequently transferred with reformation of the uncoordinated *Lewis* acid. The *Fang* group succeeded a little later in synthesizing tertiary benzyl nitriles **113** using nickel catalysis and a binaphthol-based diphosphite ligand **114** starting from α -substituted styrenes **112** and acetone cyanohydrin **19** (Scheme 17).^[83]



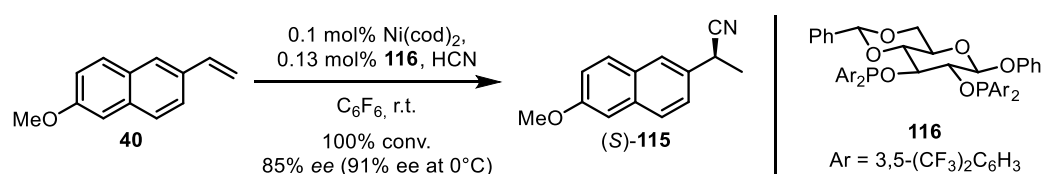
Scheme 17: Synthesis of tertiary benzyl nitriles *via Markovnikov* hydrocyanation of α -substituted styrenes.^[83]

Remarkably, they even achieved a substantial 33% *ee* for one substrate.

2.2.5. Enantioselective hydrocyanation: Initial studies

Despite the early research on hydrocyanation applied in the adiponitrile process (see Section 2.2.2.), the great success in asymmetric hydrocyanation remained elusive for a long time. Notwithstanding the attractiveness of chiral nitriles as valuable synthetic intermediates, building blocks for target molecules in natural product synthesis and pharmaceuticals, research groups focused on other metal-catalyzed asymmetric transformations until recently (see Sections 2.1. and 2.2.1.). In the last decade relevant synthesis protocols have led to major advances and the implementation of more reliable and increasingly applicable hydrocyanation sequences. Previous work has been summarized in extensive reviews by *Rajanbabu*^[40] and the *Vogt* group,^[16, 62] among others.^[44, 84] In the following, only the most important historical breakthroughs will be briefly reviewed and then present day modern works on asymmetric hydrocyanation will be discussed.

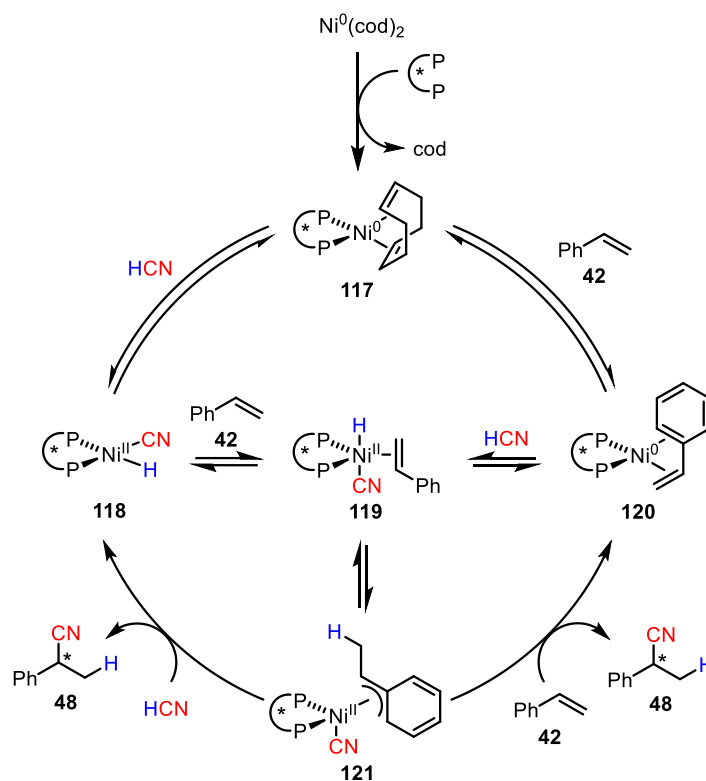
The first enantioselective approaches with low enantiomeric excesses were already examined in the 1980s. In particular, the groups of *Elmes*^[85] and *Hodsgon*^[86] were able to provide the first contributions as well as mechanistic considerations for enantioselective catalysis. They used chiral diphosphine ligands, such as (*S,S*)-DIOP, palladium as a metal catalyst, and norbornene **89** as a substrate. However, the enantiomeric excesses never exceeded 40% ee. After it was proven that the less expensive nickel catalysis gave similar results,^[87] *Rajanbabu* and *Casalnuovo* were able to achieve a sensational breakthrough with the enantioselective hydrocyanation of 2-methoxy-6-vinylnaphthalene (**40**) (Scheme 18).^[88] At that time they were interested in the asymmetric synthesis of the naproxen precursor (*S*)-**115**. Consistent with the mechanistic progression for vinylarenes (see Section 2.2.3.), the hydrocyanation sequence led to the desired branched constitution.



Scheme 18: Enantioselective hydrocyanation of 2-methoxy-6-vinylnaphthalenes (**40**) by *Rajanbabu* and *Casalnuovo*.^[88]

With the aim to establish an industrially applicable synthesis for the (*S*)-enantiomer that acts as an anti-inflammatory analgesic upon hydrolysis of the nitrile, remarkable results were obtained at exceptionally low catalyst and ligand loadings. D-Glucose-derived chiral diarylphosphinites of type **116** were utilized as asymmetry-inducing ligands. In further ligand-focused studies involving **40**, but also styrene **42** as substrates, the electron density at the phosphorus teeth showed a very strong influence.^[45] In particular, lower electron density due to electron-withdrawing aryl residues, as in the case of ligand **116**, provided the highest selectivities. The use of ligands with different electron densities at the phosphorous units could give superior enantiomeric excesses with up to 94% ee for the nitrile (*S*)-**115**,^[89] and are particularly suitable for hydrocyanation reactions, according to *Rajanbabu*.^[90] Nevertheless, the ligand system used was shown to be highly substrate specific for **40** and provided rather lower selectivities for other vinylarenes.

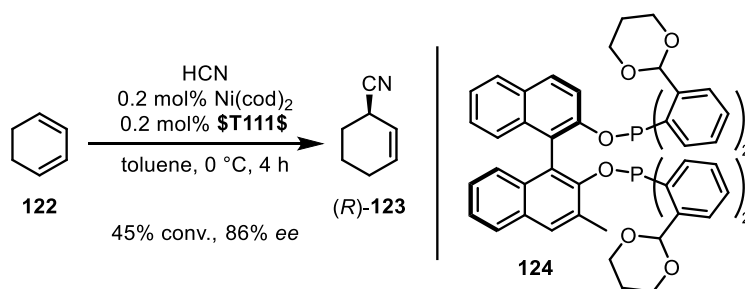
Extensive mechanistic studies by *Casalnuovo et al.*^[45] allowed a proposal of the catalytic cycle shown in Scheme 19. Ligand exchange first gives rise to the chiral catalyst complex **117**. Now, either HCN can undergo oxidative addition first, followed by coordination of the vinylarene (shown here on styrene **42**), or *vice versa* and in both cases the nickel(II) complex **119** is formed. From this, a β -H insertion allows the formation of the η^3 -benzyl complex **121**. Reductive elimination releases the product **48**, upon HCN or substrate addition to the complex. The active catalyst complexes **118** or **120** are regenerated and the cycle repeats.



Scheme 19: Proposed catalytic cycle of enantioselective hydrocyanation of vinylarenes (shown here on the reaction of styrene (**42**)).^[45]

Research by other groups quickly showed that in addition to the electronic properties studied by *Rajanbabu* and coworkers, the structural properties of the ligand were very important as well.^[91] Even the smallest modification in the steric properties caused major changes in the activity and selectivity of the catalysts. Less sterically demanding ligands even tended to form catalytically inactive bis-chelate species.^[91b] The results suggested investigation with a modular ligand system to make structural changes more accessible.

This was achieved by *Vogt* and coworkers, who were able to fine-tune a modular diphosphite ligand system with a chiral unsymmetric naphthol backbone to achieve an excellent enantiomeric excess of 86% in the hydrocyanation of 1,3-cyclohexadienes (**122**) (Scheme **20**).^[92]



Scheme 20: Asymmetric hydrocyanation of 1,3-cyclohexadiene (**122**) reported by the *Vogt* group.^[92]

However, the selectivity for styrene (**42**) was only 33% ee with the same ligand **124**. In a mechanistic study with 1,3-cyclohexadiene (**122**), they proved that in the mechanism proposed by *Rajanbabu* and coworkers (Scheme **19**), reductive elimination must be the enantioselective and rate-determining step.^[93] At the same time, there were additionally studies by the *Rajanbabu* group on aryl-conjugated 1,3-dienes.^[94]

In summary, there was some success in the enantioselective hydrocyanation of norbornene, vinylarenes, and 1,3-dienes until the late 2000s. However, the ligands predominantly showed high substrate specificity and a general protocol initially failed to emerge.

2.2.6. Enantioselective hydrocyanation: Phosphine-phosphite ligands by *Schmalz*

2.2.6.1. Highly modular phosphine-phosphite ligands

The development of new, mainly modular ligand systems still remains a key challenge in order for carrying out transition metal-catalyzed reactions efficiently and in asymmetric fashion. Despite the immense progress in computational chemistry as well as the deep mechanistic understanding of transition metal catalysis, the applicability and selectivity control of a ligand are difficult to predict. In particular, the systematic screening of a reaction with ligand libraries has proven successful in recent decades. Moreover, bidentate *P,P*-ligands with electronically differentiated phosphorus teeth gained in significance.^[95] Thus, the *Schmalz* research group developed a synthetic access to modular chiral ligands of type **124** in the 2000s and beyond (Figure **5**).^[96]

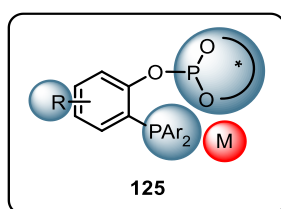


Figure 5: Modular and structurally diverse phosphine-phosphite ligands according to *Schmalz* and coworkers.

In the ligand system **124** not only the phenol-derived backbone can be diversely modified but also the phosphite unit carrying the stereo information. The phosphine unit can be further adjusted by exchanging its aryl residues. Thus, ligand libraries of type **126** or **127** (TADDOL-derived) and **128** (BINOL-derived) were prepared (Figure **6**) and successfully used in several transition metal-catalyzed transformations (see Scheme **22**). TADDOL-derived ligand **126** turned out to be highly superior in some enantioselective applications such as asymmetric copper-catalyzed conjugate addition reactions.^[97]

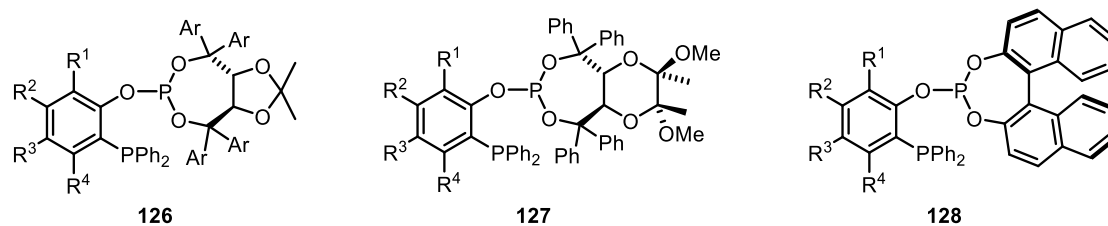
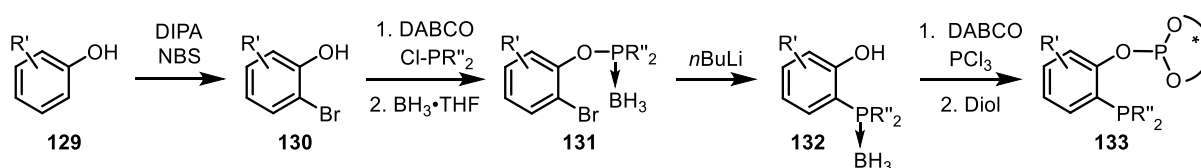


Figure 6: Developed modular ligand systems according to *Schmalz* and coworkers.

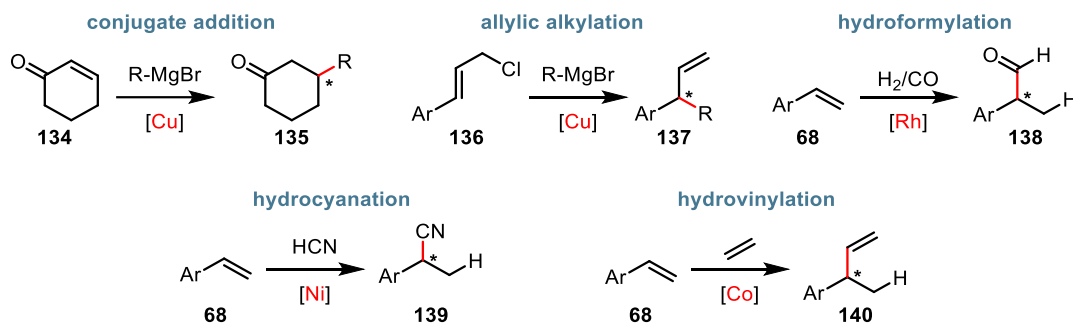
Due to an improved linear four-step synthesis route as shown in Scheme 21, the ligands can be rapidly prepared even at multigram scale.^[96c]



Scheme 21: Synthesis of phosphine-phosphite ligands from modular phenol and diol units.

Phenol building block **129** is reacted in an *ortho*-directed bromination. Subsequently, bromide **130** is mixed with a corresponding diarylphosphine chloride under basic conditions to afford phosphinite **131**, which is air-stable after borane protection. A *Fries*-type rearrangement induced with *n*BuLi affords the phosphine unit **132**.^[98] Under basic conditions, this phosphine borane complex is additionally deprotected with DABCO and, after addition to PCl_3 , attached to the chiral diol.

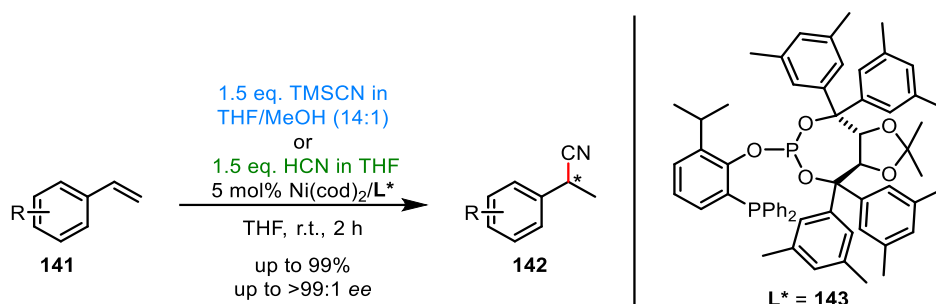
To date, many of the described ligand types (Figure 6) have been successfully applied in some transition metal-catalyzed reactions (for a selection, see Scheme 22). In most cases, the corresponding ligand/catalyst systems achieved high to excellent enantiomeric excesses and could often be implemented in the key steps of target molecule syntheses. Among the most successful enantioselective applications are copper-catalyzed 1,4-addition to cyclic enones such as **134**^[99] or allylic alkylation to allyl chlorides **136**,^[100] rhodium-catalyzed hydroformylation of vinylarenes **68** towards α -chiral aldehydes **138**,^[101] cobalt-catalyzed hydrovinylation of vinylarenes **68**,^[102] and nickel-catalyzed hydrocyanation of vinylarenes towards benzyl nitriles **24**.^[42, 103] The work and contributions to the latter are presented in more detail in the following section, as they provide the basis for the research conducted in this thesis.



Scheme 22: Overview of applications of the presented phosphine-phosphite ligands in enantioselective transition metal catalysis.

2.2.6.2. TADDOL-derived phosphine-phosphites in asymmetric hydrocyanation

In 2013, *Falk et al.* exploited the tunability of these chiral TADDOL-derived ligands of type **126** (dioxolane-bridged TADDOL building blocks) and implemented them in the nickel-catalyzed hydrocyanation of vinylarenes **141**, for which no general enantioselective protocol was established until then (Scheme 23).^[42] Among more than 15 ligand derivatives tested, phosphine-phosphite **143** proved to be the most selective in terms of conversion and enantiomeric excess. Its backbone consists of an *ortho*-isopropyl-substituted phenol and its TADDOL moiety features 3,5-dimethylphenyl as aryl substituents.



Scheme 23: Enantioselective nickel-catalyzed hydrocyanation using TADDOL-derived phosphine-phosphite ligands established by *Falk et al.*^[42, 103]

Once a substitution pattern was determined, reaction conditions and a suitable HCN surrogate had to be fine-tuned. After initial tests with acetone cyanohydrin, TMSCN/MeOH in THF was carefully chosen as the reagent solution. Crucial for the high enantioselectivities were a slow addition over 2 h to keep the HCN concentration low during the reaction in order to avoid the formation of inactive $\text{Ni}(\text{CN})_2$ species.^[16, 45] It is noteworthy that if the addition was too slow, the conversion collapsed. This indicated that the catalyst is also deactivated when too little fresh HCN is present.^[42, 84] With this methodology, a larger series of electron-rich and electron-poor substituted vinylarenes could be hydrocyanated for the first time with consistently high conversions and good to excellent enantiomeric excesses. The reaction always proceeded with absolute regioselectivity for the branched *Markovnikov* product.

In addition, to prove the principal applicability of this method in industry, the direct use of HCN was investigated and successfully integrated into the process.^[103] A selection of the substrate spectrum is shown in Figure 7 with the corresponding GC conversions (conv.) or yields (if isolated) and the enantiomeric excesses in [%]. Marked in blue are the selectivities when using TMSCN/MeOH as HCN-releasing reagent mixture and marked in green when using HCN in THF directly.

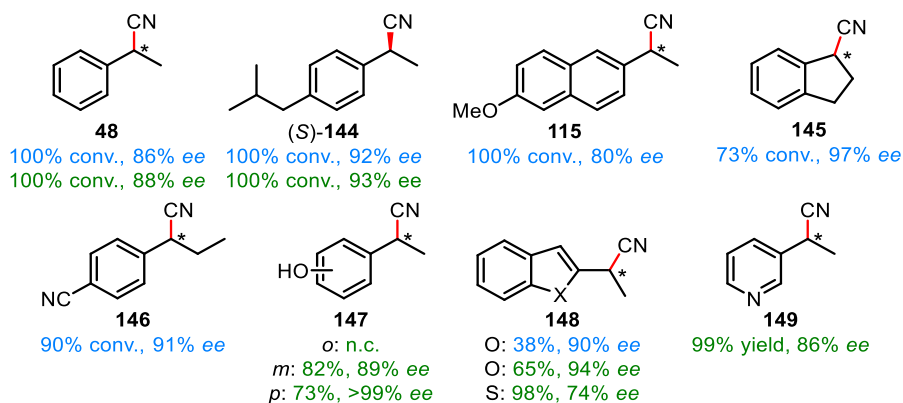


Figure 7: Selected examples of the substrate spectrum of the hydrocyanation protocol of *Falk et al.*^[42, 103]

During the optimization of ligand structure, reaction conditions and HCN source, styrene (**42**) was used as test substrate. Under the finalized conditions, complete conversions and high enantiomeric excesses were obtained for its nitrile product **48** using both TMSCN/MeOH or HCN as reagent. The same was true for the *Ibuprofen* precursor **144**. To determine the absolute configuration, the specific rotation value after hydrolysis of the nitrile was compared with the corresponding literature values and confirmed (*S*)-configuration, which is highly likely to be the same for the other structurally related hydrocyanation products with ligand **143**.^[42, 104] As a well-suited cyclic vinylarene, indene was converted to the nitrile **145** with the highest enantiomeric excess of 97% ee for the TMSCN/MeOH system. Electron-poorer systems such as **146** were accessible as well. With HCN as the most atom-economical reagent, unprotected vinylphenols and heterocycles were subjected to hydrocyanation. In this investigation, even only one enantiomer was generated of the *para*-substituted phenol **147** (within the analytical limits), which is one of the highest selectivities in an asymmetric hydrocyanation reaction to date. There was no conversion for the *ortho*-vinylphenol. It was assumed that the free hydroxy group could additionally coordinate to the nickel catalyst and prevent HCN addition to the complex. Additionally, 2-vinylindole, 2-vinylbenzofuran and 2-vinylbenzothiophene could be reacted with moderate to excellent yields and selectivities (nitriles **148**). (Un)protected indole derivatives could only be reacted to a limited extent or not at all. Likewise, *N*-methylpyrrol, nitro- or bromo-substituted styrenes did not yield any conversion. Hydrocyanation of trisubstituted α,β -dimethylstyrene, which would yield a tertiary nitrile, remained unsuccessful.

It was observed that the enantiomeric excess was slightly higher when HCN was used directly (see **48** and (*S*)-**144**), which again was explained by the complete absence of methanol, the poorer solvent in terms of enantioselectivity (compared to THF in previous solvent screening). The reaction profile of styrene **42** with direct use of HCN was established by GC monitoring and showed rapid initial conversion. Thus, under these conditions, either the reaction time could be reduced to 15 min (HCN addition time), with still full conversion and the same enantiomeric excess, or the catalyst loading could be reduced to 0.42 mol% with 2 h HCN addition time. This again underlined the potential for a more industrial setup.

In addition to indene (nitrile product **145**), other 1,2-disubstituted substrates, i.e. the alkylvinylarenes **150-153** with different *E/Z* ratios were investigated (Figure 8). While the styrene derivatives **150** and **151** showed only low conversions to give the benzyl nitriles **154** and **155**, the alkenes **152** and **153** reacted much more smoothly. It was found that in the aspect of incomplete conversion, only the (*E*)-isomer of the starting material was reisolated. This suggested a significantly higher reactivity of the (*Z*)-isomers. Moreover, this assumption could explain the higher conversions to the nitriles **156** and **157**, since the amount of (*Z*)-isomer was significantly higher in the starting compounds.

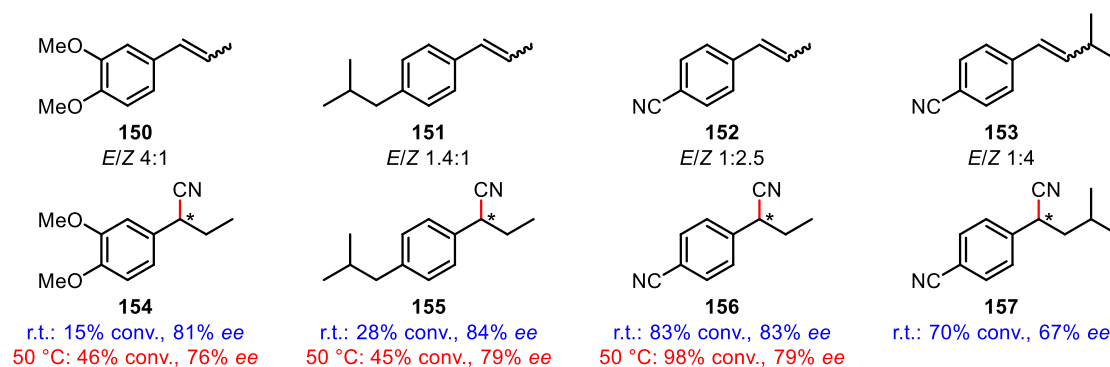


Figure 8: Selected 1,2-disubstituted substrates **150-153** and the respective nitrile products **154-157** after hydrocyanation.^[42, 84]

The fact that comparable ee values were obtained despite different *E/Z* ratios could be attributed to the verified enantioselective step (the reductive elimination)^[93] taking place *after* the β -H insertion into the double bond and, consequently, the difference between the two (*E/Z*)-isomers already being resolved (see Scheme 19, Section 2.2.5.).^[84]

In their study, *Falk et al.* were able to contribute to the generally accepted mechanism of the enantioselective hydrocyanation (see Scheme 19, Section 2.2.5.). Through ³¹P NMR experiments and elaborate X-ray single crystal analysis, they were able to elucidate the structure of the active catalyst Ni(cod)**143** (Figure 9).^[103]

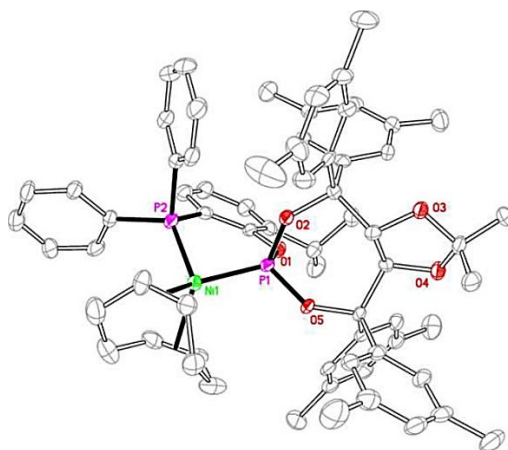
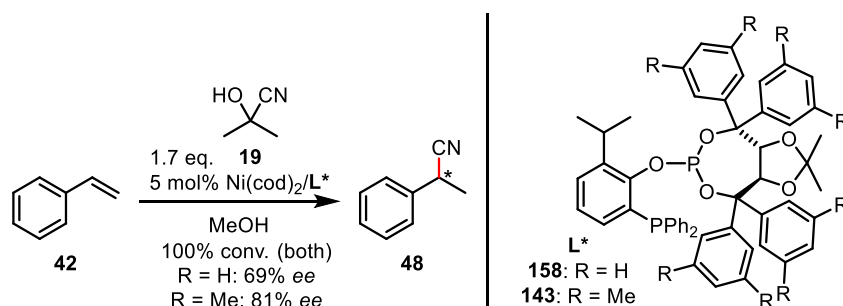


Figure 9: Crystal structure of Ni(cod)**143** complex.^[103]

When deuterated styrene- d_8 was used and the reaction was monitored by ^2D NMR, the coordination of the substrate to the catalyst was indicated by a shift of the signal set to the high field. The product spectrum recorded after HCN addition showed no hydrogen/deuterium scrambling, strongly suggesting that the β -H insertion in the reaction with styrene- d_8 was irreversible or at least reversible only to a minimal extent.

For the success of the catalysis, as discussed in Section 2.2.5, both the electronic and the structural properties of the ligand system are crucial. This was impressively demonstrated during the structural optimization of the TADDOL-derived phosphine-phosphite ligand **143**. The replacement of the H-substituents in the 3,5-positions (ligand **158**) at the chiral TADDOL phenyl units by methyl groups alone (ligand **143**) resulted in an immense increase in selectivity from 69% to 81% ee (Scheme **24**).



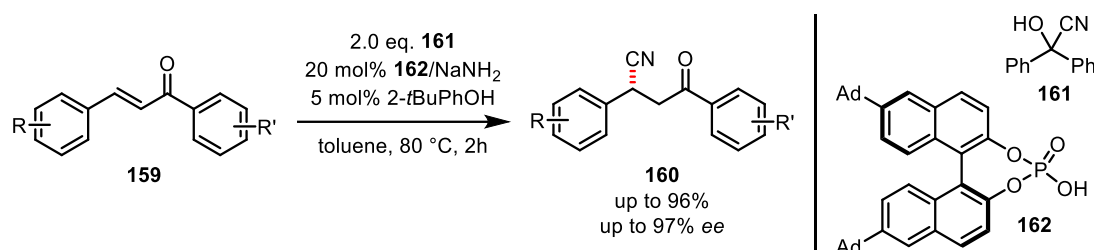
Scheme 24: Selectivity burst upon incorporation of methyl groups into the chiral TADDOL moiety during ligand optimization.^[42, 84]

Falk postulated that if other residues R were used in the 3,5-positions, stereoselectivity would be significantly affected and, above all, it cannot be ruled out that greater steric demand would even significantly increase it.^[84]

2.2.7. Enantioselective hydrocyanation: Current strategies and tactics

In recent years, in the course of ligand development and the establishment of first fundamental protocols, attention to the usefulness of enantioselective hydrocyanation has increased greatly. This is not only seen in a more frequent use of this transformation in target molecule or natural product synthesis,^[105] but in a significant number of recent publications focusing on the development of asymmetric hydrocyanation in terms of its chemo-, regio-, and enantioselectivity and, most importantly, to make it more accessible to a broader substrate scope.^[44, 46] In this regard, some research groups have even developed protocols employing highly adapted ligands or reaction sequences that bypass direct hydrocyanation by using a more established hydrofunctionalization and subsequent conversion of the introduced functional group to a nitrile. This way, some formal enantioselective hydrocyanation methods with a large substrate scope have been established. In addition to hydrocyanation, which is the focus of the methods presented below, there have been outstanding publications on copper-catalyzed cyanation reactions.^[106] These include an enantioselective borocyanation^[107] of 1-aryl-1,3-butadienes or the direct radical cyanation of benzylic C-H bonds of the *Liu* group,^[108] which gave nitriles with high enantiomeric excesses.

In 2013, the *Chen* group reported a phosphate-catalyzed, asymmetric hydrocyanation of a series of chalcones **159** using a benzophenone-derived cyanohydrin **161** as the HCN source (Scheme 25).^[109]

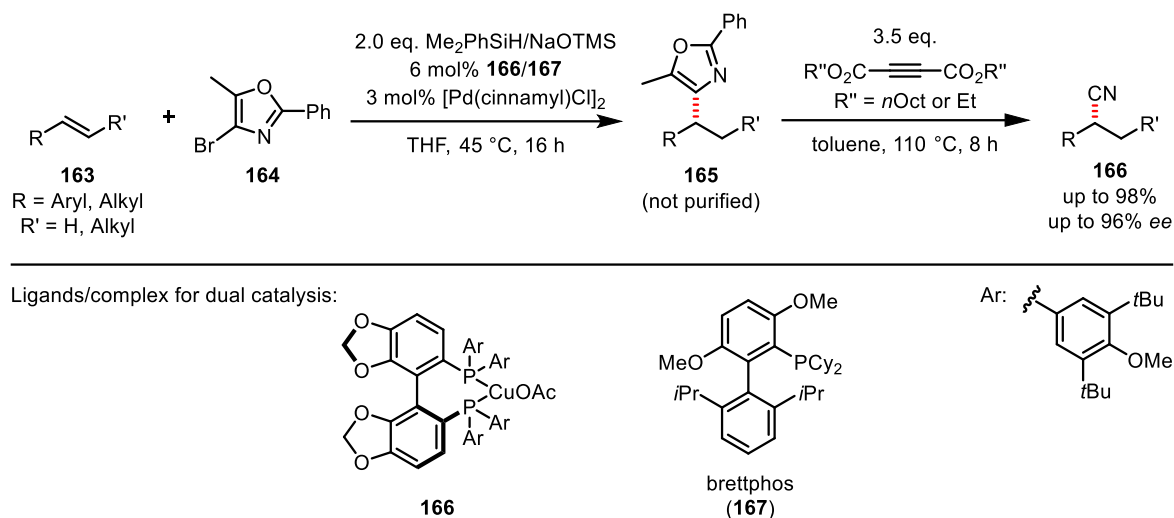


Scheme 25: Enantioselective hydrocyanation of chalcone derivatives by chiral phosphate catalysis by *Chen* and coworkers.^[109]

NaNH₂ acts as a base in this reaction to generate the active phosphate catalyst from the chiral BINOL-derived phosphoric acid **162**. According to the authors, this enables the 1,4-addition of the cyanide to the enone function in a chiral environment after coordination of the phosphate to HCN. The phenol additive 2-*t*BuPhOH was crucial to facilitate the deprotonation/protonation of the catalyst/enolate. Despite high yields and selectivities for the described chalcones, broader use of phosphate catalysts in enantioselective hydrocyanation failed to emerge, as transition metal-catalyzed variants were more versatile.

As already indicated above, some academic groups tried to circumvent the problems of the still restricted range of substrates and the use of highly toxic HCN or its surrogates. In some cases, highly complex and sophisticated reaction cascades were developed. While these were

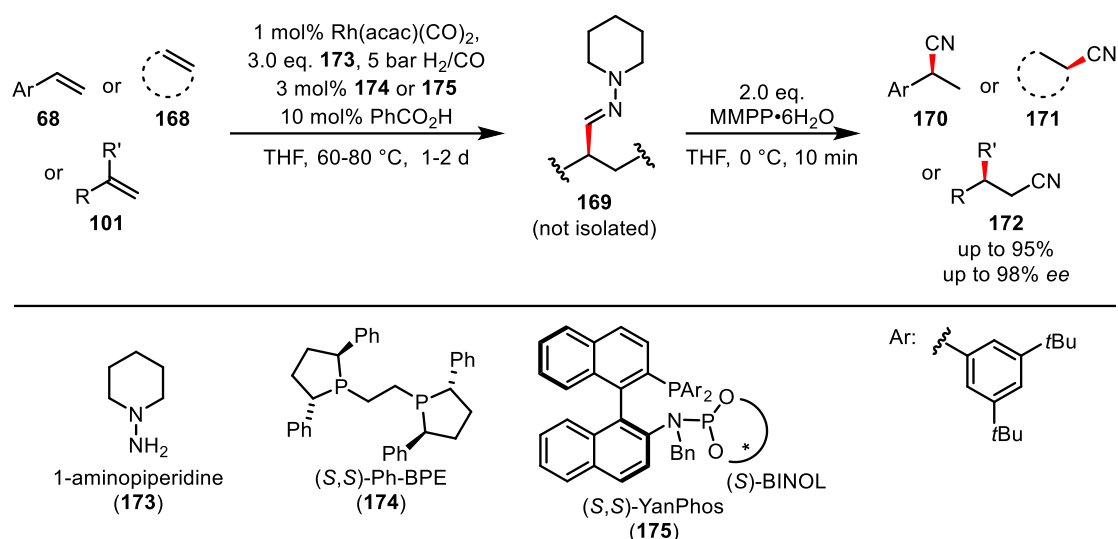
significantly less atom-economical, they could be used with remarkably high selectivities for diverse substrates. For instance, *Buchwald* and coworkers elaborated a three-step reaction sequence to nitriles starting from alkenes (Scheme 26).^[110]



Scheme 26: Formal enantioselective hydrocyanation using a hydroarylation/*Diels-Alder*/retro-*Diels-Alder* sequence by *Buchwald* and coworkers.^[110]

In their protocol, they utilized a highly enantioselective hydroarylation process to first obtain the alkyloxazole intermediate **165**. In this, a dual catalyst system was used consisting of the (*S*)-DTBM-segphos [Cu(I)] complex **166** and a Brettphos (**167**)-complexed palladium catalyst. A base (NaOTMS) and a silane (Me₂PhSiH) were used to (re-)generate the active [Cu(I)]-hydride complex. Subsequent [4+2]-cycloaddition with either ethyl- or octyl-esterified acetylenedicarboxylic acid and a retro-[4+2]-cycloaddition afforded the targeted nitrile **166** while retaining the enantiomeric excess of the hydroarylation product **165**.

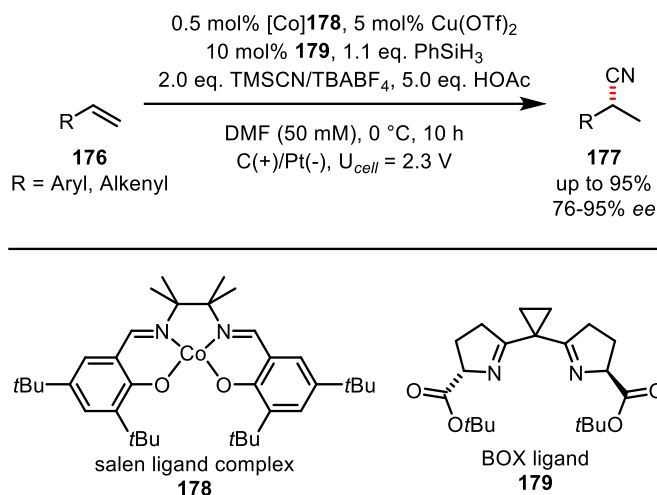
Zhang, *Lv* and coworkers were able to regio- and enantioselectively react vinylarenes of type **68**, 1,2-substituted aliphatic pentacycles **168**, and 1,1-disubstituted (non-)aryl-conjugated olefins of type **101** to chiral hydrazones of type **169** by means of asymmetric rhodium-catalysis, from which the nitrile products **170**, **171** and **172**, respectively, were obtained in good to excellent yields (Scheme 27).^[105b]



Scheme 27: Formal enantioselective hydrocyanation using a hydroformylation/condensation/aza-Cope elimination sequence by Zhang and coworkers.^[105b]

This method for a formal hydrocyanation actually exploits a rhodium-catalyzed asymmetric hydroformylation of the respective alkene substrate, a trapping of the corresponding aldehyde in an imine condensation to form the hydrazone of type **169**. Subsequent aza-Cope elimination under oxidative conditions with magnesium monoperoxyphthalate (MMPP) finally releases the nitrile. Noteworthy, the reaction conditions of the imine condensation with 1-aminopiperidine **173** had to be carefully adjusted. Addition of benzoic acid prevented racemization of the intermediate **169** by enamine formation. The applicability of the method was impressively demonstrated in a synthesis of a precursor of the diabetes drugs *Vildagliptin* and *Anagliptin*.^[105b]

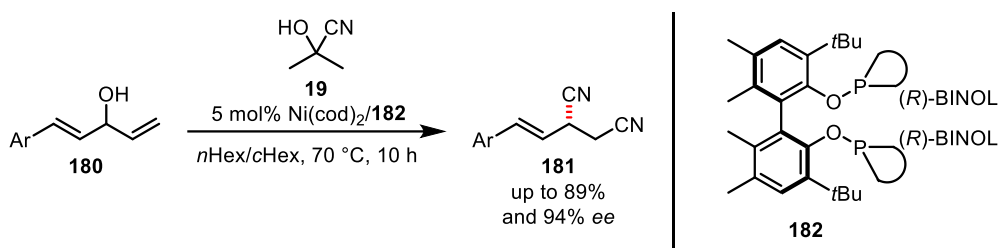
In 2020 the *Lin* group presented an impressive electrochemical pathway to generate enantioselectively branched nitriles from conjugated alkenes of type **176**. In their hydrocyanation approach, they used an electrolysis methodology in an overall oxidative process with a dual redox-catalysis system consisting of the [Co]-salen complex **178** and [Cu]-BOX ligand **179** complex (Scheme **28**).^[111]



Scheme 28: Highly enantioselective hydrocyanation of vinylarenes or 1,3-dienes using a dual electrocatalysis approach by *Lin* and coworkers.^[111]

The key step of this transformation consists, on the one hand, of the cobalt-catalyzed hydrogen atom transfer (HAT) and, on the other hand, of a copper-catalyzed cyanation cycle. The HCN source was TMSCN, the hydride source for the HAT process phenylsilane. Crucial are the electrolysis conditions with two single electron oxidation events to convert the resulting [Co(II)] and [Cu(I)] complexes back into their reactive [Co(III)] and [Cu(II)] species.^[111] Also 1,2-disubstituted derivatives such as several stilbenes, enones and allenes were converted in moderate to good yields with high enantioselectivities.

Hydrocyanation has been studied extensively by the *Fang* group in recent years. On the basis of the ligands already applied in this asymmetric nickel-catalyzed reaction, they were able to identify several BINOL-derived diphosphite ligands with either a BIPOL or TADDOL backbone that were applicable in numerous transformations. They primarily used acetone cyanohydrin (**19**) as an HCN-releasing reagent in their hydrocyanation protocols. An outstanding protocol was the synthesis of 1,3-dinitriles by merging nickel catalysis of an allylic cyanation and an enantioselective hydrocyanation (Scheme 29).^[112]

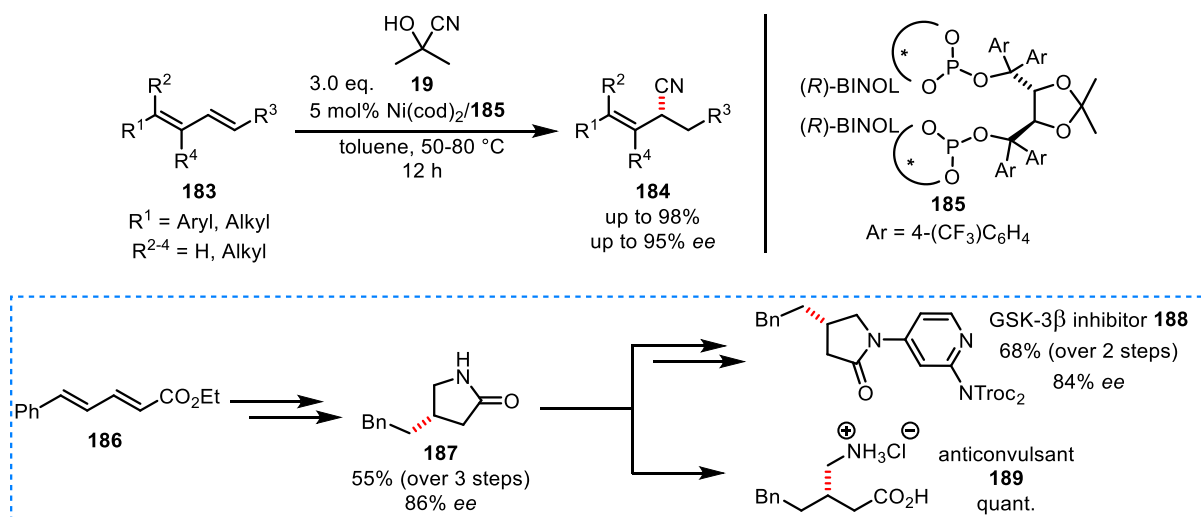


Scheme 29: Allylic cyanation/enantioselective hydrocyanation reaction cascade by *Fang* and coworkers to access 1,3-dinitriles.^[112]

Secondary (racemic) allylic alcohols of type **180** were predominantly used as substrates (primary derivatives or mixtures are also possible). According to the proposed mechanism, the allylic substitution to obtain the linear achiral nitrile occurs first to form an aryl-conjugated 1,3-

dienyl system, followed by enantioselective hydrocyanation of the terminal double bond. Among several tested bidentate *P,P*-ligands, the diphosphite ligand **182** with two (*R*)-BINOL units and a chiral biaryl as backbone turned out to be most suitable in this transformation.

Employing a different (*R,R*)-TADDOL-derived diphosphite ligand **185**, a wide range of substituted 1,3-dienes **183** could be highly selectively hydrocyanated (more than 40 examples) (Scheme 30).^[105d]



Scheme 30: Enantioselective hydrocyanation of 1,3-dienes and its application target molecule synthesis by Fang and coworkers.^[105d]

As an impressive implementation, the developed methodology was used in a new synthesis of the glycogen synthase inhibitor **188** and the anticonvulsant **189**. Starting from carboxylic acid ester **186**, the homobenzyl-substituted lactam **187** was obtained in three steps (hydrocyanation, hydrogenation, lactamization) in good yield. This building block was then converted to **189** by treatment with HCl or to **188** over two steps.

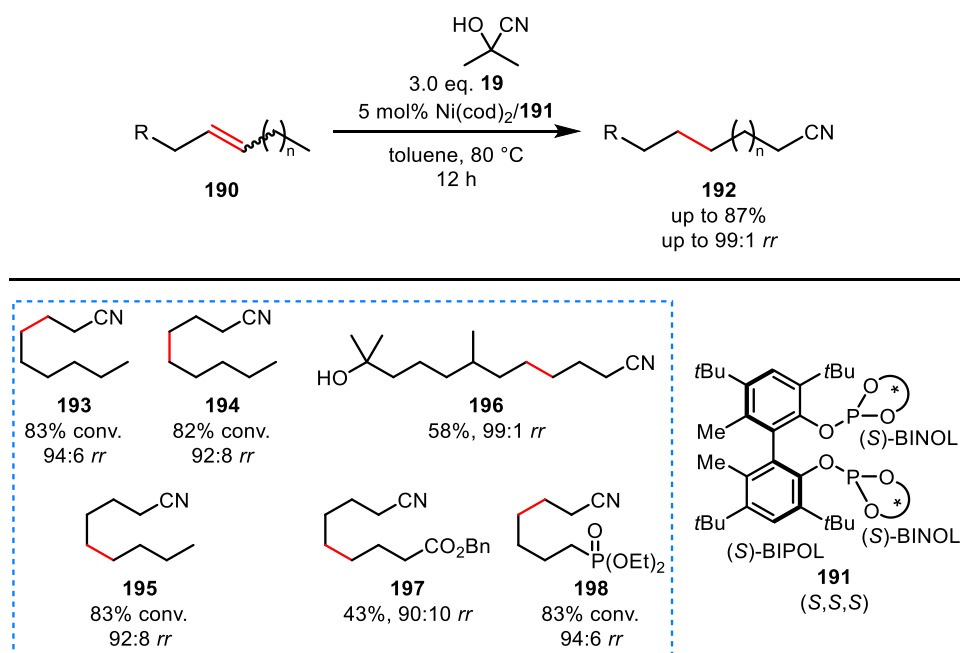
In the field of enantioselective hydrocyanation, the Fang group did not only focus on non-activated alkenes as substrates. Moreover, they have developed highly selective protocols for other interesting systems, such as methylenecyclopropanes^[113] or allenes.^[114] In conclusion, in these protocols, besides using acetone cyanohydrin (**19**) as HCN source, the application of chiral bidentate *P,P* ligands was the key to success.

After careful consideration, the Fang group took advantage of the phenomenon of nickel-catalyzed chain-walking of double bonds and implemented this for remote functionalization in several works on migratory hydrocyanation. Since the investigations of this thesis deal with hydrocyanation also under the aspect of Ni-catalyzed chain-walking, the results are briefly presented in the following section.

2.2.8. Migratory hydrocyanation *via* nickel-catalyzed chain-walking

Transition metal-catalyzed isomerization of alkenes (chain-walking) has been an established method in tandem/auto-tandem reactions to enable remote functionalization for long.^[115] Double bond isomerization in the hydrocyanation of alkenes has been known since the application in the adiponitrile process (see Section 2.2.2.). In general, the use of *Lewis* acids favors the formation of linear nitriles, as the resulting metal complexes catalyze the isomerization to terminal olefins (see Scheme 8, Section 2.2.3). Already *Morand*^[74] and *Studer*^[80] made it possible to obtain linear nitrile products from internal olefins in moderate to good regioselectivities with their work on transfer hydrocyanation (see Section 2.2.4.).

The *Fang* group, on the other hand, tried to optimize the ligand structure so that double bond migration to the terminal olefin is favored without the use of *Lewis* acids and anti-*Markovnikov* addition to give the linear nitrile is enabled. The following works by *Fang* and coworkers were published in 2020 and 2021. Employing BIPOL/BINOL diphosphite ligand **191**, it was possible to obtain linear nitriles **193-195** in relatively high regioselectivities starting from internal aliphatic 2-, 3- or 4-alkenes of type **190** (Scheme 31).^[116] Moreover, olefin isomer mixtures of the same type could be selectively converted to a single linear product.

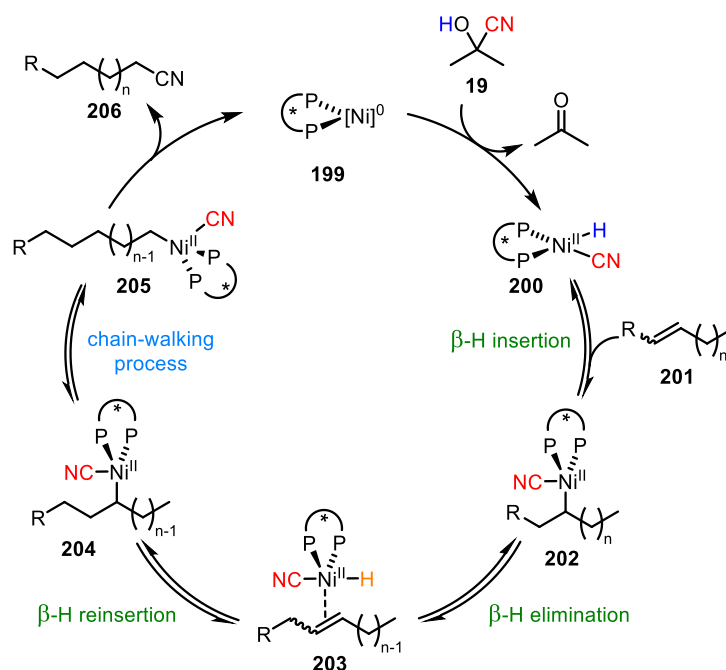


Scheme 31: Linear nitriles from internal olefins utilizing migratory hydrocyanation of *Fang* and coworkers (selected product examples shown).^[116]

Due to the absence of a *Lewis* acid, the method showed significantly higher functional group tolerance for the more than 25 substrates tested, such as for tertiary alcohol **196**, benzyl ester **197** or phosphonate **198**. To understand the regioselectivity induced by the ligand **191**, density functional theory (DFT) calculations were performed by the *Fang* group using the hydrocyanation of 1-butene as a model system. The optimized transition states of the reductive

elimination confirmed that this step was crucial for the regioselectivity. Thus, reductive elimination is favored both thermodynamically and in steric interaction with the ligand **191** to form the linear nitrile.^[116]

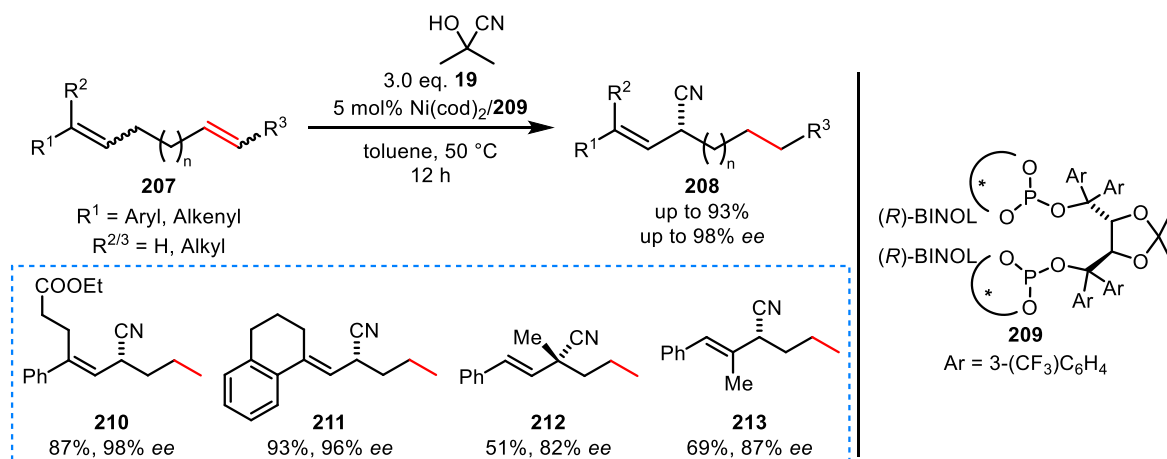
The general chain-walking process that takes place in migratory hydrocyanation can be conveniently explained by the proposed mechanism of the *Fang* group in their protocol on internal olefins (Scheme **32**).^[116]



Scheme 32: Proposed catalytic cycle of migratory hydrocyanation of internal olefins *via* nickel-catalyzed chain-walking.^[116]

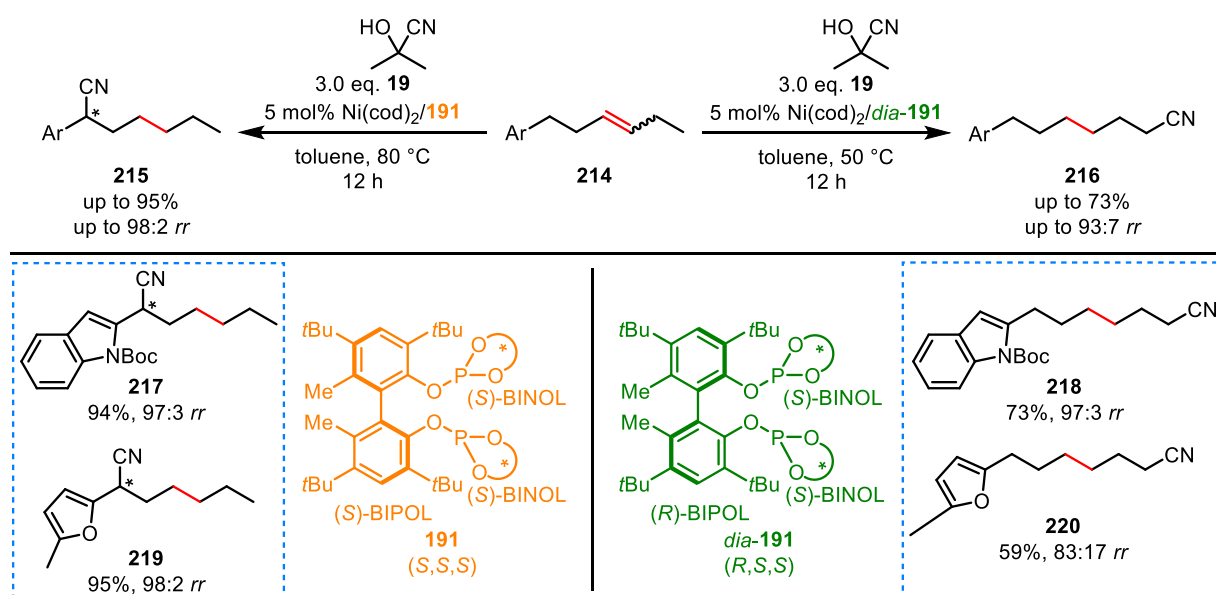
Starting from the active nickel complex **199**, oxidative addition of HCN takes place, resulting in H-[Ni]-CN complex **200**. Subsequent β -H insertion into the double bond of alkene **201** triggers a reversible β -H elimination/ β -H reinsertion cascade that can lead to multiple nickel alkyl species along the alkyl chain (for example, **202**, **204**, or **205**). According to DFT calculations, from the sterically and thermodynamically most favorable species **205**, reductive elimination takes place at the primary carbon. The linear nitrile product **206** is released and the active catalyst complex **199** recovered, which will immediately undergo oxidative addition by HCN.

Furthermore, *Fang* and coworkers succeeded in converting non-conjugated dienes of type **207** in an enantioselective migratory hydrocyanation (Scheme **33**).^[117] For this purpose, a BINOL-derived diphosphite ligand with a TADDOL backbone **209** was employed. In doing so, they only very slightly modified the ligand system **185**, which was already used for conjugated 1,3-dienes systems (see Scheme **30**, Section 2.2.7.), at the aryl units of the TADDOL backbone (change from Ar = 3-(CF₃)C₆H₄ **185** to Ar = 4-(CF₃)C₆H₄ **209**).



In this approach, the branched nitriles were obtained regioselectively, since a more stable η^3 -allyl complex can be formed during chain-walking, from which reductive elimination occurs (see Section 2.2.3.). Good yields and good to excellent enantiomeric excesses were generally obtained.

Most astonishing were the results of Yu, Rajasekar and Fang when internal olefins **214**, aryl-substituted at one end of the alkyl chain, were used as substrates (Scheme 34).^[118]



Using ligand **191**, which has already been successfully used in the migratory hydrocyanation of internal aliphatic olefins (see Scheme 31), and its diastereomer *dia*-**191**, a ligand-directed regiodivergent control was achieved. The exchange of the BIPOL backbone (either (*S*)- or (*R*)-configuration) led to a significant change in the transition state during catalysis, so that with the (*S,S,S*)-diastereomer **191** predominantly branched benzyl nitriles of type **215** were

obtained, whereas the (*R,S,S*)-diastereomer induced the formation of the linear nitriles **216** starting from the same substrates. Thereby, the products could be generated in good to excellent regioselectivities. Detailed DTF calculations proved that the spatial arrangement of the isomeric ligands differs significantly, resulting in different steric and electrical interactions in the transition states of reductive elimination.^[118] Thus, reductive elimination from either the σ -alkyl complex at the primary carbon ((*R,S,S*)-ligand *dia*-**191**) or the η^3 -benzyl complex ((*S,S,S*)-ligand **191**) is preferred (compare to Section 2.2.3., Scheme **10**).

Moreover, they were able to transfer the principle of double bond migration to an enantioselective allylic cyanation of alkenyl alcohols.^[119] Overall, these results demonstrate the importance of ligand design and structure to control nickel-catalyzed chain-walking and its utilization in migratory hydrocyanation.

2.3. Motifs and synthetic access to homostilbenes (1,3-diarylpropenes)

Since this work is the first to investigate homostilbenes in hydrocyanation, they are briefly introduced below. Structurally, homostilbene ((*E*)-**221a**) is derived from stilbene ((*E*)-**65**) by the introduction of a CH₂ unit (Figure 10). Functionalized stilbenes are present in nature mainly in plants and mostly serve as phytoalexins for the defense mechanism against diseases caused by microorganisms.^[120] Biosynthetically, (homo)stilbenes are produced *via* the aromatic amino acids L-phenylalanine and L-tyrosine derived from the shikimate pathway.^[121] Stilbene structures are often used as drugs due to their high bioactivity.^[122]

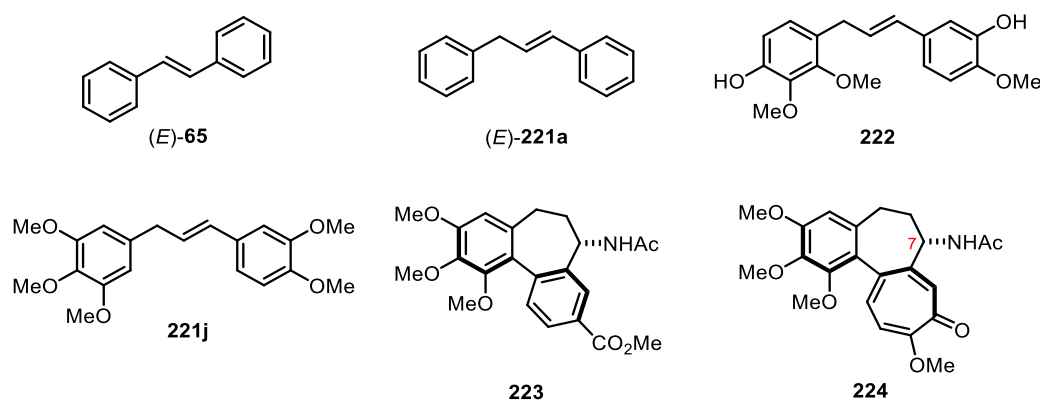
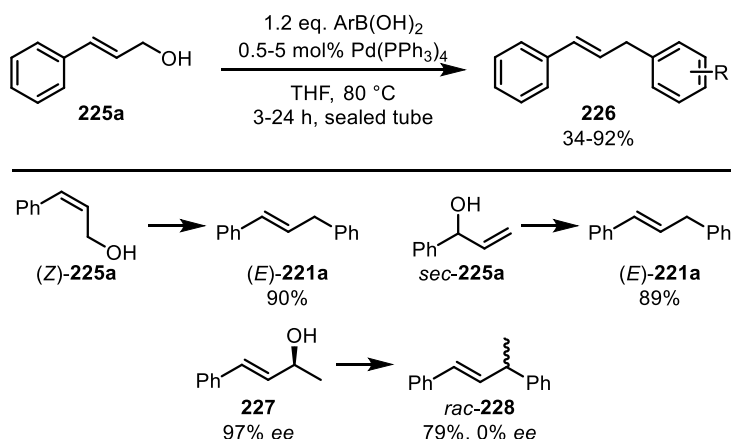


Figure 10. Structures (*E*)-stilbene (**65**), (*E*)-homostilbene (**221a**), breast cancer invasion inhibitor **221j**, cytotoxic candenatenin A (**222**), (-)-(a*R*,7*S*)-allocolchicine (**223**) and (-)-(a*R*,7*S*)-colchicine (**224**).

The homostilbenes, often referred to in the literature as 1,3-diarylpropenes, belong to the flavonoid family and have likewise a high pharmacological potential due to their cytotoxicity.^[123] For example, the natural compound candenatenin A (**222**), isolated in 2009, showed micromolar cytotoxic activity against all cancer cell lines tested.^[124] In addition, a wide range of synthetic homostilbenes such as the breast cancer invasion inhibitor **221j**^[125] exhibit in some cases efficiencies comparable to the highly bioactive colchicine (**224**).^[123, 125-126] The latter is the main alkaloid of the poisonous autumn crocus (*colchicum autumnale*) and with its derivatives one of the most important inhibitors of tubulin assembly and microtubule formation-related disease mechanisms.^[127] It is reasonable to assume that many homostilbenes attach to the colchicine binding site of the tubulin subunits due to their structural similarity (compare **221j** with **223** and **222**).^[127b] In addition to their attractiveness as targets, they are repeatedly used as synthetic intermediates in natural product and target molecule syntheses.^[128] Overall, however, homostilbenes still receive too little attention, although their incorporation into synthesis protocols is promising.

Homostilbenes can be generated *via* various established synthetic strategies.^[129] Among these, *Tsuji-Trost*-type nickel- or palladium-catalyzed allylic substitutions of cinnamyl alcohols,^[130] acetates,^[131] or even carbonates^[132] particularly stand out as reliable procedures.

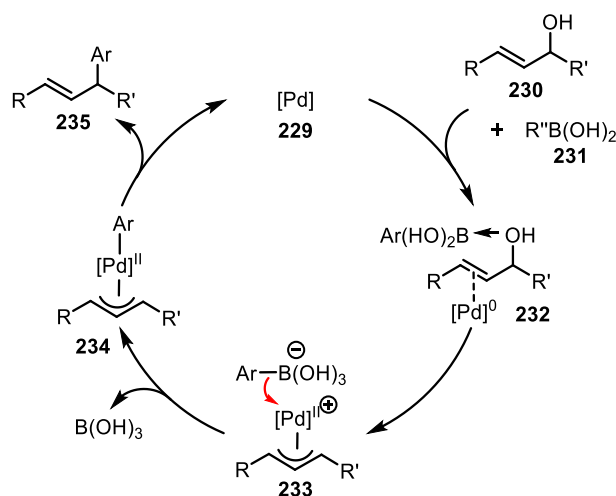
The methodology used in this work for the synthetic accession of a homostilbene library is based on a procedure of *Tsukamoto* and coworkers shown in Scheme 35, which convinced by its simplicity and efficiency in yield and selectivity.^[129a, 130a]



Scheme 35: Synthesis of homostilbenes *via* palladium-catalyzed direct cross-coupling of allylic alcohols with arylboronic acids.^[130a]

In the presence of $\text{Pd}(\text{PPh}_3)_4$ as catalyst, cinnamyl alcohol **225a** was reacted with various arylboronic acids in moderate to excellent yields. The homostilbene products were thereby obtained regioselectively in (*E*)-configuration. It was shown that when the isomers (*Z*)-**225a** or *sec*-**225a** were used, (*E*)-**221a** was again obtained in very good yields. By reacting the chiral alcohol **227**, it was shown that the stereo information is lost during catalysis as the product **228** was completely racemic.

In the proposed mechanism (Scheme 36),^[130a] the formation of a palladium π -complex **232** occurs first. Crucial for the success of the reaction was an excess (at least 20 mol%) of the Lewis-acidic boron reagents.



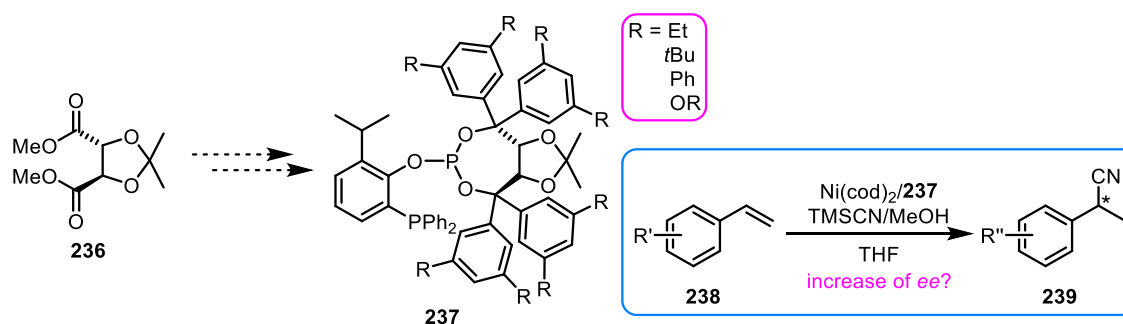
Scheme 36: Proposed catalytic cycle of palladium-catalyzed direct cross-coupling of allylic alcohols with arylboronic acids.^[130a]

This observation supported the consideration that the hydroxy group is abstracted by the boronic acid and a characteristic palladium(II) η^3 - π -allyl complex **233** is formed by oxidative addition.^[133] The same selectivities of different isomers in this reaction could be explained *via* the latter (compare, for instance, yields and regioselectivities for (*Z*)-**225a** and *sec*-**225a**). The different reaction rates, on the other hand, suggested that oxidative addition is the rate-determining step. From the boron species, the aryl residue can now be transferred in a transmetalation step. Reductive elimination from complex **234** affords the homostilbene product **235** and the Pd(0) catalyst **229** is regenerated. The observed racemization when using the chiral alcohol **227** (Scheme **35**) can be explained by the fact that the more nucleophilic Pd(0) species **229** undergoes competitive addition on the allyl system in complex **233**,^[134] thus, any stereo information is lost. To date, the *Tsukamoto* method has found little application in other synthesis protocols.^[129a] In particular, systems with bilaterally substituted aryl groups and highly substituted motifs have not been studied yet under these conditions.

3. Concept and Task

The hydrocyanation of non-activated alkenes remains a challenging task. Thus, the nickel-catalyzed enantioselective hydrocyanation of vinylarenes established by *Falk et al.*^[42, 103] should first be focused on with the aim to extend its applicability and then to elaborate its possibilities as well as to develop it further.

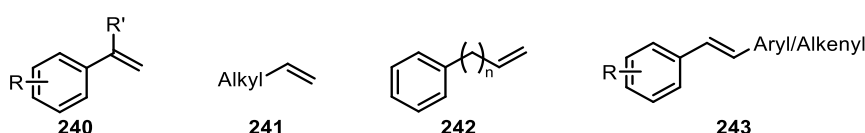
After the successful reproduction of the methodology and the synthesis of the phosphine-phosphite ligands, the 3,5-disubstitution pattern of the aryl units in the TADDOL-derived ligand backbone was to be investigated (Scheme 37). For this purpose, new ligands of type **237** should be synthesized and evaluated in the hydrocyanation protocol regarding the obtained selectivities.



Scheme 37: Envisioned new 3,5-aryl substituted phosphine-phosphite ligands of type **237** for enantioselective hydrocyanation.

As the exchange of hydrogen substituents by methyl substituents ($R = H$ to $R = Me$) already caused a strong increase in selectivity (see Scheme 24, Section 2.2.6.2.), the influence of other substituents on the reaction outcome should be inspected in detail.

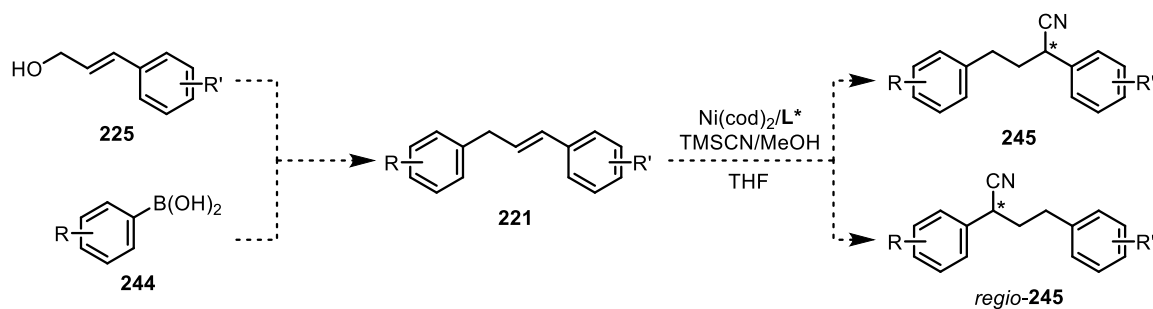
Furthermore, the substrate spectrum of this protocol should be examined regarding its scope and limitations. Therefore, 1,1-disubstituted vinylarenes of type **240**, aliphatic systems of type **241**, phenylalkenes with a terminal double bond and an alkyl spacer of type **242**, and 1,2-disubstituted vinylarenes with an aryl or alkenyl substituent of type **243** should be investigated (Scheme 38).



Scheme 38: Potential substrates for the enantioselective hydrocyanation protocol.

Since 1,3-diarylpropenes (homostilbenes) were identified as attractive substrates, this class should be investigated in more depth with the present methodology. For this purpose, a range of (new) substituted homostilbenes **221** should first be synthesized and subsequently subjected to hydrocyanation (Scheme 39). Due to the probability of migratory processes based

on nickel-catalyzed chain-walking, the chemo-, regio- and enantioselectivity of hydrocyanation of homostilbenes with electronically differentiated aryl units should be evaluated with respect to the two possible regioisomeric 2,4-diarylbutyronitrile products **245** and *regio*-**245**.



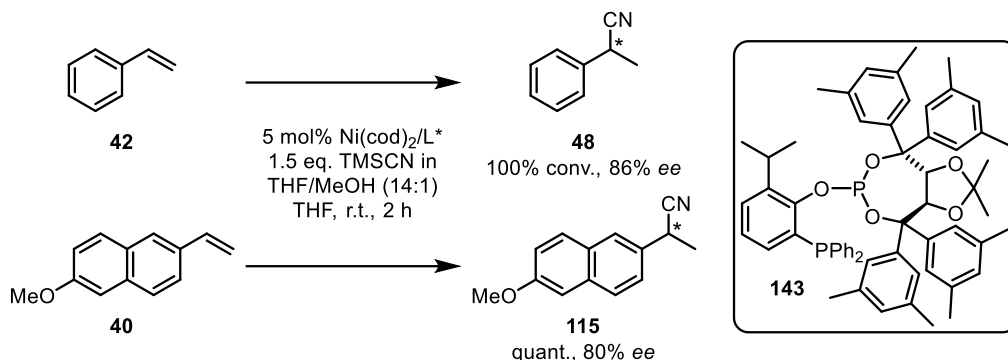
Scheme 39: Targeted synthesis and hydrocyanation of substituted homostilbenes **221**.

Furthermore, the potential of such a hydrocyanation strategy in organic syntheses should be tested on the example of a new colchinol.

4. Results and Discussion

4.1. Notes on the hydrocyanation protocol, reproducibility and ligand synthesis

To familiarize with the hydrocyanation technique established by *Falk et al.*,^[42, 103] a protocol for the hydrocyanation of styrene (**42**) and 2-methoxy-6-vinylnaphthalene (**40**) was initially reproduced (Scheme 40).

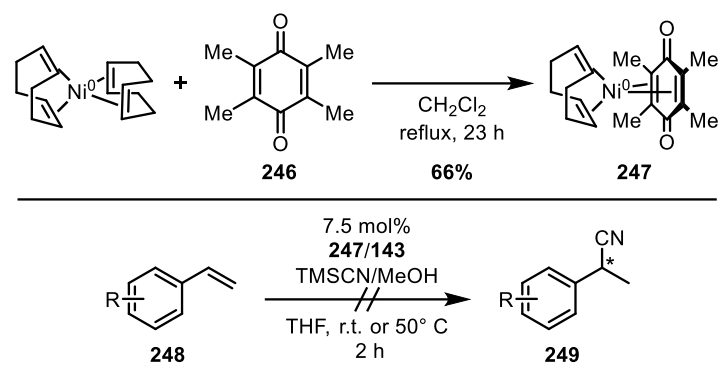


Scheme 40: Reproduction of the hydrocyanation results by *Falk et al.* with styrene (**42**) and 2-methoxy-6-vinylnaphthalene (**40**) as test substrates.

To ensure reproducibility, minor concentration adjustments of the catalyst solution (from 0.006M to 0.019M) and the TMSCN solution (from 0.125M to 0.25M) were made. While a catalyst loading of 5mol% led only to inconsistent results, which was probably often caused by catalyst deactivation, a slight increase to 7.5 mol% proved to ensure good reproducibility. Therefore, to avoid misinterpretation of any results for the research purposes in this work, a catalyst/ligand loading of 7.5 mol% was generally used. The standard reaction scale employed was 0.5 mmol regarding the substrate. The enantioselectivity outcome in the further work is defined by the enantiomeric ratio (*er*).

The most recently optimized ligand synthesis route of **143** by *Dindaroğlu* and *Falk et al.*^[96c] was successfully applied in the preparation of new phosphine-phosphite ligands (see Section 4.2.). It is noteworthy that the quality of the phosphorous trichloride was crucial for the coupling step (see Scheme 42, Section 4.2.1.). In this step, PCl_3 purchased from *Sigma Aldrich* (*ReagentPlus* 99% grade) was the only successful reagent in terms of yield and purity of the product. The coupling step is considered to be extremely moisture- and air-sensitive in most cases.

The air-stable nickel complex Ni(cod)(DQ) (**247**) developed by *Engle* and coworkers was also considered for the hydrocyanation protocol,^[135] as its use would eliminate the need for an argon to work under atmosphere during the reaction setup. The desired nickel precursor **247** was prepared accordingly in a ligand exchange reaction with duroquinone (DQ) (**246**) and Ni(cod)₂ (Scheme 41). However, attempts to implement the latter as a precatalyst in the hydrocyanation protocol failed.

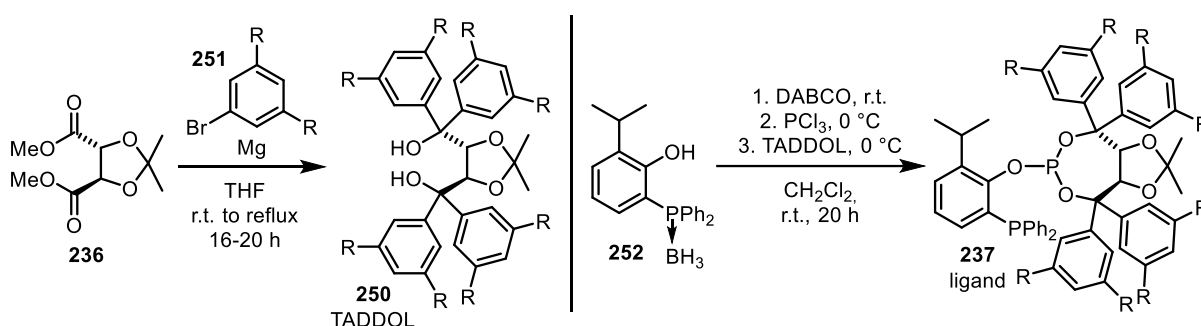


Scheme 41: Synthesis of the air-stable Ni(cod)(DQ) (**247**) according to *Engle* and coworkers^[135] and hydrocyanation attempts.

4.2. Synthesis of new phosphine-phosphite ligands for hydrocyanation

4.2.1. Derivatizing the TADDOL backbone: new phosphine-phosphite ligands

The synthesis of phosphine-phosphite ligands of type **237** was performed according to the general protocol of *Dindaroğlu et al.*^[96c] For the synthesis of the TADDOL building blocks of type **250**, the enantiomerically pure tartaric acid derivative **236** was reacted with the corresponding freshly prepared aryl *Grignard* reagents obtained from bromides of type **251** (Scheme 42). The concentration of the *Grignard* reagents was quantified by iodimetry. The starting 3,5-disubstituted-bromobenzene derivatives of type **251** were either purchased commercially (R = Me, MeO) or synthesized according to literature procedures (R = EtO, *i*PrO, Ph).



Scheme 42: Employed reaction conditions for the synthesis TADDOLs and phosphine-phosphite ligands.

The TADDOLs of type **250** were then reacted with the borane-protected phosphine building block **252** and PCl_3 in the presence of an excess of DABCO to provide the ligands of type **237**. Table 1 summarizes the results for the targeted ligand structures. The TADDOL derivatives were obtained in good to excellent yields with the exception of the tetra-phenyl substituted system **255** (entry 4).

Table 1: Results of the TADDOL and phosphine-phosphite ligand syntheses.

| entry | R | TADDOL (yield) | Ligand (yield) |
|-------|---------------|------------------|---------------------------------|
| 1 | Me | 253 (89%) | 143 (75%) |
| 2 | Et | 254 (80%) | 260 (48%) |
| 3 | <i>t</i> Bu | 255 (99%) | 261 (<5%) ^[a] |
| 4 | Ph | 256 (9%) | n.c. |
| 5 | OMe | 257 (77%) | 262 (68%) |
| 6 | OEt | 258 (50%) | 263 (63%) |
| 7 | O <i>i</i> Pr | 259 (45%) | 264 (59%) |

Isolated yields are given. ^[a]Reaction performed at 50 °C; product could not be isolated.

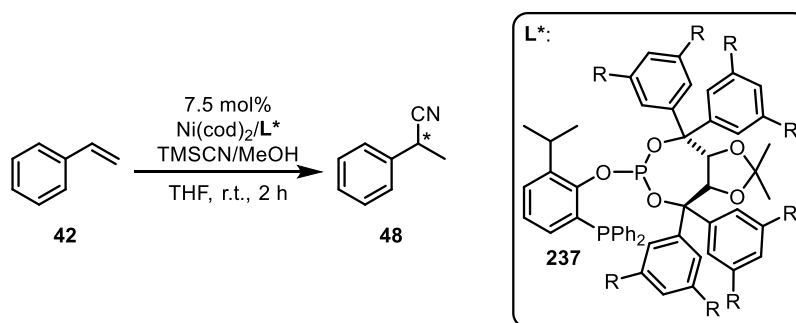
The relatively bulky 3,5-di-*tert*-butyl TADDOL **255** was even obtained in an almost quantitative yield, while the corresponding ligand **261** was formed only in trace amounts, even at higher temperatures of up to 50 °C (entry 3). The 3,5-diphenyl substituted TADDOL **255** also showed

no conversion in the attempted synthesis of the corresponding ligand (entry 4). All other TADDOL derivatives reacted as desired to give the ligands in moderate to good yields (up to 75%). Thus, four new ligands **260** and **262-264** with the envisioned 3,5-substitution pattern were successfully prepared.

4.2.2. New phosphine-phosphite ligands in enantioselective hydrocyanation

Using freshly distilled styrene (**42**) stored over molecular sieve as standard substrate, the new phosphine-phosphite ligand derivatives **260** and **262-264** were tested. The conversions and enantiomeric ratios as determined by GC are summarized in Table 2. Entry 2 shows the previously established 3,5-dimethyl substituted ligand **143**. As a reference, the selectivities obtained with the parent ligand incorporating an unsubstituted TADDOL backbone are also shown (entry 1). Except for the 3,5-diethyl substituted ligand **260** (entry 3), which led to no conversion to the nitrile **48**, hydrocyanation with the new ligands **262-264** bearing alkoxy substituents showed a complete conversion and enantioselectivities comparable to those obtained with ligand **143** (entries 4-6). Having a 3,5-diisopropyl substitution pattern, the ligand **264** provided the same enantiomeric ratio (of 93:7 *er*) as ligand **143** (entry 6).

Table 2: Testing of the new derived phosphine-phosphite ligands **237** in the hydrocyanation of styrene (**42**).



| entry | ligand | Conv. [%] | <i>er</i> ^[a] |
|-------|-------------------------------|--------------------|--------------------------|
| 1 | 158 (R = H) | 100 ^[b] | 85:15 ^[b] |
| 2 | 143 (R = Me) | 100 | 93:7 |
| 3 | 260 (R = Et) | n.c. | - |
| 4 | 262 (R = MeO) | 100 | 90:10 |
| 5 | 263 (R = EtO) | 100 | 91:9 |
| 6 | 264 (R = <i>i</i> PrO) | 100 | 93:7 |

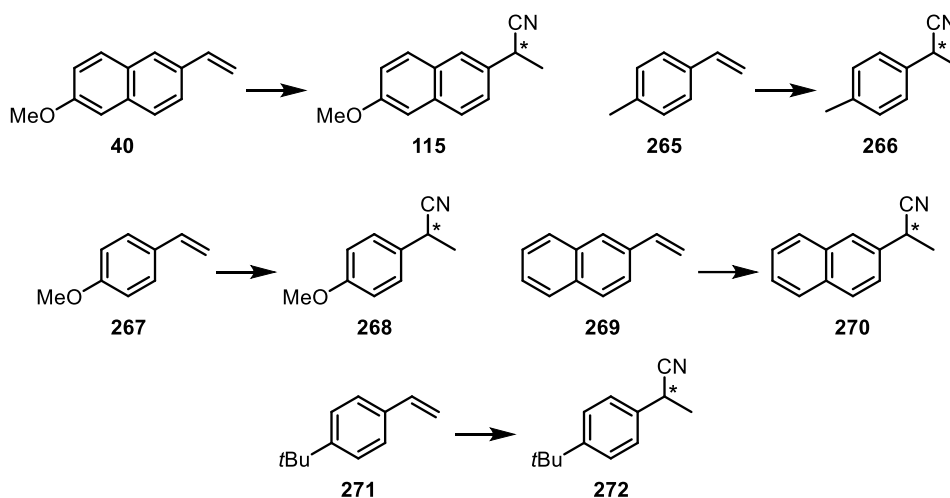
Reactions were monitored by means of GC-MS analysis. All reactions were carried out by slowly adding a solution of 1.5 equiv. TMSCN in THF/MeOH (14:1) to a solution of the styrene substrate and the chiral catalyst generated from Ni(cod)₂ and the respective ligand. ^[a]Determined by GC(FID) using a chiral stationary phase.

^[b]Result obtained by *Falk* using acetone cyanohydrin (see Scheme 24, Section 2.2.6.2.).

Remarkably, the catalyst prepared from the ethyl-substituted ligand **260** appeared to be virtually inactive in the hydrocyanation of styrene. As the phosphine-phosphite ligands had already shown high substrate specificities in previous screening experiments, ligand **260** was also tested with other substrates.

For this purpose, in addition to the established substrate **40**, the four vinylarenes **265**, **267**, **269** and **271** were selected that had not been investigated yet with the methodology by *Falk*. These were subjected to hydrocyanation with the standard ligand **143** and the tetraethylated analogue **260**. The results are shown in Table 3.

Table 3: Results of the hydrocyanation of novel vinylarenes with ligand **143** and **260**.



| entry | substrate | ligand 143 | | ligand 260 | |
|------------------|------------|-------------------|--------------------------|-------------------|--------------------------|
| | | Conv. (yield) [%] | <i>er</i> ^[a] | Conv. [%] | <i>er</i> ^[a] |
| 1 | 40 | 100 (99) | 90:10 | 100 | 89:11 |
| 2 | 265 | 100 (95) | 94:6 | 100 | 96:4 |
| 3 | 269 | 100 (99) | 89:11 | 100 | 86:14 |
| 4 | 267 | 100 (72) | 94:6 | 60 | 96:4 |
| 5 ^[b] | 271 | 100 (96) | 89:11 | n.d. | n.d. |

The reactions were carried out under the same conditions as in Table 2 at r.t. Reactions were monitored by means of GC-MS analysis; yield and conversion are given in [%]. ^[a]Determined by GC(FID) using a chiral stationary phase. ^[b]Reaction performed at 50 °C.

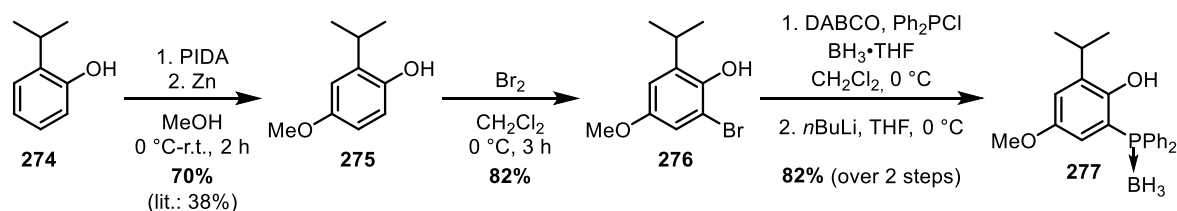
Astonishingly, hydrocyanation of 2-methoxy-6-vinylnaphthalene (**40**) with the ethyl-substituted ligand **260** showed a complete conversion and selectivities similar to ligand **143**. In the hydrocyanation of the new vinylarenes **265**, **267**, **269**, mostly high conversions and high enantiomeric excesses were obtained with both ligands. With the standard ligand **143**, even the sterically demanding 4-*tert*-butylstyrene (**271**) could be hydrocyanated at 50 °C with a complete conversion to the desired nitrile product **272** in a high enantiomeric ratio of 89:11 *er*

while at r.t. only 58% conv. was observed under the standard conditions (90:10 *er*). This substrate was not tested with the ethyl-substituted ligand **260**.

As none of the new ligands with the 3,5-disubstituted TADDOL units showed better or significantly different selectivities from the previously used catalyst system employing ligand **143**, it was concluded that the introduction of other alkyl and alkoxy residues would not further improve the enantioselectivity of this transformation.

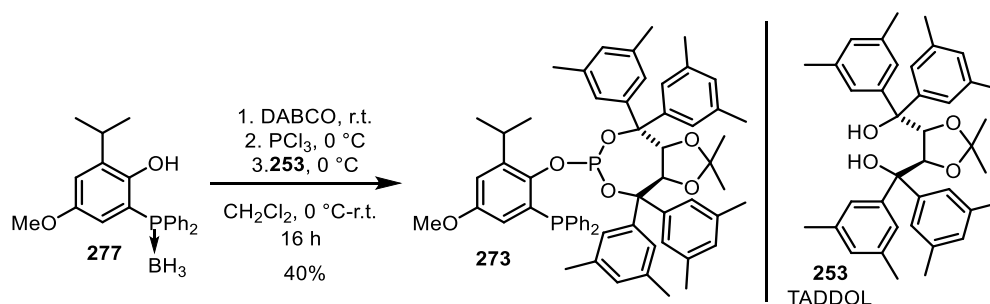
The introduction of a methoxy group in *meta*-position to the PPh₂-group at the phosphine subunit of the ligand led in experiments on the asymmetric hydrovinylation by *Movahhed et al.* to higher selectivities.^[102a] Therefore, analogous methoxy-substituted ligands appeared also promising for application in the hydrocyanation. For this reason, the methoxy-substituted new ligand **273** with the 3,5-dimethyl TADDOL substitution pattern was selected as another promising ligand.

For this purpose, the borane-protected phosphine **277**, unknown in the literature, was synthesized in good yield based on the strategy of *Dindaroğlu et al.* in 47% over four steps (Scheme 43).^[96c]



Scheme 43: Synthesis of borane-protected phosphine **277**.

Starting from 2-isopropylphenol **274**, the opening methoxylation step was performed according to *Amant et al.*^[136] By replacing the work-up procedure with a simple MTBE extraction the product **275** was cleanly obtained in a significantly improved yield of 70%. After bromination and attachment of the borane-protected phosphenyl unit to give **277**, the synthesis of ligand **273** was completed in a fair yield of 40% (Scheme 44).



Scheme 44: Synthesis of the new methoxy-substituted phosphine-phosphite ligand **273**.

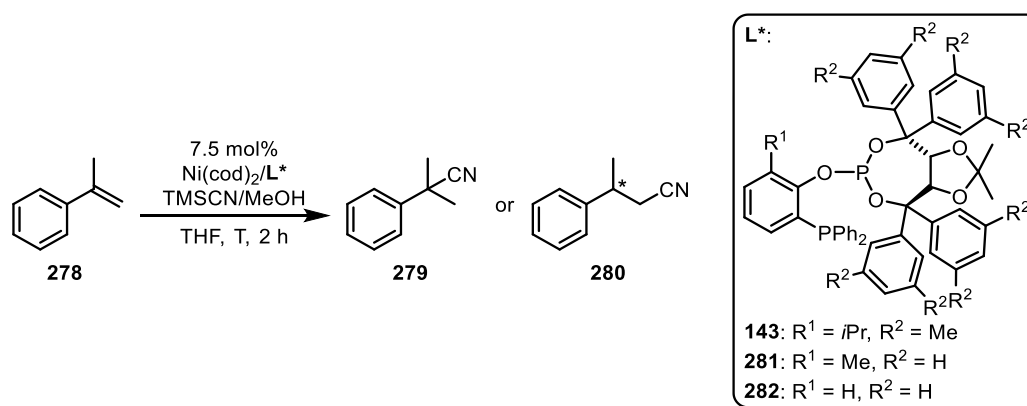
This ligand was found to be highly active in the hydrocyanation of styrene (**42**) and 2-methoxy-6-vinylnaphthalene (**40**) but provided identical selectivities (100% conv., 93:7 *er*) as the already established ligand **143** (same conditions as in Table 2).

4.3. Prospects of the substrate scope using phosphine-phosphite ligands

4.3.1. 1,1-Disubstituted vinylarenes

Besides establishing the hydrocyanation protocol for the enantioselective conversion for styrene derivatives, *Falk* also tested a few sterically more demanding 1,2-disubstituted vinylarenes (see Figure 8, Section 2.2.6.2.).^[42, 84] Likewise, 1,1-disubstituted vinylarenes such as the α -methylstyrene (**278**) are interesting substrates, since the hydrocyanation of the latter would either afford the tertiary nitrile **279** upon *Markovnikov* addition or the chiral β -methylnitrile **280** upon anti-*Markovnikov* addition (Table 4). The hydrocyanation attempts of **278** using different phosphine-phosphite ligands are summarized below.

Table 4: Experiments towards the attempted enantioselective hydrocyanation of α -methylstyrene **278**.



| entry | Ligand L^* | T [°C] | conv. [%] | comments |
|-------|---------------------|--------|-----------|----------------------------|
| 1 | 143 | r.t. | n.c. | - |
| 2 | 143 | r.t. | n.c. | 15 mol% cat./ L^* |
| 3 | 281 | r.t. | traces | - |
| 4 | 281 | 50 | 10 | - |
| 5 | 281 | 50 | n.c. | 5 h addition of TMSCN-sol. |
| 6 | 281 | 50 | 15 | 20 mol% cat./ L^* |
| 7 | 282 | 50 | <5 | 15 mol% cat./ L^* |

Reactions were monitored by means of GC-MS analysis. All reactions were carried out by slowly adding a solution of 1.5 equiv. TMSCN in THF/MeOH (14:1) to a solution of the styrene substrate and the chiral catalyst generated from $\text{Ni}(\text{cod})_2$ and the respective ligand.

Using the ligand **143**, no conversion of the starting material **278** was observed, even when the catalyst loading was increased to 15 mol% (entry 1-2). Employing the significantly less substituted ligand **281** (possessing a single methyl substituent on the phosphine subunit and an unsubstituted TADDOL backbone), product traces could be detected under standard conditions by GC-MS analysis (entry 3). When the temperature was increased to 50 °C, a conversion of up to 10% percent was observed (entry 4). Whereas a longer addition time of the TMSCN solution did not lead to any conversion (entry 5), the conversion could be slightly

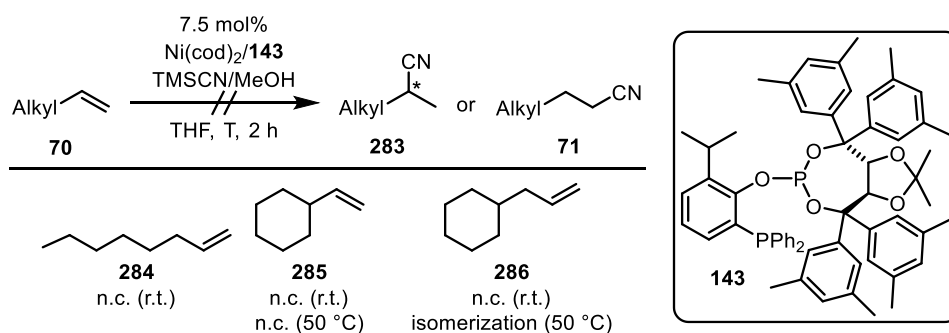
increased to 15% at a higher catalyst load of 20 mol% (entry 6). However, the products **279** or **280** could not be isolated by column chromatography at these low conversions. Even with the completely unsubstituted phosphine-phosphite ligand **282** only trace amounts were detected at a 15 mol% catalyst loading. The results suggested that the relatively rigid phosphine-phosphite ligands investigated are not suitable in the hydrocyanation of 1,1-disubstituted vinylarenes.

Possibly, the initial catalyst/starting material complex is not able to form an η^3 -benzyl complex that would lead to a tertiary nitrile **279** after reductive elimination (see Scheme 10, Section 2.2.3.). Results of the following section also suggest that when using the present phosphine-phosphite ligands, reductive elimination does not occur from a σ -alkyl complex that would have led to the linear nitrile **280**.

4.3.2. Range and limitations of the substrate spectrum

A selection of the substrates tested, which were seminal for the further investigation of the nickel-catalyzed enantioselective hydrocyanation, are presented below.

Hydrocyanation of entirely aliphatic substrates **70** never showed any conversion of the starting materials under the standard conditions with ligand **143**, as shown in Scheme 45.

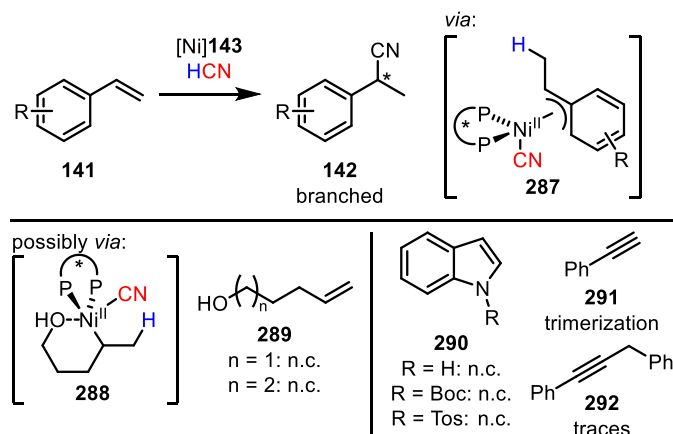


Scheme 45: Selected attempts towards the hydrocyanation of aliphatic olefins employing phosphine-phosphite ligands.

The exemplary substrates **284** and **285** shown could each be reisolated unreacted. In the case of allylcyclohexane (**286**), a mixture of isomers (1:1) of the starting compound **286** and the internal olefin 1-cyclohexylpropene *iso-286* was found at 50 °C. This double bond isomerization indicated an interaction of the nickel catalyst with the olefin. This would imply that the nickel hydride complex reacts with the double bond in a β -H insertion, but no hydrocyanation product was generated from the resulting σ -alkyl complex, since the reductive elimination does not appear to be favored (see also Scheme 10, Section 2.2.3.). At this point, studies on further ligand adaption were not continued because other diphosphine and

diphosphite ligands for the hydrocyanation of aliphatic systems had been established by other groups in the meanwhile (see Sections 2.2.4. and 2.2.8.).

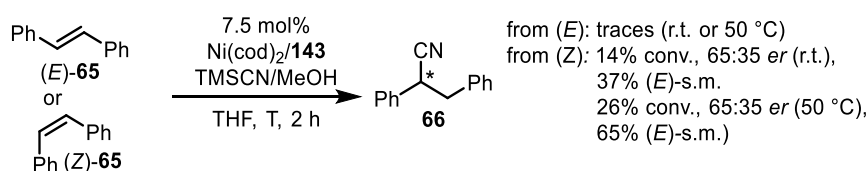
As a stabilization of the inserted nickel complex seemed to be crucial for the successful hydrocyanation of vinylarenes of type **141** through the reductive elimination from an η^3 -benzyl complex intermediate **287**, aliphatic alcohols **289** were subsequently investigated. These might undergo a stabilizing interaction of type **288**. However, this approach remained unsuccessful (Scheme 46).



Scheme 46: Hydrocyanation attempts on aliphatic alcohols, indoles and phenylacetylenes.

Vinyl-substituted heterocycles such as 2-vinylindole were successfully hydrocyanated by *Falk* (see Figure 7, Section 2.2.6.2.). However, attempts to directly subject the aromatic (protected) indole **290** to “dearomatizing” hydrocyanation did not seem feasible. When the hydrocyanation conditions were tested on alkynes, reactions of phenylacetylene derivatives **291** and **292** showed no significant conversion to the desired products. It is noteworthy that trimerization of phenylacetylene (**291**) to 1,3,5-triphenylbenzene occurred under the hydrocyanation conditions.

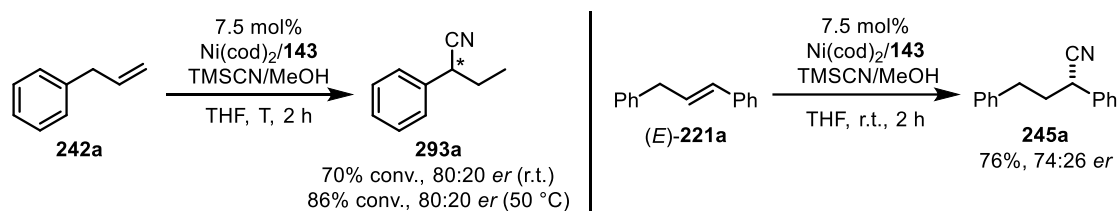
When stilbene **65** was studied, only low conversions (up to 26% at 50 °C) as well as moderate enantiomeric ratios (65:35 *er*) were obtained exclusively for the reaction of the (*Z*)-isomer (Scheme 47).



Scheme 47: Hydrocyanation approaches of (*E*)- and (*Z*)-stilbene (**65**).

The also easily accessible (*Z*)-isomer of stilbene (**65**) being the only substrate showing any reactivity is consistent with the higher reactivity of (*Z*)-configured 1,2-disubstituted vinylarenes observed by *Falk* (see Figure 8, Section 2.2.6.2.).

Two interesting substrate classes were identified during the investigation of phosphine-phosphite ligand controlled hydrocyanation: the phenylalkenes and the homostilbenes (Scheme 48). Here, the reaction of allylbenzene (**242a**) afforded the benzylic nitrile **293a** with a high selectivity (up to 86% conv., 80:20 *er* at 50 °C) through a migratory, enantioselective hydrocyanation. The (*E*)-homostilbene (**221a**) gave the hydrocyanated product **245a** in good yield (76%) and decent enantioselectivity (74:26 *er*). Remarkably, homostilbenes (1,3-diarylpropenes) have never been studied in hydrocyanation before.



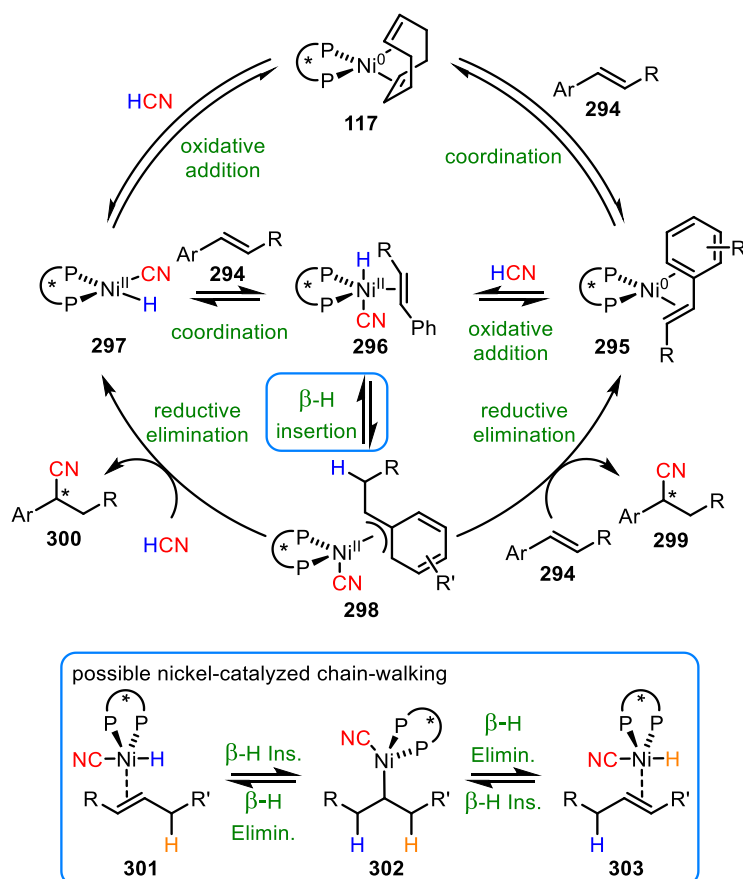
Scheme 48: Successful enantioselective hydrocyanations of allylbenzene (**242a**) and (*E*)-homostilbene (**221a**).

These two new classes of substrates for the hydrocyanation were further studied in more detail. The results of these extended studies are presented below in separate sections for each class.

4.4. Enantioselective nickel-catalyzed migratory hydrocyanation

4.4.1. Aspects of chain-walking employing phosphine-phosphite ligands

In Scheme 49 the generally accepted mechanism of the nickel-catalyzed hydrocyanation of vinylarenes is shown (here for 1,2-disubstituted substrates).^[45] After coordination of the substrate **294** to the active catalyst **117** and oxidative addition of HCN (or *vice versa*), complex **296** is formed. Starting from the latter, insertion of the olefin ligand into Nickel hydride bond affords **298** as a stabilized η^3 -benzyl complex intermediate from which reductive elimination finally leads to product **300**.



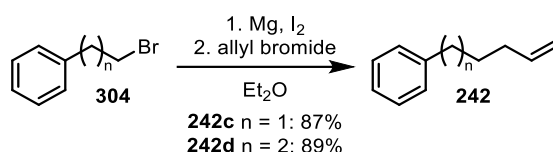
Scheme 49: Generally accepted mechanism of the enantioselective hydrocyanation highlighted in the aspect of chain-walking when using 1,2-disubstituted vinylarenes.

As β -H insertion is generally reversible (β -H elimination), migration of the double bond can occur, as the intermediate Nickel alkyl hydride complex may undergo β -H elimination to both sides (Scheme 49, blue box) until favored η^3 -benzyl complex **298** is formed from which then the irreversible reductive elimination occurs. Thus, the observed migratory hydrocyanation of allyl benzene (**242a**) can be explained (see Scheme 48, Section 4.3.2.). The double bond first migrates into conjugation before the benzyl nitrile **293a** is released from an η^3 -benzyl intermediate by reductive elimination. Further investigations of the enantioselective hydrocyanation of phenylalkenes of type **293a** are presented in the following section.

4.4.2. Migratory hydrocyanation of phenylalkenes

With regard to the observed migratory hydrocyanation of allylbenzene (**242a**), the corresponding phenylalkenes **242b-242d** with longer alkyl spacers between the phenyl ring and the terminal double bonds were investigated.

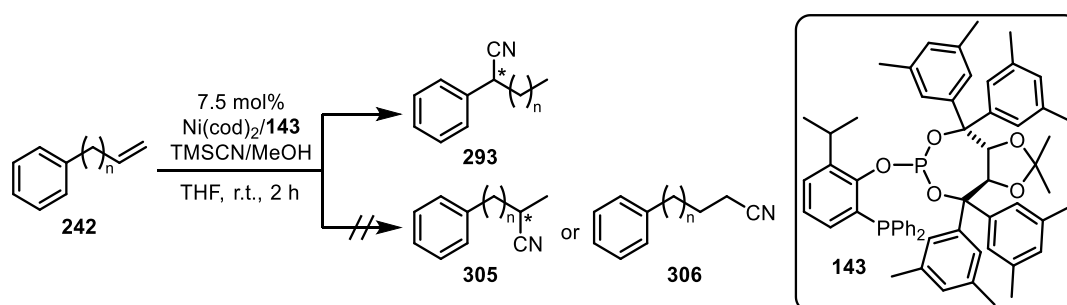
First, the literature known phenylalkenes 5-phenyl-1-pentenes (**242c**) and 6-phenyl-1-hexenes (**242d**) were prepared from the corresponding bromide of type **304** through a *Grignard* reaction with allyl bromide in very good yields (Scheme 50).^[137]



Scheme 50: Synthesis of literature known phenylalkenes **242c** and **242d**.^[137]

The phenylalkenes were all subjected to the enantioselective hydrocyanation protocol employing phosphine-phosphite ligand **143**. In all cases the benzyl nitriles of type **293** were observed as the only hydrocyanation products as expected, while none of the branched or linear isomers **305** or **306** were detected (Table 5, entry 1-4). It is noteworthy that the conversion dropped to 35% with an increasing length of the alkyl spacer for **242d** ($n = 4$, entry 4). In the case of the terminal olefins **242c** and **242d**, the reisolated olefinic material consisted mainly of isomerized internal alkenes with the respective styrene derivatives 1-phenyl-1-pentene **242e** and 1-phenyl-1-hexene **242f** as major compounds.

Table 5: Summarized results of the enantioselective hydrocyanation of phenylalkenes **242**.



| entry | substrate | yield of 293 ^[a] | <i>er</i> of 293 ^[b] |
|-------|-------------------|---------------------------------------|-------------------------------------------|
| 1 | 242a n = 1 | 45 (70) | 80:20 |
| 2 | 242b n = 2 | 60 (65) | 80:20 |
| 3 | 242c n = 3 | 50 (55) | n.d. |
| 4 | 242d n = 4 | 21 (35) ^[d] | n.d. |

All reactions were carried out by slowly adding a solution of 1.5 equiv. TMSCN in THF/MeOH (14:1) to a solution of the styrene substrate and the chiral catalyst generated from Ni(cod)₂ and the respective ligand. ^[a]Isolated yields; conversion to product **293** is given in parentheses. ^[b]Determined by GC(FID) using a chiral stationary phase. ^[c]Reaction performed at 50 °C.

The fact that no other hydrocyanation products (along the alkyl chain) than the benzyl nitriles of type **293** were formed, is consistent with the presented experiments on entirely aliphatic olefins, where no hydrocyanation (resulting from a corresponding nickel σ -alkyl complex) was observed at all. Moreover, these results demonstrate that the employed ligand **143** facilitates Nickel-catalyzed chain-walking in appropriate systems. The enantiomers of **293a** and **293b** could be separated by means of chiral GC and revealed an enantiomeric ratio of 80:20 *er*.

In order to compare the direct hydrocyanation of the internal olefins (vinylarene isomers) with the migratory hydrocyanation of the terminal olefins **242a** and **242b**, the obtained conversions and enantiomeric ratios of the hydrocyanation at 50 °C were compared (Figure 11).

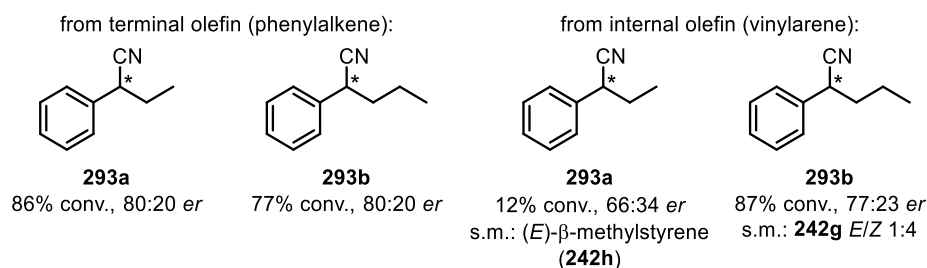


Figure 11: Hydrocyanation towards benzyl nitriles **293a** and **293b** from terminal or internal olefins at 50 °C.

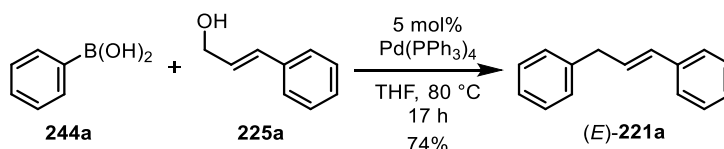
While the product **293a** from an (*E*)-configured internal vinylarene **242h** showed a significantly lower conversion and a lower enantiomeric ratio, the hydrocyanation to **293b** provided comparable results. Consistent with the observations made so far (see Section 4.3.2.), the corresponding (*Z*)-isomer-enriched internal olefin **242g** showed a significantly higher reactivity in hydrocyanation. The latter had previously been prepared in a *Wittig* reaction from benzaldehyde (**307**).^[137b]

4.5. Enantioselective hydrocyanation of homostilbenes

4.5.1. General concept & initial studies

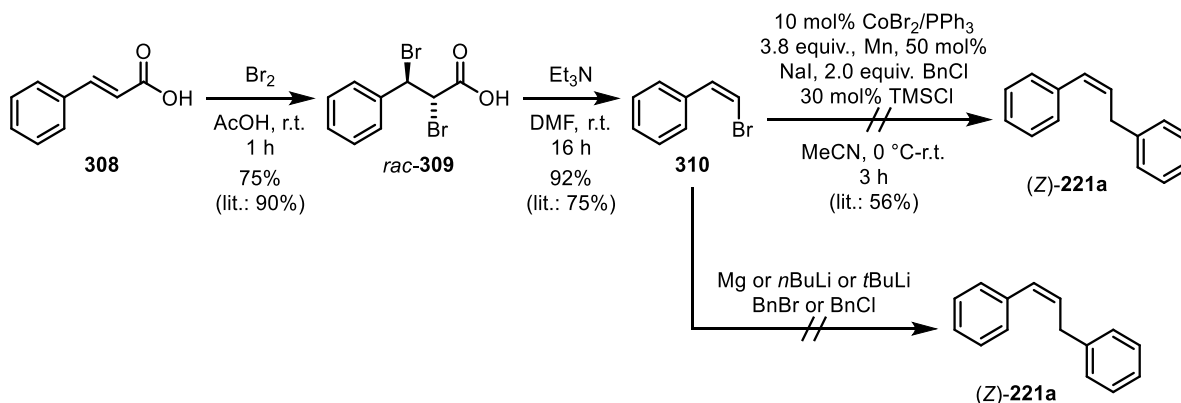
4.5.1.1. Hydrocyanation of 2,4-diphenylpropene (homostilbene) **221a**

The (*E*)-homostilbene (**221a**) was prepared in a good yield by a palladium-catalyzed coupling of phenylboronic acid (**244a**) and cinnamic alcohol (**225a**) according to a procedure by *Tsukamoto* and coworkers (Scheme 51).^[130a] The same synthetic strategy was also used for the regiospecific preparation of other (*E*)-homostilbene derivatives (see Section 4.5.1.).



Scheme 51: Synthesis of (*E*)-homostilbene (**221a**) according to *Tsukamoto* and coworkers.^[130a]

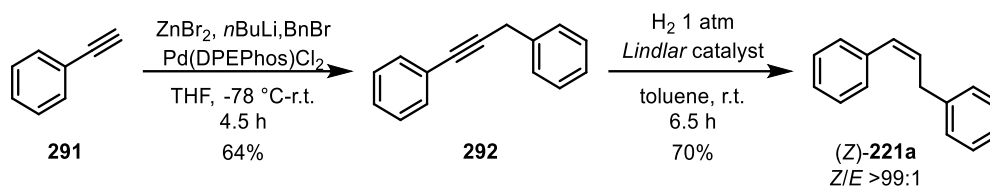
In order to also investigate the hydrocyanation of the (*Z*)-configured homostilbene (**221a**), since the (*Z*)-isomers often exhibit higher reactivity, its synthesis was first attempted starting from cinnamic acid (**308**) according to protocols known from literature (Scheme 52).^[138]



Scheme 52: Attempted synthetic strategy towards (*Z*)-homostilbene (**221a**).^[138]

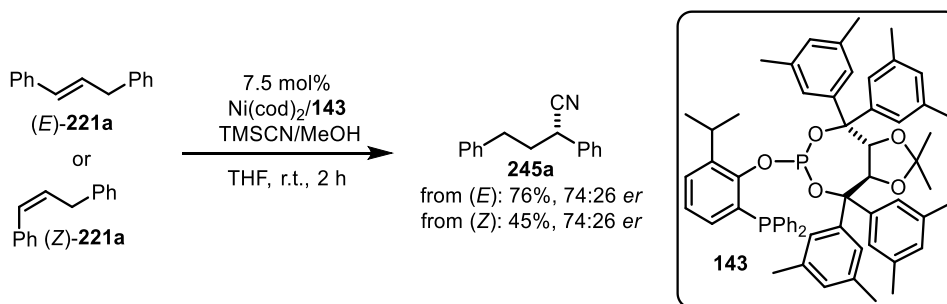
While the bromination and subsequent elimination could be realized in high yields according to a protocol by *Alexakis* and coworkers,^[138a] the envisioned cobalt-catalyzed cross-coupling according to *Cai et al.* failed.^[138b] Lithiation followed by reaction with benzyl bromide or benzyl chloride did not show any conversion to the envisioned product (*Z*)-**221a**, either, and only afforded homocoupled byproducts. As a sidenote, the prepared (*Z*)- β -bromostyrene (**310**) was also tested in hydrocyanation but showed no conversion.

Finally, the desired derivative (*Z*)-**221a** was obtained in high diastereoselectivity (*Z/E* >99:1) from the literature known alkyne **292**^[139] by *Lindlar* hydrogenation (Scheme 53).



Scheme 53: Synthesis of homostilbene (*Z*)-**221a** via a Lindlar hydrogenation of **292**.

Upon hydrocyanation using ligand **143**, both isomers of **221a** afforded the desired (*S*)-2,4-diphenylbutyronitrile (**245a**) with identical enantioselectivity (74:26 *er*). While the reaction of the (*E*)-configured homostilbene provided **245a** in a good yield of 76%, a reaction of the (*Z*)-isomer only resulted in a yield of 45% (Scheme **54**). Thus, only (*E*)-configured homostilbene derivatives were used in the following studies. Furthermore, these isomers are more easily accessible by synthesis as compared to their corresponding (*Z*)-isomers.



Scheme 54: Enantioselective hydrocyanation of (*E*)- and (*Z*)-homostilbene (**221a**). Reactions were carried out by slowly adding a solution of 1.5 equiv. TMSCN in THF/MeOH (14:1) to a solution of the styrene substrate and the chiral catalyst generated from Ni(cod)₂ and the respective ligand.

To elucidate the absolute configuration of the hydrocyanation product 2,4-diphenylbutyronitrile (**245a**) resulting from the reaction in the presence of the shown (*R,R*)-TADDOL-derived chiral ligand **143**, the experimental ECD spectrum was compared with the spectrum (*R*)-**245a** calculated by DFT-based methods (Figure **12**).^[140]

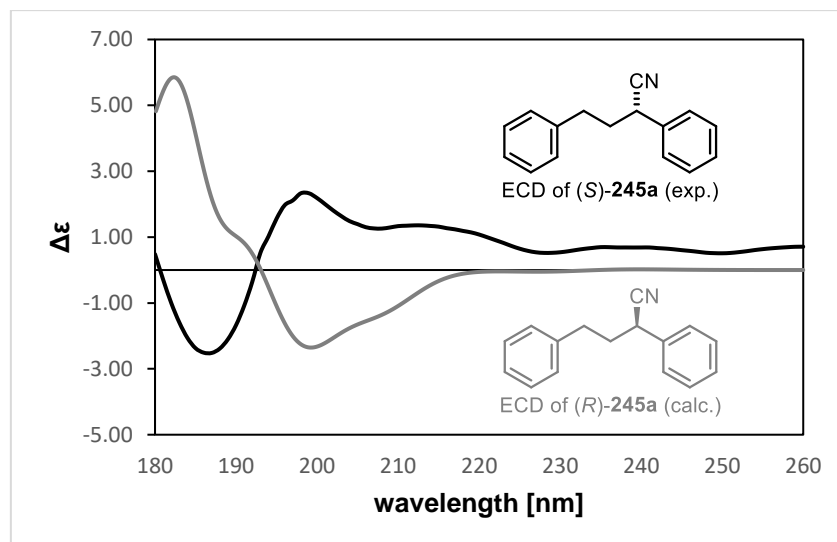
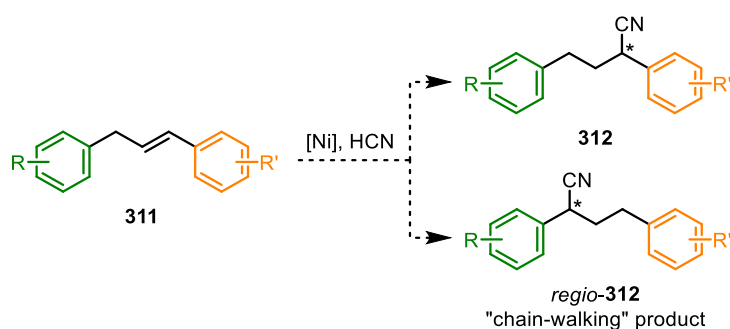


Figure 12: Comparison of the experimental ECD spectrum of prepared nitrile (*S*)-**245a** with that calculated for (*R*)-**245a** by DFT.

These results clearly determined the (*S*)-configuration for the synthesized compound **245a**. This was in line with the configurational outcome of the hydrocyanation of 4-isobutylstyrene previously determined in studies by *Falk* using the same chiral catalyst **143**. It can therefore be concluded that the related hydrocyanation products described in this work should also exhibit the (*S*)-configuration. See also Figure 16 in Section 4.5.2. which shows the crystal structure of another 2,4-diarylbutyronitrile hydrocyanation product **245e** with an (*S*)-configuration.

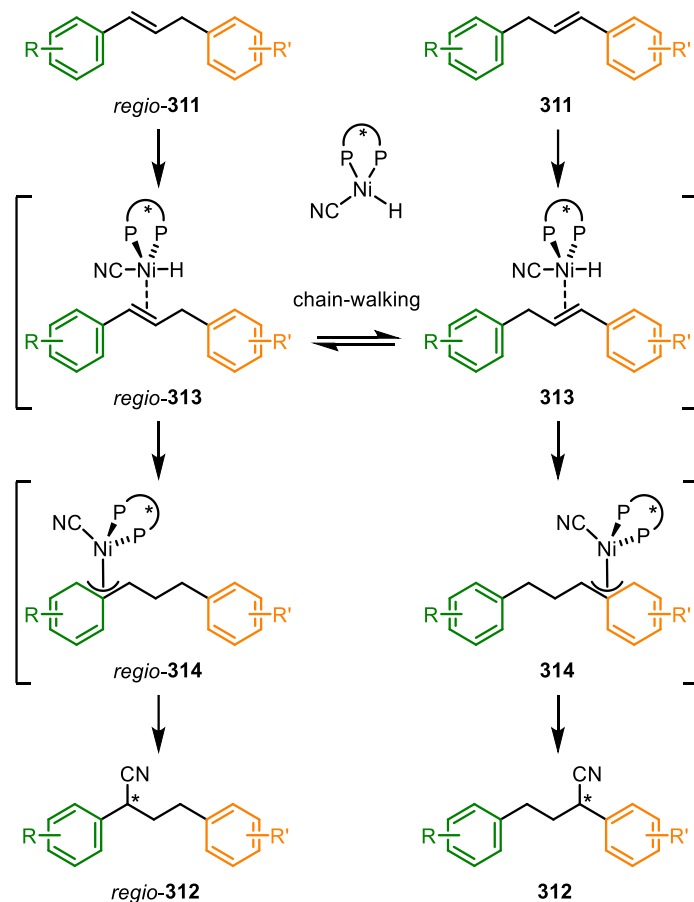
4.5.1.2. Regioselectivity under the aspect of chain-walking

Conceptually, the hydrocyanation of an unsymmetric homostilbene of type **311** should provide the corresponding 2,4-diarylbutyronitrile of type **312** if the reaction proceeds regio-retentively. The regioisomeric product of type *regio*-**312** could also be formed by a nickel-catalyzed double bond migration in the course of the reaction (Scheme 55).



Scheme 55: Schematic hydrocyanation of unsymmetric homostilbenes of type **311** and their two possible regioisomeric products **312** and *regio*-**312**.

The key question was whether the hydrocyanation of the homostilbenes *regio*-**311** or **311** would proceed regioselectively to afford *regio*-**312** or **312** without any double bond chain-walking, or whether an isomerization at the stage of the intermediates *regio*-**313** and **313** would affect the regioselectivity of the reaction (Scheme 56). In case an equilibrium between *regio*-**313** and **313** would be faster than the formation of the corresponding η^3 -benzyl complexes *regio*-**314** and **314**, the regioselectivity outcome could potentially be influenced by the electronically differentiated aryl units.



Scheme 56: Overview of the proposed nickel-catalyzed hydrocyanation mechanism of unsymmetric homostilbenes and potential influence on the regioselectivity outcome by chain-walking.

4.5.1. Preparation of a homostilbene library

To address the above-mentioned questions, a series of suitable unsymmetric homostilbenes of type **221** were prepared by means of a direct coupling of various arylboronic acids of type **244** with allylic alcohols of type **225** or their secondary isomers *sec*-**225**. For this purpose, the protocol of *Tsukamoto* and coworkers served as a basis (see Section 2.3.).^[130a]

Figure 13 shows the arylboronic acid derivatives and allylic alcohols used in the subsequent homostilbene syntheses. The building blocks in the blue box were commercially available,

whereas the compounds in the green box were prepared according to literature procedures in one or two steps each.

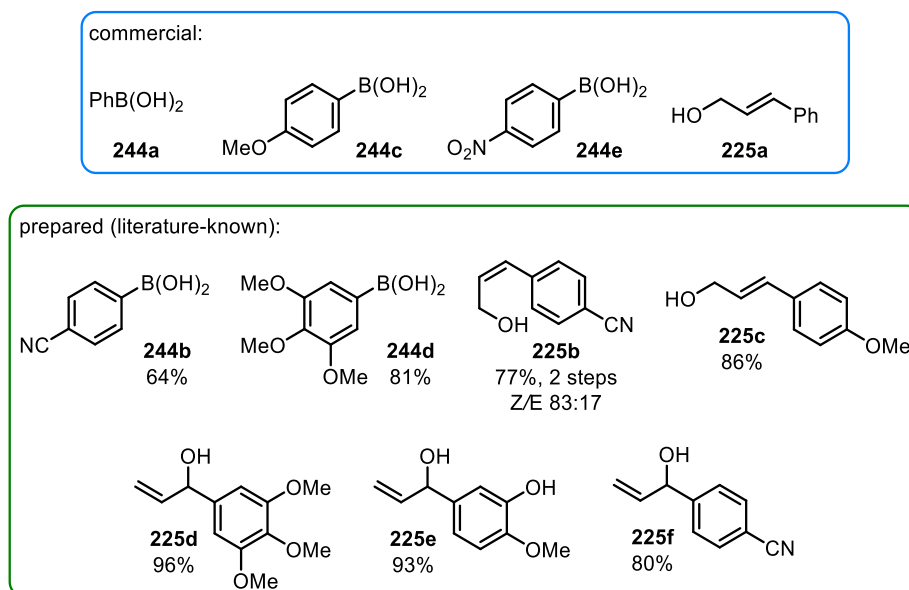
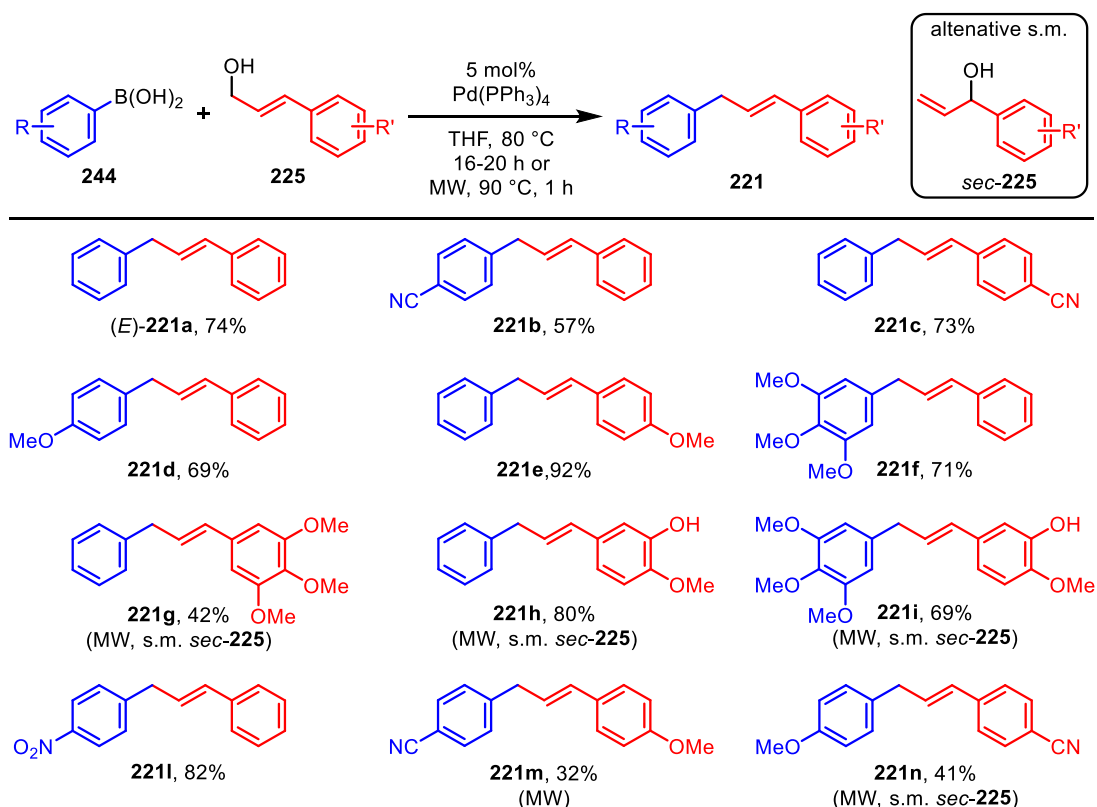


Figure 13: Employed phenylboronic acids and allylic alcohols as building blocks for various homostilbenes.

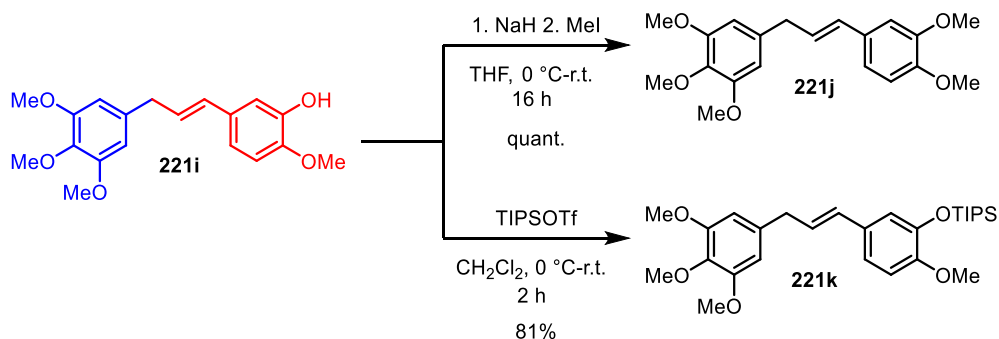
The arylboronic acids **244b** and **244d** were prepared from the corresponding aryl bromides. Noteworthy, the use of the synthetically easier accessible (*Z*)-configured allylic alcohol **225b** made no difference with respect to the (*E*)-selectivity of the homostilbene coupling (see Scheme 35, Section 2.3.). The secondary alcohol derivatives **225d-225f** were obtained in high yields from the corresponding aldehyde precursors.

The various homostilbenes of type **221** synthesized are shown in Scheme 57. The results prove that the method is applicable for both electron-poor and electron-rich substrates. In all cases, the pure (*E*)-configured products **221a-221n** were regiospecifically obtained in moderate to excellent yields without any concomitant double bond isomerization. The starting materials of type **244** and **225** were refluxed in THF in the presence of Pd(PPh₃)₄ for 16-20 h in a closed vessel. Interestingly, the reaction time was greatly shortened to 1 h by performing the reactions at 90 °C in a microwave reactor. As exemplified for the homostilbene **221i**, even a slight increase in yield to 69% could be achieved when using the microwave-assisted conditions (61% with conventional heating).



Scheme 57: Overview of the synthesized homostilbenes through palladium-catalyzed coupling of allylic alcohols.

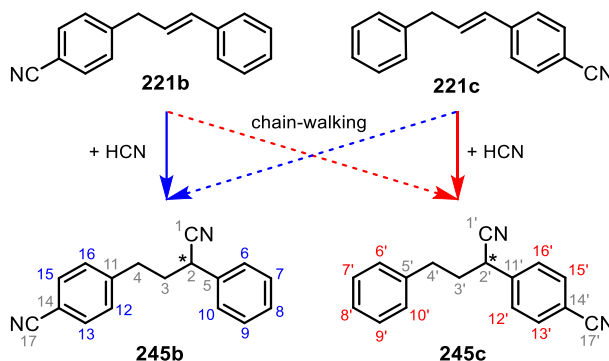
Remarkably, the aryl-isoeugenol analogues **221h** (80%) and **221i** (69%) with a free phenol group were also obtained in good yields. Subsequent quantitative methylation of the latter provided the known homostilbene **221j** in an improved overall yield of 65% over three steps starting from isovanillin (**315**). This compound had previously been shown to exhibit high bioactivity as a potent breast cancer invasion inhibitor (see Section 2.3).^[125] Moreover, TIPS-protection of **221i** to afford **221k** was also feasible in 81% yield. Thereby, the two homostilbenes **221j** and **221k** were prepared as additional potential hydrocyanation substrates (Scheme 58).



Scheme 58: Methylation and TIPS-protection of phenolic homostilbene **221j**.

4.5.2. Hydrocyanation results

With a series of substituted homostilbenes in hand, the question of regioselectivity in the hydrocyanation with respect to the occurrence of chain-walking during the course of the reaction in addition to chemo- and enantioselectivity was investigated (see section 4.5.1.2.). In initial experiments, the hydrocyanation of the two mono-cyano-substituted homostilbenes **221b** and **221c** was studied, which may lead to the regioisomeric nitriles **245b/245c** (Scheme 59).



Scheme 59: Hydrocyanation of the homostilbenes **221b** and **221c** and their regioisomeric products.

The respective regioisomeric ratios of the latter two nitriles and of the other prepared hydrocyanation products were determined by ^1H NMR analysis of well distinguishable proton signals. As an example, this analytic assignment for the hydrocyanation of **221b** and **221c** is illustrated in Figure 14 below.

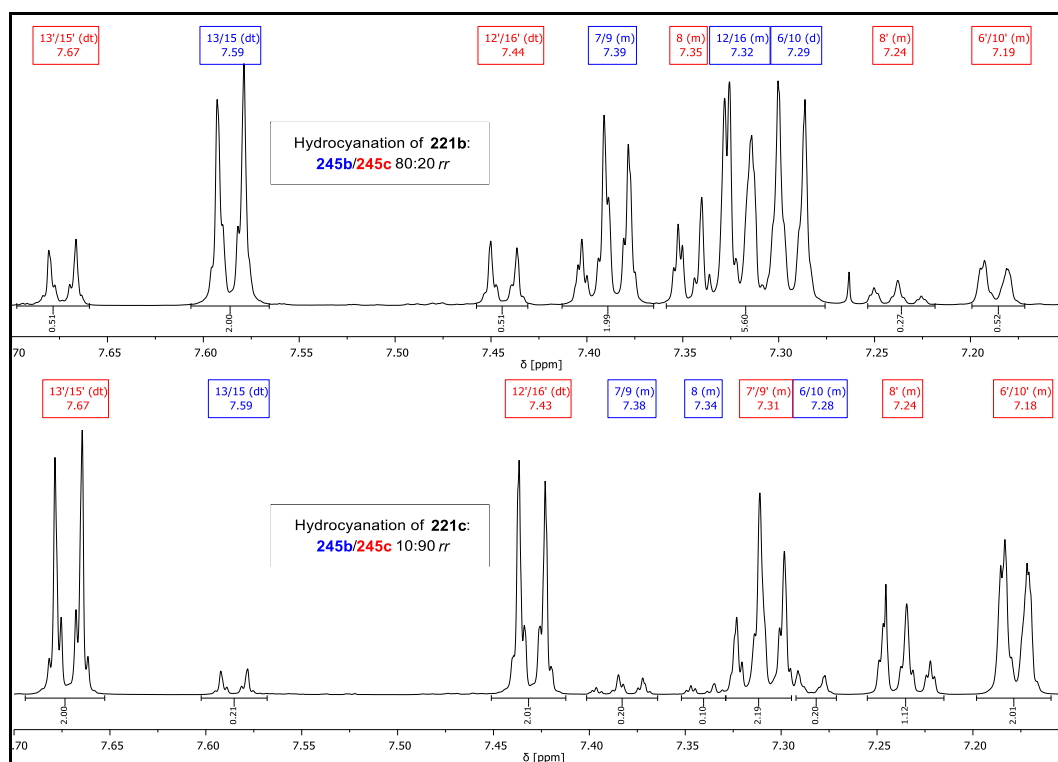
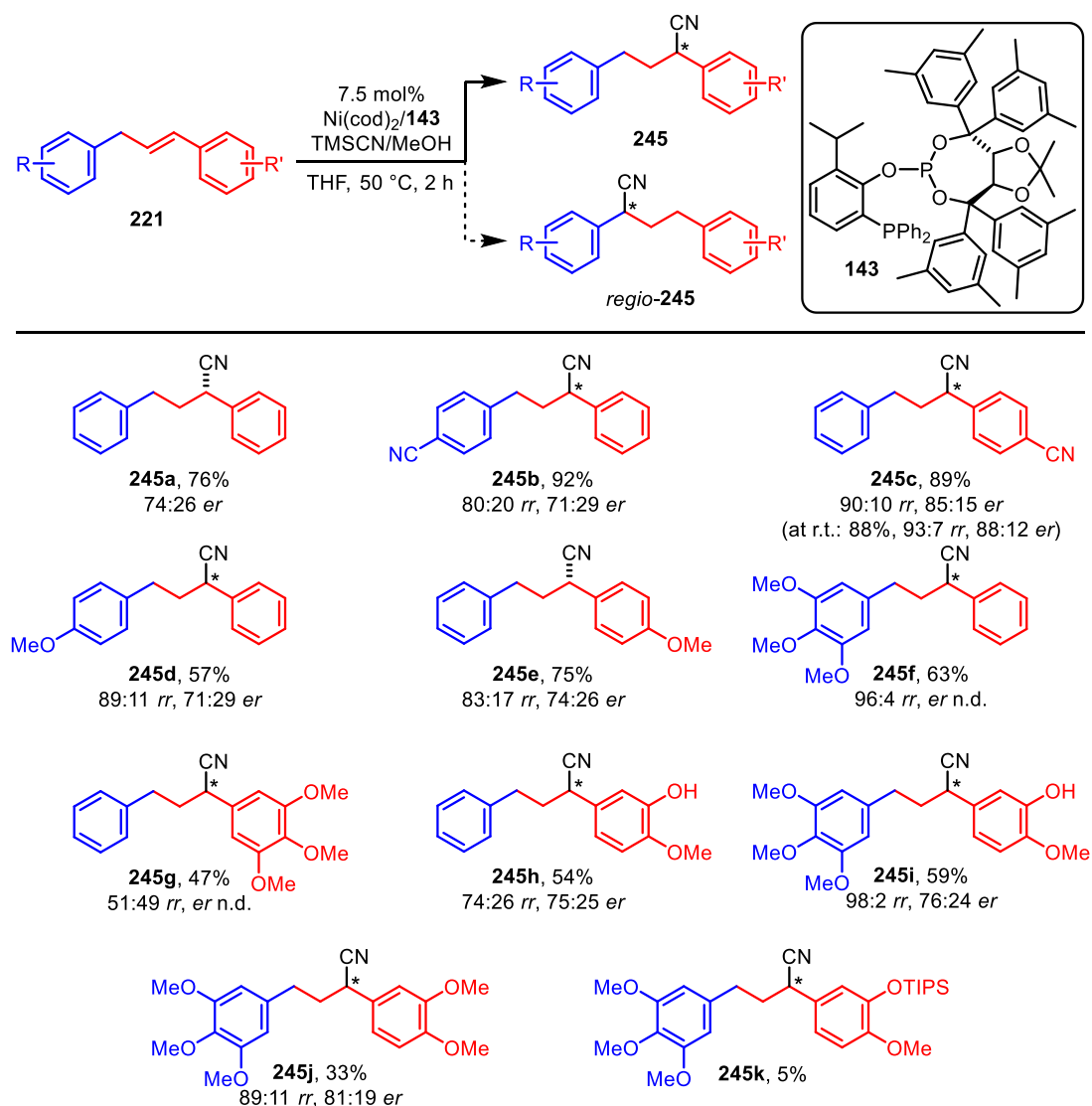


Figure 14: Regioselectivity outcome of the nickel-catalyzed hydrocyanation of homostilbenes **221b** and **221c** to the regioisomeric nitriles **245b** and **245c** analyzed by ^1H NMR spectroscopy (500 MHz, CDCl_3).

The analysis was based on the aromatic proton signals which allowed a clear distinction between the regioisomeric 2,4-diarylbutyronitrile products **245b** and **245c**. While the hydrocyanation of **221b** resulted in an 80:20 *rr* mixture of **245b/245c**, the reaction of **221c** led to **245c** as the major product with even higher regio-retention of 10:90 *rr* **245b/245c**. Thus, these experiments clearly showed a certain level of chain migration in the course of the transformations, which are, however, still regiospecific with regard to the major product corresponding to the substrate employed.

Scheme 60 summarizes the results for the enantioselective hydrocyanation of the prepared homostilbenes of type **221**. In the same way as described above, the regioselectivity of the performed hydrocyanations was analyzed. The enantiomeric purity of the respective major regioisomer was determined by HPLC on a chiral stationary phase.



Scheme 60. Overview of the obtained 2,4-diarylbutyronitriles through the hydrocyanation of homostilbenes. All reactions were carried out by slowly adding a solution of 1.5 equiv. TMSCN in THF/MeOH (14:1) to a solution of the styrene substrate and the chiral catalyst generated from Ni(cod)₂ and the respective ligand.

As discussed in Section 4.5.1.1., the (*S*)-2,4-diphenylbutyronitrile **245a** was obtained in good yield and 74:26 *er*. The cyano-substituted derivatives **245b/245c** and the related pair of methoxy-substituted compounds **245b/245c** were also obtained in good yields. Here, the comparison of the results showed some preference for the electron-poorer substrates **221b/221c**, as the cyano-substituted diarylbutyronitriles **245b** and **245c** were formed in higher yields (92% and 89%) than the methoxy derivatives **245d** and **245e** (both $\leq 75\%$). The enantioselectivities of hydrocyanation were found to be moderate for the nitrile products **245b** (71:29 *er*), **245d** (71:29 *er*) and **245e** (74:26 *er*). Remarkably, **221c** proved to be a particularly good substrate (89%, 90:10 *rr*, 85:15 *er*), reacting even at r.t. in equal yield to **245c** with even higher regio- and enantioselectivities (93:7 *rr*, 88:12 *er*).

The methoxy-substituted nitrile product **245e** crystallized and was analyzed by single crystal X-ray determination and the absolute structure of **245e** was assigned as (*S*)-configured (Figure 15).

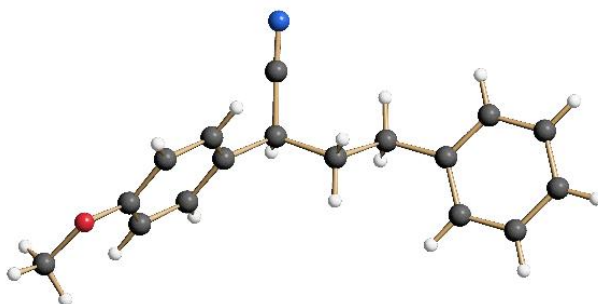


Figure 15: Structure of (*S*)-2,4-diarylbutyronitrile **245e** in the crystalline state.

This result was again consistent with the previously determined configurational outcomes with the same chiral ligand **143** (see Section 4.5.1.1.). Control measurements by chiral HPLC of the mother liquor of **245e** (81:19 *er*) and the measured single crystal (92:8 *er*) showed a significantly higher enantiomeric purity of the crystallized sample.

Interestingly, the hydrocyanation product **245f** derived from the trimethoxy-substituted homostilbene **221f** showed a high regioselectivity (96:4 *rr*) for this transformation, whereas a high degree of chain-walking was observed in the conversion of the regioisomeric homostilbene **221g** leading to an almost 1:1 mixture of regioisomeric products (**245g/245f**). It appears that the primarily formed nickel intermediate of type *regio-313/313* (see Scheme 56, Section 4.5.1.2.) with a particular electron-rich double bond has a reduced tendency to undergo β -H insertion forming the corresponding η^3 -benzyl complex (from which the product **245g** is derived). Accordingly, the system has more time to isomerize (by chain-walking) to the regioisomeric olefin complex from which the other regioisomer **245f** is formed. It is noteworthy that the enantioselectivity of these two transformations could not be determined because the

trimethoxy-substituted products **13h** and **13i** could not be separated by means of chiral chromatography.

The hydrocyanation of the aryl-isoeugenol derivatives **221h** and **221i**, both representing novel homostilbenes with an unprotected phenol group, led to the expected products **245h** and **245i** in acceptable yields and moderate enantioselectivity (75:25 *er* and 76:24 *er*). Moreover, a particularly high level of regioselectivity (98:2 *rr*) was observed for nitrile **245i**. Unfortunately, the *O*-methylated congener **221j** of the latter afforded the corresponding product **245j** in a much lower yield of 33% and only 89:11 *rr* despite an improved enantiomeric purity of 89:19 *er*. Furthermore, the TIPS-protected nitrile **245k** was obtained in only 5% yield resulting from low conversion of the starting material **221k**.

Surprisingly, disubstituted homostilbenes **221m** and **221n** bearing a methoxy substituent on the one benzene ring and a cyano-substituent on the other did not show any significant conversion (Figure 16). Why no significant conversion to the products **245m** or **245n** was observed could not be explained.

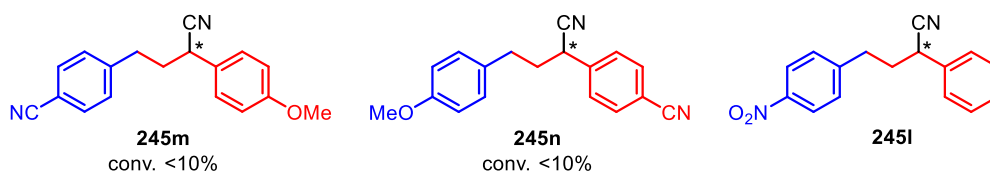
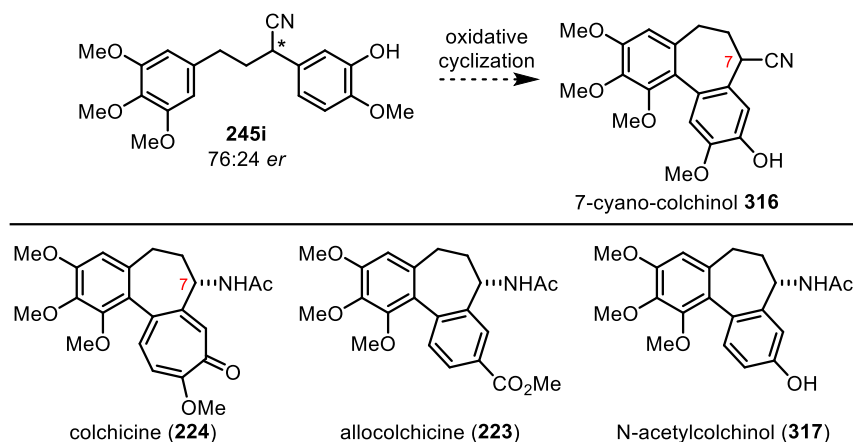


Figure 16: Envisioned 2,4-butyronitrile products that could be not obtained by hydrocyanation of the corresponding homostilbenes.

However, these compounds bear a methoxy-aryl and cyano-aryl unit displaying a donor or acceptor character, respectively, which might lead to a change of the reaction pathway due to a possible push-pull stabilization of an allylic intermediate. The reaction of the nitro-substituted homostilbene **221i** failed to give 1,4-diarylbutyronitrile **245i**. In this case, a dark red color immediately after substrate addition (before the addition of TMSCN) indicated that the nitro group might have deactivate the nickel(0) catalyst by oxidation.

4.6. Studies towards new colchicinoids from a hydrocyanated homostilbene

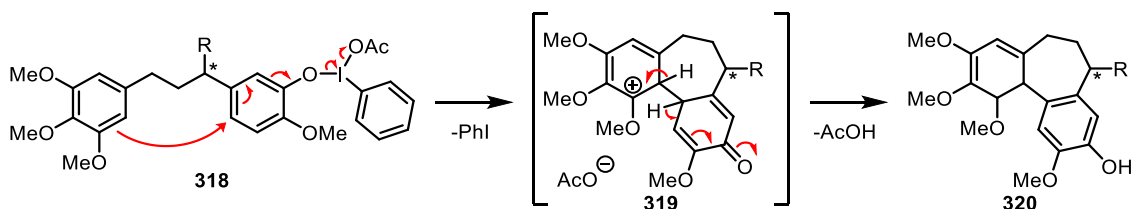
To demonstrate the potential of enantioselective hydrocyanation, especially of homostilbenes, as a useful tool in organic synthesis, the 2,4-diarylbutyronitrile **245i** obtained in high regioisomeric purity and with the specific substitution pattern was investigated as a possible precursor of the new colchicol **316** (Scheme 61).



Scheme 61: Envisioned synthesis of new colchicol derivative **316** and related natural colchicinoids.

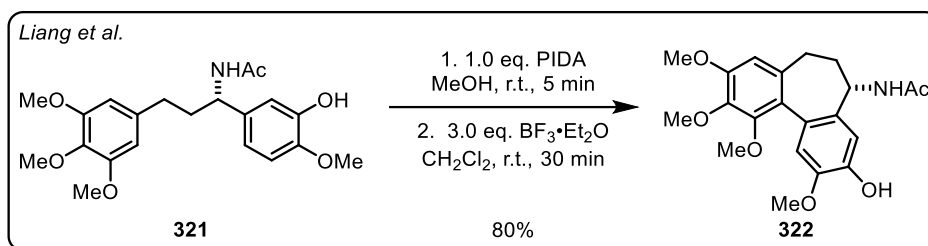
Structural analogues of the natural products colchicine (**224**), allocolchicine (**223**) and *N*-acetylcolchicol (**317**) have received considerable attention in organic synthesis^[127a, 141] and as lead structures in the development of pharmaceuticals^[127c] for decades due to their high bioactivity (see also Section 2.3.). Therefore, new derivatives are of particular value.

If oxidative cyclization of **245i** were successful, this novel strategy could provide a very short (only four linear steps) synthetic access to the targeted colchicol **316**. PIDA (phenyliodine diacetate) mediated oxidation of the nitrile **245i** was considered as a suitable reagent for the cyclization, since hypervalent iodines typically give good results in phenol oxidation reactions.^[142] Here, cyclization could proceed *via* a iodoester of type **318** formed by condensation with PIDA as shown in Scheme 62.



Scheme 62: Proposed mechanism for the anticipated PIDA-mediated oxidative cyclization of compound **245i**.

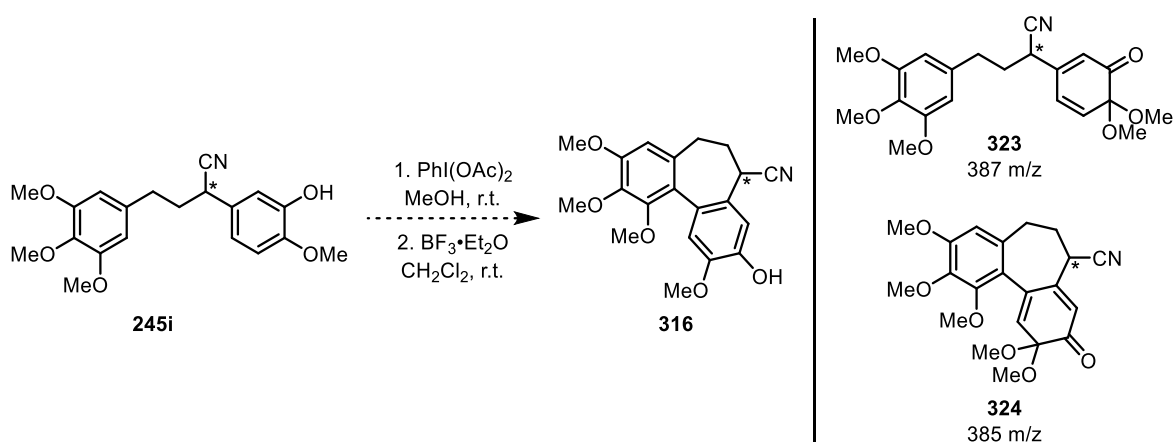
In a new synthesis of colchicine (**204**), Yang and coworkers applied a PIDA/BF₃·Et₂O-mediated oxidative cyclization to a related amide derivative **289** (Scheme 63).^[141b]



Scheme 63: Synthesis of a 7-*N*-acetylcolchicolin derivative **322** by *Liang et al.* via a PIDA/ $\text{BF}_3 \cdot \text{Et}_2\text{O}$ -mediated cyclization.^[141b]

These conditions were applied to the present system **245i** and the results are summarized in Table 6.

Table 6: Test experiments on a PIDA/ $\text{BF}_3 \cdot \text{Et}_2\text{O}$ -mediated oxidative cyclization of nitrile **245i**.



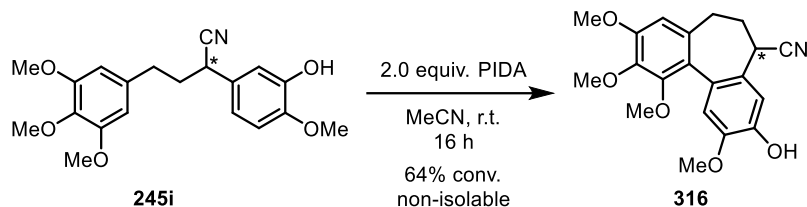
| entry | Scale [mmol] | reagent | equiv. | conversions |
|-------|--------------|--------------------------------------------------|---------|-----------------------------------------------------------------------------|
| 1 | 0.014 | 1. $\text{PhI}(\text{OAc})_2$ | 1.0 | 1. 15 min: 323/245i 80:20 |
| | | 2. $\text{BF}_3 \cdot \text{Et}_2\text{O}$ | 3.0-9.0 | 2. 20 h: no change |
| 2 | 0.014 | 1. $\text{PhI}(\text{OAc})_2$ | 1.0 | 1. 15 min: 323/245i 80:20 |
| | | 2. $\text{BF}_3 \cdot \text{Et}_2\text{O}$ | 15 | 2. 2 h: 316 + >10 byproducts |
| 3 | 0.21 | 1. $\text{PhI}(\text{OAc})_2$ | 1.5 | 1. 15 min: 323/245i 85:15 |
| | | 2. $\text{BF}_3 \cdot \text{Et}_2\text{O}^{[b]}$ | 3.0 | 2. 10 min: 358m/z/ 316/324/323 16:10:22:52; after 3 d: 32:7:32:29 |

Reactions were monitored by means of TLC and GC-MS analysis. In step 2, $\text{BF}_3 \cdot \text{Et}_2\text{O}$ solution was added to the reaction mixture. ^[a]In step 2, the reaction mixture was added dropwise over 30 min to the $\text{BF}_3 \cdot \text{Et}_2\text{O}$ solution.

With the addition of PIDA, the methanol adduct **323** was initially formed (80% conv., entry 1). This is presumably facilitated by the addition of MeOH to a corresponding iodoester of type **318** (see Scheme 62). Even with an increase from 3.0 equiv. up to 9.0 equiv. of $\text{BF}_3 \cdot \text{Et}_2\text{O}$, however, no ring closure product formed (entry 1). With a high excess of $\text{BF}_3 \cdot \text{Et}_2\text{O}$, the desired product formed to a small extent, but in a mixture of at least 10 unidentified byproducts according to GC-MS (entry 2). Increasing the PIDA equivalents still did not result in complete conversion of the starting material and facilitated overoxidation, indicated through formation of byproduct **324** (entry 3). Slowly dropping the reaction mixture to a $\text{BF}_3 \cdot \text{Et}_2\text{O}$ solution did not

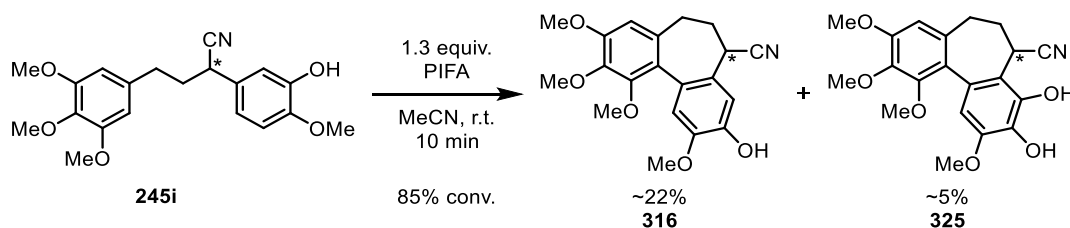
significantly increase the selectivity towards the product either. Purification attempts led only to impure mixtures of the undesired products **323** and **324** in low yields.

To avoid methanol adducts other suitable solvents (CH_2Cl_2 , THF, MeCN) were tested. Finally, a solvent switch to acetonitrile as a polar aprotic solvent with 2.0 equiv. of PIDA led to first significant conversions towards the desired compound **316** (Scheme 64).



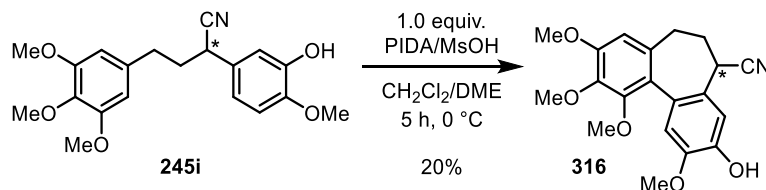
Scheme 64: PIDA-mediated synthetic approach towards colchinal **316**.

Unfortunately, the product could not be isolated starting from these reactions with different work-ups. The use of 1.3 equiv. PIFA, the hexafluoro analogue of PIDA, led to higher conversions, however, only a low yield of the desired colchinal **316** as a mixture with an overoxidized byproduct **325** was obtained (Scheme 65). In addition, the product proved to be unstable probably due to residues in the impure mixture.



Scheme 65: PIFA-mediated synthesis of colchinal **316** and byproduct **325**.

Under additional conditions tested,^[143] a reagent mixture of PIDA and methanesulfonic acid as Brønsted acid in $\text{CH}_2\text{Cl}_2/\text{DME}$ ^[143c] finally yielded the product in at least 20% yield (Scheme 66).



Scheme 66: PIDA/MsOH-mediated synthesis of colchinal **316**.

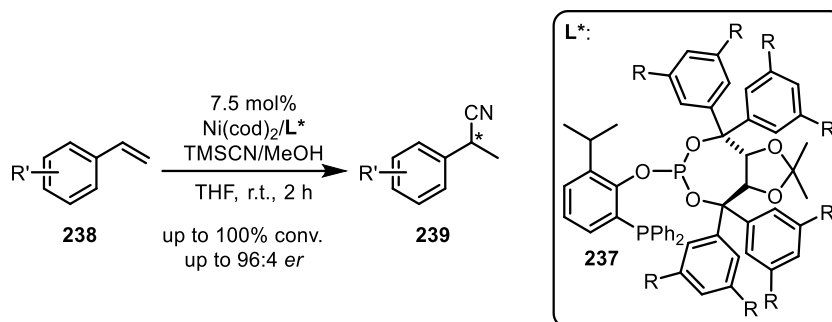
Careful adjustment of the work-up with aqueous NaHCO_3 and EtOAc extraction were crucial to prevent product decomposition. It is noteworthy that this compound formed a solvent-dependent mixture of atrop-diastereomers resulting from a hindered rotation along the biaryl axis (85:15 in CDCl_3 and 70:30 in CD_3CN).

5. Summary and Outlook

5.1. Summary

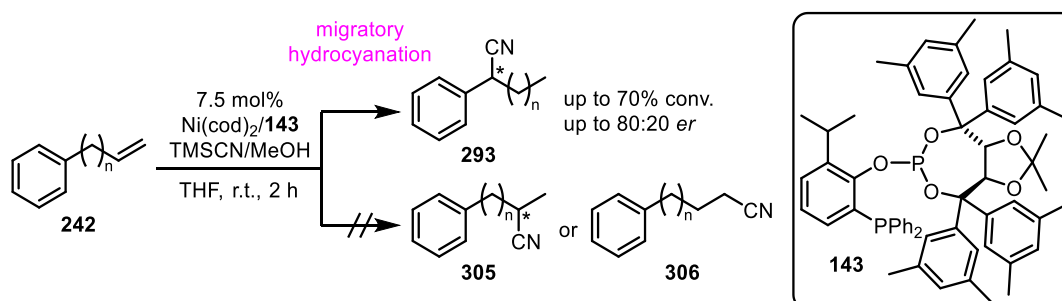
In this work, the enantioselective hydrocyanation methodology introduced by *Falk et al.*^[42] was further developed. The substrate spectrum and application potential were investigated with respect to their scope and limitations. For the first time, 1,3-diarylpropenes (homostilbenes) were thus subjected to hydrocyanation and the power of this synthetic strategy was demonstrated in the short synthesis of a new colchicol.

First, new phosphine-phosphite ligands of type **237** were synthesized and the effect of other residues in the 3,5-positions at the aryl units of the ligand's TADDOL backbone was systematically investigated with respect to the enantioselectivity of the applied hydrocyanation protocol. All ligands were found to be active and highly selective but provided only equal selectivities compared to ligand **143** (R = Me) at most (Scheme 67).



Scheme 67: Enantioselective hydrocyanation of vinylarenes employing new phosphine-phosphite ligands.

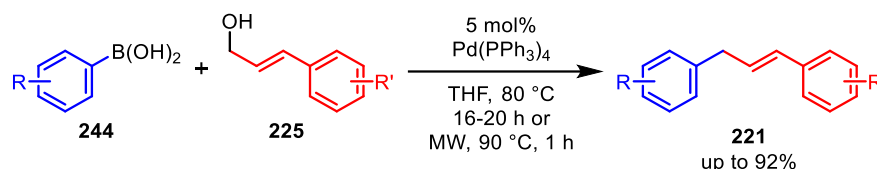
In the studies on the substrate spectrum, there was no conversion with purely aliphatic alkenes, whereas the phenylalkenes of type **242** could be converted exclusively to the benzyl nitriles of type **293** via a migratory hydrocyanation/nickel chain-walking (Scheme 68). These results were consistent with the assumption that the reductive elimination necessary for product formation using ligand **143** occurs exclusively from an η^3 -benzyl complex.



Scheme 68: Migratory enantioselective hydrocyanation of phenylalkenes of type **242**.

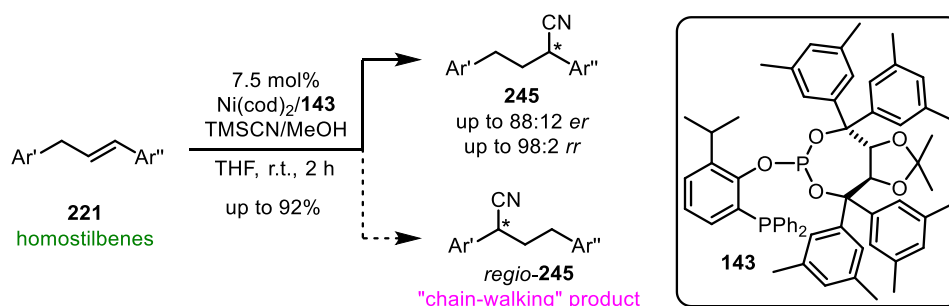
Moreover, 1,3-diarylpropenes (homostilbenes) were identified as attractive substrates for hydrocyanation. In the course of their investigation, a palladium-catalyzed direct coupling of

cinnamyl alcohols of type **225** with arylboronic acids of type **244** based on a protocol of *Tsukamoto* and coworkers^[130a] led to the regiospecific preparation of various substituted (*E*)-homostilbenes of type **221** (Scheme 69). It is noteworthy that the reaction time was greatly shortened under microwave conditions and secondary allylic alcohols were successfully employed.



Scheme 69: Palladium-catalyzed regiospecific synthesis of substituted (*E*)-homostilbenes of type **221**.

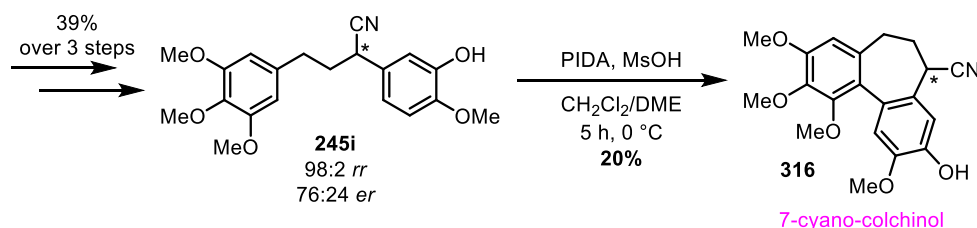
Despite chain-walking that indeed occurs with this particular catalyst system, the hydrocyanation of most homostilbene substrates proceeded with reasonable to high levels of regio-retention (up to 98:2 *rr*). Under the present hydrocyanation conditions, the resulting 2,4-diarylbutyronitriles were obtained in good to excellent yields and with enantioselectivities of up to 88:12 *er* (Scheme 70).



Scheme 70: Enantioselective nickel-catalyzed hydrocyanation of homostilbenes.

The absolute configuration of the 2,4-diarylbutyronitrile products **245** was determined by an ECD spectroscopic study for the unsubstituted parent system **245a** as (*S*)-configured. The crystal structure of another derivative (**245e**) confirmed the (*S*)-configuration, which presumably holds for all related homostilbenes generated by hydrocyanation with ligand **143**.

To confirm the application potential of the developed methodology, a short synthesis (overall four linear steps) of the new 7-cyano-colchicolin **316** using the enantio-enriched hydrocyanation product **245i** was elaborated (Scheme 71).

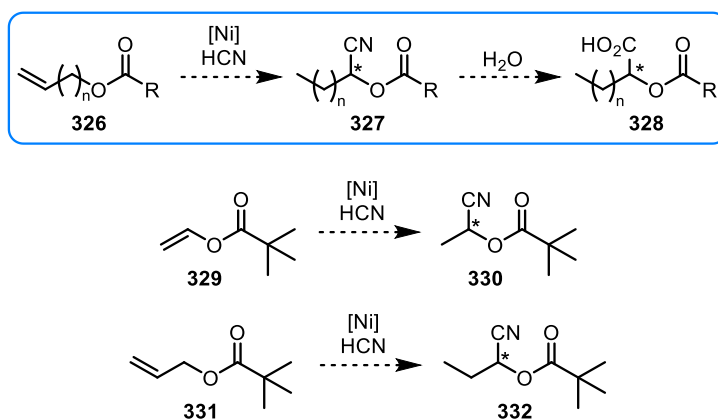


Scheme 71: Synthesis of the new 7-cyano-colchicolin **316** via the prepared 2,4-diarylbutyronitrile **245i**.

5.2. Outlook

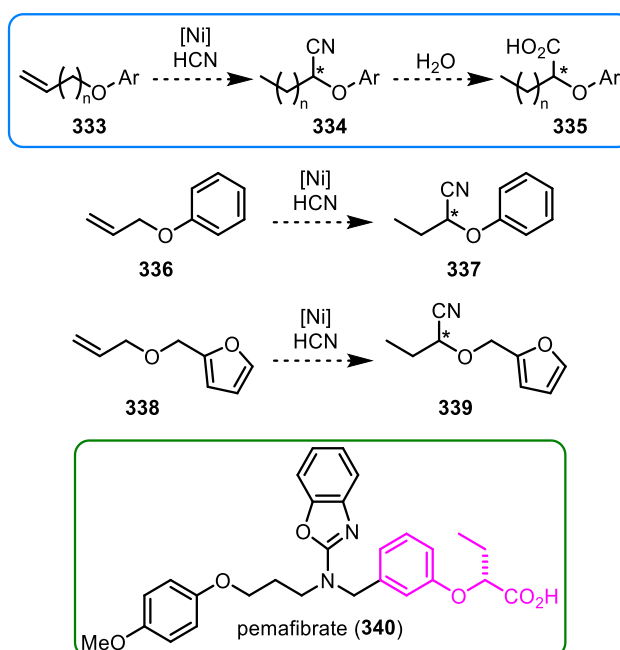
Further development of Nickel-catalyzed hydrocyanation as atom-economical and enantioselective synthetic methodology is of high urgency and remains challenging. The employment of new substrate classes can lead to synthetically very valuable products and opens new strategies towards complex target compounds.

Possibly, a (migratory) hydrocyanation of esterified (terminal) olefins or enol esters of type **326** could be used to prepare α -oxynitriles of type **327**. Upon hydrolysis of the nitrile, chiral α -functionalized carboxylic acids of type **328** would thus be formed (Scheme 72).



Scheme 72: Potential (migratory) hydrocyanation of olefins/enoethers.

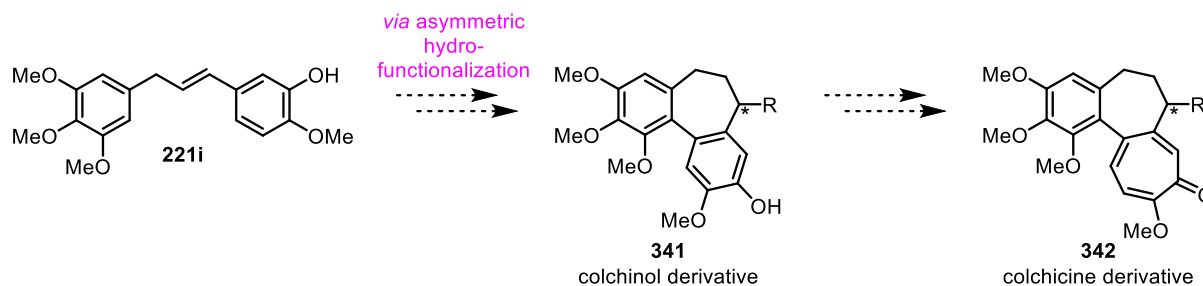
Vinyl pivalate (**329**) and allyl pivalate (**331**) could serve as initial test substrates. The development of tailored ligands for these transformations would be highly rewarding. Similarly, aryl ether substrates of type **333** would lead to α -aryloxy nitriles (Scheme 73).



Scheme 73: Potential (migratory) hydrocyanation of enoethers, for instance, as a possible access to a structural motif of pemafrate (**340**).

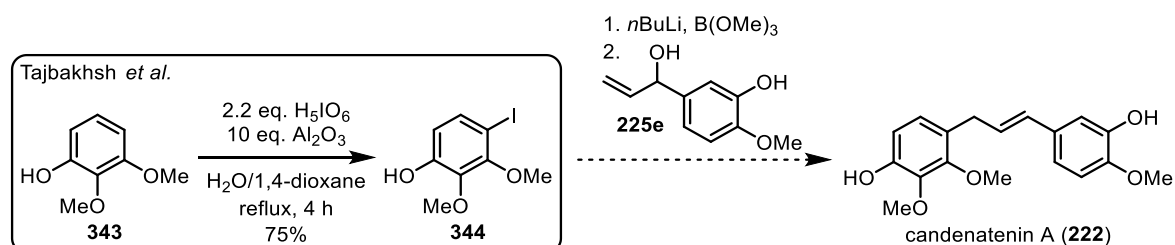
Easily accessible test substrates would be allyl phenyl ether (**336**) and allyl furfuryl ether (**338**). The resulting products such as **337** and the corresponding hydrolysis products can be found, for example, as a substructure in pemafigrate (**340**), which is used to treat the symptoms of metabolic diseases.^[144]

The homostilbene **221i** further might be converted to a range of colchicol and colchicine analogues in a few steps by a variety of available hydrofunctionalizations (Scheme **74**).^[145] The corresponding colchicinoids could then be screened for bioactivity.



Scheme 74: Possible utilization of prepared homostilbene **221i** in asymmetric hydrofunctionalizations towards a range of colchicinoids of type **341** and **342**.

Finally, the palladium-catalyzed direct coupling of allylic alcohols towards homostilbenes of type **221** could possibly be applied in a short three-step synthesis of the anticancerogenic natural product candenatenin A^[124] (**222**) starting from the literature known compounds **344**^[146] and **225e** (Scheme **75**).



Scheme 75: Potential synthetic three-step route towards anticancerogenic candenatenin A (**222**).

Part II: Studies on Chromane Natural Products

6. Introduction and State of Knowledge

6.1. Chromane natural products

6.1.1. (Toco)chromanols in the aspect of function and biosynthesis

Among the most prominent chromane-containing natural products are the tocopherols (α , β , γ , δ).^[147] These compounds, which belong to the meroterpenoids, are characterized by a phytyl side chain and differ only in divergent methyl substitution pattern at the hydroxylated chromane moiety (Figure 17). Together with the corresponding four tocotrienols, each with a farnesyl side chain, they form a group of fat-soluble antioxidants categorized as Vitamin E.^[148] The main representative and the derivative that is best metabolized in humans is (*R,R,R*)- α -tocopherol (α -345). Therefore, it is the most active form of Vitamin E.^[149]

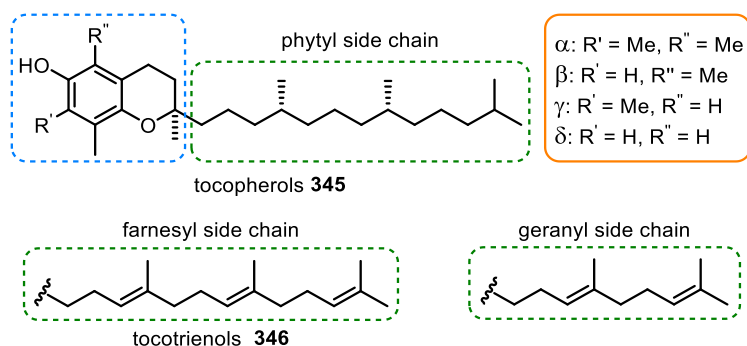
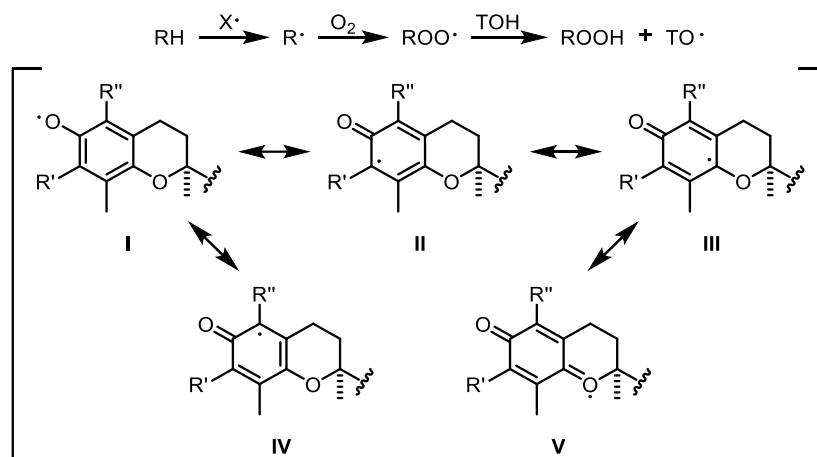


Figure 17: Structure of the tocopherols and tocotrienols grouped under the term Vitamin E and common side chain patterns for chromane natural products.^[147a, 150]

Close relatives are the tocomonoenol^[151] or the marine-derived tocopherol (MDT).^[152] Through biochemical derivatization of the farnesyl side chain, a variety of tocopherol-similar natural products, which occur in plants, have the chromanol unit in common (see Scheme 78, Section 6.1.2.).^[153] Besides, shorter and mostly functionalized geranyl side chains are common in natural chromanols (see Scheme 79).^[153d]

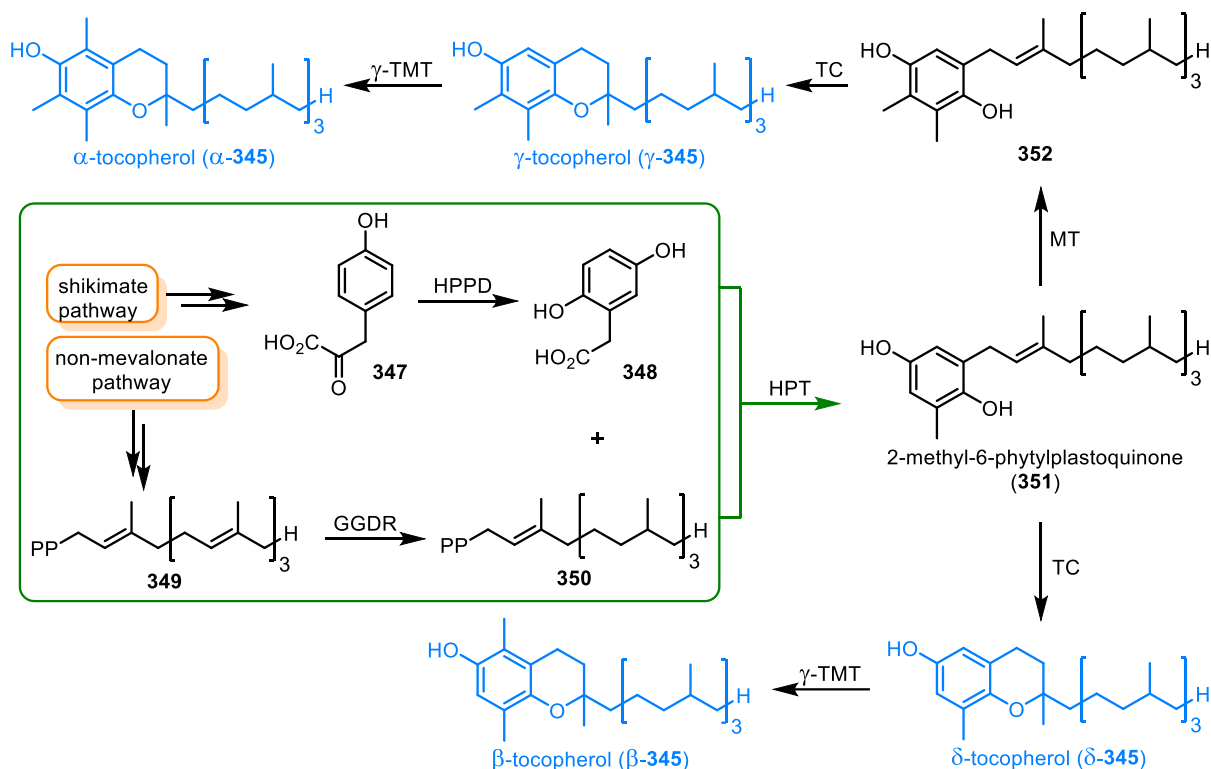
As part of the antioxidant network,^[154] tocochromanols are taken up as natural free radical scavengers in cell membranes, protecting incorporated unsaturated fatty acids from lipid peroxidation.^[155] A fatty acid peroxy radical generated by oxidative stress, which, if not quenched, leads to cell damage in a chain propagation under oxidative degradation of lipids, is terminated by H-abstraction from the chromanol moiety (Scheme 76). The resulting chromanoxyl radical (**I**) is stabilized by electronic delocalization in the aromatic ring (**II-IV**) and by oxygen lone pair conjugation (**V**) as well as hyperconjugation of any methyl substituents present on the ring.^[154, 156] Usually, the corresponding chromanol is regenerated *via* the Vitamin C cycle.^[157]



Scheme 76: Function of tocochromanols (TOH) as radical scavengers of fatty acid peroxy radicals and stabilization of the resulting chromanoxy radical.^[147a]

Vitamin E is an essential compound, as are the aromatic proteinogenic amino acids phenylalanine and tryptophan, since their biosynthesis is based on the shikimate pathway.^[158] This seven-step metabolic route does not occur in animals, so the corresponding compounds must be ingested by food.^[159] The synthesis of tocopherols in plants is well elucidated and will be explained in summary below since the biosynthesis of other chromanols can be derived from this.

The tocopherol production takes place in the photosynthetic tissues of plants (see Scheme 77).^[160] First, *p*-hydroxyphenylpyruvic acid (**347**) is derived from the shikimate pathway *via* tyrosine or prephenic acid. Subsequent conversion to homogentisic acid (**348**) occurs by *p*-hydroxyphenylpyruvic acid dioxygenase (HPPD). Phytol pyrophosphate (**350**) is derived from geranylgeranyl pyrophosphate (**349**) *via* the non-mevalonate pathway. This biocatalytic hydrogenation is facilitated by geranylgeranyl diphosphate reductase (GGDR). The following coupling step is catalyzed by homogentisate prenyltransferase (HPT). The resulting 2-methyl-6-phytylplastoquinone (**351**) is the key intermediate, as all four tocopherols **345** (α , β , γ , δ) can be synthesized from it in a few steps. In each case, the chromane cyclization is mediated by tocopherol cyclase (TC). The respective methylations occur *via* the methyltransferases 2-methyl-6-phytylhydroquinone methyltransferase (MT) or the γ -tocopherol methyltransferase (γ -TMT). The tocotrienols **346** are formed in the absence of GGDR reductase. In modified biosyntheses of different plants, different side chains are thus linked to the corresponding chromanol derivative (α -, β -, γ -, δ -pattern) and possibly functionalized.



Scheme 77: Biosynthesis of tocopherols.^[147a, 160]

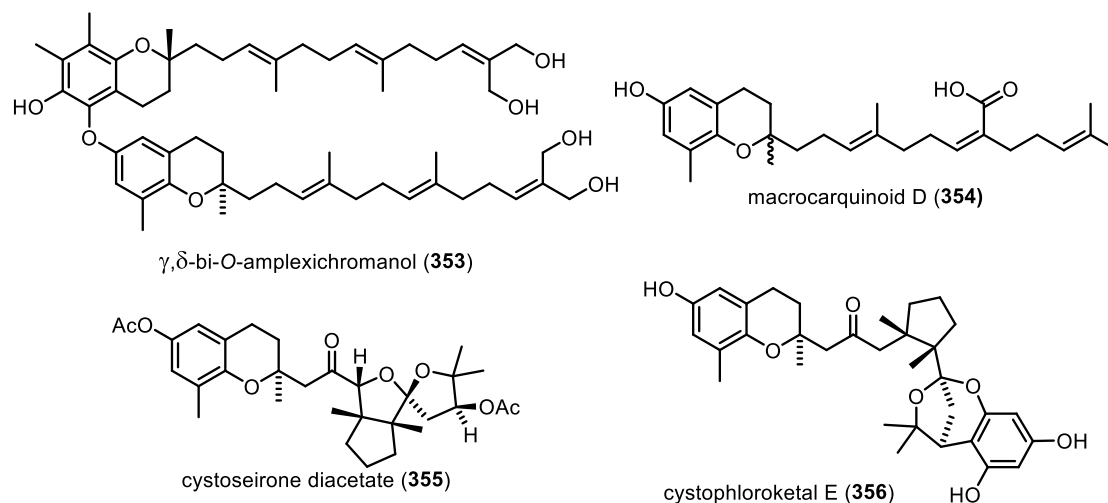
Remarkably, the corresponding δ -tocochromanol (shown here for δ -345) can be obtained directly by cyclization from the hydroquinone precursor without further methylation steps. This could be an explanation why many chromanols found in nature exhibit the δ -substitution pattern.

6.1.2. New isolated chromanes

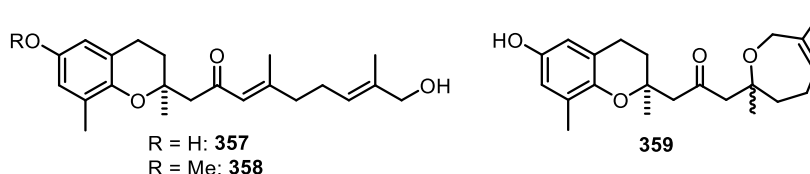
Especially in the last decades, bioactive (toco)chromanols have been increasingly isolated.^[161] Some of the isolated compounds showed high biological activities with anticancer, antiproliferative and anti-inflammatory properties.^[162]

Scheme 78 shows selected δ -tocochromanol-derived natural products that have been isolated and described in recent years. The γ, δ -bi-*O*-amplexichromanol (**353**) was isolated together with a series of tocotrienols by Guilet et al. in 2013 and showed, together with its monomers, which were also isolated, a potent antiangiogenic effect.^[153b] Recently, the δ -tocotrienol macrocarquinoid D (**354**) was isolated as an enantiomeric mixture together with known tocochromanols. It possesses a carboxylated side chain and showed good radical scavenging activity and AGE inhibitory activity.^[153e] The meroditerpenoid cystoseiron (**355**), originating from the brown alga of the genus *Cystoseira*, and some derivatives were already described as diacetates in the early 2000s and showed an unusual acetal/ether connection in the diterpene side chain.^[153a] These isolated spiro compounds were characterized by three fused

pentacycles. Without acetate protection, the compounds were found to be unstable. Other chromanols of marine origin also exhibit atypical rings and ether bridges. For example, the cystophloroketals A-E, isolated in 2015, integrate polyphenolic units into their structure.^[153c] Cystophloroketal E (**356**) showed antifouling activity in this context. A five-membered ring is incorporated in its diterpene side chain and its end is fused with a condensed polyphenol to form a bicyclic chromane unit.



But unusual δ -chromanol-derived compounds have not only been found in marine plants. In 2016, the Kingston group isolated a series of chromanols with an oxidized geranyl side chain from the North American plant *Koeberlinia spinosa* (Scheme 79).^[153d]

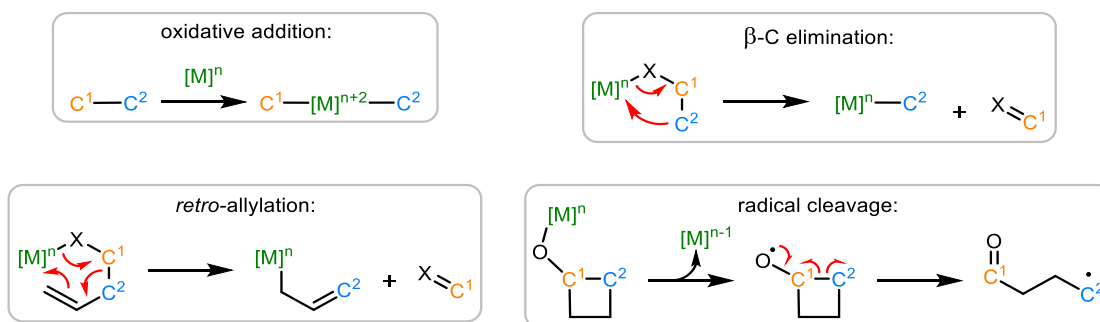


The substances were detected during the search for new compounds that could be considered as antimalarial drugs.^[163] Among others, the chromanols **357-359** were found, which showed micromolar antiplasmodial activity against the malaria parasite *Plasmodium falciparum* ($IC_{50} = 23-24 \mu M$ for **358** and **359**).^[153d] Regarding **359**, it was suggested that the oxepane moiety was formed as an artifact under acid catalysis (traces during isolation) in an oxa-*Michael*-type addition from the corresponding (*Z*)-isomer of **357**. The isolation of compound **359** as a diastereomeric mixture supported this assumption.^[153d]

6.2. Enantioselective iridium-catalyzed cyclobutanol cleavage

6.2.1. C-C bond activation

In addition to C-C bond forming reactions, C-C bond activating reactions are of interest as well. Through controlled C-C bond cleavage, more complex structures can be assembled in one step from mostly symmetric and synthetically easily accessible systems.^[164] This type of fragmentation is highly atom-economic. In contrast to the more common metal-catalyzed C-H bond activations, C-C bond activations are less frequently represented in the literature because, on the one hand, the C-C bond is comparably quite inert and sterically more difficult to access; on the other hand, the binding orbitals are highly directed compared to those of the C-H bond and can interact less well with transition metals.^[165] Scheme 80 depicts four possible metal-catalyzed mechanisms for C-C bond cleavage.^[164b, 166]



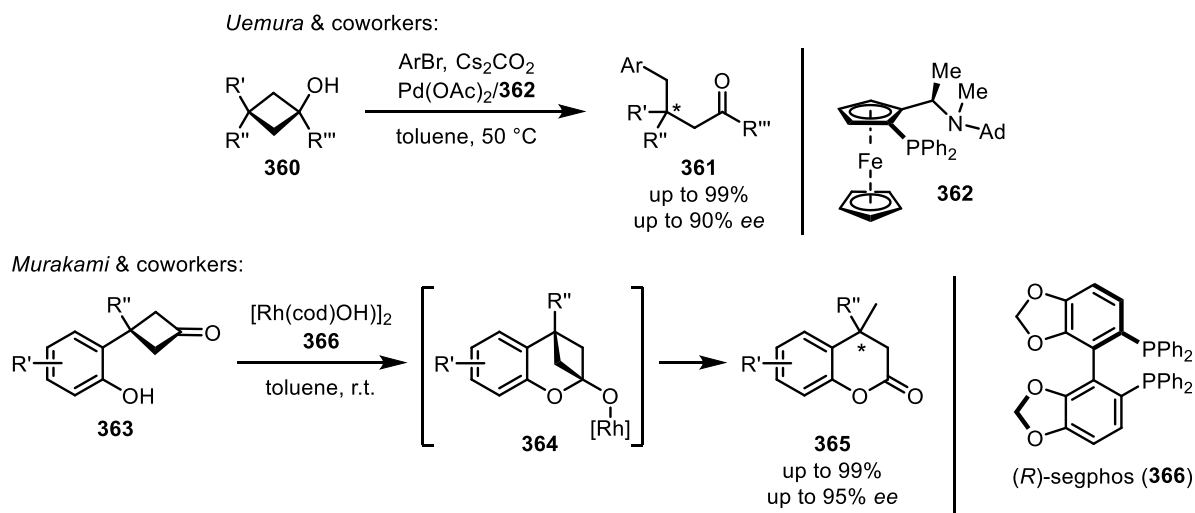
Scheme 80: Possible pathways of transition metal-catalyzed C-C bond activation to cleavage.^[166]

In principle, oxidative addition belongs to the C-C bond activating reactions. However, since the reverse step is the usually thermodynamically more favored reductive elimination, this type of bond activation is particularly suitable in the combination with the insertion of molecule groups such as carbon monoxide as well as for intramolecular rearrangements.^[166a] The driving force of the β -C elimination is mainly determined by the C=X bond strength as well as the release of the ring tension. *Retro*-allylation occurs *via* a 6-membered transition state.^[166a] The fourth mechanism *via* radical cleavage has only recently been discovered to be catalyzed through some metals e.g. silver and manganese.^[166b] Particularly strained ring systems can be fragmented well by oxidative addition, β -C elimination, or radical cleavage.^[164b] The methodology of C-C bond activation is increasingly gaining importance as a strategy in natural product syntheses.^[167] The methodology is of particular value when it comes to the construction of quaternary stereocenters, as these represent a major synthetic challenge.^[168]

6.2.2. Metal-catalyzed cyclobutanol cleavage

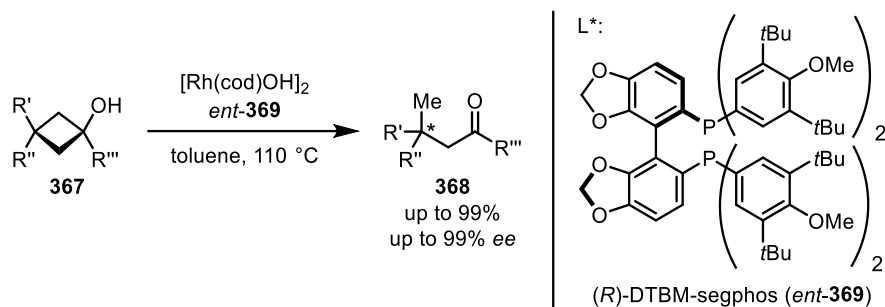
In particular the C-C bonds in cyclobutane derivatives can be activated in a metal-catalyzed manner since the energy gain from the opening of the strained four-membered ring is a major driving force.^[169] The reaction can be realized using the routes presented in Section 6.2.1. (see Scheme 80). Most notably the palladium- and rhodium-catalyzed C-C bond cleavage, which proceeds *via* β -C elimination, shows good results in such transformations coupled with further downstream reaction cascades.^[168b, 170] The use of tertiary cyclobutanols in this methodology is of particular value, as it allows the construction of β -substituted, open-chain ketones with a quaternary stereocenter.

In 2003, *Uemura* and coworkers were able to enantioselectively convert cyclobutanols of type **360** under palladium-catalysis with the transfer of an aryl group. The γ -arylated products of type **361** were obtained in high enantiomeric excess in the presence of the ferrocene-derived ligand **362** (Scheme 81).^[170a]



Scheme 81: Palladium-catalyzed asymmetric cyclobutanol cleavage by *Uemura* and coworkers^[170a] and rhodium-catalyzed asymmetric cyclobutanone fragmentation of phenolic cyclobutanones by *Murakami* and coworkers.^[170b]

The *Murakami* group^[170b] (Scheme 81) and later the *Cramer* group^[168b, 170d] (Scheme 82) developed effective rhodium systems using hydroxide complexes and segphos ligands (**366** and *ent*-**369**). The phenol-substituted cyclobutanones of type **363** were highly selectively reacted to β -substituted chromanones **365** *via* stereoselective cyclobutanone cleavage of the corresponding rhodium alkoxide intermediate **364**. *Cramer et al.* demonstrated the power of this method on tertiary **367** alcohols using the highly substituted segphos ligand *ent*-**369**. A range of ketones were synthesized in high yields and enantiomeric excesses with a quaternary carbon atom in the β -position. Extensive deuteration experiments supported β -C elimination for bond cleavage in the reaction pathway (see Scheme 84, Section 6.2.4.).



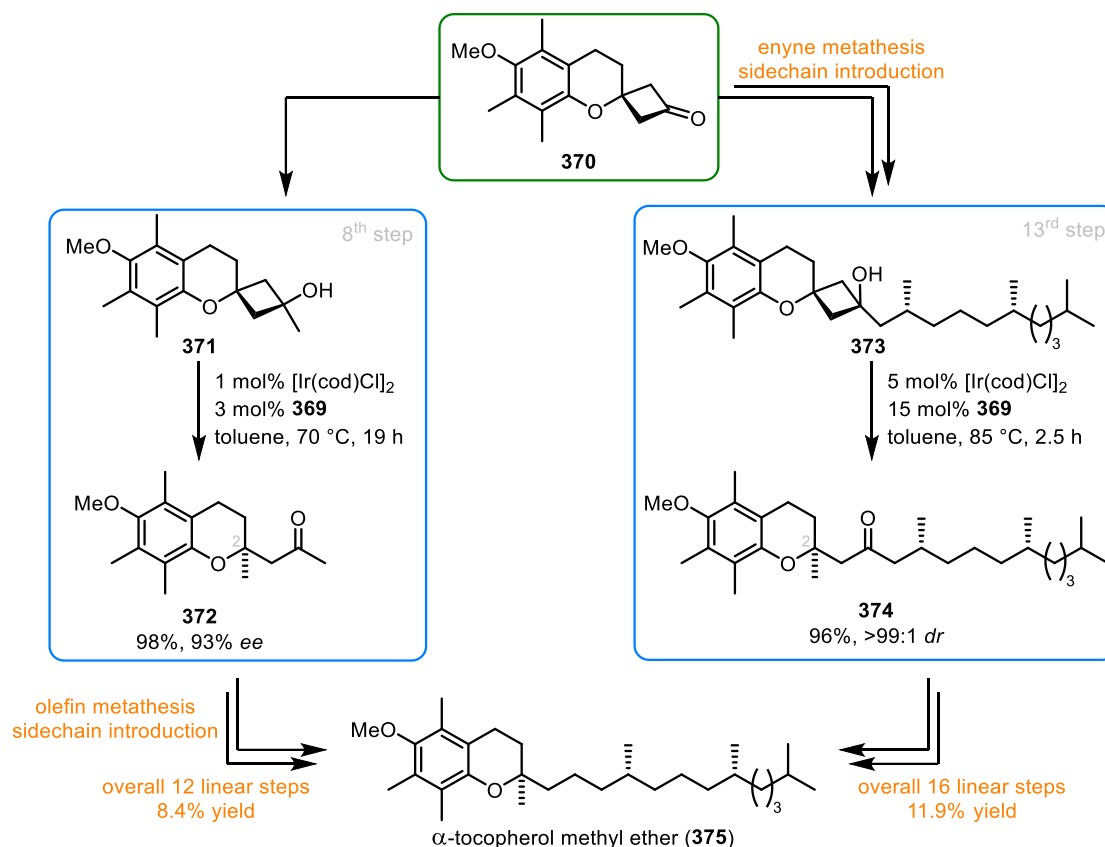
Scheme 82: Rhodium-catalyzed enantioselective cyclobutanol cleavage by *Seiser and Cramer*.^[168b, 170d]

Iridium-catalyzed C-C bond fragmentation is much less common. The first work on C-C bond activation using iridium complexes was published by *Crabtree et al.* in the 1980s.^[171] In Addition, there are only a few studies highlighting the strength of iridium-catalyzed C-C bond cleavage.^[172] A single example of an iridium-mediated cleavage of a highly strained cyclobutanol ring system was reported by *Zhu* and coworkers in 2016.^[173] Applications in total synthesis or in-depth mechanistic studies of the iridium-catalyzed desymmetrization of cyclobutanols were absent until the studies of *Ratsch* and *Schlundt et al.* presented in the following section.

6.2.3. Application in the total synthesis of α -tocopherol methyl ether

In a novel synthesis of (*R,R,R*)- α -tocopherol (α -**345**), the rhodium-catalyzed cyclobutanol fragmentation developed by *Cramer* was initially to be employed. Detailed evaluation by *Schlundt* to apply *Cramer's* method to the tocopherol system led exclusively to racemic products (0% ee) under rhodium catalysis.^[174] The use of iridium was crucial to carry out the reaction in a stereoselective manner.^[174-175]

Continuing with previously elaborated spirochromanone **370**, two different strategies were followed to introduce the side chain. One using linkage by an olefin metathesis^[174] and a second one using a previously developed enyne metathesis followed by 1,4-hydrogenation.^[176] Both routes were brought to completion by *Ratsch* in 12 and 16 linear steps (Scheme **83**). Both routes implemented the iridium-catalyzed cyclobutanol fragmentation in the 8th and 13rd steps, with great success.^[175] The spirochromanols **371** and **373** could be efficiently used to form the quaternary stereocenter in position 2 on the chromane ring. The two product ketones **372** and **374** were obtained in the desired absolute configuration. The latter two were subsequently converted to the desired α -tocopherol methyl ether (**375**), thus virtually completing the total synthesis of Vitamin E as the methyl deprotection was literature known.^[175]



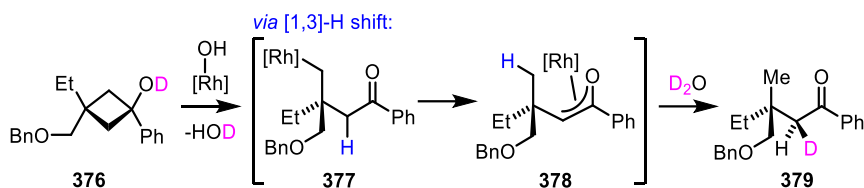
Scheme 83: Implementation of an iridium-catalyzed asymmetric cyclobutanol fragmentation as the key step in two strategically distinct syntheses of α -tocopherol methyl ether (**375**).^[175, 177]

Using the cyclobutanol fragmentation as strategy in the total synthesis of α -tocopherol methyl ether (**375**), the power of the iridium-catalyzed variant was impressively demonstrated. It proceeded in almost quantitative yields in both cases in excellent enantio- or diastereoselectivity. Based on the success of iridium as a metal catalyst in this method, the mechanism and substrate scope were investigated.^[177-178]

6.2.4. Mechanistic aspects and scope

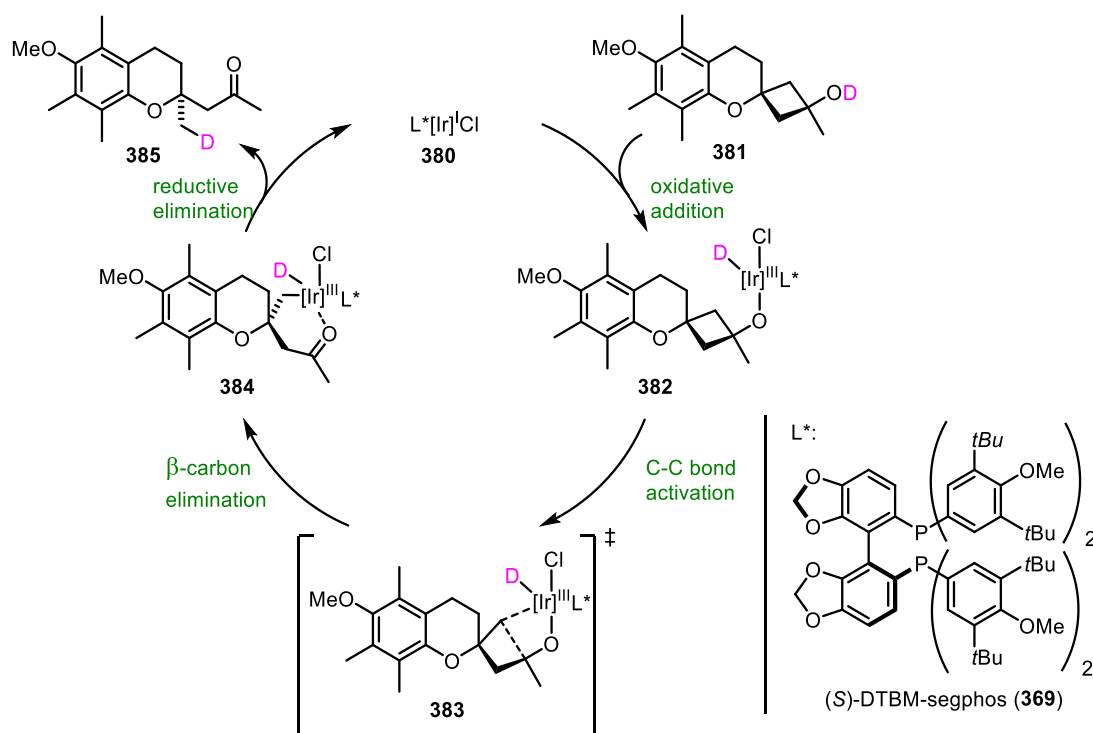
The racemic outcome (0% ee) of the rhodium-catalyzed cyclobutanol cleavage in the application for chromanol system **371** suggested distinct differences in the reaction pathways. Moreover, in the rhodium catalysis, conversion was evident only when either the hydroxide complex $[\text{Rh}(\text{cod})\text{OH}]_2$ was employed or a base was added. Iridium catalysis, on the other hand, could be carried out without base addition using the corresponding chloro complex $[\text{Ir}(\text{cod})\text{Cl}]_2$.^[174-175] Guided by these observations, *Ratsch et al.* investigated the mechanism for a better understanding and elucidation of the differences.^[177-178] For the rhodium-catalyzed cyclobutanol fragmentation, *Cramer* and *Seiser* performed deuteration experiments starting from deuterated cyclobutanol **376** (Scheme **84**).^[170c, 170d] These revealed two major findings. The deuterium remained in the end at the α -methylene group of the product **379**, and

diastereoselective deuteration also occurred, which suggested a [1,3]-H shift with the formation of an oxa- π -allylrhodium complex **378**.



Scheme 84: Mechanistic insights and results of the deuteration study of the rhodium-catalyzed cyclobutanol cleavage by *Cramer* and coworkers.^[170d]

The deuteration experiments performed with the iridium-catalyzed cyclobutanol fragmentation using spirochromanol **76** revealed a major difference: the deuterium in the product **385** was exclusively positioned at the methyl group of the formed quaternary stereocenter. KIE measurements and DFT calculations as well as further experiments supported the mechanism proposed in Scheme **85**.^[177-178]

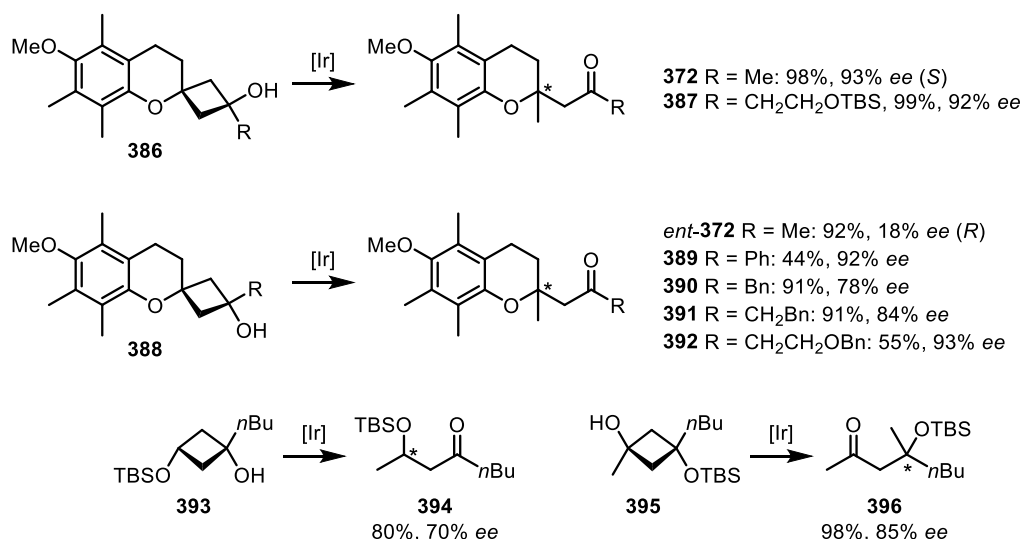


Scheme 85: Proposed mechanism of the asymmetric iridium-catalyzed cyclobutanol cleavage.^[177-178]

First, oxidative addition of the active iridium complex **380** occurs under O-D bond break. A KIE of ~ 1.7 and computational experiments confirmed that this step is most likely rate-determining. Moreover, the C-C bond activation followed by β -C elimination shown in the transition state **383** explained the experimental (*S*)-selectivity of the catalysis, based on DFT calculations. Only the (*S*)-conformational transition state **383** can form a preferential alignment with the propeller-shaped phosphorus aryl groups of the (*S*)-DTBM-segphos ligand (**369**). This makes

the β -C elimination the enantioselectivity-determining step. Reductive elimination from the iridium- σ -alkyl species subsequently releases the product.

Based on the mechanistic findings, the substrate spectrum for this novel transformation of iridium-catalyzed cyclobutanol cleavage was investigated by *Ratsch*.^[177] Different chromanol derivatives were prepared and exposed to the conditions. A selection of the successful substrates in terms of chemo- and enantioselectivity is shown in Scheme 86.^[177-178]



Scheme 86: Selection from the substrate spectrum of the developed iridium-catalyzed cyclobutanol cleavage. Reactions were performed with ligand **369**.^[177-178]

The substrate spectrum showed a rather limited functional group tolerance compared to *Cramer's* rhodium catalysis. The 2,2-disubstituted α -tocopherol related chromanes with purely aliphatic side chains were the best to react (also compare Scheme 83). The iridium-mediated reaction used for this purpose in contrast to rhodium catalysis (0% ee) displayed excellent stereo control. Potentially coordinating groups did not work or did not give the desired product. Notably, when the methyl-substituted chromane was used with the *trans*- or *cis*-configured system **386** or **388**, the other enantiomer **372** (93% ee) or *ent*-**372** (18% ee) was formed. Protected alcohols such as **387** and **392** or phenyl-substituted systems **389-391** could also be obtained in high to excellent enantiomeric excesses. Also, a non-chromane linked system was stereoselectively converted as a respective mono-TBS protected diol **393** or **395**.

Overall, the power of this method for the enantioselective assembly of quaternary carbon atom systems especially with respect to α -tocopherol related systems was impressively demonstrated.

6.3. Synthetic studies towards chromanes of *Koeberlinia spinosa*

In light of the success of the presented study for the total synthesis of α -tocopherol and the enantioselective ring opening from the prochiral spirocyclobutanol **386** to methyl ketone **387** (see Scheme **83**) using an iridium catalyst instead of the racemic-only rhodium catalysis for this transformation,^[175] it should be verified whether this methodology is transferable to the total synthesis of other natural chromanes.

In the preceding master thesis, the δ -chromanol-derived natural product **358** was investigated as a target molecule (Figure **18**).^[179] The latter has already been presented with other δ -chromanols in Section 6.1.2. The antiplasmodial chromane is methyl substituted at the phenolic hydroxy group and features a trisubstituted enone as well as a terminal alcohol in the geranyl side chain.

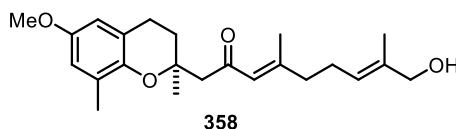
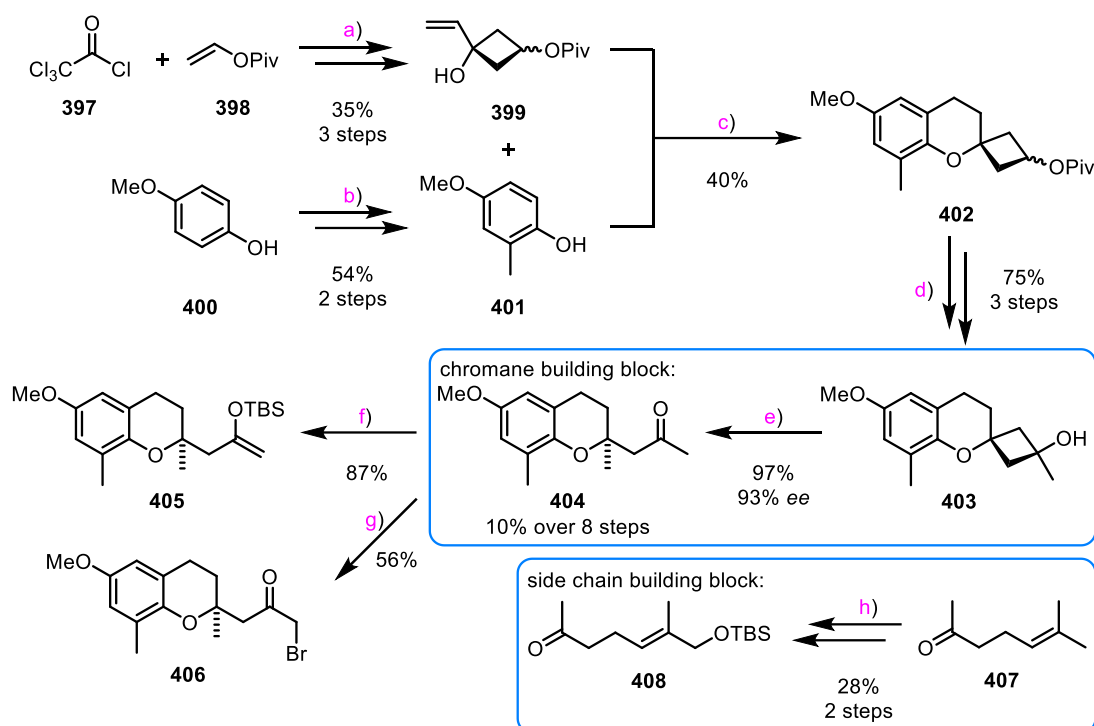


Figure 18: Structure of an antiplasmodial chromane **358** isolated from *Koeberlinia spinosa*.^[153d]

Since the δ -chromanol is an interesting motif in some tocopherol-like natural products (see Section 6.1.2.), the chromane core **404** was first synthetically developed in 8 linear steps in an overall yield of 10% (Scheme **87**), analogous to the strategy of the presented α -tocopherol synthesis (see Section 6.2.3.). The iridium-catalyzed cyclobutanol cleavage of **403** proceeded smoothly and gave excellent yields of 97% and 93% ee. The detailed reaction conditions are given in the scheme caption. This will be referred to comparatively in the later discussion (see Section 8).



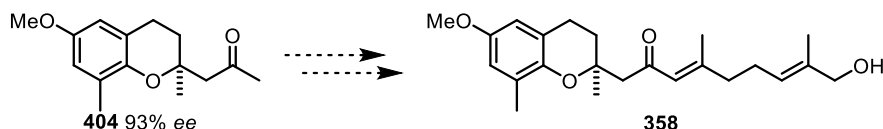
Scheme 87. Overview of the synthesis of several chromane and side chain building blocks related to the total synthetic studies towards chromane **358** elaborated in the master thesis.^[179] Conditions: **a)** 1. Zn (2.0 equiv.), Et₂O, r.t., 4 h; 2. Zn (5.0 equiv.), HOAc, 0 °C, 3 h; 3. H₂C=CHMgBr (1.5 equiv.), THF, -78 °C, 3 h; **b)** 1. MgCl₂ (3.0 equiv.), -(CH₂O)_n (5.0 equiv.), Et₃N (3.0 equiv.), THF, reflux, 16 h; 2. H₂N-NH₂·H₂O (11.0 equiv.), KOH (5.0 equiv.), (HOCH₂)₂, 150 °C, 16 h; **c)** MsOH (4.0 equiv.), CH₂Cl₂, r.t., 16 h; **d)** 1. NaOH (6.0 equiv.), EtOH, r.t., 26 h; 2. PIDA (1.2 equiv.), TEMPO (12 mol%), CH₂Cl₂, r.t., 16 h; 3. MeMgBr (1.3 equiv.), Et₂O, -78 °C, 1.5 h; **e)** **369** (17 mol%), [Ir(cod)Cl]₂ (5 mol%), MePh, 50 °C, 15 h; **f)** TBSOTf (4.0 equiv.), Et₃N (6.0 equiv.), MeCN, 0 °C, 20 min; **g)** KHMDS (1.4 equiv.), TMSCl (2.3 equiv.), NBS (1.8 equiv.), THF, -78 °C, 2.5 h; **h)** 1. TBHP (1.0 equiv.), SeO₂ (1.0 equiv.), CH₂Cl₂, r.t., 2 h; TBSCl (1.7 equiv.), DMAP (7 mol%), Et₃N (1.7 equiv.), r.t., 2 h.

The *Friedel-Crafts*-type condensation for chromane ring closure of the literature known building blocks **399** and **401** could not be carried out with BF₃·Et₂O as for the trimethyl-substituted, electron-rich α-chromane system. Only in the presence of the *Brønsted* acid MsOH could product **402** be obtained in a moderate yield.

In the master thesis, starting from methyl ketone **404**, the TBS enol ether **405** and the α-bromoketone **406** were prepared. Both derivatives were suitable as possible coupling partners for an envisioned side-chain attachment. Starting from 6-methyl-5-hepten-2-one (**407**), the TBS-protected side chain precursor **408** could be synthesized in 2 steps. Preliminary *Mukaiyama* aldol addition-type approaches with enol ether **405** were performed. However, these only led to traces of the desired product structures. A *Wittig*-like olefination approach using building block **406** remained unapproached.

7. Concept and Task

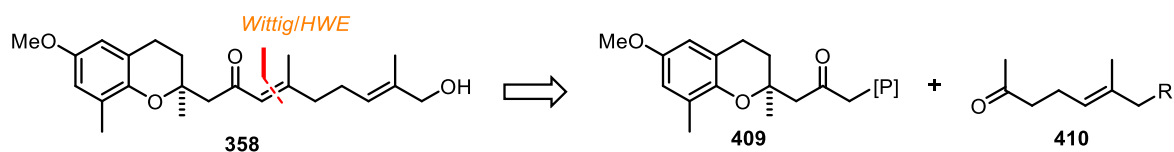
The objective of this project was to continue the total synthetic investigation of the antiplasmodial δ -chromane natural product **358** started in the master thesis.^[179] In a concise study, remaining possibilities for the side-chain introduction were to be tested to construct the desired chromane structure (**88**).



Scheme 88: Envisioned completion of the total synthesis of antiplasmodial chromane **358**.

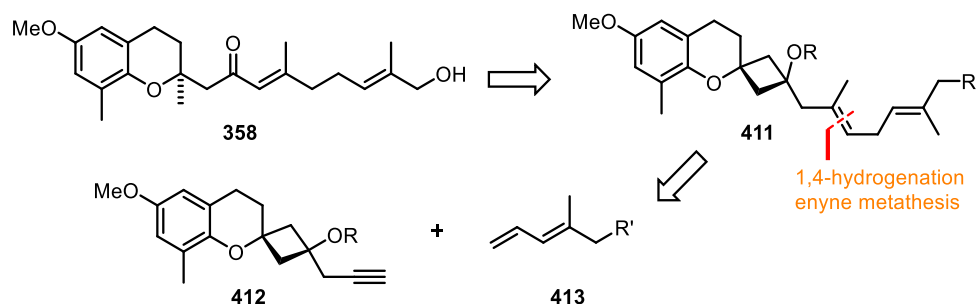
By means of common synthesis strategies, it should be verified whether the side chain could be coupled efficiently. The previously established synthesis of the desired chromane unit up to chromanone **404** should be additionally examined for further improvement possibilities.

Consequently, a Wittig/HWO-type olefination approach should be followed. By retrosynthesis, the natural product can be broken down into a chromanone-phosphorous species of type **409** and a ketone of type **410** (Scheme **89**).



Scheme 89: Retrosynthetic analysis applying a *Wittig/HWE* transformation.

A second strategy, based on the α -tocopherol synthesis developed by *Ratsch et al.*,^[175] aims to construct **358** starting from spirocyclobutanol **411** with iridium-catalyzed desymmetrization as a key step (Scheme **90**). The latter could possibly be assembled using an enyne metathesis followed by 1,4-hydrogenation. Synthetic building blocks would thus be the alkyne-substituted derivative **412** and the diene **413**.



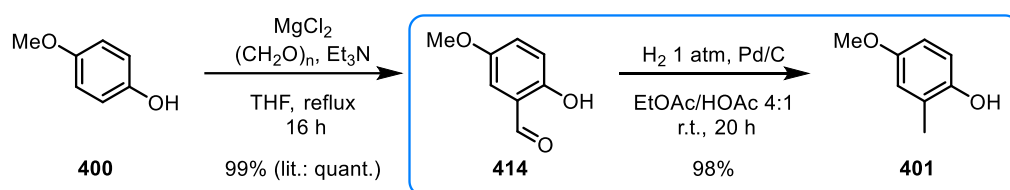
Scheme 90: Retrosynthetic analysis applying a 1,4-hydrogenation/enyne metathesis transformation.

8. Results and Discussion

8.1. Studies on the linear route towards chromanone 404

The following results refer to optimization attempts and screening experiments along the linear route towards chromanone **404** which was developed in the previous master thesis and presented in the section Introduction & State of Knowledge (see Section 6.3, Scheme **87**).

The two-step synthesis of the aromatic building block **401** was carried out *via* a literature known magnesium-mediated ortho-directed formylation of 4-methoxyphenol (**400**) in excellent yield (Scheme **91**).^[180] This was followed by a benzylic reduction of the corresponding benzaldehyde **414** to afford 4-methoxy-2-methylphenol (**401**).

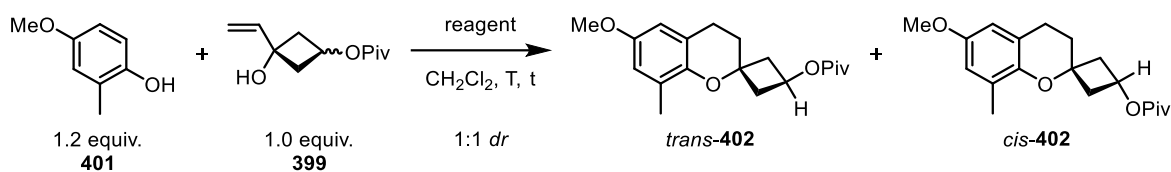


Scheme 91: Preparation of aromatic building block **401**.

Originally, the reduction of the aldehyde **414** was carried out by a *Wolff-Kishner*-type reduction with hydrazine monohydrate in a yield of 57%. Inspired by a protocol of *Hecht* and coworkers,^[181] these conditions were replaced by a palladium-catalyzed benzylic hydrogenolysis. Thus, the desired phenolic building block **401** was obtained under much milder conditions over two steps in almost quantitative overall yield (97%).

To build the chromane backbone, the aromatic building block **401** was reacted with the literature known vinylcyclobutanol **399** in a Friedel-Crafts-related condensation to give spirochromane **402** as a mixture of *cis*- and *trans*-isomers (Table **7**).^[175] While $\text{BF}_3 \cdot \text{Et}_2\text{O}$ as a *Lewis* acid for the trimethylated α -tocopherol system usually gave high yields up to 80%,^[174] only low conversion and yields were obtained for the targeted monomethylated δ -chromane system under the developed conditions (entry 1-4). Using the Brønsted acid methanesulfonic acid, a moderate yield of up to 40% was obtained (entry 5-6).

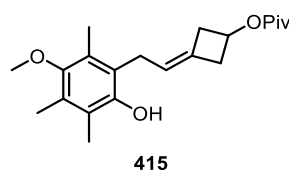
In final optimization approaches for the synthesis of **402**, the yield could not be further increased (entry 7-13). Neither an increase in concentration (entry 7) nor the use of a molecular sieve to remove H_2O (formed as condensation byproduct) were successful (both <20%). The use of other *Brønsted* acids only showed lower yields with a maximum of 13% for **402** with triflic acid (entry 9) and <10% with camphorsulfonic acid or *para*-toluenesulfonic acid (entries 10 and 11). Similar results were obtained when changing the solvent to 1,2-dichloroethane or the aromatic solvent chlorobenzene. While the unreacted phenol **401** typically was completely reisolated, the vinylcyclobutanol **399** decomposed over a longer reaction period.

Table 7: Selected screening conditions for the *Friedel-Crafts*-related condensation towards chromane **402**.

| entry | reagent | equiv. | solvent | T [°C] | T [h] | yield [%] |
|------------------|-----------------------------------------|--------|---------------------------------|---------|-------|------------------------|
| 1 ^[a] | $\text{BF}_3 \cdot \text{Et}_2\text{O}$ | 4.0 | CH_2Cl_2 (0.3M) | r.t. | 5.5 | 23 |
| 2 ^[a] | $\text{BF}_3 \cdot \text{Et}_2\text{O}$ | 2.0 | CH_2Cl_2 (0.3M) | 0-r.t. | 19 | 28 |
| 3 | $\text{BF}_3 \cdot \text{Et}_2\text{O}$ | 4.0 | CH_2Cl_2 (0.3M) | r.t.-50 | 22 | 31 |
| 4 | $\text{BF}_3 \cdot \text{Et}_2\text{O}$ | 4.0 | HCOOH (0.3M) | r.t. | 48 | <5 |
| 5 | MsOH | 4.0 | CH_2Cl_2 (0.3M) | r.t. | 18 | 38 (22) ^[b] |
| 6 ^[c] | MsOH | 4.0 | CH_2Cl_2 (0.3M) | r.t. | 72 | ~40 ^[d] |
| 7 | MsOH | 4.0 | CH_2Cl_2 (0.6M) | r.t. | 21 | 19 |
| 8 | MsOH/MS 3 Å | 4.0 | CH_2Cl_2 (0.6M) | r.t. | 21 | ~15 ^[d] |
| 9 | TfOH | 4.0 | CH_2Cl_2 (0.3M) | r.t. | 21 | 13 |
| 10 | <i>rac</i> -CSA | 4.0 | CH_2Cl_2 (0.3M) | r.t. | 51 | <10 |
| 11 | <i>p</i> TsOH | 4.0 | CH_2Cl_2 (0.3M) | r.t. | 51 | <10 |
| 12 | MsOH | 4.0 | DCE (0.3M) | r.t. | 20 | <10 |
| 13 | MsOH | 4.0 | CIPh (0.3M) | r.t. | 20 | <10 |

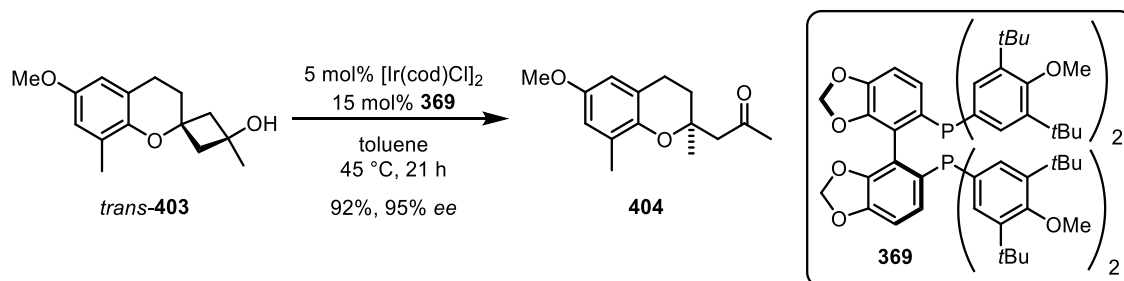
Isolated yields of combined *trans*- and *cis*-**402** (1:1 *dr*) (0.3-0.7 mmol scale). Entry 1-6 from the preceding master thesis.^[179] ^[a]Dropwise addition of **399** in corresponding solvent over 1 h. ^[b]In parentheses yield for 22 mmol scale. ^[c]Portionwise addition of **399**. ^[d]Product impure; yield is approximate based on ¹H NMR.

Overall, the comparably low conversions could possibly be explained by the significantly electron-poorer only mono-methyl-substituted phenol **401**. In the total synthesis of α -tocopherol, *Schlundt* was able to isolate the corresponding trisubstituted condensation intermediate **415** as a common byproduct (Figure 19).^[174]

**Figure 19:** Condensation byproduct in the α -tocopherol synthesis by *Schlundt*.^[174]

Since the analogous monosubstituted intermediate was never detected in the reaction of phenol **401** with cyclobutanol **399**, this suggests that even the first *Friedel-Crafts*-like alkylation step before the cyclization proceeds in low conversion. Further conversion of **402** to cyclobutanol **403** was performed according to the reactions presented in Section 6.3 (Scheme 87).

The iridium-catalyzed enantioselective cyclobutanol cleavage of chromanol *trans*-**403** is shown in Scheme 92. By lowering the temperature from 50 °C to 45 °C, a slightly increased enantiomeric excess of over 95% for desired chromanone **404** was achieved with still full conversion and excellent yield.



Scheme 92: Iridium-catalyzed cyclobutanol cleavage of chromanol **403**.

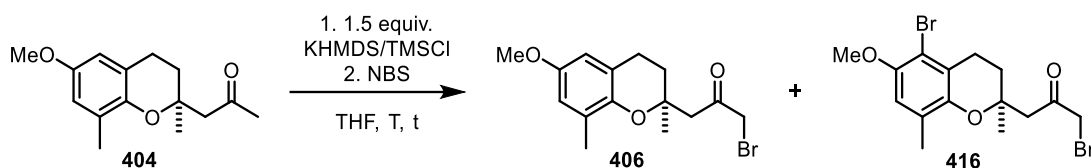
8.2. Side chain coupling attempts

8.2.1. Olefination coupling approaches

8.2.1.1. Wittig-type approach

For the preparation of a corresponding phosphonium bromide, α -bromoketone **406** was prepared starting from chromanone **404** (Table 8). Bromination was achieved through a silyl enol ether intermediate and subsequent addition of *N*-bromosuccinimide. Using 1.8 equiv. NBS product **406** was obtained in fair yield of 56% (entry 1). A longer reaction time led to the selective formation of the dibrominated chromanone **416**, which was isolated in 65% yield (entry 2).

Table 8: α -Bromination of chromanone **404**.

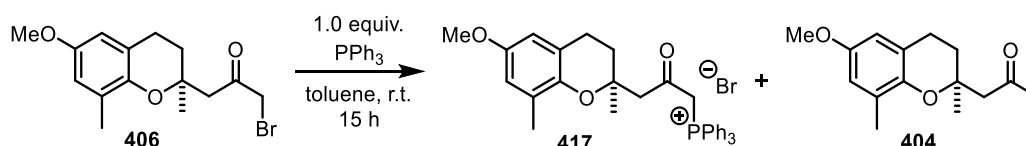


| entry | NBS equiv. | T [°C] | t [h] | yields |
|-------|------------|----------|-------|----------------------------------|
| 1 | 1.8 | -78-r.t. | 2.5 | 56% 406 |
| 2 | 2.1 | -78-r.t. | 19 | <10% 406 ; 65% 406 |
| 3 | 1.0 | -78 | 0.5 | 66 406 |
| 4 | 1.0 | -78 | 1.5 | 78 406 |

Isolated yields are given. Entry 1 from the preceding master thesis.^[179]

Further tests revealed that equimolar amounts of NBS and shorter reaction times led to an increase in selectivity. With portionwise addition of 1.0 equiv. of NBS and a reaction time of 1.5 h at -78 °C, α -bromochromane **406** was obtained in good yield (78%).

Under conditions inspired by *Liu et al.*,^[182] only a mixture of the desired phosphonium bromide **417** and the debrominated starting material **404** 0.6:1 with $\text{PPh}_3/\text{OPPh}_3$ impurities was obtained (Scheme 93)

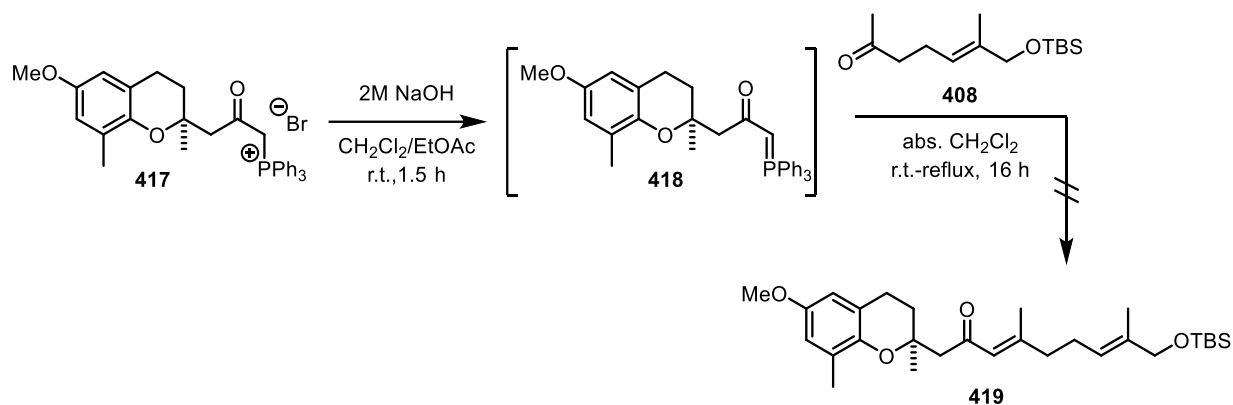


Scheme 93: Conversion of α -bromoketone **406** with PPh_3 .

The phosphonium bromide could be detected by ESI-MS. Further purification was not possible. The debromination of α -bromoketones under oxidative conditions with formation of OPPh_3 could already be described by *Borowitz et al.*^[183] To prevent this, the reaction was repeated under argon atmosphere and the nonpolar toluene phase was extracted with MeOH. HRMS and NMR spectroscopy were used to identify the desired product **7**. Recrystallization from

CH_2Cl_2 or CHCl_3 failed. The residual toluene phase contained mainly debrominated chromane **404** and $\text{PPh}_3/\text{OPPh}_3$ impurities.

Finally, by working on a larger scale and work-up by recrystallization from DCE/n-heptane, a mixture of **7** and **404** (~2:1) was obtained as a white foam. To probe at least the feasibility of the envisioned *Wittig* reaction, this mixture was reacted under basic conditions. The yellow oil, obtained after work-up, was subsequently treated with the ketone **408** and heated to reflux (Scheme 94).

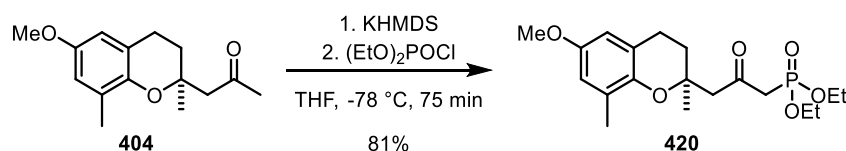


Scheme 94: Wittig-type approach for side chain introduction.

However, no conversion to the desired product **419** was observed and the ketone **408** could be completely reisolated. Since not even traces of the product were detected and it was difficult to obtain the phosphonium salt **417** in a pure form, this reaction route was not investigated further.

8.2.1.2. HWE-type approach

In order to install a phosphonate group to allow an HWE-like approach, chromane **404** was successfully reacted with KHMDs and $(\text{Et}_2\text{O})_2\text{POCl}$ to give 81% of the desired product **420** (Scheme 95).

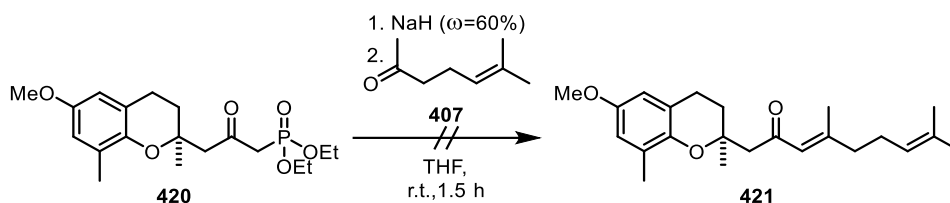


Scheme 95: Synthesis of phosphonate **420**.

According to the conditions of the *Puranik* group,^[184] a switch to shorter reaction times (67% after 5 h) and low temperature proved to be crucial for a good yield.

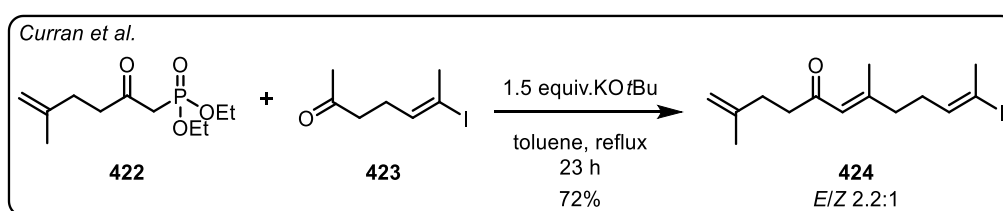
Based on several literature procedures for the synthesis of trisubstituted enones *via* HWE olefination,^[185] several conditions were screened as follows. In a first approach inspired by *Chakraborty* and coworkers, phosphonate **420** was reacted with sodium hydride and ketone

407 (Scheme 96).^[185e] The corresponding product **421** would represent the complete carbon skeleton of the natural product **358**. However, no conversion was observed again.



Scheme 96: HWE approach to construct the complete carbon skeleton of the desired natural product.

Haney and Curran were able to react an analogous ketone **423** with a β -ketophosphonate **422** in a good yield of 72% (Scheme 97).^[185b]



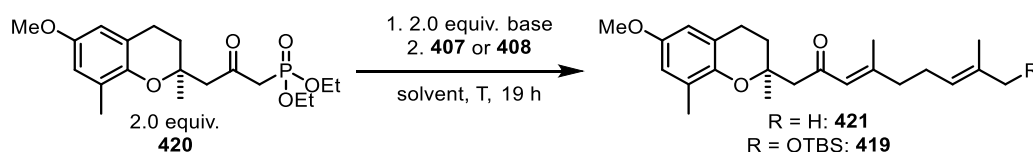
Scheme 97: HWE olefination to construct trisubstituted enone **424** by Haney and Curran.^[185b]

Under these conditions, the phosphonate **420** could not be reacted with either the ketone **407** or the side-chain building block **408** (for structure, see Scheme 94). Even under reflux conditions for several days, no traces of the respective products **421/419** were detected (see reaction scheme, Table 9). The decolorization of the reaction solution and the precipitation of a brown residue only indicated decomposition.

Even when microwave-assisted conditions^[186] were applied with 1.5 equiv. of KOtBu in THF at 90 °C, slow decomposition was always observed and only dephosphonated starting material **404**.

Table 9 summarizes final experiments on the HWE olefination approach. No conversion was detected in any of the solvents (toluene, THF, DMF) and with different bases (*n*BuLi, KOtBu, NaH, KHMDS). Mainly the starting materials **420** and **407** or **408** as well as the dephosphonated species **404** were detected in the reaction mixtures. Only in two cases, when using ketone **407** in toluene/*n*BuLi or THF/NaH, traces of the product were detected by GC-MS analysis.

Table 9: Summarized final screening results for the HWE-type olefination approach.



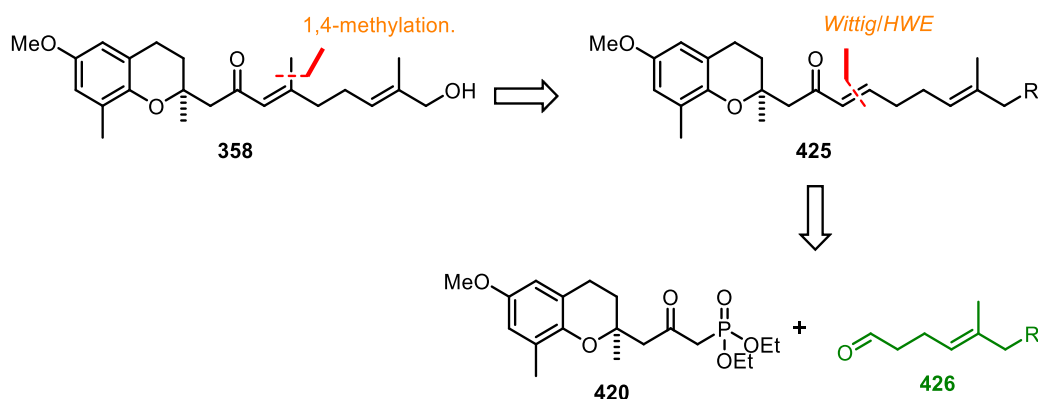
| entry | ketone | solvent | base | T [°C] | conv. |
|-------|------------|---------|--------------------|----------|-----------------------|
| 1 | 408 | toluene | <i>n</i> BuLi | r.t.-110 | - |
| 2 | 407 | toluene | KO ^t Bu | r.t.-110 | - |
| 3 | 407 | toluene | <i>n</i> BuLi | r.t.-110 | traces ^[a] |
| 4 | 407 | THF | NaH | r.t.-50 | traces ^[a] |
| 5 | 407 | THF | KHMDS | r.t.-50 | - |
| 6 | 408 | THF | KHMDS | r.t.-50 | - |
| 7 | 407 | DMF | NaH | r.t.-50 | - |
| 8 | 407 | THF | <i>n</i> -BuLi | r.t.-50 | - |

[a] Refers to the corresponding product **421**.

Since the desired *HWE* olefination did not proceed despite promising literature,^[185] an attempt was made to design the reaction system less sterically demanding.

8.2.1.3. Coupling attempts with an aldehyde side chain building block

In principle, the natural product **358** could also be derived from the only disubstituted enone **425** (Scheme **98**). After successful 1,4-methylation, the double bond might be re-introduced by means of an α -hydroxylation (e.g. *Davis* oxidation)/elimination or an analogous α -bromination/elimination sequence.^[187]

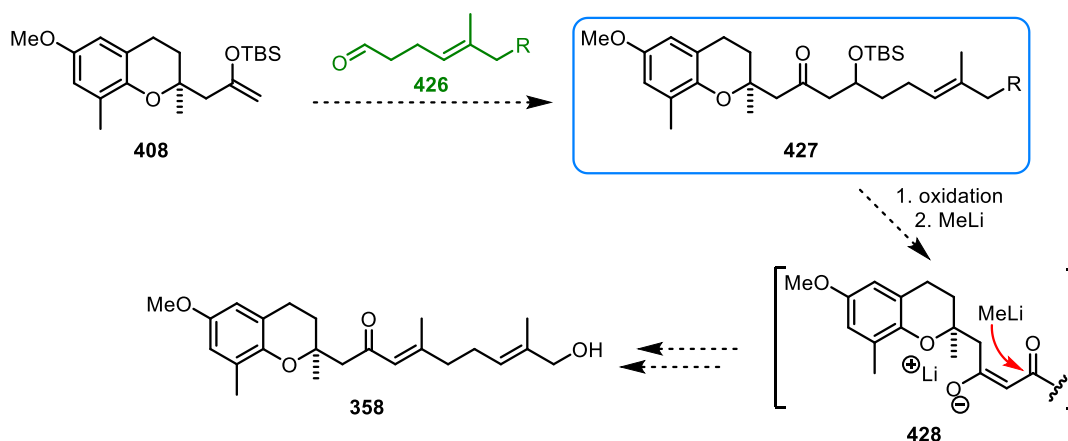


Scheme 98: Retrosynthetic analysis of chromane **358** from an aldehyde side chain unit of type **426**.

Thus, connection to the side chain might be accomplished in a sterically and kinetically more favored *HWE*-type reaction employing the aldehyde **426** as a building block.

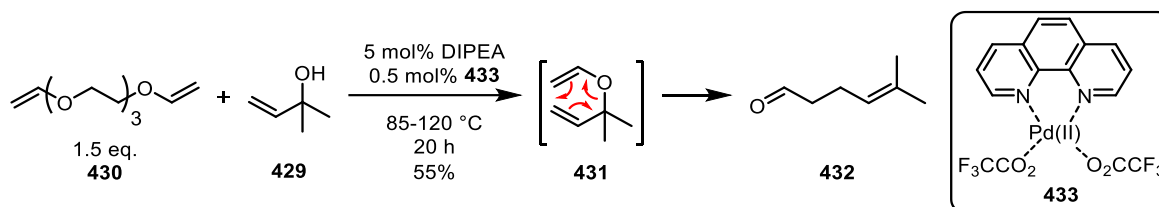
With aldehyde **426**, a *Mukaiyama* aldol addition with TBS-enol ether **405** might additionally be revisited (Scheme **99**), which afforded only product traces when using the corresponding ketone building block **408**. If successful, the TBS-protected aldol product **427** could possibly be first oxidized and then converted to an enol of type **428** by one equivalent of MeLi, followed by regioselective methylation by addition of a second equivalent of MeLi. Direct elimination of

the tertiary alcohol product rising from this transformation would lead to the desired enone structure which might be converted to the natural product **358** within a few steps.



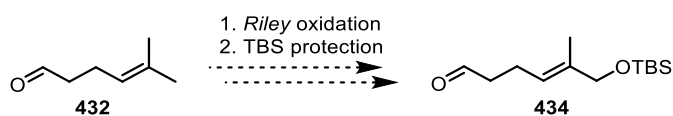
Scheme 99: Mukaiyama aldol-type synthesis plan towards chromane **358** via a regioselective 1,2-addition.

The side-chain building block with R = H, 5-methyl-4-hexenal (**432**) is known from literature.^[188] Starting from 2-methyl-3-buten-2-ol (**429**), this could be prepared based on a protocol by *Wei et al.*^[188a] using a palladium-catalyzed vinylation followed by *Claisen* rearrangement (see intermediate **431**) with a yield of 55% (Scheme **100**). Deviating from the literature protocol, the phenanthroline-palladium complex was generated *in situ* from available precursors.^[189]



Scheme 100: Synthesis of 5-methyl-4-hexenal (**432**).^[188a]

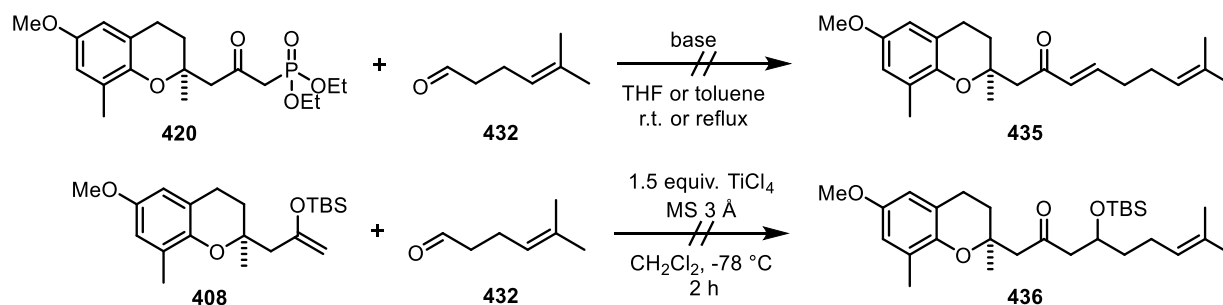
The aldehyde **432** might be functionalized using a *Riley* oxidation analogous to the strategy for ketone side chain **408** (Scheme **101**).



Scheme 101: Synthesis plan for the terminal hydroxylation of aldehyde **432**.

However, before further derivatization of the side chain building block, it should first be checked whether the aldehyde **432** can be coupled with the respective chromane building blocks **420** or **405**. In the reaction with phosphonate **420**, no conversion to the product **435** could be detected (Scheme **102**). Using KO^tBu, LiHMDS^[190] or LDA in THF or toluene with up to 10 equiv. of the aldehyde building block **432** and reflux conditions, only the corresponding

starting materials or the dephosphonation product **404** were reisolated again as in the previous HWE approaches.



Scheme 102: HWE olefination and *Mukaiyama* aldol approach using an aldehyde building block **432**.

In the *Mukaiyama* aldol approach with TBS-enol ether **405**, the deprotected starting material **404** was reisolated. Upon addition of 2.0 equiv. Et_3N as a coordinating Lewis base, an impure mixture was obtained after basic work-up and purification, which did not contain the targeted protected β -hydroxyketone **436**, but instead the condensation product **435** (<5%). In addition to GC-MS analysis, the enone **435** was moreover identified in the mixture by ^1H and 2D NMR spectroscopy and the characteristic ^1H enone signals were assigned (Figure 20).

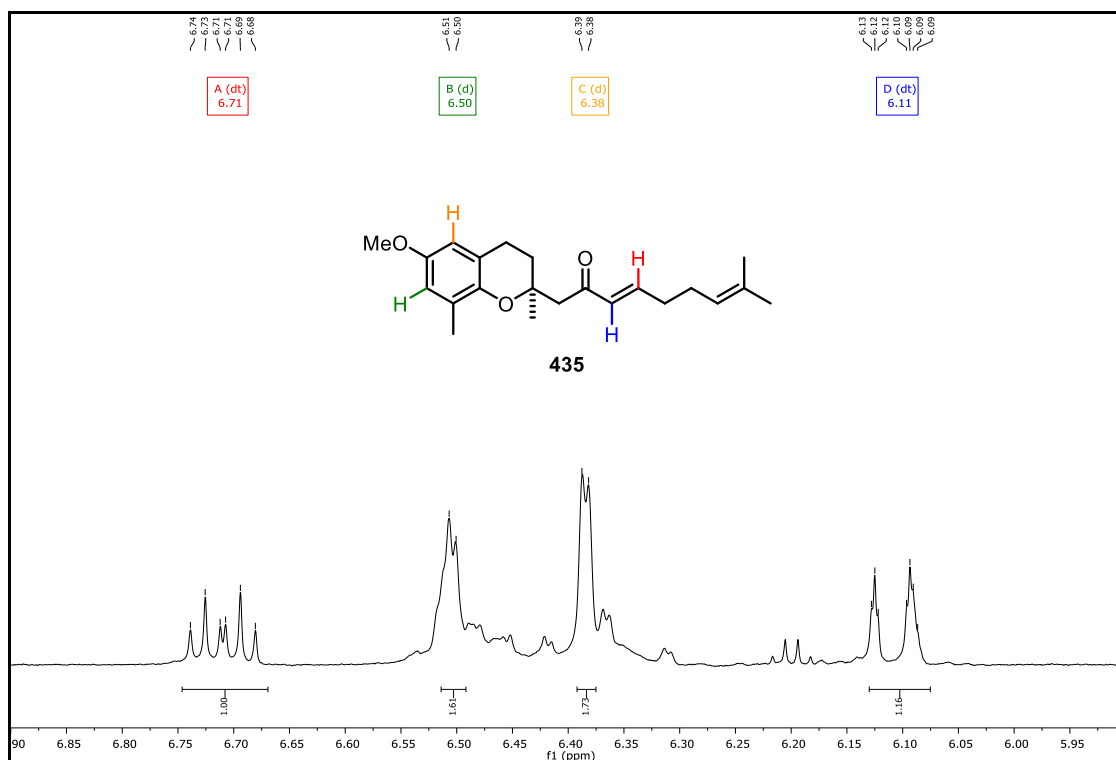
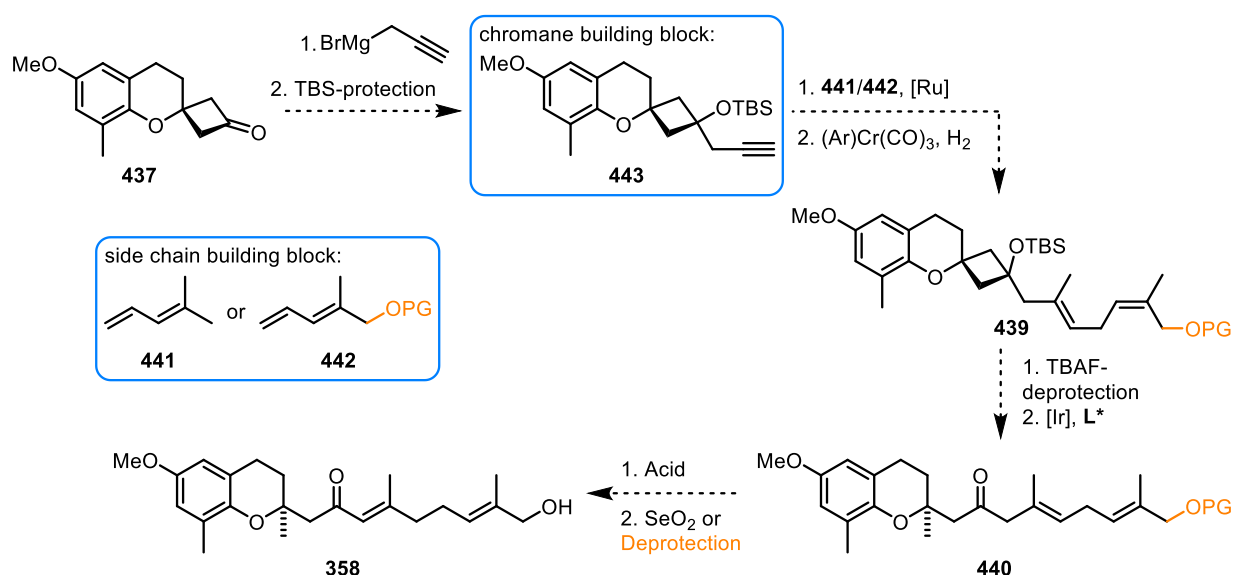


Figure 20: Excerpt of ^1H NMR spectrum showing the aromatic and enone proton signals of **435** (impure mixture).

Despite extensive experimentation the conversion could not be increased. The result was not reproducible nor did the changes in work-up^[191] lead to isolation of a clean product. Therefore, the investigation of this route was discontinued.

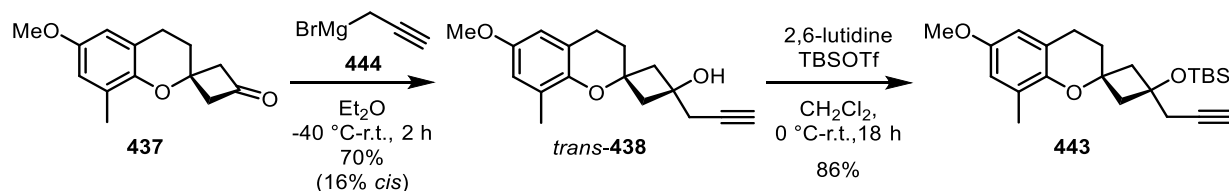
8.2.2. Enyne metathesis approach

As outlined in Section 7, a different synthesis strategy towards the natural product **358** would involve side-chain coupling by means of enyne metathesis. This key step had been successfully applied by *Ratsch* in a synthesis of α -tocopherol.^[175-177] This synthetic pathway would start from the already established spirochromanone **437** (Scheme 103). After introduction of the propargyl moiety, the chromane building block **443** would be coupled with a side-chain building block of type **441** or **442** (already with oxy function) *via* enyne metathesis. Subsequent chromium-mediated 1,4-hydrogenation would yield the protected chromane cyclobutanol **439**.^[176] After enantioselective iridium-catalyzed cyclobutanol cleavage, the expected product **440** could possibly be converted to the target structure within 2 steps *via* an acid-mediated rearrangement of the double bond and a late-stage hydroxylation or deprotection depending on the introduced side chain.



Scheme 103: Planned synthetic route towards chromane **358** employing an enyne-metathesis.

First, the propargyl-substituted spirochromanol **443** was derived from readily prepared chromanone **437** in two steps *via* a *Grignard* addition followed by TBS protection of the hydroxy group (Scheme 104).



Scheme 104: *Grignard* reaction to introduce a propargyl side chain at the spirochromanone **437**.

The required *Grignard* reagent propargylmagnesium bromide (**444**) was freshly prepared according to a protocol of *Florez* and coworkers and its concentration was determined by

iodimetry.^[192] The *trans*-selectivity (70% *trans*-**438**) can be explained by coordination of the corresponding *Grignard* magnesium cluster to the ring oxygen of the chromane core, resulting in preferential attack from the “lower” side.^[174, 179] The two diastereomers could be clearly assigned by elucidation of the structure by single X-ray crystallography (Figure 21).

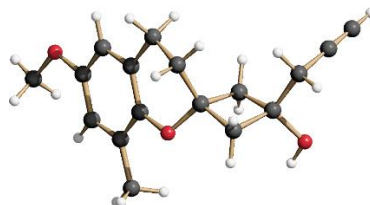
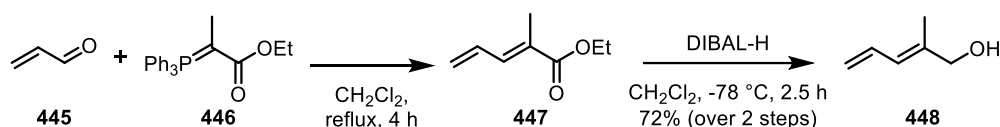


Figure 21: Crystal structure of spirochromanol *cis*-**438**.

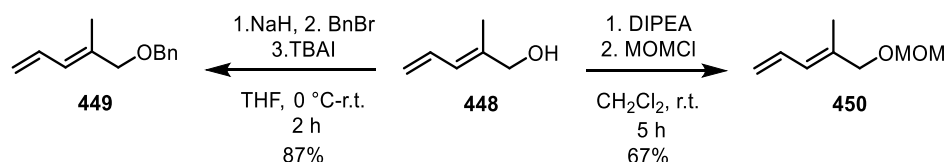
The side chain building blocks **441** and **442** (as free alcohol) are both known from literature.^[193] The diene **448** was prepared according to *Hatakeyama*^[193c] and *Coelho*^[193b] by *Wittig* olefination of acrolein (**445**) followed by DIBAL-H reduction (Scheme 105).



Scheme 105: Preparation of diene alcohol **448** via *Wittig* olefination and subsequent DIBAL-H reduction.

Acrolein (**445**) was freshly distilled and stored over hydroquinone. Deviating from the literature, the very volatile ester **447** was not purified by column chromatography, but the reaction mixture was washed only with *n*-pentane and the precipitating OPPh_3 was filtered off. The alcohol **448**, which was also volatile, was purified using *n*Pe/ Et_2O as eluent on silica and carefully concentrated. This procedure resulted in an improved yield of 72% over two steps.

According to the planned synthetic route (see Scheme 103), the alcohol had to be protected orthogonally to the TBS protecting group (see **443**, Scheme 104). Suitable protecting groups with regard to stability in the intended enyne metathesis/1,4-hydrogenation sequence^[176] were the benzyl and MOM group. Corresponding derivatives **449** and **448** were obtained in good yields under standard conditions (Scheme 106).

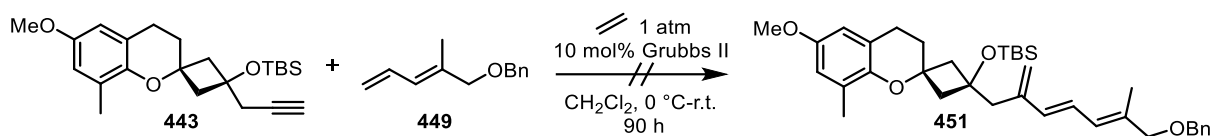


Scheme 106: Benzyl- and MOM-protection of diene alcohol **448**.

A disadvantage of the side chain attachment *via* enyne metathesis is the required large excess of the ene substrate to reach a high product selectivity. Since the conversion of benzyl-

protected alcohols had already shown good results in enyne metathesis,^[176] the benzyl derivative **449** was used in initial test experiments.

Thus the propargyl substituted spirochromanol **443** and the benzyl-protected dienol **449** were reacted under enyne metathesis conditions under an atmosphere of ethene (Scheme 107).



Scheme 107: Enyne metathesis approach employing *O*-Benzyl-(2*E*)-2-methylpenta-2,4-dienol (**449**).

Significant conversion of the alkyne **443** was observed upon reaction with at least 10 equiv. of **449**. After purification of the nonpolar mixture (SiO₂, *c*Hex/EtOAc 200:1), ~70% of the benzyl alcohol **449** were recovered. Further purification by column chromatography on Ag-doped silica and subsequent GC-MS/NMR analysis showed only the formation of the byproduct **452** typical of enyne metathesis involving ethene (Figure 22).

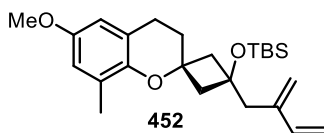


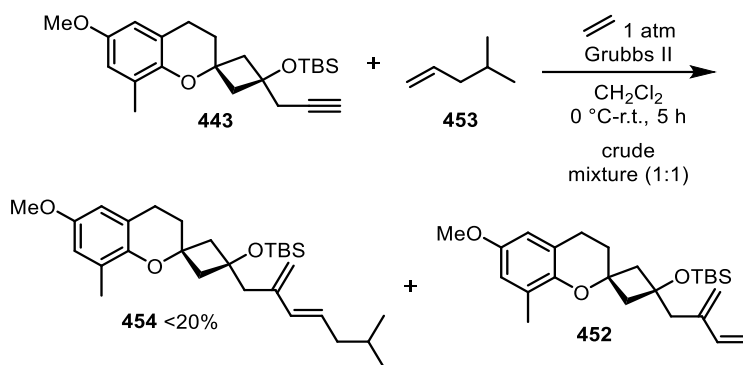
Figure 22: Observed byproduct in the enyne metathesis approach employing **443**.

Ethene, however, is necessary for correct product formation and catalyst regeneration.^[176] To keep the formation of the byproduct low, the ene substrate must be added in high excess as mentioned above (typically at least 10 equiv.).

Even with successful optimization, the subsequent selective 1,4-hydrogenation of the triene **451** would not be trivial. In order to minimize further research efforts and the difficulties in the targeted side-chain introduction, it was decided to investigate only the synthesis of a natural product model containing at least the structural enone feature.

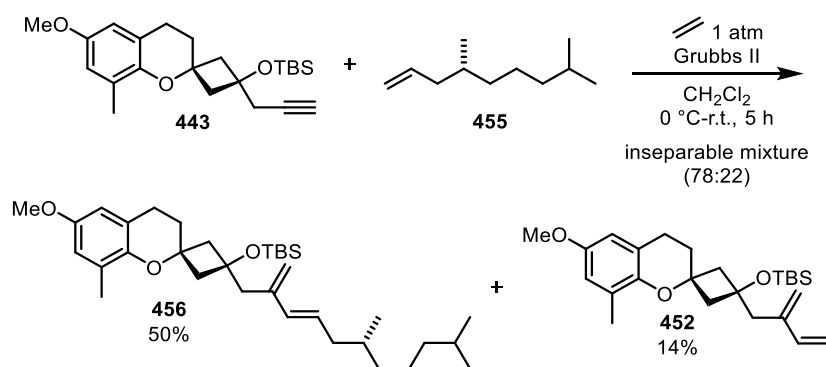
In parallel to the results collected in this work, *Ratsch* was able to show on α -tocopherol-related substrates that after iridium-catalyzed desymmetrization, double bond isomerization of the β,γ -unsaturated ketone to the α,β -enone is possible by triflic acid catalysis (see Scheme 103).^[177] Thus, if the enyne metathesis was successful, this strategy could possibly be further followed.

In a test approach, 4-methyl-1-pentene **453** (12 equiv.) was reacted with alkyne **443** (Scheme 108). After purification, the typical byproduct **452** was again obtained as the major compound besides an impure fraction of desired product **454** (<20%) and byproduct **452** as a 1:1 mixture. All attempts to purify the compounds for distinct analysis were not successful.



Scheme 108: Enyne metathesis approach employing 4-methyl-1-pentene.

Since the employed alkene **453** is highly volatile (boiling point: 54 °C), the non-volatile (*R*)-4,8-dimethylnon-1-ene (**455**), which was already employed for the side chain installation in the α -tocopherol synthesis,^[175] was used in further experiments to prevent evaporation of the alkene starting material. Under the conditions shown in Scheme 109, it was possible to achieve a significant conversion to the desired diene **456**.

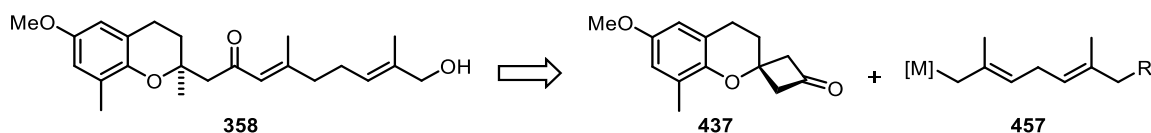


Scheme 109: Enyne metathesis approach employing (*R*)-4,8-dimethylnon-1-ene (**455**).

After multiple chromatography on Ag-doped silica, a mixture (78:22) of the diene **456** and the byproduct **452** was obtained. Compound **456** was fully characterized from the mixture. Completion of this route could not be pursued in this work.

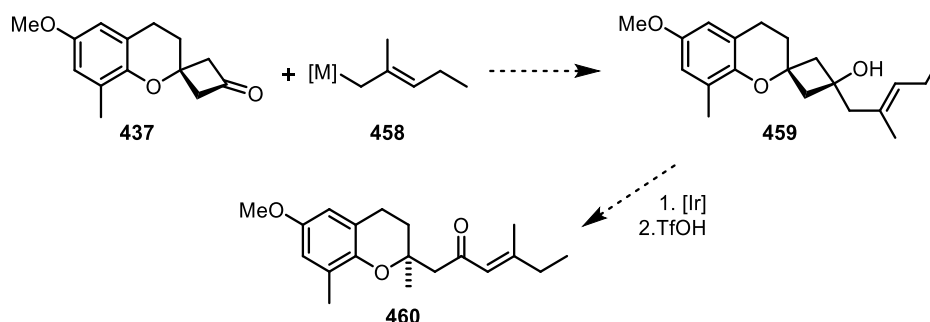
8.2.3. Grignard-type coupling approach

In addition to the routes presented so far, a Grignard-based synthetic pathway was also investigated. Retrosynthetically, natural chromane **358** could possibly be derived from spirochromanone **437** and a metalated side chain of type **457** (Scheme 110). These building blocks might be coupled *via* a Grignard reaction or similar alkylation sequence and subsequently converted by asymmetric Ir-catalyzed cyclobutanol cleavage.



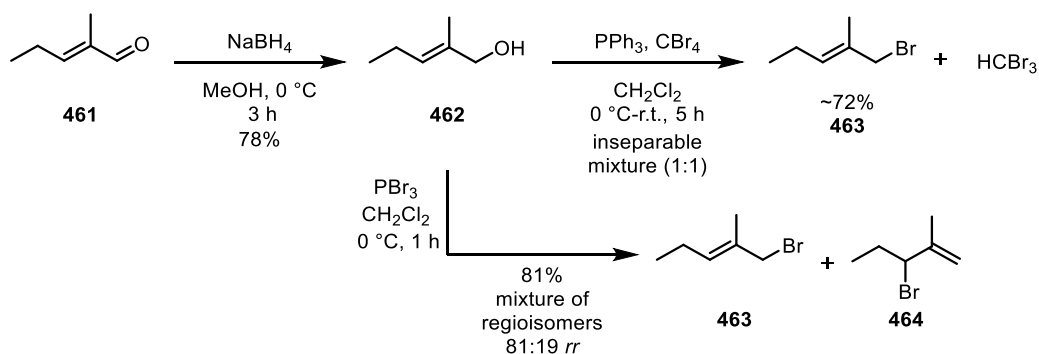
Scheme 110: Retrosynthetic analysis of chromane **358** by a 1,2-addition of metalated species **457**.

In the specific synthetic design for a model chromane of type **460**, with a trisubstituted enone as a structural entity, cyclobutanol **459** might be prepared starting from spirochromanone **437** with a metalated side chain of type **458** (Scheme **460**). Iridium-catalyzed desymmetrization followed by double bond isomerization would yield the desired model.



Scheme 111: Synthetic route for an envisioned natural product model **460**.

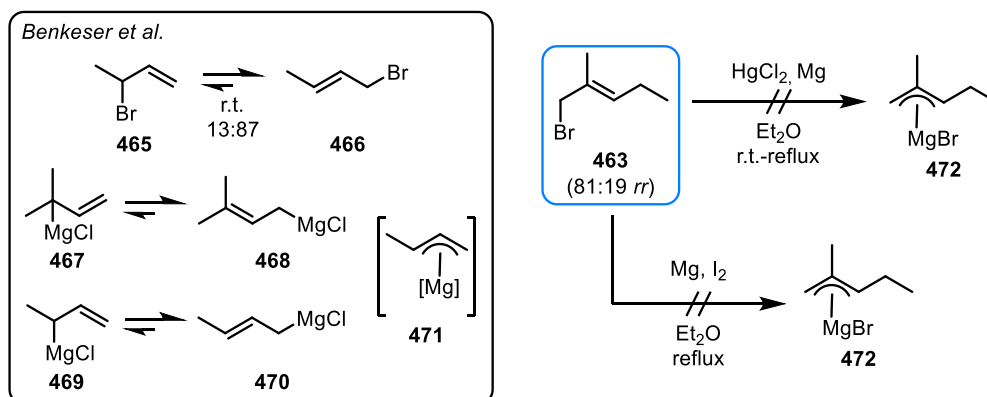
The envisioned side chain building block of type **458** can be derived from (*E*)-1-bromo-2-methyl-2-pentene (**463**). Starting from aldehyde **461**, the alcohol **462** was obtained in good yield by a literature known NaBH_4 reduction (Scheme **112**).^[194] Subsequent conversion in an *Appel*-type reaction led to the desired bromide (**463**).^[195] However, the bromoform byproduct and unknown impurities could not be separated from the impure crude product **463** by either distillation or column chromatography. In a variant carried out with PBr_3 according to Kang *et al.*,^[196] the allyl bromide **463** was obtained, as a mixture of regioisomers (81:19 *rr*) with the branched allyl bromide **464**.



Scheme 112: Synthesis of allyl bromide **463** starting from aldehyde **461**.

Early on, it was shown by *Benkeser* on similar compounds **465/466** that allyl bromides are already at r.t. in an equilibrium with their isomers (Scheme **113**, left).^[197] It was shown that the

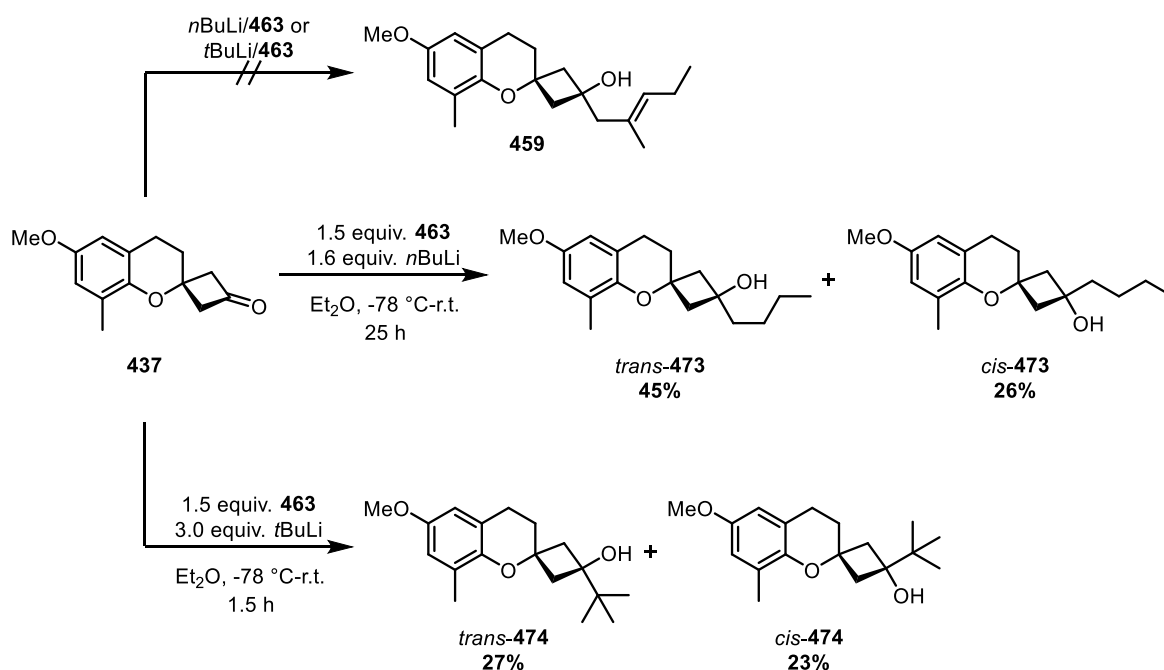
Grignard reagents studied (**467-470**) preferred the linear form (**468/470**) at equilibrium (via an η^3 -allyl complex of type **471**).



Scheme 113: Equilibrium of allyl bromide and *Grignard* reagents described by Benkeser et al. (left),^[197] and performed experiments for *Grignard* preparation (right).

No conversion was achieved in the attempted magnesium insertion to prepare the *Grignard* reagent of type **472**. The reaction mixture was analyzed by iodimetry in each case to check any reagent formation, but no reactivity was observed. Also, when directly adding ketone **369**, both starting materials remained unreacted. Also, no conversion to the *Grignard* compound **472** was observed upon addition of HgCl_2 (Scheme **453**, left).

Scheme **114** summarizes the attempts to react spirochromanone **369** with the analogous lithium species obtained by the bromine/lithium exchange with BuLi . Here, $n\text{BuLi}$ or $t\text{BuLi}$ was added to the allyl bromide **463** (81:19 *rr*) at $-78\text{ }^\circ\text{C}$ and then a solution of starting material **369** was added dropwise. However, instead of the targeted structure **459**, only the undesired 1,2-adducts of $n\text{BuLi}$ *cis/trans*-**473** or $t\text{BuLi}$ *cis/trans*-**474** were formed. Those could be cleanly isolated after purification on silica and fully characterized. These results show that the targeted lithium-halogen exchange with **463** did not occur or only to a minor extent, although at equilibrium the corresponding lithium allyl species should be preferential.^[198]



Scheme 114: Synthetic approach towards chromane **459** and resulting undesired 1,2-addition products.

The undesired chromane adducts were obtained in low to moderate yields (23–45%). The $n\text{BuLi}$ 1,2-addition showed significant *trans*-selectivity ($\sim 2:1$ *dr*), which is also typical for similar *Grignard* additions to chromane systems, possibly due to the pre-coordination of the reagent to the ring oxygen (see Section 8.2.2., Scheme **104**). In contrast, the addition of $t\text{BuLi}$ showed significantly less diastereoselectivity, which can be attributed to the poorer coordination of this sterically more demanding lithium alkyl species.

The structure of the *trans*-configured compound **474** obtained by the $t\text{BuLi}$ 1,2-addition was confirmed by single X-ray crystallography (Figure **23**).



Figure 23: Crystal structure of spirochromanol *trans*-**474**.

The structures of the $n\text{BuLi}$ adducts were clearly differentiated by $^1\text{H},^1\text{H}$ NOESY NMR spectroscopy (Figure **24** and **25**). Compound *trans*-**473** was verified by three dipolar couplings (a, b, c) between the cyclobutanol protons and the CH_2 protons of the chromane ring and the CH_2 protons of the *n*-butyl side chain (Figure **24**).

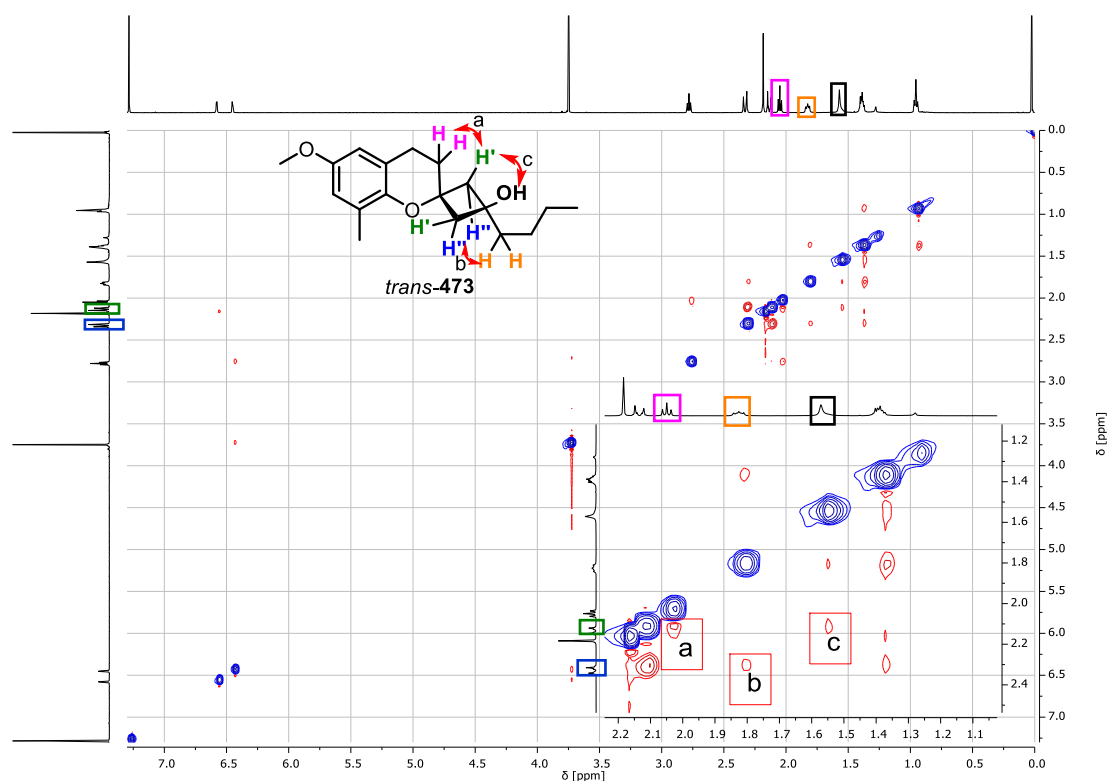


Figure 24: $^1\text{H},^1\text{H}$ NOESY spectrum of *spirochromanol trans-473* in CDCl_3 .

The $^1\text{H},^1\text{H}$ NOESY NMR spectrum of the *cis*-compound **473** confirmed the *cis*-configuration by missing interactions described above for the diastereomeric cyclobutanol *trans-473* and a weak dipolar coupling (d) between the CH_2 protons of the chromane ring and the CH_2 protons of the *n*-butyl side chain (Figure 25).

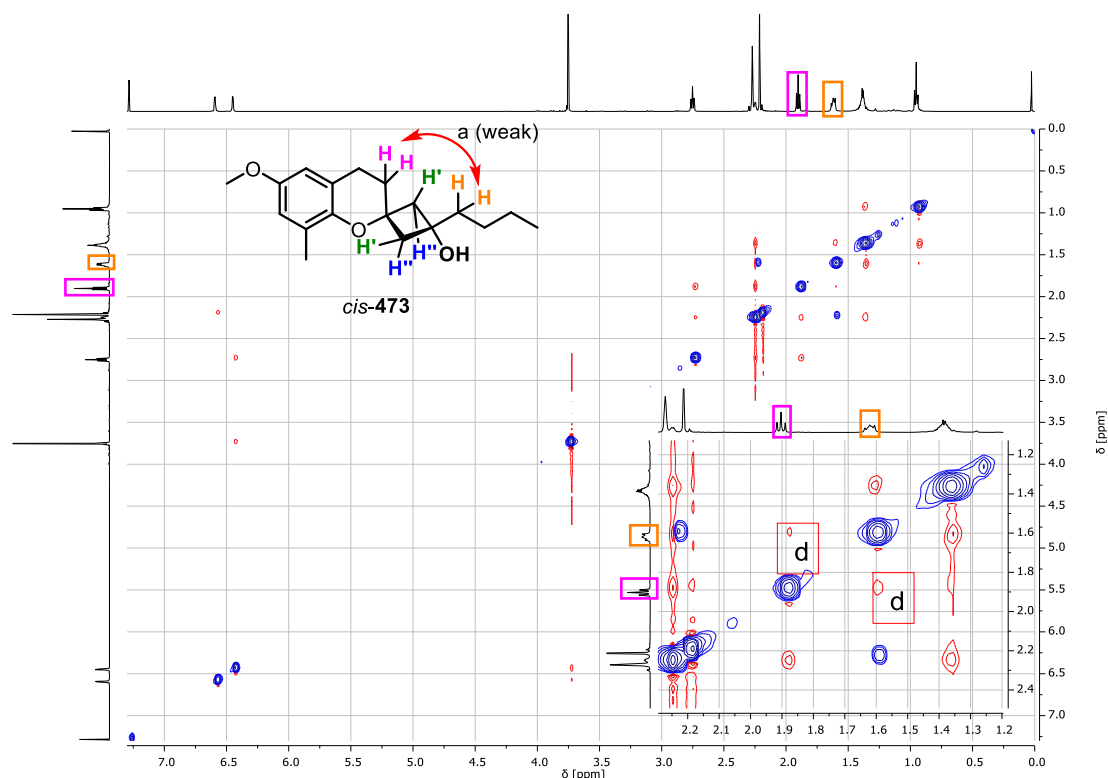
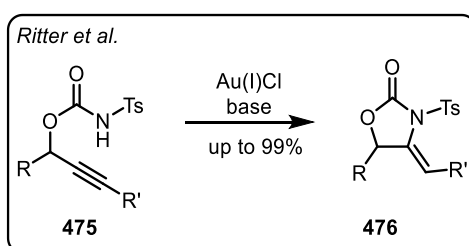


Figure 25: $^1\text{H},^1\text{H}$ NOESY spectrum of *spirochromanol cis-473* in CDCl_3 .

8.3. Prospects of enantioselective Iridium-catalyzed cyclobutanol cleavage

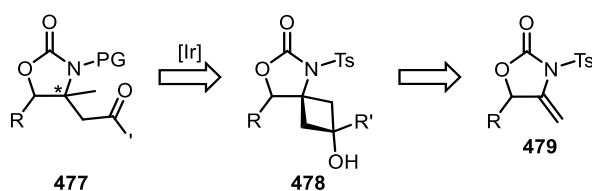
In parallel studies, *Ratsch* showed a moderate to narrow substrate scope for the developed enantioselective iridium-catalyzed cyclobutanol cleavage (see Section 6.2.4.). Nevertheless, it is highly suitable for chromane-substituted and tocopherol-related systems for which the methodology gave excellent selectivities (up to 95% ee for **404**, see Scheme 92) while the rhodium-catalyzed reaction had only racemic outcome.

In an attempt to explore other potentially interesting substrate classes, heterocycles were also considered. In 2006, the *Schmalz* group was able to develop an efficient synthesis for 4-alkylidene oxazolidinones of type **476** through a gold-catalyzed ring closure of alkyne-substituted carbamates of type **475** (Scheme 115).^[199]



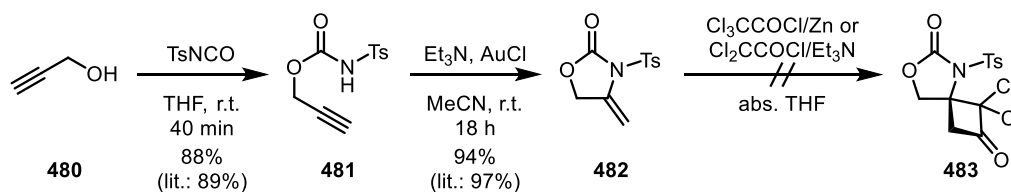
Scheme 115: Preparation of 4-alkylidene oxazolidinones of type **476** through gold-catalysis by *Ritter et al.*^[199]

This readily accessible class of heterocycles could represent interesting precursors for the synthesis of 4,4-disubstituted oxazolidinones of type **477** with an all-carbon quaternary carbon center (Scheme 116). By reacting various 4-methylene oxazolidinones of type **479** by means of a ketene [2+2]-cycloaddition, the cyclobutanol substrates of type **478** could possibly be prepared as promising precursors for the iridium-catalyzed fragmentation.



Scheme 116: Retrosynthetic analysis of 4,4-disubstituted oxazolidinones of type **477**.

First, according to *Ritter et al.*, 4-methylene oxazolidinone **482** was prepared over two steps starting from propargyl alcohol (**480**) and tosyl isocyanate in excellent yield (Scheme 117).



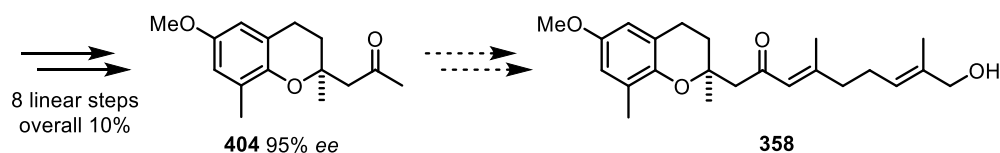
Scheme 117: Synthesis of 4-methylene oxazolidinone **482** and [2+2]-cycloaddition attempts.

However, subsequent [2+2]-cycloaddition attempts using *in situ* generated dichloroketene from either trichloroacetyl chloride/(activated) zinc^[200] or dichloroacetyl chloride/Et₃N^[201] showed no conversion of the starting material **482**.

9. Summary and Outlook

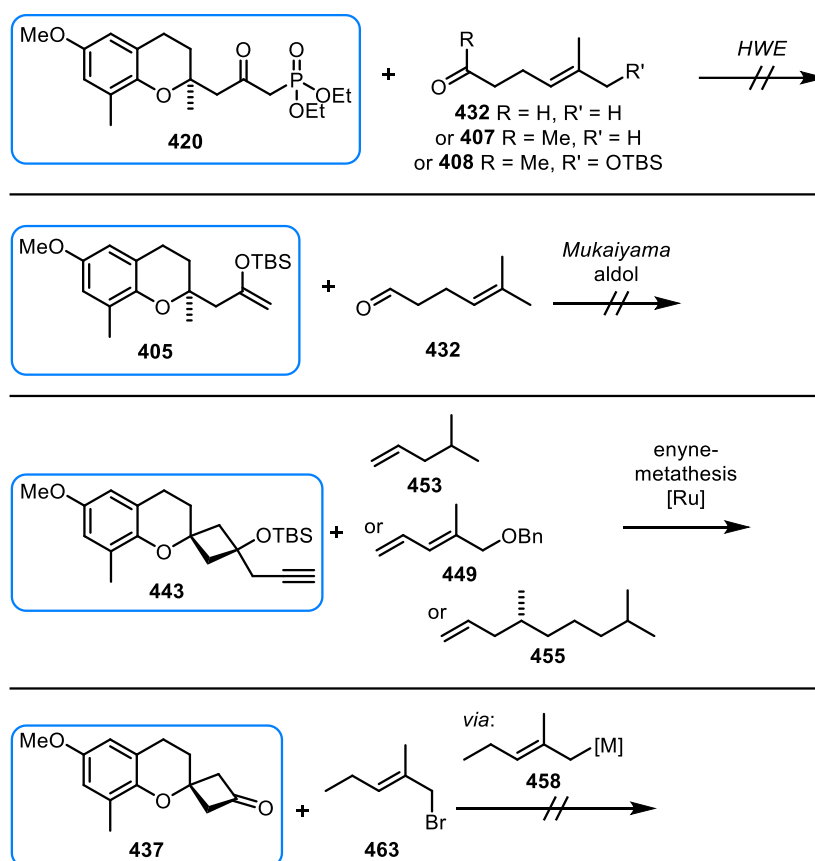
9.1. Summary

In the continuing studies aiming at the total synthesis of the antiplasmodial chromane natural product **358**, this work optimized the linear synthesis of the δ -chromanone **404** via an enantioselective iridium-catalyzed cyclobutanol cleavage and examined possibilities for the remaining side chain prolongation by common synthetic methodologies (Scheme **118**).



Scheme 118: Established δ -chromanone **404** and targeted natural chromane **358**.

Strategies for elaboration of the side chain included *Wittig/HWE* olefination, *Mukaiyama* aldol addition, enyne metathesis, and 1,2-addition (Scheme **119**).



Scheme 119: Overview of attempted side chain coupling reactions.

In the tested conditions for HWE olefination and Mukaiyama aldol addition (employing different synthetic building blocks) only traces of the desired products could be detected. While a *Wittig* olefination starting from the α -bromoketone **406** was completely unsuccessful, an impure product **456** was obtained at least in an enyne metathesis approach with olefin **455**.

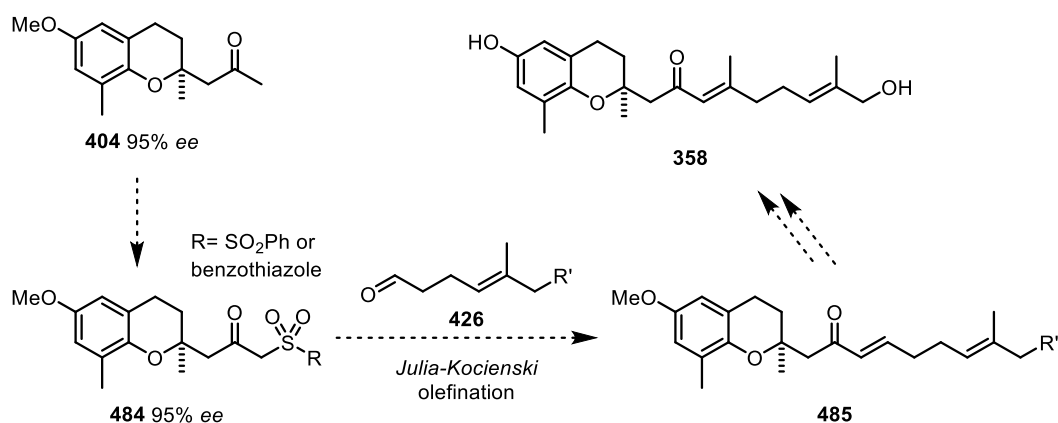
Experiments on the 1,2-addition using a metalated species derived from the allyl bromide **463** were also unsuccessful.

Thus, the completion of the synthesis of the natural product **358** could not be pursued in the frame of this work, as the side chain assembly was found to be nontrivial and the high research efforts of further investigations could no longer be justified in view of the lack of success with the synthetic strategies investigated to that point.

9.2. Outlook

For the completion of the synthesis of **358**, on the one hand, the optimization of the enyne metathesis approach was investigated. However, this route is more suitable for only a simplified analogue of the natural product and would still consist of nontrivial follow-up steps (1,4-hydrogenation, cyclobutanol cleavage and double bond isomerization; see Section 8.2.2.).

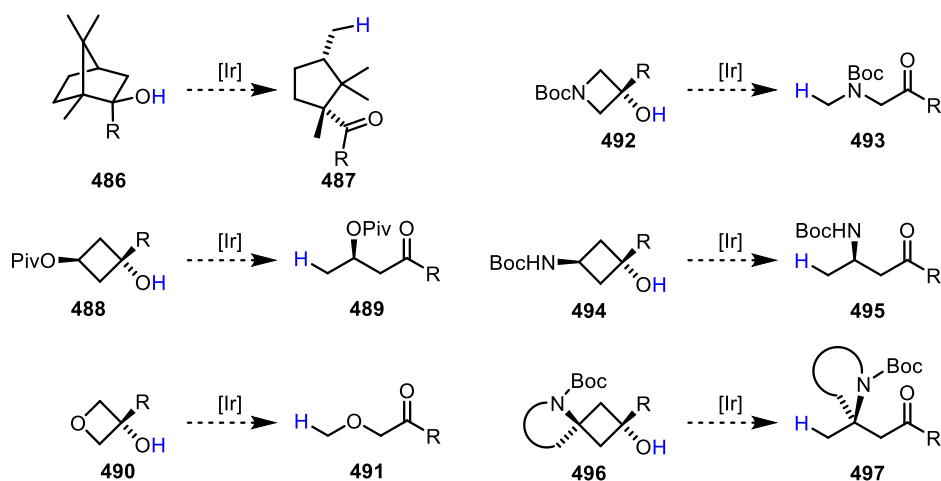
An alternative olefination approach might follow the *Julia-Kocienski* methodology. This particular approach, discovered by *Marc Julia* and further developed by *Philip Kocienski*, has shown singular success in some particularly challenging applications.^[202] Starting from the established chromanone **404**, the corresponding phenylsulfonyl or benzothiazole sulfonyl of type **484** could possibly be derived in one step (Scheme 120).



Scheme 120: Synthetic route plan towards chromane **358** employing a *Julia-Kocienski* olefination.

After the *Julia-Kocienski* olefination with aldehyde **426**, starting from the enone of type **485**, the methyl group could possibly be incorporated into the structure by a 1,4-addition/ α -functionalization/elimination sequence (see Section 8.2.1.3., Scheme **98**).

With regard to iridium-catalyzed desymmetrization/cyclobutanol cleavage, further investigation, especially of heterocycles, could provide conclusive results on the scope of this methodology (Scheme **121**). The tertiary alcohols shown might be derived from the corresponding precursor ketones via a *Grignard*-type reaction with various residues.



Scheme 121: Overview of potential (hetero)cycles with different functional groups as interesting attractive test substrates for the Ir-catalyzed cyclobutanol cleavage.

The camphor-related cyclohexanol **486** represents a good test substrate for the fragmentation of strained bicyclic systems. Cyclobutanol cleavage of oxetanes of type **490** and azetidines of type **492** type would lead to corresponding β -ketomethyl ethers of type **491** and α -(methylamino)ketones of type **493**. In addition, interesting target structures are represented by the α -aminoketones of type **495** or even in cyclized form **497**, the latter derived from the spiro compound of type **496**.

10. Experimental Part

10.1. General information

Reagents and solvents were generally purchased from commercial suppliers (*Sigma Aldrich*, *Acros Organics*, *Merck*, *ABCR*, *Carbolution*, *Alfa Aesar*, *TCI Chemicals*, *Fluka* and *BLDPharm*) and used without further purification unless otherwise stated. Technical solvents CH_2Cl_2 , CHCl_3 , cyclohexane (cHex), Et_2O , EtOAc, MTBE and *n*-pentane (*n*Pe) were distilled. Anhydrous THF and Et_2O were freshly distilled from sodium/benzophenone. Anhydrous CH_2Cl_2 was distilled from NaH. PCl_3 for ligand synthesis was purchased from *Sigma Aldrich* (*ReagentPlus* 99% grade). Organolithium reagents were titrated against *N*-benzylbenzamide. The concentration of *Grignard* reagents was determined by iodimetry.

Air and/or moisture sensitive reactions were performed in flame-dried glassware under argon (99.9997% from *Air Products*). Air-sensitive reagents were weighed in a glovebox under argon atmosphere. Substances were added in an argon counterflow or *via* septum using an argon-flushed syringe. Generally, syringes, NMR tubes and glassware for sensitive reactions were oven-dried at 60 °C. Room temperature corresponds to 25 °C \pm 2 °C. Reactions were monitored by means of TLC or GC-MS. Solvents were removed under reduced pressure using a rotary evaporator attached to a membrane pump (water bath 30 °C to 40 °C). Experiments conducted under microwave irradiation were performed in a *Discover SP* microwave reactor from *CEM* employing 10 mL of or 35 mL of vials. Pressure, temperature and power are specified in the individual experimental procedures. Products were generally purified by flash column chromatography (FCC) using “silica gel, for chromatography” (35 – 70 μm , 60 Å) or “silica gel for column chromatography, ultra-pure” (40 – 60 μm , 60 Å) from *Acros Organics*. Thin layer chromatography (TLC) analysis was performed on *Merck* 60/UV₂₅₄ silica aluminum sheets (0.25 mm layer). Chromatograms were visualized by UV light ($\lambda = 254$ nm) and/or by staining with an aqueous KMnO_4 solution (3.0 g of KMnO_4 , 20 g of K_2CO_3 , 5 mL of NaOH solution ($\omega = 5\%$), 300 mL of H_2O).

Nuclear Magnetic Resonance (NMR) spectra (^1H , ^{13}C , ^{31}P and ^{11}B) were recorded on Bruker spectrometers *Avance* 300 (300 MHz), *Avance* II 300 (300 MHz), *Avance* III 499 (500 MHz), *Avance* III 500 (500 MHz) or *Avance* II⁺ 600 (600 MHz) at 298 K in CDCl_3 (99.8% containing 0.03% TMS) unless otherwise stated. Signal assignments are based both on 1D (^1H , ^{13}C , ^{31}P , ^{11}B) and 2D spectra (^1H , ^1H -COSY, ^1H , ^{13}C -HSQC, ^1H , ^{13}C -HMBC, ^1H , ^1H -NOESY). Chemical shifts (δ) are given in ppm and coupling constants (*J*) in Hz together with the relative integrations and assignments. Atom numbering used in signal assignments does not always correspond to IUPAC nomenclature. Multiplicities are abbreviated as s (singlet), d (doublet), t (triplet), q (quartet), quint (quintet), hept (heptet), M (multiplet), br (broad) and ψ (pseudo). ^1H and ^{13}C spectra were referenced to the residual solvent signals (7.26 ppm and 77.16 ppm) or

TMS as internal standard. ^{31}P spectra were referenced to H_3PO_4 as an external standard. Other solvents were referenced corresponding to *Fulmer et al.*^[203] The spectra processing was done using *MestReNova* 12.0.

Fourier-transform infrared spectra (FT-IR) were measured with a *Perkin Elmer UATR TWO* FTIR-ATR at r.t. Signal intensities are specified as broad (br), weak (w), medium (m) or strong (s). Melting points were determined on a *Büchi B-545* instrument with a heating rate of $5\text{ }^\circ\text{C}/\text{min}$. Optical rotations were measured using an *Anton Paar* polarimeter *MPC 200* with a cell length of 10 cm in CHCl_3 at $20.0\text{ }^\circ\text{C}$.

High resolution mass spectra (HR-MS) with electrospray ionization (ESI) were measured on a *THERMO Scientific LTQ Orbitrap XL* instrument with an *XL-FTMS* analyzer at 70 eV. The spray voltage was set to 3.4 kV, the capillary and tube lens voltage to 3.0 V with $275\text{ }^\circ\text{C}$ capillary temperature. HR-MS spectra with electron impact ionization (EI) were recorded on a *Thermo Scientific Exactive GC* with *Orbitrap* analyzer at 70 eV. Low-resolution GC-MS spectra (EI) were measured on an *Agilent HP 6980* gas chromatograph employing an *MSD 5937 N* mass detector (TIC mode) using an *Optima-1-MS* capillary column (30M x 0.25 mm \varnothing) from *Machery Nagel*. Carrier gas was H_2 with a flow rate of 30 mL/min at 1.2 bar. The standard temperature program was set to $50\text{ }^\circ\text{C}$ (2 min), $50\text{ }^\circ\text{C}$ to $300\text{ }^\circ\text{C}$ (10 min), $320\text{ }^\circ\text{C}$ (5 min).

Enantiomeric analysis by means of gas chromatography at chiral stationary phase (chGC) was performed on an *Agilent Technologies GC System 7850* instrument equipped with an FID detector using H_2 as carrier gas. Column, temperature program, flow rate and retention times are given with the experimental procedures for the individual compounds. Chiral high performance liquid chromatography (chHPLC) was performed at r.t. using *HPLC* systems from *Knauer* (HPLC pump *Wellchrom Maxi Star 1000*, variable wavelength monitor, *Rheodyne 7725i* injection system, two channel degasser *K-5020*) or *Merck Hitachi* (*L-4000 A* UV-detector, *D-6000* interface, *LC-Organizer*, *D-6200A* pump, *Sonorex RK 100*). For reverse phase chromatography a *Knauer* system (HPCL pump *1001*, *K-5004* degasser, *DAD K-2700 Wellchrom*, *K-2701 Wellchrom* lamp) was employed. Details (column, eluent, detection wavelength, flow rate and retention times) are given with the experimental procedures for the individual compounds.

Crystallographic data were collected on a *Bruker NONIUS K-CCD* (Mo-anode, $\lambda = 0.71073\text{ \AA}$) or a *Bruker D8 VENTURE* (K-geometry, Cu-(microfocus)-anode, $\lambda = 1.54178\text{ \AA}$) with a *PHOTON III M14* or *PHOTON 100* detector. All measurements and structure refinements were performed employing *SHELXT* as software. ECD spectra were measured on a *Jasco j-715* CD spectropolarimeter in acetonitrile (10^{-3}M solution).

Further Comments

For the isolated hydrocyanation products (Section 10.2.3.), no measurements of the specific optical rotations were performed due to the usually small amounts of these enantiomeric mixtures. For assignment purposes, only the retention times of the major and minor enantiomers are given within the complete analytics of the compound.

The regioisomeric ratios (r) of the products in the hydrocyanation of homostilbenes (Section 10.2.3.5.) were determined by ^1H NMR analysis and 2D NMR ($^1\text{H}, ^{13}\text{C}$ -HSQC, $^1\text{H}, ^{13}\text{C}$ -HMBC, $^1\text{H}, ^1\text{H}$ -COSY) for accurate discrimination. The regioisomer signal used for ratio determination is appropriately labeled in the ^1H NMR.

Some substrates (Section 10.3.1) have been described in detail in the preceding master thesis.^[179] For these, identity and purity were confirmed by GC-MS and ^1H NMR spectroscopy (including $^1\text{H}, ^1\text{H}$ -COSY, $^1\text{H}, ^{13}\text{C}$ -HSQC, $^1\text{H}, ^{13}\text{C}$ -HMBC spectra). For completeness, some data sets were adopted for analytical properties.

10.2. Experimental procedures towards the enantioselective Ni-catalyzed hydrocyanation employing phosphine-phosphite ligands

10.2.1. Synthesis of phosphine-phosphite ligands

10.2.1.1. General procedures

10.2.1.1.1. General procedure GP1 for the preparation of TADDOLs

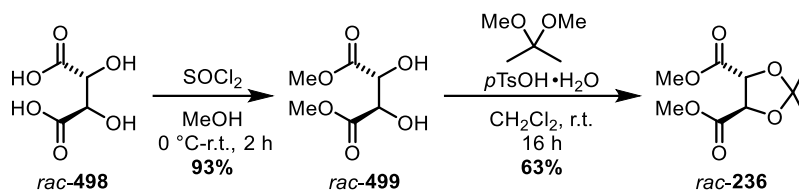
The synthesis was performed according to a procedure of *Falk et al.*^[42] Under an atmosphere of argon, a three-necked round-bottomed flask equipped with reflux condenser and dropping funnel was charged with Mg turnings (4.8 equiv.) and an I₂ crystal and the mixture was heated under vigorous stirring. Then a solution of the corresponding bromoarene (4.4 equiv.) in anhydrous THF (0.7 M) was slowly added over 30 min keeping the reaction at reflux. The suspension was heated at reflux for 4 h and stirred for 16-20 h at r.t. At 0 °C, a solution of (4*R*,5*R*)-dimethyl-2,2-dimethyl-1,3-dioxolane-4,5-dicarboxylate (**236**) (1.0 equiv.) in anhydrous THF (0.5 M) was added to the *Grignard* reagent. The reaction mixture was heated at reflux for 4-6 h (unless otherwise stated) and sat. NH₄Cl solution and H₂O were added. The aqueous phase was extracted with MTBE, the combined organic phases were dried with Na₂SO₄ and concentrated under reduced pressure. Crude material was purified by recrystallization or FCC (SiO₂, *c*Hex/EtOAc) for purification.

10.2.1.1.2. General procedure GP2 for the preparation of phosphine-phosphite ligands

The synthesis was performed according to a procedure of *Falk et al.*^[42] Under an atmosphere of argon, a *Schlenk* flask was charged with a solution of the corresponding phosphine borane complex (1.0 equiv.) and freshly sublimated DABCO (8.0 equiv.) in anhydrous CH₂Cl₂ (0.13 M) and stirred for 15-20 min at r.t. At 0 °C, a solution of PCl₃ (1.2 equiv.) in anhydrous CH₂Cl₂ (1.8 M) was added (dropwise) over 30 min by means of a syringe pump. The reaction was stirred for 30 min at 0 °C and 3-4 h at r.t. Then a solution of TADDOL (1.5 equiv.) in anhydrous CH₂Cl₂ (0.21 M) was added at 0 °C and stirred for 30 min before the ice bath was removed. The suspension was stirred for 20 h at r.t. Subsequently, it was filtered through an ultra-pure silica pad with *c*Hex/EtOAc 1:1 and concentrated under reduced pressure. Crude material was purified by FCC (ultra-pure SiO₂, *c*Hex/EtOAc) for purification.

10.2.1.2. Synthesis of the building block for racemic ligands

10.2.1.2.1. Synthesis of *rac*-(4*R*,5*R*)-dimethyl-2,2-dimethyl-1,3-dioxolane-4,5-dicarboxylate (**236**)



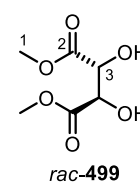
The synthesis was performed based on a modified procedure of *Dindaroğlu et al.*^[96c] A 250 mL round-bottomed flask was charged with a solution of 10.0 g of *rac*-tartaric acid (**rac-498**) (66.7 mmol, 1.0 equiv.) in 100 mL of MeOH. At 0 °C, 25.3 mL of SOCl₂ (41.5 g, 349 mmol 5.2 equiv.) were added (dropwise). The reaction mixture was stirred for 2 h at r.t. before the solvent was removed under reduced pressure. The residue was re-dissolved in 20 mL of H₂O and extracted with Et₂O (8 x 30 mL). The combined organic phases were dried with MgSO₄ and concentrated under reduced pressure to yield 11.0 g of methyl ester **rac-499** as a colorless solid (61.9 mmol, 93%, Lit.:^[204] 98%).

Under an atmosphere of argon, a 250 mL *Schlenk* flask was charged with a solution of 11.0 g of methyl ester **rac-499** (61.6 mmol, 1.0 equiv.) and 3.54 g of *p*TsOH·H₂O (20.5 mmol, 30 mol%) in 130 mL of anhydrous CH₂Cl₂. Then 37.7 mL of 2,2-dimethoxypropane (32.0 g, 308 mmol, 5.0 equiv.) were added (dropwise) and the reaction mixture was stirred at r.t. for 16 h. The solvent was removed under reduced pressure. The residue was re-suspended in 40 mL of H₂O and extracted with Et₂O (3 x 40 mL). The combined organic phases were dried with MgSO₄ and concentrated under reduced pressure. Purification of the crude material by FCC (SiO₂, *c*Hex/EtOAc 5:1) gave the product **rac-236** as an orange liquid (38.6 mmol, 63%, Lit.:^[204] 85%).

M (C₆H₁₀O₆) = 178.14 g/mol.

M.p. 88 - 90 °C.

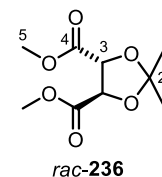
¹H NMR (300 MHz, CDCl₃) δ [ppm] = 4.57 (d, ³*J* = 6.8 Hz, 2 H, H-3), 3.87 (s, 6 H, H-1), 3.25 (brd, ³*J* = 6.8 Hz, 2 H, OH).



M (C₉H₁₄O₆) = 218.21 g/mol.

TLC (SiO₂, *c*Hex/EtOAc 10:1) R_f = 0.14.

¹H NMR (500 MHz, CDCl₃) δ [ppm] = 4.78 (s, 2 H, H-3), 3.79 (s, 3 H, H-5), 1.46 (s, 3 H, H-1).



^{13}C NMR (75 MHz, CDCl_3) δ [ppm] = 170.1 (C-4), 113.9 (C-2), 77.0 (C-3), 52.8 (C-5), 26.3 (C-1).

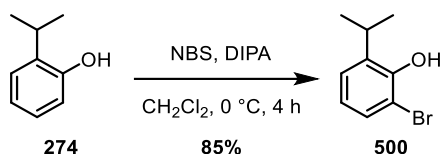
GC-MS (70 eV) m/z ([%]): 203 (100, $[\text{M}^+ - \text{CH}_3]$), 159 (28), 141 (22), 133 (10), 113 (10), 101 (23), 85 (36), 73 (51), 59 (59).

FTIR-ATR ν [cm^{-1}] = 2994 (w), 2958 (w), 2852 (s), 1740 (s), 1438 (m), 1385 (m), 1375 (m), 1348 (w), 1253 (m), 1206 (s), 1162 (m), 1106 (s), 1012 (m), 996 (m), 937 (w), 920 (w), 856 (m), 831 (w), 812 (w), 779 (w), 749 (w), 704 (w), 578 (w), 514 (w).

The analytical data are in agreement with the literature.^[205]

10.2.1.3. Synthesis of bromophenols

10.2.1.3.1. Synthesis of 2-bromo-6-isopropylphenol (**500**)



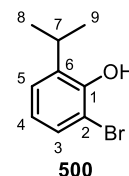
The synthesis was performed according to a procedure of *Albat et al.*^[206] A 500 mL round-bottomed flask equipped with a CaCl_2 drying tube was charged with a solution of 6.00 g of 2-isopropylphenol (**274**) (44.1 mmol, 1.0 equiv.) in 200 mL of CH_2Cl_2 and 10.0 mL of diisopropylamine (7.17 g, 70.9 mmol, 1.6 equiv.) were added after cooling the mixture to 0 °C. At this temperature, 7.08 g of NBS (39.8 mmol, 0.90 equiv.) was then added in small portions over a 2 h period. Stirring was continued for 4 h at 0 °C before 180 mL of 2M H_2SO_4 were added. The aqueous phase was extracted with CH_2Cl_2 (3 x 150 mL). The combined organic phases were dried with Na_2SO_4 and concentrated under reduced pressure to give an orange liquid. Purification by FCC (SiO_2 , *c*Hex) gave 8.03 g of **500** as a colorless oil (37.4 mmol, 85%) containing traces (<4 mol%) of a dibrominated byproduct.

M ($\text{C}_9\text{H}_{11}\text{OBr}$) = 215.09 g/mol.

TLC (SiO_2 , *c*Hex/EtOAc 10:1) R_f = 0.58.

^1H NMR (500 MHz, CDCl_3) δ [ppm] = 7.30 (dd, $^3J = 7.8$ Hz, $^4J = 1.6$ Hz, 1 H, H-3), 7.15 (dd, $^3J = 7.8$ Hz, $^4J = 1.6$ Hz, 1 H, H-5), 6.78 (t, $^3J = 7.8$ Hz, 1 H, H-4), 5.59 (s, 1 H, OH), 3.34 (hept, $^3J = 6.8$ Hz, 1 H, H-7), 1.25 (d, $^3J = 6.8$ Hz, 6 H, H-8/9).

^{13}C NMR (75 MHz, CDCl_3) δ [ppm] = 149.5 (C-1), 136.5 (C-6), 129.2 (C-3), 126.1 (C-5), 121.6 (C-4), 110.8 (C-2), 28.2 (C-7), 22.5 (C-8/9).

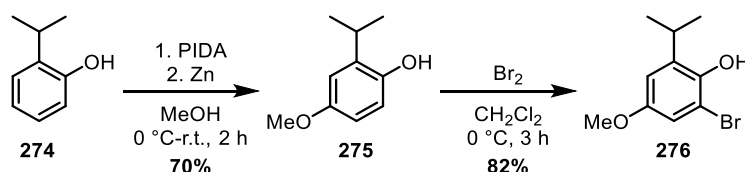


GC-MS (70 eV) m/z ([%]): 214 (30, $[M^+ - H]$), 199 (89), 120 (100), 91 (30), 77 (14), 65 (19), 51 (14).

FTIR-ATR ν [cm^{-1}] = 3511 (m), 2962 (m), 2869 (w), 1473 (m), 1440 (s), 1327 (s), 1084 (w), 1236 (s), 1206 (s), 1174 (s), 1151 (s), 1114 (m), 1048 (m), 898 (m), 828 (s), 771 (s), 733 (s), 622 (s), 553 (m).

The analytical data are in agreement with the literature.^[206]

10.2.1.3.2. Synthesis of 2-bromo-4-methoxy-6-isopropylphenol (**276**)

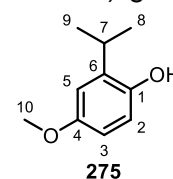


The synthesis was performed based on a modified procedure of *Amant et al.*^[136] A 500 mL round-bottomed flask was charged with a solution of 4.36 g of 2-isopropylphenol (**274**) (32.0 mmol, 1.0 equiv.) in 280 mL of MeOH. At 0 °C, a solution of 21.6 g of PIDA (67.2 mmol, 2.1 equiv.) in 40 mL of MeOH was added (dropwise) over 5 min. The reaction was stirred for 30 min at r.t. and 3.16 g of Zn (48.0 mmol, 1.5 equiv.) were added. After 1 h, the reaction slurry was concentrated under reduced pressure and re-dissolved in 200 mL of MTBE. The organic phase was washed with 20 mL of 1M HCl before the aqueous phase was re-extracted with 30 mL of MTBE and the combined organic phases were dried with Na_2SO_4 . Concentration under reduced pressure gave the crude material which was purified by FCC (SiO_2 , *c*Hex/EtOAc 6:1) to obtain 3.73 g of 2-isopropyl-4-methoxyphenol (**275**) as a peach-colored oil (22.4 mmol, 70%; lit.:^[136] 38%).

The next step was performed based on a modified procedure of *Krische* and coworkers.^[207] Under an atmosphere of argon, a 250 mL *Schlenk* flask was charged with a solution of 2.50 g of **275** (15.0 mmol, 1.0 equiv.) in 75 mL of anhydrous CH_2Cl_2 . At 0 °C, a solution of 0.77 mL of bromine (15 mmol, 1.0 equiv.) in 60 mL of anhydrous CH_2Cl_2 was slowly added over 3 h by means of a syringe pump. After addition, the reaction mixture was stirred for 5 min and 100 mL of sat. NaHCO_3 solution were added. The organic phase was separated and washed with 100 mL of brine. Then it was dried with Na_2SO_4 and concentrated under reduced pressure. Purification of the crude material by FCC (SiO_2 , *c*Hex/EtOAc 30:1) gave 3.02 g of **276** as an orange oil (12.3 mmol, 82%; Lit.:^[207] 67%).

M ($\text{C}_{10}\text{H}_{14}\text{O}_2$) = 166.22 g/mol.

TLC (SiO_2 , *c*Hex/EtOAc 6:1) R_f = 0.47.



¹H NMR (500 MHz, CDCl₃) δ [ppm] = 6.77 (d, ⁴J = 3.0 Hz, 1 H, H-5), 6.69 (d, ³J = 8.6 Hz, 1 H, H-2), 6.61 (dd, ³J = 8.6 Hz, ⁴J = 3.0 Hz, 1 H, H-3), 4.39 (m, 1 H, OH), 3.77 (s, 3 H, H-10), 3.18 (hept, ³J = 6.8 Hz, 1 H, H-7), 1.24 (d, ³J = 6.8 Hz, 6 H, H-8/9).

¹³C NMR (75 MHz, CDCl₃) δ [ppm] = 153.9 (C-4), 146.9 (C-1), 136.1 (C-6), 115.9 (C-2), 112.9 (C-5), 111.0 (C-3), 55.9 (C-10), 27.3 (C-7), 22.6 (C-8/9).

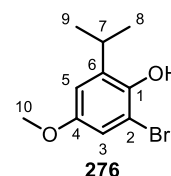
GC-MS (70 eV) m/z ([%]): 166 (58, [M⁺]), 151 (100), 136 (17), 77 (12), 91 (11).

FTIR-ATR ν [cm⁻¹] = 3401 (br), 3038 (w), 2961 (m), 2870 (w), 2834 (w), 1707 (w), 1608 (w), 1597 (w), 1506 (s), 1463 (w), 1447 (w), 1430 (s), 1382 (w), 1362 (w), 1339 (w), 1285 (s), 1200 (s), 1180 (s), 1173 (s), 1146 (m), 1112 (w), 1091 (m), 1072 (m), 1033 (s), 927 (w), 872 (m), 854 (w), 802 (m), 766 (m), 707 (m), 694 (m), 619 (w), 568 (w), 550 (w).

The analytical data are in agreement with the literature.^[136]

M (C₁₀H₁₃BrO₂) = 245.12 g/mol.

TLC (SiO₂, cHex/EtOAc 30:1) R_f = 0.48.



¹H NMR (500 MHz, CDCl₃) δ [ppm] = 6.84 (d, ⁴J = 2.9 Hz, 1 H, H-5), 6.74 (d, ⁴J = 2.9 Hz, 1 H, H-3), 5.21 (s, 1 H, OH), 3.75 (s, 3 H, H-10), 3.29 (hept, ³J = 6.9 Hz, 1 H, H-7), 1.22 (d, ³J = 6.9 Hz, 6 H, H-8/9).

¹³C NMR (126 MHz, CDCl₃) δ [ppm] = 153.7 (C-4), 143.9 (C-1), 137.1 (C-6), 113.31 (C-3), 113.29 (C-5), 110.1 (C-2), 56.0 (C-10), 28.4 (C-7), 22.5 (C-8/9).

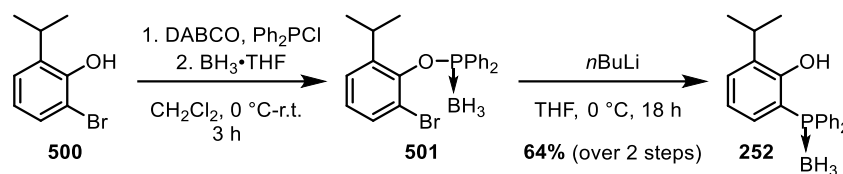
GC-MS (70 eV) m/z ([%]): 244 (49, [M⁺]), 231 (100), 77 (65), 150 (57), 51 (38).

FTIR-ATR ν [cm⁻¹] = 3517 (br), 2961 (m), 2937 (w), 2906 (w), 2869 (w), 2833 (w), 1606 (w), 1576 (m), 1473 (s), 1425 (s), 1382 (w), 1363 (w), 1330 (m), 1292 (s), 1220 (m), 1197 (s), 1175 (s), 1156 (s), 1112 (w), 1092 (w), 1038 (s), 958 (w), 938 (w), 877 (m), 849 (m), 823 (m), 798 (w), 764 (s), 754 (s), 732 (m), 611 (w), 565 (w), 537 (w).

The analytical data are in agreement with the literature.^[207]

10.2.1.4. Synthesis phosphine borane complexes

10.2.1.4.1. Synthesis of 2-(diphenylphosphino)-6-isopropylphenol borane complex (**252**)



The synthesis was performed according to a procedure of Dindaroğlu *et al.*^[96c] Under an atmosphere of argon, a 500 mL *Schlenk* flask was charged with a solution of 7.47 g of bromophenol **500** (34.7 mmol, 1.0 equiv.), 4.71 g of DABCO (42.0 mmol, 1.2 equiv.) in 110 mL of anhydrous CH_2Cl_2 . After stirring for 30 min at r.t., the clear solution was cooled to 0 °C before 7.50 mL of freshly distilled Ph_2PCl (9.15 g, 41.5 mmol, 1.2 equiv.) were slowly added by means of a syringe pump over 30 min. After stirring for 2 h at r.t., the resulting cloudy mixture was cooled to 0 °C and 70 mL of $\text{BH}_3\cdot\text{THF}$ (1.0M in THF, 70 mmol, 2.0 equiv.) were added over 10 min *via* syringe. The suspension was stirred for an additional 2 h at r.t. before 150 mL of H_2O were slowly added. The aqueous phase was extracted with MTBE (4 x 150 mL). The combined organic phases were dried with Na_2SO_4 and concentrated under reduced pressure to yield 17.1 g of crude phosphinite **501** as a colorless wax.

This material was then re-dissolved under an atmosphere of argon in 180 mL of anhydrous THF in a 500 mL *Schlenk* flask. The solution was then cooled to 0 °C before 22 mL of *n*BuLi (2.4M in *n*Hex, 53 mmol, 1.5 equiv.) were slowly added (dropwise) over a period of 35 min. The resulting white suspension was stirred for 2 h at 0 °C and 16 h at r.t. After addition of 100 mL of H_2O the mixture was extracted with MTBE (3 x 150 mL). The combined organic phases were dried with Na_2SO_4 and concentrated under reduced pressure. The crude product (orange oil) was purified by FCC (SiO_2 , *c*Hex/EtOAc 30:1) and the obtained solid recrystallized from EtOAc (5 mL) to afford 7.42 g of phosphine **252** as a colorless solid (22.2 mmol, 64%).

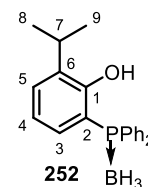
M ($\text{C}_{21}\text{H}_{24}\text{BOP}$) = 334.17 g/mol.

TLC (SiO_2 , *c*Hex/EtOAc 30:1) R_f = 0.53.

M.p. 89 - 94 °C.

$^1\text{H NMR}$ (500 MHz, CDCl_3) δ [ppm] = 7.64 (s, 1 H, OH), 7.57 – 7.50 (m, 6 H, H_{Ph}), 7.48 – 7.42 (m, 4 H, H_{Ph}), 7.37 (dd, $^3J = 7.7$ Hz, $^4J = 1.3$ Hz, 1 H, H-5), 6.86 (ψ td, $^3J = 7.7$ Hz, $^4J_{\text{P}} = 1.5$ Hz, 1 H, H-4), 6.72 (ddd, $^3J_{\text{P}} = 10.3$ Hz, $^3J = 7.7$ Hz, $^4J = 1.3$ Hz, 1 H, H-3), 3.37 (hept, $^3J = 6.9$ Hz, 1 H, H-7), 1.23 (d, $^3J = 6.9$ Hz, 1 H, H-8/9).

$^{13}\text{C NMR}$ (75 MHz, CDCl_3) δ [ppm] = 157.9 (d, $J_{\text{P}} = 9.4$ Hz, C-1), 137.9 (d, $J_{\text{P}} = 5.6$ Hz, C-6), 133.1 (d, $J_{\text{P}} = 9.9$ Hz, C_{Ph}), 131.8 (d, $J_{\text{P}} = 2.5$ Hz, C-3), 131.7 (d, $J_{\text{P}} = 3.1$ Hz, C_{Ph}), 130.6 (d, J_{P}



= 2.0 Hz, C-5), 129.0 (d, $J = 10.6$ Hz, C_{Ph}), 128.8 (d, $J_P = 3.5$ Hz, C_{Ph}), 120.6 (d, $J_P = 8.4$ Hz, C-4), 111.2 (d, $J_P = 58.8$ Hz, C-2), 26.9 (C-7), 22.6 (C-8/9).

^{11}B NMR (96 MHz, $CDCl_3$) δ [ppm] = -36.49 (d, $J = 55.7$ Hz).

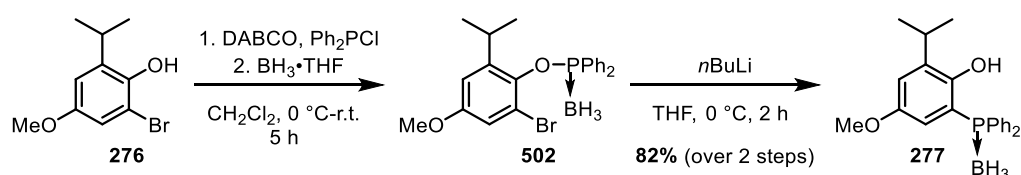
^{31}P NMR (121 MHz, $CDCl_3$) δ [ppm] = 12.58.

GC-MS (70 eV) m/z ([%]): 320 (100, $[M^+-BH_3]$), 305 (72), 292 (48), 183 (31), 165 (11), 121 (18), 78 (73).

FTIR-ATR ν [cm^{-1}] = 3404 (w), 2966 (w), 2398 (w), 2369 (w), 2325 (w), 1469 (w), 1430 (s), 1333 (m), 1219 (s), 1183 (m), 1157 (m), 1132 (m), 1105 (s), 1072 (s), 1049 (m), 999 (m), 830 (m), 759 (m), 741 (s), 692 (s), 649 (m), 608 (s), 562 (m), 495 (s).

The analytical data are in agreement with the literature.^[96c]

10.2.1.4.2. Synthesis of 2-(diphenylphosphino)-4-methoxy-6-isopropylphenol borane complex (277)



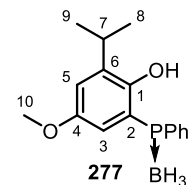
The synthesis was performed based on a modified procedure of Dindaroğlu *et al.*^[96c] Under an atmosphere of argon, a 100 mL *Schlenk* flask was charged with a solution of 1.10 g of bromophenol **276** (4.49 mmol, 1.0 equiv.) and 604 mg of DABCO (5.38 mmol, 1.2 equiv.) in 9 mL of anhydrous CH_2Cl_2 . The solution was stirred for 10 min at r.t. At 0 °C, the clear solution was slowly treated with 0.89 mL of freshly distilled Ph_2PCl (1.1 g, 4.9 mmol, 1.1 equiv.) by means of a syringe pump over 30 min. The cloudy reaction mixture was stirred for 4 h at r.t. and at 0 °C 9.0 mL of $BH_3 \cdot THF$ (1.0M in THF, 9.0 mmol, 2.0 equiv.) were added (dropwise) over 15 min. The suspension was stirred for an additional 1 h at r.t., then 5 mL of H_2O were added. The aqueous phase was extracted with MTBE (3 x 10 mL). The combined organic phases were washed with 20 mL of brine before they were dried with $MgSO_4$ and concentrated under reduced pressure to obtain the crude material **502**. This procedure was repeated and the crude material combined.

This material (9.00 mmol) was then re-dissolved under an atmosphere of argon in 10 mL of anhydrous THF in a 100 mL *Schlenk* flask. At 0 °C 2.7 mL of $nBuLi$ (2.5M in $nHex$, 6.7 mmol, 1.5 equiv.) were slowly added (dropwise) over 30 min by means of a syringe pump. Then the white suspension was stirred for 2 h at 0 °C and 30 mL of H_2O were added. This reaction cascade was repeated at the same scale and both aqueous phases were combined

for the further work-up. The combined aqueous phases were extracted with MTBE (2 x 30 mL). The combined organic phases were dried with MgSO_4 and concentrated under reduced pressure. Purification by recrystallization from *c*Hex/EtOAc (100:1) and FCC (SiO_2 , *c*Hex/EtOAc 50:1) gave 2.69 g of phosphine **277** as a colorless wax (7.39 mmol, 82%).

M ($\text{C}_{22}\text{H}_{26}\text{BO}_2\text{P}$) = 364.23 g/mol.

TLC (SiO_2 , *c*Hex/EtOAc 50:1) R_f = 0.12.



$^1\text{H NMR}$ (300 MHz, CDCl_3) δ [ppm] = 7.64 – 7.50 (m, 6 H, H_{Ph}), 7.50 – 7.39 (m, 4 H, H_{Ph}), 7.16 (d, $^4J_{\text{P}} = 1.8$ Hz, 1 H, *OH*), 6.98 (d, $^4J = 3.0$ Hz, 1 H, H-5), 6.23 (dd, $^4J_{\text{P}} = 11.4$ Hz, $^4J = 3.0$ Hz, 1 H, H-3), 3.58 (s, 3 H, H-10), 3.36 (hept, $^3J = 6.8$ Hz, 1 H, H-7), 1.23 (d, $^3J = 6.8$ Hz, 6 H, H-8/9).

$^{13}\text{C NMR}$ (75 MHz, CDCl_3) δ [ppm] = 153.1 (d, $J_{\text{P}} = 10.2$ Hz, C-4), 151.9 (d, $J_{\text{P}} = 8.7$ Hz, C-1), 139.5 (d, $J_{\text{P}} = 6.7$ Hz, C-6), 133.1 (d, $J_{\text{P}} = 9.8$ Hz, C_{Ph}), 131.7 (d, $J_{\text{P}} = 2.5$ Hz, C_{Ph}), 129.1 (d, $J_{\text{P}} = 10.6$ Hz, C_{Ph}), 128.2 (d, $J_{\text{P}} = 61.5$ Hz, C_{Ph}), 117.4 (d, $J_{\text{P}} = 2.2$ Hz, C-5), 115.3 (d, $J_{\text{P}} = 4.2$ Hz, C-3), 111.9 (d, $J_{\text{P}} = 58.1$ Hz, C-2), 55.6 (C-10), 27.2 (C-7), 22.6 (C-8/9).

$^{31}\text{P NMR}$ (121 MHz, CDCl_3) δ [ppm] = 13.93 (d, $J = 62.2$ Hz, PR_3).

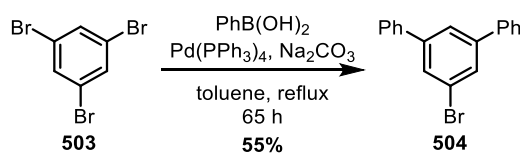
GC-MS (70 eV) m/z ([%]): 350 (100, $[\text{M}^+ - \text{BH}_3]$), 335 (63), 229 (19), 183 (23), 152 (17), 108 (21), 78 (61), 51 (31).

HR-ESI-MS m/z calculated $[\text{C}_{22}\text{H}_{26}\text{BO}_2\text{P} + \text{Na}^+]$: 387.16557; found: 387.16553.

FTIR-ATR ν [cm^{-1}] = 3395 (m), 3079 (w), 3047 (w), 3003 (w), 2957 (w), 2933 (w), 2933 (w), 2862 (w), 2832 (w), 2395 (w), 2372 (w), 2363 (w), 2324 (w), 1963 (w), 1912 (w), 1827 (w), 1735 (w), 1588 (w), 1487 (w), 1457 (s), 1434 (s), 1422 (s), 1382 (w), 1361 (w), 1340 (m), 1311 (w), 1290 (w), 1251 (m), 1208 (s), 1167 (m), 1107 (m), 1072 (s), 1045 (s), 1027 (m), 998 (m), 943 (m), 892 (w), 865 (m), 820 (w), 772 (m), 757 (m), 736 (s), 688 (s), 627 (s), 609 (m), 569 (w), 547 (w), 524 (w).

10.2.1.5. Synthesis of phenyl bromides

10.2.1.5.1. Synthesis of 1-bromo-3,5-diphenylbenzene (**504**)



The synthesis was performed according to a procedure of *Matsumoto et al.*^[208] Under an atmosphere of argon, a 250 mL two-necked round-bottomed flask equipped with a reflux condenser was charged with 3.00 g of 1,2,3-tribromobenzene (**503**) (9.53 mmol, 1.0 equiv.) and 335 mg of Pd(PPh₃)₄ (0.290 mmol, 3.0 mol%). A solution of 2.48 g of phenylboronic acid (20.3 mmol, 2.1 equiv.) in 40 mL of anhydrous toluene and 30 mL of 1M Na₂CO₃ was added. The reaction mixture was heated at reflux for 65 h and subsequently, the solvent was removed under reduced pressure. The brownish residue was re-dissolved in 100 mL of EtOAc/H₂O (1:1). The phases were separated and the aqueous phase was extracted with EtOAc (3 x 50 mL). The combined organic phases were dried with Na₂SO₄ and concentrated under reduced pressure. Purification by FCC (SiO₂, cHex) gave 1.62 g of 1-bromo-*meta*-terphenyl (**504**) (5.24 mmol, 55%; Lit.^[208] 64%). As a byproduct 0.83 g of the triphenylated species was isolated (2.72 mmol, 29%).

M (C₁₈H₁₃Br) = 309.21 g/mol.

TLC (SiO₂, cHex) R_f = 0.38.

M.p. 110 - 111 °C.

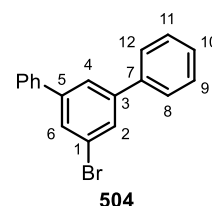
¹H NMR (500 MHz, CDCl₃) δ [ppm] = 7.72 (ψs, 3 H, H-2/4/6), 7.65 – 7.59 (m, 4 H, H-8/12), 7.52 – 7.44 (m, 4 H, H-9/11), 7.44 – 7.38 (m, 2 H, H-10).

¹³C NMR (75 MHz, CDCl₃) δ [ppm] = 143.8 (C-3/5), 139.9 (C-7), 129.1 (C-2/6/9/11), 128.1 (C-10), 127.3 (C-8/12), 125.0 (C-4), 123.4 (C-1).

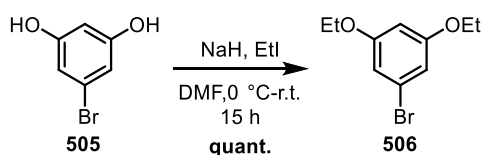
GC-MS (70 eV) m/z ([%]): 308 (69, [M⁺]), 230 (100), 152 (14), 77 (8), 51 (8).

FTIR-ATR ν [cm⁻¹] = 3060 (w), 2989 (w), 1595 (m), 1558 (s), 1497 (m), 1423 (m), 1309 (w), 1078 (w), 1046 (w), 1028 (w), 1001 (w), 870 (s), 767 (s), 750 (vs), 692 (vs), 642 (s), 611 (s), 552 (s).

The analytical data are in agreement with the literature.^[208]



10.2.1.5.2. Synthesis of 1-bromo-3,5-diethoxybenzene (506)



The synthesis was performed according to a procedure of *Yanagi et al.*^[209] Under an atmosphere of argon, a 250 mL *Schlenk* flask was charged with a solution of 1.98 g of NaH (dispersion in paraffin oil, $\omega = 60\%$, 1.19 g, 49.6 mmol, 3.0 equiv.) in 50 mL of dry DMF. At 0 °C a solution of 3.12 g of 5-bromoresorcinol (**505**) (16.5 mmol, 1.0 equiv.) in 14 mL of dry DMF was added (dropwise) over 5 min and the suspension was stirred for 1 h. Then 4.38 mL of ethyl iodide (8.50 g, 54.5 mmol, 3.3 equiv.) were added (dropwise) over 5 min. The resulting reaction mixture was stirred for 15 h before 60 mL of H₂O were added. The aqueous phase was extracted with *c*Hex/EtOAc (1:1, 3 x 70 mL) and the combined organic phase washed with 50 mL of brine and dried with Na₂SO₄. Concentration under reduced pressure gave a pale yellow liquid. Purification by FCC (SiO₂, *c*Hex/EtOAc 30:1) gave 4.05 g of **506** as a pale yellow liquid (16.5 mmol, quant.; Lit.^[209] not given).

M (C₁₀H₁₃BrO₂) = 245.12 g/mol.

TLC (SiO₂, *c*Hex/EtOAc 30:1) R_f = 0.26.

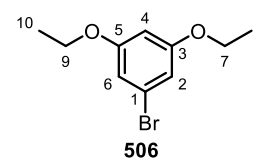
¹H NMR (500 MHz, CDCl₃) δ [ppm] = 6.62 (d, ³J = 2.2 Hz, 2 H, H-2/6), 6.35 (t, ³J = 2.2 Hz, 1 H, H-2), 3.95 (q, ³J = 7.0 Hz, 4 H, H-7/9), 1.37 (t, ³J = 7.0 Hz, 6 H, H-8/10).

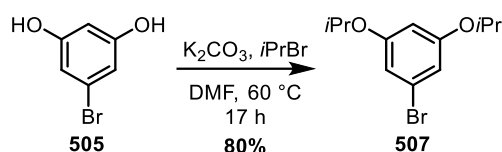
¹³C NMR (126 MHz, CDCl₃) δ [ppm] = 160.4 (C-3/5), 122.7 (C-1), 110.2 (C-2/6), 100.6 (C-4), 63.7 (C-7/9), 14.7 (C-8/10).

GC-MS (70 eV) m/z ([%]): 244 (62, [M⁺]), 216 (27), 188 (100), 172 (12), 158 (9), 137 (31), 109 (17), 91 (8), 69 (24), 51 (5).

FTIR-ATR ν [cm⁻¹] = 3091 (w), 298 (m), 2931 (m), 2881 (m), 1987 (w), 1574 (s), 1439 (m), 1390 (m), 1327 (m), 1297 (m), 1277 (m), 1244 (w), 1166 (vs), 1113 (m), 1046 (s), 988 (m), 923 (m), 815 (m), 674 (m), 583 (w).

The analytical data are in agreement with the literature.^[209]

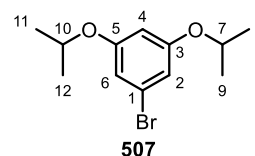


10.2.1.5.3. Synthesis of 1-bromo-3,5-isopropoxybenzene (**507**)

The synthesis was performed according to a procedure of *Procter* and coworkers.^[210] Under an atmosphere of argon, a 50 mL *Schlenk* flask was charged with a solution of 871 mg of 5-bromoresorcinol (**505**) (4.61 mmol, 1.0 equiv.) in 20 mL of dry DMF. Subsequently, 2.77 g of K_2CO_3 (20.0 mmol, 4.4 equiv.) and 1.80 mL of 2-bromopropane (2.36 g, 19.2 mmol, 4.2 equiv.) were added. The reaction mixture was heated to 60 °C for 17 h before 60 mL of H_2O were added. The aqueous phase was extracted with EtOAc (3 x 50 mL). The combined organic phases were dried with Na_2SO_4 and concentrated under reduced pressure to obtain a brown crude material. Purification by FCC (SiO_2 , cHex/EtOAc 10:1) gave 1.01 g of **507** as a pale brown oil (3.69 mmol, 80%; Lit.:^[210] 85%).

M ($\text{C}_{12}\text{H}_{17}\text{BrO}_2$) = 273.17 g/mol.

TLC (SiO_2 , cHex/EtOAc 10:1) R_f = 0.66.



$^1\text{H NMR}$ (500 MHz, CDCl_3) δ [ppm] = 6.62 (d, 3J = 2.2 Hz, 2 H, H-2/6), 6.34 (t, 3J = 2.2 Hz, 1 H, H-4), 4.47 (hept, 3J = 6.1 Hz, 2 H, H-7/10), 1.32 (d, 3J = 6.1 Hz, 12 H, H-8/9/11/12).

$^{13}\text{C NMR}$ (75 MHz, CDCl_3) δ [ppm] = 159.7 (C-3/5), 123.0 (C-1), 111.5 (C-2/6), 103.1 (C-4), 70.5 (C-7/10), 22.1 (C-8/9/11/12).

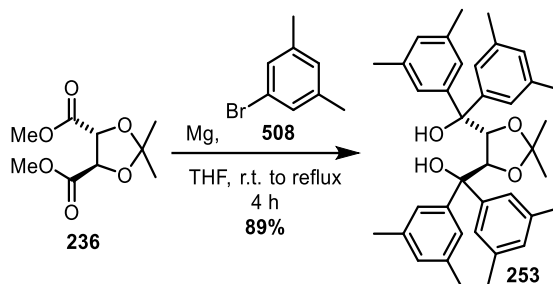
GC-MS (70 eV) m/z ([%]): 272 (23, $[\text{M}^+]$), 232 (8), 188 (100), 161 (6), 110 (7), 69 (6), 43 (7),

FTIR-ATR ν [cm^{-1}] = 2977 (m), 2934 (w), 2872 (w), 1740 (w), 1594 (s), 1570 (s), 1438 (m), 1384 (m), 1373 (m), 1351 (w), 1331 (w), 1293 (m), 1244 (w), 1182 (m), 1153 (s), 1136 (m), 1111 (s), 1032 (m), 990 (w), 955 (m), 907 (w), 863 (m), 834 (m), 811 (m), 679 (m), 619 (w), 589 (w), 546 (w).

The analytical data are in agreement with the literature.^[210]

10.2.1.6. Synthesis of TADDOLs

10.2.1.6.1. Synthesis of 3,5-dimethyl-TADDOL 253



According to the general procedure **GP1**, 3.45 g of Mg turnings (142 mmol, 4.8 equiv.) and 24.1 g of bromoarene **508** (130 mmol, 4.4 equiv.) were reacted with 6.44 g of ester **236** (29.5 mmol, 1.0 equiv.). Repeated recrystallization from MTBE (1 mL/g) and purification of the concentrated mother liquor by FCC (cHex/EtOAc 10:1) gave 15.2 g of 3,5-dimethyl-TADDOL **253** as a colorless foam (26.3 mmol, 89%; lit.:^[42] 75%).

M (C₃₉H₄₆O₄) = 578.79 g/mol.

TLC (SiO₂, cHex/EtOAc 10:1) R_f = 0.45.

M.p. 94 - 98 °C.

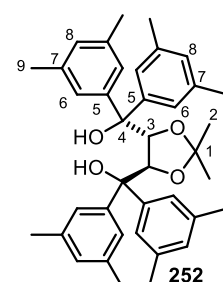
¹H NMR (500 MHz, CDCl₃) δ [ppm] = 7.15 (s, 4 H, H-6), 6.94 (s, 6 H, H-6/8), 6.86 (s, 2 H, H-8), 4.57 (s, 2 H, H-3), 3.75 (s, 2 H, OH), 2.32 (s, 12 H, H-9), 2.24 (s, 12 H, H-9), 1.08 (s, 6 H, H-2).

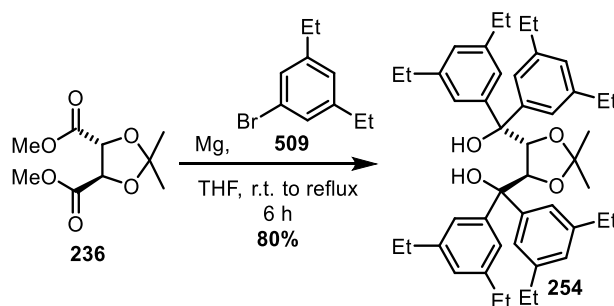
¹³C NMR (75 MHz, CDCl₃) δ [ppm] = 146.1 (C-5), 142.9 (C-5), 137.5 (C-7), 136.5 (C-7), 129.3 (C-8), 128.8 (C-8), 126.5 (C-6), 125.5 (C-6), 109.4 (C-1), 81.3 (C-3), 78.1 (C-4), 27.1 (C-2), 21.7 (C-9).

FTIR-ATR ν [cm⁻¹] = 3284 (w), 2984 (w), 2915 (w), 2884 (w), 1603 (w), 1454 (w), 1370 (w), 1237 (m), 1222 (w), 1160 (m), 1063 (s), 1038 (m), 891 (w), 849 (vs), 754 (s), 734 (s), 724 (s), 692 (w), 601 (w), 504 (w).

Specific rotation (c = 0.505 g/100 mL, CHCl₃, [α]_D^T): [α]₃₆₅^{20.0} = - 153.9 °, [α]₄₃₆^{20.0} = - 80.9 °, [α]₅₄₆^{20.0} = - 49.4 °, [α]₅₇₉^{20.0} = - 44.4 °, [α]₅₈₉^{20.0} = - 44.6 °.

The analytical data are in agreement with the literature.^[42]



10.2.1.6.2. Synthesis of 3,5-diethyl-TADDOL **254**

According to the general procedure **GP1**, 537 mg of Mg turnings (22.1 mmol, 4.9 equiv.) and 4.27 g of bromoarene **509** (20.0 mmol, 4.4 equiv.) were reacted with 988 mg of ester **236** (4.52 mmol, 1.0 equiv.). Purification by FCC (cHex/EtOAc 20:1) gave 2.49 g of 3,5-diethyl-TADDOL **254** as a colorless resin 3.61 mmol, 80%).

M (C₄₇H₆₂O₄) = 691.01 g/mol.

TLC (SiO₂, cHex/EtOAc 10:1) R_f = 0.49.

¹H NMR (500 MHz, CDCl₃) δ [ppm] = 7.23 (d, ⁴J = 1.6 Hz, 4 H, H-6), 7.04 (d, ⁴J = 1.6 Hz, 4 H, H-6), 7.00 (t, ⁴J = 1.6 Hz, 2 H, H-8), 6.94 (t, ⁴J = 1.6 Hz, 2 H, H-8), 4.70 (s, 2 H, H-3), 3.83 (s, 2 H, OH), 2.65 (q, ³J = 7.6 Hz, 8 H, H-9), 2.58 (q, ³J = 7.6 Hz, 8 H, H-9), 1.25 (t, ³J = 7.6 Hz, 12 H, H-10), 1.17 (t, ³J = 7.6 Hz, 12 H, H-10), 0.98 (s, 6 H, H-2).

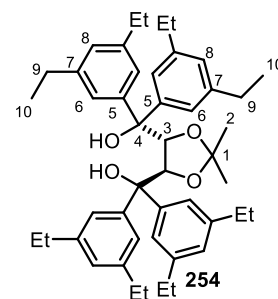
¹³C NMR (126 MHz, CDCl₃) δ [ppm] = 146.1 (C-5), 143.8 (C-7), 143.0 (C-7), 142.8 (C-5), 126.7 (C-8), 126.3 (C-8), 126.0 (C-6), 124.8 (C-6), 109.4 (C-1), 81.1 (C-3), 78.4 (C-4), 29.2 (C-9), 29.1 (C-9), 27.2 (C-2), 16.1 (C-10), 15.6 (C-10).

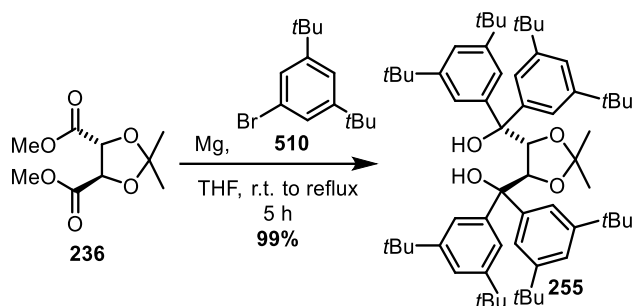
HR-ESI-MS m/z calculated [C₄₇H₆₂O₄+Na⁺]: 713.4540316; found: 713.45462.

FTIR-ATR ν [cm⁻¹] = 3279 (br), 2963 (s), 2932 (m), 2873 (m), 1980 (w), 1770 (w), 1600 (m), 1457 (s), 1370 (m), 1319 (w), 1239 (m), 1217 (w), 1163 (m), 1064 (s), 1001 (w), 968 (w), 943 (w), 871 (s), 850 (w), 815 (w), 784 (w), 745 (m), 704 (m), 673 (w), 659 (w), 627 (w), 509 (w).

Specific rotation (c = 0.625 g/100 mL, CHCl₃, [α]_D^T): [α]₃₆₅^{20.0} = + 68.8 °, [α]₄₃₆^{20.0} = + 32.8 °, [α]₅₄₆^{20.0} = + 15.4 °, [α]₅₇₉^{20.0} = + 13.0 °, [α]₅₈₉^{20.0} = + 12.2 °.

The analytical data are in agreement with the literature.^[211]



10.2.1.6.3. Synthesis of 3,5-di-*tert*-butyl-TADDOL **255**

According to the general procedure **GP1**, 960 mg of Mg turnings (39.5 mmol, 7.3 equiv.) and 9.69 g of bromoarene **510** (36.0 mmol, 6.6 equiv.) were reacted with 1.18 g of ester **236** (5.45 mmol, 1.0 equiv.). Purification by repeated FCC (cHex/EtOAc 15:1 and 50:1) gave 4.92 g of 3,5-di-*tert*-butyl-TADDOL **255** as a pale yellow foam (5.37 mmol, 99%).

M (C₆₃H₉₄O₄) = 915.44 g/mol.

TLC (SiO₂, cHex/EtOAc 50:1) R_f = 0.31.

M.p. 158 - 161 °C.

¹H NMR (500 MHz, CDCl₃) δ [ppm] = 7.42 (d, ⁴J = 1.8 Hz, 4 H, H-6), 7.31 (t, ⁴J = 1.8 Hz, 2 H, H-8), 7.25 (t, ⁴J = 1.8 Hz, 2 H, H-8), 7.18 (d, ⁴J = 1.8 Hz, 4 H, H-6), 4.70 (s, 2 H, H-3), 3.69 (s, 2 H, OH), 1.30 (s, 36 H, H-10), 1.20 (s, 36 H, H-10), 0.93 (s, 6 H, H-2).

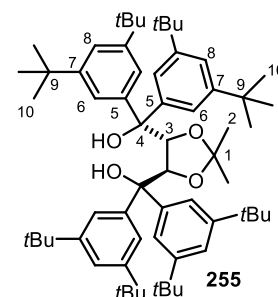
¹³C NMR (126 MHz, CDCl₃) δ [ppm] = 149.8 (C-7), 149.2 (C-7), 145.3 (C-5), 141.9 (C-5), 123.1 (C-6), 122.3 (C-6), 121.0 (C-8), 120.6 (C-8), 108.4 (C-1), 82.0 (C-3), 79.0 (C-4), 35.1 (C-9), 35.0 (C-9), 31.8 (C-10), 31.6 (C-10), 27.0 (C-2).

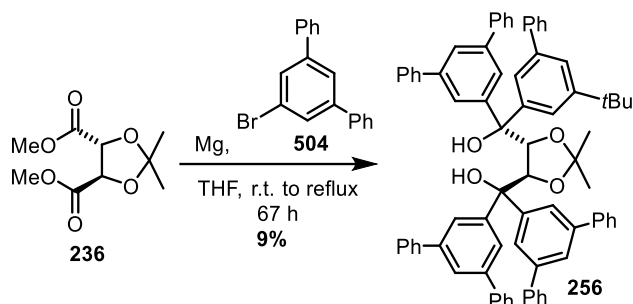
HR-ESI-MS m/z calculated [C₆₃H₉₄O₄+Na⁺]: 937.7044325; found: 937.70339.

FTIR-ATR ν [cm⁻¹] = 3284 (br), 2954 (vs), 2904 (m), 2867 (m), 1597 (s), 1477 (s), 1451 (s), 1393 (m), 1379 (w), 1362 (s), 1248 (vs), 1201 (s), 1047 (s), 877 (s), 879 (s), 863 (m), 826 (m), 795 (w), 735 (s), 711 (m), 511 (w).

Specific rotation (c = 0.500 g/100 mL, CHCl₃, [α]_λ^T): [α]₃₆₅^{20.0} = - 511.3 °, [α]₄₃₆^{20.0} = + 54.0 °, [α]₅₄₆^{20.0} = + 27.8 °, [α]₅₇₉^{20.0} = + 22.6 °, [α]₅₈₉^{20.0} = + 19.8 °.

The analytical data are in agreement with the literature.^[212]



10.2.1.6.4. Synthesis of 3,5-diphenyl-TADDOL **256**

According to the general procedure **GP1**, 247 mg of Mg turnings (10.2 mmol, 4.9 equiv.) and 2.83 g of bromoarene **504** (9.15 mmol, 4.4 equiv.) were reacted with 452 mg of ester **236** (2.08 mmol, 1.0 equiv.). Purification by repeated FCC (cHex/EtOAc 5:1) gave 196 mg of 3,5-diphenyl-TADDOL **256** as a pale yellow foam (0.18 mmol, 9%).

M ($C_{79}H_{62}O_4$) = 1075.36 g/mol.

TLC (SiO_2 , cHex/EtOAc 5:1) R_f = 0.32.

M.p. 125 - 128 °C.

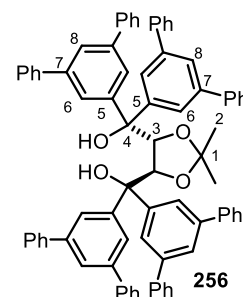
1H NMR (500 MHz, $CDCl_3$) δ [ppm] = 8.14 (d, 4J = 1.7 Hz, 4 H, H-6), 7.96 (t, 4J = 1.7 Hz, 2 H, H-8), 7.93 (d, 4J = 1.8 Hz, 4 H, H-6), 7.84 – 7.77 (m, 10 H, H-8, H_{Ph}), 7.66 – 7.62 (m, 8 H, H_{Ph}), 7.55 – 7.37 (m, 24 H, H_{Ph}), 5.25 (s, 2 H, H-3), 4.90 (brs, 2 H, OH), 1.29 (s, 6 H, H-2).

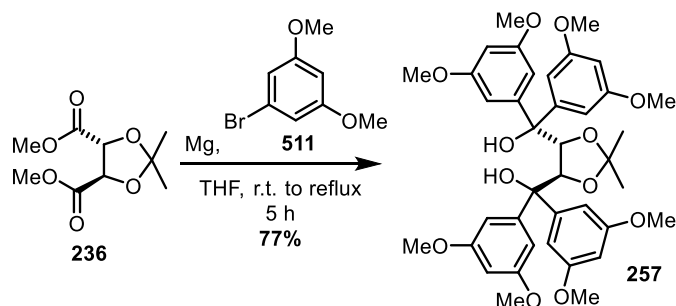
^{13}C NMR (126 MHz, $CDCl_3$) δ [ppm] = 146.9 (C-5), 143.8 (C-5), 141.6 (C_{Ph}), 141.20 (C-7), 141.17 (C-7), 140.9 (C_{Ph}), 128.9 (C_{Ph}), 128.8 (C_{Ph}), 127.5 (C_{Ph}), 127.44 (C_{Ph}), 127.36 (C_{Ph}), 127.35 (C_{Ph}), 126.5 (C-6), 125.8 (C-8), 125.6 (C-6), 125.5 (C-8), 110.1 (C-1), 81.8 (C-3), 78.7 (C-4), 27.5 (C-2).

FTIR-ATR ν [cm^{-1}] = 3296 (br), 3059 (w), 3034 (w), 2988 (w), 2924 (m), 2852 (w), 2051 (w), 1980 (w), 1947 (w), 1883 (w), 1739 (w), 1595 (m), 1576 (w), 1498 (w), 1452 (w), 1428 (w), 1413 (w), 1246 (w), 1380 (w), 1371 (w), 1246 (w), 1310 (w), 1241 (w), 1220 (w), 1164 (m), 1076 (s), 1050 (s), 967 (w), 917 (w), 879 (m), 808 (w), 758 (s), 741 (s), 727 (w), 695 (s), 640 (w), 614 (m), 557 (w).

Specific rotation (c = 0.550 g/100 mL, $CHCl_3$, $[\alpha]_D^{20}$): $[\alpha]_{365}^{20.0} = -2245.9^\circ$, $[\alpha]_{436}^{20.0} = +111.2^\circ$, $[\alpha]_{546}^{20.0} = +51.7^\circ$, $[\alpha]_{579}^{20.0} = +43.9^\circ$, $[\alpha]_{589}^{20.0} = +41.6^\circ$.

The analytical data are in agreement with the literature.^[213]



10.2.1.6.5. Synthesis of 3,5-dimethoxy-TADDOL **257**

According to the general procedure **GP1**, 636 mg of Mg turnings (26.2 mmol, 4.8 equiv.) and 5.20 g of bromoarene **511** (24.0 mmol, 4.4 equiv.) were reacted with 1.19 g of ester **236** (5.45 mmol, 1.0 equiv.). Purification by FCC (cHex/EtOAc 15:1) gave 2.96 g of 3,5-dimethoxy-TADDOL **257** as a pale yellow foam (4.19 mmol, 77%).

M ($C_{39}H_{46}O_{12}$) = 706.79 g/mol.

TLC (SiO_2 , cHex/EtOAc 2:1) R_f = 0.40.

M.p. 89 - 92 °C.

1H NMR (300 MHz, $CDCl_3$) δ [ppm] = 6.75 (d, 4J = 2.3 Hz, 4 H, H-6), 6.54 (d, 4J = 1.8 Hz, 4 H, H-6)*, 6.38 (t, 4J = 1.8 Hz, 2 H, H-8), 6.30 (t, 4J = 1.8 Hz, 2 H, H-8), 4.56 (s, 2 H, H-3), 3.84 (s, 2 H, OH), 3.75 (s, 12 H, H-9), 3.69 (s, 12 H, H-9), 1.17 (s, 6 H, H-2).

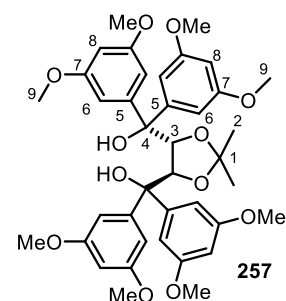
^{13}C NMR (75 MHz, $CDCl_3$) δ [ppm] = 160.4 (C-7), 160.0 (C-7), 147.6 (C-5), 145.2 (C-5), 109.3 (C-1), 106.8 (C-6), 106.2 (C-6), 99.5 (C-8), 99.2 (C-8), 81.7 (C-3), 78.2 (C-4), 55.5 (C-9), 55.4 (C-9), 27.5 (C-2).

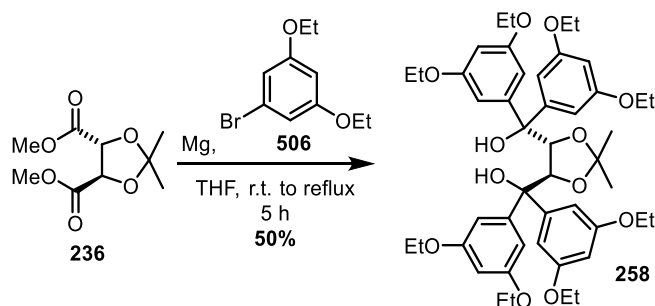
HR-ESI-MS m/z calculated [$C_{39}H_{46}O_{12}+Na^+$]: 729.2881479; found: 729.28693.

FTIR-ATR ν [cm^{-1}] = 3324 (w), 2937 (w), 2836 (w), 1591 (s), 1455 (s), 1424 (s), 1371 (w), 1348 (m), 1308 (m), 1242 (w), 1203 (s), 1150 (vs), 1048 (s), 924 (m), 894 (w), 839 (m), 751 (m), 735 (s), 689 (w), 541 (w), 506 (w).

Specific rotation (c = 0.500 g/100 mL, $CHCl_3$, $[\alpha]_D^{20}$): $[\alpha]_{365}^{20.0} = -5.4^\circ$, $[\alpha]_{436}^{20.0} = -17.2^\circ$, $[\alpha]_{546}^{20.0} = -15.5^\circ$, $[\alpha]_{579}^{20.0} = -14.5^\circ$, $[\alpha]_{589}^{20.0} = -15.5^\circ$.

The analytical data are in agreement with the literature.^[214]



10.2.1.6.6. Synthesis of 3,5-diethoxy-TADDOL **258**

According to the general procedure **GP1**, 437 mg of Mg turnings (18.0 mmol, 4.9 equiv.) and 3.92 g of bromoarene **506** (16.0 mmol, 4.4 equiv.) were reacted with 797 mg of ester **236** (3.65 mmol, 1.0 equiv.). Purification by FCC (cHex/EtOAc 9:1) gave 1.49 g of 3,5-diethoxy-TADDOL **258** as a colorless foam (1.82 mmol, 50%).

M (C₄₇H₆₂O₁₂) = 818.42 g/mol.

TLC (SiO₂, cHex/EtOAc 4:1) R_f = 0.31.

M.p. 77 - 79 °C.

¹H NMR (600 MHz, CDCl₃) δ [ppm] = 6.70 (d, ⁴J = 1.6 Hz, 4 H, H-6), 6.51 (d, ⁴J = 1.6 Hz, 4 H, H-6), 6.37 (t, ⁴J = 1.6 Hz, 2 H, H-8), 6.28 (t, ⁴J = 1.6 Hz, 2 H, H-8), 4.58 (s, 2 H, H-3), 3.91 (q, ³J = 6.9 Hz, 8 H, H-9), 3.88 (q, ³J = 7.0 Hz, 8 H, H-9), 3.81 (s, 2 H, OH) 1.36 (t, ³J = 6.9 Hz, 12 H, H-10), 1.34 (t, ³J = 7.0 Hz, 12 H, H-10), 1.13 (s, 6 H, H-2).

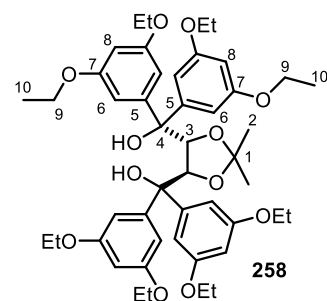
¹³C NMR (151 MHz, CDCl₃) δ [ppm] = 159.5 (C-7), 159.1 (C-7), 147.7 (C-5), 144.9 (C-5), 109.2 (C-1), 107.4 (C-6), 106.4 (C-6), 100.3 (C-8), 100.1 (C-8), 81.4 (C-3), 78.2 (C-4), 63.5 (C-9), 63.4 (C-9), 27.3 (C-2), 14.8 (C-10), 14.7 (C-10).

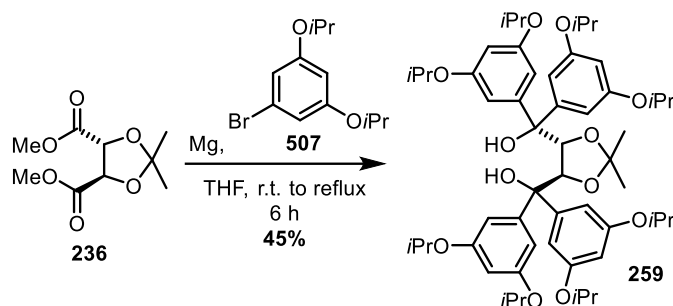
HR-ESI-MS m/z calculated [C₄₇H₆₂O₁₂+Na⁺]: 841.4133484; found: 841.41403.

FTIR-ATR ν [cm⁻¹] = 3312 (br), 2978 (m), 2932 (m), 2880 (m), 1748 (w), 1591 (s), 1440 (m), 1389 (m), 1306 (m), 1209 (m), 1246 (m), 1218 (w), 1165 (vs), 1113 (m), 1045 (vs), 844 (m), 819 (m), 757 (m), 740 (m), 693 (m), 623 (w), 587 (w), 507 (w).

Specific rotation (c = 0.500 g/100 mL, CHCl₃, [α]_D^T): [α]₃₆₅^{20.0} = - 42.2 °, [α]₄₃₆^{20.0} = - 14.2 °, [α]₅₄₆^{20.0} = - 11.0 °, [α]₅₇₉^{20.0} = - 10.2 °, [α]₅₈₉^{20.0} = - 10.5 °.

The analytical data are in agreement with the literature.^[215]



10.2.1.6.7. Synthesis of 3,5-diisopropoxy-TADDOL **259**

According to the general procedure **GP1**, 92 mg of Mg turnings (3.79 mmol, 4.8 equiv.) and 952 mg of bromoarene **507** (3.49 mmol, 4.4 equiv.) were reacted with 172 mg of ester **236** (0.790 mmol, 1.0 equiv.). Purification by FCC (cHex/EtOAc10:1) gave 332 mg of 3,5-diisopropoxy-TADDOL **259** as a pale yellow resin (0.36 mmol, 45%).

M (C₅₅H₇₈O₁₂) = 931.22 g/mol.

TLC (SiO₂, cHex/EtOAc 10:1) R_f = 0.19.

¹H NMR (600 MHz, CDCl₃) δ [ppm] = 6.69 (d, ⁴J = 2.3 Hz, 4 H, H-6), 6.52 (d, ⁴J = 2.3 Hz, 4 H, H-6), 6.36 (t, ⁴J = 2.3 Hz, 2 H, H-8), 6.28 (t, ⁴J = 1.6 Hz, 2 H, H-8), 4.62 (s, 2 H, H-3), 4.52 – 4.44 (m, 6 H, OH, H-9), 4.38 (hept, ³J = 7.0 Hz, 4 H, H-9), 1.32 – 1.19 (m, 48 H, H-10).

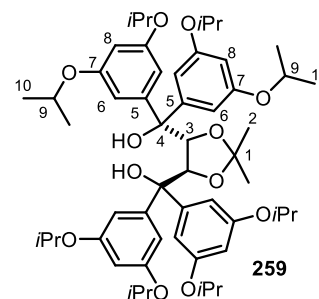
¹³C NMR (151 MHz, CDCl₃) δ [ppm] = 158.6 (C-7), 158.1 (C-7), 148.1 (C-5), 145.0 (C-5), 109.6 (C-1), 109.3 (C-6), 107.9 (C-6), 103.5 (C-8), 103.0 (C-8), 81.6 (C-3), 78.3 (C-4), 70.0 (C-9), 69.9 (C-9), 27.3 (C-2), 22.4 (C-10), 22.2 (C-10), 22.1 (C-10), 22.1 (C-10).

HR-ESI-MS m/z calculated [C₅₅H₇₈O₁₂+Na⁺]: 953.5385488; found: 953.53774.

FTIR-ATR ν [cm⁻¹] = 3344 (br), 2976 (m), 2933 (w), 1980 (w), 1748 (w), 1590 (s), 1438 (m), 1383 (w), 1371 (m), 1346 (w), 1332 (m), 1287 (m), 1249 (w), 1217 (w), 1182 (m), 1150 (s), 1134 (s), 1111 (s), 1026 (s), 998 (w), 964 (w), 936 (w), 907 (w), 897 (w), 839 (s), 818 (w), 760 (w), 742 (m), 627 (w), 592 (w).

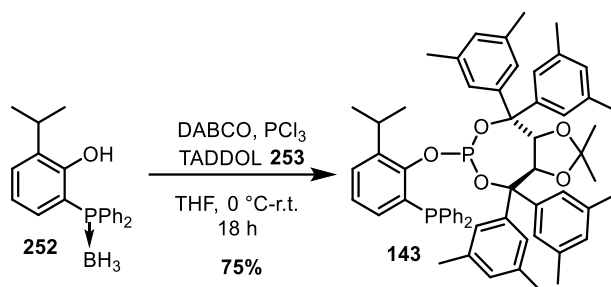
Specific rotation (c = 0.425 g/100 mL, CHCl₃, [α]_D^T): [α]₃₆₅^{20.0} = + 51.5 °, [α]₄₃₆^{20.0} = - 15.9 °, [α]₅₄₆^{20.0} = - 13.4 °, [α]₅₇₉^{20.0} = - 12.1 °, [α]₅₈₉^{20.0} = - 12.5 °.

The analytical data are in agreement with the literature.^[215]



10.2.1.7. Phosphine-Phosphite Ligand assembly

10.2.1.7.1. Synthesis of phosphine-phosphite ligand 143

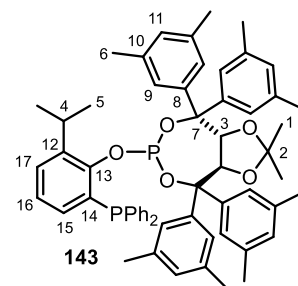


According to the general procedure **GP2**, 1.00 g of phosphine **252** (3.00 mmol, 1.0 equiv.) and 2.70 g of DABCO (24.1 mmol, 8.0 equiv.) were reacted with 0.31 mL of PCl_3 (0.49 g, 3.6 mmol, 1.2 equiv.) and 2.60 g of TADDOL **253** (4.49 mmol, 1.5 equiv.). Purification by FCC (ultra-pure SiO_2 , cHex/EtOAc 50:1) gave 2.10 g of ligand **143** as a colorless foam (2.27 mmol, 75%; lit.:^[42] 42%).

M ($\text{C}_{60}\text{H}_{64}\text{O}_5\text{P}_2$) = 927.11 g/mol.

TLC (SiO_2 , cHex/EtOAc 30:1) R_f = 0.23.

M.p. 111 - 115 °C.



$^1\text{H NMR}$ (500 MHz, CDCl_3) δ [ppm] = 7.54 (s, 2 H, H-9), 7.26 (dd, $^3J = 7.6$ Hz, $^4J = 1.7$ Hz, 1 H, H-17), 7.24 – 7.09 (m, 10 H, H_{Ph}), 7.09 – 7.02 (m, 6 H, H-9), 6.99 (t, $^3J = 7.6$ Hz, $^4J_{\text{P}} = 1.1$ Hz, 1 H, H-16), 6.86 (s, 1 H, H-11), 6.82 (s, 2 H, H-11), 6.79 (s, 1 H, H-11), 6.71 (ddd, $^3J = 7.6$ Hz, $^3J_{\text{P}} = 3.4$ Hz, $^4J = 1.7$ Hz, 1 H, H-15), 4.99 (dd, $^3J = 8.2$ Hz, $^3J_{\text{H,P}} = 2.5$ Hz, 1 H, H-3), 4.94 (d, $^3J = 8.2$ Hz, 1 H, H-3), 3.92 (hept, $^3J = 7.0$ Hz, 1 H, H-4), 2.25 (s, 6 H, H-6), 2.23 (s, 6 H, H-6), 2.20 (s, 6 H, H-6), 2.12 (s, 6 H, H-6), 1.30 (s, 3 H, H-1), 1.19 (d, $^3J = 7.0$ Hz, 3 H, H-5), 1.15 (d, $^3J = 7.0$ Hz, 3 H, H-5), 0.36 (s, 3 H, H-1).

$^{13}\text{C NMR}$ (126 MHz, CDCl_3) δ [ppm] = 152.85 (dd, $J_{\text{P}} = 21.0$ Hz, $J_{\text{P}} = 1.3$ Hz, C-13), 146.16 (C-8), 145.72 (d, $J_{\text{P}} = 1.6$ Hz, C-8), 141.7 (d, $J_{\text{P}} = 2.5$ Hz, C-12), 141.4 (d, $J_{\text{P}} = 1.6$ Hz, C-8), 140.9 (C-8), 137.9 – 137.7 (ψ_{m} , C_{Ph}), 137.2 (C-10), 136.8 (C-10), 136.6 (C-10), 136.2 (C-10), 133.9 (C_{Ph}), 133.7 (C_{Ph}), 133.6 (C_{Ph}), 132.3 (d, $J_{\text{P}} = 9.0$ Hz, C-15), 130.5 (dd, $J_{\text{P}} = 13.0$ Hz, $J_{\text{P}} = 2.9$ Hz, C-14), 129.2 (C-11), 128.3 (ψ_{d} , C-11), 128.22 (C_{Ph}), 128.2 (C_{Ph}), 128.1 (d, $J_{\text{P}} = 4.1$ Hz, C_{Ph}), 127.6 (C-17), 127.2 (C-9), 126.9 (dd, $J_{\text{P}} = 5.0$ Hz, $J_{\text{P}} = 2.6$ Hz, C-9), 125.4 (C-9), 125.2 (C-9), 124.7 (C-16), 123.9 (C_{Ph}), 112.2 (C-2), 84.1 (d, $J_{\text{P}} = 2.9$ Hz, C-7), 83.1 – 82.2 (ψ_{m} , C-3/7), 27.7 (C-1), 27.0 (C-4), 25.9 (C-1), 23.9 (C-5), 23.1 (C-5), 21.8 (d, $J_{\text{P}} = 1.8$ Hz, C-6), 21.7 – 21.6 (ψ_{m} , C-6).

^{31}P NMR (121 MHz, CDCl_3) δ [ppm] = 149.61 (d, $J = 73.3$ Hz, $\text{P}(\text{OR})_3$), -18.70 (d, $J = 73.3$ Hz, PR_3).

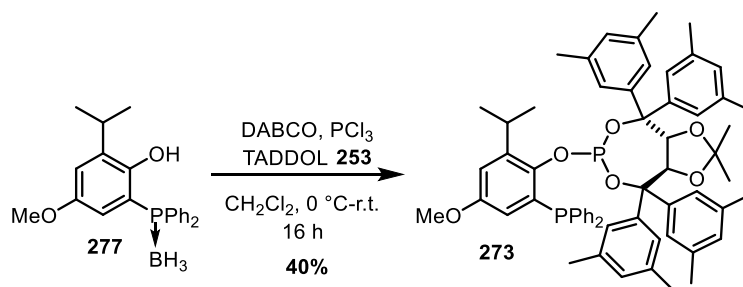
HR-ESI-MS m/z calculated [$\text{C}_{60}\text{H}_{64}\text{O}_5\text{P}_2 + \text{Na}^+$]: 949.4121192; found: 949.41186.

FTIR-ATR ν [cm^{-1}] = 2916 (w), 2867 (w), 2361 (w), 1601 (w), 1456 (w), 1434 (w), 1418 (w), 1381 (w), 1337 (w), 1248 (w), 1212 (w), 1161 (m), 1084 (w), 1067 (m), 1043 (s), 941 (w), 886 (m), 853 (s), 803 (s), 761 (s), 741 (s), 691 (s), 603 (w), 501 (m).

Specific rotation ($c = 0.510$ g/100 mL, CHCl_3 , $[\alpha]_{\lambda}^T$): $[\alpha]_{365}^{20.0} = -550.6^\circ$, $[\alpha]_{436}^{20.0} = -307.5^\circ$, $[\alpha]_{546}^{20.0} = -166.1^\circ$, $[\alpha]_{579}^{20.0} = -145.2^\circ$, $[\alpha]_{589}^{20.0} = -140.5^\circ$.

The analytical data are in agreement with the literature.^[42]

10.2.1.7.2. Synthesis of phosphine-phosphite ligand **273**



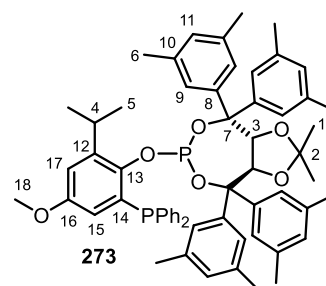
According to the general procedure **GP2**, 500 mg of phosphine **277** (1.37 mmol, 1.0 equiv.) and 1.12 g of DABCO (11.0 mmol, 8.0 equiv.) were reacted with 0.14 mL of PCl_3 (0.23 g, 1.7 mmol, 1.2 equiv.) and 1.19 g of TADDOL **253** (2.06 mmol, 1.5 equiv.). Purification by FCC (ultra-pure SiO_2 , $c\text{Hex}/\text{EtOAc}$ 50:1) gave 530 mg of ligand **273** as a colorless foam (0.554 mmol, 40%).

M ($\text{C}_{61}\text{H}_{66}\text{O}_6\text{P}_2$) = 957.14 g/mol.

TLC (SiO_2 , $c\text{Hex}/\text{EtOAc}$ 30:1) $R_f = 0.40$.

M.p. 116 - 119 $^\circ\text{C}$.

^1H NMR (500 MHz, CDCl_3) δ [ppm] = 7.55 (d, 2 H, H-9), 7.26 – 7.12 (m, 8 H, H_{Ph}), 7.11 – 7.06 (m, 6 H, H-9), 7.02 (s, 2 H, H-11), 6.86 (s, 1 H, H-17), 6.81 (s, 2 H, H_{Ph}), 6.79 (d, $^4J = 2.7$ Hz, 2 H, H-11), 6.20 (ψ t, $^3J_{\text{P}} = 3.2$ Hz, $^4J_{\text{P}} = 3.2$ Hz, 1 H, H-15), 5.00 (dd, $^3J = 8.2$ Hz, $^4J_{\text{P}} = 2.5$ Hz, 1 H, H-3), 4.93 (d, $^3J = 8.2$ Hz, 1 H, H-3), 3.90 (hept, $^3J = 6.8$ Hz, 1 H, H-4), 3.53 (s, 3 H, H-18), 2.25 (s, 3 H, H-6), 2.24 (s, 3 H, H-6), 2.20 (s, 3 H, H-6), 2.14 (s, 3 H, H-6), 1.31 (s, 3 H, H-1), 1.17 (d, $^3J = 6.8$ Hz, 3 H, H-5), 1.15 (d, $^3J = 6.8$ Hz, 3 H, H-5), 0.36 (s, 3 H, H-1).



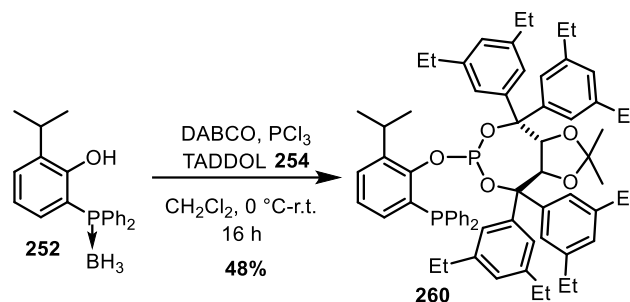
¹³C NMR (126 MHz, CDCl₃) δ [ppm] = 156.1 (d, J_P = 1.4 Hz, C-16), 146.5 (d, J_P = 20.8 Hz, C-13), 146.2 (C-8), 145.8 (d, J_P = 1.5 Hz, C-8), 142.9 (d, J_P = 2.6 Hz, C-12), 141.4 (d, J_P = 1.5 Hz, C-8), 140.9 (C-8), 137.7 – 137.4 (ψm, C_{Ph}), 137.1 (C-10), 136.7 (C-10), 136.5 (C-10), 136.2 (C-10), 134.2 – 133.5 (ψm, C_{Ph}), 131.6 (dd, J_P = 14.6 Hz, J_P = 2.9 Hz, C-14), 129.4 – 128.7 (ψm, C-11), 128.4 – 128.1 (ψm C_{Ph}), 127.2 (C-9), 127.0 – 126.9 (ψm, C-9), 125.4 (C-11), 125.2 (C-9), 116.3 (C-15), 113.4 (C-17), 112.2 (C-2), 84.0 (d, J_P = 2.8 Hz, C-7), 83.0 – 82.2 (ψm, C-3), 55.3 (d, J_P = 2.6 Hz, C-18), 27.7 (C-1), 27.3 (C-4), 25.9 (C-1), 23.9 (C-5), 23.0 (C-5), 21.9 – 21.4 (ψm, C-6).

³¹P NMR (202 MHz, CDCl₃) δ [ppm] = 149.64 (d, J = 66.8 Hz, P(OR)₃), -17.05 (d, J = 66.8 Hz, PR₃).

HR-ESI-MS m/z calculated [C₆₁H₆₆O₆P₂+Na⁺]: 979.4226839; found: 979.42389.

FTIR-ATR ν [cm⁻¹] = 3071 (w), 3053 (w), 2987 (w), 2963 (w), 2916 (w), 2866 (w), 2731 (w), 2246 (w), 1739 (w), 1599 (w), 1452 (m), 1433 (m), 1424 (m), 1381 (w), 1341 (w), 1291 (w), 1245 (w), 1216 (w), 1194 (m), 1162 (m), 1084 (m), 1067 (m), 1039 (s), 940 (m), 906 (s), 887 (m), 852 (s), 801 (m), 760 (m), 732 (s), 691 (s), 649 (w), 603 (w).

Specific rotation (c = 0.560 g/100 mL, CHCl₃, [α]_λ^T): [α]₃₆₅^{20.0} = - 589.3 °, [α]₄₃₆^{20.0} = - 321.5 °, [α]₅₄₆^{20.0} = - 171.7 °, [α]₅₇₉^{20.0} = - 147.9 °, [α]₅₈₉^{20.0} = - 141.4 °.

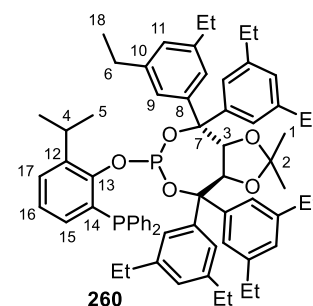
10.2.1.7.3. Synthesis of phosphine-phosphite ligand **260**

According to the general procedure **GP2**, 500 mg of phosphine **252** (1.50 mmol, 1.0 equiv.) and 1.36 g of DABCO (12.1 mmol, 8.1 equiv.) were reacted with 0.16 mL of PCl_3 (0.25 g, 1.8 mmol, 1.2 equiv.) and 1.55 g of TADDOL **254** (2.24 mmol, 1.5 equiv.). Purification by FCC (ultra-pure SiO_2 , cHex/EtOAc 50:1) gave 755 mg of ligand **260** as a colorless foam (0.727 mmol, 48%).

M ($\text{C}_{68}\text{H}_{80}\text{O}_5\text{P}_2$) = 1039.33 g/mol.

TLC (SiO_2 , cHex/EtOAc 50:1) R_f = 0.73.

M.p. 75 - 79 °C.



$^1\text{H NMR}$ (600 MHz, CDCl_3) δ [ppm] = 7.54 (d, $^4J = 1.6$ Hz, 2 H, H-9), 7.35 – 7.31 (m, 1 H, H-17), 7.26 – 7.13 (m, 8 H, H-9, H_{Ph}), 7.12 – 7.06 (m, 8 H, H-9, H_{Ph}), 7.01 (ddd, $^3J = 8.4$ Hz, $^3J = 7.6$ Hz, $^4J_{\text{P}} = 1.3$ Hz, 1 H, H-16), 6.90 (t, $^4J = 1.6$ Hz, 1 H, H-11), 6.88 (t, $^4J = 1.6$ Hz, 1 H, H-11), 6.86 (t, $^4J = 1.7$ Hz, 1 H, H-11), 6.84 (t, $^4J = 1.7$ Hz, 1 H, H-11), 6.75 (ddd, $^3J = 7.6$ Hz, $^3J_{\text{P}} = 3.3$ Hz, $^4J = 1.7$ Hz, 1 H, H-15), 5.11 (dd, $^3J = 8.3$ Hz, $^3J_{\text{P}} = 2.1$ Hz, 1 H, H-3), 5.07 (d, $^3J = 8.3$ Hz, 1 H, H-3), 3.89 (hept, $^3J = 6.8$ Hz, 1 H, H-4), 2.63 – 2.48 (m, 12 H, H-6), 2.47 – 2.39 (m, 4 H, H-6), 1.22 (s, 3 H, H-1), 1.20 – 1.09 (m, 24 H, H-5/18), 1.02 (t, $^3J = 7.6$ Hz, 6 H, H-18), 0.28 (s, 3 H, H-1).

$^{13}\text{C NMR}$ (151 MHz, CDCl_3) δ [ppm] = 153.0 (d, $J_{\text{P}} = 20.6$ Hz, C-13), 146.1 (C-8), 145.7 (C-8), 143.5 (C-10), 143.1 (C-10), 143.0 (C-10), 142.6 (C-10), 141.8 – 141.5 (ψm , C-12), 141.3 (d, $J_{\text{P}} = 1.6$ Hz, C-8), 141.0 (C-8), 138.2 – 137.8 (ψm , C_{Ph}), 133.9 – 133.4 (ψm , C_{Ph}) 133.3 (C-16), 132.7 (d, $J_{\text{P}} = 9.0$ Hz, C-15), 130.3 (dd, $J_{\text{P}} = 13.2$ Hz, $J_{\text{P}} = 2.2$ Hz, C-14), 129.1 (C_{Ph}), 128.8 (C-17), 128.2 – 128.0 (ψm , C_{Ph}), 127.9 (C_{Ph}), 127.6 (C_{Ph}), 126.8 – 126.2 (ψm , C-9/11), 124.8 (C-9), 124.5 (C-9), 112.0 (C-2), 84.5 (d, $J_{\text{P}} = 2.6$ Hz, C-7), 83.3 – 82.4 (m, C-3/7), 29.2 (C-6), 29.1 (C-6), 29.0 (C-6), 29.0 (C-6), 27.7 (C-1), 27.0 (C-4), 25.6 (C-1), 23.9 (C-5), 23.1 (C-5), 16.1 (C-18), 15.9 (C-18), 15.57 (C-18), 15.56 (C-18).

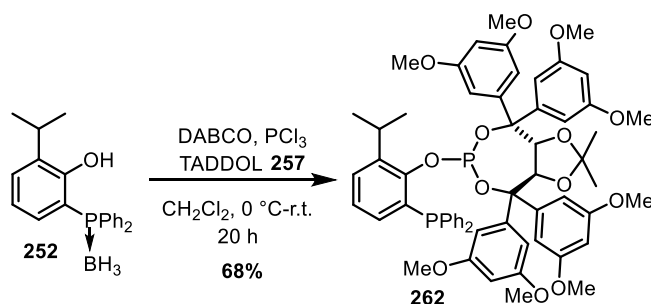
^{31}P NMR (122 MHz, CDCl_3) δ [ppm] = 149.73 (d, $J = 79.8$ Hz, $\text{P}(\text{OR})_3$), -19.62 (d, $J = 77.2$ Hz, PR_3).

HR-ESI-MS m/z calculated [$\text{C}_{68}\text{H}_{80}\text{O}_5\text{P}_2+\text{Na}^+$]: 1061.5373197; found: 1061.54031.

FTIR-ATR ν [cm^{-1}] = 3054 (w), 2963 (m), 2931 (w), 2871 (w), 1770 (w), 1685 (w), 1600 (w), 1457 (m), 1434 (w), 1418 (w), 1381 (w), 1371 (w), 1335 (w), 1249 (w), 1212 (w), 1161 (m), 1119 (w), 1089 (w), 1065 (m), 1051 (m), 1036 (m), 999 (w), 968 (w), 872 (s), 853 (w), 805 (m), 741 (s), 695 (s), 643 (w), 624 (w), 590 (w), 571 (w), 537 (w).

Specific rotation ($c = 0.550$ g/100 mL, CHCl_3 , $[\alpha]_{\lambda}^T$): $[\alpha]_{365}^{20.0} = -374.7^\circ$, $[\alpha]_{436}^{20.0} = -205.8^\circ$, $[\alpha]_{546}^{20.0} = -109.3^\circ$, $[\alpha]_{579}^{20.0} = -94.6^\circ$, $[\alpha]_{589}^{20.0} = -90.4^\circ$.

10.2.1.7.4. Synthesis of phosphine-phosphite ligand **262**



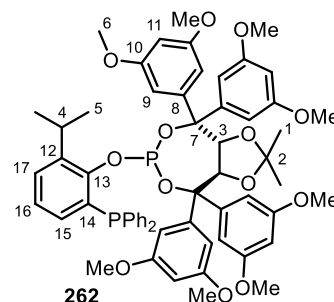
According to the general procedure **GP2**, 500 mg of phosphine **252** (1.50 mmol, 1.0 equiv.) and 1.35 g of DABCO (12.0 mmol, 8.0 equiv.) were reacted with 0.16 mL of PCl_3 (0.25 g, 1.8 mmol, 1.2 equiv.) and 1.59 g of TADDOL **257** (2.25 mmol, 1.5 equiv.). Purification by FCC (ultra-pure SiO_2 , $c\text{Hex}/\text{EtOAc}$ 2:1) gave 1.08 g of ligand **262** as a colorless foam (1.02 mmol, 68%).

M ($\text{C}_{60}\text{H}_{64}\text{O}_{13}\text{P}_2$) = 1055.11 g/mol.

TLC (SiO_2 , $c\text{Hex}/\text{EtOAc}$ 2:1) $R_f = 0.57$.

M.p. 111 - 116 $^\circ\text{C}$.

^1H NMR (500 MHz, CDCl_3) δ [ppm] = 7.25 (dd, $^3J = 7.7$ Hz, $^4J = 1.7$ Hz, 1 H, H-17), 7.23 – 7.09 (m, 6 H, H_{Ph}), 7.06 (d, $^4J = 2.4$ Hz, 2 H, H-9), 7.05 – 6.95 (m, 5 H, H-16, H_{Ph}), 6.76 (ddd, $^3J = 7.6$ Hz, $^3J_{\text{P}} = 3.3$ Hz, $^4J = 1.7$ Hz, 1 H, H-15), 6.74 (d, $^4J = 2.3$ Hz, 2 H, H-9), 6.69 (d, $^4J = 2.3$ Hz, 2 H, H-9), 6.66 (d, $^4J = 2.3$ Hz, 2 H, H-9), 6.35 (t, $^4J = 2.3$ Hz, 1 H, H-11), 6.32 (ψq , $^4J = 2.4$ Hz, 2 H, H-11), 6.28 (t, $^4J = 2.3$ Hz, 1 H, H-11), 5.05 (dd, $^3J = 8.5$ Hz, $^4J_{\text{P}} = 2.4$ Hz, 1 H, H-3), 4.86 (d, $^3J = 8.5$ Hz, 1 H, H-3), 3.91 (hept, $^3J = 6.9$ Hz, 1 H, H-4), 3.72 (s, 3 H, H-6), 3.68



(s, 3 H, H-6), 3.62 (s, 3 H, H-6), 3.50 (s, 3 H, H-6), 1.40 (s, 3 H, H-1), 1.19 (d, $^3J = 6.9$ Hz, 3 H, H-5), 1.16 (d, $^3J = 6.9$ Hz, 3 H, H-5), 0.39 (s, 3 H, H-1).

^{13}C NMR (126 MHz, CDCl_3) δ [ppm] = 160.3 (C-10), 160.1 (C-10), 160.1 (C-10), 159.8 (C-10), 152.5 (dd, $J_P = 21.6$ Hz, $J_P = 3.0$ Hz, C-13), 148.1 (C-8), 147.5 (d, $J_P = 2.1$ Hz, C-8), 143.2 (d, $J_P = 1.6$ Hz, C-8), 142.7 (C-8), 141.6 (d, $J_P = 2.5$ Hz, C-12), 137.6 (dd, $J_P = 13.2$ Hz, $J_P = 4.6$ Hz, C_{Ph}), 137.3 (dd, $J_P = 11.6$ Hz, $J_P = 2.7$ Hz, C_{Ph}), 133.8 – 133.32 (ψm , C_{Ph}), 133.0 (C-15), 130.2 (dd, $J_P = 13.6$ Hz, $J_P = 2.3$ Hz, C-14), 128.3 – 128.0 (ψm , C_{Ph}), 127.9 (C-17), 124.8 (C-16), 111.9 (C-2), 108.2 (C-9), 107.2 (C-9), 106.1 (C-9), 105.7 (C-9), 100.2 (C-11), 99.7 (C-11), 99.2 (C-11), 99.0 (C-11), 83.2 – 82.3 (ψm , C-3/7), 55.7 – 55.0 (ψm , C-6), 27.8 (C-1), 27.1 (C-4), 25.5 (C-1), 23.7 (C-5), 23.4 (C-5).

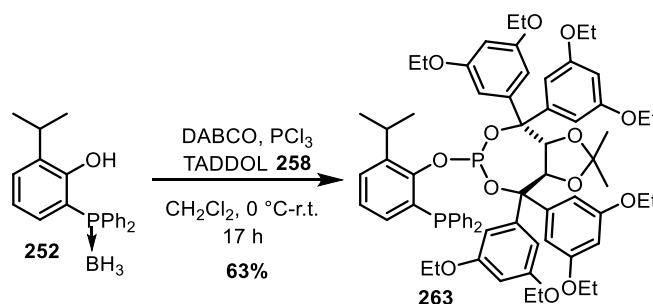
^{31}P NMR (122 MHz, CDCl_3) δ [ppm] = 150.21 (d, $J = 85.9$ Hz, $\text{P}(\text{OR})_3$), -20.36 (d, $J = 87.4$ Hz, PR_3).

HR-ESI-MS m/z calculated [$\text{C}_{60}\text{H}_{64}\text{O}_{13}\text{P}_2 + \text{Na}^+$]: 1077.3714360; found: 1077.37299.

FTIR-ATR ν [cm^{-1}] = 2936 (w), 2835 (w), 1592 (s), 1456 (m), 1423 (s), 1382 (w), 1347 (w), 1311 (m), 1278 (w), 1252 (w), 1203 (s), 1151 (s), 1060 (m), 1039 (s), 999 (m), 926 (w), 890 (m), 860 (s), 802 (m), 741 (s), 695 (m), 620 (w), 542 (w), 502 (m), 466 (w).

Specific rotation ($c = 0.510$ g/100 mL, CHCl_3 , $[\alpha]_{\lambda}^T$): $[\alpha]_{365}^{20.0} = -439.1^\circ$, $[\alpha]_{436}^{20.0} = -246.3^\circ$, $[\alpha]_{546}^{20.0} = -134.5^\circ$, $[\alpha]_{579}^{20.0} = -117.9^\circ$, $[\alpha]_{589}^{20.0} = -114.9^\circ$.

10.2.1.7.5. Synthesis of phosphine-phosphite ligand 263

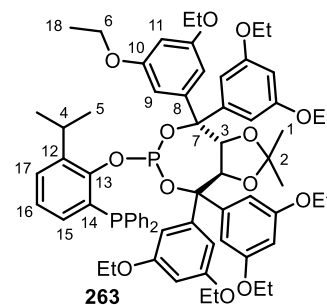


According to the general procedure **GP2**, 375 mg of phosphine **252** (1.12 mmol, 1.0 equiv.) and 1.01 g of DABCO (9.00 mmol, 8.0 equiv.) were reacted with 0.12 mL of PCl_3 (0.19 g, 1.3 mmol, 1.2 equiv.) and 1.38 g of TADDOL **258** (1.69 mmol, 1.5 equiv.). Purification by FCC (ultra-pure SiO_2 , $c\text{Hex}/\text{EtOAc}$ 10:1) gave 820 mg of ligand **263** as a colorless foam (0.703 mmol, 63%).

M ($C_{68}H_{80}O_{13}P_2$) = 1167.32 g/mol.

TLC (SiO_2 , cHex/EtOAc 10:1) R_f = 0.20.

M.p. 57 - 60 °C.



1H NMR (500 MHz, $CDCl_3$) δ [ppm] = 7.25 (d, $^3J = 7.6$ Hz, 1 H, H-17), 7.22 – 7.09 (m, 6 H, H_{Ph}), 7.10 – 6.97 (m, 7 H, H-9/16, H_{Ph}), 6.78 (dd, $J = 7.9$ Hz, $^3J_P = 3.4$ Hz, 1 H, H-15), 6.73 (s, 2 H, H-9), 6.69 (d, $^4J = 2.2$ Hz, 2 H, H-9), 6.64 (d, $^4J = 2.2$ Hz, 2 H, H-9), 6.35 (s, 1 H, H-11), 6.31 (s, 2 H, H-11), 6.27 (s, 1 H, H-11), 5.07 (d, $^3J = 8.5$ Hz, 1 H, H-3), 4.91 (d, $^3J = 8.5$ Hz, 1 H, H-3), 4.09 – 3.54 (m, 17 H, H-4/6), 1.40 (s, 3 H, H-1), 1.33 (ψq , $^3J_{18H,6H} = 6.5$ Hz, 12 H, H-18) 1.26 – 1.09 (m, 18 H, H-5/18), 0.41 (s, 3 H, H-1).

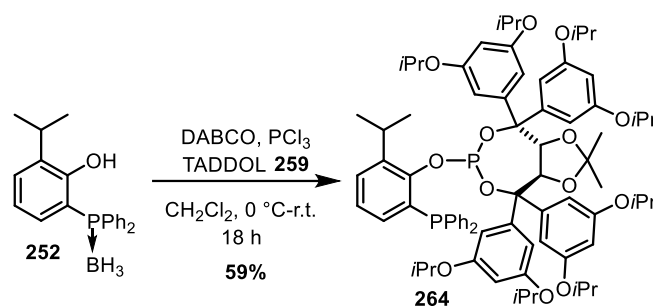
^{13}C NMR (126 MHz, $CDCl_3$) δ [ppm] = 159.6 (C-10), 159.3 (C-10), 159.3 (C-10), 159.1 (C-10), 152.6 (d, $J_P = 21.2$ Hz, C-13), 148.1 (C-8), 147.4 (C-8), 143.0 (C-8), 142.6 (C-8), 141.5 (C-12), 137.8 – 137.2 (ψm , C_{Ph}), 133.8 (C_{Ph}), 133.6 (C_{Ph}), 133.4 (C_{Ph}), 133.3 (C_{Ph}), 132.8 (C-15), 130.4 (d, $J_P = 14.0$ Hz, C-14), 128.3 – 127.9 (ψm , C_{Ph}), 127.7 (C-17), 124.6 (C-16), 111.8 (C-2), 108.7 (C-9), 107.7 (C-9), 106.5 (C-9), 106.2 (C-9), 101.3 (C-11), 100.5 (C-11), 100.2 (C-11), 99.9 (C-11), 83.3 – 82.4 (ψm , C-3/7), 63.5 (C-6), 63.5 (C-6), 63.3 (C-6), 63.3 (C-6), 27.8 (C-1), 27.0 (C-4), 25.5 (C-1), 23.6 (C-5), 23.3 (C-5), 14.9 (C-18), 14.8 (C-18).

^{31}P NMR (202 MHz, $CDCl_3$) δ [ppm] = 150.16 (d, $J = 84.6$ Hz, $P(OR)_3$), -20.38 (d, $J = 84.5$ Hz, PR_3).

HR-ESI-MS m/z calculated [$C_{68}H_{80}O_{13}P_2 + Na^+$]: 1189.4966365; found: 1189.49666.

FTIR-ATR ν [cm^{-1}] = 2978 (m), 2931 (w), 2901 (w), 2882 (w), 1592 (s), 1436 (m), 1419 (w), 1390 (m), 1371 (w), 1337 (w), 1310 (w), 1292 (w), 1277 (w), 1252 (w), 1212 (w), 1167 (s), 1114 (m), 1085 (w), 1044 (s), 995 (w), 933 (w), 885 (w), 859 (s), 817 (w), 804 (m), 763 (w), 742 (s), 694 (s), 647 (w), 621 (w), 588 (w), 545 (w).

Specific rotation ($c = 0.550$ g/100 mL, $CHCl_3$, $[\alpha]_{\lambda}^T$): $[\alpha]_{365}^{20.0} = -337.9^\circ$, $[\alpha]_{436}^{20.0} = -190.4^\circ$, $[\alpha]_{546}^{20.0} = -103.0^\circ$, $[\alpha]_{579}^{20.0} = -89.2^\circ$, $[\alpha]_{589}^{20.0} = -85.6^\circ$.

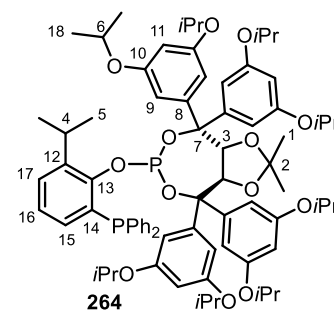
10.2.1.7.6. Synthesis of phosphine-phosphite ligand **264**

According to the general procedure **GP2**, 63 mg of phosphine **252** (0.18 mmol, 1.0 equiv.) and 165 mg of DABCO (1.46 mmol, 8.1 equiv.) were reacted with 0.12 μL of PCl_3 (30 mg, 0.22 mmol, 1.2 equiv.) and 256 mg of TADDOL **259** (0.275 mmol, 1.5 equiv.). Purification by FCC (ultra-pure SiO_2 , *c*Hex/EtOAc 10:1) gave 137 mg of ligand **264** as a colorless foam (0.107 mmol, 59%).

M ($\text{C}_{76}\text{H}_{96}\text{O}_{13}\text{P}_2$) = 1279.54 g/mol.

TLC (SiO_2 , *c*Hex/EtOAc 10:1) R_f = 0.28.

M.p. 68 - 70 $^\circ\text{C}$.



^1H NMR (600 MHz, CDCl_3) δ [ppm] = 7.25 (dd, $^3J = 7.6$ Hz, $^3J = 1.6$ Hz, 1 H, H-17), 7.21 – 7.07 (m, 6 H, H_{Ph}), 7.07 – 6.96 (m, 5 H, H-16, H_{Ph}), 7.01 (d, $^4J = 2.2$ Hz, 2 H, H-9), 6.76 (ddd, $^3J = 7.5$ Hz, $^3J_{\text{P}} = 3.3$ Hz, $^4J = 1.6$ Hz, 1 H, H-15), 6.67 (d, $^4J = 2.2$ Hz, 2 H, H-9), 6.63 (d, $^4J = 2.2$ Hz, 2 H, H-9), 6.58 (d, $^4J = 2.2$ Hz, 2 H, H-9), 6.33 (t, $^4J = 2.2$ Hz, 1 H, H-11), 6.28 (ψ p, $^4J = 2.2$ Hz, 2 H, H-11), 6.24 (t, $^4J = 2.2$ Hz, 1 H, H-11), 5.08 (dd, $^3J = 8.4$ Hz, $^4J_{\text{P}} = 2.1$ Hz, 1 H, H-3), 4.91 (d, $^3J = 8.4$ Hz, 1 H, H-3), 4.47 – 4.31 (m, 6 H, H-6), 4.18 (hept, $^3J = 6.2$ Hz, 2 H, H-6), 3.84 (hept, $^3J = 6.6$ Hz, 1 H, H-4), 1.33 (s, 3 H, H-1), 1.25 – 1.10 (m, 54 H, H-5/8), 0.41 (s, 3 H, H-2).

^{13}C NMR (151 MHz, CDCl_3) δ [ppm] = 158.6 (C-10), 158.3 (C-10), 158.2 (C-10), 157.97 (C-10), 152.75 (d, $J_{\text{P}} = 4.6$ Hz, C-13), 148.1 (C-8), 147.4 (C-8), 143.3 (C-8), 142.8 (C-8), 141.5 (C-12), 137.9 – 137.5 (ψ m, C_{Ph}), 133.9 (C_{Ph}), 133.8 (C_{Ph}), 133.6 (C_{Ph}), 133.4 (C_{Ph}), 132.8 (C-15), 130.45 (C-14), 130.54 – 127.9 (ψ m, C_{Ph}), 127.7 (C-17), 124.6 (C-16), 111.8 (C-2), 110.0 (C-9), 109.3 (C-9), 107.8 (C-9), 107.4 (C-9), 104.8 (C-11), 103.29 (C-11), 103.26 (C-11), 102.7 (C-11), 77.0 (C-6), 70.0 (C-6), 69.9 (C-6), 69.7 (C-6), 69.6 (C-6), 27.7 (C-1), 27.1 (C-4), 25.4 (C-1), 23.7 (C-5), 23.3 (C-5), 22.5 – 21.9 (ψ m, C-18).

^{31}P NMR (122 MHz, CDCl_3) δ [ppm] = 149.60 (d, J = 80.0 Hz, $\text{P}(\text{OR})_3$), -20.11 (d, J = 80.0 Hz, PR_3).

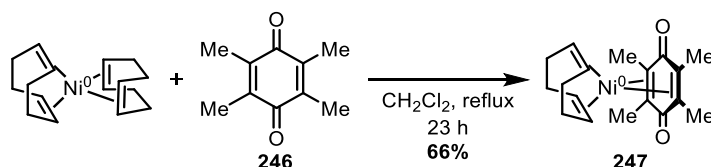
HR-ESI-MS m/z calculated [$\text{C}_{76}\text{H}_{96}\text{O}_{13}\text{P}_2+\text{Na}^+$]: 1301.6218370; found: 1301.62248.

FTIR-ATR ν [cm^{-1}] = 2978 (w), 2932 (w), 2901 (w), 2882 (w), 1592 (s), 1436 (m), 1419 (w), 1390 (w), 1371 (w), 1337 (w), 1310 (w), 1292 (w), 1277 (w), 1252 (w), 1212 (w), 1167 (s), 1114 (m), 1085 (w), 1043 (s), 995 (w), 933 (w), 885 (w), 859 (s), 817 (w), 804 (m), 763 (w), 742 (s), 694 (m), 647 (w), 621 (w), 588 (w), 545 (w).

Specific rotation (c = 0.525 g/100 mL, CHCl_3 , $[\alpha]_{\lambda}^T$): $[\alpha]_{365}^{20.0} = -5393.0^\circ$, $[\alpha]_{436}^{20.0} = -151.3^\circ$, $[\alpha]_{546}^{20.0} = -81.8^\circ$, $[\alpha]_{579}^{20.0} = -71.0^\circ$, $[\alpha]_{589}^{20.0} = -68.1^\circ$.

10.2.1.8. Synthesis of an air-stable nickel catalyst precursor

10.2.1.8.1. Synthesis of Ni(cod)(DQ) (**247**)

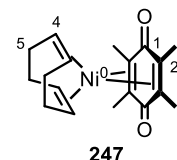


The synthesis was performed according to a procedure of *Engle & Coworkers*.^[135] Under an atmosphere of argon, a 10 mL GC-headspace vial was charged with a solution 500 mg of Ni(cod)₂ (1.82 mmol, 1.0 equiv.) and 299 mg of duroquinone (**246**) (1.82 mmol, 1.0 equiv.) in 6 mL of anhydrous CH₂Cl₂. The reddish-brown reaction mixture was heated at reflux for 22 h and the suspension filtered over a *Cellite* pad. Subsequently, the resulting solution was concentrated under reduced pressure to give an oily residue. Then 5 mL of CH₂Cl₂ and 20 mL of *n*Pe were added. The resulting red precipitate was washed with *n*Pe/CH₂Cl₂ (50:1, 2 x 20 mL) and the solid was dried by *Schlenk* line vacuum to give 394 mg of **247** as a dark red powder (1.19 mmol, 66%; Lit.:^[135] 79%).

M ($\text{C}_{18}\text{H}_{24}\text{NiO}_2$) = 331.08 g/mol.

TLC (SiO_2 , *c*Hex/EtOAc 9:1) R_f = 0.00.

M.p. >200 °C decomposition.



^1H NMR (500 MHz, benzene-*d*₆) δ [ppm] = 3.48 – 3.44 (m, 4 H, H-4), 1.96 (s, 12 H, H-3), 1.85 – 1.79 (m, 4 H, H-5), 1.59 – 1.48 (m, 4 H, H-5).

^{13}C NMR (126 MHz, benzene-*d*₆) δ [ppm] = 155.0 (C-1), 112.5 (C-2), 100.0 (C-4), 29.4 (C-5), 12.7 (C-3).

FTIR-ATR ν [cm^{-1}] = 2987 (w), 2913 (w), 2886 (w), 1657 (w), 1587 (w), 1549 (s), 1426 (m), 1375 (w), 1364 (s), 1333 (w), 1307 (w), 1283 (w), 1274 (w), 1227 (w), 1177 (w), 1149 (w), 1118 (w), 1076 (w), 1027 (w), 994 (w), 977 (w), 891 (w), 860 (m), 820 (m), 779 (m), 735 (m), 687 (s), 616 (m), 554 (w).

The analytical data are in agreement with the literature.^[135]

10.2.2. Synthesis of homostilbenes (1,3-diarylpropenes)

10.2.2.1. General procedures

10.2.2.1.1. General procedure GP3 for the preparation of homostilbenes by conventional heating

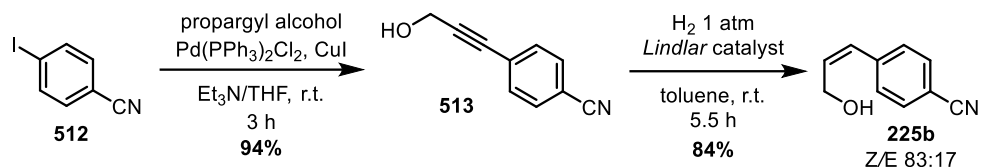
The synthesis was performed based on a modified procedure of *Tsukamoto et al.*^[130a] A 10 mL GC-headspace vial was charged with a solution of the corresponding allylic alcohol (2.0 mmol, 1.0 equiv.), boronic acid (2.4 mmol, 1.2 equiv.) and $\text{Pd}(\text{PPh}_3)_4$ (0.10 mmol, 5 mol%) in 6.6 mL of anhydrous THF (0.3 M). The reaction mixture was heated at 80 °C for 16-20 h. The orange brown reaction mixture was filtered over *Celite*, washed with CH_2Cl_2 or EtOAc, and concentrated under reduced pressure. The crude material was purified by FCC (SiO_2 , cHex/EtOAc). Bigger reaction scales were performed in several 10 mL GC-headspace vials at the same time and combined for work-up.

10.2.2.1.2. General procedure GP4 for the microwave-assisted preparation of homostilbenes

The synthesis was performed based on a modified procedure of *Tsukamoto et al.*^[130a] A 35 mL microwave vessel was charged with a solution of the corresponding allylic alcohol (5.0 mmol, 1.0 equiv.), boronic acid (6.0 mmol, 1.2 equiv.) and $\text{Pd}(\text{PPh}_3)_4$ (250 μmol , 5 mol%) in 16 mL of anhydrous THF (0.3 M). The reaction mixture was heated at 90 °C for 1 h with an average of 5-8 W at 2-3 bar (set maxima: 150 W/10 bar). After microwave irradiation the yellow solution was treated with 30 mL of sat. NH_4Cl solution before it was extracted with CH_2Cl_2 (3 x 30 mL). After drying with Na_2SO_4 , the combined organic phases were concentrated under reduced pressure. The crude material was purified by FCC (SiO_2 , cHex/EtOAc).

10.2.2.2. Synthesis of allylic alcohol and boronic acid building blocks

10.2.2.2.1. Synthesis of (Z)-4-cyanocinnamic alcohol (225b)



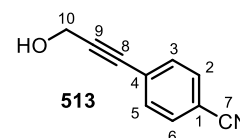
The synthesis was performed according to a procedure of *Xu et al.*^[216] Under an atmosphere of argon, a 250 mL *Schlenk* flask was charged with a solution of 70 mg of Pd(PPh₃)₂Cl₂ (0.10 mmol, 1 mol%) and 38 mg of CuI (0.20 mmol, 2 mol%) in 20 mL of Et₃N. Then a solution of 2.29 g of 4-iodobenzonitrile (**512**) (10.0 mmol, 1.0 equiv.) and 0.64 mL of propargyl alcohol (11 mmol, 1.1 equiv.) in 20 mL of anhydrous THF/Et₃N 1:1 was added (dropwise). The reaction mixture was stirred at r.t. for 20 h and the resulting suspension was filtered over *Celite* before it was washed with EtOAc (4 x 15 mL). The combined organic phases were concentrated under reduced pressure to give a brown crude product. Purification by FCC (SiO₂, cHex/EtOAc 3:1) gave 1.48 g of alkyne **513** as a yellow solid (9.39 mmol, 94%, lit.^[216] not given).

The synthesis was performed according to a procedure of *Tambar* and coworkers.^[217] Under an atmosphere of argon, a 100 mL round-bottomed flask was charged with a suspension of 1.03 g of alkyne **513** (6.52 mmol, 1.0 equiv.) and 358 mg of *Lindlar* catalyst ($\omega(\text{Pd}) = 5\%$, 0.17 mmol, 2.6 mol%) in 21 mL of dry toluene. Argon was removed by *Schlenk* line vacuum and H₂ atmosphere (1 atm.) was applied. The reaction mixture was stirred for 5.5 h. The suspension was filtered over *Celite* and concentrated under reduced pressure to give a grey crude product. After purification by FCC (SiO₂, cHex/EtOAc 4:1) 872 mg of (Z)-**225b** as a pale yellow solid were obtained (5.48 mmol, 84%, *E/Z* >83:17, lit.^[217] not given).

M (C₁₀H₉NO) = 157.17 g/mol.

TLC (SiO₂, cHex/EtOAc 3:1) R_f = 0.14.

M.p. 93 - 96 °C.



¹H NMR (300 MHz, CDCl₃) δ [ppm] = 7.59 (d, ³J = 8.5 Hz, 2 H, H-2/6), 7.49 (d, ³J = 8.5 Hz, 2 H, H-3/5), 4.53 (d, ³J = 5.4 Hz, 2 H, H-10), 2.35 (t, ³J = 5.4 Hz, 1 H, OH).

¹³C NMR (75 MHz, CDCl₃) δ [ppm] = 132.2 (C-3/5), 132.1 (C-2/6), 127.2 (C-4), 118.5 (C-7), 111.3 (C-1), 91.6 (C-9), 85.7 (C-8), 52.0 (C-10).

GC-MS (70 eV) m/z ([%]): 156 (29, [M-H⁺]), 140 (100), 115 (49), 89 (13), 63 (18), 39 (10).

FTIR-ATR ν [cm⁻¹] = 3346 (m), 3087 (w), 3046 (w), 2989 (w), 2916 (w), 2978 (w), 2823 (w), 2680 (w), 2547 (w), 2236 (m), 2051 (w), 1981 (w), 1936 (w), 1807 (w), 1684 (w), 1604 (m), 1503 (m), 1464 (w), 1425 (m), 1397 (m), 1288 (m), 1272 (m), 1255 (m), 1235 (m), 1182 (m),

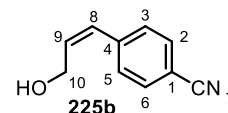
1110 (m), 1032 (s), 996 (m), 947 (m), 840 (s), 784 (m), 722 (w), 653 (w), 579 (m), 556 (s), 523 (m).

The analytical data are in agreement with the literature.^[216]

M (C₁₀H₇NO) = 159.19 g/mol.

TLC (SiO₂, cHex/EtOAc 4:1) R_f = 0.08.

M.p. 58 - 60 °C.



¹H NMR (300 MHz, CDCl₃) δ [ppm] = 7.63 (d, ³J = 8.3 Hz, 2 H, H-2/6), 7.32 (d, ³J = 8.3 Hz, 2 H, H-3/5), 6.57 (d, ³J = 11.9 Hz, 1 H, H-8), 6.04 (dt, ³J = 11.9 Hz, ³J = 5.5 Hz, 1 H, H-9), 4.40 (d, ³J = 5.5 Hz, 2 H, H-10), 1.82 (s, 1 H, OH).

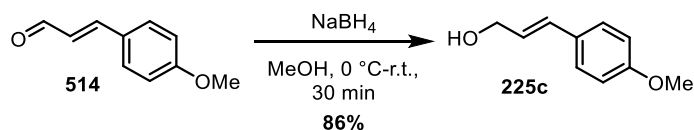
¹³C NMR (75 MHz, CDCl₃) δ [ppm] = 142.5 (C-4), 134.4 (C-9), 132.2 (C-2/6), 129.6 (C-8), 129.5 (C-3/5), 118.9 (C-7), 110.9 (C-1), 59.5 (C-10).

GC-MS (70 eV) m/z ([%]): 159 (26, [M⁺]), 140 (27), 117 (100), 103 (47), 77 (14), 51 (8).

FTIR-ATR ν [cm⁻¹] = 3838 (w), 3482 (s), 3087 (w), 3058 (w), 3040 (w), 3019 (w), 2962 (m), 2905 (m), 2833 (m), 2667 (w), 2585 (w), 2408 (b), 2354 (w), 2235 (s), 2183 (w), 2052 (w), 2023 (w), 1949 (w), 1928 (w), 1711 (m), 1634 (w), 1603 (s), 1501 (s), 1452 (w), 1416 (m), 1397 (s), 1337 (m), 1297 (m), 1252 (m), 1196 (m), 1182 (m), 1170 (m), 1117 (m), 1099 (m), 1043 (m), 1014 (s), 989 (s), 949 (m), 858 (vs), 826 (m), 807 (m), 763 (m), 729 (s), 692 (m), 651 (m), 617 (m), 558 (vs), 553 (s), 519 (s).

The analytical data are in agreement with the literature.^[217]

10.2.2.2.2. Synthesis of (E)-4-methoxycinnamic alcohol (225c)



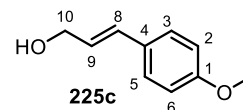
The synthesis was performed according to a procedure of Wang *et al.*^[130b] A 100 mL round-bottomed flask was charged with a solution of 4.87 g of 4-methoxycinnamic aldehyde (**514**) (30.0 mmol, 1.0 equiv.) in 100 mL of MeOH. At 0 °C, 1.14 g of NaBH₄ (30.0 mmol, 1.0 equiv.) were added in small portions over 10 min. The decolorized solution was stirred for 10 min at 0 °C and 20 min at r.t. Then 20 mL of sat. NH₄Cl solution and 20 mL of H₂O were added. The aqueous phase was extracted with MTBE (3 x 50 mL) and the combined organic phases were washed with 50 mL of H₂O and 50 mL of brine. Subsequently, the organic phase was dried

with Na₂SO₄ and concentrated under reduced pressure. Purification of the crude material by FCC (SiO₂, cHex/EtOAc 3:1) gave 4.26 g of product **225c** as a colorless solid (25.9 mmol, 86%, lit.:^[130b] 97%).

M (C₁₀H₁₂O₂) = 164.20 g/mol.

TLC (SiO₂, cHex/EtOAc 3:1) R_f = 0.23.

M.p. 78 - 80 °C.



¹H NMR (500 MHz, CDCl₃) δ [ppm] = 7.32 (d, ³J = 8.7 Hz, 2 H, H-3/5), 6.86 (d, J = 8.7 Hz, 2 H, H-2/6), 6.55 (d, ³J = 16.1 Hz, 1 H, H-8), 6.23 (dtd, ³J = 16.1 Hz, ³J = 5.8 Hz, ³J = 1.2 Hz, 1 H, H-9), 4.29 (d, ³J = 5.8 Hz, 2 H, H-10), 3.81 (s, 3 H, H-7), 1.78 – 1.43 (m, 1 H, OH).

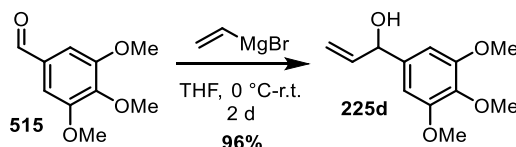
¹³C NMR (75 MHz, CDCl₃) δ [ppm] = 159.3 (C-1), 130.8 (C-8), 129.6 (C-4), 127.7 (C-3/5), 126.4 (C-9), 114.1 (C-2/6), 63.8 (C-7), 55.3 (C-10).

GC-MS (70 eV) m/z ([%]): 164 (8, [M⁺]), 148 (78), 133 (18), 121 (100), 105 (17), 91 (17), 77 (20), 65 (4), 51 (4), 39 (3).

FTIR-ATR ν [cm⁻¹] = 3354 (br), 3077 (w), 3034 (w), 3018 (w), 2970 (w), 2914 (w), 2864 (w), 1891 (w), 1772 (w), 1652 (w), 1604 (s), 1575 (w), 1510 (s), 1458 (m), 1443 (m), 1422 (w), 1367 (w), 1326 (w), 1306 (m), 1270 (m), 1242 (s), 1206 (w), 1189 (w), 1174 (s), 1153 (w), 931 (w), 1086 (s), 1025 (s), 1007 (s), 968 (s), 961 (w), 931 (w), 918 (w), 837 (s), 801 (m), 776 (m), 755 (w), 710 (w), 637 (m), 626 (m), 577 (w), 537 (m), 519 (m).

The analytical data are in agreement with the literature.^[130b]

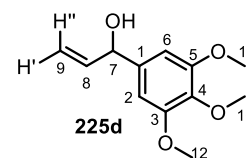
10.2.2.2.3. Synthesis of trimethoxy-allylic alcohol **225d**



The synthesis was performed according to a procedure of *Miles-Barrett et al.*^[218] Under an atmosphere of argon, a 500 mL *Schlenk* flask was charged with a solution of 3.02 g of 3,4,5-trimethoxybenzaldehyde (**515**) (15.4 mmol, 1.0 equiv.) in 75 mL of anhydrous THF. At 0 °C, 17 mL of vinylmagnesium bromide (1.0M in THF, 17 mmol, 1.1 equiv.) were added (dropwise) and the reaction mixture was stirred for 2 d. Subsequently, 50 mL of sat. NH₄Cl solution were added and the mixture was diluted with 200 mL of EtOAc. The organic phase was washed with 50 mL of H₂O before it was dried with Na₂SO₄ and concentrated under reduced pressure to give 3.11 g of **225d** as a yellow orange oil (14.7 mmol, 96%, lit.:^[218] quant.).

M (C₁₂H₁₆O₄) = 224.26 g/mol.

TLC (SiO₂, cHex/EtOAc 4:1) R_f = 0.09.



¹H NMR (500 MHz, CDCl₃) δ [ppm] = 6.59 (s, 2 H, H-2/6), 6.02 (ddd, ³J = 17.2 Hz, ³J = 10.4 Hz, ³J = 6.0 Hz, 1 H, H-8), 5.36 (dt, ³J = 17.5 Hz, ⁴J = 1.5 Hz, 1 H, H''-9), 5.20 (dt, ³J = 10.4 Hz, ⁴J = 1.5 Hz, 1 H, H'-9), 5.12 (d, ³J = 6.0 Hz, 1 H, H-7), 3.85 (s, 6 H, H-11/12), 3.82 (s, 3 H, H-10).

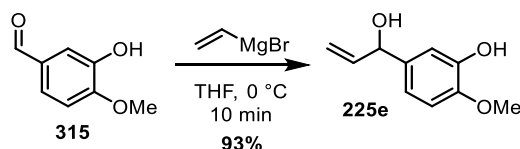
¹³C NMR (75 MHz, CDCl₃) δ [ppm] = 153.3 (C-3/5), 140.0 (C-8), 138.4 (C-1), 137.3 (C-4), 115.2 (C-9), 103.1 (C-2/6), 75.4 (C-7), 60.8 (C-10), 56.1 (C-11/12).

GC-MS (70 eV) m/z ([%]): 224 (100, [M⁺]), 209 (12), 193 (13). 169 (13).

FTIR-ATR ν [cm⁻¹] = 3676 (w), 3455 (br), 2988 (w), 2971 (br), 2940 (w), 2902 (w), 2839 (w), 2111 (w), 1736 (w), 1640 (w), 1591 (s), 1505 (m), 1456 (m), 1417 (m), 1395 (w), 1375 (w), 1327 (m), 1230 (s), 1183 (w), 1120 (s), 1066 (w), 1046 (w), 1003 (m), 922 (m), 898 (w), 835 (m), 787 (w), 758 (w), 726 (m), 688 (w), 670 (w), 634 (w), 529 (w), 463 (w), 418 (w).

The analytical data are in agreement with the literature.^[218]

10.2.2.2.4. Synthesis of phenolic-allylic alcohol 225e

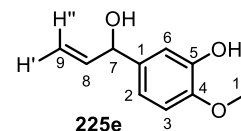


The synthesis was performed according to a procedure of Yang and coworkers.^[141b] Under an atmosphere of argon, a 500 mL *Schlenk* flask was charged with a solution of 1.52 g of 3-hydroxy-4-methoxy-benzaldehyde (**315**) (10.0 mmol, 1.0 equiv.) in 150 mL of anhydrous THF. At 0 °C, 40 mL of vinylmagnesium bromide (1.0M in THF, 40 mmol, 4.0 equiv.) were added rapidly. The resulting suspension was stirred for 10 min and subsequently, 30 mL of sat. NH₄Cl solution and 100 mL of H₂O were added. The aqueous phase was extracted with EtOAc (3 x 100 mL). The combined organic phases were washed with 50 mL H₂O before they were dried with Na₂SO₄ and concentrated under reduced pressure to give an orange crude product. Purification by FCC (SiO₂, cHex/EtOAc 2:1) gave 1.68 g of **225e** as a pale yellow solid (9.33 mmol, 93%, lit.:^[141b] quant. without purification).

M (C₁₀H₁₂O₃) = 180.20 g/mol.

TLC (SiO₂, cHex/EtOAc 2:1) R_f = 0.20.

M.p. 97 - 100 °C.



¹H NMR (300 MHz, CDCl₃) δ [ppm] = 6.94 (d, ⁴J = 2.0 Hz, 1 H, H-6), 6.86 (dd, ³J = 8.3 Hz, ⁴J = 2.0 Hz, 1 H, H-2), 6.82 (d, ³J = 8.3 Hz, 1 H, H-3), 6.02 (ddd, ³J = 17.5 Hz, ³J = 10.5 Hz, ³J = 5.6 Hz, 1 H, H-8), 5.67 (s, 1 H, OH_{Ar}), 5.33 (d, ³J = 17.5 Hz, 1 H, H''-9), 5.17 (d, ³J = 10.5 Hz, 1 H, H'-9), 5.11 (d, ³J_{H,H} = 5.6 Hz, 1 H, H-7), 3.88 (s, 3 H, H-10), 1.97 (brs, 1 H, OH).

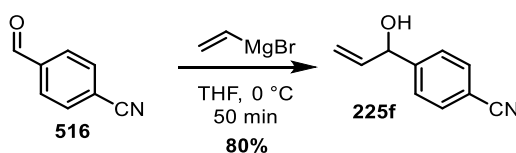
¹³C NMR (75 MHz, CDCl₃) δ [ppm] = 146.9 (C-5), 146.4 (C-4), 140.9 (C-8), 136.8 (C-1), 118.7 (C-2), 115.6 (C-9), 113.5 (C-6), 111.3 (C-3), 75.7 (C-7), 56.8 (C-10).

GC-MS (70 eV) m/z ([%]): 180 (100, [M⁺]), 162 (60), 147 (60), 125 (46), 109 (12), 93 (49), 77 (22), 55 (39), 39 (10).

FTIR-ATR ν [cm⁻¹] = 3353 (br), 3082 (w), 3008 (w), 2970 (w), 2935 (w), 2839 (w), 2275 (w), 2031 (w), 1869 (w), 1731 (w), 1639 (w), 1618 (w), 1590 (w), 1509 (s), 1437 (s), 1348 (m), 1257 (s), 1242 (s), 1216 (s), 1174 (w), 1153 (w), 1122 (s), 1040 (s), 1020 (s), 995 (m), 970 (w), 866 (m), 904 (m), 866 (m), 820 (w), 761 (s), 734 (w), 690 (w), 633 (w), 587 (w).

The analytical data are in agreement with the literature.^[141b]

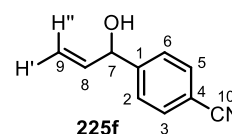
10.2.2.2.5. Synthesis of cyano-allylic alcohol **225f**



The synthesis was performed according to a procedure of *Killoran et al.*^[219] Under an atmosphere of argon, a 500 mL *Schlenk* flask was charged with a solution of 1.97 g of 4-cyanobenzaldehyde (**516**) (15.0 mmol, 1.0 equiv.) in 75 mL of anhydrous THF. At 0 °C, 20 mL of vinylmagnesium bromide (1.0M in THF, 20 mmol, 1.3 equiv.) were added rapidly. The resulting dark red suspension was stirred for 50 min and then 80 mL of sat. NH₄Cl solution were added. Subsequently, 80 mL of EtOAc were added, the organic phase separated and washed with 150 mL of brine. Drying with MgSO₄ and concentration under reduced pressure yielded a brown crude product. Purification by FCC (SiO₂, cHex/EtOAc 4:1) gave 1.58 g of **225f** as a pale yellow solid (12.1 mmol, 80%, lit.:^[219] 93%).

M (C₁₀H₉NO) = 159.19 g/mol.

TLC (SiO₂, cHex/EtOAc 4:1) R_f = 0.21.



$^1\text{H NMR}$ (300 MHz, CDCl_3) δ [ppm] = 7.63 (d, $^3J = 8.3$ Hz, 2 H, H-3/5), 7.49 (d, $^3J = 8.3$ Hz, 2 H, H-2,6), 5.97 (ddd, $^3J = 16.9$ Hz, $^3J = 10.4$ Hz, $^3J = 6.3$ Hz, 1 H, H-8), 5.41 – 5.31 (m, 2 H, H-7, H''-9), 5.26 – 5.21 (m, 1 H, H'-9).

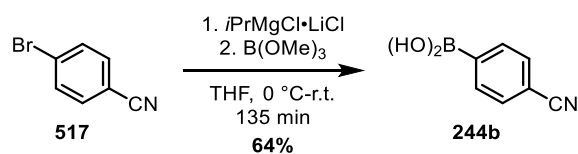
$^{13}\text{C NMR}$ (75 MHz, CDCl_3) δ [ppm] = 147.8 (C-1), 139.4 (C-8), 132.4 (C-3/5), 127.0 (C-2/6), 118.9 (C-10), 116.7 (C-9), 111.3 (C-4), 74.8 (C-7).

GC-MS (70 eV) m/z ([%]): 158 (100, $[\text{M}-\text{H}^+]$), 130 (88), 104 (59), 77 (32), 55 (20).

FTIR-ATR ν [cm^{-1}] = 3676 (w), 3419 (br), 3084 (w), 2988 (m), 2901 (m), 2229 (s), 2124 (w), 1930 (w), 1688 (w), 1640 (w), 1608 (m), 1568 (w), 1503 (w), 1408 (s), 1321 (w), 1242 (w), 1197 (w), 1173 (w), 1104 (w), 1065 (w), 1045 (w), 1018 (w), 989 (m), 927 (s), 852 (s), 818 (s), 759 (w), 706 (w), 642 (w), 558 (s), 506 (w), 419 (w).

The analytical data are in agreement with the literature.^[219]

10.2.2.2.6. Synthesis of 4-cyanophenylboronic acid (**244b**)



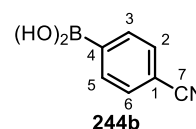
The synthesis was performed according to a procedure of *Colobert* and coworkers.^[220] Under an atmosphere of argon, a 250 mL *Schlenk* flask was charged with a solution of 7.29 g of 4-cyanobromobenzene (**517**) (40.0 mmol, 1.0 equiv.) in 40 mL of anhydrous THF. At 0 °C, 38 mL of *iPrMgCl*·*LiCl* (1.3M in THF, 49 mmol, 1.2 equiv.) were added (dropwise) and the brown solution was stirred for 2 h. At 0 °C, 9 mL of trimethyl borate were added rapidly and the suspension was stirred for 15 min at r.t. before 35 mL of 1M HCl were added (pH ~2). The aqueous phase was extracted with EtOAc (3 x 50 mL), the combined organic phases were dried with Na_2SO_4 and concentrated under reduced pressure. The crude solid was recrystallized from 110 mL of hot H_2O before it was dried for 2 d on air (to prevent anhydride formation) and by *Schlenk* line vacuum to give 3.76 g of the desired **244b** as a beige solid (25.6 mmol, 64%, lit.:^[220] 72%).

M ($\text{C}_7\text{H}_6\text{BNO}_2$) = 146.94 g/mol.

TLC (SiO_2 , *cHex*/*EtOAc* 9:1) R_f = 0.05.

M.p. >300 °C decomposition.

$^1\text{H NMR}$ (300 MHz, $\text{DMSO}-d_6$) δ [ppm] = 8.40 (brs, 2 H, BOH), 7.94 (d, $^3J = 8.1$ Hz, 2 H, H-3/5), 7.77 (d, $^3J = 8.1$ Hz, 2 H, H-2/6).



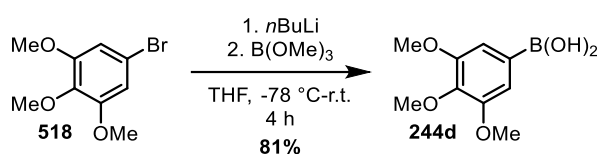
$^{13}\text{C NMR}$ (75 MHz, $\text{DMSO-}d_6$) δ [ppm] = 134.7 (C-3/5), 131.0 (C-2/6), 119.1 (C-7), 112.5 (C-1).

$^{11}\text{B NMR}$ (160 MHz, $\text{DMSO-}d_6$) δ [ppm] = 28.5.

FTIR-ATR ν [cm^{-1}] = 3508 (br), 3332 (br), 3070 (w), 3056 (w), 3028 (w), 2989 (w), 2324 (w), 2229 (s), 2177 (w), 1939 (w), 1800 (w), 1684 (w), 1610 (w), 1587 (w), 1557 (w), 1506 (w), 1484 (w), 1444 (w), 1416 (w), 1397 (w), 1371 (w), 1341 (s), 1316 (w), 1275 (m), 1209 (w), 1189 (w), 1156 (s), 1114 (w), 1061 (s), 1004 (s), 834 (s), 820 (w), 772 (m), 735 (m), 658 (w), 645 (w), 629 (w), 679 (s), 545 (w), 513 (w).

The analytical data are in agreement with the literature.^[220]

10.2.2.2.7. Synthesis of 3,4,5-trimethoxyphenylboronic acid (**244d**)



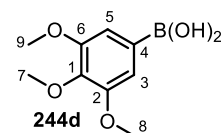
The synthesis was performed according to a procedure of *Rosen et al.*^[221] Under an atmosphere of argon, a 500 mL *Schlenk* flask was charged with a solution of 5.00 g of 3,4,5-trimethoxybromobenzene (**518**) (20.2 mmol, 1.0 equiv.) in 170 mL of anhydrous THF and cooled to -78°C . Subsequently, 9.7 mL of *n*BuLi (2.3 M, in *n*Hex, 23 mmol, 1.1 equiv.) were added (dropwise) over 10 min and the reaction mixture was stirred for 30 min. Then 7.0 mL of trimethyl borate (6.5 g, 63 mmol, 3.1 equiv.) were added over 5 min and the clear solution was warmed up to r.t. and stirred for 3.5 h. At -20°C , 10 mL of HCl ($\omega = 10\%$) were added (pH ~ 2 -3) and diluted with 100 mL of EtOAc and 100 mL of H_2O . The phases were separated and the aqueous phase extracted with EtOAc (2 x 100 mL). The combined organic phases were washed with 50 mL of brine before they were dried with Na_2SO_4 and concentrated under reduced pressure until a white precipitate formed. Precipitation was completed by the addition of 250 mL of *c*Hex. The white solid was filtered off before it was dried for 2 h on air (to prevent anhydride formation) and by *Schlenk* line vacuum to obtain 3.454 g of product **244d** as a white powder (16.3 mmol, 81%; lit.:^[221] 95%).

M ($\text{C}_9\text{H}_{13}\text{BO}_5$) = 212.01 g/mol.

TLC (SiO_2 , *c*Hex/EtOAc 2:1) $R_f = 0.00$.

M.p. $>200^\circ\text{C}$ decomposition.

$^1\text{H NMR}$ (300 MHz, CDCl_3) δ [ppm] = 7.99 (brs, 1 H, BOH), 7.11 (s, 2 H, H-3/5), 3.77 (s, 6 H, H-8/9), 3.67 (s, 3 H, H-7).



^{13}C NMR (75 MHz, CDCl_3) δ [ppm] = 152.3 (C-2/6), 139.4 (C-1), 111.2 (C-3/5), 60.0 (C-7), 55.8 (C-8/9).

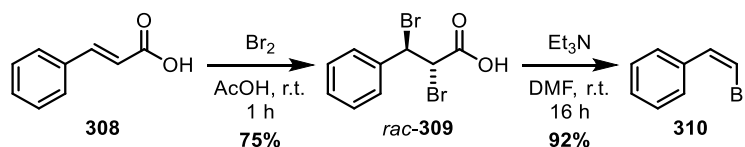
^{11}B NMR (160 MHz, $\text{DMSO}-d_6$) δ [ppm] = 19.9.

FTIR-ATR ν [cm^{-1}] = 3442 (br), 3358 (br), 3010 (w), 2038 (w), 2839 (w), 2114 (w), 1583 (m), 1511 (w), 1457 (m), 1448 (m), 1410 (s), 1342 (s), 1292 (m), 1247 (m), 1231 (m), 1184 (m), 1129 (s), 1083 (s), 1040 (w), 994 (m), 920 (w), 887 (m), 846 (m), 792 (w), 775 (m), 741 (w), 712 (w), 694 (s), 611 (s), 559 (w), 336 (w), 507 (w).

The analytical data are in agreement with the literature.^[221]

10.2.2.3. Synthesis studies towards (Z)-homostilbene

10.2.2.3.1. Synthesis of (Z)- β -bromostyrene (310)

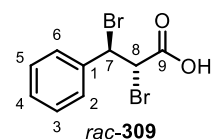


The synthesis was performed according to a procedure of Alexakis and coworkers.^[138a] A 250 mL round-bottomed flask was charged with a suspension of 14.9 g of (*E*)-cinnamic acid (**308**) (10.1 mmol, 1.0 equiv.) in 50 mL of AcOH and 5.70 mL of Br_2 (17.6 g, 110 mmol, 1.1 equiv.) were added rapidly. The resulting brown solution decolorized quickly and was stirred for 1 h at r.t. before 50 mL of 1M $\text{Na}_2\text{S}_2\text{O}_3$ were added. The white precipitate was filtered off, then washed with H_2O (3 x 20mL) and CH_3Cl (3 x 30 mL) before it was dried with Na_2SO_4 and concentrated under reduced pressure to give 23.0 g of **309** as a colorless powder (74.6 mmol, 75%, Lit.:^[138a] 90% with 12% s.m. impurity).

A 250 mL round-bottomed flask equipped with a CaCl_2 drying tube was charged with a suspension of 12.4 g of dibromo acid **309** (40.1 mmol, 1.0 equiv.) in 50 mL of DMF . At 0 °C, 11.6 mL of Et_3N (8.42 g, 83.2 mmol, 2.1 equiv.) were added (dropwise) over 5 min. The suspension cleared and the resulting solution was stirred for 16 h at r.t. Then 50 mL of H_2O were added and the aqueous phase was extracted with *n*Pe (2 x 80 mL). The combined organic phases were washed with 50 mL of H_2O before they were dried with Na_2SO_4 and concentrated under reduced pressure to obtain 6.76 g of **310** as a pale brown oil (36.9 mmol, 92%, Lit.:^[138a] 75%).

M ($\text{C}_9\text{H}_8\text{Br}_2\text{O}_2$) = 307.97 g/mol.

M.p. >204 °C decomposition.



¹H NMR (500 MHz, DMSO-*d*₆) δ [ppm] = 7.65 – 7.58 (m, 2 H, H-2/6), 7.41 – 7.30 (m, 3 H, H-3/4/5), 5.53 (d, ³*J* = 11.8 Hz, 1 H, H-7), 5.30 (d, ³*J* = 11.8 Hz, 1 H, H-8).

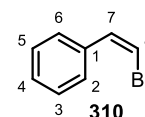
¹³C NMR (75 MHz, DMSO-*d*₆) δ [ppm] = 169.1 (C-9), 138.2 (C-1), 129.1 (C-4), 128.7 (C-3/5), 128.4 (C-2/6), 51.9 (C-7), 47.3 (C-8).

FTIR-ATR ν [cm⁻¹] = 3008 (w), 2857 (br), 1711 (s), 1496 (w), 1455 (w), 1429 (m), 1318 (w), 1297 (w), 1277 (s), 1219 (m), 1199 (w), 1164 (w), 1146 (m), 1108 (w), 1088 (w), 1061 (w), 1031 (w), 1001 (w), 910 (s), 838 (w), 780 (w), 767 (m), 690 (s), 657 (m), 622 (w), 597 (s), 558 (s), 525 (s), 474 (w).

The analytical data are in agreement with the literature.^[138a]

M (C₈H₇Br) = 183.05 g/mol.

TLC (SiO₂, cHex) R_f = 0.55.



¹H NMR (500 MHz, CDCl₃) δ [ppm] = 7.73 – 7.61 (m, 2 H, H-2/6), 7.39 – 7.35 (m, 2 H, H-3/5), 7.33 – 7.29 (m, 1 H, H-4), 7.05 (d, ³*J* = 8.2 Hz, 1 H, H-7), 6.42 (d, ³*J* = 8.2 Hz, 1 H, H-8).

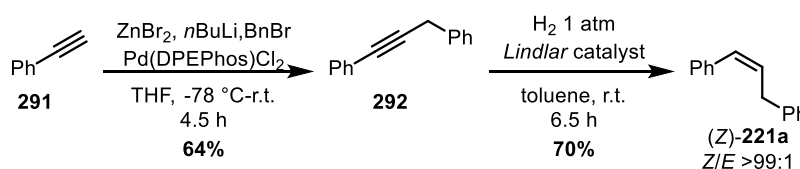
¹³C NMR (75 MHz, CDCl₃) δ [ppm] = 135.0 (C-1), 132.5 (C-7), 129.1 (C-2/6), 128.44 (C-4), 128.35 (C-3/5), 106.5 (C-8).

GC-MS (70 eV) m/z ([%]): 182 (83, [M⁺]), 103 (100), 77 (74), (41).

FTIR-ATR ν [cm⁻¹] = 3078 (w), 3054 (w), 3025 (w), 3000 (w), 2917 (w), 1950 (w), 1879 (w), 1804 (w), 1752 (w), 1679 (w), 1614 (w), 1575 (w), 1537 (w), 1480 (m), 1445 (m), 1385 (w), 1323 (s), 1316 (s), 1298 (w), 1212 (w), 1183 (w), 1169 (w), 1073 (w), 1029 (w), 1001 (w), 967 (w), 924 (w), 913 (w), 827 (m), 766 (s), 691 (s), 679 (s), 623 (s), 571 (s), 511 (s), 468 (w).

The analytical data are in agreement with the literature.^[138a]

10.2.2.3.2. Synthesis of (*Z*)-1,3-diphenylpropene ((*Z*)-221a)



The synthesis was performed according to a procedure of *Negishi* and coworkers.^[139] Under an atmosphere of argon, a 100 mL *Schlenk* flask was charged with a solution of 1.3 mL of phenylacetylene (**291**) (1.2 g, 12 mmol, 1.2 equiv.) in 30 mL of anhydrous THF. This solution

was cooled to $-78\text{ }^{\circ}\text{C}$ and treated (dropwise) with 5.2 mL of *n*BuLi (2.3M in *n*Hex, 12 mmol, 1.2 equiv.) over 5 min. The orange solution was stirred for 30 min before a solution of 2.70 g of ZnBr_2 (12.0 mmol, 1.2 equiv.) in 10 mL of anhydrous THF was added. The reaction was warmed up to r.t. over 30 min. Subsequently, 1.2 mL of BnBr (1.7 g, 10 mmol, 1.0 equiv.) and 68 mg of $\text{Pd}(\text{DPEPhos})\text{Cl}_2$ (95 μmol , 1 mol%) were added. The resulting yellow solution was stirred for 4.5 h before 30 mL of 1M HCl were added. The aqueous phase was extracted with MTBE (3 x 50 mL) and the combined organic phases washed with 50 mL of sat. NaHCO_3 solution. Drying with MgSO_4 and concentration under reduced pressure gave a yellow crude material. Purification by FCC (SiO_2 , *c*Hex) gave 1.48 g of **292** as a pale yellow liquid (7.70 mmol, 64%; lit.:^[139] 91%).

Under an atmosphere of argon, a 50 mL *Schlenk* flask was charged with a suspension of 600 mg of **292** (3.12 mmol, 1.0 equiv.) and 332 mg of *Lindlar* catalyst ($\omega(\text{Pd}) = 5\%$, 0.156 mmol, 5.0 mol%) in 12 mL of dry toluene. Argon was removed by *Schlenk* line vacuum and H_2 atmosphere (1 atm.) was applied. The reaction mixture was stirred for 6.5 h. The suspension was filtered over *Celite* and concentrated under reduced pressure to give a yellow crude material. After purification by FCC (SiO_2 , *c*Hex) 405 mg of (*Z*)-**221a** as a colorless liquid were obtained (2.20 mmol, 70%, *E/Z* >99:1).

M ($\text{C}_{15}\text{H}_{12}$) = 192.26 g/mol.

TLC (SiO_2 , *c*Hex) $R_f = 0.29$.

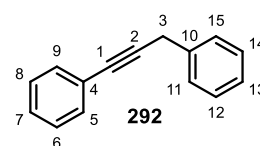
$^1\text{H NMR}$ (300 MHz, CDCl_3) δ [ppm] = 7.49 – 7.37 (m, 4 H, H-5/9/11/15), 7.36 – 7.16 (m, 6 H, H-6/7/8/12/13/14), 3.81 (s, 2 H, H-3).

$^{13}\text{C NMR}$ (75 MHz, CDCl_3) δ [ppm] = 136.9 (C-4), 131.8 (C-11/15), 128.7 (C-6/8), 128.4 (C-12/14), 128.1 (C-5/9), 127.9 (C-13), 126.8 (C-7), 123.8 (C-10), 87.7 (C-2), 82.8 (C-1), 25.9 (C-3).

GC-MS (70 eV) m/z ([%]): 192 (100, $[\text{M}^+]$), 165 (28), 139 (4), 115 (24), 94 (8), 77 (3), 63 (7).

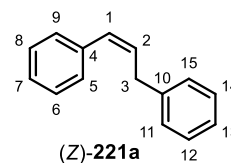
FTIR-ATR ν [cm^{-1}] = 3062 (w), 3029 (w), 2989 (w), 2901 (w), 2235 (w), 2200 (w), 1949 (w), 1880 (w), 1805 (w), 1598 (m), 1490 (s), 1453 (m), 1442 (m), 1417 (w), 1394 (w), 1337 (w), 1318 (w), 1289 (w), 1250 (w), 1204 (w), 1177 (w), 1157 (w), 1070 (m), 1028 (m), 939 (w), 914 (w), 754 (s), 732 (m), 711 (m), 689 (s), 621 (w), 603 (m), 527 (m), 512 (w), 486 (w), 454 (w).

The analytical data are in agreement with the literature.^[139]



M (C₁₅H₁₄) = 194.28 g/mol.

TLC (SiO₂, cHex) R_f = 0.36.



¹H NMR (500 MHz, CDCl₃) δ [ppm] = 7.38 – 7.27 (m, 6 H, H-5/6/8/9/11/15), 7.26 – 7.16 (m, 4 H, H-7/12/13/14), 6.59 (dt, ³J = 11.5 Hz, ⁴J = 1.8 Hz, 1 H, H-1), 5.86 (dt, ³J = 11.5 Hz, ³J = 7.5 Hz, 1 H, H-2), 3.68 (dd, ³J = 7.5 Hz, ⁴J = 1.8 Hz, 2 H, H-3).

¹³C NMR (75 MHz, CDCl₃) δ [ppm] = 140.9 (C-10), 137.4 (C-4), 130.8 (C-2), 130.1 (C-1), 128.8 (C-5/9), 128.7 (C-11/15), 128.5 (C-6/8), 128.4 (C-12/14), 127.0 (C-13), 126.2 (C-7), 34.8 (C-3).

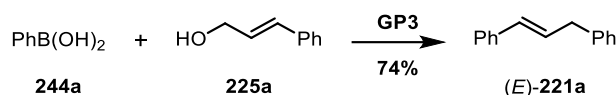
GC-MS (70 eV) m/z ([%]): 194 (100, [M⁺]), 179 (61), 165 (18), 115 (83), 103 (19), 91 (35), 65 (16).

FTIR-ATR ν [cm⁻¹] = 3082 (w), 3060 (w), 3024 (w), 2989 (w), 2901 (w), 1946 (w), 1880 (w), 1805 (w), 1741 (w), 1601 (w), 1494 (s), 1452 (m), 1447 (m), 1404 (w), 1330 (w), 1250 (w), 1179 (w), 1156 (w), 1075 (m), 1057 (w), 1029 (m), 966 (w), 916 (w), 888 (w), 823 (w), 808 (w), 795 (w), 766 (s), 735 (s), 695 (w), 619 (w), 594 (w), 497 (s), 470 (m), 404 (w).

The analytical data are in agreement with the literature.^[222]

10.2.2.4. Homostilbenes by direct coupling of allylic alcohols with boronic acids

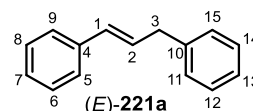
10.2.2.4.1. Synthesis of (*E*)-homostilbene (221a)



According to the general procedure **GP3**, 813 mg of cinnamic alcohol (**225a**) (6.06 mmol, 1.0 equiv.) were reacted with 887 mg of phenylboronic acid (**244a**) (7.27 mmol, 1.2 equiv.) and 337 mg of Pd(PPh₃)₄ (0.292 mmol, 4.8 mol%). Purification by FCC (cHex) gave 870 mg of **221a** as a colorless liquid (4.48 mmol, 74%; lit.:^[130a] 66%).

M (C₁₅H₁₄) = 194.28 g/mol.

TLC (SiO₂, cHex) R_f = 0.15.



¹H NMR (500 MHz, CDCl₃) δ [ppm] = 7.34 (d, ³J = 7.8 Hz, 2 H, H-5/9), 7.31 – 7.24 (m, 4 H, H-6/8/12/14), 7.24 – 7.21 (m, 2 H, H-11/15), 7.20 – 7.15 (m, 2 H, H-7/13), 6.44 (d, ³J = 15.9 Hz, 1 H, H-1), 6.35 (dt, ³J = 15.9 Hz, ³J = 6.8 Hz, 1 H, H-2), 3.53 (d, ³J = 6.8 Hz, 1 H, H-3).

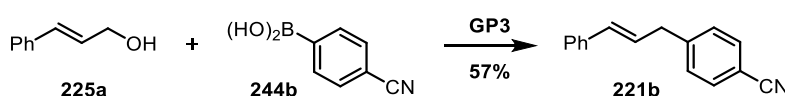
¹³C NMR (75 MHz, CDCl₃) δ [ppm] = 140.3 (C-10), 137.6 (C-4), 131.2 (C-1), 129.4 (C-2), 128.8 (C-11/15), 128.6 (C-6/8/12/14), 127.2 (C-7), 126.31 (C-13), 126.26 (C-5/9), 39.5 (C-3).

GC-MS (70 eV) m/z ([%]): 194 (98, [M⁺]), 179 (54), 165 (20), 115 (100), 91 (61), 77 (26), 65 (27), 51 (28).

FTIR-ATR ν [cm⁻¹] = 3083 (w), 3061 (w), 3026 (w), 3001 (w), 2989 (w), 2955 (w), 2901 (w), 2241 (w), 1948 (w), 1875 (w), 1806 (w), 1751 (w), 1653 (w), 1601 (w), 1495 (m), 1453 (m), 1430 (w), 1394 (w), 1307 (w), 1250 (w), 1210 (w), 1179 (w), 1156 (w), 1076 (w), 1057 (w), 1029 (w), 1003 (w), 964 (s), 935 (w), 909 (w), 857 (w), 843 (w), 790 (w), 738 (s), 692 (s), 620 (w), 612 (w), 598 (w), 584 (w), 571 (w), 555 (w).

The analytical data are in agreement with the literature.^[130a]

10.2.2.4.2. Synthesis of homostilbene **221b**

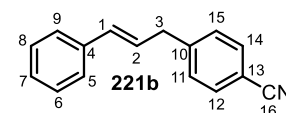


According to the general procedure **GP3**, 524 mg of cinnamic alcohol (**225a**) (3.91 mmol, 1.0 equiv.) were reacted with 887 mg of phenylboronic acid **244b** (4.57 mmol, 1.2 equiv.) and 227 mg of Pd(PPh₃)₄ (0.196 mmol, 5.0 mol%). Purification by FCC (cHex/EtOAc 15:1) gave 488 mg of **221b** as a pale yellow solid (2.23 mmol, 57%).

M (C₁₆H₁₃N) = 219.29 g/mol.

TLC (SiO₂, cHex/EtOAc 15:1) R_f = 0.25.

M.p. 46 - 48 °C.



¹H NMR (500 MHz, CDCl₃) δ [ppm] = 7.60 (d, ³J = 8.3 Hz, 2 H, H-12/14), 7.38 – 7.34 (m, 4 H, H-5/9/11/15), 7.34 – 7.29 (m, 2 H, H-6/8), 7.25 – 7.20 (m, 1 H, H-7), 6.48 (d, ³J = 15.7 Hz, 1 H, H-1), 6.30 (dt, ³J = 15.7 Hz, ³J = 6.9 Hz, 1 H, H-2), 3.61 (d, ³J = 6.9 Hz, 2 H, H-3).

¹³C NMR (75 MHz, CDCl₃) δ [ppm] = 145.9 (C-4), 137.0 (C-10), 132.5 (C-1), 132.4 (C-12/14), 129.6 (C-11/15), 128.7 (C-6/8), 127.6 (C-7), 127.3 (C-2), 126.3 (C-5/9), 119.1 (C-16), 110.2 (C-13), 39.4 (C-3).

GC-MS (70 eV) m/z ([%]): 219 (100, [M⁺]), 204 (69), 190 (20), 165 (11), 140 (43), 115 (69), 91 (54), 77 (36), 51 (23).

FTIR-ATR ν [cm⁻¹] = 3061 (w), 3059 (w), 3027 (w), 2844 (w), 2227 (m), 1606 (w), 1495 (m), 1448 (w), 1111 (m), 965 (s), 829 (m), 748 (s), 692 (s), 561 (s).

The analytical data are in agreement with the literature.^[130a]

10.2.2.4.3. Synthesis of homostilbene 221c

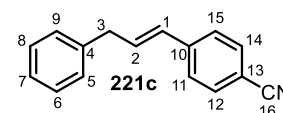


According to the general procedure **GP3**, 1.12 g of cinnamic alcohol **225b** (6.73 mmol, 1.0 equiv.) were reacted with 1.36 g of phenylboronic acid (**244a**) (8.74 mmol, 1.3 equiv.) and 410 mg of Pd(PPh₃)₄ (0.355 mmol, 5.3 mol%). Purification by FCC (cHex/EtOAc 15:1) gave 1.07 g of **221c** as a colorless solid (4.88 mmol, 73%; *E/Z* 96:4).

M (C₁₆H₁₃N) = 219.29 g/mol.

TLC (SiO₂, cHex/EtOAc 15:1) R_f = 0.36.

M.p. 53 - 56 °C.



¹H NMR (500 MHz, CDCl₃) δ [ppm] = 7.54 (d, ³J = 8.4 Hz, 2 H, H-12/14), 7.40 (d, ³J = 8.4 Hz, 2 H, H-11/15), 7.32 (dd, ³J = 6.7 Hz, 2 H, H-6/8), 7.23 (m, 3 H, H-5/7/9), 6.57 (dt, ³J = 15.8 Hz, ³J = 6.5 Hz, 1 H, H-2), 6.44 (d, ³J = 15.8 Hz, 1 H, H-1), 3.57 (d, ³J = 6.5 Hz, 2 H, H-3).

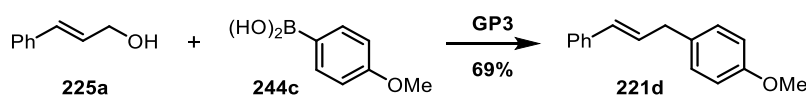
¹³C NMR (75 MHz, CDCl₃) δ [ppm] = 142.0 (C-10), 139.3 (C-4), 133.7 (C-2), 132.4 (C-12/14), 129.6 (C-1), 128.8 (C-5/9), 128.74 (C-6/8), 126.7 (C-11/15), 126.6 (C-7), 119.1 (C-16), 110.4 (C-13), 39.5 (C-3).

GC-MS (70 eV) m/z ([%]): 219 (100, [M⁺]), 204 (34), 190 (9), 140 (18), 115 (19), 91 (16).

FTIR-ATR ν [cm⁻¹] = 3676 (w), 3398 (w), 3084 (w), 3061 (w), 3027 (w), 3003 (w), 2901 (w), 2224 (m), 2173 (w), 1917 (w), 1806 (w), 1751 (w), 1648 (m), 1603 (m), 1507 (m), 1494 (m), 1453 (m), 1428 (w), 1411 (m), 1342 (w), 1305 (w), 1257 (w), 1197 (w), 1175 (m), 1156 (w), 1108 (w), 1076 (w), 1051 (w), 1029 (w), 1018 (w), 1003 (w), 968 (m), 934 (w), 866 (m), 840 (m), 819 (m), 781 (m), 750 (m), 697 (s), 648 (w), 615 (w), 586 (m), 546 (s).

The analytical data are in agreement with the literature.^[129b]

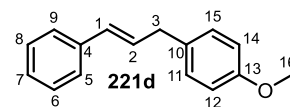
10.2.2.4.4. Synthesis of homostilbene 221d



According to the general procedure **GP3**, 570 mg of cinnamic alcohol **225a** (4.25 mmol, 1.0 equiv.) were reacted with 762 mg of phenylboronic acid **244c** (5.01 mmol, 1.2 equiv.) and 226 mg of Pd(PPh₃)₄ (0.196 mmol, 4.6 mol%). Purification by FCC (cHex) gave 623 mg of **221d** as a yellow oil (2.78 mmol, 69%).

M (C₁₆H₁₆O) = 224.30 g/mol.

TLC (SiO₂, cHex) R_f = 0.19.



¹H NMR (500 MHz, CDCl₃) δ [ppm] = 7.37 – 7.31 (m, 2 H, H-5/9), 7.31 – 7.24 (m, 2 H, H-6/8), 7.24 – 7.11 (m, 3 H, H-7/11/15), 6.93 – 6.79 (m, 2 H, H-12/14), 6.49 – 6.39 (m, 1 H, H-1), 6.39 – 6.26 (m, 1 H, H-2), 3.80 – 3.72 (m, 3 H, H-16), 3.51 – 3.43 (m, 2 H, H-3).

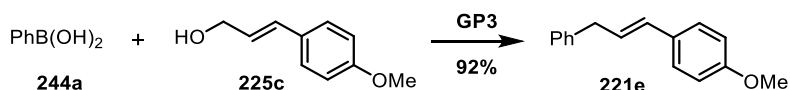
¹³C NMR (75 MHz, CDCl₃) δ [ppm] = 158.2 (C-13), 137.7 (C-4), 132.3 (C-10), 130.9 (C-1), 129.8 (C-2), 129.7 (C-11/15), 128.6 (C-6/8), 127.2 (C-7), 126.2 (C-5/9), 114.0 (C-12/14), 55.4 (C-16), 38.6 (C-3).

GC-MS (70 eV) m/z ([%]): 224 (89, [M⁺]), 209 (20), 193 (28), 178 (23), 165 (25), 115 (100), 102 (30), 91 (63), 78 (74), 63 (32), 51 (45).

FTIR-ATR ν [cm⁻¹] = 3081 (w), 3059 (w), 3026 (w), 3001 (w), 2954 (w), 2933 (w), 2902 (w), 2834 (w), 2058 (w), 1950 (w), 1880 (w), 1651 (w), 1610 (m), 1584 (w), 1510 (s), 1497 (w), 1463 (w), 1449 (w), 1441 (w), 1320 (w), 1300 (m), 1242 (s), 1175 (m), 1107 (w), 1074 (w), 1034 (m), 965 (m), 919 (w), 862 (w), 826 (s), 812 (m), 755 (m), 727 (s), 691 (s), 639 (w), 610 (w), 562 (w), 515 (w).

The analytical data are in agreement with the literature.^[130a]

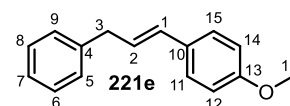
10.2.2.4.5. Synthesis of homostilbene 221e



According to the general procedure **GP3**, 988 mg of cinnamic alcohol **225c** (6.02 mmol, 1.0 equiv.) were reacted with 888 mg of phenylboronic acid (**244a**) (7.28 mmol, 1.2 equiv.) and 348 mg of Pd(PPh₃)₄ (0.301 mmol, 5.0 mol%). Purification by FCC (cHex/EtOAc 10:1) gave 1.24 g of **221e** as a pale yellow oil (5.52 mmol, 92%).

M (C₁₆H₁₆O) = 224.30 g/mol.

TLC (SiO₂, cHex/EtOAc 9:1) R_f = 0.62.



¹H NMR (500 MHz, CDCl₃) δ [ppm] = 7.33 – 7.25 (m, 4 H, H-6/8/11/15), 7.24 – 7.15 (m, 3 H, H-5/7/9), 6.81 (d, ³J = 8.8 Hz, 2 H, H-12/14), 6.38 (d, ³J = 15.7 Hz, 1 H, H-1), 6.19 (dt, ³J = 15.7 Hz, ³J = 6.9 Hz, 1 H, H-2), 3.77 (s, 3 H, H-16), 3.51 (d, ³J = 6.9 Hz, 2 H, H-3).

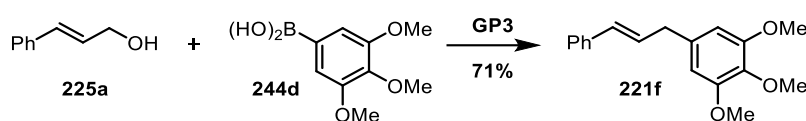
¹³C NMR (75 MHz, CDCl₃) δ [ppm] = 159.0 (C-13), 140.6 (C-4), 130.6 (C-1), 130.4 (C-10), 128.8 (C-5/9), 128.6 (C-6/8), 127.4 (C-11/15), 127.2 (C-2), 126.2 (C-7), 114.1 (C-12/14), 55.4 (C-16), 39.5 (C-3).

GC-MS (70 eV) m/z ([%]): 224 (100, $[M^+]$), 209 (19), 193 (23), 178 (16), 165 (14), 147 (8), 134 (8), 121 (52), 115 (25), 103 (7), 91 (17), 77 (10).

FTIR-ATR ν [cm^{-1}] = 3061 (w), 3027 (w), 3001 (w), 2956 (w), 2934 (w), 2902 (w), 2834 (w), 2548 (w), 2059 (w), 1948 (w), 1948 (w), 1882 (w), 1808 (w), 1739 (w), 1652 (w), 1606 (m), 1577 (w), 1509 (s), 1494 (w), 1464 (w), 1453 (w), 1441 (w), 1419 (w), 1294 (w), 1242 (s), 1174 (m), 1109 (w), 1075 (w), 1032 (m), 965 (m), 932 (m), 861 (w), 832 (m), 780 (m), 739 (m), 713 (w), 697 (s), 639 (w), 609 (w), 579 (w), 568 (w), 547 (w), 519 (m).

The analytical data are in agreement with the literature.^[129b]

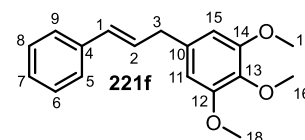
10.2.2.4.6. Synthesis of homostilbene **221f**



According to the general procedure **GP3**, 538 mg of cinnamic alcohol **225a** (4.00 mmol, 1.0 equiv.) were reacted with 1.02 g of phenylboronic acid **244d** (4.80 mmol, 1.2 equiv.) and 229 mg of $\text{Pd}(\text{PPh}_3)_4$ (0.19 mmol, 5.0 mol%). Purification by repeated FCC (cHex/EtOAc 9:1 and 15:1) gave 925 mg of a pale yellow oil with 1,2,3-trimethoxybenzene as inseparable byproduct ($w(\text{TMB}) = 13\%$, 805 mg of **221f**, 2.83 mmol, 71%).

M ($\text{C}_{18}\text{H}_{20}\text{O}_3$) = 284.36 g/mol.

TLC (SiO_2 , cHex/EtOAc 9:1) $R_f = 0.27$.



$^1\text{H NMR}$ (600 MHz, CDCl_3) δ [ppm] = 7.42 – 7.36 (m, 2 H, H-5/9), 7.33 – 7.28 (m, 2 H, H-6/8), 7.25 – 7.20 (m, 1 H, H-7), 6.48 (d, $^3J = 15.7$ Hz, 1 H, H-1), 6.47 (s, 2 H, H-11/15), 6.35 (dt, $^3J = 15.7$ Hz, $^3J = 6.9$ Hz, 1 H, H-2), 3.86 (s, 6 H, H-17/18), 3.85 (s, 3 H, H-16), 3.50 (dd, $^3J = 6.9$ Hz, $^3J = 1.3$ Hz, 2 H, H-3).

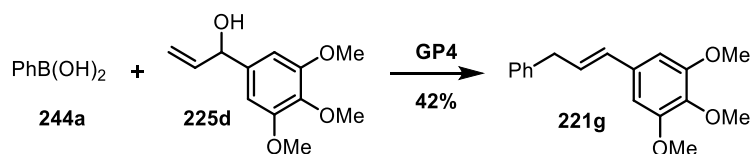
$^{13}\text{C NMR}$ (151 MHz, CDCl_3) δ [ppm] = 153.4 (C-12/14), 137.5 (C-4), 136.5 (C-13), 136.0 (C-10), 131.3 (C-1), 129.1 (C-2), 128.6 (C-6/8), 127.3 (C-7), 126.3 (C-5/9), 105.6 (C-11/15), 61.0 (C-16), 56.2 (C-17/18), 39.8 (C-3).

GC-MS (70 eV) m/z ([%]): 284 (100, $[M^+]$), 269 (19), 253 (56), 237 (15), 209 (19), 194 (23), 165 (18), 115 (31).

FTIR-ATR ν [cm^{-1}] = 3058 (w), 2989 (w), 2961 (w), 2937 (w), 2902 (w), 2836 (w), 2100, 1951 (w), 1885 (w), 1677 (w), 1649 (w), 1589 (s), 1506 (m), 1496 (m), 1477 (w), 1455 (m), 1418 (m), 1329 (m), 1297 (w), 1233 (s), 1183 (w), 1148 (w), 1124 (s), 1110 (s), 1067 (w), 1039 (w), 1058 (w), 1007 (s), 967 (m), 940 (w), 914 (w), 866 (w), 827 (w), 803 (w), 777 (w), 739 (m), 694 (m), 670 (w), 646 (w), 620 (w), 576 (w), 527 (w), 495 (w).

The analytical data are in agreement with the literature.^[223]

10.2.2.4.7. Synthesis of homostilbene **221g**

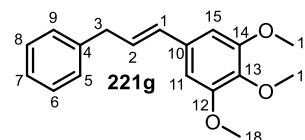


According to the general procedure **GP4**, 1.15 g of allylic alcohol **225d** (5.10 mmol, 1.0 equiv.) were reacted with 733 mg of phenylboronic acid (**244a**) (4.81 mmol, 1.2 equiv.) and 292 mg of Pd(PPh₃)₄ (0.253 mmol, 5.0 mol%). Purification by FCC (cHex/EtOAc 3:1) gave 609 mg of **221g** as a pale yellow solid (2.14 mmol, 42%).

M (C₁₈H₂₀O₃) = 284.36 g/mol.

TLC (SiO₂, cHex/EtOAc 3:1) R_f = 0.45.

M.p. 51 - 59 °C.



¹H NMR (500 MHz, CDCl₃) δ [ppm] = 7.32 (t, ³J = 7.5 Hz, 2 H, H-6/8), 7.27 – 7.21 (m, 3 H, H-5/7/9), 6.58 (s, 2 H, H-11/15), 6.38 (dt, ³J = 15.8 Hz, ⁴J = 1.4 Hz, 1 H, H-1), 6.27 (dt, ³J = 15.8 Hz, ³J = 6.7 Hz, 1 H, H-2), 3.86 (s, 6 H, H-17/18), 3.83 (s, 3 H, H-16), 3.55 (dd, ³J = 6.7 Hz, ¹J = 1.4 Hz, 2 H, H-3).

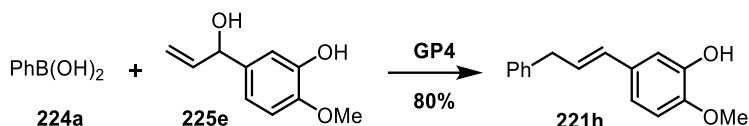
¹³C NMR (75 MHz, CDCl₃) δ [ppm] = 153.4 (C-12/14), 140.2 (C-4), 137.6 (C-13), 133.4 (C-10), 131.1 (C-1), 129.0 (C-2), 128.9 (C-5/9), 128.7 (C-6/8), 126.4 (C-7), 103.3 (C-11/15), 61.1 (C-16), 56.2 (C-17/18), 39.4 (C-3).

GC-MS (70 eV) m/z ([%]): 284 (100, [M⁺]), 253 (46), 115 (23).

FTIR-ATR ν [cm⁻¹] = 3676 (w), 3430 (w), 3061 (w), 2989 (br), 2971 (w), 2937 (w), 2902 (w), 2837 (w), 2120 (w), 1959 (w), 1735 (w), 1651 (w), 1580 (s), 1506 (m), 1496 (w), 1463 (w), 1452 (m), 1416 (s), 1395 (w), 1346 (w), 1325 (w), 1237 (s), 1184 (w), 1151 (w), 1123 (s), 1076 (w), 1067 (w), 1046 (w), 1028 (w), 1005 (m), 964 (m), 922 (w), 849 (w), 826 (w), 778 (w), 751 (m), 699 (s), 644 (w), 632 (w), 620 (w), 569 (w), 528 (w), 510 (w), 494 (w), 459 (w), 418 (w).

The analytical data are in agreement with the literature.^[224]

10.2.2.4.8. Synthesis of homostilbene 221h

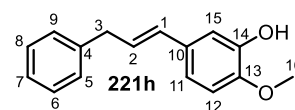


According to the general procedure **GP4**, 901 mg of allylic alcohol **225e** (5.00 mmol, 1.0 equiv.) were reacted with 731 mg of phenylboronic acid (**244a**) (6.00 mmol, 1.2 equiv.) and 289 mg of $\text{Pd}(\text{PPh}_3)_4$ (0.250 mmol, 5.0 mol%). Purification by FCC (cHex/EtOAc 5:1) gave 958 mg of **221g** as a pale yellow solid (3.99 mmol, 80%).

M ($\text{C}_{16}\text{H}_{16}\text{O}_2$) = 240.30 g/mol.

TLC (SiO_2 , cHex/EtOAc 5:1) R_f = 0.29.

M.p. 61 - 63 °C.



$^1\text{H NMR}$ (600 MHz, CDCl_3) δ [ppm] = 7.32 – 7.26 (m, 2 H, H-6/8), 7.24 – 7.16 (m, 3 H, H-5/7/9), 6.98 (d, 4J = 2.1 Hz, 1 H, H-15), 6.80 (dd, 3J = 8.3 Hz, 4J = 2.1 Hz, 1 H, H-11), 6.74 (d, 3J = 8.3 Hz, 1 H, H-12), 6.34 (dt, 3J = 15.7 Hz, 4J = 1.5 Hz, 1 H, H-1), 6.19 (dt, 3J = 15.7 Hz, 3J = 6.9 Hz, 1 H, H-2), 5.59 (s, 1 h, OH), 3.82 (s, 3 H, H-16), 3.50 (d, 3J = 6.9 Hz, 2 H, H-3).

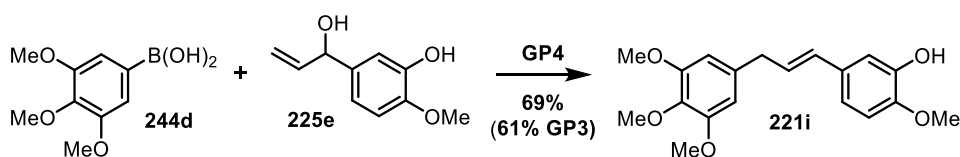
$^{13}\text{C NMR}$ (151 MHz, CDCl_3) δ [ppm] = 146.0 (C-13), 145.7 (C-14), 140.5 (C-4), 131.4 (C-10), 130.6 (C-1), 128.7 (C-5/9), 128.6 (C-6/8), 127.7 (C-2), 126.2 (C-7), 118.6 (C-11), 111.9 (C-15), 110.7 (C-12), 56.1 (C-16), 39.4 (C-3).

GC-MS (70 eV) m/z ([%]): 240 (100, $[\text{M}^+]$), 223 (12), 207 (19), 179 (20), 152 (6), 131 (7), 115 (30), 91 (20), 65 (6).

HR-EI-MS m/z calculated [$\text{C}_{16}\text{H}_{16}\text{O}_2^+$]: 240.11448; found: 240.11414.

FTIR-ATR ν [cm^{-1}] = 3438 (br), 3080 (w), 3038 (w), 3024 (w), 3002 (w), 2958 (w), 2932 (w), 2915 (w), 2882 (w), 2838 (w), 2285 (w), 2113 (w), 2037 (w), 1981 (w), 1958 (w), 1885 (w), 1850 (w), 1813 (w), 1740 (w), 1654 (w), 1603 (w), 1590 (m), 1523 (s), 1493 (m), 1462 (w), 1450 (w), 1436 (s), 1426 (w), 1358 (w), 1335 (w), 1310 (w), 1257 (w), 1273 (w), 1257 (w), 1234 (s), 1207 (s), 1199 (w), 1160 (w), 1125 (s), 1063 (w), 1022 (s), 967 (s), 930 (w), 886 (w), 870 (s), 845 (w), 809 (s), 778 (w), 755 (s), 727 (s), 695 (s), 632 (w), 535 (w), 598 (w), 569 (m), 535 (m), 500 (m), 459 (s).

10.2.2.4.9. Synthesis of homostilbene 221i

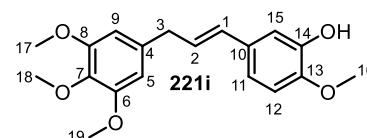


According to the general procedure **GP4**, 902 mg of allylic alcohol **225e** (5.01 mmol, 1.0 equiv.) were reacted with 1.28 g of phenylboronic acid **244d** (6.01 mmol, 1.2 equiv.) and 290 mg of Pd(PPh₃)₄ (0.251 mmol, 5.0 mol%). Purification by FCC (cHex/EtOAc 3:1) gave 1.14 g of **221i** as a pale yellow solid (3.46 mmol, 69%; 61% following **GP3**).

M (C₁₉H₂₂O₅) = 330.38 g/mol.

TLC (SiO₂, cHex/EtOAc 2:1) R_f = 0.36.

M.p. 96 - 100 °C.



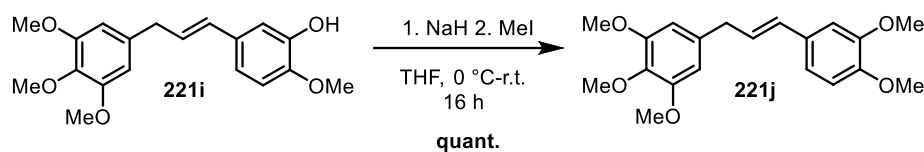
¹H NMR (500 MHz, CDCl₃) δ [ppm] = 7.04 (d, ⁴J = 2.1 Hz, 1 H, H-15), 6.86 (dd, ³J = 8.3 Hz, ⁴J = 2.1 Hz, 1 H, H-11), 6.80 (d, ³J = 8.3 Hz, 1 H, H-12), 6.48 (s, 2 H, H-5/9), 6.39 (d, ³J = 15.7 Hz, 1 H, H-1), 6.21 (dt, ³J = 15.7 Hz, ³J = 6.9 Hz, 1 H, H-2), 5.77 (s, 1 H, OH), 3.87 (ψs, 12 H, H-16/17/18/19), 3.48 (d, ³J = 6.9 Hz, 2 H, H-3).

¹³C NMR (126 MHz, CDCl₃) δ [ppm] = 153.2 (C-6/8), 146.1 (C-13), 145.7 (C-14), 136.3 (C-7), 136.2 (C-4), 131.2 (C-10), 130.7 (C-1), 127.2 (C-2), 118.5 (C-11), 111.8 (C-15), 110.6 (C-12), 105.5 (C-5/9), 60.8 (C-18), 56.1 (C-17/19), 56.0 (C-16), 39.6 (C-3).

GC-MS (70 eV) m/z ([%]): 330 (100, [M⁺]), 315 (11), 299 (29), 283 (11), 268 (7), 240 (7), 225 (4), 207 (44), 182 (13), 167 (13), 139 (55), 124 (11), 109 (13), 93 (4), 77 (18), 53 (11).

HR-ESI-MS m/z calculated [C₁₉H₂₂O₅+Na⁺]: 353.1359450; found: 353.13610.

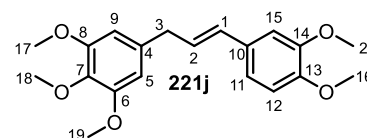
FTIR-ATR ν [cm⁻¹] = 3315 (br), 3006 (w), 2934 (w), 2838 (w), 2136 (w), 2104 (w), 1980 (w), 1843 (w), 1733 (w), 1615 (w), 1592 (m), 1581 (m), 1509 (m), 1459 (m), 1451 (m), 1437 (m), 1420 (m), 1339 (w), 1313 (w), 1279 (m), 1263 (m), 1240 (m), 1231 (m), 1184 (w), 1174 (w), 1149 (w), 1125 (s), 1052 (w), 1047 (w), 1026 (m), 1011 (m), 964 (m), 931 (w), 908 (w), 883 (w), 868 (w), 833 (w), 824 (w), 799 (m), 781 (w), 766 (w), 755 (w), 745 (w), 681 (w), 647 (w), 605 (m), 594 (w), 577 (w), 527 (w), 500 (w), 466 (w).

10.2.2.4.10. Synthesis of homostilbene **221j**

Under an atmosphere of argon, a 50 mL *Schlenk* flask was charged with a solution of 550 mg of homostilbene **221i** (1.67 mmol, 1.0 equiv.) in 5 mL of anhydrous THF. At 0 °C 157 mg of NaH (dispersion in paraffin oil, $\omega = 60\%$, 94 mg, 3.93 mmol, 2.4 equiv.) were added in small portions over 10 min. When the gas formation stopped, the reaction mixture was stirred for 20 min at r.t. before 0.41 mL of MeI (0.93 g, 6.6 mmol, 4.0 equiv.) were slowly added over 5 min. The orange suspension was stirred for 16 h and then 10 mL of brine were added. Extraction with EtOAc (3 x 15 mL), drying with Na₂SO₄ was followed by concentration under reduced pressure to give a brown crude product. Purification by FCC (SiO₂, cHex/EtOAc 4:1) gave 570 mg of **221i** as a pale orange oil (1.66 mmol, quant.).

M (SiO₂, C₂₀H₂₄O₅) = 344.41 g/mol.

TLC (cHex/EtOAc 3:1) R_f = 0.26.



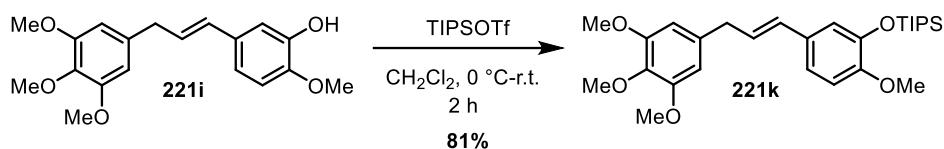
¹H NMR (500 MHz, CDCl₃) δ [ppm] = 6.93 (d, ⁴J = 2.0 Hz, 1 H, H-15), 6.90 (dd, ³J = 8.2 Hz, ⁴J = 2.0 Hz, 1 H, H-11), 6.81 (d, ³J = 8.2 Hz, 1 H, H-12), 6.46 (s, 2 H, H-5/9), 6.40 (dt, ³J = 15.7 Hz, ⁴J = 1.6 Hz, 1 H, H-1), 6.20 (dt, ³J = 15.7 Hz, ³J = 6.9 Hz, 1 H, H-2), 3.88 (s, 3 H, H-16/20), 3.87 (s, 3 H, H-16/20), 3.85 (s, 6 H, H-17/19), 3.83 (s, 3 H, H-18), 3.47 (dd, ³J = 6.9 Hz, ³J = 1.6 Hz, 2 H, H-3).

¹³C NMR (126 MHz, CDCl₃) δ [ppm] = 153.3 (C-17/19), 149.1 (C-14), 148.6 (C-13), 136.4 (C-7), 136.2 (C-4), 130.8 (C-10), 130.6 (C-1), 127.1 (C-2), 119.2 (C-11), 111.2 (C-12), 108.7 (C-15), 105.6 (C-5/9), 60.9 (C-18), 56.2 (C-17/19), 56.0 (C-16/20), 55.9 (d, C-20), 39.8 (C-3).

GC-MS (70 eV) m/z ([%]): 344 (100, [M⁺]), 329 (21), 313 (47), 297 (6), 282 (7), 207 (6), 191 (7), 175 (6).

FTIR-ATR ν [cm⁻¹] = 3070 (w), 2990 (w), 2960 (w), 2935 (w), 2921 (w), 2836 (w), 2252 (w), 2162 (w), 2085 (w), 2035 (w), 2000 (w), 1838 (w), 1767 (w), 1735 (w), 1588 (s), 1505 (s), 1454 (s), 1420 (s), 1329 (m), 1260 (s), 1228 (s), 1181 (m), 1124 (s), 1021 (m), 1010 (m), 990 (s), 976 (m), 924 (w), 815 (s), 805 (m), 768 (s), 733 (m), 617 (w), 596 (m), 564 (w), 522 (m), 454 (m).

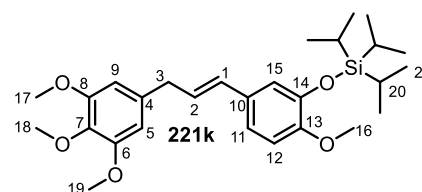
The analytical data are in agreement with the literature.^[225]

10.2.2.4.11. Synthesis of homostilbene **221k**

The synthesis was performed based on a modified procedure of *Sugimoto et al.*^[226] Under an atmosphere of argon, a 50 mL *Schlenk* flask was charged with a solution of 346 mg of homostilbene **221i** (*E/Z* 92:8 isomer mixture, 1.05 mmol, 1.0 equiv.) in 8 mL of anhydrous CH_2Cl_2 . At 0 °C, 0.25 mL of Et_3N (0.18 g, 1.8 mmol, 1.7 equiv.) and 0.42 mL of TIPSOTf (0.48 g, 1.6 mmol, 1.5 equiv.) were added. The bright yellow reaction mixture was stirred for 2 h at r.t., then diluted with 30 mL of CH_2Cl_2 . The organic phase was washed with 20 mL of 1M HCl and 20 mL of NaHCO_3 . It was then dried with MgSO_4 and concentrated under reduced pressure to obtain a yellow crude material. Purification by FCC (SiO_2 , cHex/EtOAc 4:1) gave 464 mg of a colorless oil with TIPSOH as inseparable byproduct ($\omega(\text{TIPSOH}) = 11\%$, 413 mg of **221k**, 0.849 mmol, 81%, *E/Z* 92:8).

M (SiO_2 , $\text{C}_{28}\text{H}_{42}\text{O}_5\text{Si}$) = 486.72 g/mol.

TLC (cHex/EtOAc 4:1) $R_f = 0.49$.



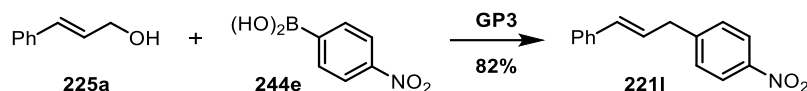
$^1\text{H NMR}$ (600 MHz, CDCl_3) δ [ppm] = 6.93 (d, $^4J = 2.2$ Hz, 1 H, H-15), 6.88 (dd, $^3J = 8.4$ Hz, $^4J = 2.2$ Hz, 1 H, H-11), 6.76 (d, $^3J = 8.4$ Hz, 1 H, H-12), 6.45 (s, 2 H, H-5/9), 6.34 (dt, $^3J = 15.7$ Hz, $^4J = 1.6$ Hz, 1 H, H-1), 6.13 (dt, $^3J = 15.7$ Hz, $^3J = 6.9$ Hz, 1 H, H-2), 3.84 (s, 6 H, H-17/19), 3.83 (s, 3 H, H-18), 3.78 (s, 3 H, H-16), 3.53 – 3.29 (m, 2 H, H-3), 1.29 – 1.19 (m, 3 H, H-20), 1.09 (d, $^3J = 7.5$ Hz, 18 H, H-21).

$^{13}\text{C NMR}$ (151 MHz, CDCl_3) δ [ppm] = 153.3 (C-6/8), 150.5 (C-13), 145.6 (C-14), 136.4 (C-7), 136.3 (C-4), 131.0 (C-1), 130.6 (C-10), 126.6 (C-2), 119.7 (C-11), 118.0 (C-15), 112.0 (C-12), 105.6 (C-5/9), 61.0 (C-18), 56.2 (C-17/19), 55.6 (C-16), 39.7 (C-3), 18.0 (C-21), 13.0 (C-20).

GC-MS (70 eV) m/z ([%]): 486 (97, $[\text{M}^+]$), 428 (100), 413 (11), 397 (28), 259 (6), 237 (24), 222 (26), 206 (5), 191 (7), 175 (8), 151 (15).

HR-ESI-MS m/z calculated $[\text{C}_{28}\text{H}_{42}\text{O}_5\text{Si}+\text{H}^+]$: 487.2874274; found: 487.28823.

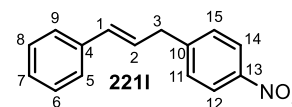
FTIR-ATR ν [cm^{-1}] = 2942 (m), 2896 (w), 2866 (m), 2837 (w), 2059 (w), 1740 (w), 1693 (w), 1589 (m), 1508 (s), 1462 (m), 1443 (w), 1419 (m), 1384 (w), 1328 (w), 1308 (w), 1270 (m), 1229 (s), 1183 (w), 1165 (w), 1127 (s), 1071 (w), 1032 (w), 999 (m), 964 (m), 936 (w), 920 (w), 881 (m), 834 (s), 798 (w), 778 (w), 761 (w), 746 (w), 732 (w), 703 (w), 678 (s), 614 (w), 590 (w), 557 (w), 528 (w), 506 (w), 465 (w).

10.2.2.4.12. Synthesis of homostilbene **221I**

According to the general procedure **GP3**, 537 mg of cinnamic alcohol **225a** (4.00 mmol, 1.0 equiv.) were reacted with 804 mg of phenylboronic acid **244e** (4.82 mmol, 1.2 equiv.) and 234 mg of Pd(PPh₃)₄ (0.202 mmol, 5.1 mol%). Purification by FCC (cHex/EtOAc 15:1 and 20:1) gave 781 mg of **221I** as a pale orange solid (3.26 mmol, 82%).

M (C₁₅H₁₃NO₂) = 239.27 g/mol.

TLC (SiO₂, cHex/EtOAc 8:1) R_f = 0.50.



M.p. 55 - 58 °C.

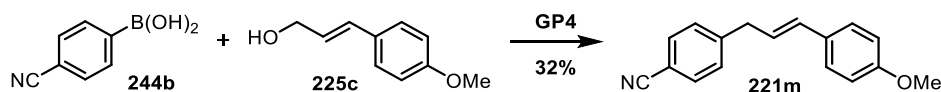
¹H NMR (500 MHz, CDCl₃) δ [ppm] = 8.16 (d, ³J = 8.7 Hz, 2 H, H-12/14), 7.41 – 7.37 (m, 2 H, H-11/15), 7.37 – 7.34 (m, 2 H, H-5/9), 7.33 – 7.28 (m, 2 H, H-6/8), 7.26 – 7.19 (m, 1 H, H-7), 6.49 (dt, ³J = 16.0 Hz, ⁴J = 1.6 Hz, 1 H, H-1), 6.30 (dt, ³J = 16.0 Hz, ³J = 6.9 Hz, 1 H, H-2), 3.64 (dd, ³J = 6.9 Hz, ⁴J = 1.6 Hz, 1 H, H-3).

¹³C NMR (75 MHz, CDCl₃) δ [ppm] = 148.1 (C-10), 146.7 (C-13), 137.0 (C-4), 132.7 (C-1), 129.6 (C-11/15), 128.7 (C-12/14), 127.7 (C-7), 127.1 (C-2), 126.3 (C-6/8), 123.9 (C-5/9), 39.2 (C-3).

GC-MS (70 eV) m/z ([%]): 239 (100, [M⁺]), 222 (36), 208 (22), 192 (57), 178 (50), 165 (41), 152 (35), 103 (17), 91 (45), 77 (12).

FTIR-ATR ν [cm⁻¹] = 3105 (w), 3079 (w), 3058 (w), 3027 (w), 2940 (w), 2902 (w), 2847 (w), 2450 (w), 1928 (w), 1880 (w), 1800 (w), 1702 (w), 1652 (w), 1597 (m), 1513 (s), 1495 (w), 1448 (w), 1433 (w), 1341 (s), 1259 (w), 1211 (w), 1179 (w), 1157 (w), 1109 (m), 1076 (w), 1029 (w), 1015 (w), 965 (s), 929 (w), 853 (m), 842 (m), 788 (m), 739 (s), 691 (s), 641 (w), 611 (w), 526 (w).

The analytical data are in agreement with the literature.^[227]

10.2.2.4.13. Synthesis of homostilbene **221m**

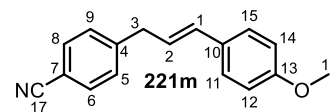
According to the general procedure **GP4**, 821 mg of cinnamic alcohol **225c** (5.00 mmol, 1.0 equiv.) were reacted with 881 mg of phenylboronic acid **244b** (6.00 mmol, 1.2 equiv.) and

290 mg of Pd(PPh₃)₄ (0.251 mmol, 5.0 mol%). Purification by FCC (cHex/EtOAc 20:1) gave 401 mg of **221m** as a white solid (1.61 mmol, 32%).

M (SiO₂, C₁₇H₁₅NO) = 249.31 g/mol.

TLC (cHex/EtOAc 15:1) R_f = 0.19.

M.p. 69 - 71 °C.



¹H NMR (600 MHz, CDCl₃) δ [ppm] = 7.76 – 7.54 (m, 2 H, H-6/8), 7.35 (dt, ³J = 8.9 Hz, ⁴J = 0.7 Hz, 2 H, H-5/9), 7.33 – 7.26 (m, 2 H, H-11/15), 6.85 (d, ³J = 8.7 Hz, 2 H, H-12/14), 6.42 (dt, ³J = 15.7 Hz, ⁴J = 1.5 Hz, 1 H, H-1), 6.15 (dt, ³J = 15.7 Hz, ³J = 6.9 Hz, 1 H, H-2), 3.80 (s, 3 H, H-16), 3.58 (d, ³J = 6.9 Hz, 2 H, H-3).

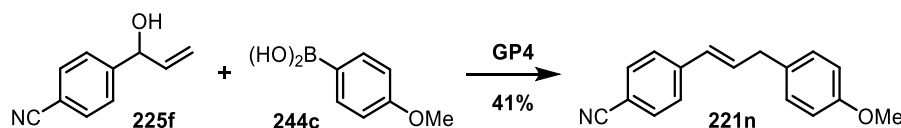
¹³C NMR (151 MHz, CDCl₃) δ [ppm] = 159.3 (C-13), 146.3 (C-4), 132.4 (C-6/8), 131.9 (C-1), 129.8 (C-10), 129.5 (C-5/9), 127.4 (C-11/15), 125.0 (C-2), 119.2 (C-17), 114.1 (C-12/14), 110.1 (C-7), 55.4 (C-16), 39.4 (C-3).

GC-MS (70 eV) m/z ([%]): 249 (100, [M⁺]), 234 (20), 218 (23), 203 (4), 190 (6), 140 (18), 121 (20), 103 (3), 89 (6).

HR-ESI-MS m/z calculated [C₁₇H₁₅NO+Na⁺]: 272.1045853; found: 272.10455.

FTIR-ATR ν [cm⁻¹] = 3034 (w), 3012 (w), 2963 (w), 2936 (w), 2898 (w), 2835 (w), 2227 (s), 1931 (w), 1905 (w), 1811 (w), 1779 (w), 1660 (w), 1645 (w), 1605 (s), 1575 (w), 1512 (s), 1456 (w), 1439 (m), 1414 (w), 1315 (w), 1302 (w), 1260 (s), 1238 (s), 1179 (s), 1147 (w), 1110 (m), 1026 (s), 990 (s), 961 (w), 881 (m), 840 (s), 817 (m), 785 (m), 773 (m), 735 (m), 708 (m), 638 (w), 606 (w), 559 (s), 531 (m), 519 (m), 436 (w).

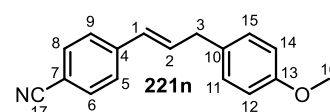
10.2.2.4.14. Synthesis of homostilbene **221n**



According to the general procedure **GP4**, 951 mg of allylic alcohol **225f** (5.97 mmol, 1.0 equiv.) were reacted with 1.09 g of phenylboronic acid **244c** (7.19 mmol, 1.2 equiv.) and 347 mg of Pd(PPh₃)₄ (0.300 mmol, 5.0 mol%). Purification by FCC (cHex/EtOAc 9:1) gave 607 mg of **221n** as a pale yellow oil (2.435 mmol, 41%).

M (C₁₇H₁₅NO) = 249.31 g/mol.

TLC (SiO₂, cHex/EtOAc 9:1) R_f = 0.36.



¹H NMR (600 MHz, CDCl₃) δ [ppm] = 7.56 (d, ³J = 8.4 Hz, 2 H, H-6/8), 7.41 (d, ³J = 8.4 Hz, 2 H, H-5/9), 7.15 (d, ³J = 8.7 Hz, 2 H, H-11/15), 6.88 (d, ³J = 8.7 Hz, 2 H, H-12/14), 6.49 (dt, ³J = 15.8 Hz, ³J = 6.7 Hz, 1 H, H-2), 6.42 (dt, ³J = 15.8 Hz, ⁴J = 1.4 Hz, 1 H, H-1), 3.80 (s, 3 H, H-16), 3.52 (d, ³J = 6.7 Hz, 2 H, H-3).

¹³C NMR (151 MHz, CDCl₃) δ [ppm] = 158.4 (C-13), 142.1 (C-4), 134.2 (C-2), 132.4 (C-6/8), 131.2 (C-10), 129.7 (C-11/15), 129.3 (C-1), 126.6 (C-5/9), 119.2 (C-17), 114.1 (C-12/14), 110.3 (C-7), 55.4 (C-16), 38.6 (C-3).

GC-MS (70 eV) m/z ([%]): 249 (100, [M⁺]), 234 (21), 218 (23), 190 (11), 165 (2), 140 (23), 121 (22), 103 (7), 77 (13).

HR-ESI-MS m/z calculated [C₁₇H₁₅NO+Na⁺]: 272.1045853; found: 272.10455.

FTIR-ATR ν [cm⁻¹] = 3031 (w), 3003 (w), 2955 (w), 2934 (w), 2904 (w), 2835 (w), 2224 (m), 2059 (w), 1991 (w), 1917 (w), 1647 (w), 1604 (s), 1584 (w), 1509 (s), 1464 (w), 1441 (w), 1412 (w), 1300 (m), 1243 (s), 1175 (s), 1107 (w), 1033 (s), 969 (m), 919 (w), 871 (w), 845 (w), 829 (s), 818 (s), 747 (w), 704 (s), 647 (w), 638 (w), 599 (w), 571 (w), 545 (s), 508 (m).

10.2.3. Enantioselective Ni-catalyzed hydrocyanation

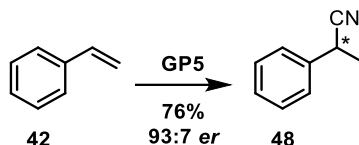
10.2.3.1. General procedures

10.2.3.1.1. General procedure GP5 for the hydrocyanation of vinylarenes

The synthesis was performed according to a procedure of *Falk et al.*^[42] Under an atmosphere of argon, a 25 mL *Schlenk* flask was charged with 10.3 mg of Ni(cod)₂ (37.5 μmol, 7.5 mol%) and 34.8 mg of ligand **143** ((37.5 μmol, 7.5 mol%). Subsequently, 1.0 mL of dry toluene (0.038 M) was added and the yellow solution was stirred for 5 min at r.t. Then the solvent was removed by *Schlenk* line vacuum to give the air-sensitive Ni(cod)**143**^[103] catalyst which was re-dissolved in 2.0 mL of anhydrous THF (0.019 M). The corresponding substrate (0.50 mmol, 1.0 equiv.) was added to give an orange solution. At r.t. or 50 °C, a solution of 74 mg of TMSCN (94 μL, 0.75 mmol, 1.5 equiv.) in 3.0 mL of THF/MeOH (14:1, 0.25 M) was slowly added over 2 h to the substrate solution by means of a syringe pump. Temporary red coloring indicated an active catalysis. After finished addition, a pale yellow solution was obtained and concentrated by *Schlenk* line vacuum (**Caution:** Operation must be performed in a fume hood; removal of residual HCN in cooling trap) and the crude material was purified by FCC (SiO₂, cHex/EtOAc) for purification. Racemic standards for stereochemical analysis were synthesized employing racemic ligand *rac*-**143**.

10.2.3.2. Hydrocyanation of Vinylarenes

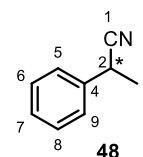
10.2.3.2.1. Synthesis of 2-phenylpropionitrile (**48**)



According to the general procedure **GP5**, 58 μL of styrene (**42**) (52 mg, 0.50 mmol, 1.0 equiv.) were reacted at r.t. and purification by FCC (cHex/EtOAc 40:1) gave 52 mg of a colorless liquid (~4 mg of EtOAc/H₂O residues; 48 mg of **48**, 0.47 mmol, 76%, 100% GC-conv., 93:7 *er*; Lit.:^[42] 100% GC-conv., 93:7 *er*). **Attention:** Product is volatile.

M (C₉H₉N) = 131.17 g/mol.

TLC (SiO₂, cHex/EtOAc 40:1) R_f = 0.20.



¹H NMR (500 MHz, CDCl₃) δ [ppm] = 7.45 – 7.26 (m, 5 H, H-5/6/7/8/9), 3.90 (q, ³J = 7.3 Hz, 1 H, H-2), 1.64 (d, ³J = 7.3 Hz, 3 H, H-3).

¹³C NMR (126 MHz, CDCl₃) δ [ppm] = 37.2 (C-4), 129.2 (C-6/8), 128.1 (C-7), 126.8 (C-5/9), 121.7 (C-1), 31.33 (C-2), 21.6 (C-3).

GC-MS (70 eV) m/z ([%]): 131 (33, [M⁺]), 116 (100), 104 (21), 89 (13), 77 (12), 63 (8), 51 (13).

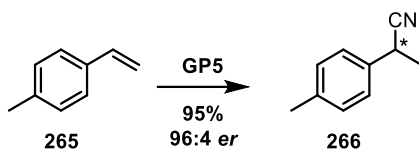
FTIR-ATR ν [cm⁻¹] = 3032 (w), 2987 (w), 2242 (w), 1736 (w), 1601 (w), 1496 (m), 1452 (s), 1379 (w), 1243 (w), 1079 (w), 1031 (w), 1004 (w), 988 (w), 913 (w), 756 (s), 670 (vs), 623 (w), 570 (s), 509 (s).

Specific rotation (c = 0.510 g/100 mL, CHCl₃, [α] _{λ} ^T): [α]₃₆₅^{20.0} = - 72.9 °, [α]₄₃₆^{20.0} = - 43.6 °, [α]₅₄₆^{20.0} = - 24.7 °, [α]₅₇₉^{20.0} = - 23.3 °, [α]₅₈₉^{20.0} = - 24.3 °.

Enantiomeric separation by chGC column: MEGA DEX BETA (30M x 0.25 mm Ø), temperature program: 50 °C, 50 °C – 180 °C (1 °C/min). Flow rate: 3 mL/min. Major enantiomer T_R = 41.9 min; minor enantiomer T_R = 45.9 min.

The analytical data are in agreement with the literature.^[42]

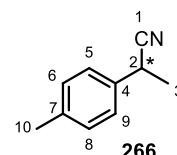
10.2.3.2.2. Synthesis of 2-(4-methylphenyl)-propionitrile (**266**)



According to the general procedure **GP5**, 67 μL of 4-methylstyrene (**265**) (0.50 mmol, 1.0 equiv.) were reacted at r.t. and purification by FCC (cHex/EtOAc 40:1) gave 75 mg of a colorless oil (~6 mg of cHex/EtOAc residues; 69 mg of **266**, 0.48 mmol, 95%, 96:4 *er*).

M ($\text{C}_{10}\text{H}_{11}\text{N}$) = 145.21 g/mol.

TLC (SiO_2 , cHex/EtOAc 40:1) R_f = 0.19.



$^1\text{H NMR}$ (500 MHz, CDCl_3) δ [ppm] = 7.24 (d, 3J = 8.0 Hz, 2 H, H-5/9), 7.19 (d, 3J = 8.0 Hz, 2 H, H-6/8), 3.86 (q, 3J = 7.3 Hz, 1 H, H-2), 2.36 (s, 3 H, H-10), 1.63 (d, 3J = 7.3 Hz, 3 H, H-3).

$^{13}\text{C NMR}$ (151 MHz, CDCl_3) δ [ppm] = 138.0 (C-7), 134.2 (C-4), 129.9 (C-6/8), 126.7 (C-5/9), 121.9 (C-1), 31.0 (C-2), 21.6 (C-3), 21.1 (C-10).

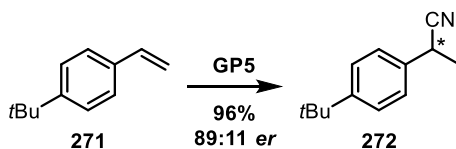
GC-MS (70 eV) m/z ([%]): 145 (33, $[\text{M}^+]$), 130 (100), 103 (18), 91 (13), 77 (10).

FTIR-ATR ν [cm^{-1}] = 3026 (w), 2986 (w), 2926 (w), 2876 (w), 2241 (w), 1903 (w), 1737 (w), 1651 (w), 1607 (w), 1514 (m), 1453 (m), 1416 (w), 1378 (w), 1329 (w), 1304 (w), 1242 (w), 1215 (w), 1187 (w), 1159 (w), 1116 (w), 1083 (w), 1045 (w), 1022 (w), 995 (w), 941 (w), 815 (s), 732 (w), 701 (w), 640 (w), 570 (m), 514 (s).

Enantiomeric separation by chGC column: MEGA DEX BETA (30M x 0.25 mm \varnothing), temperature program: 50 $^\circ\text{C}$, 50 $^\circ\text{C}$ – 180 $^\circ\text{C}$ (1 $^\circ\text{C}/\text{min}$). Flow rate: 3 mL/min. Major enantiomer T_R = 51.7 min; minor enantiomer T_R = 55.7 min.

The analytical data are in agreement with the literature.^[73]

10.2.3.2.3. Synthesis of 2-(4-*tert*-butylphenyl)-propionitrile (**272**)

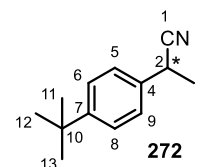


According to the general procedure **GP5**, 80 mg of 4-*tert*-butylstyrene (**271**) (0.50 mmol, 1.0 equiv.) were reacted at 50 $^\circ\text{C}$ and purification by FCC (cHex/EtOAc 40:1) gave 90 mg of **272** as a colorless oil (0.48 mmol, 96%, 89:11 *er*, at r.t. 58% GC-conv. and 90:10 *er*).

M (C₁₃H₁₇N) = 187.29 g/mol.

TLC (SiO₂, cHex/EtOAc 40:1) R_f = 0.24.

M.p. 49 - 52 °C.



¹H NMR (500 MHz, CDCl₃) δ [ppm] = 7.41 (d, ³J = 8.6 Hz, 2 H, H-6/8), 7.30 (d, ³J = 8.6 Hz, 2 H, H-5/9), 3.88 (q, ³J = 7.3 Hz, 1 H, H-2), 1.64 (d, ³J = 7.3 Hz, 3 H, H-3), 1.33 (s, 9 H, H-11/12/13).

¹³C NMR (75 MHz, CDCl₃) δ [ppm] = 151.2 (C-7), 134.1 (C-4), 126.5 (C-5/9), 126.2 (C-6/8), 121.9 (C-1); 34.7 (C-10), 31.4 (C-11/12/13), 30.9 (C-2), 21.5 (C-3).

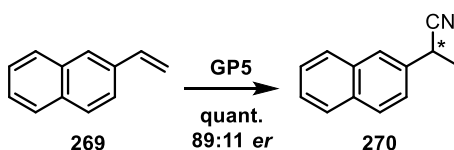
GC-MS (70 eV) m/z ([%]): 187 (16, [M⁺]), 172 (100), 144 (24), 131 (19), 117 (39), 105 (32), 91 (31), 77 (18), 63 (17), 57 (18).

FTIR-ATR ν [cm⁻¹] = 3676 (w), 2964 (s), 2904 (m), 2870 (m), 2242 (w), 1909 (w), 1682 (w), 1607 (w), 1513 (m), 1476 (w), 1459 (m), 1408 (w), 1395 (w), 1378 (w), 1365 (m), 1331 (w), 1304 (w), 1270 (m), 1203 (w), 1112 (m), 1084 (w), 1059 (w), 1020 (w), 990 (w), 924 (w), 831 (s), 772 (w), 741 (w), 707 (w), 672 (w), 639 (w), 582 (s), 546 (m).

Enantiomeric separation by chGC column: MEGA DEX BETA (30M x 0.25 mm Ø), temperature program: 50 °C, 50 °C – 180 °C (1 °C/min). Flow rate: 3 mL/min. Major enantiomer T_R = 72.9 min; minor enantiomer T_R = 74.6 min.

The analytical data are in agreement with the literature.^[73]

10.2.3.2.4. Synthesis of 2-(naphthalen-2-yl)-propionitrile (270)

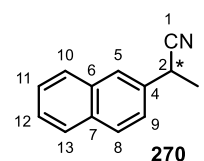


According to the general procedure **GP5**, 80 mg of 2-vinylnaphthalene (**269**) (0.52 mmol, 1.0 equiv.) were reacted at r.t. and purification by FCC (cHex/EtOAc 15:1) gave 94 mg of **270** as a colorless solid (0.52 mmol, quant., 89:11 *er*).

M (C₁₃H₁₁N) = 181.24 g/mol.

TLC (SiO₂, cHex/EtOAc 15:1) R_f = 0.26.

M.p. 89 - 90 °C.



¹H NMR (500 MHz, CDCl₃) δ [ppm] = 7.88 (d, ³J = 8.5 Hz, 1 H, H-8) 7.86 – 7.82 (m, 3 H, H-5/11/13), 7.54 – 7.49 (m, 2 H, H-10/12), 7.44–7.42 (dd, 1 H, ³J = 8.5 Hz, ⁴J = 1.8 Hz, H-9), 4.07 (q, ³J = 7.3 Hz, 1 H, H-2), 1.74–1.73 (d, 3 H, ³J = 7.3 Hz, H-3).

¹³C NMR (75 MHz, CDCl₃) δ [ppm] = 134.3 (C-4), 133.3 (C-6), 132.8 (C-7), 129.2 (C-8), 127.9 (C-11/13), 127.7 (C-11/13), 126.7 (C-10/12), 126.5 (C-10/12), 125.6 (C-5), 124.4 (C-9), 121.6 (C-1), 31.4 (C-2), 21.4 (C-3).

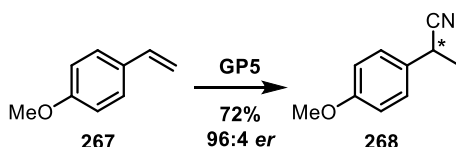
GC-MS (70 eV) m/z ([%]): 181 (55, [M⁺]), 166 (100), 139 (14).

FTIR-ATR ν [cm⁻¹] = 3676 (w), 3056 (w), 2989 (br), 2972 (w), 2944 (w), 2925 (w), 2902 (w), 2288 (w), 2239 (m), 2114 (w), 1968 (w), 1922 (w), 1847 (w), 1819 (w), 1778 (w), 1711 (w), 1692 (w), 1632 (w), 1599 (w), 1506 (m), 1457 (w), 1408 (w), 1394 (w), 1377 (m), 1366 (w), 1295 (w), 1276 (w), 1260 (w), 1211 (w), 1171 (m), 1145 (w), 1127 (w), 1081 (s), 1066 (w), 1057 (w), 1028 (w), 1020 (w), 991 (w), 967 (m), 955 (w), 924 (w), 901 (m), 866 (m), 822 (s), 771 (w), 752 (s), 697 (w), 656 (m), 623 (w), 583 (w), 569 (w), 538 (w), 522 (w), 503 (w), 480 (s), 472 (w), 447 (w), 420 (w).

Enantiomeric separation by chGC column: MEGA DEX BETA (30M x 0.25 mm Ø), temperature program: 50 °C, 50 °C – 180 °C (1 °C/min). Flow rate: 3 mL/min. Major enantiomer T_R = 99.3 min; minor enantiomer T_R = 101.5 min.

The analytical data are in agreement with the literature.^[228]

10.2.3.2.5. Synthesis of 2-(4-methoxyphenyl)-propionitrile (**268**)

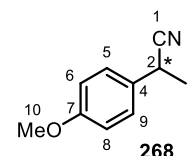


According to the general procedure **GP5**, 67 μL of 4-methoxystyrene (**267**) (67 mg, 0.50 mmol, 1.0 equiv.) were reacted at r.t. and purification by FCC (cHex/EtOAc 15:1) gave 58 mg of **268** as a colorless solid (0.36 mmol, 72%, 100% GC-conv., 94:6 er).

M (C₁₀H₁₁NO) = 161.20 g/mol.

TLC (SiO₂, cHex/EtOAc 10:1) R_f = 0.26.

M.p. 55 - 59 °C.



¹H NMR (500 MHz, CDCl₃) δ [ppm] = 7.26 (d, ³J = 8.7 Hz, 2 H, H-6/8), 6.89 (d, ³J = 8.7 Hz, 2 H, H-5/9), 3.84 (q, ³J = 7.3 Hz, 1 H, H-2), 3.80 (s, 3 H, H-10), 1.60 (d, ³J = 7.3 Hz, 3 H, H-3).

¹³C NMR (75 MHz, CDCl₃) δ [ppm] = 159.4 (C-7), 129.2 (C-4), 127.9 (C-5/9), 122.0 (C-1), 114.6 (C-6/8), 55.4 (C-10), 30.5 (C-2), 21.6 (C-3).

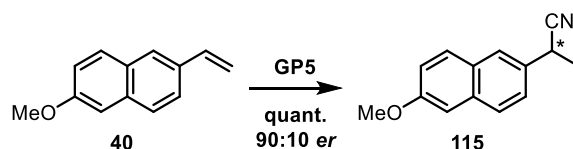
GC-MS (70 eV) m/z ([%]): 161 (32, [M⁺]), 146 (100), 116 (4), 91 (6), 77 (3).

FTIR-ATR ν [cm⁻¹] = 3020 (w), 2991 (w), 2965 (w), 2942 (w), 2910 (w), 2878 (w), 2839 (w), 2239 (w), 2044 (w), 1886 (w), 1611 (m), 1584 (w), 1511 (s), 1454 (m), 1379 (w), 1304 (w), 1269 (w), 1242 (s), 1178 (s), 1113 (w), 1086 (w), 1060 (w), 1025 (s), 989 (w), 830 (s), 819 (s), 804 (m), 733 (w), 635 (w), 592 (w), 572 (s), 531 (s).

Enantiomeric separation by chGC column: MEGA DEX BETA (30M x 0.25 mm Ø), temperature program: 50 °C, 50 °C – 180 °C (1 °C/min). Flow rate: 3 mL/min. Major enantiomer T_R = 72.9 min; minor enantiomer T_R = 74.6 min.

The analytical data are in agreement with the literature.^[73]

10.2.3.2.6. Synthesis of 2-(6-methoxynaphthalen-2-yl)-propionitrile (**115**)

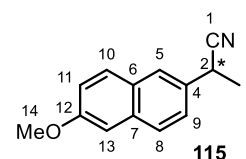


According to the general procedure **GP5**, 89 mg of 2-methoxy-6-vinylnaphthalene (**40**) (0.48 mmol, 1.0 equiv.) were reacted at r.t. and purification by FCC (cHex/EtOAc 15:1) gave 102 mg of **115** as a colorless solid (0.48 mmol, quant., 90:10 *er*, Lit.:^[42] quant., 90:10 *er*).

M (C₁₄H₁₃NO) = 211.26 g/mol.

TLC (SiO₂, cHex/EtOAc 15:1) R_f = 0.20.

M.p. 93 - 94 °C.



¹H NMR (500 MHz, CDCl₃) δ [ppm] = 7.75 (m, 3 H, H-5/8/10), 7.39 (dd, ³J = 8.4 Hz, ⁴J = 2.0 Hz, 1 H, H-9), 7.19 (dd, ³J = 8.9 Hz, ⁴J = 2.6 Hz, 1 H, H-11), 7.14 (d, ⁴J = 2.6 Hz, 1H, H-13), 4.03 (q, ³J = 7.3 Hz, 1 H, H-2), 3.93 (s, 3 H, H-14), 1.71 (d, ³J = 7.3 Hz, 3 H, H-3).

¹³C NMR (75 MHz, CDCl₃) δ [ppm] = 158.2 (C-12), 134.2 (C-7), 132.1 (C-4), 129.5 (C-10), 128.9 (C-6), 128.0 (C-8), 125.5 (C-5), 125.1 (C-9), 121.9 (C-1), 119.7 (C-11), 105.8 (C-13), 55.5 (C-14), 31.4 (C-2), 21.6 (C-3).

GC-MS (70 eV) m/z ([%]): 211 (29, [M⁺]), 196 (60), 171 (100), 153 (20), 141 (65), 128 (60), 115 (47).

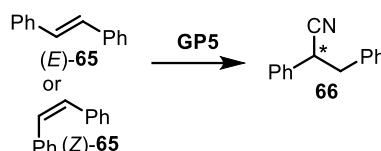
FTIR-ATR ν [cm^{-1}] = 2991 (w), 2963 (w), 2942 (w), 2241 (w), 1629 (w), 1603 (s), 1506 (m), 1482 (m), 1465 (w), 1449 (m), 1436 (w), 1419 (w), 1258 (s), 1232 (w), 1212 (s), 1187 (m), 1164 (s), 1085 (m), 1023 (s), 961 (w), 891 (m), 856 (vs), 816 (s), 750 (w), 675 (m), 630 (w), 592 (w), 524 (w), 476 (s), 469 (m).

Specific rotation ($c = 0.510$ g/100 mL, CHCl_3 , $[\alpha]_{\lambda}^T$): $[\alpha]_{365}^{20.0} = -104.2^\circ$, $[\alpha]_{436}^{20.0} = -52.0^\circ$, $[\alpha]_{546}^{20.0} = -27.5^\circ$, $[\alpha]_{579}^{20.0} = -24.8^\circ$, $[\alpha]_{589}^{20.0} = -26.0^\circ$.

Enantiomeric separation by chGC column: MEGA DEX BETA (30M x 0.25 mm \varnothing), temperature program: 50 $^\circ\text{C}$, 50 $^\circ\text{C}$ – 180 $^\circ\text{C}$ (1 $^\circ\text{C}/\text{min}$). Flow rate: 3 mL/min. Major enantiomer $T_R = 125.6$ min; minor enantiomer $T_R = 126.6$ min.

The analytical data are in agreement with the literature.^[42]

10.2.3.2.7. Synthesis of 2,3-diphenylpropionitrile (**66**)

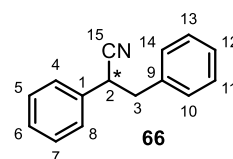


According to the general procedure **GP5**, 90 mg of (*E*)-stilbene ((*E*)-**65**) or 89 μL of (*Z*)-stilbene ((*Z*)-**65**) (90 mg, 0.50 mmol, 1.0 equiv.) were reacted at r.t. or 50 $^\circ\text{C}$ (from (*E*)-**65**: traces r.t./50 $^\circ\text{C}$; from (*Z*)-**65**: at r.t. 14% GC-conv. and 65:35 *er*; at 50 $^\circ\text{C}$ 26% GC-conv. and 65:35 *er*). For analytics, purification of the combined crude fractions (3 x 0.5 mmol scale) by FCC (cHex/EtOAc 60:1) gave 15 mg of **66** as a colorless solid (72 μmol , <5%).

M ($\text{C}_{15}\text{H}_{13}\text{N}$) = 207.28 g/mol.

TLC (SiO_2 , cHex/EtOAc 60:1) $R_f = 0.18$.

M.p. 49 - 52 $^\circ\text{C}$.



^1H NMR (500 MHz, CDCl_3) δ [ppm] = 7.41 – 7.19 (m, 8 H, H-4/5/6/7/8/11/12/13), 7.15 – 7.07 (m, 2 H, H-10/14), 3.98 (dd, $^3J = 8.4$ Hz, $^3J = 6.4$ Hz 1 H, H-2), 3.16 (dd, $^2J = 13.6$ Hz, $^3J = 8.4$ Hz, 1 H, H-3), 3.11 (dd, $^2J = 13.6$ Hz, $^3J = 6.4$ Hz, 1 H, H-3).

^{13}C NMR (75 MHz, CDCl_3) δ [ppm] = 136.3 (C-9), 135.3 (C-1), 129.3 (C-10/14), 129.0 (C-5/7), 128.6 (C-11/13), 128.2 (C-6), 127.5 (C-4/8), 127.4 (C-12), 120.4 (C-15), 42.2 (C-3), 39.8 (C-2).

GC-MS (70 eV) m/z ([%]): 207 (8, $[\text{M}^+]$), 179 (5), 116 (19), 91 (100), 77 (5), 65 (22), 51 (18).

FTIR-ATR ν [cm^{-1}] = 3088 (w), 3064 (w), 3031 (w), 2930 (w), 2860 (w), 2241 (w), 1952 (w), 1879 (w), 1808 (w), 1751 (w), 1601 (w), 1586 (w), 1497 (m), 1455 (m), 1343 (w), 1260 (w), 1182 (w), 1157 (w), 1109 (w), 1074 (w), 1031 (w), 1004 (w), 975 (w), 913 (w), 869 (w), 846

(w), 797 (w), 754 (s), 742 (m), 696 (s), 645 (w), 609 (w), 620 (w), 597 (w), 573 (m), 562 (m), 526 (w).

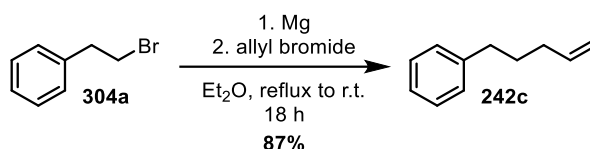
Enantiomeric separation by chGC column: MEGA DEX BETA (30M x 0.25 mm Ø), temperature program: 50 °C, 50 °C – 180 °C (0.5 °C/min). Flow rate: 3 mL/min. Major enantiomer $T_R = 179.7$ min; minor enantiomer $T_R = 181.8$ min.

The analytical data are in agreement with the literature.^[73]

10.2.3.3. Synthesis of phenylalkenes for hydrocyanation

Phenylalkenes 3-phenyl-1-propene (**242a**), 4-phenyl-1-butene (**242b**) and 1-phenyl-1-propene (**242h**) were purchased commercially.

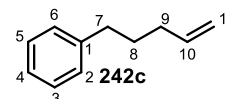
10.2.3.3.1. Synthesis of 5-phenyl-1-pentene (**242c**)



The synthesis was performed according to a procedure of *Aguilar et al.*^[229] Under an atmosphere of argon, a 50 mL round-bottomed flask equipped with a reflux condenser was charged with 413 mg of Mg turnings (17.0 mmol, 1.1 equiv.) and an I₂ crystal and the mixture was heated under vigorous stirring. Then a solution of 2.10 mL of (2-bromoethyl)benzene (**304a**) (2.85 g, 15.4 mmol, 1.0 equiv.) in 6.0 mL of anhydrous Et₂O was slowly added over 10 min. The resulting reaction mixture was heated at reflux for 1 h. At 15 °C, a solution of 1.8 mL of allyl bromide (2.5 g, 21 mmol, 1.4 equiv.) in 6.0 mL of Et₂O was added over 1 h by means of a syringe pump. The suspension was stirred for 18 h at r.t. and then 8 mL of sat. NH₄Cl solution and 5 mL of H₂O were added. The aqueous phase was extracted with MTBE (3 x 20 mL). The combined organic phases were dried with MgSO₄ and concentrated under reduced pressure (**attention**: product is volatile) to give 2.06 g of a pale yellow liquid (~95 mg of MTBE residues; 1.96 g of product **242c**, 13.4 mmol, 87%).

M (C₁₁H₁₄) = 146.23 g/mol.

TLC (SiO₂, cHex/EtOAc 60:1) $R_f = 0.73$.



¹H NMR (500 MHz, CDCl₃) δ [ppm] = 7.26 (t, $^3J = 7.7$ Hz, 2 H, H-3/5), 7.20 – 7.13 (m, 3 H, H-2/4/6), 5.83 (ddt, $^3J = 16.9$ Hz, $^3J = 10.2$ Hz, $^3J = 6.6$ Hz, 1 H, H-10), 5.02 (dd, $^3J = 16.9$ Hz, $^4J = 1.8$ Hz, 1 H, H-11), 4.99 – 4.93 (m, 1 H, H-11), 2.82 – 2.42 (m, 2 H, H-7), 2.21 – 1.87 (m, 2 H, H-9), 1.84 – 1.59 (m, 2 H, H-8).

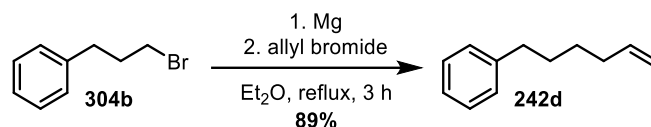
^{13}C NMR (75 MHz, CDCl_3) δ [ppm] = 142.6 (C-1), 138.7 (C-10), 128.6 (C-2/6), 128.4 (C-3/5), 125.8 (C-4), 114.8 (C-11), 35.5 (C-7), 33.4 (C-9), 30.8 (C-8).

GC-MS (70 eV) m/z ([%]): 146 (5, $[\text{M}^+]$), 131 (6), 117 (11), 104 (100), 91 (91), 77 (13), 65 (23), 51 (11).

FTIR-ATR ν [cm^{-1}] = 3079 (w), 3064 (w), 3027 (w), 3001 (w), 2977 (w), 2931 (m), 2858 (w), 1943 (w), 1865 (w), 1801 (w), 1747 (w), 1641 (w), 1604 (w), 1584 (w), 1496 (m), 1453 (m), 1412 (w), 1349 (w), 1109 (w), 1074 (w), 1031 (w), 991 (m), 909 (s), 845 (w), 803 (w), 742 (s), 697 (s), 635 (w), 581 (w), 566 (w).

The analytical data are in agreement with the literature.^[229]

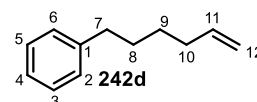
10.2.3.3.2. Synthesis of 6-phenyl-1-hexene (242d)



The synthesis was performed according to a procedure of *Mulpuri et al.*^[137a] Under an atmosphere of argon, a 50 mL round-bottomed flask equipped with a reflux condenser was charged with 413 mg of Mg turnings (17.0 mmol, 1.1 equiv.) and an I_2 crystal and the mixture was heated under vigorous stirring. Then a solution of 2.30 mL of (3-bromopropyl)benzene (**304b**) (3.01 g, 15.4 mmol, 1.0 equiv.) in 6.0 mL of anhydrous Et_2O was slowly added over 10 min. The resulting reaction mixture was heated at reflux for 1.5 h. At r.t., a solution of 1.4 mL of allyl bromide (2.0 g, 16 mmol, 1.1 equiv.) in 6.0 mL of Et_2O was added over 5 min and the suspension was heated at reflux for 3 h. Then 10 mL of sat. NH_4Cl solution and 10 mL of H_2O were added. The aqueous phase was extracted with MTBE (3 x 15 mL). The combined organic phases were dried with MgSO_4 and concentrated under reduced pressure (**attention**: product is volatile) to give 2.28 g of a pale yellow liquid (~135 mg of MTBE residues; 2.15 g of product **242d**, 13.4 mmol, 89%).

M ($\text{C}_{12}\text{H}_{16}$) = 160.26 g/mol.

TLC (SiO_2 , cHex/EtOAc 60:1) R_f = 0.74.



^1H NMR (300 MHz, CDCl_3) δ [ppm] = 7.26 (t, 3J = 7.6 Hz, 2 H, H-3/5), 7.18 – 7.11 (m, 3 H, H-2/4/6), 5.79 (ddt, 3J = 17.0 Hz, 3J = 10.2 Hz, 3J = 6.7 Hz, 1 H, H-11), 4.99 (dd, 3J = 16.9 Hz, 4J = 2.0 Hz, 1 H, H-12), 4.95 – 4.90 (m, 1 H, H-12), 2.59 (t, 3J = 7.9 Hz, 2 H, H-7), 2.07 (ψ q, 3J = 7.1 Hz, 2 H, H-10), 1.70 – 1.56 (m, 2 H, H-8), 1.43 (ψ p, 3J = 7.5 Hz, 2 H, H-9).

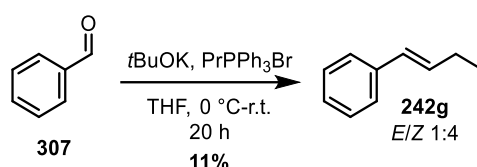
^{13}C NMR (75 MHz, CDCl_3) δ [ppm] = 142.8 (C-1), 139.0 (C-11), 128.5 (C-2/6), 128.4 (C-3/5), 125.8 (C-4), 114.5 (C-12), 36.0 (C-7), 33.8 (C-10), 31.1 (C-8), 28.7 (C-9).

GC-MS (70 eV) m/z ([%]): 160 (9, $[\text{M}^+]$), 131 (6), 117 (33), 104 (70), 91 (100), 77 (11), 65 (24), 51 (10).

FTIR-ATR ν [cm^{-1}] = 3079 (w), 3064 (w), 3027 (w), 3001 (w), 2977 (w), 2930 (m), 2857 (w), 1942 (w), 1802 (w), 1641 (w), 1603 (w), 1587 (w), 1496 (m), 1453 (m), 1414 (w), 1260 (w), 1077 (w), 1030 (w), 992 (w), 909 (m), 808 (w), 744 (s), 697 (s), 636 (w), 568 (w).

The analytical data are in agreement with the literature.^[137a]

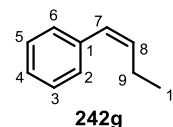
10.2.3.3.3. Synthesis of 1-phenyl-1-butene (242g)



The synthesis was performed according to a procedure of *Yu et al.*^[137b] Under an atmosphere of argon, a 50 mL *Schlenk* flask was charged with a solution of 6.36 g of PrPPh_3Br (16.5 mmol, 1.1 equiv.) in 20 mL of dry THF. At 0 °C, the solution was treated with 1.89 g of $\text{KO}t\text{Bu}$ (16.9 mmol, 1.1 equiv.). The reaction mixture was stirred for 30 min at r.t. Then 1.5 mL of benzaldehyde (**307**) (1.6 g, 15 mmol, 1.0 equiv.) were added and the reaction was stirred for 20 h. Subsequently, 10 mL of sat. NH_4Cl solution were added and the aqueous phase was extracted with Et_2O (3 x 30 mL). The combined organic phases were dried with Na_2SO_4 and concentrated under reduced pressure (**attention**: product is volatile). Purification by FCC ($\text{cHex}/\text{Et}_2\text{O}$ 9:1) gave 210 mg of **242g** as a pale yellow liquid (1.60 mmol, 11%, *E/Z* 1:4; Lit.:^[137b] not given).

M ($\text{C}_{10}\text{H}_{12}$) = 132.21 g/mol.

TLC (SiO_2 , cHex/EtOAc 9:1) R_f = 0.86.



^1H NMR (300 MHz, CDCl_3) δ [ppm] = 7.48 – 7.25 (m, 5 H, H-2/3/4/5/6), 6.48 (d, $^3J = 11.8$ Hz, 1 H, H-7), 5.95 – 5.62 (m, 1 H, H-8), 2.54 – 2.37 (m, 2 H, H-9), 1.27 – 1.07 (m, 3 H, H-10).

^{13}C NMR (75 MHz, CDCl_3) δ [ppm] = 137.9 (C-1), 134.9 (C-8), 128.9 (C-2/6), 128.4 (C-7), 128.2 (C-3/5), 126.6 (C-4), 22.1 (C-9), 14.6 (C-10).

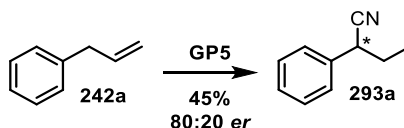
GC-MS (70 eV) m/z ([%]): 132 (50, $[\text{M}^+]$), 117 (100), 91 (23), 77 (5), 51 (3).

FTIR-ATR ν [cm^{-1}] = 3082 (w), 3058 (w), 3025 (w), 3009 (w), 2964 (m), 2933 (w), 2875 (w), 1945 (w), 1880 (w), 1803 (w), 1642 (w), 1600 (w), 1576 (w), 1493 (m), 1456 (w), 1447 (m), 1407 (w), 1375 (w), 1307 (w), 1263 (w), 1180 (w), 1156 (w), 1070 (m), 1029 (w), 964 (m), 915 (m), 841 (w), 794 (m), 765 (s), 741 (m), 697 (s), 618 (w), 606 (w), 531 (m).

The analytical data are in agreement with the literature.^[137b]

10.2.3.4. Hydrocyanation of phenylalkenes

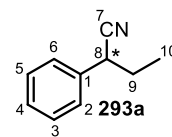
10.2.3.4.1. Synthesis of 2-phenylbutyronitrile (**293a**)



According to the general procedure **GP5**, 66 μL of 3-phenyl-1-propene (**242a**) (59 mg, 0.50 mmol, 1.0 equiv.) were reacted at r.t. and purification by FCC (cHex/EtOAc 60:1) gave 33 mg of benzyl nitrile **293a** as a colorless liquid (0.23 mmol, 45%, 80:20 *er*; from internal olefin **242h**: 66:34 *er*). **Attention:** Product is volatile.

M ($\text{C}_{10}\text{H}_{11}\text{N}$) = 145.21 g/mol.

TLC (SiO_2 , cHex/EtOAc 60:1) R_f = 0.17.



$^1\text{H NMR}$ (500 MHz, CDCl_3) δ [ppm] = 7.41 – 7.36 (m, 2 H, H-3/5), 7.35 – 7.30 (m, 3 H, H-2/4/6), 3.74 (t, 3J = 7.2 Hz, 1 H, H-8), 2.01 – 1.79 (m, 2 H, H-9), 1.08 (t, 3J = 7.4 Hz, 3 H, H-10).

$^{13}\text{C NMR}$ (75 MHz, CDCl_3) δ [ppm] = 135.8 (C-1), 129.1 (C-3/5), 128.1 (C-4), 127.4 (C-2/6), 120.8 (C-7), 39.0 (C-8), 29.3 (C-9), 11.5 (C-10).

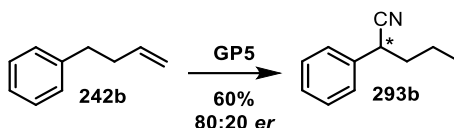
GC-MS (70 eV) m/z ([%]): 145 (45, $[\text{M}^+]$), 117 (100), 104 (8), 89 (42), 77 (10), 63 (14), 51 (15).

FTIR-ATR ν [cm^{-1}] = 3065 (w), 3032 (w), 2972 (m), 2936 (w), 2879 (w), 2240 (w), 1952 (w), 1876 (w), 1807 (w), 1724 (w), 1602 (w), 1493 (m), 1454 (m), 1384 (w), 1343 (w), 1233 (w), 1073 (w), 1031 (w), 942 (w), 911 (w), 891 (w), 823 (w), 799 (w), 759 (s), 697 (s), 649 (w), 640 (w), 619 (w), 593 (w), 554 (w), 511 (w).

Enantiomeric separation by chGC column: MEGA DEX BETA (30M x 0.25 mm \varnothing), temperature program: 50 $^\circ\text{C}$, 50 $^\circ\text{C}$ – 180 $^\circ\text{C}$ (1 $^\circ\text{C}/\text{min}$). Flow rate: 3 mL/min. Major enantiomer T_R = 47.7 min; minor enantiomer T_R = 51.7 min.

The analytical data are in agreement with the literature.^[230]

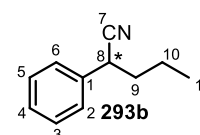
10.2.3.4.2. Synthesis of 2-phenylvaleronitrile (**293b**)



According to the general procedure **GP5**, 75 μL of 4-phenyl-1-butene (**242b**) (66 mg, 0.50 mmol, 1.0 equiv.) were reacted at r.t. and purification by FCC (cHex/EtOAc 60:1) gave 53 mg of a pale yellow liquid (~5 mg of cHex/EtOAc residues; 48 mg of benzyl nitrile product **293b**, 0.30 mmol, 60%, 80:20 *er*, from internal olefin **242g**: 77:23 *er*).

M ($\text{C}_{11}\text{H}_{13}\text{N}$) = 159.23 g/mol.

TLC (SiO_2 , cHex/EtOAc 60:1) R_f = 0.19.



$^1\text{H NMR}$ (500 MHz, CDCl_3) δ [ppm] = 7.44 – 7.28 (m, 5 H, H-2/3/4/5/6), 3.79 (dd, $^3J = 8.5$ Hz, $^3J = 6.3$ Hz, 1 H, H-8), 2.01 – 1.74 (m, 2 H, H-9), 1.65 – 1.45 (m, 2 H, H-10), 0.97 (t, $^3J = 7.3$ Hz, 3 H, H-11).

$^{13}\text{C NMR}$ (75 MHz, CDCl_3) δ [ppm] = 136.2 (C-1), 129.1 (C-3/5), 128.1 (C-4), 127.3 (C-2/6), 121.0 (C-8), 38.0 (C-9), 37.3 (C-8), 20.4 (C-10), 13.5 (C-11).

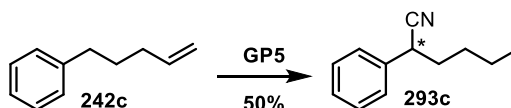
GC-MS (70 eV) m/z ([%]): 159 (18, $[\text{M}^+]$), 117 (100), 103 (8), 89 (20), 77 (12), 51 (14).

FTIR-ATR ν [cm^{-1}] = 3062 (w), 3032 (w), 2961 (m), 2933 (m), 2875 (w), 2239 (w), 2217 (w), 1720 (w), 1602 (w), 1494 (w), 1466 (m), 1455 (m), 1382 (w), 1345 (w), 1271 (w), 1248 (w), 1159 (w), 1111 (w), 1073 (w), 1030 (w), 940 (w), 914 (w), 856 (w), 756 (s), 698 (s), 639 (w), 620 (w), 573 (w), 509 (w).

Enantiomeric separation by chGC column: MEGA DEX B-SE (30M x 0.25 mm \varnothing), temperature program: 50 $^\circ\text{C}$, 50 $^\circ\text{C}$ – 180 $^\circ\text{C}$ (0.25 $^\circ\text{C}/\text{min}$). Flow rate: 4 mL/min. Major enantiomer T_R = 140.5 min; minor enantiomer T_R = 135.1 min.

The analytical data are in agreement with the literature.^[116]

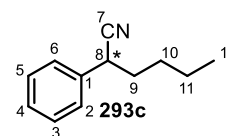
10.2.3.4.3. Synthesis of 2-phenylhexanenitrile (**293c**)



According to the general procedure **GP5**, 83 μL of 5-phenyl-1-pentene (**242c**) (73 mg, 0.50 mmol, 1.0 equiv.) were reacted at r.t. and purification by FCC (cHex/EtOAc 60:1) gave 48 mg of benzyl nitrile **293c** as a pale yellow liquid (0.23 mmol, 50%).

M (C₁₂H₁₅N) = 173.26 g/mol.

TLC (SiO₂, cHex/EtOAc 60:1) R_f = 0.19.



¹H NMR (500 MHz, CDCl₃) δ [ppm] = 7.43 – 7.35 (m, 2 H, H-3/5), 7.35 – 7.29 (m, 3 H, H-2/4/6), 3.77 (dd, ³J = 8.6 Hz, ³J = 6.2 Hz, 1 H, H-8), 1.99 – 1.77 (m, 2 H, H-9), 1.53 – 1.45 (m, 2 H, H-10), 1.41 – 1.32 (m, 2 H, H-11), 0.91 (t, ³J = 7.3 Hz, 3 H, H-12).

¹³C NMR (75 MHz, CDCl₃) δ [ppm] = 136.2 (C-1), 129.2 (C-3/5), 128.1 (C-4), 127.4 (C-2/6), 121.1 (C-7), 37.5 (C-8), 35.7 (C-9), 29.2 (C-10), 22.2 (C-11), 13.9 (C-12).

GC-MS (70 eV) m/z ([%]): 173 (17, [M⁺]), 117 (100), 104 (10), 91 (18), 77 (9), 63 (8), 57 (10), 21 (10).

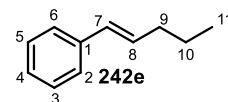
FTIR-ATR ν [cm⁻¹] = 3065 (w), 3029 (w), 2958 (m), 2931 (m), 2863 (w), 2241 (w), 2215 (w), 1721 (w), 1601 (w), 1495 (w), 1466 (w), 1455 (m), 1380 (w), 1270 (w), 1246 (w), 1116 (w), 1103 (w), 1075 (w), 1031 (w), 911 (w), 877 (w), 853 (w), 753 (s), 698 (s), 639 (w), 620 (w), 581 (w), 538 (w), 518 (w).

The analytical data are in agreement with the literature.^[118]

Analytical data of isomerized starting material 1-phenyl-1-pentene **242e** (colorless liquid).

M (C₁₁H₁₄) = 146.23 g/mol.

TLC (SiO₂, cHex/EtOAc 60:1) R_f = 0.71.



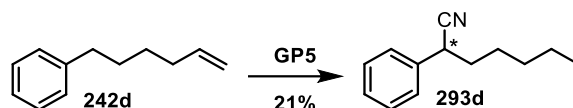
¹H NMR (500 MHz, CDCl₃) δ [ppm] = 7.40 – 7.35 (m, 2 H, H-2/6), 7.34 – 7.28 (m, 2 H, H-3/5), 7.21 (dd, ³J = 7.0 Hz, ⁴J = 1.4 Hz, 1 H, H-4), 6.41 (d, ³J = 15.8 Hz, 1 H, H-7), 6.26 (dt, ³J = 15.7 Hz, ³J = 6.8 Hz, 1 H, H-8), 2.22 (ψqd, ³J = 7.1 Hz, ⁴J = 1.4 Hz, 2 H, H-9), 1.53 (ψh, ³J = 7.4 Hz, 2 H, H-10), 0.99 (t, ³J = 7.4 Hz, 3 H, H-11).

¹³C NMR (75 MHz, CDCl₃) δ [ppm] = 138.1 (C-1), 131.1 (C-8), 130.1 (C-7), 128.6 (C-3/5), 126.9 (C-4), 126.1 (C-2/6), 35.3 (C-9), 22.7 (C-10), 13.9 (C-11).

GC-MS (70 eV) m/z ([%]): 146 (32, [M⁺]), 117 (100), 104 (30), 91 (34), 77 (8), 65 (9), 51 (10).

FTIR-ATR ν [cm⁻¹] = 3081 (w), 3061 (w), 3025 (w), 2989 (w), 2959 (m), 2928 (m), 2904 (w), 2872 (m), 1942 (w), 1871 (w), 1798 (w), 1741 (w), 1703 (w), 1654 (w), 1598 (w), 1577 (w), 1493 (w), 1450 (w), 1434 (w), 1405 (w), 1379 (w), 1339 (w), 1261 (w), 1072 (m), 1049 (w), 1029 (w), 962 (s), 909 (w), 808 (w), 774 (w), 736 (s), 713 (w), 691 (s), 605 (w), 518 (w).

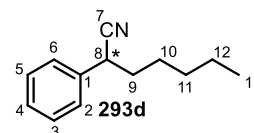
The analytical data are in agreement with the literature.^[231]

10.2.3.4.4. Synthesis of 2-phenylheptanenitrile (**293c**)

According to the general procedure **GP5**, 90 μL of 6-phenyl-1-hexene (**242d**) (80 mg, 0.50 mmol, 1.0 equiv.) were reacted at 50 $^{\circ}\text{C}$ and purification by FCC (cHex/EtOAc 60:1) gave 20 mg of benzyl nitrile **293d** as a pale yellow liquid (0.11 mmol, 21%).

M ($\text{C}_{13}\text{H}_{17}\text{N}$) = 187.29 g/mol.

TLC (SiO_2 , cHex/EtOAc 60:1) R_f = 0.16.



$^1\text{H NMR}$ (500 MHz, CDCl_3) δ [ppm] = 7.33 – 7.27 (m, 2 H, H-3/5), 7.27 – 7.21 (m, 3 H, H-2/4/6), 3.69 (dd, $^3J = 8.7$ Hz, $^3J = 6.2$ Hz, 1 H, H-8), 1.92 – 1.67 (m, 2 H, H-9), 1.48 – 1.38 (m, 4 H, H-10/11), 1.27 – 1.19 (m, 2 H, H-12), 0.87 – 0.75 (m, 3 H, H-13).

$^{13}\text{C NMR}$ (75 MHz, CDCl_3) δ [ppm] = 136.2 (C-1), 129.1 (C-3/5), 128.1 (C-4), 127.3 (C-2/6), 121.1 (C-7), 37.5 (C-8), 36.0 (C-9), 31.2 (C-10), 26.8 (C-11), 22.5 (C-12), 14.0 (C-13).

GC-MS (70 eV) m/z ([%]): 187 (13, $[\text{M}^+]$), 160 (4), 129 (4), 117 (100), 104 (14), 91 (22), 77 (6), 65 (5), 56 (83), 51 (6).

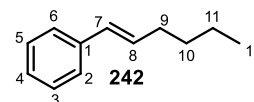
FTIR-ATR ν [cm^{-1}] = 2989 (w), 2957 (m), 2929 (s), 2862 (w), 2240 (w), 2217 (w), 1956 (w), 1876 (w), 1810 (w), 1722 (w), 1601 (w), 1495 (w), 1466 (w), 1454 (m), 1407 (w), 1394 (w), 1380 (w), 1242 (w), 1075 (m), 1068 (m), 1057 (m), 900 (w), 857 (w), 805 (w), 753 (m), 698 (s), 640 (w), 618 (w), 607 (w), 580 (w), 538 (w), 520 (w), 507 (w).

The analytical data are in agreement with the literature.^[232]

Analytical data of isomerized starting material 1-phenyl-1-hexene **242f** (colorless liquid).

M ($\text{C}_{12}\text{H}_{16}$) = 160.26 g/mol.

TLC (SiO_2 , cHex/EtOAc 60:1) R_f = 0.74.



$^1\text{H NMR}$ (500 MHz, CDCl_3) δ [ppm] = 7.41 – 7.34 (m, 2 H, H-2/6), 7.34 – 7.28 (m, 2 H, H-3/5), 7.25 – 7.14 (m, 1 H, H-4), 6.41 (d, $^3J = 15.7$ Hz, 1 H, H-7), 6.26 (dt, $^3J = 15.7$ Hz, $^3J = 6.9$ Hz, 1 H, H-8), 2.25 (ψq , $^3J = 6.9$ Hz, 2 H, H-9), 1.55 – 1.49 (m, 2 H, H-10), 1.45 – 1.38 (m, 2 H, H-11), 1.09 – 0.86 (m, 3 H, H-12).

$^{13}\text{C NMR}$ (75 MHz, CDCl_3) δ [ppm] = 138.1 (C-1), 131.3 (C-8), 129.9 (C-7), 128.6 (C-3/5), 126.9 (C-4), 126.0 (C-2/6), 32.9 (C-9), 31.7 (C-10), 22.4 (C-11), 14.1 (C-12).

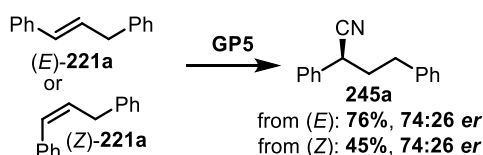
GC-MS (70 eV) m/z ([%]): 160 (7, [M⁺]), 131 (7), 117 (7), 104 (18), 91 (100), 77 (5), 65 (17), 51 (7).

FTIR-ATR ν [cm⁻¹] = 3081 (w), 3062 (w), 3025 (w), 2958 (m), 2925 (m), 2872 (m), 2856 (m), 1945 (w), 1871 (w), 1802 (w), 1736 (w), 1652 (w), 1599 (w), 1495 (w), 1453 (w), 1407 (w), 1394 (w), 1378 (w), 1308 (w), 1242 (w), 1158 (w), 1067 (m), 1057 (m), 963 (s), 933 (w), 906 (w), 891 (w), 866 (w), 775 (w), 742 (s), 691 (s), 614 (w), 606 (w), 571 (w), 516 (w).

The analytical data are in agreement with the literature.^[233]

10.2.3.5. Hydrocyanation of homostilbenes (1,3-diarylpropenes)

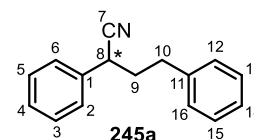
10.2.3.5.1. Synthesis of 1,4-diphenylbutyronitrile (**245a**)



According to the general procedure **GP5**, 96 μL of (*E*)-homostilbene ((*E*)-**221a**) or 97 μL of (*Z*)-homostilbene ((*Z*)-**221a**) (97 mg, 0.50 mmol, 1.0 equiv.) were reacted at r.t. and purification by FCC (cHex/EtOAc 40:1) gave 84 mg of product **245a** starting from (*E*)-**221a** (0.38 mmol, 76%, 74:26 *er*) or 50 mg of **245a** starting from (*Z*)-**221a** (0.23 mmol, 45%, 74:26 *er*) as a colorless oil. The absolute (*S*)-configuration was confirmed by comparison of the experimental and calculated ECD spectrum.

M (C₁₆H₁₅N) = 221.30 g/mol.

TLC (SiO₂, cHex/EtOAc 40:1) R_f = 0.19.



¹H NMR (500 MHz, CDCl₃) δ [ppm] = 7.42 – 7.36 (m, 2 H, H-3/5), 7.35 – 7.29 (m, 5 H, H-2/4/6/13/15), 7.26 – 7.18 (m, 3 H, H-12/14/16), 3.75 (dd, ³*J* = 9.0 Hz, ³*J* = 6.0 Hz, 1 H, H-8), 3.10 – 2.58 (m, 2 H, H-10), 2.28 (ψ ddd, ²*J* = 14.6 Hz, ³*J* = 8.8 Hz, ³*J* = 5.8 Hz, 1 H, H-9), 2.18 (dddd, ²*J* = 13.6 Hz, ³*J* = 8.9 Hz, ³*J* = 7.4 Hz, ³*J* = 6.0 Hz, 1 H, H-9).

¹³C NMR (75 MHz, CDCl₃) δ [ppm] = 139.9 (C-11), 135.8 (C-1), 129.3 (C-3/5), 128.8 (C-12/16), 128.6 (C-13/15), 128.3 (C-4), 127.4 (C-2/6), 126.6 (C-14), 120.8 (C-7), 37.5 (C-9), 36.7 (C-8), 33.2 (C-10).

GC-MS (70 eV) m/z ([%]): 221 (42, [M⁺]), 194 (40), 179 (19), 165 (8), 130 (28), 117 (34), 105 (68), 91 (100), 77 (45), 65 (33), 51 (33).

FTIR-ATR ν [cm⁻¹] = 3086 (w), 3063 (w), 3029 (w), 2956 (w), 2929 (m), 2863 (w), 2343 (w), 2241 (w), 1951 (w), 1878 (w), 1808 (w), 1718 (w), 1602 (w), 1586 (w), 1495 (m), 1454 (m),

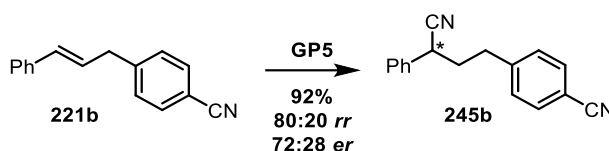
1394 (w), 1381 (w), 1344 (w), 1266 (w), 1183 (w), 1158 (w), 1082 (w), 1029 (w), 1004 (w), 986 (w), 967 (w), 910 (w), 857 (w), 786 (w), 748 (s), 696 (s), 641 (w), 620 (w), 598 (w), 571 (w), 555 (w), 518 (w).

Specific rotation ($c = 0.540$ g/100 mL, CHCl_3 , $[\alpha]_{\lambda}^T$): $[\alpha]_{365}^{20.0} = -53.8^\circ$, $[\alpha]_{436}^{20.0} = -34.6^\circ$, $[\alpha]_{546}^{20.0} = -20.3^\circ$, $[\alpha]_{579}^{20.0} = -18.0^\circ$, $[\alpha]_{589}^{20.0} = -17.4^\circ$.

Enantiomeric separation by chGC column: MEGA DEX B-SE (30M x 0.25 mm \varnothing), temperature program: 50 $^\circ\text{C}$, 50 $^\circ\text{C}$ – 180 $^\circ\text{C}$ (0.5 $^\circ\text{C}/\text{min}$). Flow rate: 4 mL/min. Major enantiomer $T_R = 196.1$ min; minor enantiomer $T_R = 198.4$ min.

The analytical data are in agreement with the literature.^[234]

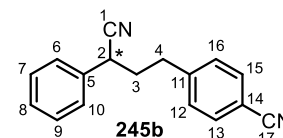
10.2.3.5.2. Synthesis of 1,4-diarylbutyronitrile **245b**



According to the general procedure **GP5**, 112 mg cyanohomostilbene **221b** (0.511 mmol, 1.0 equiv.) were reacted at 50 $^\circ\text{C}$ and purification by FCC (cHex/EtOAc 9:1) gave 116 mg of **245b** as a colorless oil (0.471 mmol, 92%, 80:20 *rr*, 71:29 *er*).

M ($\text{C}_{17}\text{H}_{14}\text{N}_2$) = 246.31 g/mol.

TLC (SiO_2 , cHex/EtOAc 40:1) $R_f = 0.09$.



$^1\text{H NMR}$ (500 MHz, CDCl_3) δ [ppm] = 7.61 – 7.55 (m, 2 H, H-13/15), 7.41 – 7.37 (m, 2 H, H-7/9), 7.36 – 7.33 (m, 1 H, H-8), 7.33 – 7.30 (m, 2 H, H-12/16), 7.30 – 7.28 (m, 2 H, H-6/10), 3.78 (dd, $^3J = 8.8$ Hz, $^3J = 6.0$ Hz, 1 H, H-2), 2.91 – 2.76 (m, 2 H, H-4), 2.30 – 2.22 (m, 1 H, H-3), 2.21 – 2.13 (m, 1 H, H-3).

$^{13}\text{C NMR}$ (151 MHz, CDCl_3) δ [ppm] = 145.5 (C-11), 135.1 (C-5), 132.5 (C-13/15), 129.29 (C-7/9), 129.27 (C-6/10), 128.4 (C-8), 127.2 (C-12/16), 120.3 (C-1), 118.8 (C-17), 110.5 (C-14), 36.72 (C-3), 36.71 (C-2), 33.2 (C-4).

GC-MS (70 eV) m/z ([%]): 246 (16, $[\text{M}^+]$), 130 (83), 117 (100), 102 (42), 89 (31), 77 (23), 51 (14).

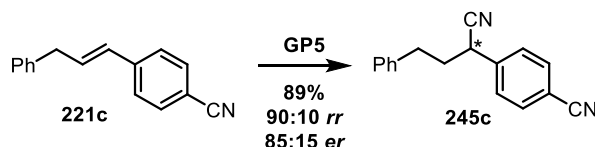
HR-ESI-MS m/z calculated $[\text{C}_{17}\text{H}_{14}\text{N}_2 + \text{H}^+]$: 247.1229750; found: 247.12335.

FTIR-ATR ν [cm^{-1}] = 3092 (w), 3064 (w), 3009 (w), 2952 (w), 2931 (w), 2865 (w), 2228 (m), 1922 (w), 1809 (w), 1736 (w), 1608 (m), 1505 (m), 1495 (m), 1455 (m), 1415 (w), 1344 (w), 1290 (w), 1193 (w), 1778 (w), 1159 (w), 1080 (w), 1021 (w), 1004 (w), 969 (w), 913 (w), 891

(w), 872 (w), 827 (s), 752 (s), 698 (s), 647 (w), 620 (w), 586 (w), 568 (m), 552 (s), 517 (w), 442 (w), 422 (w).

Enantiomeric separation by chHPLC column: Diacel Chiralpak AD-H (No 39), eluent mixture: *n*Hex/*i*PrOH 95:5, detection at 254 nm. Flow rate: 0.5 mL/min. Major enantiomer $T_R = 86.9$ min; minor enantiomer $T_R = 81.3$ min.

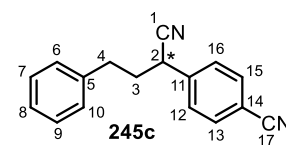
10.2.3.5.3. Synthesis of 1,4-diarylbutyronitrile **245c**



According to the general procedure **GP5**, 110 mg of cyanohomostilbene **221c** (0.500 mmol, 1.0 equiv.) were reacted at 50 °C and purification by FCC (*c*Hex/EtOAc 9:1) gave 117 mg of a colorless oil (~8 mg of EtOAc residues; 109 mg of **245c**, 0.443 mmol, 89%, 90:10 *rr*, 85:15 *er*). At r.t., 114 mg of a colorless oil were obtained (~6 mg of EtOAc/H₂O residues; 108 mg of **245c**, 0.438 mmol, 88%, 93:7 *rr*, 88:12 *er*).

M (C₁₇H₁₄N₂) = 246.31 g/mol.

TLC (SiO₂, *c*Hex/EtOAc 9:1) $R_f = 0.19$.



¹H NMR (600 MHz, CDCl₃) δ [ppm] = 7.71 – 7.66 (m, 2 H, H-13/15), 7.48 – 7.42 (m, 2 H, H-12/16), 7.34 – 7.30 (m, 2 H, H-7/9), 7.26 – 7.23 (m, 1 H, H-8), 7.21 – 7.17 (m, 2 H, H-6/10), 3.80 (dd, ³*J* = 9.3 Hz, ³*J* = 5.8 Hz, 1 H, H-2), 2.92 – 2.75 (m, 2 H, H-4), 2.27 (dddd, ²*J* = 13.8 Hz, ³*J* = 9.3 Hz, ³*J* = 8.3 Hz, ³*J* = 5.6 Hz, 1 H, H-3), 2.21 – 2.11 (m, 1 H, H-3).

¹³C NMR (151 MHz, CDCl₃) δ [ppm] = 141.0 (C-11), 139.2 (C-5), 133.1 (C-13/15), 129.0 (C-7/9), 128.5 (C-6/10), 128.3 (C-12/6), 126.9 (C-8), 119.5 (C-1), 118.2 (C-17), 112.5 (C-14), 37.3 (C-3), 36.7 (C-2), 33.1 (C-4).

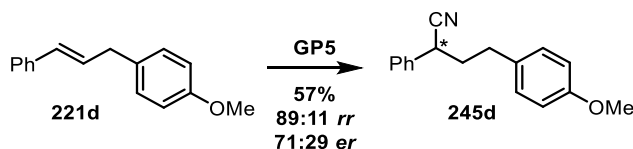
GC-MS (70 eV) *m/z* ([%]): 246 (65, [M⁺]), 207 (14), 155 (46), 141 (22), 114 (18), 105 (83), 92 (100), 77 (43), 51 (24).

FTIR-ATR ν [cm⁻¹] = 3063 (w), 3028 (w), 2989 (w), 2955 (w), 2928 (w), 2865 (w), 2230 (s), 1927 (w), 1809 (w), 1735 (m), 1608 (m), 1506 (m), 1497 (m), 1455 (m), 1414 (m), 1338 (w), 1285 (w), 1258 (w), 1205 (w), 1179 (w), 1156 (w), 1114 (w), 1080 (w), 1066 (w), 1029 (w), 1021 (w), 968 (w), 911 (w), 834 (s), 792 (w), 749 (s), 699 (s), 646 (w), 621 (w), 599 (m), 566 (s), 495 (w), 469 (w), 417 (w).

HR-ESI-MS *m/z* calculated [C₁₇H₁₄N₂+Na⁺]: 269.1049197; found: 269.10513.

Enantiomeric separation by chHPLC column: Diacel Chiralpak AD-H (No 39), eluent mixture: *n*Hex/*i*PrOH 95:5, detection at 254 nm. Flow rate: 0.5 mL/min. Major enantiomer $T_R = 78.6$ min; minor enantiomer $T_R = 57.4$ min.

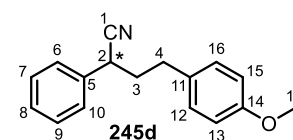
10.2.3.5.4. Synthesis of 1,4-diarylbutyronitrile **245d**



According to the general procedure **GP5**, 112 mg methoxyhomostilbene **221d** (0.499 mmol, 1.0 equiv.) were reacted at 50 °C and purification by FCC (*c*Hex/*E*tOAc 20:1) gave 72 mg of **245d** as a colorless oil (0.29 mmol, 57%, 89:11 *rr*, 71:29 *er*).

M ($C_{17}H_{17}NO$) = 251.33 g/mol.

TLC (SiO_2 , *c*Hex/*E*tOAc 9:1) $R_f = 0.36$.



1H NMR (500 MHz, $CDCl_3$) δ [ppm] = 7.42 – 7.36 (m, 2 H, H-7/9), 7.35 – 7.29 (m, 3 H, H-6/8/10), 7.15 – 7.09 (m, 2 H, H-12/16), 6.89 – 6.84 (m, 2 H, H-13/15), 3.80 (s, 3 H, H-17), 3.73 (dd, $^3J = 9.0$ Hz, $^3J = 6.0$ Hz, 1 H, H-2), 2.90 – 2.67 (m, 2 H, H-4), 2.32 – 2.19 (m, 1 H, H-3), 2.19 – 2.08 (m, 1 H, H-3).

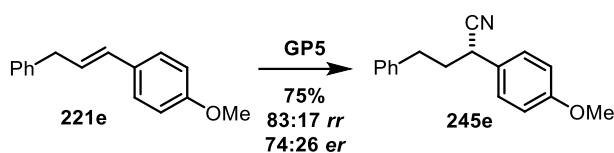
^{13}C NMR (126 MHz, $CDCl_3$) δ [ppm] = 158.4 (C-14), 135.8 (C-5), 131.9 (C-11), 129.5 (C-12/16), 129.2 (C-7/9), 128.2 (C-8), 127.4 (C-6/10), 120.8 (C-1), 114.2 (C-13/15), 55.4 (C-17), 37.7 (C-3), 36.6 (C-2), 32.3 (C-4).

GC-MS (70 eV) m/z ([%]): 251 (19, $[M^+]$), 135 (21), 121 (100), 116 (47), 105 (25), 91 (82), 77 (76), 51 (42).

FTIR-ATR ν [cm^{-1}] = 3063 (w), 3031 (w), 2990 (w), 2954 (w), 2932 (w), 2863 (w), 2836 (w), 2240 (w), 2058 (w), 1956 (w), 1883 (w), 1734 (w), 1684 (w), 1611 (m), 1584 (w), 1511 (s), 1495 (w), 1464 (w), 1454 (m), 1442 (w), 1421 (w), 1394 (w), 1381 (w), 1344 (w), 1301 (m), 1244 (s), 1178 (m), 1109 (w), 1079 (w), 1066 (w), 1032 (s), 959 (w), 891 (w), 826 (m), 812 (w), 752 (m), 698 (s), 654 (w), 638 (w), 588 (w), 542 (w), 511 (m).

Enantiomeric separation by chHPLC column: Diacel Chiralpak AD-H (No 14), eluent mixture: *n*Hex/*i*PrOH 99:1 (90:10 for racemic standard), detection at 254 nm. Flow rate: 0.5 mL/min (1 mL/min for racemic standard). Major enantiomer $T_R = 29.5$ min; minor enantiomer $T_R = 35.4$ min.

The analytical data are in agreement with the literature.^[235]

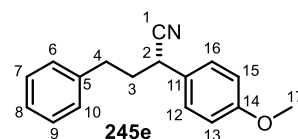
10.2.3.5.5. Synthesis of 1,4-diarylbutyronitrile **245e**

According to the general procedure **GP5**, 112 mg methoxyhomostilbene **221e** (0.499 mmol, 1.0 equiv.) were reacted at 50 °C and purification by FCC (cHex/EtOAc 20:1) gave 94 mg of **245e** as a colorless solid (0.37 mmol, 75%, 83:17 *rr*, 74:26 *er*). The absolute (*S*)-configuration was confirmed by X-ray crystallography.

M (C₁₇H₁₇NO) = 251.33 g/mol.

TLC (SiO₂, cHex/EtOAc 9:1) R_f = 0.33.

M.p. 49 - 52 °C.



¹H NMR (500 MHz, CDCl₃) δ [ppm] = 7.34 – 7.28 (m, 2 H, H-7/9), 7.26 – 7.21 (m, 3 H, H-6/8/10), 7.21 – 7.17 (m, 2 H, H-12/16), 6.95 – 6.88 (m, 2 H, H-13/15), 3.81 (s, 3 H, H-17), 3.69 (dd, ³J = 9.0 Hz, ³J = 6.3 Hz, 1 H, H-2), 2.79 (ϕtt, ²J = 14.2 Hz, ²J = 6.8 Hz, 2 H, H-4), 2.31 – 2.19 (m, 1 H, H-3), 2.14 (dddd, ²J = 13.5 Hz, ³J = 8.7 Hz, ³J = 7.3 Hz, ³J = 6.2 Hz, 1 H, H-3).

¹³C NMR (75 MHz, CDCl₃) δ [ppm] = 159.5 (C-14), 140.0 (C-5), 128.8 (C-7/9), 128.6 (C-6/10), 127.7 (C-12/16), 126.6 (C-8), 121.0 (C-1), 114.6 (C-13/15), 55.5 (C-17), 37.5 (C-3), 35.9 (C-2), 33.1 (C-4).

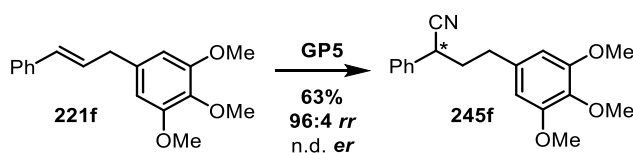
GC-MS (70 eV) m/z ([%]): 251 (20, [M⁺]), 224 (9), 160 (11), 146 (46), 134 (19), 121 (18), 105 (37), 91 (100), 77 (48), 64 (20), 51 (35).

FTIR-ATR ν [cm⁻¹] = 3090 (w), 3064 (w), 3032 (w), 3010 (w), 2958 (w), 2929 (w), 2863 (w), 2837 (w), 2241 (w), 2040 (w), 1980 (w), 1952 (w), 1887 (w), 1761 (w), 1610 (m), 1584 (m), 1512 (s), 1498 (w), 1456 (m), 1443 (w), 1425 (w), 1362 (w), 1349 (w), 1336 (w), 1303 (m), 1289 (w), 1220 (s), 1179 (s), 1110 (w), 1080 (w), 1025 (s), 971 (w), 958 (w), 932 (w), 908 (w), 892 (w), 828 (s), 819 (w), 773 (w), 753 (m), 737 (s), 699 (s), 637 (w), 621 (w), 603 (m), 594 (w), 561 (m), 532 (m).

Enantiomeric separation by chHPLC column: Diacel Chiralpak AD-H (No 14), eluent mixture: *n*Hex/*i*PrOH 90:10, detection at 254 nm. Flow rate: 1 mL/min. Major enantiomer T_R = 10.97 min; minor enantiomer T_R = 9.00 min.

The analytical data are in agreement with the literature.^[234]

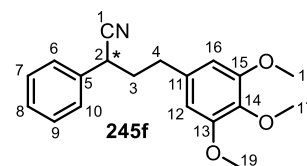
10.2.3.5.6. Synthesis of 1,4-diarylbutyronitrile **245f**



According to the general procedure **GP5**, 163 mg of trimethoxyhomostilbene **221f** (\cong 142 mg, $\omega(\text{TMB}) = 13\%$, 0.500 mmol, 1.0 equiv.) were reacted at 50 °C and purification by FCC (cHex/EtOAc 9:1) gave 98 mg of **245f** as a colorless oil (0.32 mmol, 63%, 96:4 *rr*, *er* n.d.).

M ($\text{C}_{19}\text{H}_{21}\text{NO}_3$) = 311.38 g/mol.

TLC (SiO_2 , cHex/EtOAc 9:1) $R_f = 0.14$.



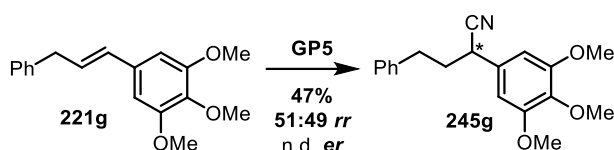
$^1\text{H NMR}$ (500 MHz, CDCl_3) δ [ppm] = 7.42 – 7.37 (m, 2 H, H-7/9), 7.36 – 7.31 (m, 3 H, H-6/8/10), 6.40 (s, 2 H, H-12/16), 3.85 (s, 6 H, H-18/19), 3.83 (s, 3 H, H-17), 3.76 (dd, $^3J = 9.2$ Hz, $^3J = 5.9$ Hz, 1 H, H-2), 2.86 – 2.65 (m, 2 H, H-4), 2.30 – 2.20 (m, 1 H, H-3), 2.20 – 2.11 (m, 1 H, H-3).

$^{13}\text{C NMR}$ (126 MHz, CDCl_3) δ [ppm] = 153.5 (C-13/15), 136.7 (C-14), 135.7 (C-11), 135.6 (C-5), 129.3 (C-7/9), 128.3 (C-8), 127.4 (C-6/10), 120.8 (C-1), 105.4 (C-12/16), 61.0 (C-17), 56.3 (C-18/19), 37.5 (C-3), 36.7 (C-2), 33.7 (C-4).

GC-MS (70 eV) m/z ([%]): 311 (100, $[\text{M}^+]$), 182 (96), 167 (21), 151 (25), 16 (4), 116 (5), 77 (3), 51 (2).

HR-EI-MS m/z calculated $[\text{C}_{19}\text{H}_{21}\text{NO}_3\text{-CH}_3^+]$: 296.12812; found: 296.12766.

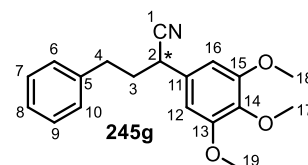
FTIR-ATR ν [cm^{-1}] = 3676 (br), 3061 (w), 2988 (w), 2968 (w), 2954 (w), 2989 (w), 2924 (m), 2241 (w), 2103 (w), 1991 (w), 1966 (w), 1897 (w), 1821 (w), 1736 (w), 1590 (s), 1507 (m), 1495 (m), 1455 (s), 1420 (m), 1365 (w), 1347 (w), 1333 (m), 1282 (w), 1238 (s), 1183 (w), 1149 (w), 1126 (s), 1078 (w), 1066 (w), 1057 (w), 1043 (m), 1021 (w), 1004 (s), 974 (w), 917 (w), 890 (w), 871 (w), 853 (w), 827 (m), 816 (m), 771 (s), 751 (w), 704 (s), 670 (m), 650 (w), 637 (w), 620 (w), 595 (m), 574 (w), 526 (w), 437 (w).

10.2.3.5.7. Synthesis of 1,4-diarylbutyronitrile **245g**

According to the general procedure **GP5**, 162 mg trimethoxyhomostilbene **221g** (0.570 mmol, 1.0 equiv.) were reacted at 50 °C and purification by FCC (cHex/EtOAc 9:1) gave 84 mg of **245g** as a pale yellow oil (0.27 mmol, 47%, 51:49 *rr*, *er* n.d.). For distinct analysis, a small product sample of **245g** was separated from its regioisomer **245f** by repeated FCC (cHex/EtOAc 15:1).

M (C₁₉H₂₁NO₃) = 311.38 g/mol.

TLC (SiO₂, cHex/EtOAc 9:1) R_f = 0.08.



¹H NMR (500 MHz, CDCl₃) δ [ppm] = 7.32 (t, ³J = 7.5 Hz, 2 H, H-7/9), 7.25 – 7.18 (m, 3 H, H-6/8/10), 6.50 (s, 2 H, H-12/16), 3.86 (s, 3 H, H-18/19), 3.84 (s, 3 H, H-17), 3.72 – 3.63 (m, 1 H, H-2), 3.00 – 2.70 (m, 2 H, H-4), 2.34 – 2.21 (m, 1 H, H-3), 2.17 (dddd, ²J = 13.5 Hz, ³J = 9.0 Hz, ³J = 7.2 Hz, ³J = 6.2 Hz, 1 H, H-3).

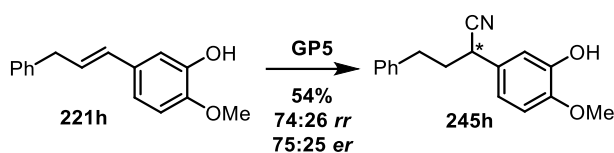
¹³C NMR (126 MHz, CDCl₃) δ [ppm] = 153.8 (C-13/15), 139.8 (C-5), 137.9 (C-14), 131.3 (C-11), 128.8 (C-7/9), 128.6 (C-6/10), 126.7 (C-8), 120.8 (C-1), 104.5 (C-12/16), 61.0 (C-17), 56.4 (C-18/19), 37.4 (C-3), 36.9 (C-2), 33.2 (C-4).

GC-MS (70 eV) m/z ([%]): 311 (39, [M⁺]), 207 (100), 192 (24), 176 (41), 105 (23), 91 (55).

HR-ESI-MS m/z calculated [C₁₉H₂₁NO₃+Na⁺]: 334.1413647; found: 334.14154.

FTIR-ATR ν [cm⁻¹] = 3063 (w), 3027 (w), 3001 (w), 2930 (br), 2841 (w), 2240 (w), 2106 (w), 1952 (w), 1737 (w), 1592 (m), 1508 (m), 1498 (m), 1456 (m), 1422 (m), 1337 (m), 1238 (m), 1184 (w), 1124 (s), 1029 (w), 1004 (m), 979 (w), 923 (w), 826 (m), 782 (w), 749 (m), 700 (m), 655 (w), 572 (w), 528 (w), 489 (w).

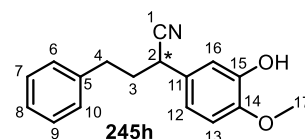
10.2.3.5.8. Synthesis of 1,4-diarylbutyronitrile **245h**



According to the general procedure **GP5**, 120 mg of eugenol derivative **221h** (0.500 mmol, 1.0 equiv.) were reacted at 50 °C and purification by FCC (cHex/EtOAc 5:1) gave 72 mg of **245h** as a pale yellow oil (0.27 mmol, 54%, 74:26 *rr*, 75:25 *er*).

M (C₁₇H₁₇NO₂) = 267.33 g/mol.

TLC (SiO₂, cHex/EtOAc 5:1) R_f = 0.18.



¹H NMR (600 MHz, CDCl₃) δ [ppm] = 7.33 – 7.29 (m, 2 H, H-7/9), 7.25 – 7.21 (m, 1 H, H-8), 7.19 (d, ³J = 6.9 Hz, 2 H, H-6/10), 6.87 (d, ⁴J = 2.0 Hz, 1 H, H-16), 6.84 (d, ³J = 8.3 Hz, 1 H, H-13), 6.81 (dd, ³J = 8.3 Hz, ⁴J = 2.0 Hz, 1 H, H-12), 3.89 (s, 3 H, H-17), 3.64 (dd, ³J = 8.8 Hz, ³J = 6.2 Hz, 1 H, H-2), 2.84 – 2.75 (m, 2 H, H-4), 2.30 – 2.18 (m, 1 H, H-3), 2.18 – 2.08 (m, 1 H, H-3).

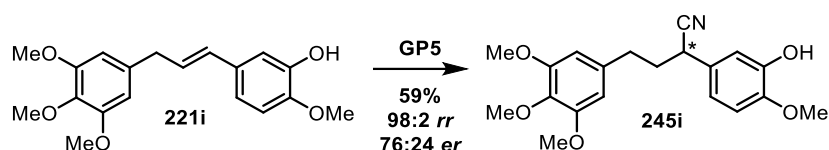
¹³C NMR (151 MHz, CDCl₃) δ [ppm] = 146.5 (C-15), 146.2 (C-14), 140.0 (C-5), 129.2 (C-11), 128.8 (C-7/9), 128.6 (C-6, C-10), 126.6 (C-8), 120.9 (C-1), 119.1 (C-12), 113.7 (C-16), 111.0 (C-13), 56.2 (C-17), 37.4 (C-3), 36.0 (C-2), 33.1 (C-4).

GC-MS (70 eV) m/z ([%]): 267 (100, [M⁺]), 175 (46), 163 (92), 148 (21), 131 (19), 105 (67), 91 (43), 77 (22), 51 (17).

HR-ESI-MS m/z calculated [C₁₇H₁₇NO₂+H⁺]: 268.1332053; found: 268.13320.

FTIR-ATR ν [cm⁻¹] = 3504 (br), 3414 (br), 3063 (s), 3028 (s), 2952 (s), 2933 (w), 2862 (w), 2842 (w), 2241 (w), 1952 (w), 1732 (w), 1593 (m), 1510 (s), 1454 (m), 1441 (m), 1357 (w), 1272 (s), 1236 (s), 1212 (s), 1176 (m), 1153 (w), 1130 (s), 1081 (w), 1026 (s), 958 (w), 914 (w), 867 (w), 805 (m), 762 (s), 752 (s), 699 (s), 634 (w), 614 (w), 589 (w), 572 (w), 537 (w), 491 (w), 447 (w).

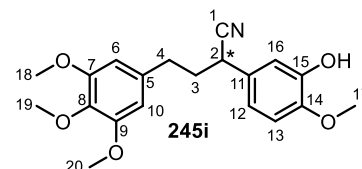
Enantiomeric separation by chHPLC column: Diacel Chiralpak AD-H (No 39), eluent mixture: *n*Hex/*i*PrOH 90:10, detection at 254 nm. Flow rate: 0.5 mL/min. Major enantiomer T_R = 82.5 min; minor enantiomer T_R = 77.8 min.

10.2.3.5.9. Synthesis of 1,4-diarylbutyronitrile **245i**

According to the general procedure **GP5**, 120 mg of trimethoxyhomostilbene **221i** (0.500 mmol, 1.0 equiv.) were reacted at 50 °C and purification by FCC (cHex/EtOAc 3:1) gave 105 mg of **245i** as a pale yellow oil (0.30 mmol, 59%, 98:2 *rr*, 76:24 *er*).

M (C₂₀H₂₃NO₅) = 357.41 g/mol.

TLC (SiO₂, cHex/EtOAc 2:1) R_f = 0.19.



¹H NMR (600 MHz, CDCl₃) δ [ppm] = 6.87 (d, ⁴J = 2.0 Hz, 1 H, H-16), 6.83 (d, ³J = 8.1 Hz, 1 H, H-13), 6.81 (dd, ³J = 8.3 Hz, ⁴J = 2.0 Hz, 1 H, H-12), 6.39 (s, 2 H, H-6/10), 3.88 (s, 3 H, H-17), 3.84 (s, 6 H, H-18/20), 3.82 (s, 3 H, H-19), 3.65 (dd, ³J = 8.8 Hz, ³J = 6.1 Hz, 1 H, H-2), 2.81 – 2.66 (m, 2 H, H-4), 2.26 – 2.16 (m, 1 H, H-3), 2.12 (dddd, ²J = 13.5 Hz, ³J = 9.0 Hz, ³J = 7.3 Hz, ³J = 6.2 Hz, 1 H, H-3).

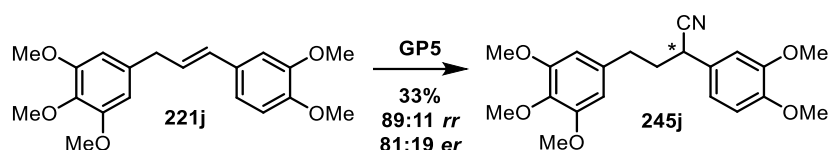
¹³C NMR (151 MHz, CDCl₃) δ [ppm] = 153.4 (C-7/9), 146.5 (C-15), 146.2 (C-14), 136.6 (C-8), 135.7 (C-5), 128.6 (C-11), 120.9 (C-1), 119.0 (C-12), 113.7 (C-16), 111.0 (C-13), 105.4 (C-6/10), 61.0 (C-19), 56.2 (C-18/20), 56.1 (C-17), 37.3 (C-3), 36.0 (C-2), 33.5 (C-4).

GC-MS (70 eV) m/z ([%]): 357 (47, [M⁺]), 182 (100), 167 (22), 151 (29), 137 (5), 119 (4), 105 (2), 91 (4), 77 (4).

HR-ESI-MS m/z calculated [C₂₀H₂₃NO₅+Na⁺]: 380.1468440; found: 380.14702.

FTIR-ATR ν [cm⁻¹] = 3392 (br), 3005 (w), 2937 (w), 2840 (w), 2241 (w), 2100 (w), 1733 (w), 1590 (s), 1508 (s), 1457 (m), 1421 (m), 1350 (w), 1332 (m), 1275 (m), 1237 (s), 1182 (w), 1122 (s), 1025 (m), 1004 (m), 958 (w), 912 (w), 865 (w), 807 (m), 778 (w), 763 (m), 731 (w), 669 (w), 632 (w), 594 (w), 528 (w).

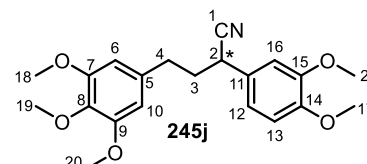
Enantiomeric separation by chHPLC column: Diacel Chiralpak AD-RH (No 36), eluent mixture: MeCN/iPrOH 80:20, detection at 220 nm. Flow rate: 0.2 mL/min. Major enantiomer T_R = 49.8 min; minor enantiomer T_R = 60.1 min.

10.2.3.5.10. Synthesis of 1,4-diarylbutyronitrile **245j**

According to the general procedure **GP5**, 172 mg of trimethoxyhomostilbene **221j** (0.500 mmol, 1.0 equiv.) were reacted at 50 °C and purification by FCC (cHex/EtOAc 3:1) gave 62 mg of **245j** as a pale yellow oil (0.17 mmol, 33%, 89:11 *rr*, 81:19 *er*).

M (C₂₁H₂₅NO₅) = 371.43 g/mol.

TLC (SiO₂, cHex/EtOAc 2:1) R_f = 0.24.



¹H NMR (600 MHz, CDCl₃) δ [ppm] = 6.84 (ψd, 2 H, H-13/16), 6.80 (s, 1 H, H-12), 6.39 (s, 2 H, H-6/10), 3.88 (s, 3 H, H-17), 3.87 (s, 3 H, H-21), 3.84 (s, 6 H, H-18/20), 3.82 (s, 3 H, H-19), 3.69 (dd, ³J = 9.1 Hz, ³J = 6.0 Hz, 1 H, H-2), 2.83 – 2.65 (m, 2 H, H-4), 2.29 – 2.18 (m, 1 H, H-3), 2.13 (dddd, ²J = 13.5 Hz, ³J = 9.2 Hz, ³J = 7.3 Hz, ³J = 6.1 Hz, 1 H, H-3).

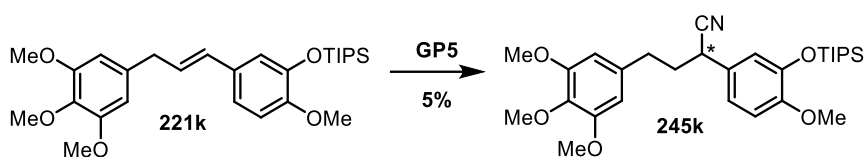
¹³C NMR (151 MHz, CDCl₃) δ [ppm] = 153.4 (C-7/9), 149.5 (C-14/15), 149.0 (C-14/15), 136.6 (C-8), 135.6 (C-5), 128.0 (C-11), 121.0 (C-1), 119.7 (C-12), 111.5 (C-16), 110.4 (C-13), 105.4 (C-6/10), 60.9 (C-19), 56.2 (C-18/20), 56.1 (C-17/21), 56.0 (C-17/21), 37.4 (C-3), 36.2 (C-2), 33.6 (C-4).

GC-MS (70 eV) m/z ([%]): 371 (43, [M⁺]), 344 (6), 313 (4), 182 (100), 167 (22), 151 (30).

HR-EI-MS m/z calculated [C₂₁H₂₅NO₅+Na⁺]: 371.17272; found: 371.17200.

FTIR-ATR ν [cm⁻¹] = 2989 (w), 2959 (w), 2937 (w), 2838 (w), 2239 (w), 2103 (w), 1735 (w), 1590 (m), 1515 (m), 1509 (m), 1373 (w), 1332 (w), 1236 (s), 1184 (w), 1141 (w), 1123 (s), 1066 (w), 1026 (m), 1007 (m), 946 (w), 921 (w), 848 (w), 810 (m), 764 (m), 700 (w), 638 (w), 617 (w), 600 (w), 528 (w), 460 (w).

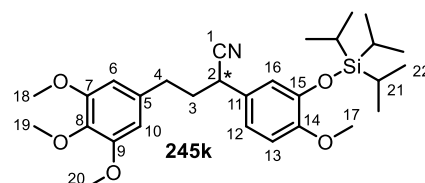
Enantiomeric separation by chHPLC column: Diacel Chiralpak AD-H (No 39), eluent mixture: *n*Hex/*i*PrOH 90:10, detection at 254 nm. Flow rate: 0.6 mL/min. Major enantiomer T_R = 63.7 min; minor enantiomer T_R = 60.0 min.

10.2.3.5.11. Synthesis of 1,4-diarylbutyronitrile **245k**

According to the general procedure **GP5**, 272 mg of trimethoxyhomostilbene **221k** (\cong 243 mg, ω (TIPSOH) = 11%, 0.500 mmol, 1.0 equiv.) were reacted at 50 °C and purification by FCC (cHex/EtOAc 15:1) gave 12 mg of **245k** as a colorless oil (0.023 mmol, 5%; contains minor impurities).

M (C₂₉H₄₃NO₅Si) = 513.75 g/mol.

TLC (SiO₂, cHex/EtOAc 9:1) R_f = 0.13.



¹H NMR (500 MHz, CDCl₃) δ [ppm] = 6.80 – 6.76 (m, 1 H, H-13), 6.73 (ψ dd, 2 H, H-12/16), 6.50 (s, 2 H, H-6/10), 3.86 (s, 6 H, H-18/20), 3.84 (s, 3 H, H-19), 3.79 (s, 3 H, H-17), 3.60 (dd, 3J = 9.3 Hz, 3J = 6.0 Hz, 1 H, H-2), 2.83 – 2.65 (m, 2 H, H-4), 2.25 – 2.17 (m, 1 H, H-3), 2.11 – 2.02 (m, 1 H, H-3), 1.31 – 1.17 (m, 3 H, H-21), 1.09 (d, 3J = 7.4 Hz, 18 H, H-22).

¹³C NMR (151 MHz, CDCl₃) δ [ppm] = 153.8 (C-7/9), 149.7 (C-15), 145.7 (C-14), 137.9 (C-8), 132.1 (C-11), 131.5 (C-5), 121.4 (C-12), 120.81 (C-1), 120.76 (C-16), 112.3 (C-13), 104.5 (C-6/10), 61.0 (C-19), 56.4 (C-18/20), 55.6 (C-17), 37.6 (C-3), 36.7 (C-2), 32.4 (C-4), 18.1 (C-22), 13.1 (C-21).

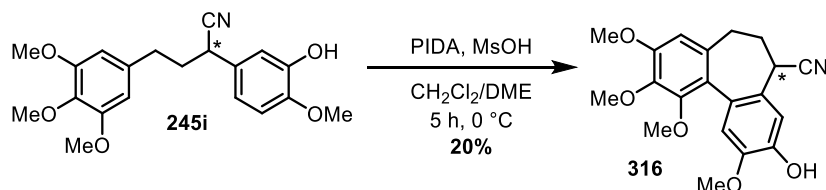
GC-MS (70 eV) m/z ([%]): 470 (100, [M-*i*Pr⁺]), 276 (38), 249 (10), 135 (16), 207 (17), 192 (6), 176 (10), 149 (8).

HR-ESI-MS m/z calculated [C₂₉H₄₃NO₅Si+Na⁺]: 536.2802711; found: 536.28017.

FTIR-ATR ν [cm⁻¹] = 3001 (w), 2943 (m), 2866 (w), 2240 (w), 1739 (w), 1692 (w), 1592 (m), 1509 (s), 1462 (m), 1423 (m), 1383 (w), 1335 (w), 1281 (m), 1232 (s), 1184 (w), 1159 (w), 1127 (s), 1072 (w), 1031 (w), 996 (m), 945 (w), 921 (w), 882 (m), 829 (m), 742 (w), 731 (w), 681 (s), 657 (m), 592 (w), 559 (w), 505 (w), 467 (w).

10.2.3.6. Synthesis of a colchicine analogue

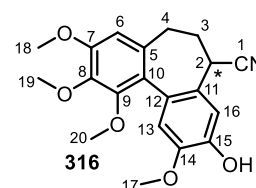
10.2.3.6.1. Synthesis of 7-cyano-colchicol 316



The synthesis was performed based on a modified procedure of *Takubo et al.*^[143c] Under an atmosphere of argon, a 5 mL *Schlenk* tube was charged with a solution of 21 mg of benzyl nitrile **245i** (59 μmol , 1.0 equiv.) in 0.6 mL of anhydrous $\text{CH}_2\text{Cl}_2/\text{DME}$ (1:1). At 0 $^\circ\text{C}$, the colorless solution was treated with 19 mg of PIDA (59 μmol , 1.0 equiv.) and 3.5 μL of MsOH (5.2 mg, 56 μmol , 0.95 equiv.). The reaction mixture was stirred for 5 h before 0.6 mL of sat. NaHCO_3 solution were added. The aqueous phase was extracted with EtOAc (4 x 1 mL). The combined organic phases were dried with MgSO_4 and concentrated under reduced pressure to give a grey crude material. Purification by FCC (SiO_2 , *c*Hex/EtOAc 3:1) gave 4 mg of 7-cyano-colchicol **316** as a colorless wax (11 μmol , 20%). Atrop-diastereomer ratio in CDCl_3 : 85:15 (70:30 in D_3CCN).

M ($\text{C}_{20}\text{H}_{21}\text{NO}_5$) = 355.39 g/mol.

TLC (SiO_2 , *c*Hex/EtOAc 2:1) R_f = 0.30.



$^1\text{H NMR}$ (500 MHz, CDCl_3) δ [ppm] = 7.27 (s, 1 H, H-16), 7.03 (s, 1 H, H-13), 6.58 (s, 1 H, H-6), 5.73 (s, 1 H, OH), 3.92 (s, 3 H, H-19), 3.91 (s, 3 H, H-17), 3.90 (s, 3 H, H-18), 3.61 (s, 3 H, H-20), 3.60 – 3.58 (m, 1 H, H-2), 2.54 – 2.42 (m, 2 H, H-3/4), 2.35 – 2.25 (m, 2 H, H-3/4).

$^{13}\text{C NMR}$ (151 MHz, CDCl_3) δ [ppm] = 153.1 (C-7), 151.1 (C-9), 146.0 (C-14), 145.3 (C-15), 141.5 (C-8), 134.0 (C-5), 126.7 (C-12), 125.5 (C-11), 124.4 (C-10), 120.9 (C-1), 113.2 (C-13), 112.2 (C-16), 108.0 (C-6), 61.3 (C-19), 61.1 (C-20), 56.3 (C-17/18), 56.2 (C-17/18), 38.5 (C-3), 32.0 (C-2), 30.8 (C-4).

GC-MS (70 eV) m/z ([%]): 355 (100, $[\text{M}^+]$), 340 (8), 324 (1), 308 (9), 226 (3).

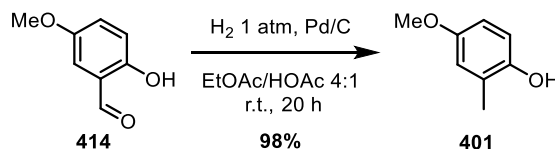
HR-ESI-MS m/z calculated [$\text{C}_{20}\text{H}_{21}\text{NO}_5 + \text{Na}^+$]: 378.1311939; found: 378.13115.

FTIR-ATR ν [cm^{-1}] = 3431 (br), 2959 (m), 2929 (m), 2874 (w), 2860 (w), 2088 (w), 1719 (s), 1578 (w), 1505 (w), 1462 (m), 1408 (w), 1380 (w), 1265 (s), 1247 (s), 1172 (w), 1154 (w), 1115 (s), 1101 (s), 1019 (m), 979 (w), 959 (w), 908 (w), 874 (w), 795 (w), 771 (w), 729 (s), 633 (w), 499 (w).

10.3. Experimental procedures towards chromane natural products by Ir-catalyzed asymmetric desymmetrization

10.3.1. Synthetic studies towards chromane natural products

10.3.1.1. Synthesis of 4-methoxy-2-methylphenol (**401**)

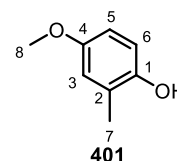


The synthesis was performed based on a modified procedure of *Hecht et al.*^[181] Under an atmosphere of argon, a 500 mL three-necked round-bottomed flask was charged with a suspension of 7.59 g of aldehyde **414** (49.9 mmol, 1.0 equiv.) and 2.81 g of Pd/C ($\omega(\text{Pd}) = 10\%$, 2.63 mmol, 5.3 mol%) in 220 mL of EtOAc/HOAc (4:1). Argon was removed by *Schlenk* line vacuum and H₂ atmosphere (1 atm.) was applied. The reaction mixture was stirred for 20 h. The suspension was diluted with 100 mL of EtOAc and filtered over *Celite*. Evaporation under reduced pressure gave a greenish crude material. After purification by FCC (SiO₂, cHex/EtOAc 5:1) 7.06 g of a beige solid were obtained (~329 mg of HOAc residues; 6.73 g of product **401**, 48.7 mmol, 98%).

M (C₈H₁₀O₂) = 138.17 g/mol.

TLC (SiO₂, cHex/EtOAc 5:1) R_f = 0.30.

M.p.^[179] 71 - 72 °C.



¹H NMR^[179] (500 MHz, CDCl₃) δ [ppm] = 6.72 (d, ³J = 3.1 Hz, 1 H, H-3), 6.70 (d, ³J = 8.6 Hz, 1 H, H-6), 6.64 (dd, ³J = 8.7 Hz, ³J = 3.1 Hz, 1 H, H-5), 5.12 (s, 1 H, OH), 3.77 (s, 3 H, H-8), 2.25 (s, 3 H, H-7).

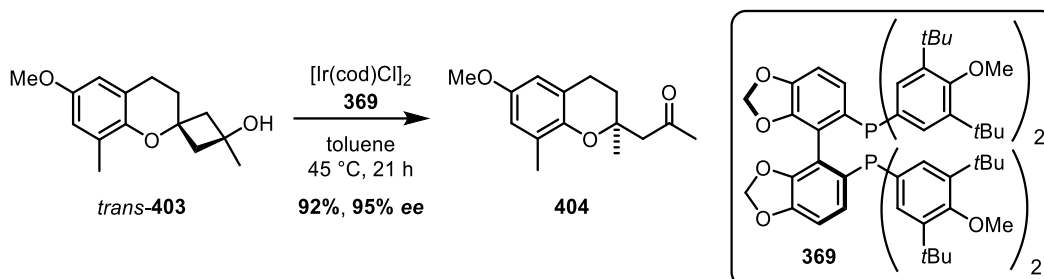
¹³C NMR^[179] (75 MHz, CDCl₃) δ [ppm] = 153.6 (C-4), 148.0 (C-1), 125.2 (C-2), 116.8 (C-3), 115.7 (C-6), 112.0 (C-5), 55.9 (C-8), 16.2 (C-7).

GC-MS^[179] (70 eV) m/z ([%]): 161 (12, [M+Na⁺]), 138 (20, [M⁺]), 123 (100), 95 (22), 77 (45), 68 (35), 54 (13).

FTIR-ATR^[179] ν [cm⁻¹] = 3676 (w), 3254 (br, m), 3037 (w), 3007 (w), 2952 (w), 2835 (w), 1831 (w), 1721 (w), 1619 (w), 1609 (w), 1600 (w), 1510 (m), 1452 (m), 1430 (m), 1400 (m), 1375 (w), 1290 (m), 1268 (w), 1251 (w), 1204 (s), 1184 (s), 1151 (m), 1116 (m), 1045 (s), 924 (w), 861 (s), 809 (m), 799 (m), 760 (m), 718 (s), 704 (m).

The analytical data are in agreement with the literature.^[236]

10.3.1.2. Synthesis of 2,2-disubstituted chromane 404

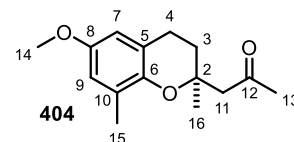


The synthesis was performed based on a modified procedure of *Schlundt et al.*^[175] Under an atmosphere of argon, a 10 mL GC-headspace vial was charged with 50.5 mg of (*S*)-DTBM-segphos ligand (**369**) (0.0428 mmol, 15 mol%) and 9.5 mg of $[\text{Ir}(\text{cod})\text{Cl}]_2$ catalyst (0.0143 mmol, 5 mol%). Then a solution of 71 mg of alcohol *trans*-**403** (0.29 mmol, 1.0 equiv.) in 2.8 mL of anhydrous toluene was added and the reaction mixture was stirred for 30 min at r.t. The resulting yellow solution was heated at 45 °C (color change to orange). After 21 h of stirring, the mixture was cooled down to r.t. A spatula tip of *QuadraSil* AP was added and the suspension was stirred for 10 min. By *Celite* filtration and concentration under reduced pressure a brown oil was obtained. The crude product was purified by FCC (SiO_2 , *c*Hex/EtOAc 15:1) to obtain 66 mg of chromanylpropanone **404** as a beige solid (0.266 mmol, 93%; 95% ee). The absolute (*S*)-configuration was confirmed by X-ray crystallography.^[178-179]

M ($\text{C}_{15}\text{H}_{20}\text{O}_3$) = 248.32 g/mol.

TLC (SiO_2 , *c*Hex/EtOAc 5:1) R_f = 0.38.

M.p.^[179] <30 °C.



$^1\text{H NMR}$ ^[179] (600 MHz, CDCl_3) δ [ppm] = 6.58 (d, $^4J = 2.6$ Hz, 1 H, H-9), 6.45 (d, $^4J = 2.6$ Hz, 1 H, H-7), 3.73 (s, 3 H, H-14), 2.80 (d, $^2J = 14.0$ Hz, 1 H, H-11), 2.77 – 2.67 (m, 2 H, H-4), 2.63 (d, $^2J = 14.0$ Hz, 1 H, H-11), 2.23 (s, 3 H, H-13), 2.16 (s, 3 H, H-15), 1.94 (ddd, $^2J = 13.5$ Hz, $^3J = 8.0$ Hz, $^3J = 6.5$ Hz, 1 H, H-3), 1.84 (dt, $^2J = 13.5$ Hz, $^3J = 6.5$ Hz, 1 H, H-3), 1.35 (s, 3 H, H-16).

$^{13}\text{C NMR}$ ^[179] (151 MHz, CDCl_3) δ [ppm] = 207.9 (C-12), 152.7 (C-8), 145.4 (C-6), 127.4 (C-10), 120.8 (C-5), 115.3 (C-9), 111.2 (C-7), 74.9 (C-2), 55.8 (C-14), 53.0 (C-11), 32.4 (C-13), 31.7 (C-3), 24.4 (C-16), 22.7 (C-4), 16.5 (C-15).

GC-MS^[179] (70 eV) m/z ([%]): 248 (100, $[\text{M}^+]$), 230 (20), 215 (25), 206 (19), 191 (19), 175 (45), 150 (70), 135 (15), 115 (21), 91 (77), 77 (50), 65 (21), 53 (19).

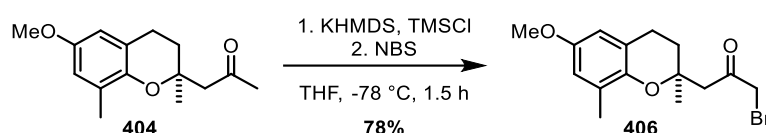
HR-ESI-MS^[179] m/z calculated $[\text{C}_{15}\text{H}_{20}\text{O}_3 + \text{Na}^+]$: 271.1304657; found: 271.13080.

FTIR-ATR^[179] ν [cm⁻¹] = 3676 (w), 2971 (m), 2936 (m), 2838 (w), 1705 (m), 1606 (w), 1481 (s), 1453 (m), 1440 (m), 1376 (w), 1358 (m), 1325 (w), 1311 (w), 1281 (w), 1207 (s), 1175 (m), 1149 (s), 1098 (s), 1057 (s), 1007 (w), 978 (w), 950 (m), 914 (m), 855 (m), 837 (w), 790 (w), 736 (w), 717 (w), 679 (w), 649 (w).

Specific rotation (c = 0.420 g/100 mL, CHCl₃, $[\alpha]_D^{20}$): $[\alpha]_{365}^{20.0} = -51.2^\circ$, $[\alpha]_{436}^{20.0} = +19.1^\circ$, $[\alpha]_{546}^{20.0} = +9.6^\circ$, $[\alpha]_{579}^{20.0} = +8.4^\circ$, $[\alpha]_{589}^{20.0} = -6.9^\circ$.

Enantiomeric separation by chGC column: MEGA DEX B-SE (30M x 0.25 mm Ø), temperature program: 50 °C, 50 °C – 145 °C (2 °C/min), 145 °C – 170 °C (1 °C/min). Flow rate: 5 mL/min. Major enantiomer T_R = 65.3 min; minor enantiomer T_R = 66.6 min.

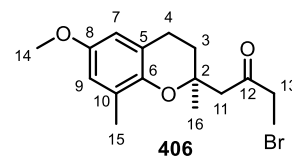
10.3.1.3. Synthesis of monobrominated chromane 406



The synthesis was performed based on a modified procedure of the preceding master thesis.^[179] Under an atmosphere of argon, a 10 mL *Schlenk* tube was charged with a solution of 40 mg of chromane **404** (0.16 mmol, 1.0 equiv.) in 0.4 mL of anhydrous THF. Subsequently, 0.04 mL of TMSCl (34 mg, 0.31 mmol, 1.9 equiv.) were added. This resulting solution was added (dropwise) over 5 min to a suspension of 64 mg of KHMDS (0.32 mmol, 2.0 equiv.) in 0.14 mL of anhydrous THF at -78 °C. After 30 min of stirring, 29 mg of NBS (0.16 mmol, 1.0 equiv.) were added at -78 °C. The reaction mixture was warmed up to r.t. and after 1 h of stirring, 5 mL of sat. NaHCO₃ solution and 5 mL of H₂O were added. The aqueous phase was extracted with CH₂Cl₂ (3 x 15 mL). The combined organic phases were dried with Na₂SO₄ and concentrated under reduced pressure to obtain an orange residue. Purification by FCC (SiO₂, cHex/EtOAc 60:1) gave 41 mg of monobrominated chromane **406** as a colorless oil (0.13 mmol, 78%).

M (C₁₅H₁₉BrO₃) = 327.22 g/mol.

TLC (SiO₂, cHex/EtOAc 5:1) R_f = 0.58.



¹H NMR^[179] (500 MHz, CDCl₃) δ [ppm] = 6.59 (d, ⁴J = 2.8 Hz, 1 H, H-9), 6.45 (d, ⁴J = 2.8 Hz, 1 H, H-7), 4.10 (d, ²J = 13.1 Hz, 1 H, H-13), 4.04 (d, ²J = 13.1 Hz, 1 H, H-13), 3.73 (s, 3 H, H-14), 3.00 (d, ²J = 13.9 Hz, 1 H, H-11), 2.83 (d, ²J = 13.9 Hz, 1 H, H-11), 2.80 – 2.68 (m, 2 H, H-4), 2.15 (s, 3 H, H-15), 1.94 (ddd, ²J = 14.0 Hz, ³J = 8.7 Hz, ³J = 6.3 Hz, 1 H, H-3), 1.85 (dt, ²J = 14.0 Hz, ³J = 6.3 Hz, 1 H, H-3), 1.35 (s, 3 H, H-16).

^{13}C NMR^[179] (126 MHz, CDCl_3) δ [ppm] = 199.9 (C-12), 153.0 (C-8), 145.0 (C-6), 127.3 (C-10), 120.6 (C-5), 115.4 (C-9), 111.3 (C-7), 75.2 (C-2), 55.8 (C-14), 49.7 (C-11), 36.6 (C-13), 31.67 (C-3), 24.1 (C-16), 22.5 (C-4), 16.6 (C-15).

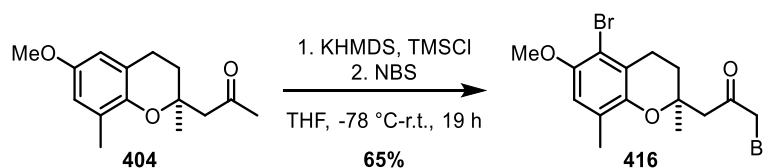
GC-MS^[179] (70 eV) m/z ([%]): 326 (17, $[\text{M}^+]$), 248 (12), 229 (12), 215 (6), 205 (9), 189 (47), 175 (28), 163 (10), 151 (100), 135 (10), 122 (16), 109 (22), 91 (31), 77 (27), 65 (22), 55 (22).

HR-ESI-MS^[179] m/z calculated $[\text{C}_{15}\text{H}_{19}\text{BrO}_3 + \text{Na}^+]$: 349.0409783; found: 349.04116.

FTIR-ATR^[179] ν [cm^{-1}] = 2974 (w), 2936 (w), 2850 (w), 2837 (w), 1723 (m), 1605 (w), 1481 (s), 1453 (m), 1440 (m), 1379 (m), 1343 (w), 1325 (w), 1313 (w), 1280 (w), 1262 (w), 1208 (s), 1192 (m), 1148 (s), 1058 (s), 1005 (w), 978 (w), 953 (w), 936 (w), 920 (w), 901 (w), 855 (w), 839 (w), 790 (w), 738 (w), 717 (w), 654 (w).

Specific rotation ($c = 0.500$ g/100 mL, CHCl_3 , $[\alpha]_{\lambda}^T$): $[\alpha]_{365}^{20.0} = -269.5^\circ$, $[\alpha]_{436}^{20.0} = +105.5^\circ$, $[\alpha]_{546}^{20.0} = +48.4^\circ$, $[\alpha]_{579}^{20.0} = +41.4^\circ$, $[\alpha]_{589}^{20.0} = +38.9^\circ$.

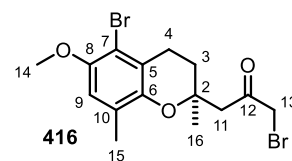
10.3.1.4. Synthesis of dibrominated chromane 416



The synthesis was performed based on a modified procedure of the preceding master thesis.^[179] Under an atmosphere of argon, a 10 mL *Schlenk* tube was charged with a solution of 58 mg of chromane **404** (0.23 mmol, 1.0 equiv.) in 0.5 mL of anhydrous THF. Subsequently, 0.05 mL of TMSCl (43 mg, 0.39 mmol, 1.7 equiv.) were added. This solution was added (dropwise) over 25 min to a stirred solution of 70 mg of KHMDS (0.35 mmol, 1.5 equiv.) in 0.4 mL of anhydrous THF at -78°C . After 1.5 h of stirring, 90 mg of NBS (0.51 mmol, 2.1 equiv.) were added at -78°C . After 1.5 h, the reaction mixture was warmed up to r.t. and stirred for 16 h. Then 5 mL of sat. NaHCO_3 solution and 5 mL of H_2O were added. The aqueous phase was extracted with CH_2Cl_2 (3 x 15 mL). The combined organic phases were dried with Na_2SO_4 and concentrated under reduced pressure to obtain an orange oil. Purification by FCC (SiO_2 , $c\text{Hex}/\text{EtOAc}$ 60:1) gave 68 mg of a pale yellow oil (~6 mg, ~8% monobrominated product **406**; 62 mg of dibrominated chromane **416**, 0.153 mmol, 65%).

M ($\text{C}_{15}\text{H}_{18}\text{Br}_2\text{O}_3$) = 406.11 g/mol.

TLC (SiO_2 , $c\text{Hex}/\text{EtOAc}$ 2:1) $R_f = 0.50$.



¹H NMR (300 MHz, CDCl₃) δ [ppm] = 6.65 (s, 1 H, H-9), 4.11 – 3.95 (ψq, ²J = 12.9 Hz, 2 H, H-13), 3.83 (s, 3 H, H-14), 3.00 (d, ²J = 14.1 Hz, 1 H, H-11), 2.84 (d, ²J = 14.1 Hz, 1 H, H-11), 2.79 – 2.73 (m, 2 H, H-4), 2.15 (s, 3 H, H-15), 2.05 – 1.83 (m, 2 H, H-3), 1.35 (s, 3 H, H-16).

¹³C NMR (75 MHz, CDCl₃) δ [ppm] = 199.6 (C-12), 149.6 (C-8), 145.8 (C-6), 125.8 (C-10), 121.7 (C-5), 113.2 (C-9), 111.2 (C-7), 75.1 (C-2), 57.0 (C-14), 49.2 (C-11), 36.4 (C-13), 31.7 (C-3), 24.1 (C-16), 23.7 (C-4), 16.6 (C-15).

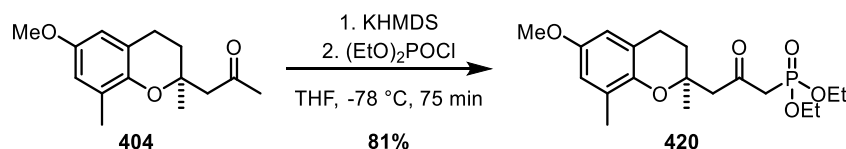
GC-MS (70 eV) m/z ([%]): 406 (100, [M⁺]), 325 (18), 309 (15), 269 (80), 245 (45), 228 (77), 203 (22), 189 (60), 175 (18), 149 (16), 121 (16), 91 (20), 77 (17), 43 (44).

HR-ESI-MS m/z calculated [C₁₅H₁₈Br₂O₃+Na⁺]: 426.9514908; found: 426.95160.

FTIR-ATR ν [cm⁻¹] = 2974 (w), 2935 (w), 2849 (w), 1722 (m), 1595 (w), 1468 (s), 1439 (m), 1398 (w), 1379 (w), 1339 (w), 1318 (w), 1286 (w), 1232 (s), 1197 (w), 1172 (w), 1152 (m), 1082 (s), 1059 (w), 1046 (w), 1018 (w), 984 (w), 961 (m), 918 (w), 872 (w), 837 (m), 819 (w), 753 (w), 716 (w), 637 (w), 601 (w), 584 (w), 557 (w), 518 (w).

Specific rotation (c = 0.520 g/100 mL, CHCl₃, [α]_λ^T): [α]₃₆₅^{20.0} = + 154.7 °, [α]₄₃₆^{20.0} = + 63.2 °, [α]₅₄₆^{20.0} = + 29.1 °, [α]₅₇₉^{20.0} = + 23.1 °, [α]₅₈₉^{20.0} = + 18.6 °.

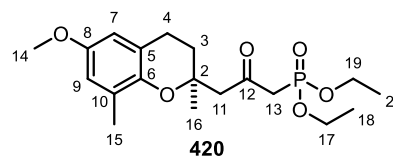
10.3.1.5. Synthesis of phosphonated chromane 420



The synthesis was performed based on a modified procedure of *Pandey et al.*^[184] Under an atmosphere of argon, a 5 mL *Schlenk* tube was charged with a solution of 60 mg of chromanylpropanone **404** (0.24 mmol, 1.0 equiv.) in 0.8 mL of anhydrous THF. This solution was added (dropwise) to a -78 °C cold suspension of 100 mg of KHMDS (0.500 mmol, 2.1 equiv.) in 1.0 mL of anhydrous THF. The resulting mixture was treated (dropwise) with 0.07 mL of (EtO)₂POCl (83 mg, 0.48 mmol, 2.0 equiv.) over 3 min at -78 °C. The reaction mixture was stirred for 75 min before 2 mL of sat. NaHCO₃ solution and 5 mL of H₂O were added. The aqueous phase was extracted with CH₂Cl₂ (3 x 10 mL). The combined organic phases were dried with Na₂SO₄ and the solvent was removed under reduced pressure to obtain a brown crude material. Purification by FCC (SiO₂, cHex/EtOAc 3:1) gave 75 mg of phosphonated chromane **420** as a pale yellow oil (0.195 mmol, 81%).

M (C₁₉H₂₉O₆P) = 384.41 g/mol.

TLC (SiO₂, cHex/EtOAc 2:1) R_f = 0.20.



¹H NMR (600 MHz, CDCl₃) δ [ppm] = 6.56 (d, ⁴J = 3.0 Hz, 1 H, H-9), 6.44 (d, ⁴J = 3.0 Hz, 1 H, H-7), 5.00 (t, ²J_P = 2.1 Hz, 1 H, H-13), 4.59 (t, ²J_P = 2.1 Hz, 1 H, H-13), 4.25 – 4.01 (m, 4 H, H-17/19), 3.73 (s, 3 H, H-14), 2.75 (ψt, ³J = 6.8 Hz, 2 H, H-4), 2.52 (d, ²J = 14.5 Hz, 1 H, H-11), 2.47 (d, ²J = 14.5 Hz, 1 H, H-11), 2.14 (s, 3 H, H-15), 1.90 (dt, ²J = 13.7 Hz, ³J = 6.9 Hz, 1 H, H-3), 1.83 (dt, ²J = 13.7 Hz, ³J = 6.9 Hz, 1 H, H-3), 1.36 (s, 3 H, H-16), 1.34 (dd, ³J = 7.0 Hz, ⁴J_P = 0.9 Hz, 6 H, H-18/20).

¹³C NMR (151 MHz, CDCl₃) δ [ppm] = 152.5 (C-8), 152.0 (C-12), 145.7 (C-6), 127.5 (C-10), 120.7 (C-5), 115.1 (C-9), 111.1 (C-7), 101.0 (C-13), 74.8 (C-2), 64.4 (C-17/19), 55.8 (C-14), 44.7 (C-11), 31.3 (C-3), 24.7 (C-16), 22.7 (C-4), 16.4 (C-15), 16.2 (C-18/20).

³¹P NMR (121 MHz, CDCl₃) δ [ppm] = -6.96 (t, J = 8.2 Hz).

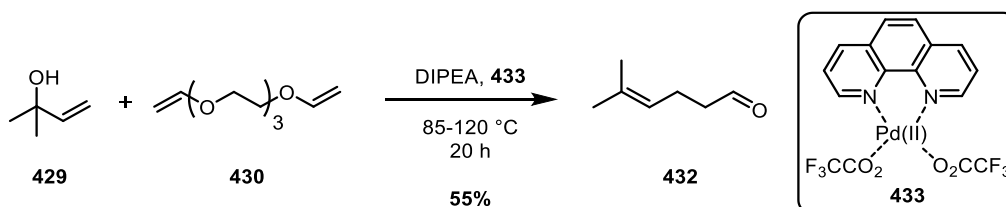
GC-MS (70 eV) m/z ([%]): 384 (68, [M⁺]), 230 (43), 215 (100), 191 (54), 175 (29), 151 (21), 99 (36), 81 (18).

HR-ESI-MS m/z calculated [C₁₉H₂₉O₆P+Na⁺]: 407.1593963; found: 407.15945.

FTIR-ATR ν [cm⁻¹] = 2981 (w), 2932 (w), 2852 (w), 2837 (w), 1736 (w), 1652 (w), 1606 (w), 1481 (m), 1442 (w), 1393 (w), 1378 (w), 1337 (w), 1316 (w), 1273 (m), 1219 (m), 1166 (w), 1150 (w), 1127 (w), 1093 (w), 1059 (w), 1023 (s), 1004 (s), 954 (w), 917 (w), 865 (w), 856 (w), 816 (w), 799 (w), 753 (w), 718 (w), 655 (w), 617 (w), 585 (w), 514 (w).

Specific rotation (c = 0.575 g/100 mL, CHCl₃, [α]_λ^T): [α]₃₆₅^{20.0} = - 3.5 °, [α]₄₃₆^{20.0} = - 2.3 °, [α]₅₄₆^{20.0} = - 1.3 °, [α]₅₇₉^{20.0} = - 1.3 °, [α]₅₈₉^{20.0} = - 3.7 °.

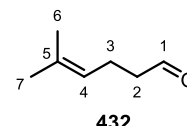
10.3.1.6. Synthesis of 5-methyl-4-hexenal (432)



The synthesis was performed based on a modified procedure of *Wei et al.*^[188a] A 10 mL round-bottomed flask equipped with a reflux condenser was charged with a solution 8.3 mg of Pd(O₂CCF₃)₂ (0.025 mmol, 0.5 mol%) and 5.1 mg of 1,10-phenanthroline (0.028 mmol,

0.57 mol%.) in 1.5 mL of triethylene glycol divinyl ether (**430**) (1.5 g, 7.5 mmol, 1.5 equiv.). To this solution 0.52 mL of 2-methyl-3-buten-2-ol (**429**) (5.0 mmol, 1.0 equiv.) and 0.04 mL of DIPEA (32 mg, 0.25 mmol, 0.05 equiv.) were added. The reaction mixture was heated at 85 °C for 19 h and 1 h at 120 °C for conversion completion. The brown crude product was directly submitted to FCC (SiO₂, *n*Pe/Et₂O 5:1) and carefully concentrated under reduced pressure (**attention**: product is volatile). Thus, 342 mg of a pale yellow liquid were obtained (~33 mg of *n*Pe residues; 6.73 g of product **432**, 48.7 mmol, 55%). For an analytical sample, the solvent was removed completely.

M (C₇H₁₂O) = 112.17 g/mol.



TLC (SiO₂, *c*Hex/EtOAc 5:1) R_f = 0.87.

¹H NMR (500 MHz, CDCl₃) δ [ppm] = 9.76 (t, ³J = 1.7 Hz, 1 H, H-1), 5.09 (ψtt, ³J = 7.1 Hz, ⁴J = 1.5 Hz, ⁴J = 1.2 Hz, 1 H, H-4), 2.46 (td, ³J = 7.4 Hz, ³J = 1.7 Hz, 2 H, H-2), 2.36 – 2.28 (m, 2 H, H-3), 1.69 (d, ⁴J = 1.5 Hz, 3 H, H-7), 1.63 (d, ⁴J = 1.2 Hz, 3 H, H-6).

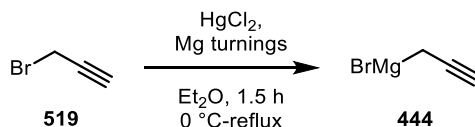
¹³C NMR (75 MHz, CDCl₃) δ [ppm] = 202.7 (C-1), 129.1 (C-5), 122.3 (C-4), 44.1 (C-2), 25.8 (C-7), 21.0 (C-3), 17.8 (C-6).

GC-MS (70 eV) m/z ([%]): 112 (13, [M⁺]), 91 (27), 79 (30), 69 (100), 53 (41).

FTIR-ATR ν [cm⁻¹] = 3433 (br), 2968 (m), 1917 (m), 2861 (w), 2822 (w), 2721 (w), 1809 (w), 1724 (s), 1685 (m), 1638 (w), 1604 (w), 1448 (m), 1410 (s), 1377 (m), 1342 (w), 1324 (w), 1257 (w), 1200 (w), 1171 (w), 1113 (w), 1066 (w), 984 (w), 937 (w), 871 (w), 826 (w), 776 (w), 685 (w), 515 (w).

The analytical data are in agreement with the literature.^[237]

10.3.1.7. Preparation of propargyl magnesium bromide (**444**)

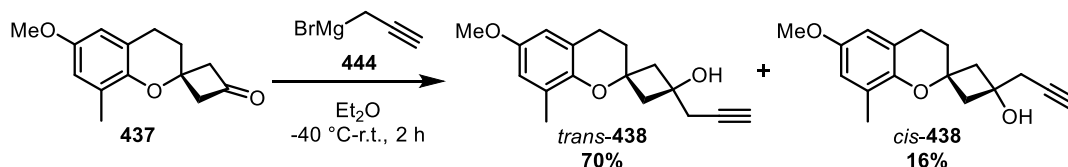


The synthesis was performed according to a procedure of by *Florez et al.*^[192] Under an atmosphere of argon, a 25 mL *Schlenk* flask was charged with 240 mg of Mg turnings (9.98 mmol, 1.7 equiv.) and flame-dried under vigorous stirring. At r.t. 6.3 mg of HgCl₂ (0.023 mmol, 0.004 equiv.) were added and the mixture was dissolved in 2.0 mL of anhydrous Et₂O. Then a solution of 0.65 mL of propargyl bromide (**519**) (ω = 80% in toluene, 0.69 g, 5.8 mmol, 1.0 equiv.) in 8.0 mL of anhydrous Et₂O were added (dropwise) over 15 min. During the addition, the reaction mixture was kept at mild reflux. Subsequently, the grey suspension

was stirred for 1.5 h at r.t. The concentration of the *Grignard* reagent **444** in Et₂O was determined by iodimetry ($c = 0.51 \text{ mol/L}$).

$M (\text{C}_{17}\text{H}_{20}\text{O}_3) = 272.34 \text{ g/mol}$.

10.3.1.8. Synthesis of *spirochromanol* **438**



The synthesis was performed based on a modified procedure of *Ratsch et al.*^[175] Under an atmosphere of argon, a 25 mL *Schlenk* flask was charged with 2.2 mL of *Grignard* reagent **444** (0.51M in Et₂O, 1.1 mmol, 2.6 equiv.) and cooled to -40 °C before a solution of 100 mg of chromanone **437** (0.431 mmol, 1.0 equiv.) in 2.5 mL of anhydrous Et₂O were slowly added by means of a syringe pump over 30 min. The bright yellow solution was stirred for 30 min and warmed up to r.t. and stirred for 1.5 h. The resulting suspension was treated with 15 mL of sat. NH₄Cl solution and diluted with 10 mL of H₂O. The aqueous phase was extracted with Et₂O (3 x 20 mL). The combined organic phases were dried with Na₂SO₄ and concentrated under reduced pressure to obtain a yellow oil. Purification by FCC (SiO₂, *c*Hex/EtOAc 12:1 to 5:1) gave 83 mg of *spirochromanol trans*-**438** as a pale yellow oil (0.30 mmol, 70%) and 19 mg of *cis*-**438** as a pale yellow oil (0.070 mmol, 16%). Determination of the absolute configuration of product *cis*-**438** was done by X-ray crystallography (see Appendix).

$M (\text{C}_{17}\text{H}_{20}\text{O}_3) = 272.34 \text{ g/mol}$.

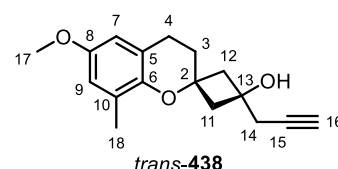
TLC (SiO₂, *c*Hex/EtOAc 5:1) $R_f = 0.14$.

¹H NMR (500 MHz, CDCl₃) δ [ppm] = 6.57 (d, ⁴ $J = 3.0 \text{ Hz}$, 1 H, H-9), 6.43 (d, ⁴ $J = 3.0 \text{ Hz}$, 1 H, H-7), 3.73 (s, 3 H, H-17), 2.78 – 2.73 (m, 4 H, H-4/14), 2.43 (s, 1 H, OH), 2.41 – 2.35 (m, 2 H, H-11/12), 2.24 – 2.19 (m, 2 H, H-11/12), 2.17 (s, 3 H, H-18), 2.06 (t, ⁴ $J = 2.6 \text{ Hz}$, 1 H, H-16), 2.01 (t, ³ $J = 6.6 \text{ Hz}$, 2 H, H-3).

¹³C NMR (126 MHz, CDCl₃) δ [ppm] = 152.9 (C-8), 145.7 (C-6), 127.4 (C-10), 121.9 (C-5), 114.9 (C-9), 111.2 (C-7), 80.4 (C-15), 72.4 (C-2), 71.1 (C-16), 69.2 (C-13), 55.7 (C-17), 46.3 (C-11/12), 32.8 (C-14), 31.8 (C-3), 22.6 (C-4), 16.4 (C-18).

GC-MS (70 eV) m/z ([%]): 272 (30, [M⁺]), 190 (100), 175 (23), 151 (20), 91 (8), 77 (7).

HR-ESI-MS m/z calculated [C₁₇H₂₀O₃+Na⁺]: 295.1304657; found: 295.13073.

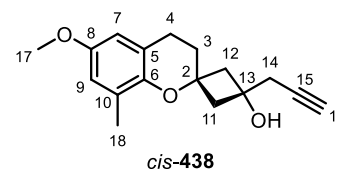


FTIR-ATR ν [cm^{-1}] = 3428 (br), 3287 (w), 2975 (w), 2931 (w), 2838 (w), 2118 (w), 1714 (w), 1606 (w), 1480 (s), 1441 (w), 1411 (w), 1378 (w), 1350 (w), 1334 (w), 1310 (w), 1286 (m), 1252 (w), 1204 (s), 1178 (m), 1152 (w), 1132 (w), 1101 (w), 1055 (s), 981 (w), 937 (m), 921 (w), 898 (w), 878 (w), 854 (w), 766 (w), 735 (w), 719 (w), 638 (m), 554 (w), 549 (w), 530 (w).

M ($\text{C}_{17}\text{H}_{20}\text{O}_3$) = 272.34 g/mol.

TLC (cHex/EtOAc 5:1) R_f = 0.24.

M.p. 80 °C.



$^1\text{H NMR}$ (500 MHz, CDCl_3) δ [ppm] = 6.57 (d, 4J = 3.0 Hz, 1 H, H-9), 6.43 (d, 4J = 3.0 Hz, 1 H, H-7), 3.73 (s, 3 H, H-17), 2.74 (t, 3J = 6.6 Hz, 2 H, H-4), 2.63 (s, 1 H, OH), 2.53 (d, 4J = 2.6 Hz, 2 H, H-14), 2.46 – 2.39 (m, 2 H, H-11/12), 2.36 – 2.30 (m, 2 H, H-11/12), 2.19 (s, 3 H, H-18), 2.07 (t, 4J = 2.6 Hz, 1 H, H-16), 1.90 (t, 3J = 6.6 Hz, 2 H, H-3).

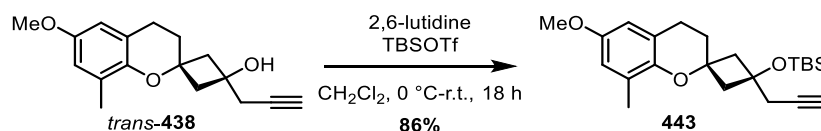
$^{13}\text{C NMR}$ (126 MHz, CDCl_3) δ [ppm] = 152.9 (C-8), 145.5 (C-6), 127.6 (C-10), 121.6 (C-5), 115.0 (C-9), 111.1 (C-7), 80.5 (C-15), 72.0 (C-2), 70.9 (C-16), 68.9 (C-13), 55.7 (C-17), 46.8 (C-11/12), 31.6 (C-14), 30.7 (C-3), 22.8 (C-4), 16.4 (C-18).

GC-MS (70 eV) m/z ([%]): 272 (30, $[\text{M}^+]$), 190 (100), 175 (23), 151 (20), 91 (8), 77 (7).

HR-ESI-MS m/z calculated [$\text{C}_{17}\text{H}_{20}\text{O}_3 + \text{Na}^+$]: 295.1304657; found: 295.13067.

FTIR-ATR ν [cm^{-1}] = 3303 (br), 3280 (m), 2994 (w), 2978 (w), 2962 (w), 2930 (w), 2842 (w), 2117 (w), 1981 (w), 1703 (w), 1616 (w), 1598 (w), 1482 (m), 1467 (w), 1444 (m), 1421 (w), 1380 (w), 1353 (w), 1332 (w), 1308 (w), 1300 (w), 1283 (m), 1243 (w), 1207 (s), 1183 (w), 1154 (w), 1142 (m), 1109 (w), 1061 (s), 1045 (w), 1025 (w), 1010 (w), 982 (w), 968 (w), 950 (w), 941 (w), 913 (w), 897 (w), 879 (w), 853 (m), 842 (w), 813 (w), 778 (w), 736 (w), 721 (w), 693 (w), 654 (s), 605 (w), 589 (w), 528 (w), 506 (w).

10.3.1.9. Synthesis of *tert*-butylsilyl chromane ether 443



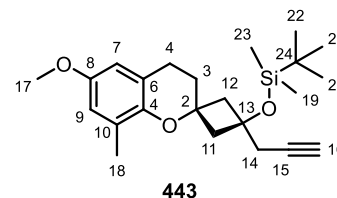
The synthesis was performed based on a modified procedure of *Ratsch et al.*^[175] Under an atmosphere of argon a 10 mL *Schlenk* flask was charged with a solution of 68 mg of *spirochromanol trans*-438 (0.25 mmol, 1.0 equiv.) in 1.5 mL of anhydrous CH_2Cl_2 and cooled to 0 °C. Then 87 μL 2,2-lutidine (80 mg, 0.75 mmol, 3.0 equiv.) were added and the solution was treated with 0.10 mL of TBSOTf (0.12 g, 0.35 mmol, 1.7 equiv.). The pale yellow reaction mixture was stirred at 0 °C for 2 h. Additional 0.09 mL of TBSOTf (0.1 g, 0.38 mmol, 1.5 equiv.)

were added to complete conversion and the reaction was stirred at r.t. for 16 h. The brown solution was treated with 10 mL of H₂O and extracted with CH₂Cl₂ (3 x 10 mL). The combined organic phases were washed with 5 mL of brine before they were dried with Na₂SO₄ and concentrated under reduce pressure to give an orange residue. Purification by FCC (SiO₂, cHex/EtOAc 60:1) gave 83 mg of *tert*-butylsilyl chromane ether **443** as a nearly colorless oil (0.215 mmol, 86%).

M (C₂₃H₃₄O₃Si) = 386.61 g/mol.

TLC (SiO₂, cHex/EtOAc 20:1) R_f = 0.36.

M.p. <20 °C.



¹H NMR (500 MHz, CDCl₃) δ [ppm] = 6.56 (d, ⁴J = 3.0 Hz, 1 H, H-9), 6.43 (d, ⁴J = 3.0 Hz, 1 H, H-7), 3.73 (s, 3 H, H-17), 2.82 – 2.67 (m, 4 H, H-4/14), 2.55 – 2.37 (m, 2 H, H-11/12), 2.22 – 2.18 (m, 2 H, H-11/12), 2.17 (s, 3 H, H-18), 1.99 – 1.93 (m, 3 H, H-3/16), 0.91 (s, 9 H, H-20/21/22), 0.13 (s, 6 H, H-19/23).

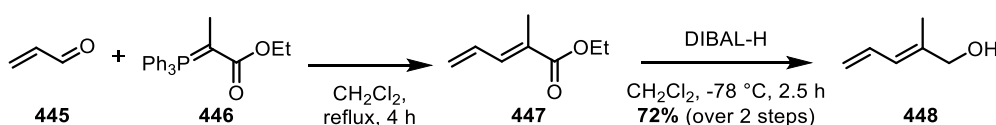
¹³C NMR (126 MHz, CDCl₃) δ [ppm] = 152.9 (C-8), 145.9 (C-6), 127.6 (C-10), 121.9 (C-5), 114.9 (C-9), 111.12 (C-7), 81.8 (C-15), 72.7 (C-2), 71.2 (C-16), 70.0 (C-13), 55.7 (C-17), 47.6 (C-11/12), 33.1 (C-14), 32.4 (C-3), 25.9 (C-20/21/22), 22.7 (C-4), 18.1 (C-19/23), 16.40 (C-19/23), 16.39 (C-18).

GC-MS (70 eV) m/z ([%]): 386 (15, [M⁺]), 329 (8), 190 (100), 175 (12), 151 (9), 91 (5), 75 (13).

HR-ESI-MS m/z calculated [C₂₃H₃₄O₃Si+Na⁺]: 409.2169426; found: 409.21718.

FTIR-ATR ν [cm⁻¹] = 3313 (w), 3290 (w), 2951 (w), 2930 (m), 2856 (w), 2121 (w), 1723 (w), 1607 (w), 1481 (m), 1440 (w), 1410 (w), 1389 (w), 1381 (w), 1361 (w), 1335 (w), 1311 (w), 1286 (m), 1254 (w), 1205 (s), 1192 (m), 1182 (s), 1153 (w), 1139 (w), 1108 (w), 1083 (m), 1059 (s), 1027 (w), 1003 (w), 982 (w), 951 (m), 938 (w), 912 (w), 876 (w), 855 (w), 832 (s), 774 (s), 723 (w), 708 (w), 674 (w), 635 (m), 573 (w), 547 (w), 528 (w).

10.3.1.10. Synthesis of (2*E*)-2-methylpenta-2,4-dienol (**448**)



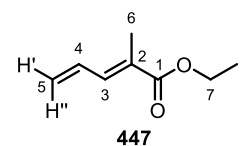
The synthesis was performed based on a modified procedure of *Hatakeyama et al.*^[193c] Under an atmosphere of argon, a 50 mL round-bottomed flask equipped with a reflux condenser was charged with a solution of 2.09 g of phosphor ylide **446** (ω = 94%, 1.97 g, 5.43 mmol, 1.0 equiv.) in 6.0 mL of anhydrous CH₂Cl₂. Subsequently, 0.36 mL of acrolein (**445**) (freshly

distilled, 0.30 g, 5.4 mmol, 1.0 equiv.) were added and the yellow reaction mixture was heated at reflux for 4 h. At r.t. 40 mL of *n*Pe were added under vigorous stirring. Precipitated PPh₃O was filtered off and the clear solution was concentrated carefully under reduced pressure (**attention**: product is volatile). The washing step with *n*Pe was repeated twice until no further PPh₃O precipitated. The desired product **447** was obtained as a crude mixture of 1.23 g still containing PPh₃O and *n*Pe. For analysis, a small product sample was purified completely.

The next step was performed based on a modified procedure of *Coelho et al.*^[193b] and *Morken et al.*^[238] Under an atmosphere of argon, a 100 mL *Schlenk* flask was charged with a solution of 1.2 g of crude material **447** in 19.0 mL of anhydrous CH₂Cl₂ and cooled to -78 °C. Subsequently, 12.3 mL of DIBAL-H (13.6 mmol, 2.5 equiv.) were slowly added over 15 min. The reaction mixture was stirred for 2.5 h and diluted with 30 mL of CH₂Cl₂ before 20 mL of sat. NH₄Cl solution were added. For phase separation, *Seignette's* salt solution (ω = 10%) was added and the mixture was stirred for 2 d. The aqueous phase was extracted with CH₂Cl₂ (5 x 40 mL). The combined organic phases were dried with Na₂SO₄ and after careful evaporation (**attention**: product is volatile) 731 mg of a pale yellow liquid were obtained. Purification by FCC (SiO₂, *n*Pe/Et₂O 5:1) gave 494 mg of a colorless liquid (~93 mg of *n*Pe/Et₂O/H₂O residues; 385 mg of product **448**, 3.9 mmol, 72% over two steps). For analysis, a small product sample was purified completely.

M (C₈H₁₂O₂) = 140.18 g/mol.

TLC (SiO₂, *c*Hex/EtOAc 50:1) R_f = 0.30.



¹H NMR (500 MHz, CDCl₃) δ [ppm] = 7.16 (dq, ³J = 11.3 Hz, ⁴J = 1.2 Hz, 1 H, H-3), 6.65 (ddd, ³J = 16.8 Hz, ³J = 11.3 Hz, ³J = 10.1 Hz, 1 H, H-4), 5.55 (d, ³J = 16.8 Hz, 1 H, H'-5), 5.44 (d, ³J = 10.1 Hz, 1 H, H'-5), 4.21 (q, ³J = 10.1 Hz, 2 H, H-7), 1.95 (d, ⁴J = 1.2 Hz, 3 H, H-6), 1.30 (t, ³J = 10.1 Hz, 3 H, H-8).

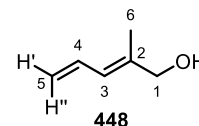
¹³C NMR (126 MHz, CDCl₃) δ [ppm] = 168.5 (C-1), 138.3 (C-3), 132.4 (C-4), 128.3 (C-2), 124.2 (C-5), 60.8 (C-7), 14.4 (C-8), 12.8 (C-6).

GC-MS (70 eV) m/z ([%]): 140 (78, [M⁺]), 112 (83), 95 (97), 67 (100), 41 (59).

FTIR-ATR ν [cm⁻¹] = 3091 (w), 2982 (w), 2957 (w), 2932 (w), 2876 (w), 2107 (w), 1704 (s), 1634 (w), 1596 (w), 1518 (w), 1479 (w), 1464 (w), 1446 (w), 1421 (w), 1392 (w), 1367 (w), 1341 (w), 1293 (w), 1242 (s), 1195 (w), 1176 (s), 1098 (s), 1055 (w), 1034 (w), 1008 (w), 989 (m), 871 (w), 850 (w), 786 (w), 758 (m), 733 (w), 693 (w), 652 (m), 518 (w).

The analytical data are in agreement with the literature.^[193c]

M (C₆H₁₀O) = 98.15 g/mol.



TLC (SiO₂, cHex/EtOAc 5:1) R_f = 0.25.

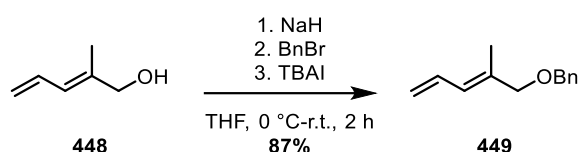
¹H NMR (500 MHz, CDCl₃) δ [ppm] = 6.59 (ddd, ³J = 16.8 Hz, ³J = 10.9 Hz, ³J = 10.2 Hz, 1 H, H-4), 6.08 (dq, ³J = 10.9 Hz, ⁴J = 1.4 Hz, 1 H, H-3), 5.21 (d, ³J = 16.8 Hz, 1 H, H'-5), 5.11 (d, ³J = 10.2 Hz, 1 H, H'-5), 4.07 (s, 2 H, H-1), 1.79 (m, 3 H, H-6).

¹³C NMR (126 MHz, CDCl₃) δ [ppm] = 137.9 (C-2), 132.7 (C-4), 125.5 (C-3), 117.2 (C-5), 68.4 (C-1), 14.2 (C-6).

FTIR-ATR ν [cm⁻¹] = 3313 (br), 3086 (w), 3048 (w), 3012 (w), 2970 (w), 2916 (w), 2860 (w), 1808 (w), 1659 (w), 1602 (w), 1446 (w), 1421 (w), 1381 (w), 1358 (w), 1339 (8w), 1292 (w), 1208 (w), 1144 (w), 1069 (m), 988 (s), 955 (w), 941 (w), 899 (s), 818 (w), 660 (m), 615 (m), 588 (w).

The analytical data are in agreement with the literature.^[193c]

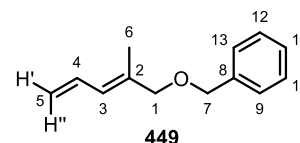
10.3.1.11. Synthesis of *O*-Benzyl-(2*E*)-2-methylpenta-2,4-dienol (**449**)



The synthesis was performed based on a modified procedure of *Lam et al.*^[239] Under an atmosphere of argon, a 50 mL *Schlenk* flask was charged with a solution 245 mg of alcohol **448** (2.49 mmol, 1.0 equiv.) in 5.0 mL of anhydrous THF which was cooled to 0 °C. Then 299 mg of NaH (dispersion in paraffin oil, ω = 60%, 179 mg, 7.48 mmol, 3.0 equiv.) were added. After 15 min, the suspension was treated with 1.75 mL of BnBr (2.56 g, 15.0 mmol, 6.00 eq). After 10 min, 927 mg of TBAI (2.51 mmol, 1.0 equiv.) were added and the reaction mixture was stirred for 15 min at 0 °C, then for 2 h at r.t. At 0 °C, the reaction mixture was acidified with 10 mL of 2M HCl and diluted with 20 mL of Et₂O and 10 mL of H₂O. The aqueous phase was extracted with Et₂O (4 x 15 mL). The combined organic phases were dried with Na₂SO₄ and evaporated under reduced pressure to give a yellow crude material. Purification by FCC (SiO₂, *n*Pe/EtOAc 100:1) and careful concentration under reduced pressure (**attention**: product is volatile) yielded 514 mg of a colorless oil (~17 mg of alcohol **448** and ~42 mg of *n*Pe residues; 455 mg of product **449**, 2.42 mmol, 87%). For analysis, a small product sample was purified completely.

M (C₁₃H₁₆O) = 188.27 g/mol.

TLC(SiO₂, cHex/EtOAc 30:1) R_f = 0.44.



¹H NMR (500 MHz, CDCl₃) δ [ppm] = 7.35 (ψs, 2 H, H-9/13), 7.30 (ψs, 2 H, H-10/12), 7.32 – 7.27 (m, 1 H, H-11), 6.62 (ddd, ³J = 16.9 Hz, ³J = 11.3 Hz, ³J = 10.2 Hz, 1 H, H-4), 6.11 (dq, ³J = 11.3 Hz, ⁴J = 1.4 Hz, 1 H, H-3), 5.23 (d, ³J = 16.9 Hz, 1 H, H''-5), 5.13 (d, ³J = 10.2 Hz, 1 H, H'-5), 4.49 (s, 2 H, H-7), 3.98 (s, 2 H, H-1), 1.82 (s, 2 H, H-6).

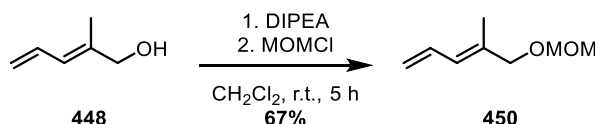
¹³C NMR (125 MHz, CDCl₃) δ [ppm] = 138.5 (C-7), 135.5 (C-2), 132.7 (C-4), 128.5 (C-9/13), 127.9 (C-10/12), 127.7 (C-11), 127.6 (C-3), 117.3 (C-5), 75.7 (C-1), 71.9 (C-7), 14.5 (C-6).

GC-MS (70 eV) m/z ([%]): 188 (<1, [M⁺]), 130 (11), 91 (100), 77 (10), 65 (13), 51 (8).

FTIR-ATR ν [cm⁻¹] = 3086 (w), 3063 (w), 3031 (w), 3009 (w) 2972 (w), 2916 (w), 2853 (w), 2788 (w), 1950 (w), 1869 (w), 1810 (w), 1726 (w), 1656 (w), 1601 (w), 1497 (w), 1453 (w), 1421 (w), 1408 (w), 1381 (w), 1363 (w), 1353 (w), 1308 (w), 1292 (w), 1255 (w), 1205 (w), 1175 (w), 1146 (w), 1090 (s), 1071 (s), 1028 (m), 987 (m), 940 (w), 902 (s), 846 (w), 817 (w), 734 (s), 696 (s), 662 (w), 639 (w), 606 (w), 591 (w).

The analytical data are in agreement with the literature.^[239]

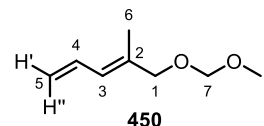
10.3.1.12. Synthesis of O-MOM-(2E)-2-methylpenta-2,4-dienol 450



The synthesis was performed based on a modified procedure of *Schmidt et al.*^[240] Under an atmosphere of argon, a 25 mL *Schlenk* flask was charged with a solution of 50 mg of alcohol **448** (0.51 mmol, 1.0 equiv.) in 4.0 mL of anhydrous CH₂Cl₂ and 216 μL DIPEA (164 mg, 1.27 mmol, 2.5 equiv.) were added. After 10 min of stirring at r.t., 58 μL MOMCl (61 mg, 0.76 mmol, 1.5 equiv.) were added. After 5 h, the reaction mixture was treated with 5 mL of sat. NH₄Cl solution and diluted with 5 mL of CH₂Cl₂ and 5 mL of H₂O. The aqueous phase was extracted with CH₂Cl₂ (3 x 10 mL). The combined organic phases were washed with 20 mL of 1M HCl before they were dried with Na₂SO₄ and carefully concentrated under reduced pressure (**attention**: product is volatile) to give a yellow liquid. Purification by FCC (SiO₂, *n*Pe/EtOAc 100:1) gave 70 mg of a colorless liquid (~22 mg of H₂O/*n*Pe residues; 48 mg of product **450**, 0.34 mmol, 67%). For analysis, a small product sample was purified completely.

M (C₈H₁₄O₂) = 142.20 g/mol.

TLC (SiO₂, cHex/EtOAc 5:1) R_f = 0.75.



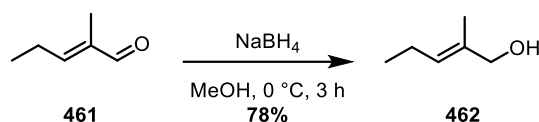
¹H NMR (500 MHz, CDCl₃) δ [ppm] = 6.59 (ddd, ³J = 16.9 Hz, ³J = 10.9 Hz, ³J = 10.2 Hz, 1 H, H-4), 6.09 (dq, ³J = 10.9 Hz, ⁴J = 1.4 Hz, 1 H, H-3), 5.21 (d, ³J = 16.9 Hz, 1 H, H''-5), 5.11 (d, ³J = 10.2 Hz, 1 H, H'-5), 4.64 (s, 2 H, H-7), 4.00 (s, 3 H, H-8), 3.39 (s, 2 H, H-1), 1.80 (d, ⁴J = 1.2 Hz, 3 H, H-6).

¹³C NMR (125 MHz, CDCl₃) δ [ppm] = 134.9 (C-2), 132.7 (C-4), 127.5 (C-3), 117.4 (C-5), 95.6 (C-7), 72.69 (C-1), 55.5 (C-8), 14.6 (C-6).

GC-MS (70 eV) m/z ([%]): 142 (9, [M⁺]), 110 (19), 95 (15), 81 (100), 67 (51), 53 (40).

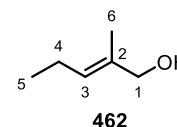
FTIR-ATR ν [cm⁻¹] = 3086 (w), 3049 (w), 2930 (w), 2884 (w), 2824 (w), 2777 (w), 1728 (w), 1658 (w), 1602 (w), 1451 (w), 1422 (w), 1401 (w), 1377 (w), 1290 (w), 1264 (w), 1212 (w), 1149 (s), 1101 (m), 1041 (s), 990 (m), 968 (w), 916 (m), 902 (s), 877 (w), 818 (w), 734 (w), 661 (w), 630 (w), 569 (w).

10.3.1.13. Synthesis of (*E*)-2-methyl-2-penten-1-ol (**462**)



The synthesis was performed according to a procedure of *Kulshrestha et al.*^[194] Under an atmosphere of argon, a 500 mL *Schlenk* flask was charged with a solution of 3.00 mL of aldehyde **461** (2.58 g, 26.3 mmol, 1.0 equiv.) in 200 mL of dry MeOH. At 0 °C the solution was treated with 2.69 g of NaBH₄ (71.0 mmol, 2.7 equiv.) in small portions over 15 min. The reaction mixture was stirred for 3 h at 0 °C before 20 mL of sat. NaHCO₃ solution were added. The MeOH was removed under reduced pressure (**attention**: product is volatile). The residue was re-dissolved in 100 mL of H₂O and extracted with EtOAc (3 x 80 mL). The combined organic phases were dried with MgSO₄ and carefully evaporated to yield 2.92 g of a colorless liquid (~879 mg of EtOAc residues; 2.04 g of product **462**, 20.4 mmol, 78%; lit.^[194] quant.). For analysis, a small product sample was purified completely.

M (C₆H₁₂O) = 100.16 g/mol.



TLC (SiO₂, cHex/EtOAc 5:1) R_f = 0.35.

¹H NMR (600 MHz, CDCl₃) δ [ppm] = 5.40 (tq, ³J = 7.2 Hz, ⁴J = 1.5 Hz, ⁴J = 1.4 Hz, 1 H, H-3), 3.98 (d, ⁴J = 1.4 Hz, 2 H, H-1), 2.14 – 1.90 (m, 2 H, H-4), 1.65 (d, ⁴J = 1.5 Hz, 3 H, H-6), 1.49 (s, 1 H, OH), 0.96 (t, ³J = 7.5 Hz, 3 H, H-5).

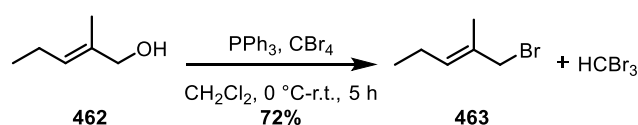
¹³C NMR (151 MHz, CDCl₃) δ [ppm] = 134.2 (C-2), 128.3 (C-3), 69.1 (C-1), 21.0 (C-4), 14.2 (C-5), 13.6 (C-6).

FTIR-ATR ν [cm⁻¹] = 3323 (br), 2963 (m), 2933 (w), 2920 (w), 2873 (w), 1673 (w), 1457 (w), 1438 (w), 1414 (w), 1377 (w), 1328 (m), 1305 (w), 1239 (w), 1214 (w), 1117 (w), 1070 (m), 1006 (s), 905 (w), 854 (w), 821 (w), 748 (w), 665 (w), 595 (w).

The analytical data are in agreement with the literature.^[194]

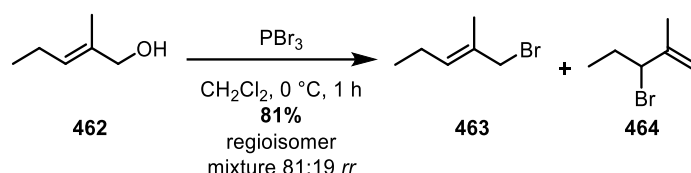
10.3.1.14. Synthesis of (*E*)-1-bromo-2-methyl-2-pentene (463)

Procedure 1



The synthesis was performed based on a modified procedure of *Magoulas et al.*^[195] Under an atmosphere of argon, a 20 mL *Schlenk* tube was charged with a solution of 302 mg of alcohol (**462**) (3.02 mmol, 1.0 equiv.) and 787 mg of PPh₃ (3.00 mmol, 1.0 equiv.) in 1.0 mL of anhydrous CH₂Cl₂. At 0 °C, the resulting solution was treated with 996 mg of CBr₄ (3.00 mmol, 1.0 equiv.) in small portions. The reaction mixture was stirred at r.t. for 5 h and then carefully concentrated under reduced pressure (**attention**: product is volatile) to obtain a yellow crude material. Purification by FCC (SiO₂, *n*Pe/Et₂O 50:1) gave 932 mg of a colorless liquid (~447 mg of HBr and ~133 mg of *n*Pe residues; 352 mg of product **463**, 2.16 mmol, 72%). HBr impurities could not be removed.

Procedure 2

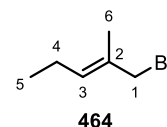


The synthesis was performed based on a modified procedure of *Zhang et al.*^[196] Under an atmosphere of argon, a 50 mL *Schlenk* flask was charged with a solution of 778 mg of alcohol (**462**) (7.76 mmol, 1.0 equiv.) in 16 mL of anhydrous CH₂Cl₂. At 0 °C, a solution of 0.75 mL of PBr₃ (2.1 g, 7.9 mmol, 1.0 equiv.) in 8 mL of anhydrous CH₂Cl₂ was added (dropwise). After

1 h, the reaction mixture was treated with 60 mL of sat. NaHCO₃ solution. The aqueous phase was extracted with 3 x 15 mL of CH₂Cl₂. The combined organic phases were dried with Na₂SO₄ and after careful concentration under reduced pressure (**attention**: product is volatile) a colorless liquid was obtained. Purification by FCC (SiO₂, *n*Pe/Et₂O 50:1) yielded 1.28 g of a colorless liquid (~241 mg of *n*Pe residues; 1.04 g of isomeric product mixture, 3.65 mmol, 81%; **463/464** 81:19 *rr*).

M (C₆H₁₁Br) = 163.06 g/mol.

TLC (SiO₂, *c*Hex/EtOAc 5:1) R_f = 0.89.



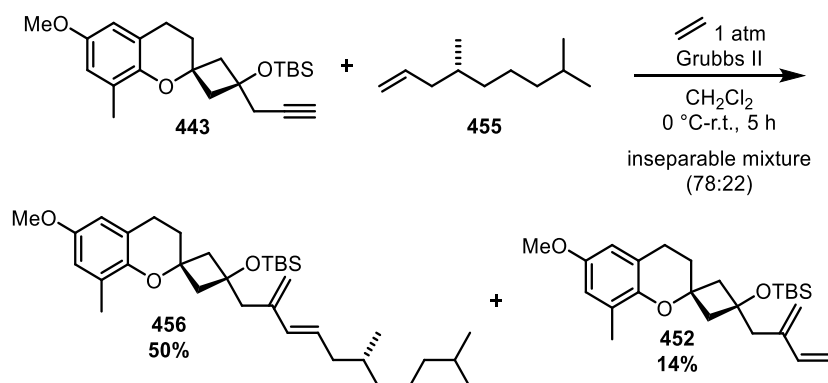
¹H NMR (500 MHz, CDCl₃) δ [ppm] = 5.67 – 5.51 (m, 1 H, H-3), 3.97 (d, ⁴*J* = 0.7 Hz, 2 H, H-1), 2.13 – 1.96 (m, 2 H, H-4), 1.77 – 1.70 (m, 3 H, H-6), 1.03 – 0.92 (m, 3 H, H-5).

¹³C NMR (125 MHz, CDCl₃) δ [ppm] = 133.4 (C-3), 131.5 (C-2), 42.1 (C-1), 21.7 (C-4), 14.6 (C-6), 13.7 (C-5).

GC-MS (70 eV) *m/z* ([%]): 162 (3, [M⁺]), 83 (65), 67 (27), 55 (100).

FTIR-ATR ν [cm⁻¹] = 2966 (m), 2934 (w), 2875 (w), 1661 (w), 1643 (w), 1454 (w), 1438 (w), 1378 (w), 1305 (w), 1280 (w), 1222 (w), 1201 (m), 1180 (w), 1148 (w), 1104 (w), 1086 (w), 1069 (w), 1039 (w), 998 (w), 969 (w), 904 (w), 879 (w), 851 (w), 820 (w), 803 (w), 750 (w), 637 (w), 607 (s), 542 (w).

10.3.1.15. Synthesis of chromanyldiene **456**



The synthesis was performed based on a modified procedure of *Ratsch et al.*^[175] Under an atmosphere of argon, a 10 mL *Schlenk* flask was charged with 20.4 mg of *Grubbs II* (0.0240 mmol, 10 mol%) and cooled to 0 °C before ethylene atmosphere (1 atm.) was applied. A solution of 92 mg of *tert*-butylsilyl chromane ether **443** (0.238 mmol, 1.0 equiv.) and 451 mg of (*R*)-4,8-dimethylnon-1-ene (**455**) (2.92 mmol, 12.3 equiv.) in 0.5 mL of anhydrous CH₂Cl₂ was added. Subsequently, the purple reaction mixture was stirred for 5 h at r.t. Then it was

diluted with 2 mL of CH_2Cl_2 and a spatula tip of activated charcoal was added. After 20 min, the suspension was filtered over *Celite* and evaporated under reduced pressure to give a brown liquid. Purification by repeated FCC (Ag-doped SiO_2 , cHex/EtOAc 270:1 and cHex/EtOAc 600:1 to 150:1) gave 79 mg of an inseparable mixture of **456/452** 78:22 (65 mg of **456**, 0.12 mmol, 50%; 14 mg of **452**, 0.034 mmol, 14%). Analytical data is given from the mixture.

M ($\text{C}_{34}\text{H}_{56}\text{O}_3\text{Si}$) = 540.90 g/mol.

TLC (SiO_2 , cHex/EtOAc 15:1) R_f = 0.59.

$^1\text{H NMR}$ (500 MHz, CDCl_3) δ [ppm] = 6.90 (d, 4J = 3.0 Hz, 1 H, H-9), 6.42 (d, 4J = 3.0 Hz, 1 H, H-7), 6.08 (d, 3J = 15.6 Hz, 1 H, H-16), 5.68 (dt, 3J = 15.6 Hz, 3J = 7.3 Hz, 1 H, H-17), 5.06 (d, 4J = 3.0 Hz, 2 H, H-18), 3.72 (s, 3 H, H-19), 2.78 – 2.70 (m, 4 H, H-4/14), 2.56 – 2.43 (m, 2 H, H-11/12), 2.26 – 2.18 (m, 2 H, H-11/12), 2.14 (s, 3 H, H-20), 2.12 – 2.04 (m, 1 H, H-27), 1.97 (t, 3J = 6.6 Hz, 2 H, H-3), 1.94 – 1.87 (m, 1 H, H-27), 1.58 – 1.41 (m, 2 H, H-28/32), 1.36 – 1.19 (m, 3 H, H-29/31), 1.17 – 1.03 (m, 2 H, H-29/30), 0.88 (s, 9 H, H-22/23/24), 0.91 – 0.83 (m, 9 H, H-33/34/35), 0.06 (s, 6 H, H-12/25).

$^{13}\text{C NMR}$ (126 MHz, CDCl_3) δ [ppm] = 152.7 (C-8), 146.1 (C-6), 141.3 (C-15), 135.2 (C-16), 128.2 (C-17), 127.5 (C-10), 122.0 (C-5), 116.1 (C-18), 114.8 (C-9), 111.2 (C-7), 73.5 (C-2), 71.8 (C-13), 55.7 (C-19), 48.5 (C-11/12), 43.6 (C-14), 40.6 (C-27), 39.4 (C-30), 37.0 (C-29), 33.5 (C-28), 32.4 (C-3), 28.1 (C-32), 26.0 (C-22/23/24), 25.0 (C-31), 22.9 (C-33), 22.8 (C-4/34), 19.7 (C-35), 18.1 (C-26), 16.5 (C-20), -2.6 (C-21/25).

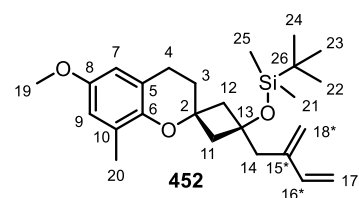
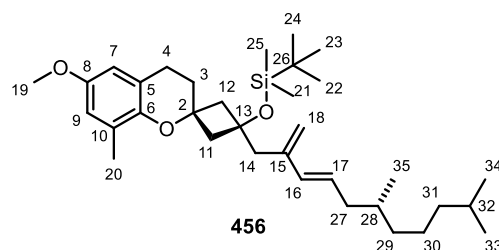
GC-MS (70 eV) m/z ([%]): 540 (5, [M^+]), 347 (6), 293 (5), 249 (5), 190 (100), 151 (7), 73 (18), 57 (6).

HR-ESI-MS m/z calculated [$\text{C}_{34}\text{H}_{56}\text{O}_3\text{Si}+\text{Na}^+$]: 563.3890933; found: 563.38972.

M ($\text{C}_{25}\text{H}_{38}\text{O}_3\text{Si}$) = 414.66 g/mol.

TLC (SiO_2 , cHex/EtOAc 15:1) R_f = 0.51.

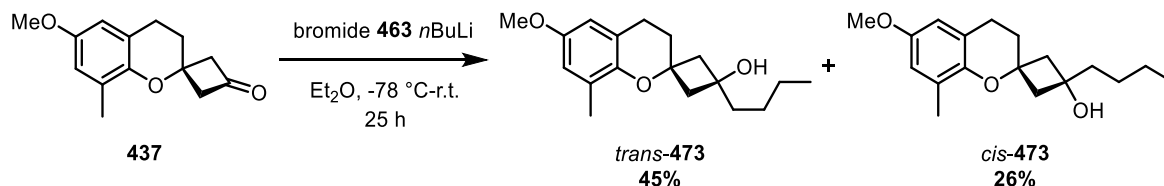
$^1\text{H NMR}$ (500 MHz, CDCl_3) δ [ppm] = 6.90 (d, 4J = 3.0 Hz, 1 H, H-9), 6.42 (d, 4J = 3.1 Hz, 1 H, H-7), 6.41 – 6.37 (m, 1 H, H-16*), 5.28 – 5.16 (m, 3 H, H-17*/18*), 5.03 – 4.97 (m, 1 H, H-18*), 3.72 (s, 3 H, H-19), 2.78 – 2.70 (m, 4 H, H-4/14), 2.56 – 2.43 (m, 2 H, H-11/12), 2.26 – 2.18



(m, 2 H, H-11/12), 2.14 (s, 3 H, H-20), 1.97 (t, $^3J = 6.6$ Hz, 2 H, H-3), 0.88 (s, 9 H, H-22/23/24), 0.06 (s, 6 H, H-21/25).

GC-MS (70 eV) m/z ([%]): 414 (18, $[M^+]$), 357 (8), 281 (22), 207 (27), 190 (100), 151 (8), 87 (9), 73 (15).

10.3.1.16. Synthetic 1,2-addition approach with chromanylketone **437**



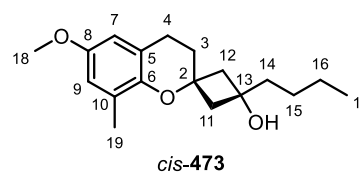
Under an atmosphere of argon, a 50 mL *Schlenk* flask was charged with a solution of 105 mg of bromide **463** (0.646 mmol, 1.5 equiv.) in 4.0 mL of anhydrous Et₂O and cooled to -78 °C. Then 0.45 mL of *n*BuLi (1.5M in *n*Hex, 0.675 mmol, 1.6 equiv.) were added (dropwise) over 5 min and the solution was stirred for 1.5 h until a solution of 100 mg of chromanylketone **437** (0.432 mmol, 1.0 equiv.) in 3.0 mL of anhydrous Et₂O was slowly added over 10 min at -78 °C. The reaction mixture was stirred for 1.5 h and warmed up to r.t. before it was stirred for 25 h. The orange suspension was treated with 20 mL of sat. NH₄Cl solution and 10 mL of H₂O. The aqueous phase was extracted with CH₂Cl₂ (3 x 25 mL). The combined organic phases were washed with 10 mL of brine before they were dried with Na₂SO₄ and concentrated under reduced pressure to give a yellow crude material. Purification by FCC (SiO₂, *c*Hex/EtOAc 12:1 to 6:1) gave 57 mg of non-desired *spirochromanol cis*-**473** (0.196 mmol, 45%) and 33 mg of *trans*-**473** (0.114 mmol, 26%) both as a pale yellow oil. Configurations of the stereoisomers were confirmed by ¹H,¹H NOESY correlation spectroscopy.

M (C₁₈H₂₆O₃) = 290.40 g/mol.

TLC (SiO₂, *c*Hex/EtOAc 5:1) R_f = 0.41.

¹H NMR (500 MHz, CDCl₃) δ [ppm] = 6.57 (d, $^4J = 3.1$ Hz, 1 H, H-9), 6.43 (d, $^4J = 3.1$ Hz, 1 H, H-7), 3.73 (s, 3 H, H-18), 2.73 (t, $^3J = 6.6$ Hz, 2 H, H-4), 2.26 – 2.21 (m, 4 H, H-11/12), 2.19 (s, 3 H, H-19), 1.88 (t, $^3J = 6.6$ Hz, 2 H, H-3), 1.63 – 1.54 (m, 2 H, H-14), 1.41 – 1.31 (m, 4 H, H-15/16), 0.93 (t, $^3J = 7.0$ Hz, 3 H, H-17).

¹³C NMR (126 MHz, CDCl₃) δ [ppm] = 152.9 (C-8), 145.7 (C-6), 127.5 (C-10), 121.7 (C-5), 114.9 (C-9), 111.1 (C-7), 73.05 (C-2), 70.6 (C-13), 55.7 (C-18), 47.9 (C-11/12), 41.1 (C-14), 31.0 (C-3), 25.9 (C-15), 23.1 (C-16), 22.9 (C-4), 16.5 (C-19), 14.3 (C-17).

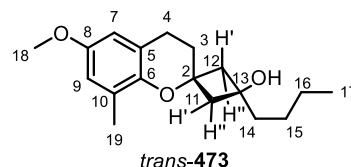


GC-MS (70 eV) m/z ([%]): 290 (8, $[M^+]$), 272 (8), 229 (6), 215 (5), 206 (7), 190 (100), 175 (30), 151 (28), 121 (7), 91 (10), 77 (9), 57 (9), 41 (9).

FTIR-ATR ν [cm^{-1}] = 3436 (br), 2951 (w), 2927 (m), 2869 (w), 2858 (w), 2838 (w), 1786 (w), 1606 (w), 1481 (s), 1440 (m), 1378 (w), 1352 (w), 1335 (w), 1286 (w), 1236 (w), 1204 (s), 1149 (m), 1101 (w), 1085 (w), 1059 (s), 1041 (m), 1003 (w), 981 (w), 955 (w), 918 (w), 877 (w), 855 (w), 783 (w), 732 (w), 717 (w), 680 (w), 647 (w), 599 (w).

M ($\text{C}_{18}\text{H}_{26}\text{O}_3$) = 290.40 g/mol.

TLC (SiO_2 , $c\text{Hex}/\text{EtOAc}$ 5:1) R_f = 0.19.



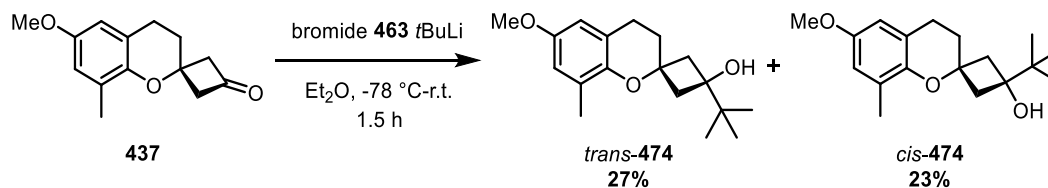
$^1\text{H NMR}$ (500 MHz, CDCl_3) δ [ppm] = 6.56 (d, 4J = 3.0 Hz, 1 H, H-9), 6.43 (d, 4J = 3.0 Hz, 1 H, H-7), 3.73 (s, 3 H, H-18), 2.76 (t, 3J = 6.6 Hz, 2 H, H-4), 2.34 – 2.26 (m, 2 H, H''-11/12), 2.16 (s, 3 H, H-19), 2.14 – 2.08 (m, 2 H, H'-11/12), 2.03 (t, 3J = 6.6 Hz, 2 H, H-3), 1.87 – 1.76 (m, 2 H, H-14), 1.60 (s, 1 H, OH), 1.44 – 1.32 (m, 4 H, H-15/16), 0.96 – 0.86 (t, 3J = 6.9 Hz, 3 H, H-17).

$^{13}\text{C NMR}$ (126 MHz, CDCl_3) δ [ppm] = 152.8 (C-8), 146.0 (C-6), 127.5 (C-10), 122.0 (C-5), 114.8 (C-9), 111.1 (C-7), 72.81 (C-2), 70.9 (C-13), 55.7 (C-18), 47.1 (C-11/12), 42.1 (C-14), 32.0 (C-3), 25.6 (C-15), 23.1 (C-16), 22.7 (C-4), 16.3 (C-19), 14.3 (C-17).

GC-MS (70 eV) m/z ([%]): 290 (8, $[M^+]$), 272 (8), 229 (6), 215 (5), 190 (100), 175 (30), 151 (28), 121 (7), 91 (10), 77 (9), 57 (9), 41 (9).

FTIR-ATR ν [cm^{-1}] = 3421 (br), 2954 (w), 2927 (m), 2871 (w), 2858 (w), 1717 (w), 1606 (w), 1481 (s), 1467 (m), 1441 (w), 1409 (w), 1378 (w), 1334 (w), 1309 (w), 1285 (m), 1234 (w), 1206 (s), 1149 (m), 1106 (w), 1089 (w), 1059 (s), 1039 (m), 1005 (w), 981 (w), 956 (w), 939 (w), 908 (w), 879 (w), 856 (w), 838 (w), 784 (w), 767 (w), 732 (w), 718 (w), 668 (w), 601 (w), 570 (w), 505 (w).

10.3.1.17. Synthetic 1,2-addition approach with chromanylketone 437



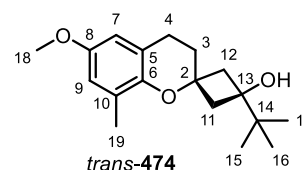
Under an atmosphere of argon, a 50 mL *Schlenk* flask was charged with a solution of 105 mg of bromide **463** (0.646 mmol, 1.5 equiv.) in 4.0 mL of anhydrous Et_2O and cooled to $-78\text{ }^\circ\text{C}$.

Then 0.76 mL of *t*BuLi (1.7M in *n*Pe, 1.29 mmol, 3.0 equiv.) were added (dropwise) over 10 min and the reaction mixture was stirred for 1 h until a solution of 100 mg of chromanylketone **437** (0.432 mmol, 1.0 equiv.) in 3.0 mL of anhydrous Et₂O was slowly added over 10 min and stirred for 1.5 h at -78 °C. After stirring for an additional 6 h at r.t., the orange suspension was treated with 5 mL of sat. NH₄Cl solution and 10 mL of H₂O. The aqueous phase was extracted with CH₂Cl₂ (4 x 20 mL). The combined organic phases were dried with Na₂SO₄ and concentrated under reduced pressure to give a brown crude product. Purification by FCC (SiO₂, *c*Hex/EtOAc 12:1) gave 35 mg of non-desired spirochromanol *trans*-**474** (0.117 mmol, 27%) as a yellow solid and 29 mg of spirochromanol *cis*-**474** (0.010 mmol, 23%) as a colorless oil. Determination of the configuration of *trans*-**474** was performed by X-ray crystallography.

M (C₁₈H₂₆O₃) = 290.40 g/mol.

TLC (SiO₂, *c*Hex/EtOAc 5:1) R_f = 0.50.

M.p. 79 - 80 °C.



¹H NMR (600 MHz, CDCl₃) δ [ppm] = 6.55 (d, ⁴*J* = 2.9 Hz, 1 H, H-9), 6.44 (d, ⁴*J* = 3.0 Hz, 1 H, H-7), 3.73 (s, 3 H, H-18), 2.79 (t, ³*J* = 6.6 Hz, 2 H, H-4), 2.54 – 2.44 (m, 2 H, H-11/12), 2.14 (s, 3 H, H-19), 2.12 (t, ³*J* = 6.6 Hz, 2 H, H-3), 1.96 – 1.90 (m, 2 H, H-11/12), 1.55 (s, 1 H, OH), 0.96 (s, 9 H, H-15/16/17).

¹³C NMR (151 MHz, CDCl₃) δ [ppm] = 152.8 (C-8), 146.0 (C-6), 127.6 (C-10), 122.1 (C-5), 114.8 (C-9), 111.0 (C-7), 75.9 (C-13), 71.8 (C-2), 55.7 (C-18), 42.7 (C-11/12), 36.2 (C-14), 31.7 (C-3), 24.4 (C-15/16/17), 22.6 (C-4), 16.2 (C-19).

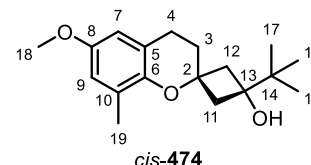
GC-MS (70 eV) *m/z* ([%]): 290 (15, [M⁺]), 190 (100), 175 (13), 151 (21), 91 (8), 57 (20), 41 (8).

FTIR-ATR *v* [cm⁻¹] = 3525 (m), 2995 (w), 2949 (m), 2922 (m), 2871 (w), 2851 (w), 1723 (w), 1607 (w), 1479 (m), 1466 (m), 1450 (w), 1433 (w), 1411 (w), 1392 (w), 1378 (w), 1365 (w), 1341 (w), 1324 (w), 1283 (m), 1210 (s), 1170 (m), 1151 (m), 1130 (m), 1102 (w), 1053 (s), 1029 (w), 1003 (w), 970 (w), 957 (w), 936 (m), 896 (m), 875 (m), 848 (w), 830 (m), 785 (m), 725 (w) 709 (w), 604 (w), 659 (w), 533 (w), 518 (w).

M (C₁₈H₂₆O₃) = 290.40 g/mol.

TLC (SiO₂, *c*Hex/EtOAc 5:1) R_f = 0.24.

M.p. 78 °C.



¹H NMR (600 MHz, CDCl₃) δ [ppm] = 6.57 (d, ⁴*J* = 2.9 Hz, 1 H, H-9), 6.43 (d, ⁴*J* = 3.0 Hz, 1 H, H-7), 3.73 (s, 3 H, H-18), 2.73 (t, ³*J* = 6.6 Hz, 2 H, H-4), 2.70 (s, 1 H, OH), 2.45 – 2.29 (m, 2 H,

H-11/12), 2.20 (s, 3 H, H-19), 1.99 – 1.91 (m, 2 H, H-11/12), 1.86 (t, $^3J = 6.6$ Hz, 2 H, H-3), 0.93 (s, 9 H, H-15/16/17).

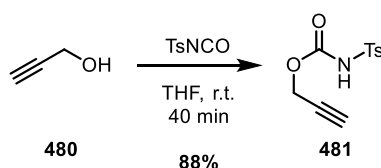
^{13}C NMR (151 MHz, CDCl_3) δ [ppm] = 153.0 (C-8), 145.6 (C-6), 127.5 (C-10), 121.9 (C-5), 114.9 (C-9), 111.3 (C-7), 78.4 (C-13), 75.1 (C-2), 55.7 (C-18), 42.6 (C-11/12), 5.2 (C-14), 30.5 (C-3), 24.6 (C-15/16/17), 22.9 (C-4), 16.6 (C-19).

GC-MS (70 eV) m/z ([%]): 290 (15, $[\text{M}^+]$), 190 (100), 175 (13), 151 (21), 91 (8), 57 (20), 41 (8).

FTIR-ATR ν [cm^{-1}] = 3674 (w), 3571 (w), 22948 (m), 2915 (w), 2871 (w), 2839 (w), 1606 (w), 1480 (s), 1440 (w), 1405 (w), 1394 (w), 1376 (w), 1364 (w), 1334 (w), 1310 (w), 1286 (w), 1240 (w), 1201 (s), 1169 (w), 1149 (m), 1130 (m), 1100 (w), 1058 (s), 1006 (w), 981 (w), 951 (w), 938 (w), 915 (w), 877 (w), 857 (w), 837 (w), 813 (w), 764 (w), 724 (w), 705 (w), 632 (w), 602 (w), 562 (w).

10.3.1.18. Substrate synthesis for Ir-catalyzed desymmetrization

10.3.1.18.1. Synthesis of 3-propynyl-*N*-tosyl carbamate (**481**)

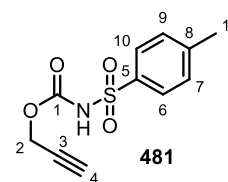


The synthesis was performed according to a procedure of *Zhao et al.*^[200] Under an atmosphere of argon, a 250 mL *Schlenk* flask was charged with a solution of 1.00 mL of propargyl alcohol (**480**) (0.972 g, 17.3 mmol, 1.0 equiv.) in 85 mL of anhydrous THF. At 0 °C, 2.9 mL of tosyl isocyanate (3.76 g, 19.1 mmol, 1.1 equiv.) were added (dropwise) over 10 min. The reaction mixture was stirred for 40 min at r.t. and was then concentrated under reduced pressure. The colorless oil was re-dissolved in 100 mL of $\text{Et}_2\text{O}/\text{H}_2\text{O}$ 1:1 added. The aqueous phase was extracted with Et_2O (3 x 50 mL). The combined organic phases were dried with Na_2SO_4 and concentrated under reduced pressure to obtain a nearly colorless oil. Purification by FCC (SiO_2 , cHex/EtOAc 5:1) gave 4.15 g of 3-propynyl-*N*-tosyl carbamate (**481**) as a white solid (~275 mg of EtOAc residues; 3.88 g of product, 15.3 mmol, 88%; lit.:^[200] 89%).

M ($\text{C}_{11}\text{H}_{11}\text{NO}_4\text{S}$) = 253.27 g/mol.

TLC (SiO_2 , cHex/EtOAc 3:1) $R_f = 0.16$.

M.p. 84 °C.



¹H NMR (500 MHz, CDCl₃) δ [ppm] = 7.94 (d, ³J = 8.3 Hz, 2 H, H-6/10), 7.78 (brs, 1 H, NH), 7.35 (d, ³J = 8.3 Hz, 2 H, H-7/9), 4.67 (d, ⁴J = 2.5 Hz, 2 H, H-2), 2.49 (t, ⁴J = 2.5 Hz, 1 H, H-4), 2.45 (s, 3 H, H-11).

¹³C NMR (126 MHz, CDCl₃) δ [ppm] = 149.8 (C-1), 145.5 (C-8), 135.2 (C-5), 129.8 (C-7/9), 128.6 (C-6/10), 76.4 (C-3), 76.3 (C-4), 54.3 (C-2), 21.8 (C-11).

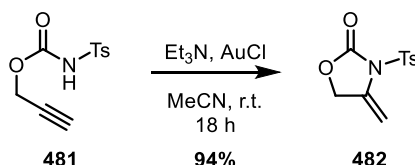
GC-MS (70 eV) m/z ([%]): 253 (8, [M⁺]), 155 (45), 91 (100), 65 (29), 39 (11).

HR-ESI-MS m/z calculated [C₁₁H₁₁NO₄S+Na⁺]: 276.0300997; found: 276.03049.

FTIR-ATR ν [cm⁻¹] = 3284 (w), 3223 (m), 3096 (w), 3067 (w), 2937 (w), 2920 (w), 2809 (w), 2133 (w), 1759 (m), 1658 (w), 1597 (w), 1529 (w), 1495 (w), 1459 (m), 1446 (m), 1402 (w), 1367 (w), 1349 (m), 1308 (w), 1291 (w), 1238 (w), 1217 (m), 1187 (w), 1153 (s), 1086 (m), 1044 (w), 1018 (w), 987 (w), 974 (w), 861 (m), 817 (m), 795 (w), 762 (m), 753 (m), 704 (w), 663 (m), 643 (m), 635 (w), 576 (s), 542 (s), 516 (m).

The analytical data are in agreement with the literature.^[200]

10.3.1.18.2. Synthesis of 4-methylene oxazolidinone **482**

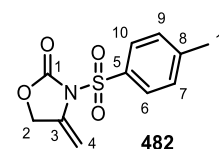


The synthesis was performed according to a procedure of *Ritter et al.*^[199] A 25 mL round-bottomed flask was charged with a solution of 1.00 g of 3-propynyl-*N*-tosyl carbamate (**481**) (3.95 mmol, 1.0 equiv.) in 8.0 mL of dry MeCN. Subsequently, 27.5 μL Et₃N (19.5 mg, 0.197 mmol, 0.05 equiv.) and 44.2 mg of AuCl (0.190 mmol, 4.8 mol%) were added. The pale yellow solution was stirred for 18 h at r.t. The brown suspension was filtered over a *Celite* and washed with 100 mL of CH₂Cl₂. The organic phase was concentrated under reduced pressure to give a yellow crude material. After purification by FCC (SiO₂, *c*Hex/EtOAc 3:1) 939 mg of 4-methylene oxazolidinone **482** was obtained as a white solid (3.71 mmol, 94%; lit.:^[199] 97%).

M (C₁₁H₁₁NO₄S) = 253.27 g/mol.

TLC (SiO₂, *c*Hex/EtOAc 3:1) R_f = 0.20.

M.p. 139 °C.



¹H NMR (500 MHz, CDCl₃) δ [ppm] = 7.96 (d, ³J = 8.2 Hz, 2 H, H-6/10), 7.37 (d, ³J = 8.2 Hz, 2 H, H-7/9), 5.53 (ψq, ⁴J = 2.5 Hz, 1 H, H-4), 4.79 (t, ⁴J = 2.5 Hz, 2 H, H-2), 4.52 (ψq, ⁴J = 2.5 Hz, 1 H, H-4), 2.46 (s, 3 H, H-11).

^{13}C NMR (126 MHz, CDCl_3) δ [ppm] = 151.7 (C-1), 146.4 (C-8), 135.2 (C-3), 134.4 (C-5), 130.1 (C-7/9), 128.4 (C-6/10), 90.9 (C-4), 67.2 (C-2), 21.9 (C-11).

GC-MS (70 eV) m/z ([%]): 253 (10, $[\text{M}^+]$), 155 (62), 91 (100), 65 (28), 39 (7).

HR-ESI-MS m/z calculated $[\text{C}_{11}\text{H}_{11}\text{NO}_4\text{S}+\text{Na}^+]$: 276.0300997; found: 276.03044.

FTIR-ATR ν [cm^{-1}] = 3141 (w), 1810 (w), 1791 (m), 1746 (w), 1667 (w), 1597 (w), 1516 (w), 1490 (w), 1453 (w), 1399 (w), 1380 (w), 1370 (m), 1357 (m), 1298 (w), 1284 (m), 1215 (w), 1191 (m), 1177 (m), 1156 (s), 1122 (w), 1083 (s), 1032 (m), 1015 (w), 999 (w), 974 (w), 953 (w), 915 (w), 862 (m), 839 (w), 813 (w), 802 (w), 756 (m), 731 (w), 702 (m), 672 (s), 648 (m), 582 (s), 569 (s), 544 (s).

The analytical data are in agreement with the literature.^[199]

11. List of References

- [1] L. E. Orgel, *Sci. Am.* **1994**, *271*, 76-83.
- [2] L. J. Boucher, ACS Publications, **1989**.
- [3] P. Prajapat, *J. Nanomed. Res.* **2018**, *7*, 69-70.
- [4] K. Smith, D. A. Evans, G. A. El-Hiti, *Philos. Trans. R. Soc. Lond., B, Biol. Sci.* **2008**, *363*, 623-637.
- [5] a) H. A. Wittcoff, B. G. Reuben, J. S. Plotkin, *Industrial organic chemicals*, John Wiley & Sons, **2012**; b) H. Li, H. A. Aguirre-Villegas, R. D. Allen, X. Bai, C. H. Benson, G. T. Beckham, S. L. Bradshaw, J. L. Brown, R. C. Brown, V. S. Cecon, *Green Chem.* **2022**.
- [6] a) A. Ravishankara, Y. Rudich, J. A. Pyle, *Chem. Rev.* **2015**, *115*, 3679-3681; b) P. M. Gschwend, D. M. Imboden, *Environmental organic chemistry*, John Wiley & Sons, **2016**.
- [7] K. C. Nicolaou, *Proc. R. Soc. A: Math. Phys. Eng. Sci.* **2014**, *470*, 20130690.
- [8] M. T. Reetz, *Pure Appl. Chem.* **1988**, *60*, 1607-1614.
- [9] N. Chhabra, M. L. Aseri, D. Padmanabhan, *Int. J. Appl. Basic Med.* **2013**, *3*, 16.
- [10] S.-A. Lim, *Ann. Acad. Med. Singap.* **2006**, *35*, 274.
- [11] A. J. J. Straathof, S. Panke, A. Schmid, *Curr. Opin. Biotechnol.* **2002**, *13*, 548-556.
- [12] O. García Mancheño, M. Waser, *Eur. J. Org. Chem.* **2022**, e202200950.
- [13] a) P. J. Guiry, C. P. Saunders, *Adv. Synth. Catal.* **2004**, *346*, 497-537; b) M. Diéguez, O. Pàmies, A. Ruiz, Y. Díaz, S. Castellón, C. Claver, *Coord. Chem. Rev.* **2004**, *248*, 2165-2192; c) P. W. N. M. v. Leeuwen, P. C. J. Kamer, C. Claver, O. Pamies, M. Dieguez, *Chem. Rev.* **2011**, *111*, 2077-2118; d) A. Fanourakis, P. J. Docherty, P. Chuentragool, R. J. Phipps, *ACS Catal.* **2020**, *10*, 10672-10714.
- [14] a) F. F. Fleming, *Nat. Prod. Rep.* **1999**, *16*, 597-606; b) X. Wang, Y. Wang, X. Li, Z. Yu, C. Song, Y. Du, *RCS Med. Chem.* **2021**; c) Y. Monguchi, *Science* **2022**, *376*, 1382-1383.
- [15] R. C. Larock, *Comprehensive organic transformations*, Wiley Online Library, **1989**.
- [16] L. Bini, C. Müller, D. Vogt, *ChemCatChem* **2010**, *2*, 590-608.
- [17] a) B. Clement, *Drug Metab. Rev.* **2002**, *34*, 565-579; b) N. Mahanta, D. M. Szantai-Kis, E. J. Petersson, D. A. Mitchell, *ACS Chem. Biol.* **2019**, *14*, 142-163; c) F. Jin, Q. Hu, H. Fei, H. Lv, S. Wang, B. Gui, J. Zhang, W. Tu, Y. Zhang, L. Zhang, *ACS Med. Chem. Lett.* **2021**, *12*, 195-201.
- [18] R. C. Cheng, D. B. Tikhonov, B. S. Zhorov, *J. Biol. Chem.* **2009**, *284*, 28332-28342.
- [19] T. K. Warren, R. Jordan, M. K. Lo, A. S. Ray, R. L. Mackman, V. Soloveva, D. Siegel, M. Perron, R. Bannister, H. C. Hui, *Nature* **2016**, *531*, 381-385.
- [20] M. L. Agostini, E. L. Andres, A. C. Sims, R. L. Graham, T. P. Sheahan, X. Lu, E. C. Smith, J. B. Case, J. Y. Feng, R. Jordan, *Mbio* **2018**, *9*, e00221-00218.
- [21] a) D. Siegel, H. C. Hui, E. Doerffler, M. O. Clarke, K. Chun, L. Zhang, S. Neville, E. Carra, W. Lew, B. Ross, *J. Med. Chem.* **2017**, *60*, 1648-1661; b) A. Shannon, N. T.-T. Le, B. Selisko, C. Eydoux, K. Alvarez, J.-C. Guillemot, E. Decroly, O. Peersen, F. Ferron, B. Canard, *Antivir. Res.* **2020**, *178*, 104793.
- [22] D. S. Seigler, G. S. Rosenthal, M. R. Berenbaum, *Cyanide and cyanogenic glycosides*, **1991**.
- [23] R. M. Gleadow, I. E. Woodrow, *J. Chem. Ecol.* **2002**, *28*, 1301-1313.
- [24] M. Sharma, N. N. Sharma, T. C. Bhalla, *Enzyme Microb. Technol.* **2005**, *37*, 279-294.
- [25] D. A. Jones, *Phytochemistry* **1998**, *47*, 155-162.
- [26] N. Wiberg, E. Wiberg, A. F. Holleman, Walter de Gruyter, Berlin, **2007**.
- [27] G. R. Maxwell, V. H. Edwards, M. Robertson, K. Shah, *J. Hazard. Mater.* **2007**, *142*, 677-684.
- [28] A. H. Hall, B. H. Rumack, *Ann. Emerg. Med.* **1986**, *15*, 1067-1074.
- [29] P. J. Macquer, *Examen chymique du bleu de Prusse*, **1756**.
- [30] M. Köckinger, C. A. Hone, C. O. Kappe, *Org. Lett.* **2019**, *21*, 5326-5330.
- [31] L. Andrussow, *Angew. Chem.* **1935**, *48*, 593-595.

- [32] R. Horn, R. Schlögl, *Catal. Lett.* **2015**, *145*, 23-39.
- [33] E. Gail, S. Gos, R. Kulzer, J. Lorösch, A. Rubo, M. Sauer, R. Kellens, J. Reddy, N. Steier, W. Hasenpusch, in *Ullmann's Encyclopedia of Industrial Chemistry*, Wiley-VCH, Weinheim, **2000**.
- [34] D. Medina, C. G. Anderson, *Metals* **2020**, *10*, 897.
- [35] C. Boulanger, *J. Electron. Mater.* **2010**, *39*, 1818-1827.
- [36] a) R. O. Duthaler, *Tetrahedron* **1994**, *50*, 1539-1650; b) K. Drauz, I. Grayson, A. Kleemann, H. P. Krimmer, W. Leuchtenberger, C. Weckbecker, in *Ullmann's Encyclopedia of industrial chemistry*, Wiley-VCH, Weinheim, **2000**.
- [37] a) J. Wang, X. Liu, X. Feng, *Chem. Rev.* **2011**, *111*, 6947-6983; b) V. V. Kouznetsov, C. E. P. Galvis, *Tetrahedron* **2018**, *74*, 773-810.
- [38] E. Pawar, *IOSR J. Mech. Civ. Eng.* **2016**, *13*, 1-4.
- [39] K. Nagai, *Appl. Catal. A: Gen.* **2001**, *221*, 367-377.
- [40] T. V. RajanBabu, in *Comprehensive Organic Synthesis II (Second Edition)*, Vol. 75, John Wiley & Sons, Inc., **2014**, pp. 1-73.
- [41] M. de Greef, B. Breit, *Angew. Chem. Int. Ed.* **2009**, *121*, 559-562.
- [42] A. Falk, A. L. Göderz, H. G. Schmalz, *Angew. Chem. Int. Ed.* **2013**, *52*, 1576-1580.
- [43] a) S. Arai, *Chem. Pharm. Bull.* **2019**, *67*, 397-403; b) L. Peng, Z. Hu, H. Wang, L. Wu, Y. Jiao, Z. Tang, X. Xu, *RSC Adv.* **2020**, *10*, 10232-10244.
- [44] N. Kurono, T. Ohkuma, *ACS Catal.* **2016**, *6*, 989-1023.
- [45] A. L. Casalnuovo, T. V. RajanBabu, T. A. Ayers, T. H. Warren, *J. Am. Chem. Soc.* **1994**, *116*, 9869-9882.
- [46] H. Zhang, X. Su, K. Dong, *Org. Biomol. Chem.* **2020**, *18*, 391-399.
- [47] a) C. A. Tolman, *Chem. Rev.* **1977**, *77*, 313-348; b) C. A. Tolman, *J. Chem. Educ.* **1986**, *63*, 199-201.
- [48] T. Li, W. D. Jones, *Organometallics* **2011**, *30*, 547-555.
- [49] T. Betke, M. Maier, H. Gruber-Wöfler, H. Gröger, *Nat. Commun.* **2018**, *9*, 1-9.
- [50] a) S. Van de Vyver, Y. Román-Leshkov, *Catal. Sci. Technol.* **2013**, *3*, 1465-1479; b) W. Deng, L. Yan, B. Wang, Q. Zhang, H. Song, S. Wang, Q. Zhang, Y. Wang, *Angew. Chem. Int. Ed.* **2021**, *60*, 4712-4719.
- [51] P. Elsner, P. Eyerer, T. Hirth, *Kunststoffe: Eigenschaften und Anwendungen*, Springer, **2012**.
- [52] A. Arévalo, J. J. García, *Eur. J. Inorg. Chem* **2010**, *2010*, 4063-4074.
- [53] C. Tolman, R. McKinney, W. Seidel, J. Druliner, W. Stevens, in *Adv. Catal.*, Vol. 33, Elsevier, **1985**, pp. 1-46.
- [54] W. Seidel, C. Tolman, *Ann. N. Y. Acad. Sci.* **1983**, *415*, 201-201.
- [55] C. A. Tolman, W. C. Seidel, L. W. Gosser, *J. Am. Chem. Soc.* **1974**, *96*, 53-60.
- [56] C. A. Tolman, *J. Am. Chem. Soc.* **1970**, *92*, 2956-2965.
- [57] a) J.-E. Bäckvall, O. S. Andell, *J. Chem. Soc., Chem. Commun.* **1981**, 1098-1099; b) J.-E. Bäckvall, O. S. Andell, *J. Chem. Soc., Chem. Commun.* **1984**, 260-261.
- [58] a) R. J. McKinney, D. C. Roe, *J. Am. Chem. Soc.* **1985**, *107*, 261-262; b) R. J. McKinney, D. C. Roe, *J. Am. Chem. Soc.* **1986**, *108*, 5167-5173.
- [59] P. Arthur Jr, D. England, B. Pratt, G. Whitman, *J. Am. Chem. Soc.* **1954**, *76*, 5364-5367.
- [60] C. A. Tolman, W. C. Seidel, J. D. Druliner, P. J. Domaille, *Organometallics* **1984**, *3*, 33-38.
- [61] a) J. Druliner, *Organometallics* **1984**, *3*, 205-208; b) R. J. McKinney, W. A. Nugent, *Organometallics* **1989**, *8*, 2871-2875.
- [62] L. Bini, C. Müller, D. Vogt, *Chem. Commun.* **2010**, *46*, 8325-8334.
- [63] W. A. Nugent, R. J. McKinney, *J. Org. Chem.* **1985**, *50*, 5370-5372.
- [64] L. Bini, E. A. Pidko, C. Müller, R. A. van Santen, D. Vogt, *Chem. Eur. J.* **2009**, *15*, 8768-8778.
- [65] a) M. Kranenburg, C. J. Paul, P. W. N. M. ávan Leeuwen, D. Vogt, W. Keim, *J. Chem. Soc., Chem. Commun.* **1995**, 2177-2178; b) P. C. J. Kamer, P. W. N. M. Van Leeuwen, J. N. H. Reek, *Acc. Chem. Res.* **2001**, *34*, 895-904.

- [66] M. D. K. Boele, L. A. van der Veen, P. C. J. Kamer, P. W. N. M. van Leeuwen, *Journal of the Chemical Society, Dalton Transactions* **1998**, 2981-2988.
- [67] L. Bini, C. Müller, J. Wilting, L. von Chrzanowski, A. L. Spek, D. Vogt, *J. Am. Chem. Soc.* **2007**, *129*, 12622-12623.
- [68] A. P. Göthlich, M. Tensfeldt, H. Rothfuss, M. E. Tauchert, D. Haap, F. Rominger, P. Hofmann, *Organometallics* **2008**, *27*, 2189-2200.
- [69] K. Nemoto, T. Nagafuchi, K.-i. Tominaga, K. Sato, *Tetrahedron Lett.* **2016**, *57*, 3199-3203.
- [70] G. Wang, X. Xie, W. Xu, Y. Liu, *Org. Chem. Front.* **2019**, *6*, 2037-2042.
- [71] a) W. Li, J. K. Boon, Y. Zhao, *Chem. Sci.* **2018**, *9*, 600-607; b) S. Thapa, R. K. Dhungana, R. T. Magar, B. Shrestha, K. Shekhar, R. Giri, *Chem. Sci.* **2018**, *9*, 904-909.
- [72] J. Huang, C. M. Haar, S. P. Nolan, J. E. Marccone, K. G. Moloy, *Organometallics* **1999**, *18*, 297-299.
- [73] X. Shu, Y.-Y. Jiang, L. Kang, L. Yang, *Green Chem.* **2020**, *22*, 2734-2738.
- [74] a) X. Fang, P. Yu, B. Morandi, *Science* **2016**, *351*, 832-836; b) H.-G. Schmalz, *Science* **2016**, *351*, 817-817.
- [75] a) N. M. Brunkan, D. M. Brestensky, W. D. Jones, *J. Am. Chem. Soc.* **2004**, *126*, 3627-3641; b) Y. Nakao, A. Yada, S. Ebata, T. Hiyama, *J. Am. Chem. Soc.* **2007**, *129*, 2428-2429; c) M. Tobisu, N. Chatani, *Chem. Soc. Rev.* **2008**, *37*, 300-307.
- [76] S.-F. Ni, T.-L. Yang, L. Dang, *Organometallics* **2017**, *36*, 2746-2754.
- [77] P. Yu, B. Morandi, *Angew. Chem. Int. Ed.* **2017**, *129*, 15899-15903.
- [78] B. N. Bhawal, J. C. Reisenbauer, C. Ehinger, B. Morandi, *J. Am. Chem. Soc.* **2020**, *142*, 10914-10920.
- [79] J. C. Reisenbauer, B. N. Bhawal, N. Jelmini, B. Morandi, *Org. Process Res. Dev.* **2022**, *26*, 1165-1173.
- [80] A. Bhunia, K. Bergander, A. Studer, *J. Am. Chem. Soc.* **2018**, *140*, 16353-16359.
- [81] N. L. Frye, A. Bhunia, A. Studer, *Org. Lett.* **2020**, *22*, 4456-4460.
- [82] P. Orecchia, W. Yuan, M. Oestreich, *Angew. Chem. Int. Ed.* **2019**, *58*, 3579-3583.
- [83] Y. Xing, R. Yu, X. Fang, *Org. Lett.* **2020**, *22*, 1008-1012.
- [84] A. Falk, *Dissertation* **2014**, University of Cologne.
- [85] a) P. S. Elmes, W. R. Jackson, *J. Am. Chem. Soc.* **1979**, *101*, 6128-6129; b) P. S. Elmes, W. R. Jackson, *Ann. N. Y. Acad. Sci.* **1980**, *333*, 225-228; c) P. S. Elmes, W. R. Jackson, *Aust. J. Chem.* **1982**, *35*, 2041-2051.
- [86] a) M. Hodgson, D. Parker, *J. Organomet. Chem.* **1987**, *325*, C27-C30; b) M. Hodgson, D. Parker, R. J. Taylor, G. Ferguson, *Organometallics* **1988**, *7*, 1761-1766.
- [87] M. J. Baker, P. G. Pringle, *J. Chem. Soc., Chem. Commun.* **1991**, 1292-1293.
- [88] T. V. RajanBabu, A. L. Casalnuovo, *J. Am. Chem. Soc.* **1992**, *114*, 6265-6266.
- [89] T. V. RajanBabu, A. L. Casalnuovo, *Pure Appl. Chem.* **1994**, *66*, 1535-1542.
- [90] T. V. RajanBabu, A. L. Casalnuovo, *J. Am. Chem. Soc.* **1996**, *118*, 6325-6326.
- [91] a) M. Yan, Q.-Y. Xu, A. S. Chan, *Tetrahedron Asymmetry* **2000**, *11*, 845-849; b) W. Goertz, P. C. Kamer, P. W. van Leeuwen, D. Vogt, *Chem. Eur. J.* **2001**, *7*, 1614-1618.
- [92] J. Wilting, M. Janssen, C. Müller, M. Lutz, A. L. Spek, D. Vogt, *Adv. Synth. Catal.* **2007**, *349*, 350-356.
- [93] J. Wilting, M. Janssen, C. Müller, D. Vogt, *J. Am. Chem. Soc.* **2006**, *128*, 11374-11375.
- [94] B. Saha, T. V. RajanBabu, *Org. Lett.* **2006**, *8*, 4657-4659.
- [95] a) H. Fernandez-Perez, P. Etayo, A. Panossian, A. Vidal-Ferran, *Chem. Rev.* **2011**, *111*, 2119-2176; b) S. Lühr, J. Holz, A. Boerner, *ChemCatChem* **2011**, *3*, 1708-1730.
- [96] a) F. Blume, S. Zemolka, T. Fey, R. Kranich, H. G. Schmalz, *Adv. Synth. Catal.* **2002**, *344*, 868-883; b) J. Velder, T. Robert, I. Weidner, J. M. Neudörfl, J. Lex, H. G. Schmalz, *Adv. Synth. Catal.* **2008**, *350*, 1309-1315; c) M. Dindaroğlu, A. Falk, H.-G. Schmalz, *Synthesis* **2013**, *45*, 527-535.
- [97] a) A. Cernijenko, R. Risgaard, P. S. Baran, *J. Am. Chem. Soc.* **2016**, *138*, 9425-9428; b) J. Guo, B. Li, W. Ma, M. Pitchakuntla, Y. Jia, *Angew. Chem. Int. Ed.* **2020**, *59*, 15195-

- 15198; c) D. Vargová, I. Némethová, R. Šebesta, *Org. Biomol. Chem.* **2020**, *18*, 3780-3796.
- [98] D. Moulin, S. Bago, C. Bauduin, C. Darcel, S. Jugé, *Tetrahedron Asymmetry* **2000**, *11*, 3939-3956.
- [99] a) T. Robert, J. Velder, H. G. Schmalz, *Angew. Chem. Int. Ed.* **2008**, *120*, 7832-7835; b) Q. Naeemi, T. Robert, D. P. Kranz, J. Velder, H.-G. Schmalz, *Tetrahedron Asymmetry* **2011**, *22*, 887-892.
- [100] a) W. Lölsberg, S. Ye, H. G. Schmalz, *Adv. Synth. Catal.* **2010**, *352*, 2023-2031; b) W. Lölsberg, S. Werle, J. r.-M. Neudörfl, H.-G. n. Schmalz, *Org. Lett.* **2012**, *14*, 5996-5999.
- [101] T. Robert, Z. Abiri, J. Wassenaar, A. J. Sandee, S. Romanski, J. r.-M. Neudörfl, H.-G. n. Schmalz, J. N. Reek, *Organometallics* **2010**, *29*, 478-483.
- [102] a) S. Movahhed, J. Westphal, M. Dindaroğlu, A. Falk, H. G. Schmalz, *Chem. Eur. J.* **2016**, *22*, 7381-7384; b) S. Movahhed, J. Westphal, A. Kempa, C. E. Schumacher, J. Sperlich, J. M. Neudörfl, N. Teusch, M. Hochgürtel, H. G. Schmalz, *Chem. Eur. J.* **2021**, *27*, 11574-11579; c) C. E. Schumacher, M. Rausch, T. Greven, J. M. Neudörfl, T. Schneider, H. G. Schmalz, *Eur. J. Org. Chem.* **2022**, e202200058.
- [103] A. Falk, A. Cavalieri, G. S. Nichol, D. Vogt, H. G. Schmalz, *Adv. Synth. Catal.* **2015**, *357*, 3317-3320.
- [104] P. Kocienski, *Synfacts* **2013**, *9*, 0351-0351.
- [105] a) K. Matsumoto, S. Arai, A. Nishida, *Tetrahedron* **2018**, *74*, 2865-2870; b) X. Li, C. You, J. Yang, S. Li, D. Zhang, H. Lv, X. Zhang, *Angew. Chem. Int. Ed.* **2019**, *58*, 10928-10931; c) M. Jiao, J. Gao, X. Fang, *Org. Lett.* **2020**, *22*, 8566-8571; d) R. Yu, Y. Xing, X. Fang, *Org. Lett.* **2021**, *23*, 930-935.
- [106] F. Wang, P. Chen, G. Liu, *Acc. Chem. Res.* **2018**, *51*, 2036-2046.
- [107] T. Jia, M. J. Smith, A. P. Pulis, G. J. Perry, D. J. Procter, *ACS Catal.* **2019**, *9*, 6744-6750.
- [108] a) W. Zhang, F. Wang, S. D. McCann, D. Wang, P. Chen, S. S. Stahl, G. Liu, *Science* **2016**, *353*, 1014-1018; b) D. Kuiling, *Prog. Chem.* **2017**, *29*, 13.
- [109] Y. F. Wang, W. Zeng, M. Sohail, J. Guo, S. Wu, F. X. Chen, *Eur. J. Org. Chem.* **2013**, *2013*, 4624-4633.
- [110] A. W. Schuppe, G. M. Borrajo-Calleja, S. L. Buchwald, *J. Am. Chem. Soc.* **2019**, *141*, 18668-18672.
- [111] L. Song, N. Fu, B. G. Ernst, W. H. Lee, M. O. Frederick, R. A. DiStasio, S. Lin, *Nat. Chem.* **2020**, *12*, 747-754.
- [112] J. Long, R. Yu, J. Gao, X. Fang, *Angew. Chem. Int. Ed.* **2020**, *59*, 6785-6789.
- [113] R. Yu, X. Fang, *Org. Lett.* **2019**, *22*, 594-597.
- [114] J. Long, J. Gao, X. Fang, *Org. Lett.* **2020**, *22*, 376-380.
- [115] D. Fiorito, S. Scaringi, C. Mazet, *Chem. Soc. Rev.* **2021**, *50*, 1391-1406.
- [116] J. Gao, J. Ni, R. Yu, G.-J. Cheng, X. Fang, *Org. Lett.* **2020**, *23*, 486-490.
- [117] R. Yu, S. Rajasekar, X. Fang, *Angew. Chem. Int. Ed.* **2020**, *59*, 21436-21441.
- [118] J. Gao, M. Jiao, J. Ni, R. Yu, G. J. Cheng, X. Fang, *Angew. Chem. Int. Ed.* **2021**, *133*, 1911-1918.
- [119] Y. Ding, J. Long, F. Sun, X. Fang, *Org. Lett.* **2021**, *23*, 6073-6078.
- [120] a) J. Chong, A. Poutaraud, P. Huguene, *Plant Sci.* **2009**, *177*, 143-155; b) P. Jeandet, B. Delaunois, A. Conreux, D. Donnez, V. Nuzzo, S. Cordelier, C. Clément, E. Courot, *BioFactors* **2010**, *36*, 331-341.
- [121] a) A. Dubrovina, K. Kiselev, *Planta* **2017**, *246*, 597-623; b) A. Valletta, L. M. Iozia, F. Leonelli, *Plants* **2021**, *10*, 90.
- [122] P. Pecyna, J. Wargula, M. Murias, M. Kucinska, *Biomolecules* **2020**, *10*, 1111.
- [123] J.-W. Jung, J.-K. Kim, J.-G. Jun, *Chem. Pharm. Bull.* **2016**, c16-00089.
- [124] S. Cheenpracha, C. Karalai, C. Ponglimanont, A. Kanjana-Opas, *J. Nat. Prod.* **2009**, *72*, 1395-1398.
- [125] F. M. A. Bar, M. A. Khanfar, A. Y. Elnagar, F. A. Badria, A. M. Zaghloul, K. F. Ahmad, P. W. Sylvester, K. A. El Sayed, *Bioorg. Med. Chem.* **2010**, *18*, 496-507.

- [126] A. S. Tan, J. Singh, N. S. Rezali, M. Muhamad, N. N. S. Nik Mohamed Kamal, Y. Six, M. N. Azmi, *Molecules* **2022**, *27*, 5373.
- [127] a) T. Graening, H. G. Schmalz, *Angew. Chem.* **2004**, *116*, 3292-3318; b) Y. Lu, J. Chen, M. Xiao, W. Li, D. D. Miller, *Pharm. Res.* **2012**, *29*, 2943-2971; c) I. A. Gracheva, E. S. Shchegravina, H.-G. Schmalz, I. P. Beletskaya, A. Y. Fedorov, *J. Med. Chem.* **2020**, *63*, 10618-10651.
- [128] a) B. Kramer, S. R. Waldvogel, *Angew. Chem. Int. Ed.* **2004**, *43*, 2446-2449; b) C.-R. Su, Y.-C. Shen, P.-C. Kuo, Y.-L. Leu, A. G. Damu, Y.-H. Wang, T.-S. Wu, *Bioorg. Med. Chem. Lett.* **2006**, *16*, 6155-6160; c) K. N. Mewett, S. P. Fernandez, A. K. Pasricha, A. Pong, S. O. Devenish, D. E. Hibbs, M. Chebib, G. A. Johnston, J. R. Hanrahan, *Bioorg. Med. Chem.* **2009**, *17*, 7156-7173.
- [129] a) F. C. Pigge, *Synthesis* **2010**, *2010*, 1745-1762; b) Y. Zhao, L. Sun, T. Zeng, J. Wang, Y. Peng, G. Song, *Org. Biomol. Chem.* **2014**, *12*, 3493-3498.
- [130] a) H. Tsukamoto, T. Uchiyama, T. Suzuki, Y. Kondo, *Org. Biomol. Chem.* **2008**, *6*, 3005-3013; b) G. Wang, Y. Gan, Y. Liu, *Chin. J. Chem.* **2018**, *36*, 916-920.
- [131] S. A. Ghorpade, D. N. Sawant, D. Renn, A. Zernickel, W. Du, N. Sekar, J. Eppinger, *New J. Chem.* **2018**, *42*, 6210-6214.
- [132] Y. Lee, S. Shabbir, S. Lee, H. Ahn, H. Rhee, *Green Chem.* **2015**, *17*, 3579-3583.
- [133] a) C. G. Frost, J. Howarth, J. M. Williams, *Tetrahedron Asymmetry* **1992**, *3*, 1089-1122; b) F. K. Sheffy, J. Godschalx, J. Stille, *J. Am. Chem. Soc.* **1984**, *106*, 4833-4840.
- [134] K. L. Granberg, J. E. Baekvall, *J. Am. Chem. Soc.* **1992**, *114*, 6858-6863.
- [135] V. T. Tran, Z. Q. Li, O. Apolinar, J. Derosa, M. V. Joannou, S. R. Wisniewski, M. D. Eastgate, K. M. Engle, *Angew. Chem. Int. Ed.* **2020**, *59*, 7409-7413.
- [136] A. S. Amant, C. Frazier, B. Newmeyer, K. Fruehauf, J. R. De Alaniz, *Org. Biomol. Chem.* **2016**, *14*, 5520-5524.
- [137] a) S. V. Mulpuri, J. Shin, B.-G. Shin, A. Greiner, D. Y. Yoon, *Polymer* **2011**, *52*, 4377-4386; b) W.-L. Yu, J.-Q. Chen, Y.-L. Wei, Z.-Y. Wang, P.-F. Xu, *Chem. Commun.* **2018**, *54*, 1948-1951.
- [138] a) D. Müller, A. Alexakis, *Chem. Eur. J.* **2013**, *19*, 15226-15239; b) Y. Cai, A. D. Benischke, P. Knochel, C. Gosmini, *Chem. Eur. J.* **2017**, *23*, 250-253.
- [139] M. Qian, E.-i. Negishi, *Tetrahedron Lett.* **2005**, *46*, 2927-2930.
- [140] M. J. Frisch, G. W. Trucks, H. B. Schlegel, G. E. Scuseria, M. A. Robb, J. R. Cheeseman, G. Scalmani, V. Barone, G. A. Petersson, H. Nakatsuji, X. Li, M. Caricato, A. V. Marenich, J. Bloino, B. G. Janesko, R. Gomperts, B. Mennucci, H. P. Hratchian, J. V. Ortiz, A. F. Izmaylov, J. L. Sonnenberg, Williams, F. Ding, F. Lipparini, F. Egidi, J. Goings, B. Peng, A. Petrone, T. Henderson, D. Ranasinghe, V. G. Zakrzewski, J. Gao, N. Rega, G. Zheng, W. Liang, M. Hada, M. Ehara, K. Toyota, R. Fukuda, J. Hasegawa, M. Ishida, T. Nakajima, Y. Honda, O. Kitao, H. Nakai, T. Vreven, K. Throssell, J. A. Montgomery Jr., J. E. Peralta, F. Ogliaro, M. J. Bearpark, J. J. Heyd, E. N. Brothers, K. N. Kudin, V. N. Staroverov, T. A. Keith, R. Kobayashi, J. Normand, K. Raghavachari, A. P. Rendell, J. C. Burant, S. S. Iyengar, J. Tomasi, M. Cossi, J. M. Millam, M. Klene, C. Adamo, R. Cammi, J. W. Ochterski, R. L. Martin, K. Morokuma, O. Farkas, J. B. Foresman, D. J. Fox, Wallingford, CT, **2016**.
- [141] a) B. Chen, X. Liu, Y.-J. Hu, D.-M. Zhang, L. Deng, J. Lu, L. Min, W.-C. Ye, C.-C. Li, *Chem. Sci.* **2017**, *8*, 4961-4966; b) X. Liang, L. Li, K. Wei, Y.-R. Yang, *Org. Lett.* **2021**, *23*, 2731-2735.
- [142] F. V. Singh, T. Wirth, *Chem. Asian J.* **2014**, *9*, 950-971.
- [143] a) M. G. Banwell, M.-A. Fam, R. W. Gable, E. Hamel, *J. Chem. Soc., Chem. Commun.* **1994**, 2647-2649; b) K. Hackelöer, G. Schnakenburg, S. R. Waldvogel, *J. Org. Chem.* **2011**, 6314-6319; c) K. Takubo, K. Furutsu, T. Ide, H. Nemoto, Y. Ueda, K. Tsujikawa, T. Ikawa, T. Yoshimitsu, S. Akai, *Eur. J. Org. Chem.* **2016**, *2016*, 1562-1576.
- [144] S. Yamashita, D. Masuda, Y. Matsuzawa, *Curr. Atheroscler. Rep.* **2020**, *22*, 1-17.
- [145] aJ. Chen, Z. Lu, *Org. Chem. Front.* **2018**, *5*, 260-272; bJ. Guo, Z. Cheng, J. Chen, X. Chen, Z. Lu, *Acc. Chem. Res.* **2021**, *54*, 2701-2716; cJ. L. Kennemur, R. Maji, M. J.

- Scharf, B. List, *Chem. Rev.* **2021**, *121*, 14649-14681; dX.-Y. Sun, B.-Y. Yao, B. Xuan, L.-J. Xiao, Q.-L. Zhou, *Chem Catalysis* **2022**.
- [146] M. A. Khalilzadeh, A. Hosseini, M. Shokrollahzadeh, M. R. Halvagar, D. Ahmadi, F. Mohannazadeh, M. Tajbakhsh, *Tetrahedron Lett.* **2006**, *47*, 3525-3528.
- [147] a) L. M. Nollet, F. Toldrá, *Handbook of analysis of active compounds in functional foods*, CRC Press, **2012**; b) M. A. Müller, C. Schäfer, G. Litta, A. M. Klünter, M. G. Traber, A. Wyss, T. Ralla, M. Eggersdorfer, W. Bonrath, *Eur. J. Org. Chem.* **2022**, *2022*, e202201190.
- [148] M. L. Colombo, *Molecules* **2010**, *15*, 2103-2113.
- [149] A. Azzi, *Redox. Biol.* **2019**, *26*, 101259.
- [150] J.-M. Zingg, *Mol. Asp. Med.* **2007**, *28*, 400-422.
- [151] a) M. H. Ng, Y. M. Choo, A. N. Ma, C. H. Chuah, M. A. Hashim, *Lipids* **2004**, *39*, 1031-1035; b) A. Fiorentino, C. Mastellone, B. D'Abrosca, S. Pacifico, M. Scognamiglio, G. Cefarelli, R. Caputo, P. Monaco, *Food Chem.* **2009**, *115*, 187-192; c) B. Butinar, M. Bučar-Miklavčič, C. Mariani, P. Raspor, *Food Chem.* **2011**, *128*, 505-512.
- [152] Y. Yamamoto, N. Maita, A. Fujisawa, J. Takashima, Y. Ishii, W. C. Dunlap, *J. Nat. Prod.* **1999**, *62*, 1685-1687.
- [153] a) G. Navarro, J. J. Fernández, M. Norte, *J. Nat. Prod.* **2004**, *67*, 495-499; b) A. Lavaud, P. Richomme, M. Litaudon, R. Andriantsitohaina, D. Guilet, *J. Nat. Prod.* **2013**, *76*, 2246-2252; c) M. El Hattab, G. g. Genta-Jouve, N. Bouzidi, A. Ortalo-Magne, C. Hellio, J.-P. Maréchal, L. Piovetti, O. P. Thomas, G. Culioli, *J. Nat. Prod.* **2015**, *78*, 1663-1670; d) C. C. Presley, A. L. Valenciano, M. L. Fernández-Murga, Y. Du, N. Shanaiah, M. B. Cassera, M. Goetz, J. A. Clement, D. G. Kingston, *J. Nat. Prod.* **2017**, *81*, 475-483; e) S. Shinoda, S.-i. Kurimoto, T. Kubota, M. Sekiguchi, *Heterocycles* **2022**, *104*, 1141-1147.
- [154] L. Packer, S. U. Weber, G. Rimbach, *J. Nutr.* **2001**, *131*, 369S-373S.
- [155] E. Niki, M. G. Traber, *Ann. Nutr. Metab.* **2012**, *61*, 207-212.
- [156] G. W. Burton, T. Doba, E. Gabe, L. Hughes, *J. Am. Chem. Soc.* **1985**, *107*, 7053-7065.
- [157] E. Niki, *Ann. N. Y. Acad. Sci.* **1987**, *498*, 186-199.
- [158] E. Haslam, *Shikimic acid: metabolism and metabolites*, Wiley, **1993**.
- [159] D. J. Wilson, S. Patton, G. Florova, V. Hale, K. A. Reynolds, *J. Ind. Microbiol. Biotechnol.* **1998**, *20*, 299-303.
- [160] D. Hofius, U. Sonnewald, *Trends Plant Sci.* **2003**, *8*, 6-8.
- [161] a) P. Dörmann, *Planta* **2007**, *225*, 269-276; b) L. Mène-Saffrané, D. DellaPenna, *Plant Physiol. Biochem.* **2010**, *48*, 301-309.
- [162] a) C. Constantinou, A. Papas, A. I. Constantinou, *Int. J. Cancer* **2008**, *123*, 739-752; b) S. Wada, *Forum Nutr.* **2009**, *61*, 204-216.
- [163] W. H. Organization, *World malaria report 2015*, World Health Organization, **2015**.
- [164] a) C.-H. Jun, *Chem. Soc. Rev.* **2004**, *33*, 610-618; b) G. Dong, N. Cramer, *CC bond activation*, Vol. 346, Springer, **2014**.
- [165] a) Y. Xia, G. Lu, P. Liu, G. Dong, *Nature* **2016**, *539*, 546-550; b) L. Deng, G. Dong, *Trends Chem.* **2020**, *2*, 183-198.
- [166] a) L. Souillart, N. Cramer, *Chem. Rev.* **2015**, *115*, 9410-9464; b) L. Huan, C. Zhu, *Org. Chem. Front.* **2016**, *3*, 1467-1471.
- [167] X. Bi, Q. Zhang, Z. Gu, *Chin. J. Chem.* **2021**, *39*, 1397-1412.
- [168] a) J. Christoffers, A. Baro, *Adv. Synth. Catal.* **2005**, *347*, 1473-1482; b) N. Cramer, T. Seiser, *Synlett* **2011**, *2011*, 449-460.
- [169] P. R. Khoury, J. D. Goddard, W. Tam, *Tetrahedron* **2004**, *60*, 8103-8112.
- [170] a) S. Matsumura, Y. Maeda, T. Nishimura, S. Uemura, *J. Am. Chem. Soc.* **2003**, *125*, 8862-8869; b) T. Matsuda, M. Shigeno, M. Murakami, *J. Am. Chem. Soc.* **2007**, *129*, 12086-12087; c) T. Seiser, N. Cramer, *Angew. Chem. Int. Ed.* **2008**, *47*, 9294-9297; d) T. Seiser, N. Cramer, *J. Am. Chem. Soc.* **2010**, *132*, 5340-5341.
- [171] R. H. Crabtree, R. P. Dion, D. J. Gibboni, D. V. McGrath, E. M. Holt, *J. Am. Chem. Soc.* **1986**, *108*, 7222-7227.

- [172] a) M. Murakami, K. Itami, M. Ubukata, I. Tsuji, Y. Ito, *J. Org. Chem.* **1998**, *63*, 4-5; b) T. Nishimura, T. Yoshinaka, Y. Nishiguchi, Y. Maeda, S. Uemura, *Org. Lett.* **2005**, *7*, 2425-2427.
- [173] J. Yu, H. Yan, C. Zhu, *Angew. Chem.* **2016**, *128*, 1155-1158.
- [174] W. Schlundt, *Dissertation* **2018**, University of Cologne.
- [175] F. Ratsch, W. Schlundt, D. Albat, A. Zimmer, J. M. Neudörfel, T. Netscher, H. G. Schmalz, *Chem. Eur. J.* **2019**, *25*, 4941-4945.
- [176] F. Ratsch, H.-G. Schmalz, *Synlett* **2018**, *29*, 785-792.
- [177] F. Ratsch, *Dissertation* **2020**, University of Cologne.
- [178] F. Ratsch, J. P. Strache, W. Schlundt, J. M. Neudörfel, A. Adler, S. Aziz, B. Goldfuss, H. G. Schmalz, *Chem. Eur. J.* **2021**, *27*, 4640-4652.
- [179] J. P. Strache, *Master Thesis* **2019**, University of Cologne.
- [180] A. J. Fugard, B. K. Thompson, A. M. Slawin, J. E. Taylor, A. D. Smith, *Organic Letters* **2015**, *17*, 5824-5827.
- [181] U. S. Singh, R. T. Scannell, H. An, B. J. Carter, S. M. Hecht, *J. Am. Chem. Soc.* **1995**, *117*, 12691-12699.
- [182] X.-D. Liu, H.-Y. Ma, C.-H. Xing, L. Lu, *Chin. Chem. Lett.* **2017**, *28*, 1780-1783.
- [183] I. J. Borowitz, L. I. Grossman, *Tetrahedron Lett.* **1962**, *3*, 471-474.
- [184] G. Pandey, R. Kumar, P. Banerjee, V. G. Puranik, *Eur. J. Org. Chem.* **2011**, *2011*, 4571-4587.
- [185] a) J. P. Clayton, K. Luk, N. H. Rogers, *J. Chem. Soc., Perkin trans.* **1979**, 308-313; b) B. P. Haney, D. P. Curran, *J. Org. Chem.* **2000**, *65*, 2007-2013; c) G. H. Posner, S. T. Lee, H. J. Kim, S. Peleg, P. Dolan, T. W. Kensler, *Bioorg. Med. Chem.* **2005**, *13*, 2959-2966; d) Z.-J. Yang, W.-Z. Ge, Q.-Y. Li, Y. Lu, J.-M. Gong, B.-J. Kuang, X. Xi, H. Wu, Q. Zhang, Y. Chen, *J. Med. Chem.* **2015**, *58*, 7007-7020; e) N. Singh, K. K. Pulukuri, T. K. Chakraborty, *Tetrahedron* **2015**, *71*, 4608-4615.
- [186] Y. A. Jasem, R. El-Esawi, T. Thiemann, *J. Chem. Res.* **2014**, *38*, 453-463.
- [187] F. A. Davis, *Tetrahedron* **2018**, *74*, 3198-3214.
- [188] a) X. Wei, J. C. Lorenz, S. Kapadia, A. Saha, N. Haddad, C. A. Busacca, C. H. Senanayake, *J. Org. Chem.* **2007**, *72*, 4250-4253; b) A. R. Jadhav, R. S. Thombal, P. Nigam, V. H. Jadhav, *Tetrahedron Lett.* **2015**, *56*, 5235-5237.
- [189] P. M. Weintraub, C.-H. R. King, *J. Org. Chem.* **1997**, *62*, 1560-1562.
- [190] T. M. Ross, S. J. Burke, W. P. Malachowski, *Tetrahedron Lett.* **2014**, *55*, 4616-4618.
- [191] J. M. Faber, C. M. Williams, *Chem. Commun.* **2011**, *47*, 2258-2260.
- [192] M. G. Suero, R. De la Campa, L. Torre-Fernández, S. García-Granda, J. Florez, *Chem. Eur. J.* **2012**, *18*, 7287-7295.
- [193] a) P. S. Mariano, E. Bay, D. G. Watson, T. Rose, C. Bracken, *J. Org. Chem.* **1980**, *45*, 1753-1762; b) R. S. Porto, M. L. A. A. Vasconcellos, E. Ventura, F. Coelho, *Synthesis* **2005**, *2005*, 2297-2306; c) J. Ishihara, O. Tokuda, K. Shiraishi, K. Takahashi, S. Hatakeyama, *Heterocycles* **2010**, *80*, 1067-1079; d) S. M. A. H. Siddiki, A. S. Touchy, K. Kon, K. i. Shimizu, *Chem. Eur. J.* **2016**, *22*, 6111-6119.
- [194] A. Kulshrestha, N. Salehi Marzijarani, K. Dilip Ashtekar, R. Staples, B. Borhan, *Org. Lett.* **2012**, *14*, 3592-3595.
- [195] G. E. Magoulas, S. E. Bariamis, C. M. Athanassopoulos, A. Haskopoulos, P. G. Dedes, M. G. Krokidis, N. K. Karamanos, D. Kletsas, D. Papaioannou, G. Maroulis, *Eur. J. Med. Chem.* **2011**, *46*, 721-737.
- [196] Y. F. Kang, W. J. Yan, T. W. Zhou, F. Dai, X. Z. Li, X. Z. Bao, Y. T. Du, C. H. Yuan, H. B. Wang, X. R. Ren, J. Zhang, *Chem. Eur. J.* **2014**, *20*, 8904-8908.
- [197] R. A. Benkeser, *Synthesis* **1971**, *1971*, 347-358.
- [198] Y. Yamamoto, N. Asao, *Chem. Rev.* **1993**, *93*, 2207-2293.
- [199] S. Ritter, Y. Horino, J. Lex, H.-G. Schmalz, *Synlett* **2006**, *19*, 3309-3313.
- [200] Y. Yin, W. Ma, Z. Chai, G. Zhao, *J. Org. Chem.* **2007**, *72*, 5731-5736.
- [201] a) A. R. de Faria, C. R. R. Matos, C. R. D. Correia, *Tetrahedron Lett.* **1993**, *34*, 27-30; b) P. C. M. Miranda, C. R. D. Correia, *Tetrahedron Lett.* **1999**, *40*, 7735-7738.

- [202] a) C. Aissa, *Eur. J. Org. Chem.* **2009**, 2009, 1831-1844; b) P. X. T. Rinu, S. Radhika, G. Anilkumar, *ChemistrySelect* **2022**, 7, e202200760.
- [203] G. R. Fulmer, A. J. Miller, N. H. Sherden, H. E. Gottlieb, A. Nudelman, B. M. Stoltz, J. E. Bercaw, K. I. Goldberg, *Organometallics* **2010**, 29, 2176-2179.
- [204] J. Westphal, *Dissertation* **2017**, University of Cologne.
- [205] X. Gao, J. Han, L. Wang, *Org. Lett.* **2015**, 17, 4596-4599.
- [206] D. Albat, M. Reiher, J. M. Neudörfl, H. G. Schmalz, *Eur. J. Org. Chem.* **2021**, 2021, 4237-4242.
- [207] J. Feng, F. Noack, M. J. Krische, *J. Am. Chem. Soc.* **2016**, 138, 12364-12367.
- [208] K. Matsumoto, K. Hatano, N. Umezawa, T. Higuchi, *Synthesis* **2004**, 2004, 2181-2185.
- [209] T. Yanagi, K. Nogi, H. Yorimitsu, *Chem. Eur. J.* **2020**, 26, 783-787.
- [210] C. W. Cavanagh, M. H. Aukland, A. Hennessy, D. J. Procter, *Chem. Commun.* **2015**, 51, 9272-9275.
- [211] L. T. Kliman, S. N. Mlynarski, J. P. Morken, *J. Am. Chem. Soc.* **2010**, 132, 13949-13949.
- [212] C. Schmitz, W. Leitner, G. Franciò, *Chem. Eur. J.* **2015**, 21, 10696-10702.
- [213] a) K. Hong, J. P. Morken, *J. Org. Chem.* **2011**, 76, 9102-9108; b) Y.-X. Wang, S.-L. Qi, Y.-X. Luan, X.-W. Han, S. Wang, H. Chen, M. Ye, *J. Am. Chem. Soc.* **2018**, 140, 5360-5364.
- [214] Y. Kurihara, M. Nishikawa, Y. Yamanoi, H. Nishihara, *Chem. Commun.* **2012**, 48, 11564-11566.
- [215] A. A. Szymaniak, C. Zhang, J. R. Coombs, J. P. Morken, *ACS Catal.* **2018**, 8, 2897-2901.
- [216] B. Xu, J. A. Gartman, U. K. Tambar, *Tetrahedron* **2017**, 73, 4150-4159.
- [217] B. Xu, U. K. Tambar, *J. Am. Chem. Soc.* **2016**, 138, 12073-12076.
- [218] D. M. Miles-Barrett, A. R. Neal, C. Hand, J. R. Montgomery, I. Panovic, O. S. Ojo, C. S. Lancefield, D. B. Cordes, A. M. Slawin, T. Lebl, *Org. Biomol. Chem.* **2016**, 14, 10023-10030.
- [219] P. M. Killoran, S. B. Rossington, J. A. Wilkinson, J. A. Hadfield, *Tetrahedron Lett.* **2016**, 57, 3954-3957.
- [220] T. Leermann, F. R. Leroux, F. Colobert, *Org. Lett.* **2011**, 13, 4479-4481.
- [221] B. M. Rosen, D. A. Wilson, C. J. Wilson, M. Peterca, B. C. Won, C. Huang, L. R. Lipski, X. Zeng, G. Ungar, P. A. Heiney, *J. Am. Chem. Soc.* **2009**, 131, 17500-17521.
- [222] Y. Zhang, Y. Tanabe, S. Kuriyama, Y. Nishibayashi, *Chem. Eur. J.* **2022**.
- [223] C.-K. Chan, Y.-L. Tsai, M.-Y. Chang, *Tetrahedron* **2017**, 73, 3368-3376.
- [224] H. Wang, M. Yang, Y. Wang, X. Man, X. Lu, Z. Mou, Y. Luo, H. Liang, *Org. Lett.* **2021**, 23, 8183-8188.
- [225] V. Pathak, I. Ahmad, A. K. Kahlon, M. Hasanain, S. Sharma, K. K. Srivastava, J. Sarkar, K. Shankar, A. Sharma, A. Gupta, *RSC Adv.* **2014**, 4, 35171-35185.
- [226] K. Sugimoto, K. Tamura, N. Ohta, C. Tohda, N. Toyooka, H. Nemoto, Y. Matsuya, *Bioorg. Med. Chem. Lett.* **2012**, 22, 449-452.
- [227] K. Balaraman, C. Wolf, *Org. Lett.* **2021**, 23, 8994-8999.
- [228] Y. Huang, Y. Yu, Z. Zhu, C. Zhu, J. Cen, X. Li, W. Wu, H. Jiang, *J. Org. Chem.* **2017**, 82, 7621-7627.
- [229] A. A. A. Aguilar, G. N. Ledesma, B. Tirloni, T. S. Kaufman, E. L. Larghi, *Synthesis* **2019**, 51, 4253-4262.
- [230] X. Qian, J. Han, L. Wang, *Adv. Synth. Catal.* **2016**, 358, 940-946.
- [231] S. Fu, N.-Y. Chen, X. Liu, Z. Shao, S.-P. Luo, Q. Liu, *J. Am. Chem. Soc.* **2016**, 138, 8588-8594.
- [232] W. Ma, S. Cui, H. Sun, W. Tang, D. Xue, C. Li, J. Fan, J. Xiao, C. Wang, *Chem. Eur. J.* **2018**, 24, 13118-13123.
- [233] M. H. Aukland, F. J. Talbot, J. A. Fernández-Salas, M. Ball, A. P. Pulis, D. J. Procter, *Angewandte Chemie* **2018**, 130, 9933-9937.
- [234] G. Wu, Y. Deng, C. Wu, Y. Zhang, J. Wang, *Angew. Chem. Int. Ed.* **2014**, 53, 10510-10514.

- [235] S. H. Shaber, *Rohm and Haas Company* **1992**, *US Patent* 5,087,635.
- [236] C. Viglianisi, M. G. Bartolozzi, G. F. Pedulli, R. Amorati, S. Menichetti, *Chem. Eur. J.* **2011**, *17*, 12396-12404.
- [237] N. J. Harris, J. J. Gajewski, *J. Am. Chem. Soc.* **1994**, *116*, 6121-6129.
- [238] L. T. Kliman, S. N. Mlynarski, G. E. Ferris, J. P. Morken, *Angew. Chem. Int. Ed.* **2012**, *51*, 521-524.
- [239] S. E. Korkis, D. J. Burns, H. W. Lam, *J. Am. Chem. Soc.* **2016**, *138*, 12252-12257.
- [240] B. Schmidt, O. Kunz, *Beilstein J. Org. Chem.* **2013**, *9*, 2544-2555.

12. Appendix

12.1. List of abbreviations

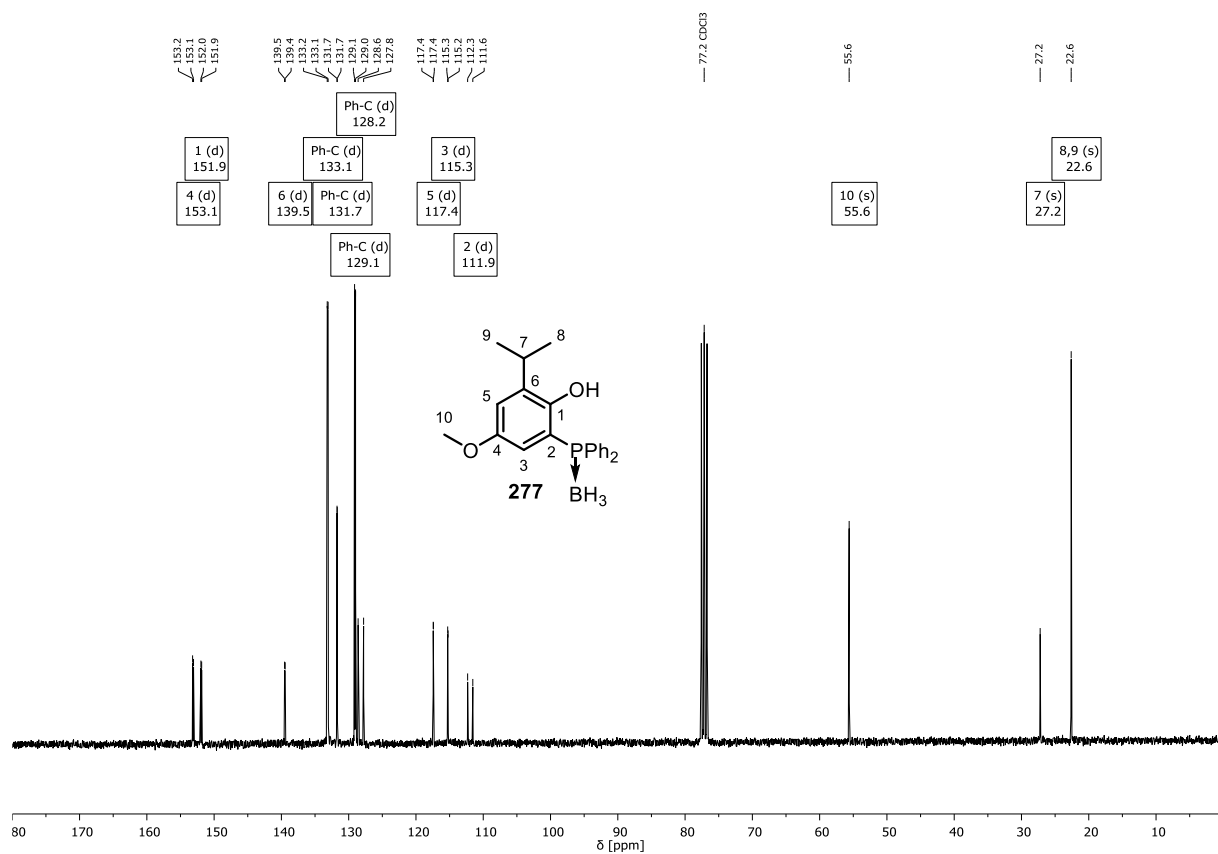
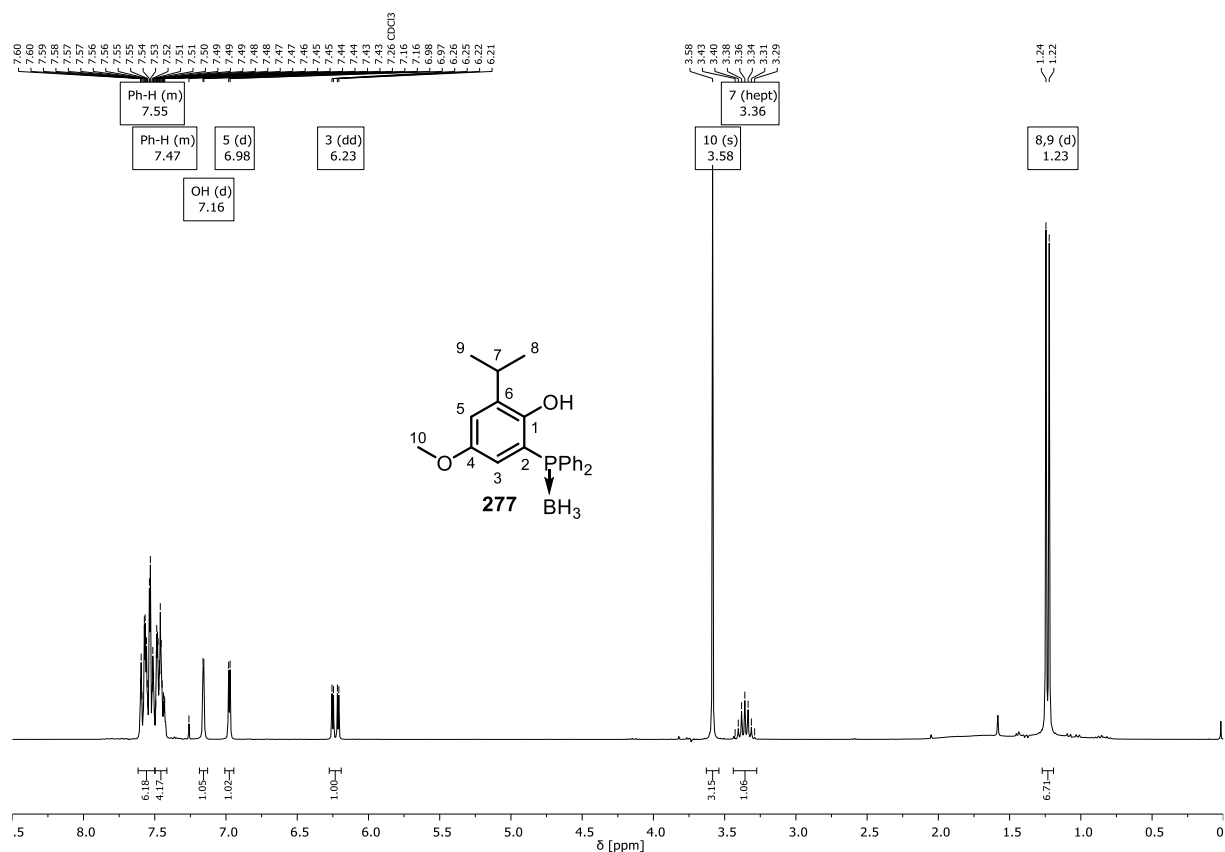
| | |
|---------------------------------|---------------------------------------------|
| Å | Ångstrom (10^{-10} m) |
| Ac | acetyl |
| Ad | adamantyl |
| AGE | advanced glycation end products |
| Ar | aryl, arene |
| atm | standard atmosphere |
| ATP | adenosine triphosphate |
| BINAP | 2,2'-bis(diphenylphosphino)-1,1'-binaphthyl |
| BINOL | 1,1'-bi-2-naphthol |
| BIPOL | 1,1'-bi-2-phenol |
| Bn | benzyl |
| Boc | <i>tert</i> -butyloxycarbonyl |
| br | broad |
| °C | degree <i>Celsius</i> |
| CH ₂ Cl ₂ | dichloromethane |
| cHex | cyclohexane |
| cod | 1,5-cyclooctadiene |
| conv. | conversion |
| CSA | camphorsulfonic acid |
| Cy | cyclohexyl |
| d | doublet |
| DABCO | 1,4-diazabicyclo[2.2.2]octane |
| | 1,2-dichloroethane |
| δ | chemical shift |
| DFT | density functional theory |
| DIBAL-H | diisobutylaluminum hydride |
| DIPA | diisopropylamine |
| DIPEA | diisopropylethylamine |
| DME | 1,2-dimethoxyethane |
| DMF | <i>N,N</i> -dimethylformamide |
| DMAP | 4-(dimethylamino)pyridine |
| DMP | <i>Dess-Martin</i> periodinane |

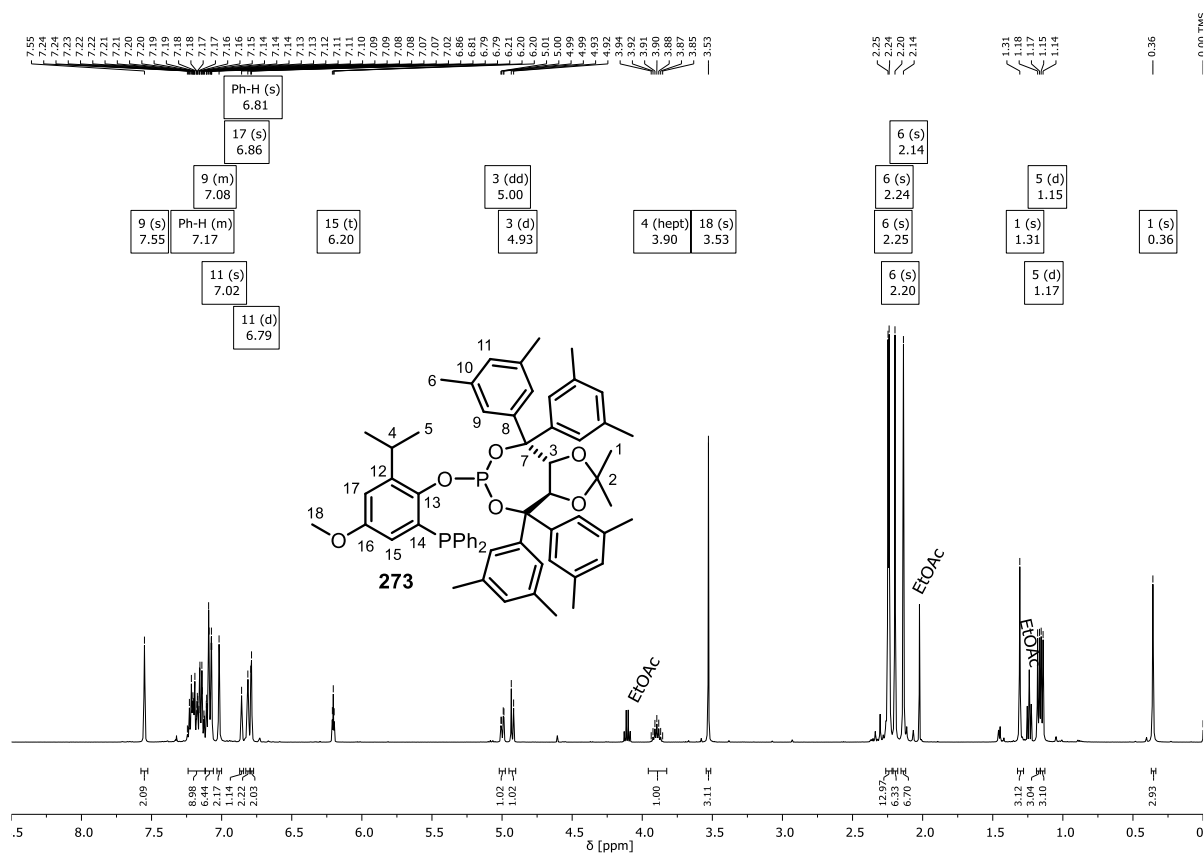
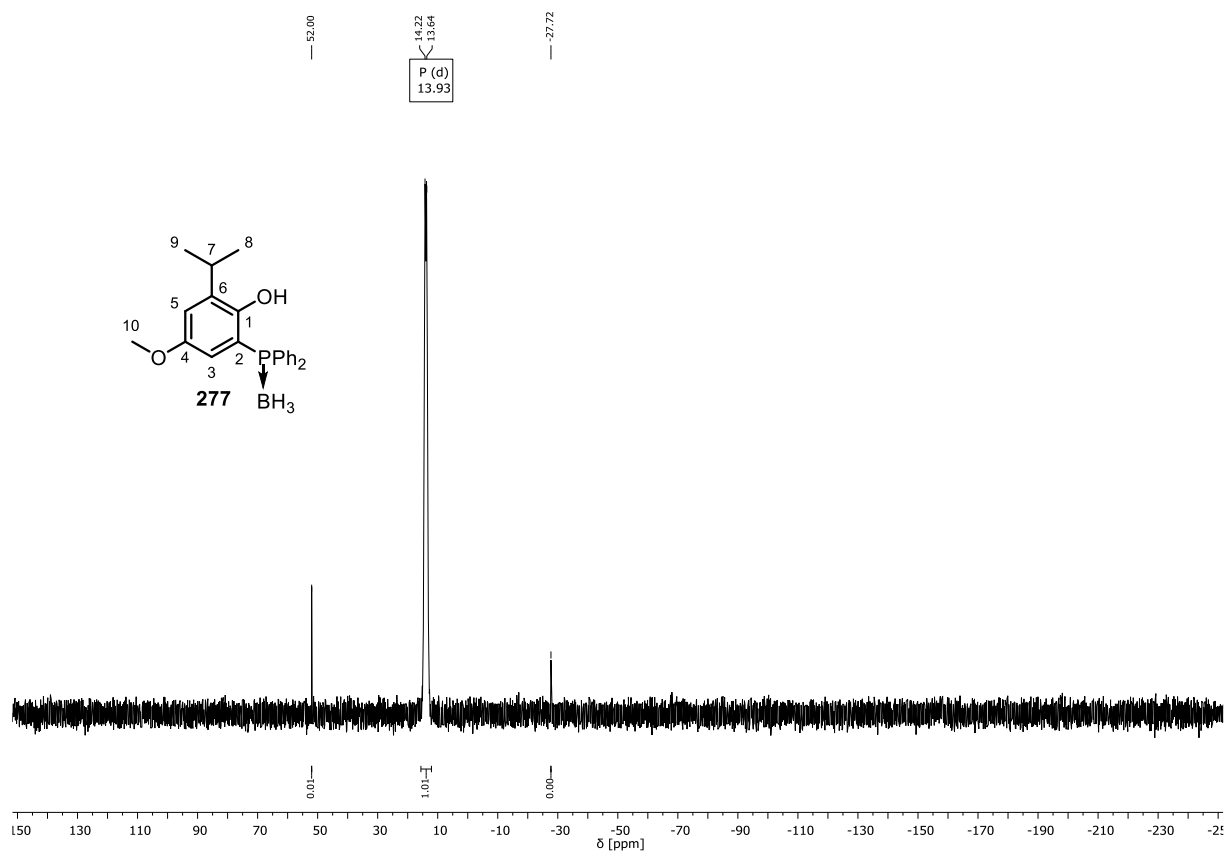
| | |
|-------------------|---------------------------------------------------------------------------------------------------------------------|
| DMSO | dimethyl sulfoxide |
| DIOP | 2,3- <i>O</i> -isopropylidene-2,3-dihydroxy-1,4-bis(diphenylphosphino)butane |
| DPEPhos | [oxydi(2,1-phenylene)]bis(diphenylphosphane) |
| dppp | 1,3-bis(diphenylphosphino)propane |
| DQ | duroquinone |
| <i>dr</i> | diastereomeric ratio |
| ECD | electronic circular dichroism |
| <i>ee</i> | enantiomeric excess |
| EI | electron impact ionization |
| equiv. | equivalent(s) |
| <i>er</i> | enantiomeric ratio |
| ESI | electrospray ionization |
| Et | ethyl |
| Et ₂ O | diethyl ether |
| Et ₃ N | triethylamine |
| EtOAc | ethyl acetate |
| eV | electron volt |
| FCC | flash column chromatography |
| GC | gas chromatography |
| <i>Grubbs II</i> | [1,3-bis-(2,4,6-trimethylphenyl)-2-imidazolidinylidene]-dichloro(phenylmethylene)-(tricyclohexylphosphino)ruthenium |
| h | hours(s) |
| hept. | heptet |
| Hz | <i>Hertz</i> |
| IUPAC | International Union of Pure and Applied Chemistry |
| K | degree <i>Kelvin</i> |
| KHMDS | potassium bis(trimethylsilyl)amide |
| KIE | kinetic isotope effect |
| L | ligand |
| LA | <i>Lewis acid</i> |
| LDA | lithium diisopropylamide |
| lit. | literature |
| M | molar |

| | |
|---------------------|----------------------------------------|
| m | meter or multiplet (in NMR analysis) |
| max. | maximum |
| min | minute(s) |
| min. | minimum |
| Me | methyl |
| MeCN | acetonitrile |
| mL | milliliter |
| mm | millimeter |
| MMPP | magnesium monoperoxyphthalate |
| MOM | Methoxymethyl |
| MsOH | methanesulfonic acid |
| MS | molecular sieves 3-4 Å |
| Ms | mesyl/methanesulfonyl |
| MTBE | <i>tert</i> -butylmethylether |
| MW | microwave |
| NBS | <i>N</i> -bromosuccinimide |
| <i>n</i> Bu | <i>n</i> -butyl |
| n.c. | no conversion |
| n.d. | not determined |
| <i>n</i> Hex | <i>n</i> -hexane |
| nm | nanometer(s) (10 ⁻⁹ m) |
| NMR | nuclear magnetic resonance |
| <i>n</i> Pe | <i>n</i> -pentane |
| PG | protecting group |
| PIDA | phenyliodine(III) diacetate |
| PIFA | phenyliodine(III) di(trifluoroacetate) |
| Piv | pivalate |
| ppm | parts per million |
| Pr | propyl |
| ψ | pseudo |
| PTFE | polytetrafluoroethylene |
| q | quartet |
| quant. | quantitative |
| <i>QuadraSil</i> AP | <i>QuadraSil</i> aminopropyl |
| quin. | quintet |

| | |
|---------------------------|------------------------------------------------------------------------------------------------|
| <i>rac</i> | racemic, racemate |
| rct. | reaction |
| R _f | retention factor |
| <i>rr</i> | regioisomeric ratio |
| r.t. | room temperature (25 °C ± 2 °C) |
| s | singlet |
| sat. | saturated |
| (S)-DTBM-segphos | (S)-5,5'-bis[di(3,5-di- <i>tert</i> -butyl-4-methoxyphenyl)phosphino]-4,4'-bi-1,3-benzodioxole |
| s.m. | starting material |
| T | temperature |
| t | triplet |
| TADDOL | α,α,α',α'-tetraaryl-2,2-disubstituted 1,3-dioxolane-4,5-dimethanol |
| TBAF | tetra- <i>N</i> -butylammonium fluoride |
| TBAI | tetrabutylammonium iodide |
| TBS | <i>tert</i> -butyldimethylsilyl |
| TBSOTf | <i>tert</i> -butyldimethylsilyl triflate |
| <i>t</i> Bu | <i>tert</i> -butyl |
| TEMPO | (2,2,6,6-tetramethylpiperidin-1-yl)oxyl |
| Tf | triflyl |
| TBHP | <i>tert</i> -butyl hydroperoxide |
| TIPS | triisopropylsilyl |
| TLC | thin layer chromatography |
| TMB | 1,2,3-trimethoxybenzene |
| TMS (in NMR) | tetramethylsilane |
| TMS (as protecting group) | trimethylsilyl |
| TPPO | triphenylphosphine oxide |
| T _R | retention time |
| Troc | 2,2,2-trichloroethoxycarbonyl |
| Ts/Tosyl | <i>p</i> -toluenesulfonyl |
| W (unit) | watt |

12.2. NMR spectra of selected compounds





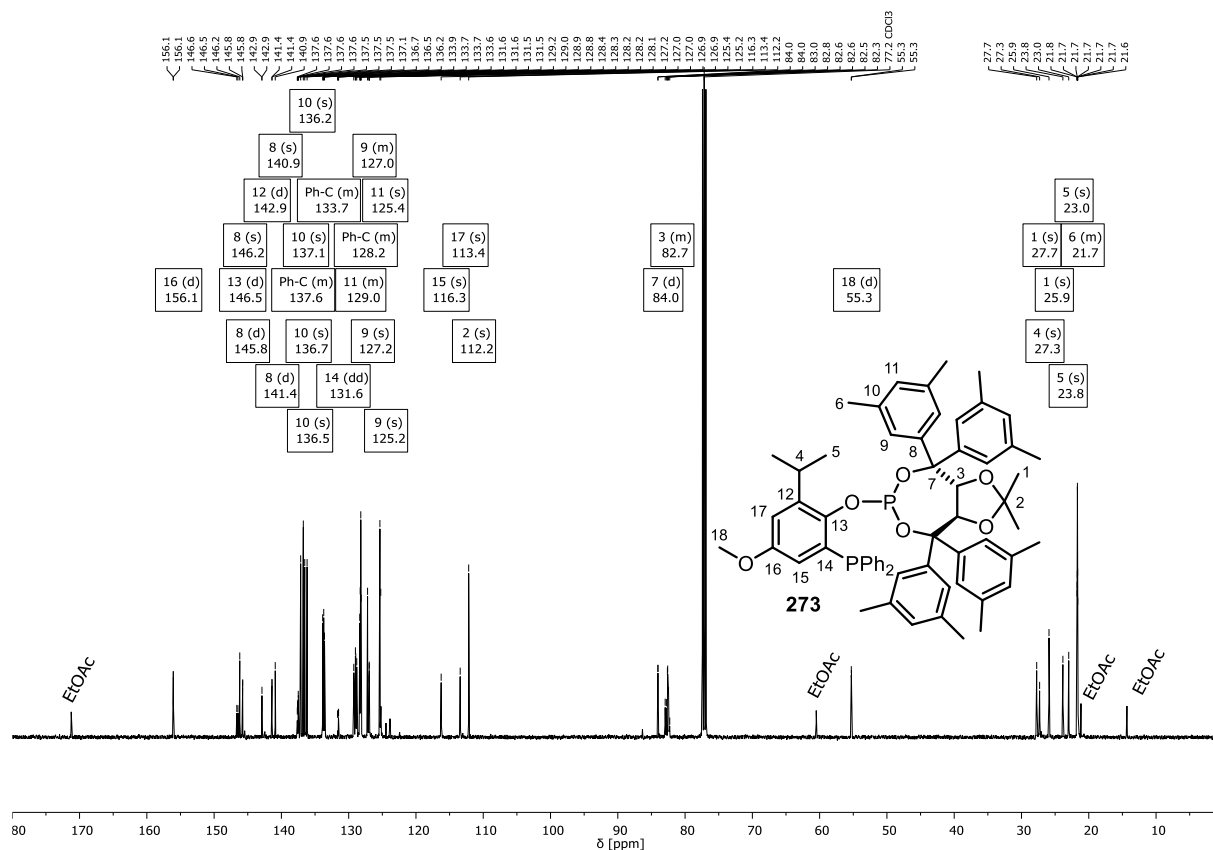


Figure 30: ^{13}C NMR (126 MHz, CDCl_3) spectrum of phosphine-phosphite ligand **273**.

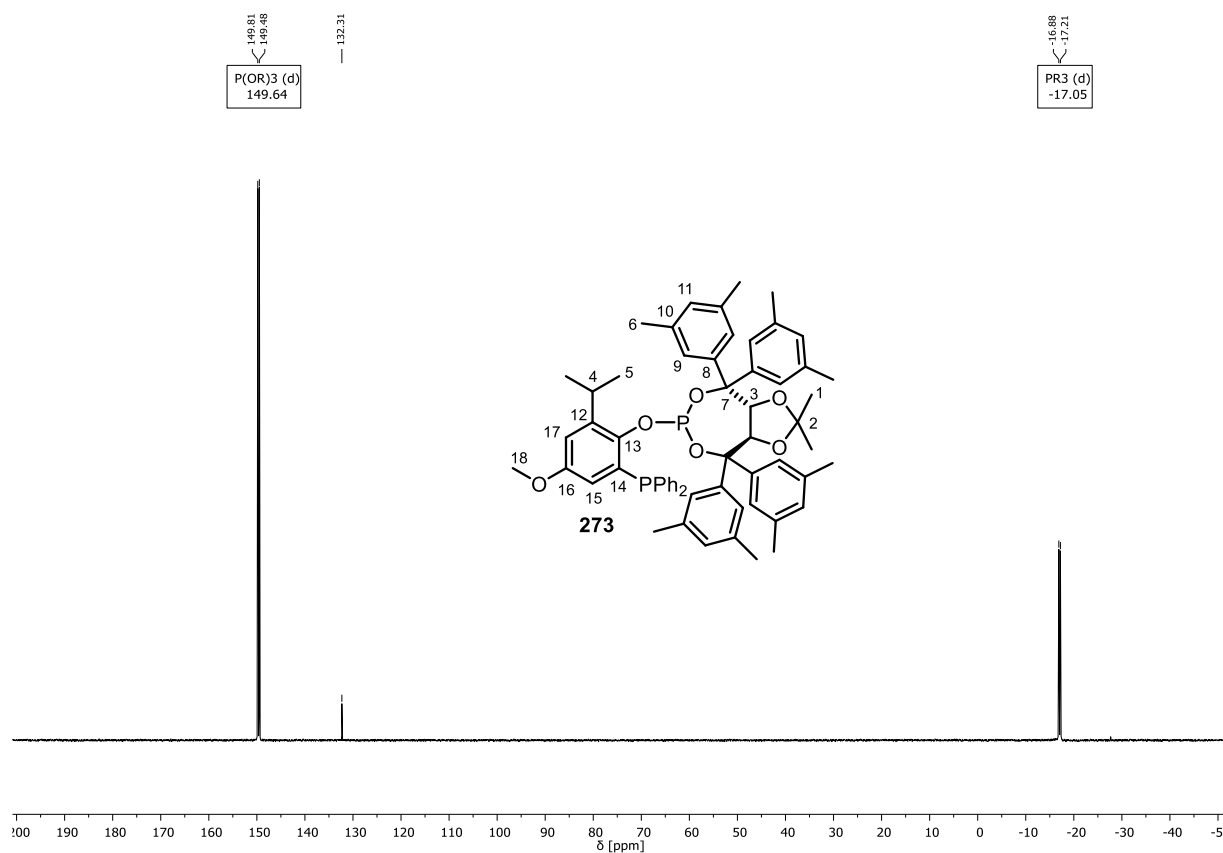


Figure 31: ^{31}P NMR (202 MHz, CDCl_3) spectrum of phosphine-phosphite ligand **273**.

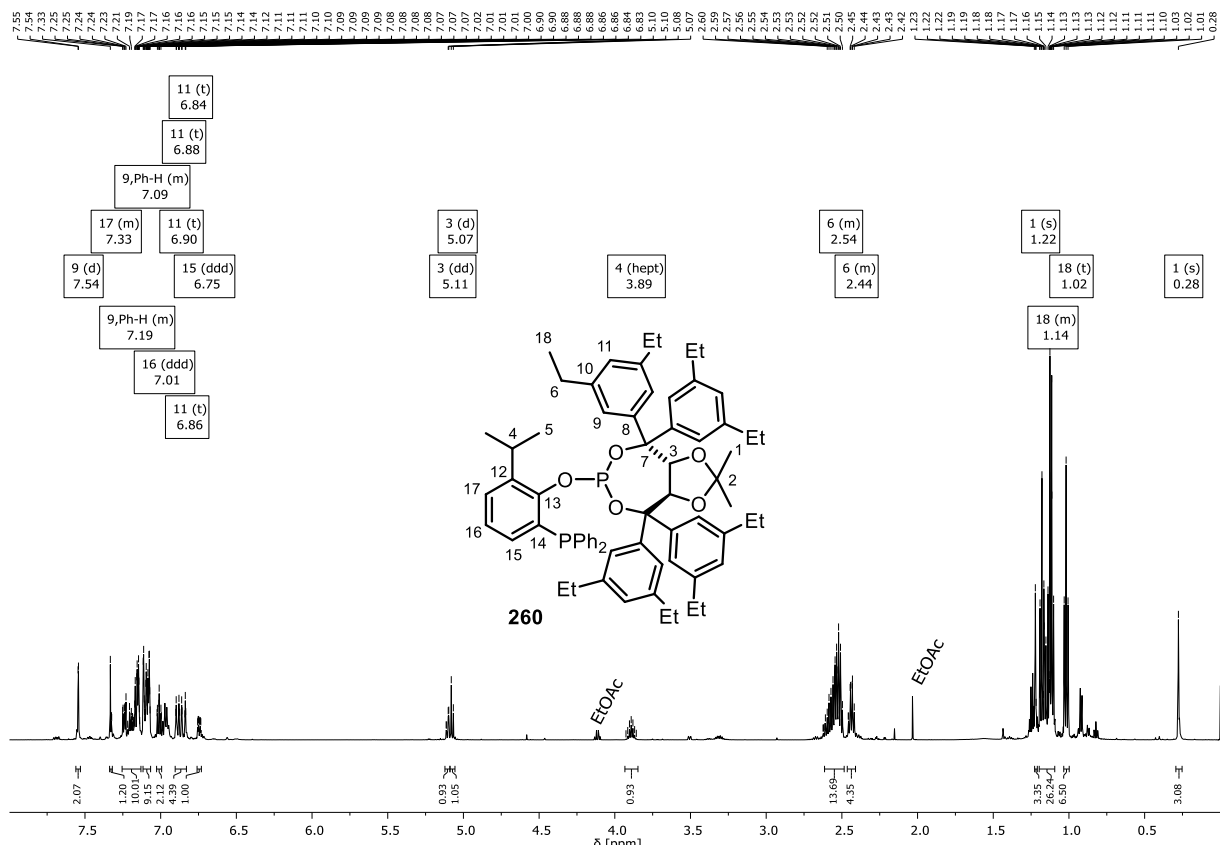


Figure 32: ¹H NMR (600 MHz, CDCl₃) spectrum of phosphine-phosphite ligand **260.**

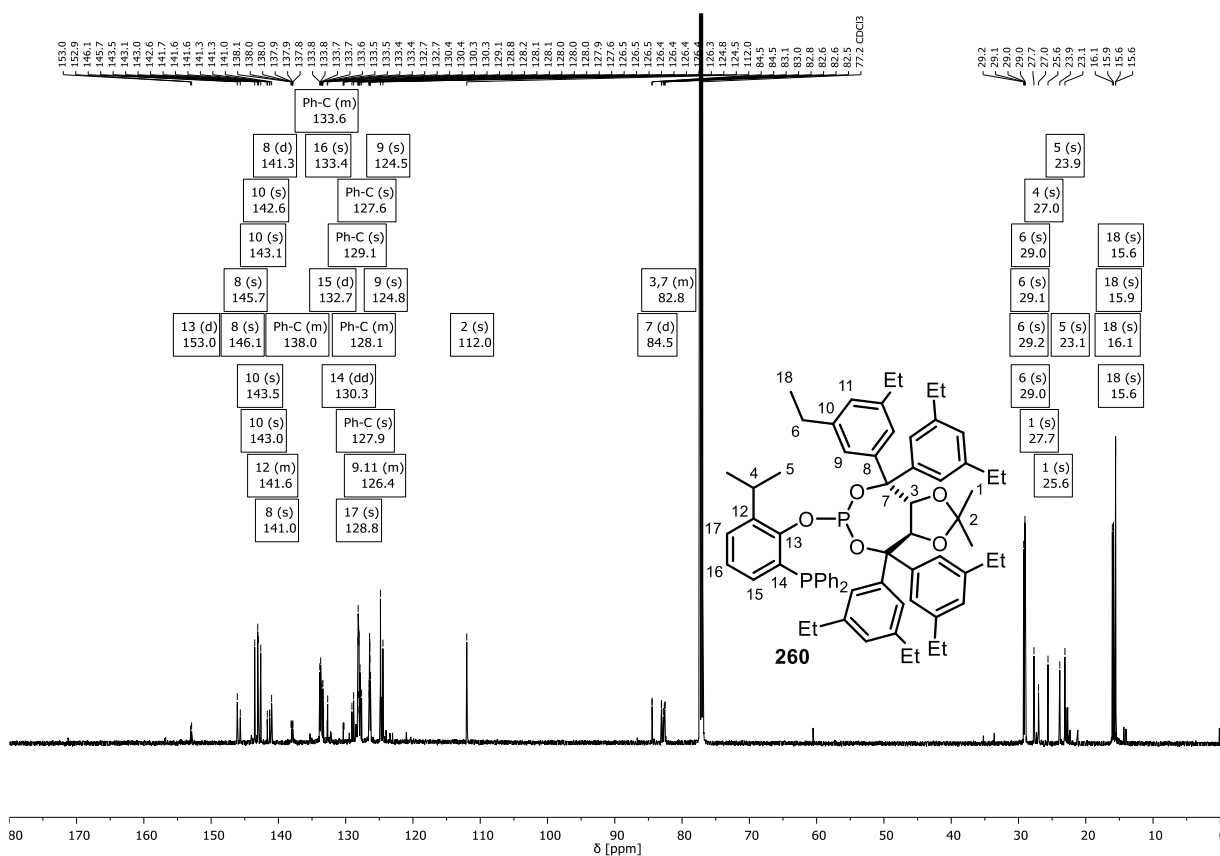
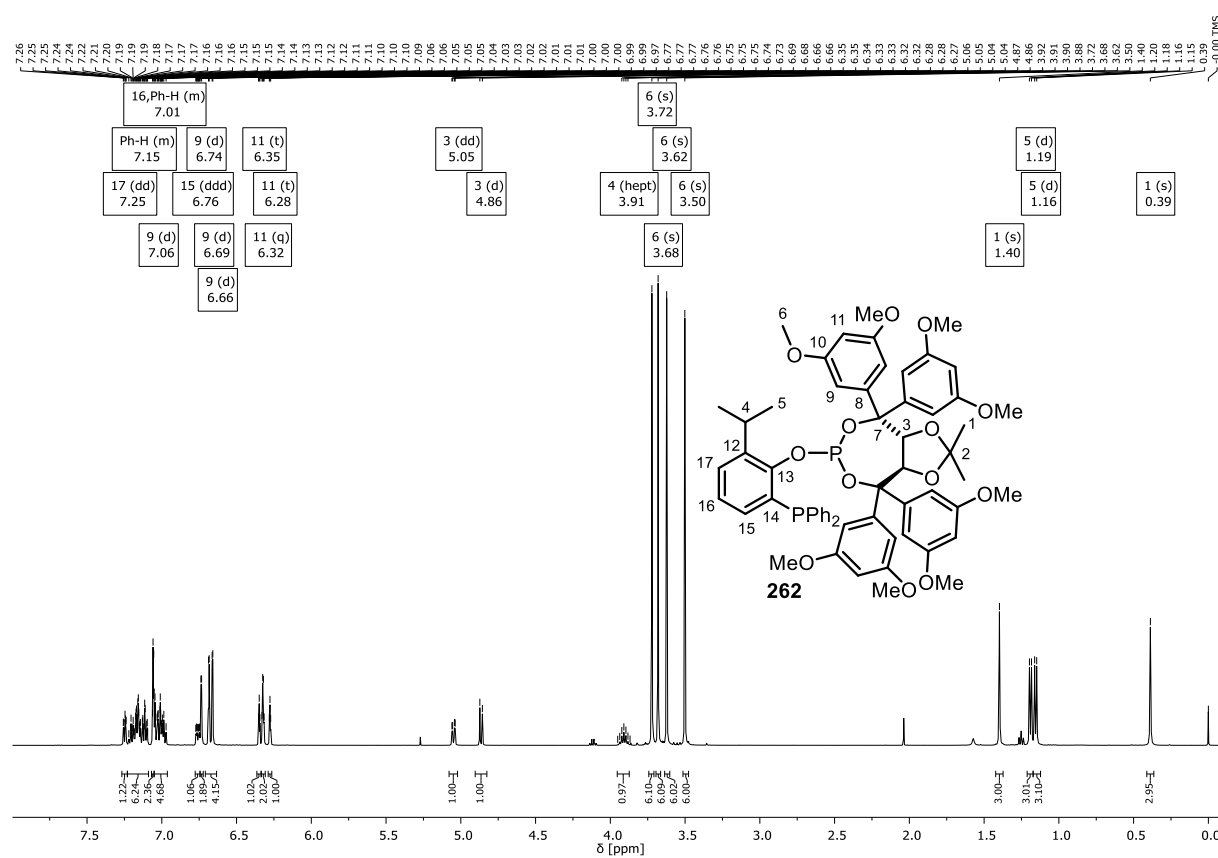
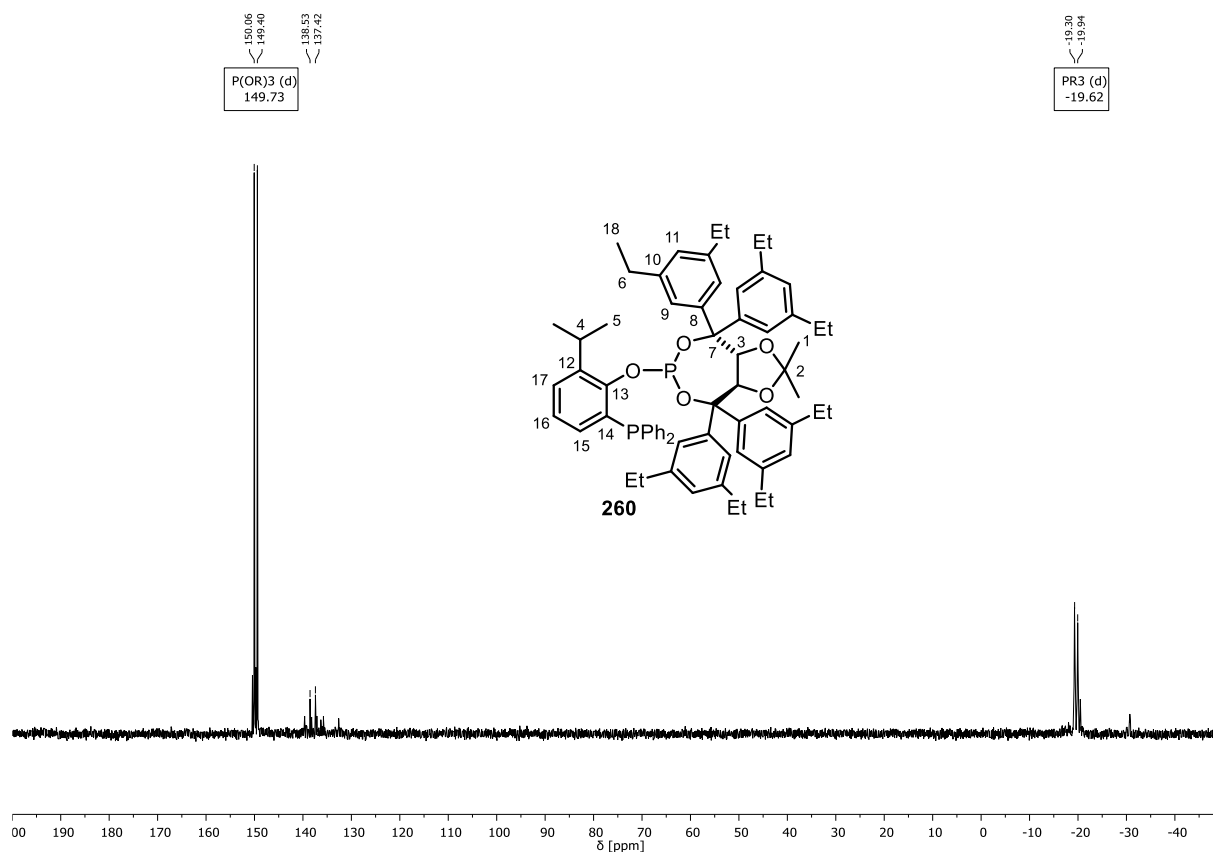


Figure 33: ¹³C NMR (151 MHz, CDCl₃) spectrum of phosphine-phosphite ligand **260.**



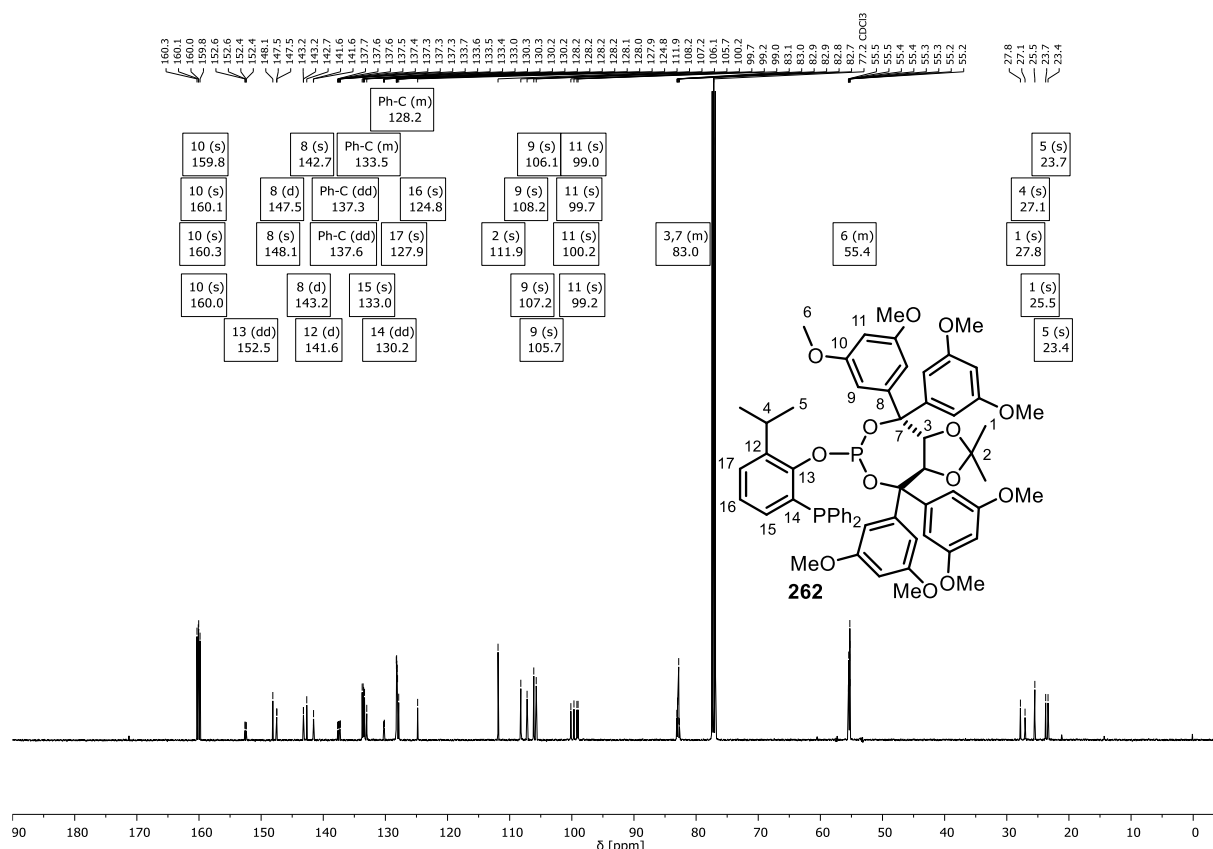


Figure 36: ^{13}C NMR (126 MHz, CDCl_3) spectrum of phosphine-phosphite ligand **262**.

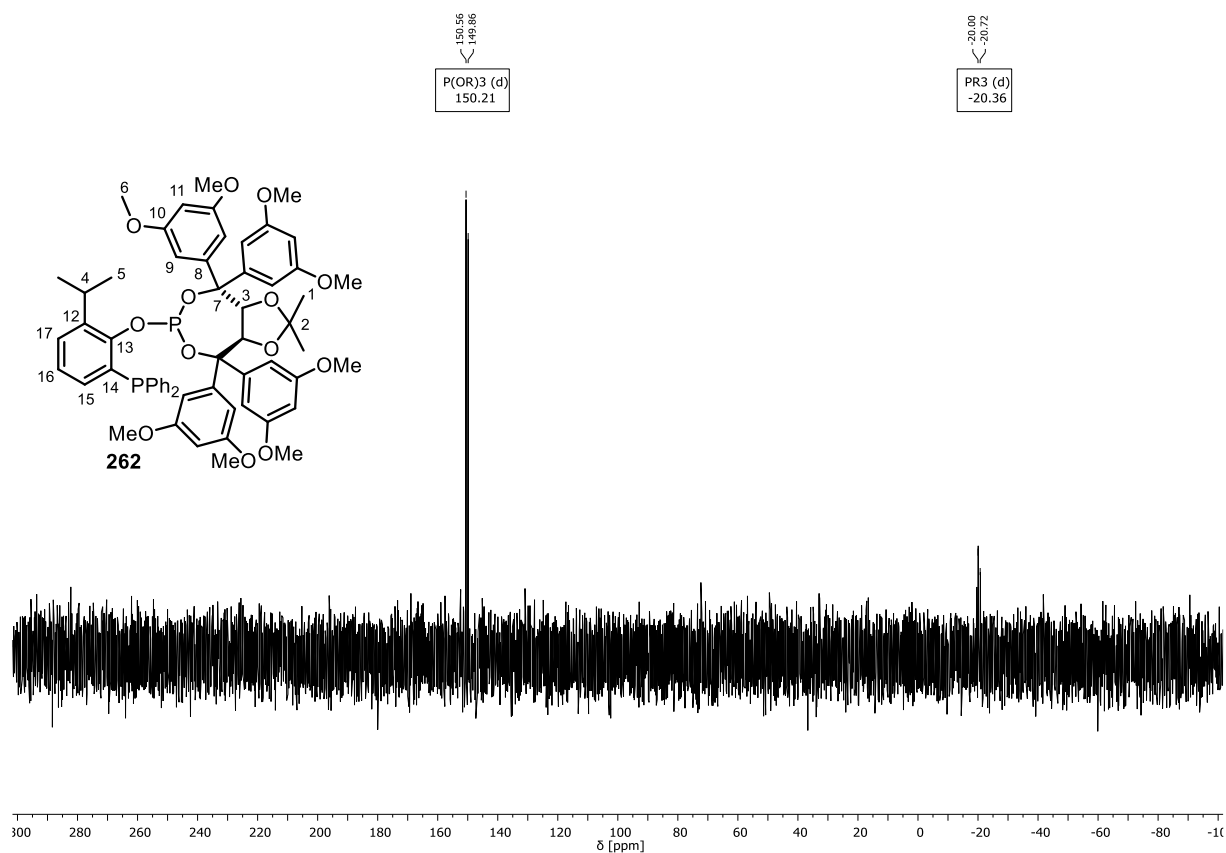


Figure 37: ^{31}P NMR (122 MHz, CDCl_3) spectrum of phosphine-phosphite ligand **262**.

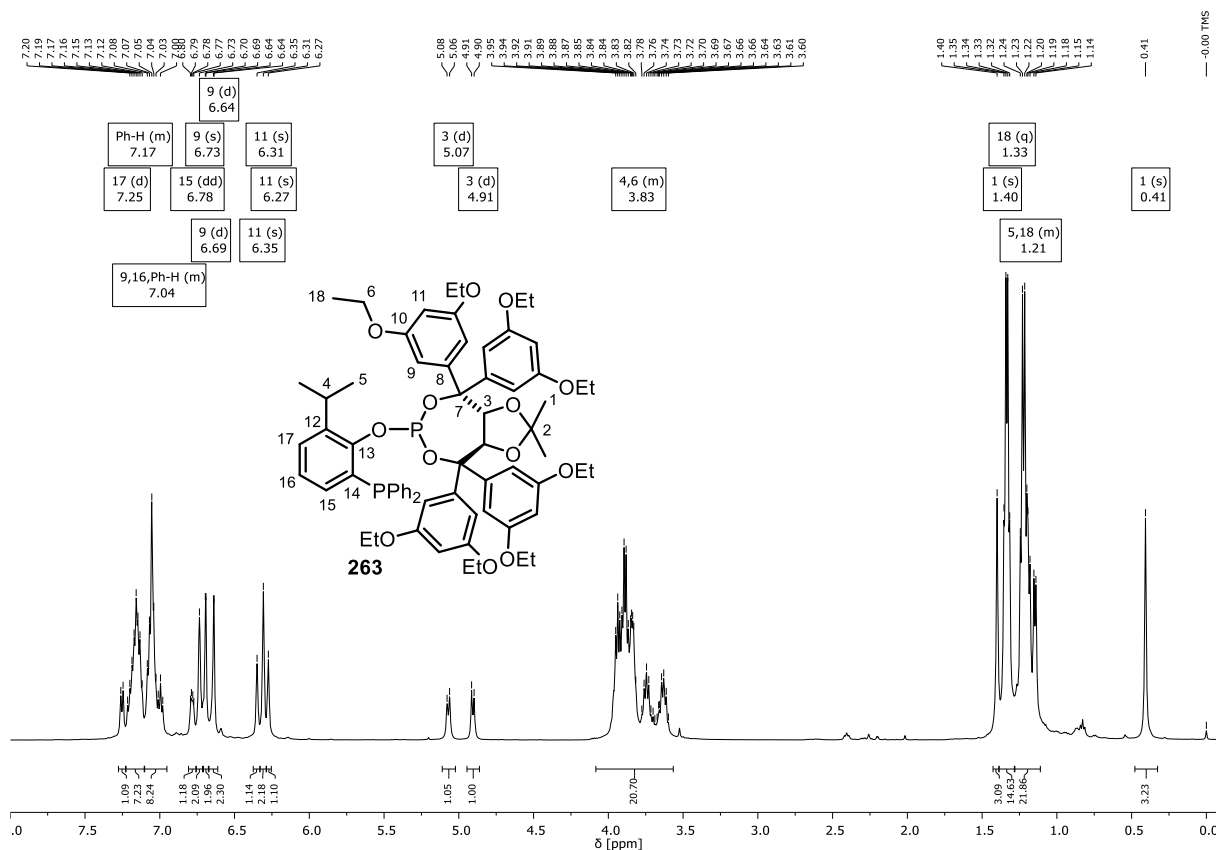


Figure 38: $^1\text{H NMR}$ (500 MHz, CDCl_3) spectrum of phosphine-phosphite ligand **263**.

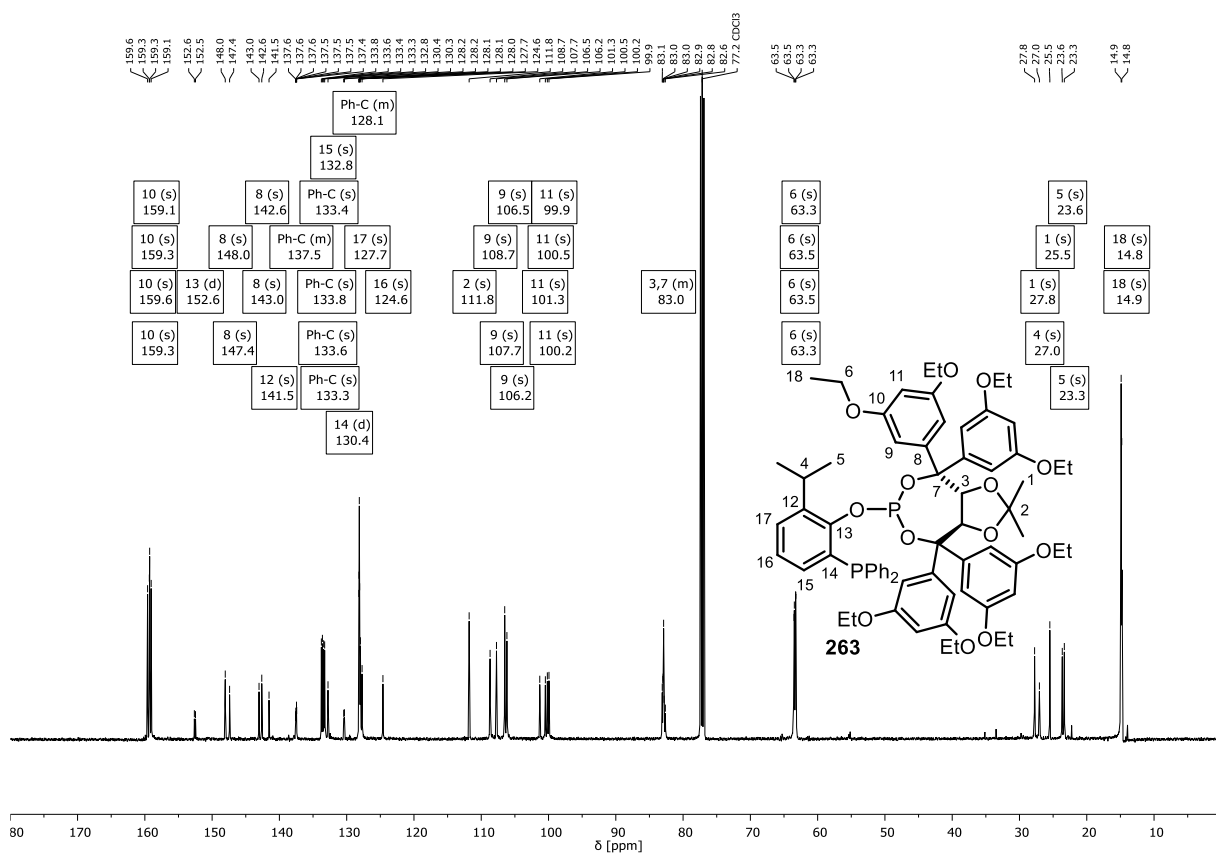
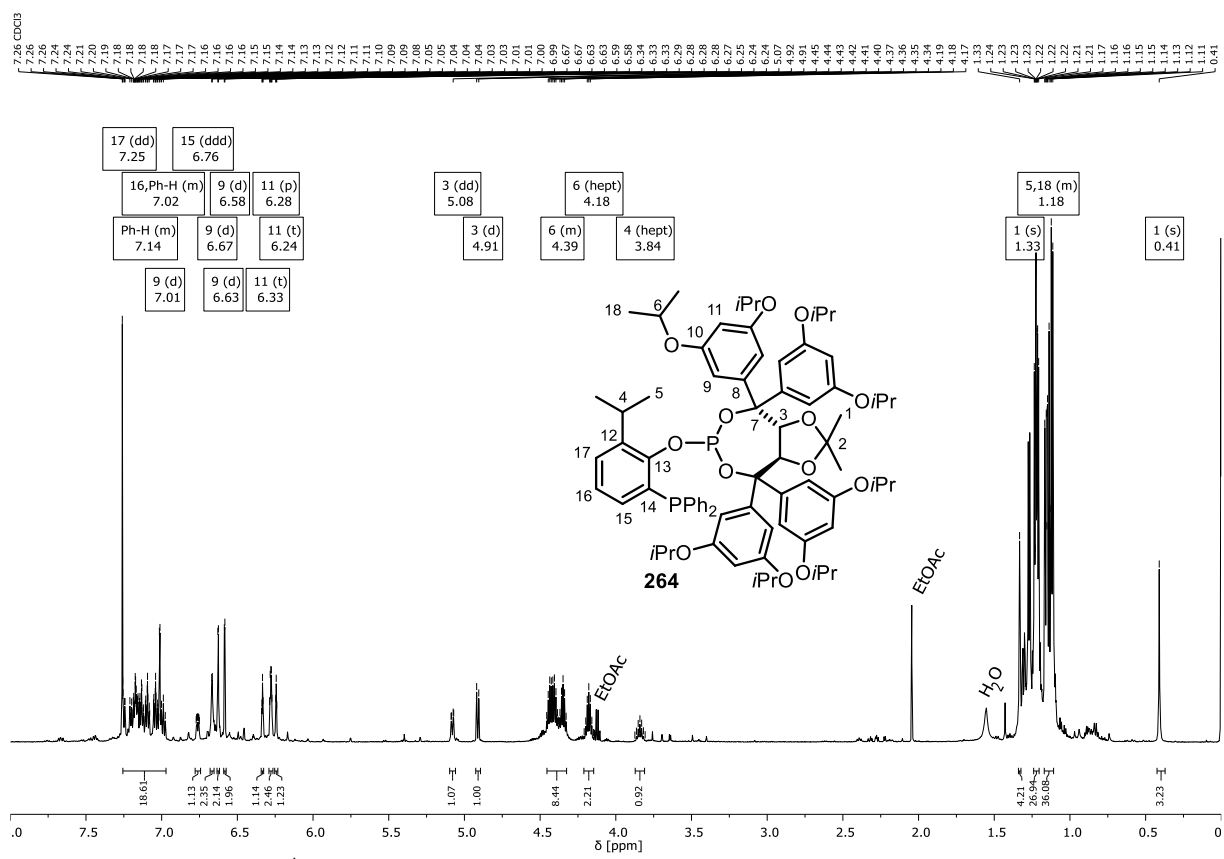
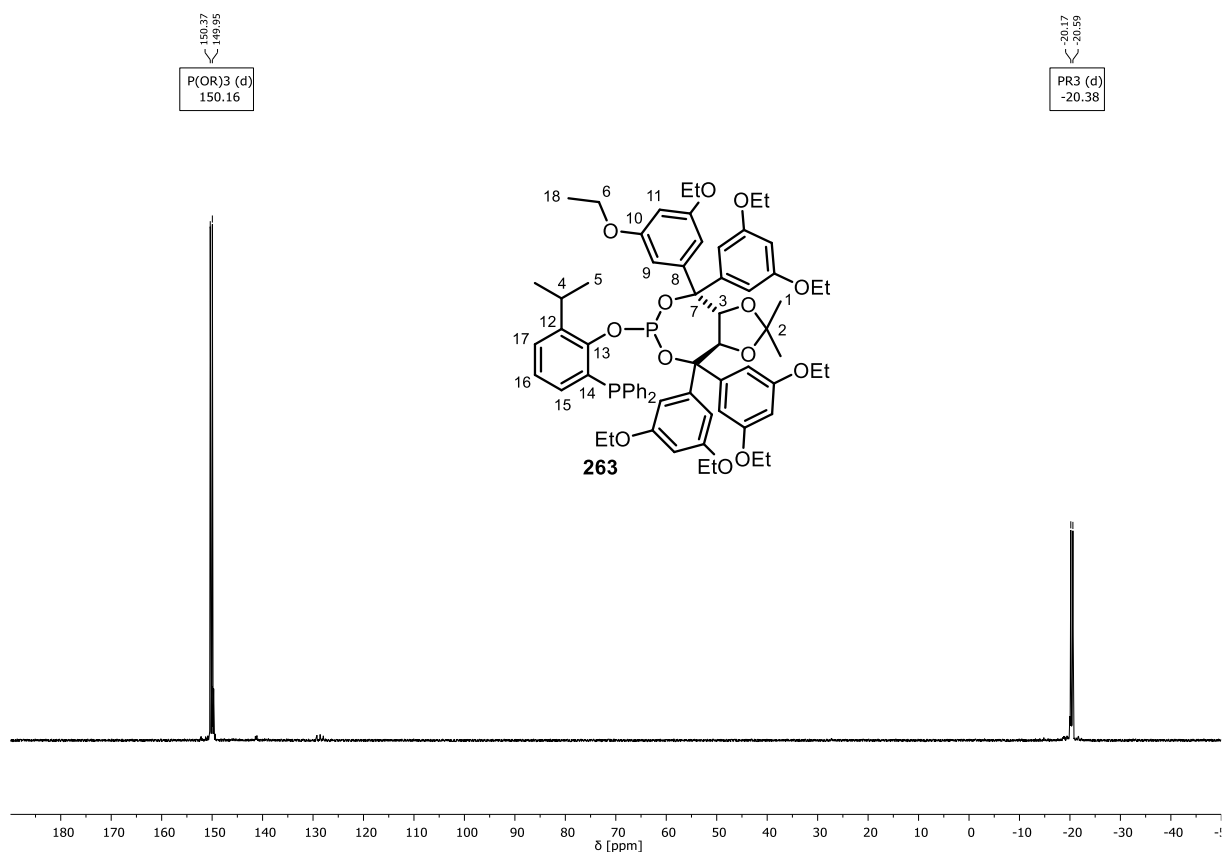


Figure 39: $^{13}\text{C NMR}$ (126 MHz, CDCl_3) spectrum of phosphine-phosphite ligand **263**.



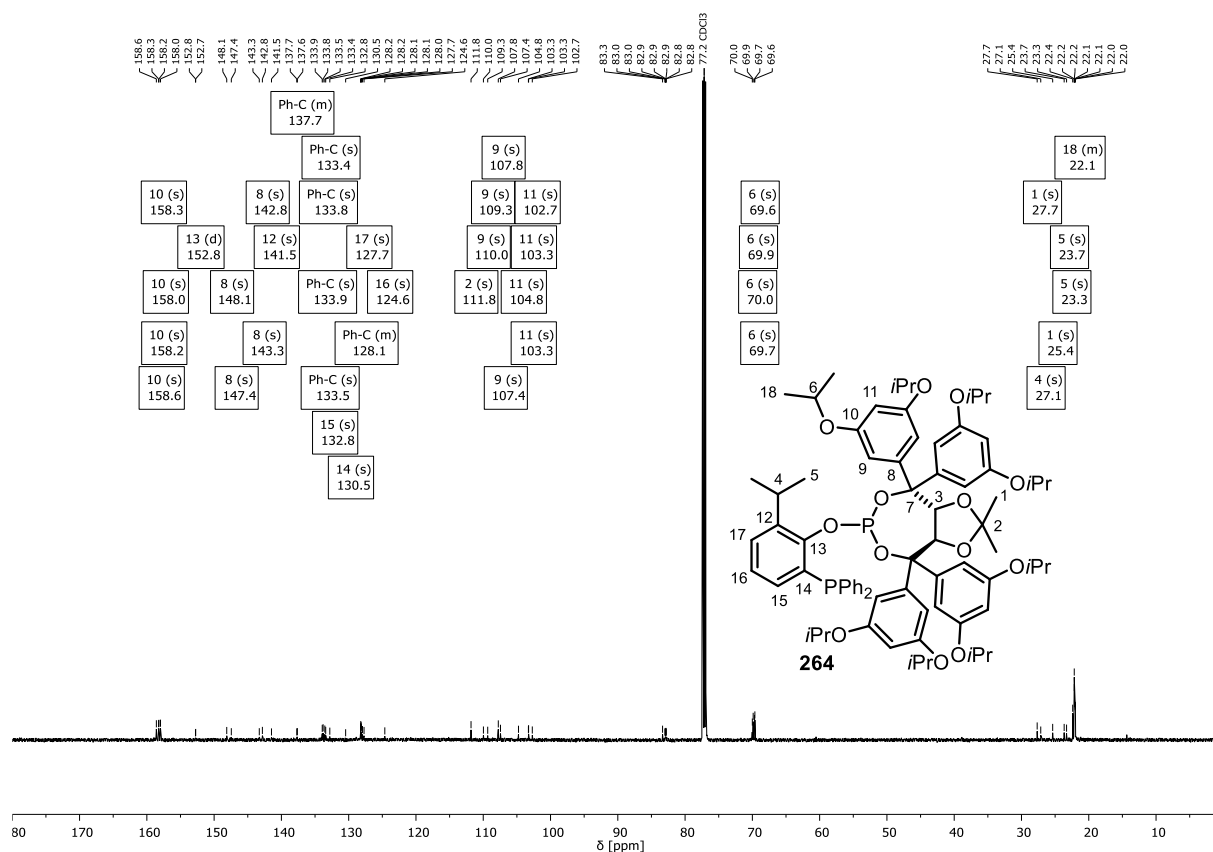


Figure 42: ^{13}C NMR (151 MHz, CDCl₃) spectrum of phosphine-phosphite ligand **264**.

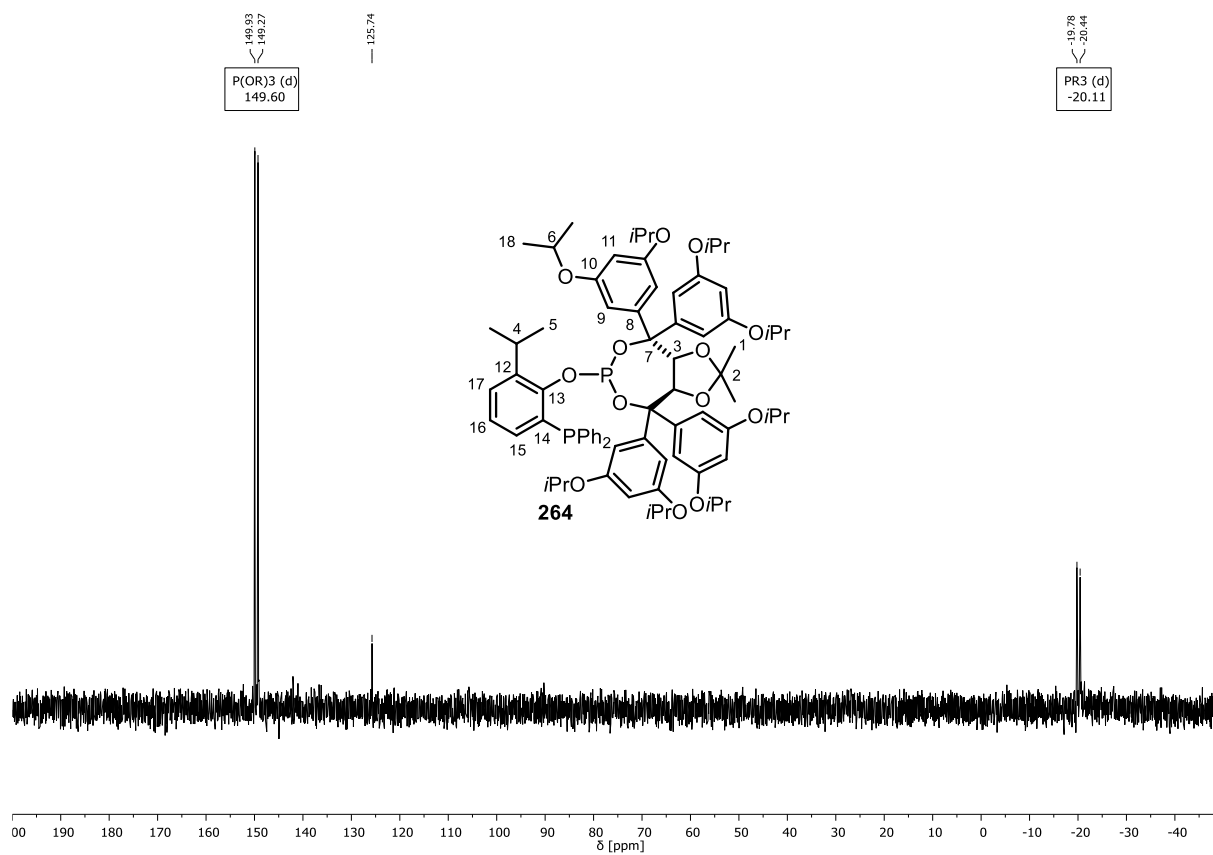


Figure 43: ^{31}P NMR (122 MHz, CDCl₃) spectrum of phosphine-phosphite ligand **264**.

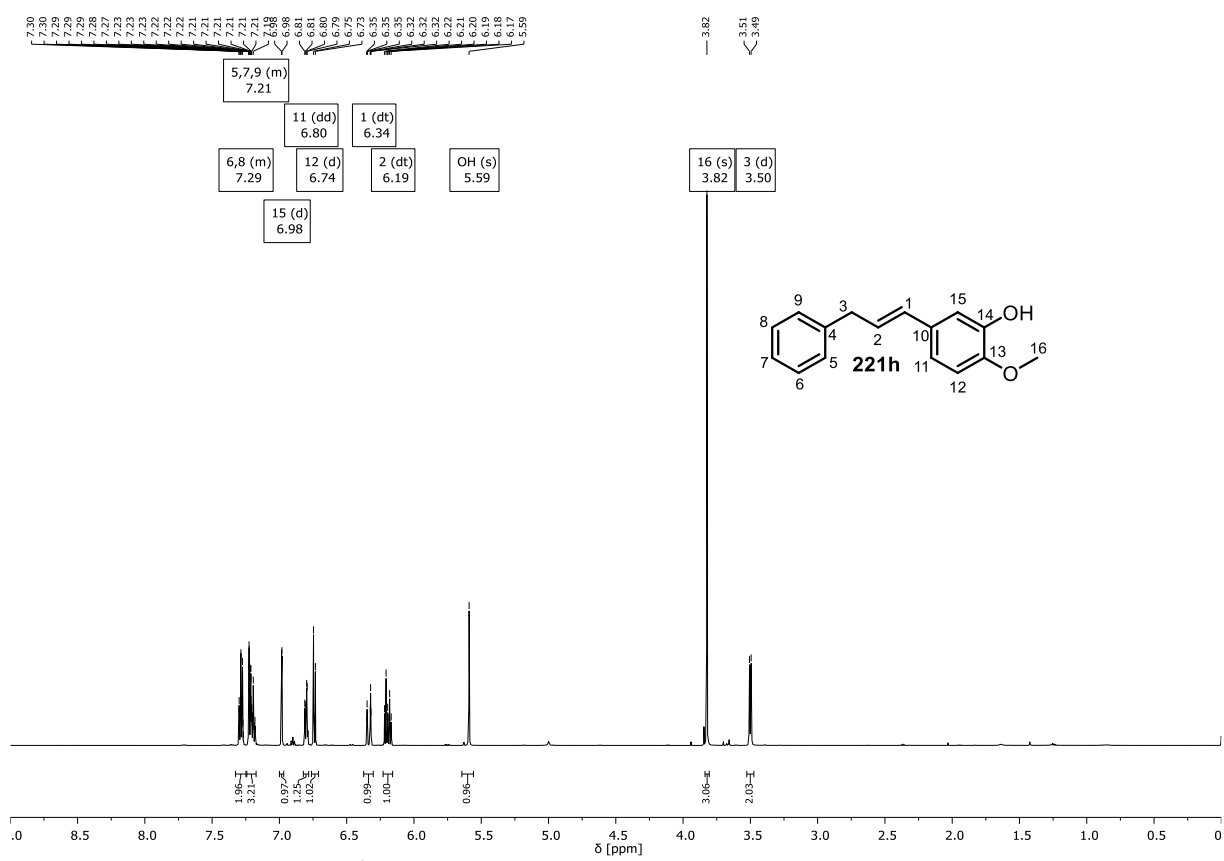


Figure 44: ¹H NMR (600 MHz, CDCl₃) spectrum of homostilbene **221h**.

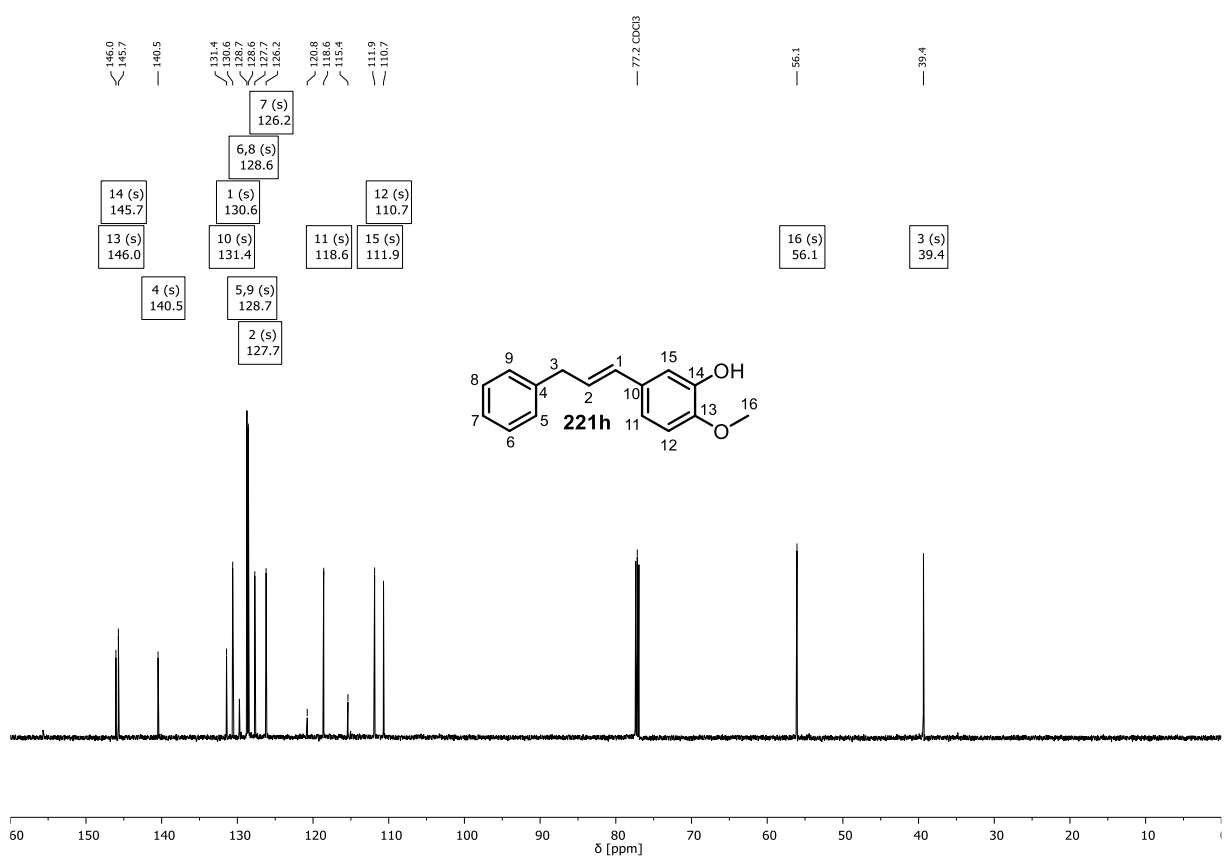
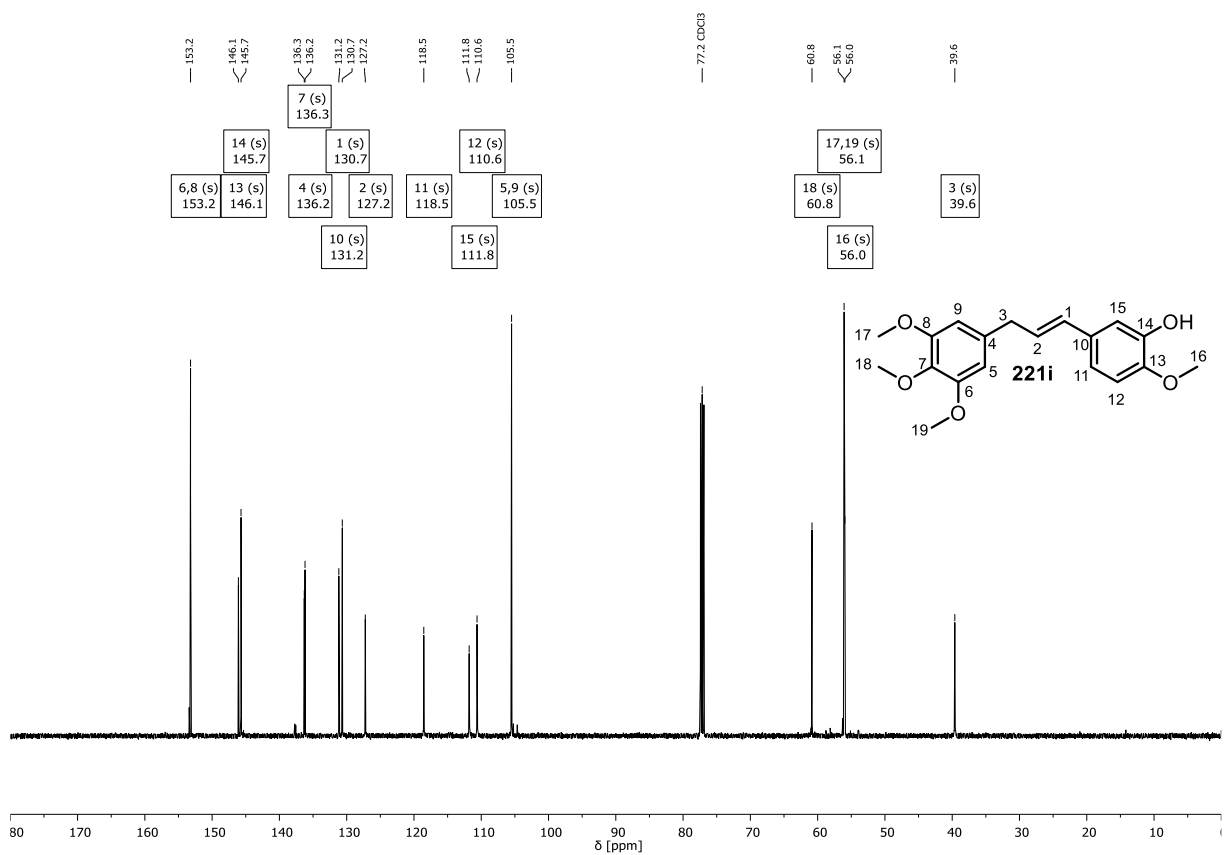
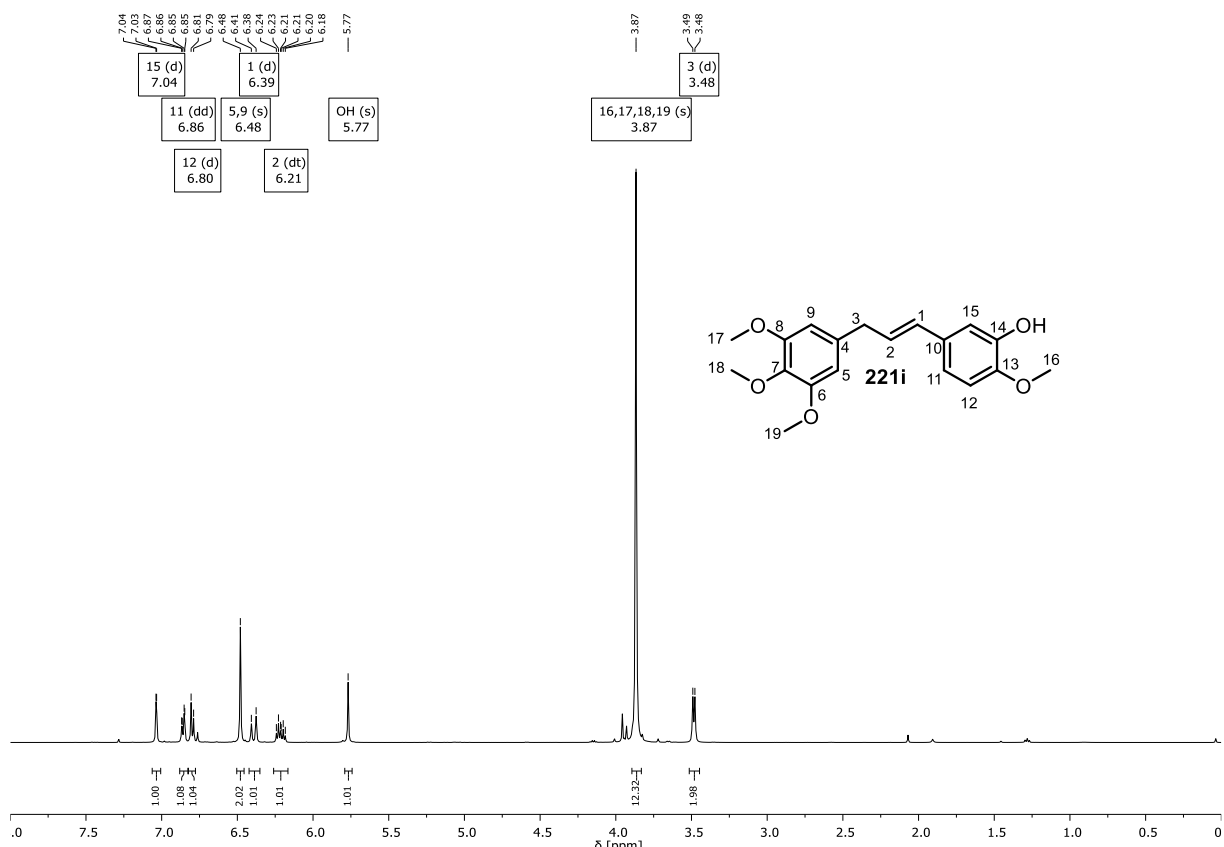
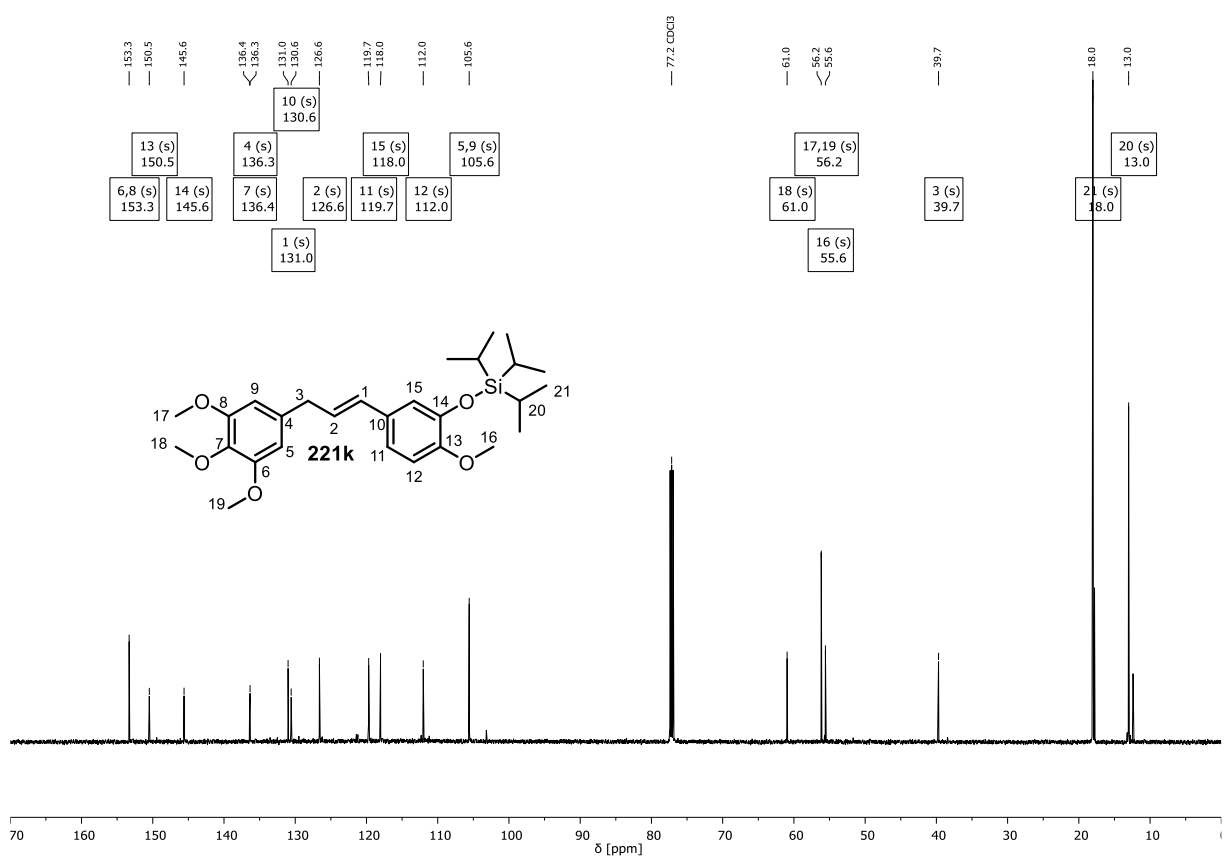
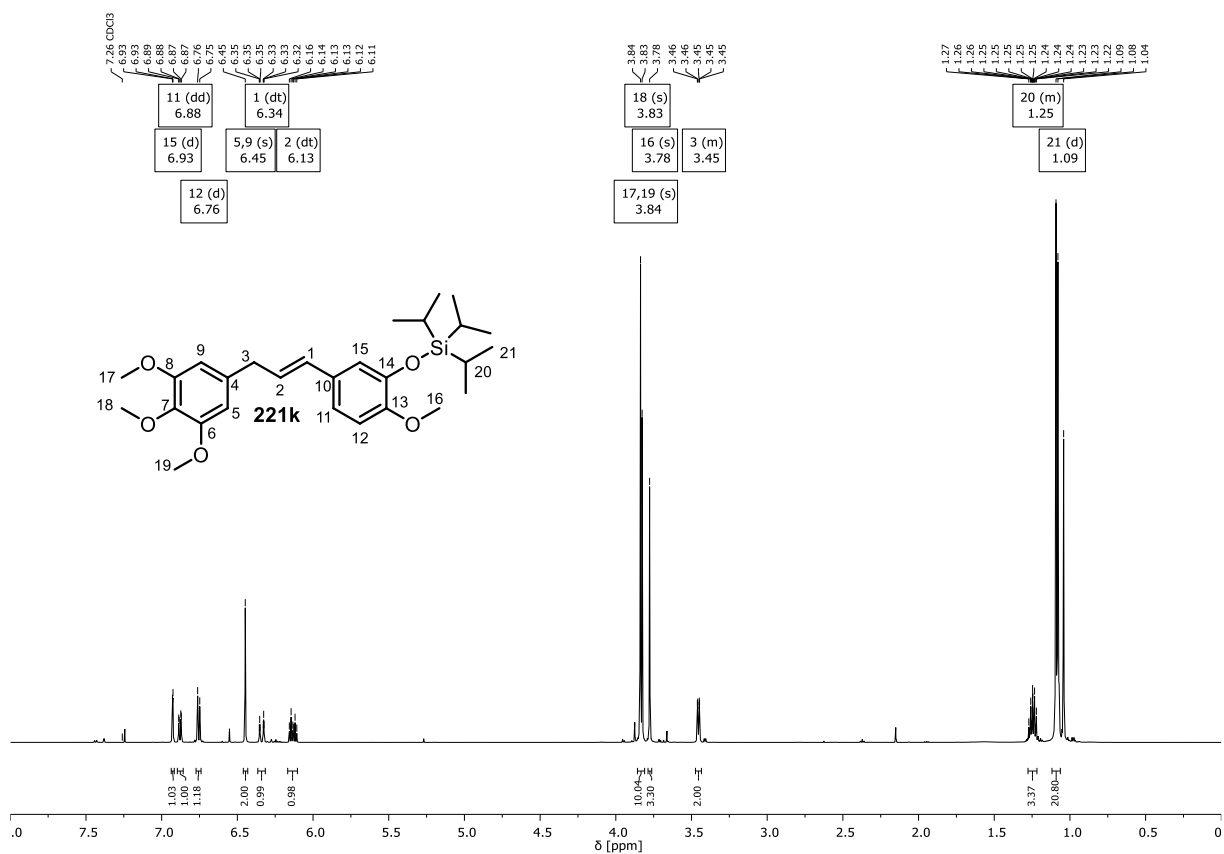


Figure 45: ¹³C NMR (151 MHz, CDCl₃) spectrum of homostilbene **221h**.





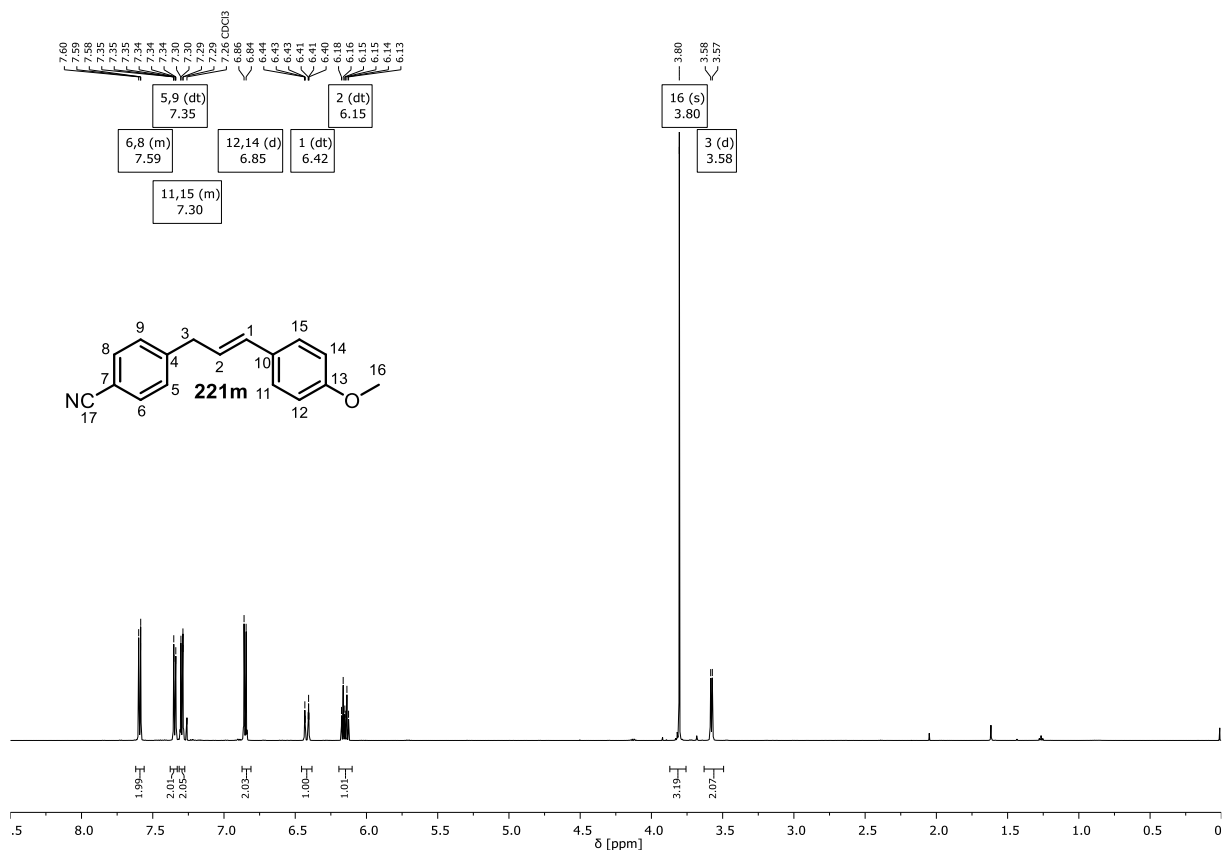


Figure 50: ^1H NMR (600 MHz, CDCl_3) spectrum of homostilbene **221m**.

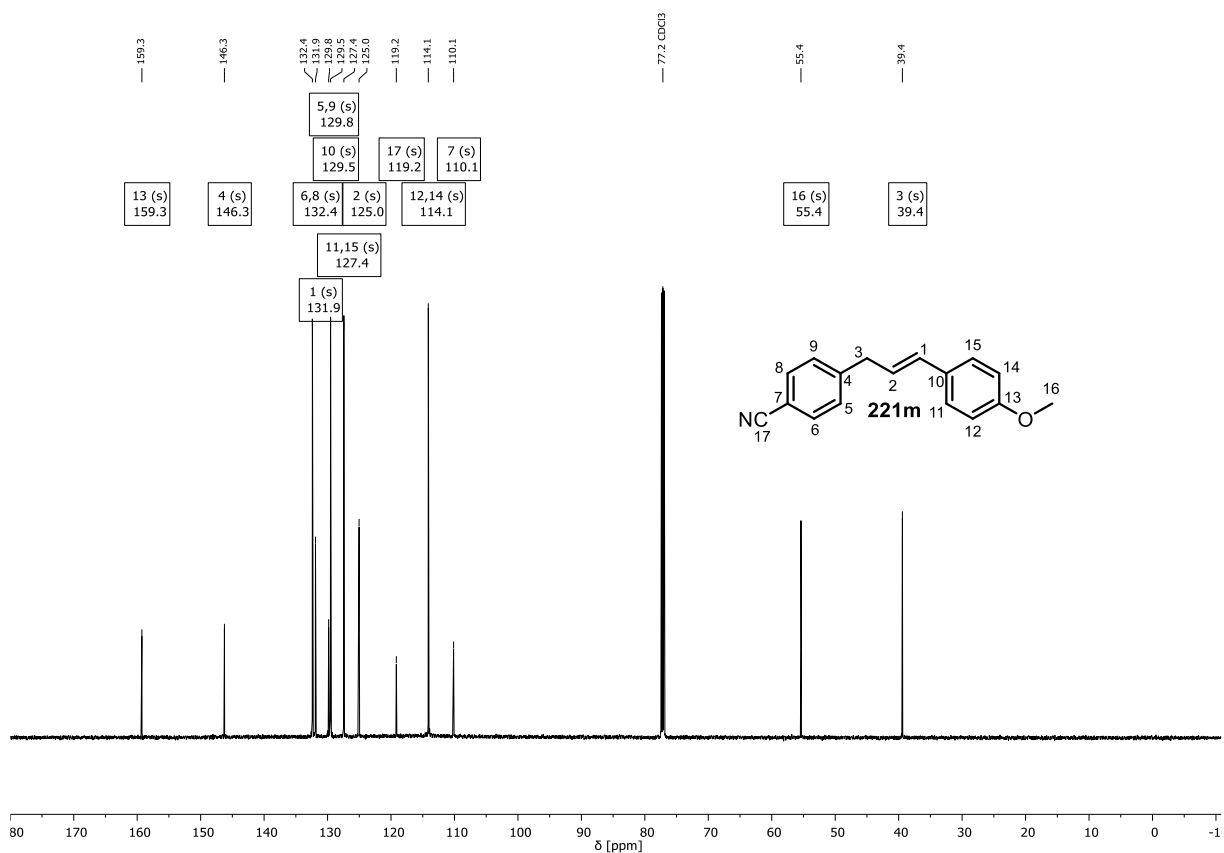


Figure 51: ^{13}C NMR (151 MHz, CDCl_3) spectrum of homostilbene **221m**.

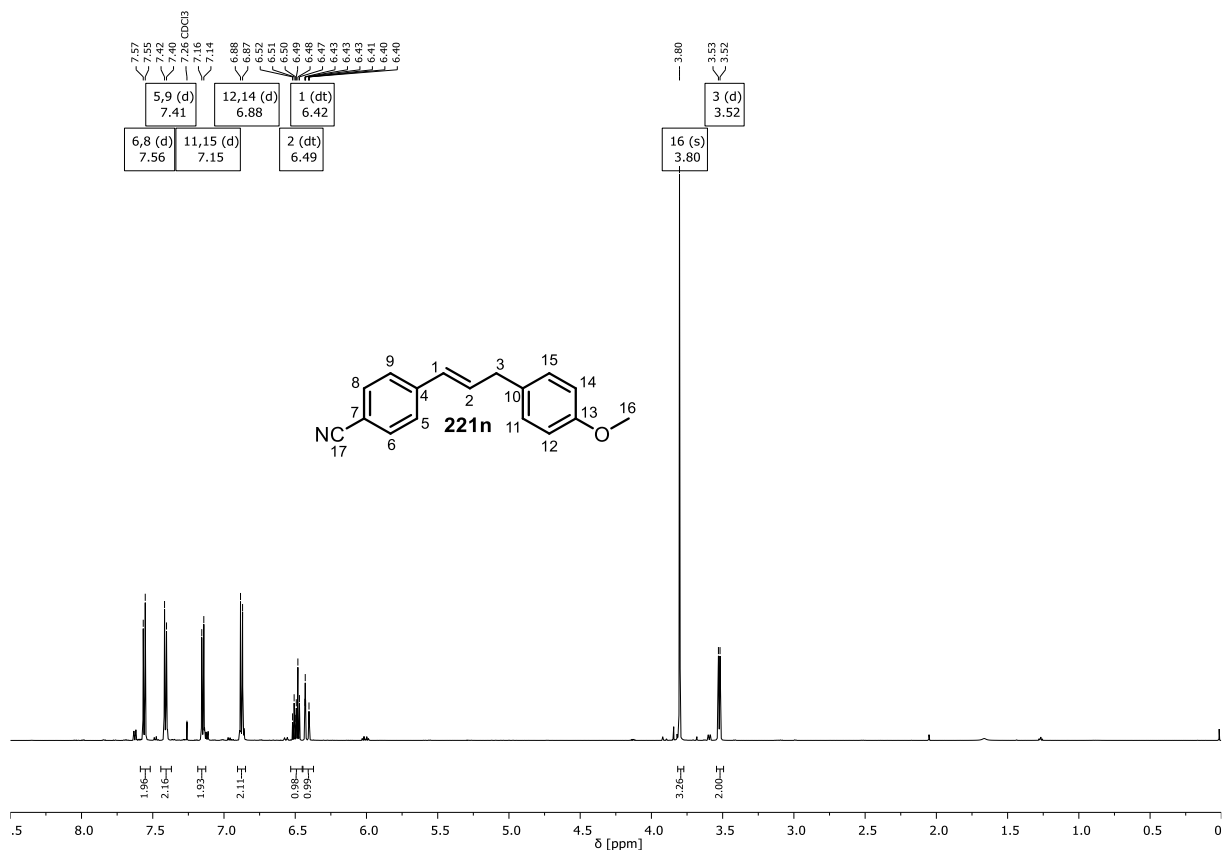


Figure 52: ^1H NMR (600 MHz, CDCl_3) spectrum of homostilbene **221n**.

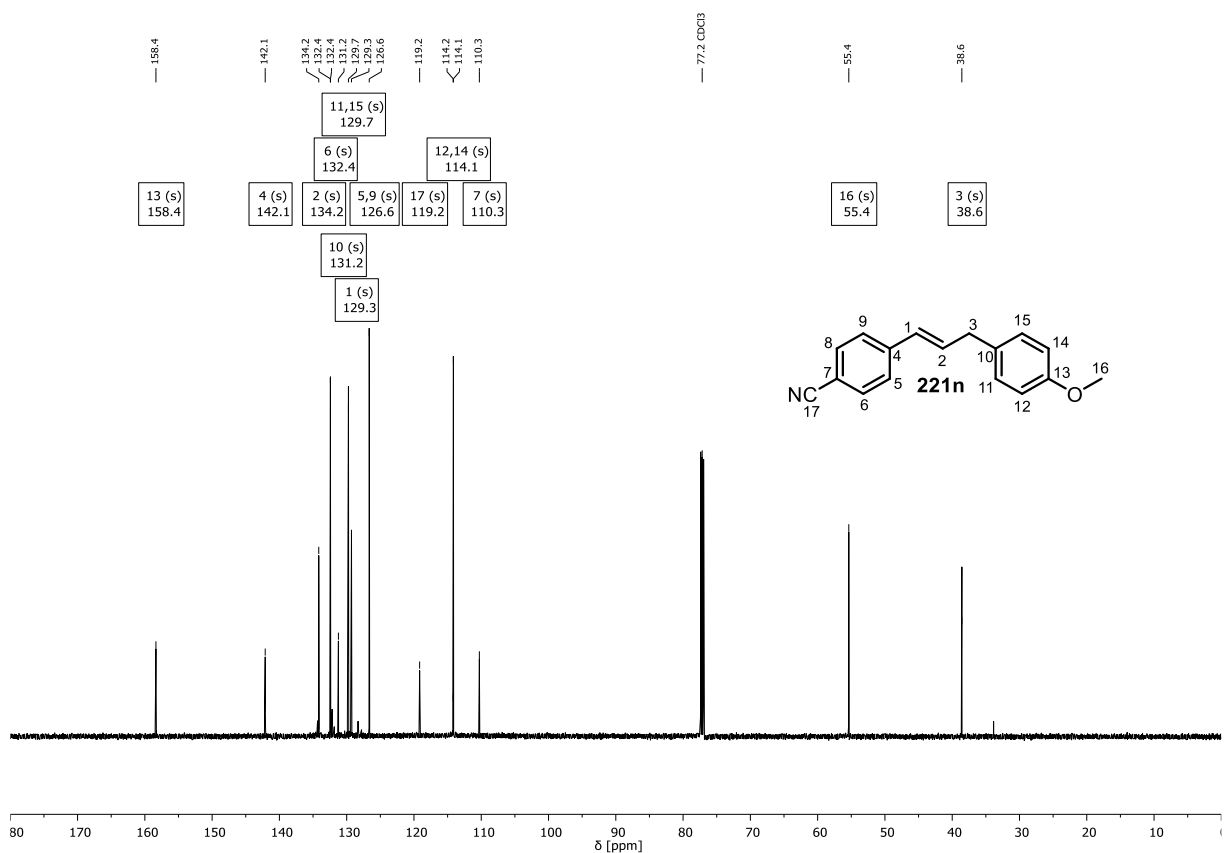


Figure 53: ^{13}C NMR (151 MHz, CDCl_3) spectrum of homostilbene **221n**.

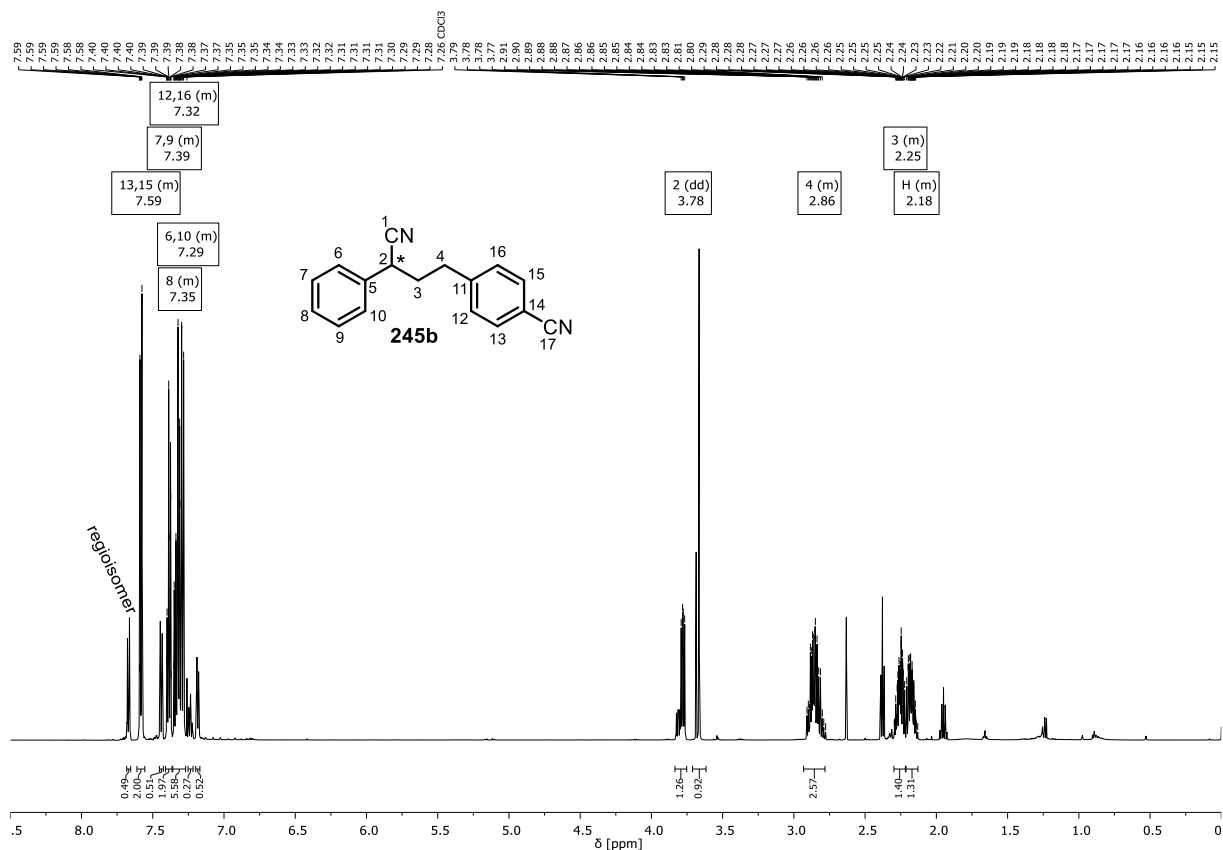


Figure 54: ^1H NMR (600 MHz, CDCl_3) spectrum of 2,4-diarylbutyronitrile **245b** (80:20 *rr*).

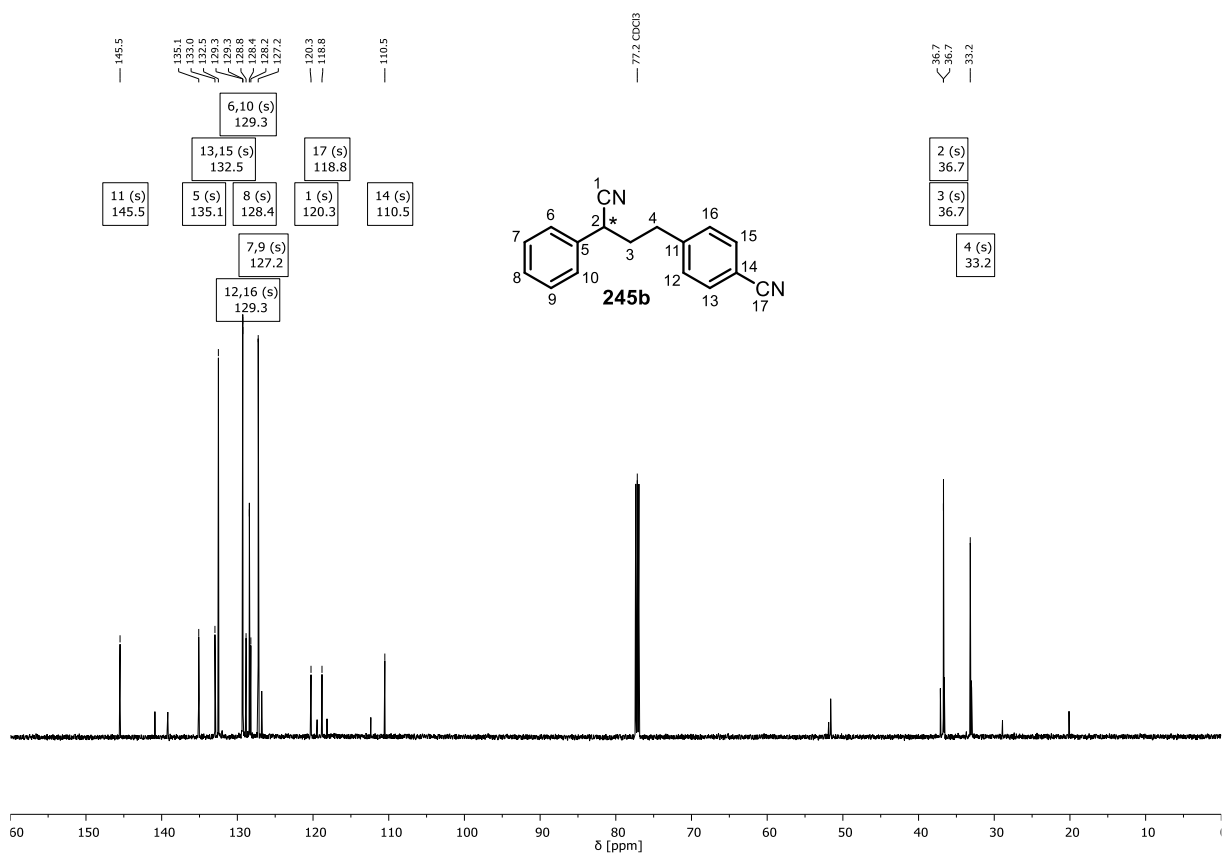


Figure 55: ^{13}C NMR (151 MHz, CDCl_3) spectrum of 2,4-diarylbutyronitrile **245b** (80:20 *rr*).

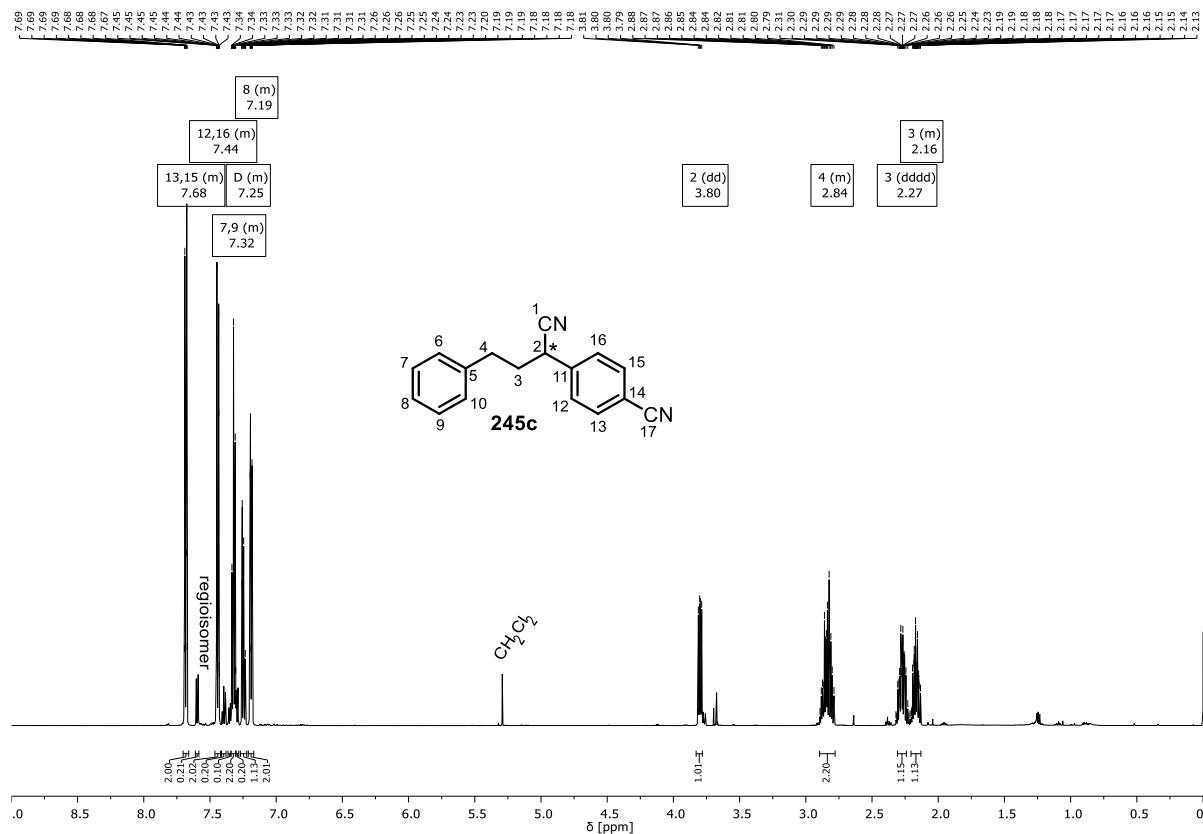


Figure 56: ^1H NMR (600 MHz, CDCl_3) spectrum of 2,4-diarylbutyronitrile **245c** (90:10 *rr*).

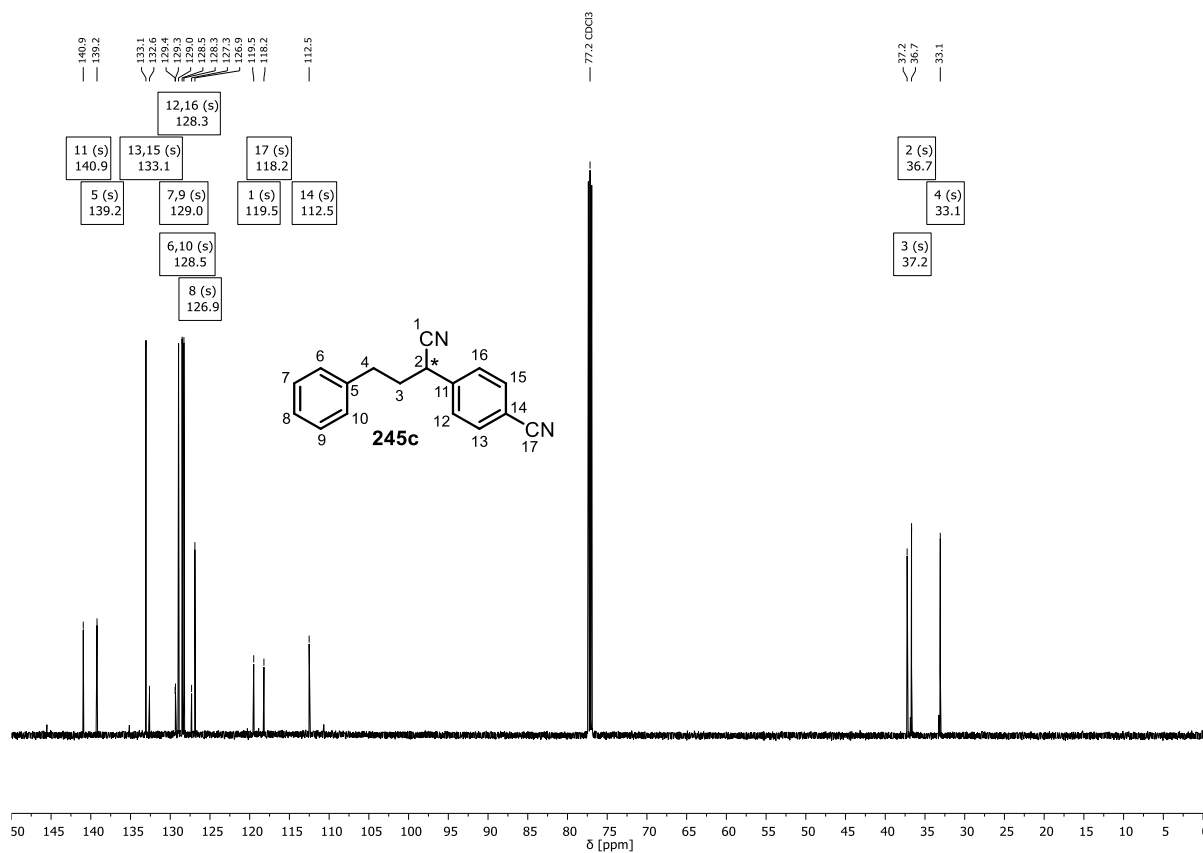


Figure 57: ^{13}C NMR (151 MHz, CDCl_3) spectrum of 2,4-diarylbutyronitrile **245c** (90:10 *rr*).

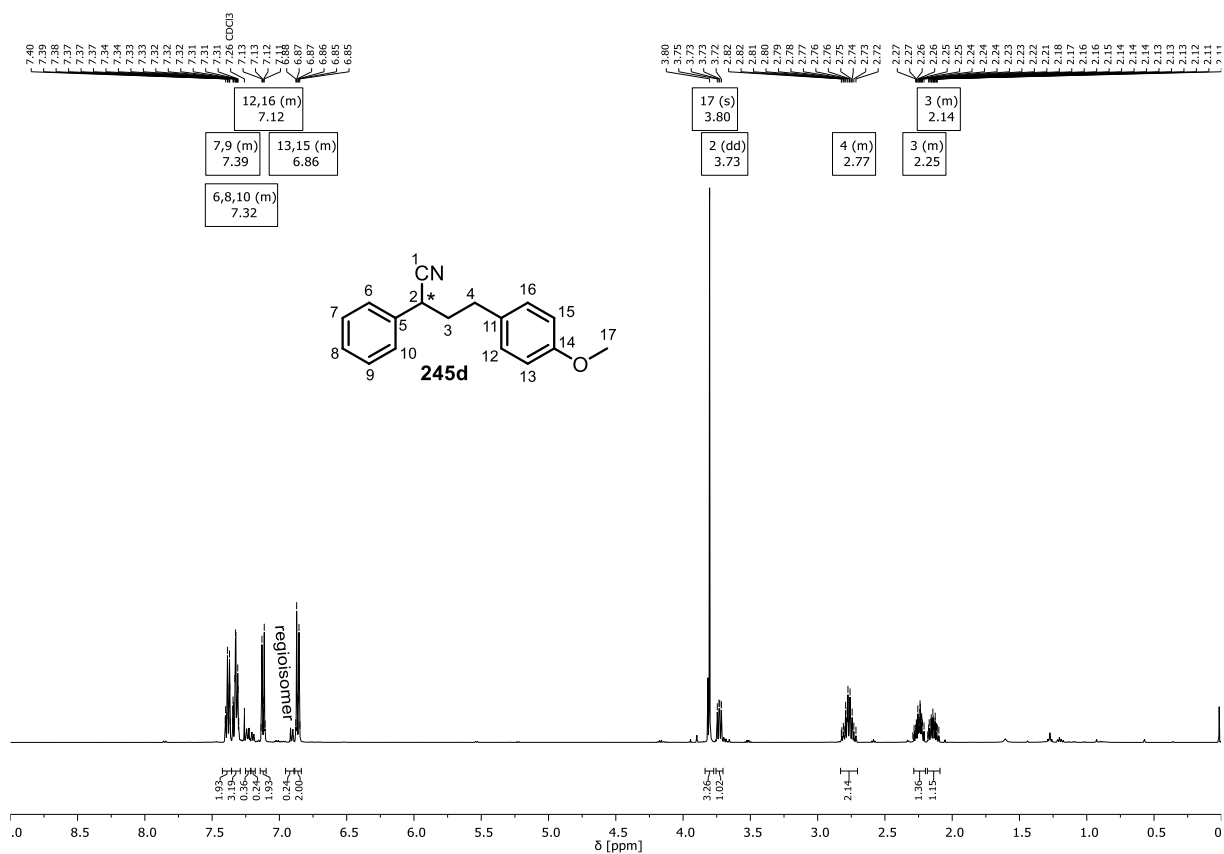


Figure 58: ^1H NMR (500 MHz, CDCl_3) spectrum of 2,4-diarylbutyronitrile **245d** (89:11 *rr*).

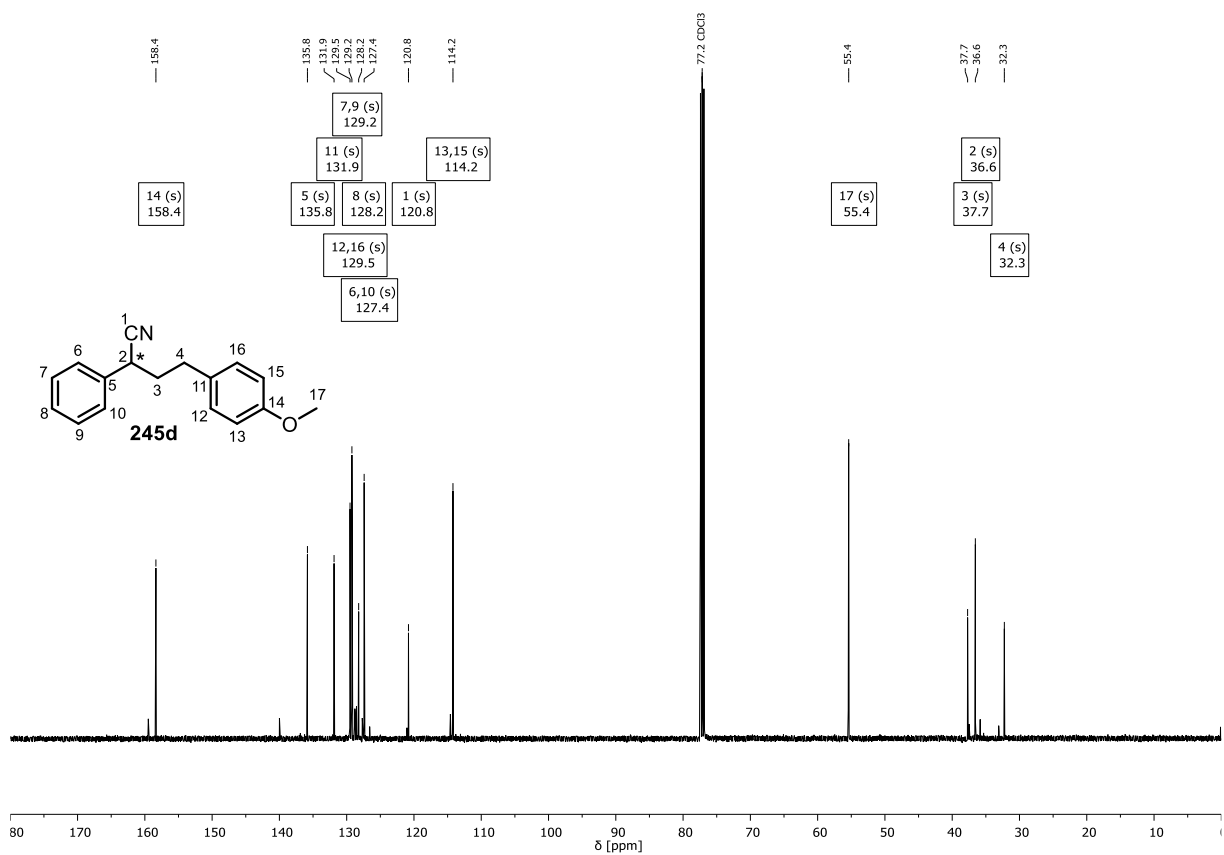


Figure 59: ^{13}C NMR (126 MHz, CDCl_3) spectrum of 2,4-diarylbutyronitrile **245d** (89:11 *rr*).

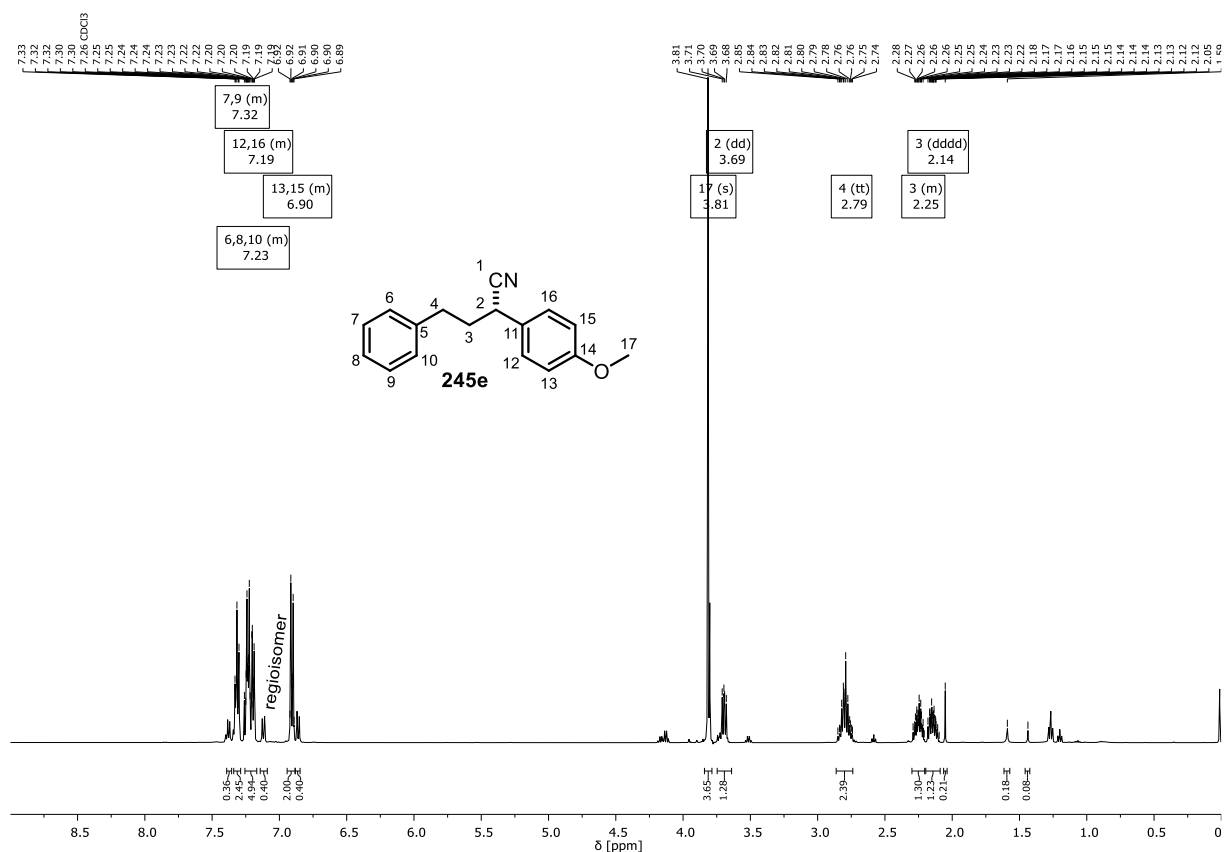


Figure 60: ^1H NMR (500 MHz, CDCl_3) spectrum of 2,4-diarylbutyronitrile **245e** (83:17 *rr*).

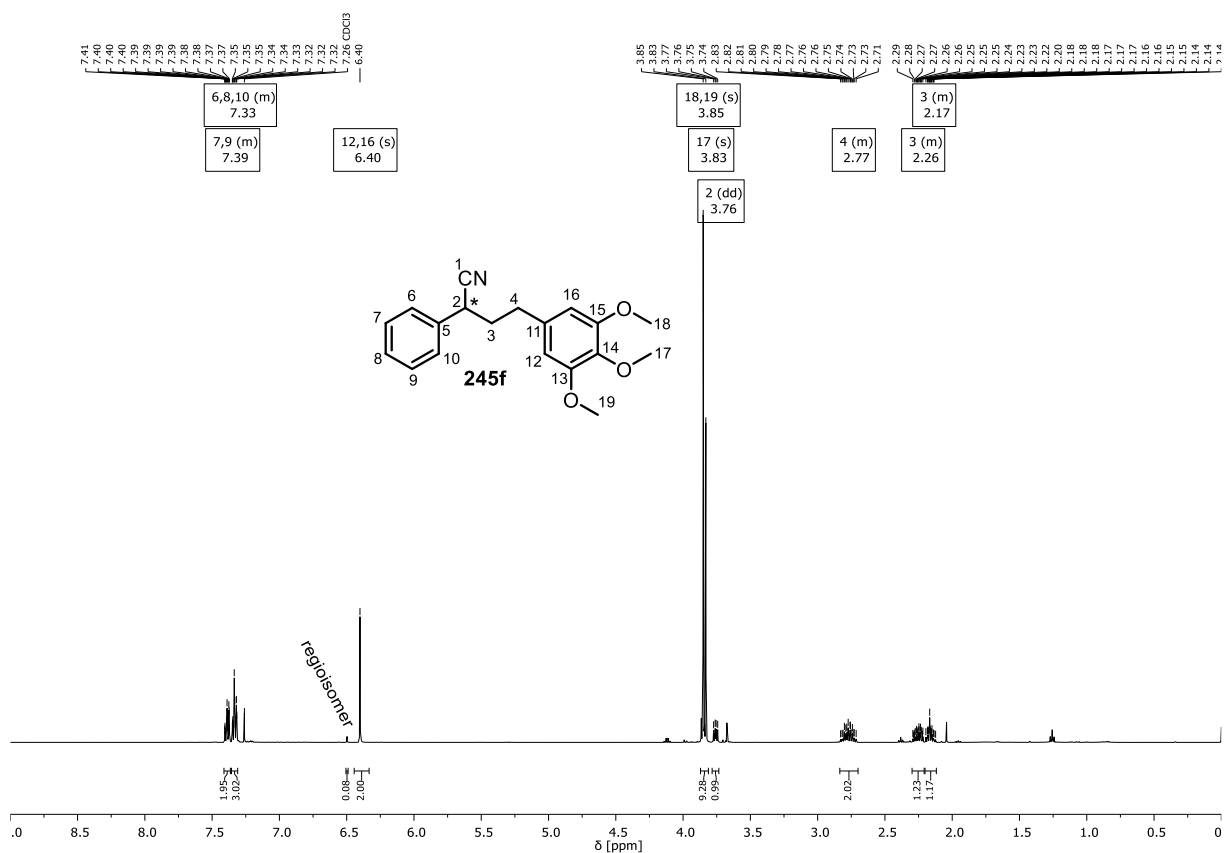
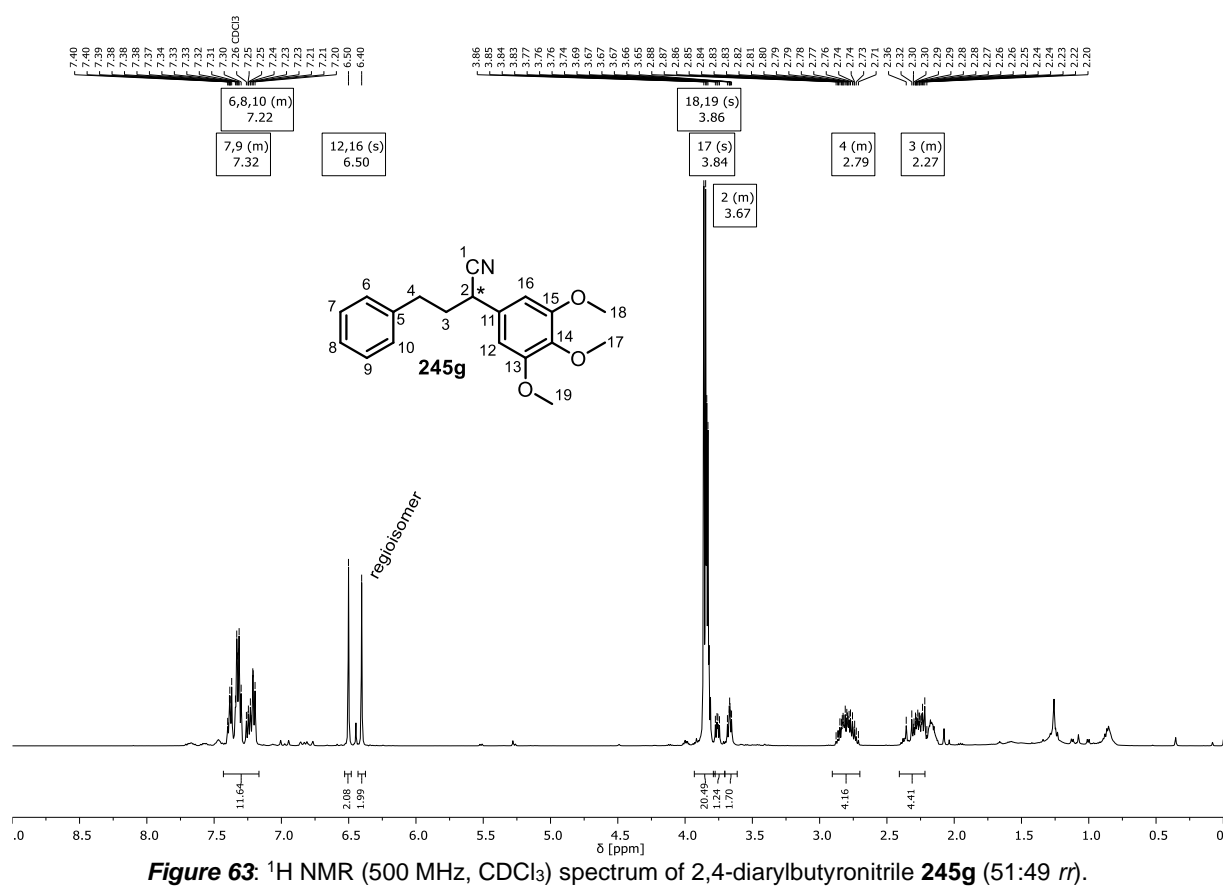
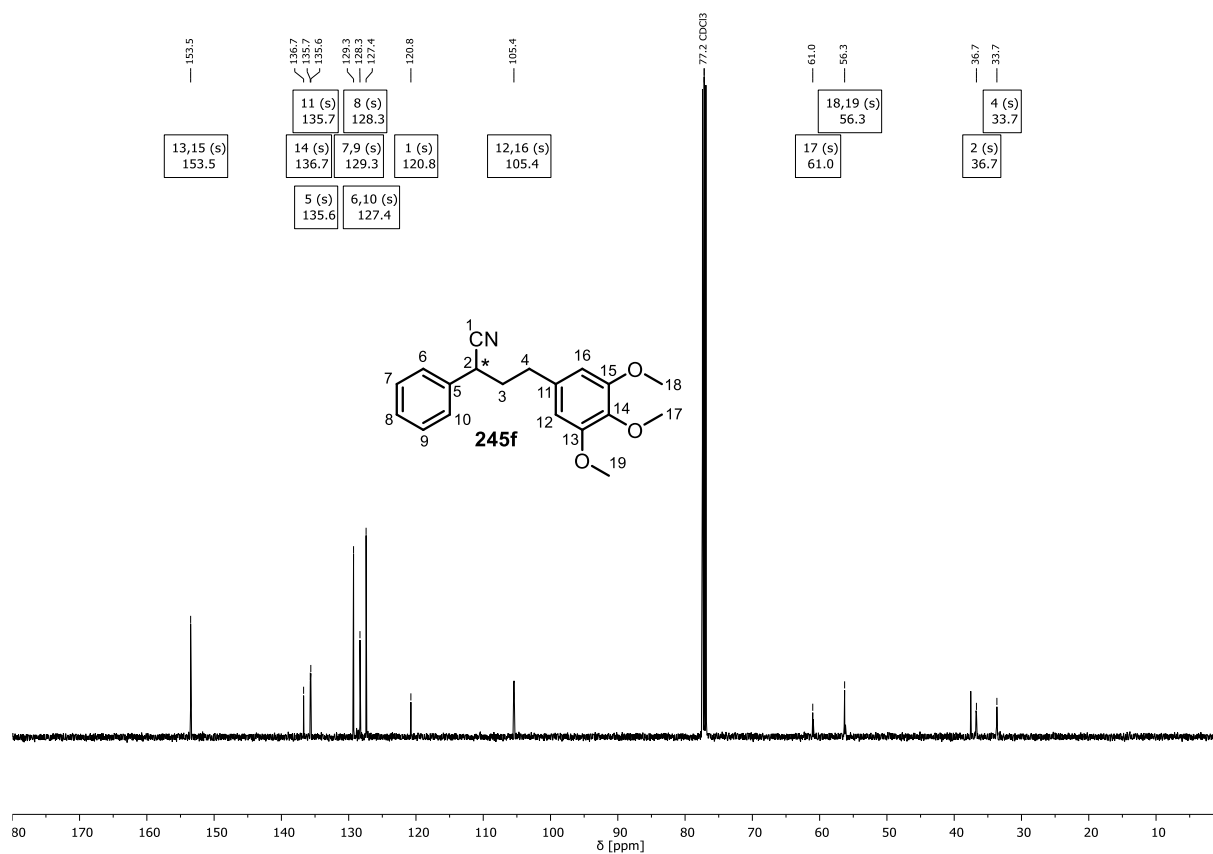


Figure 61: ^1H NMR (500 MHz, CDCl_3) spectrum of 2,4-diarylbutyronitrile **245f** (96:4 *rr*).



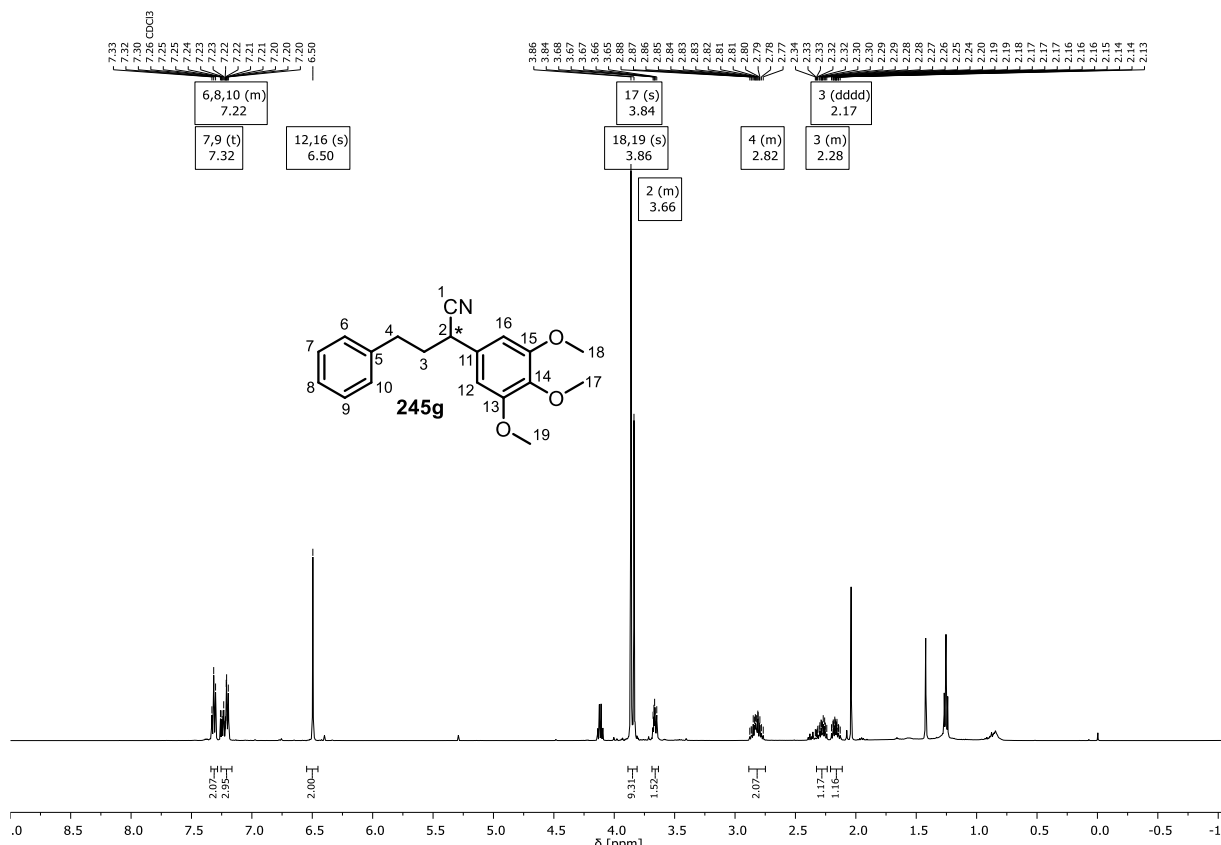


Figure 64: ^1H NMR (500 MHz, CDCl_3) spectrum of 2,4-diarylbutyronitrile **245g** (separated from its regioisomer **245f**).

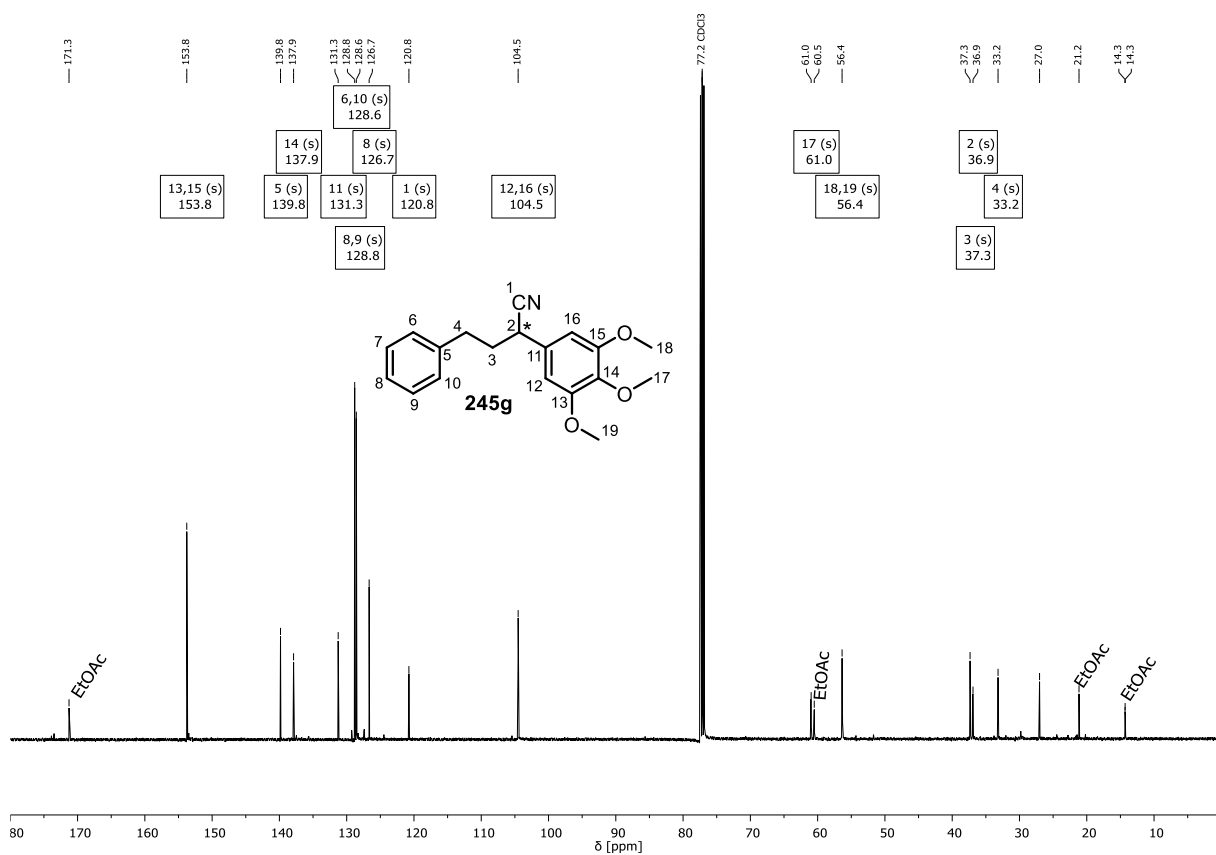


Figure 65: ^{13}C NMR (126 MHz, CDCl_3) spectrum of 2,4-diarylbutyronitrile **245g** (separated from its regioisomer **245f**).

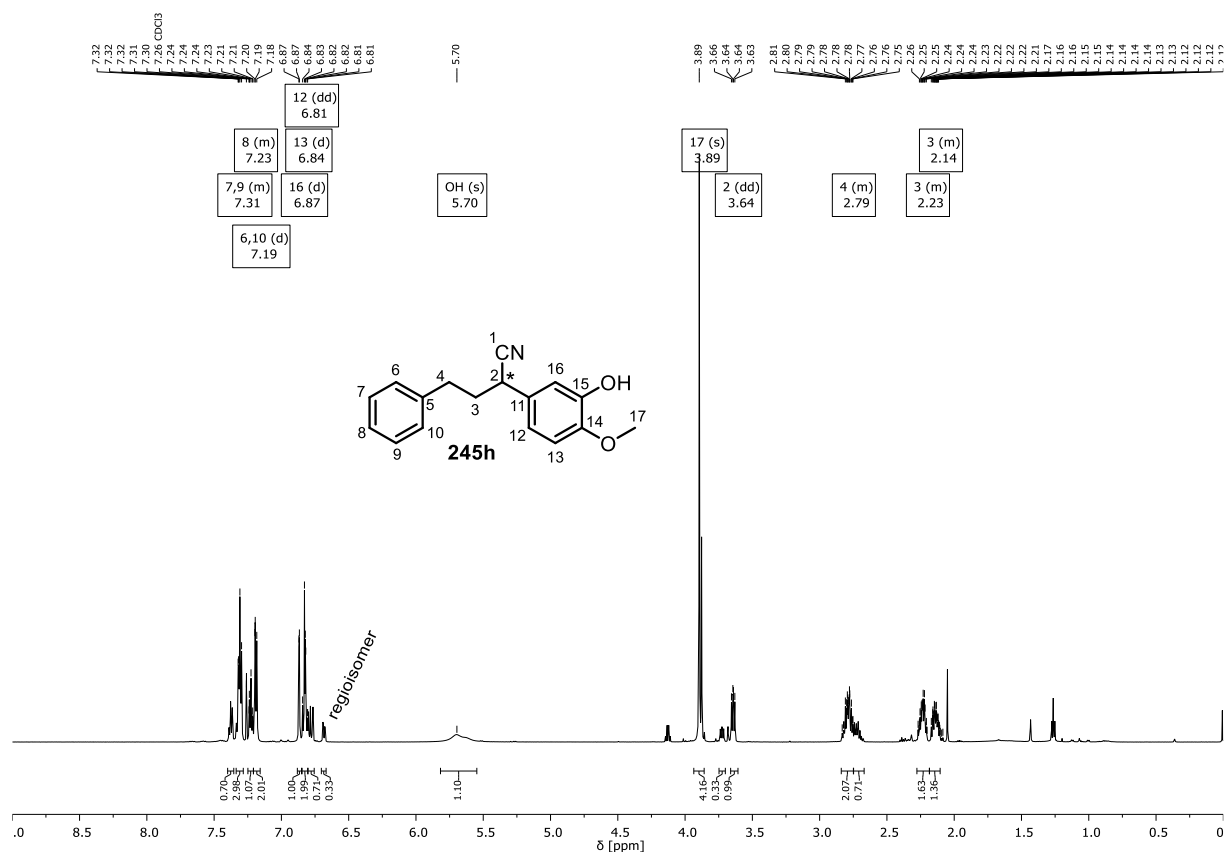


Figure 66: $^1\text{H NMR}$ (500 MHz, CDCl_3) spectrum of 2,4-diarylbutyronitrile **245h** (75:25 *rr*).

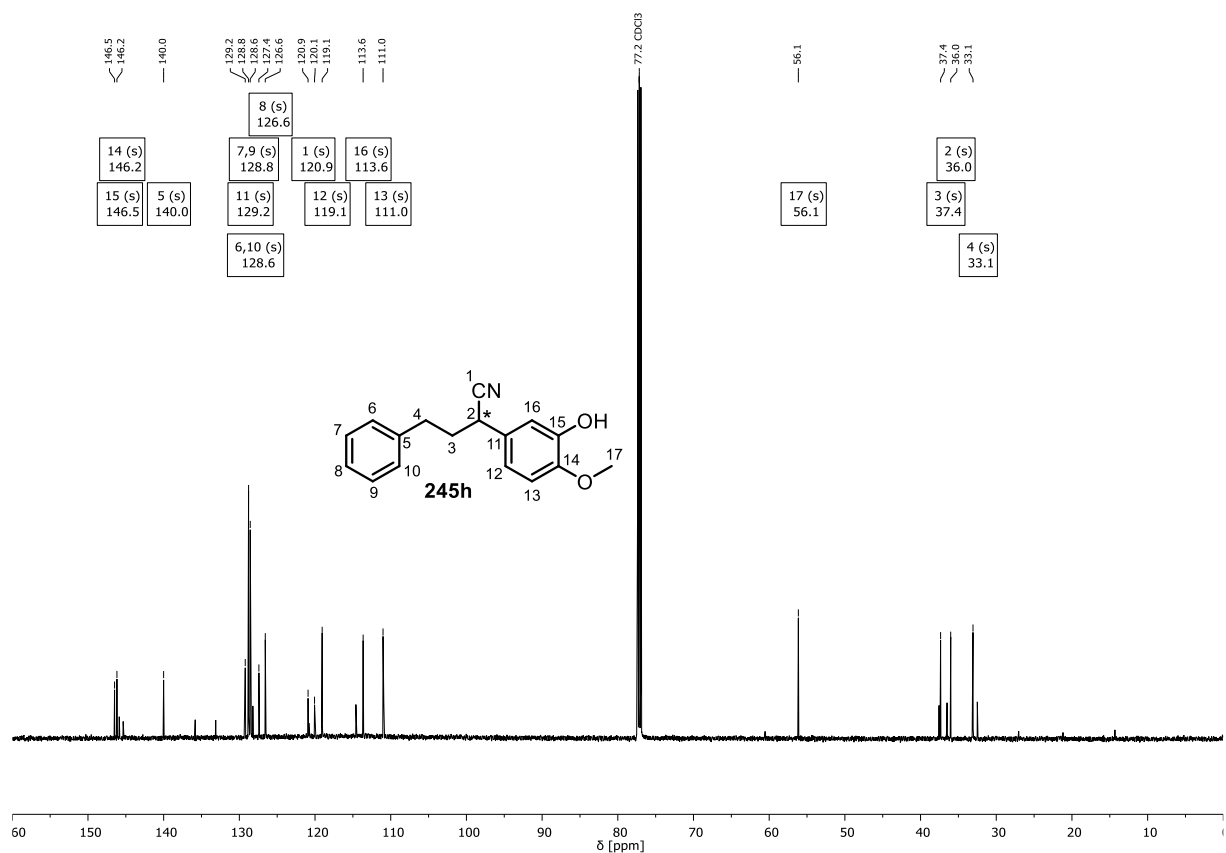


Figure 67: $^{13}\text{C NMR}$ (151 MHz, CDCl_3) spectrum of 2,4-diarylbutyronitrile **245h** (75:25 *rr*).

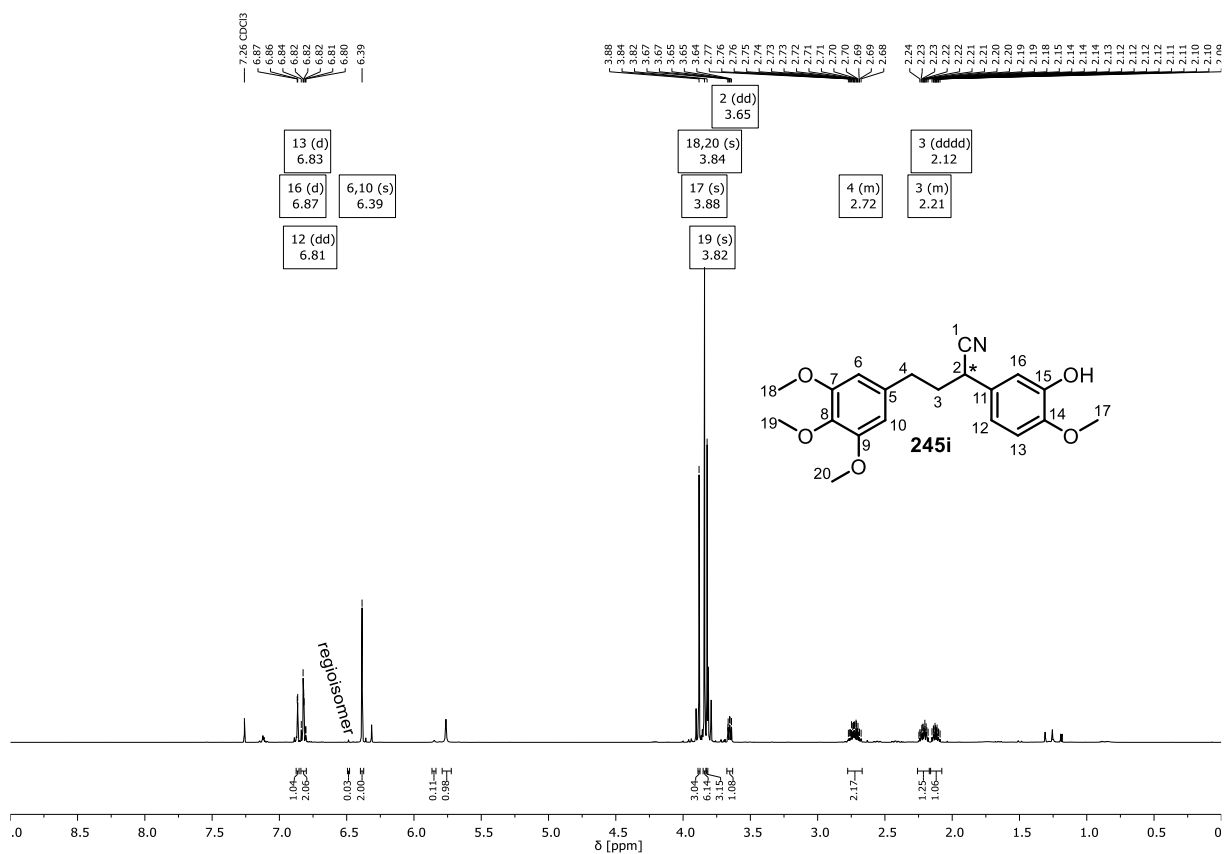


Figure 68: ^1H NMR (600 MHz, CDCl_3) spectrum of 2,4-diarylbutyronitrile **245i** (98:2 *r*).

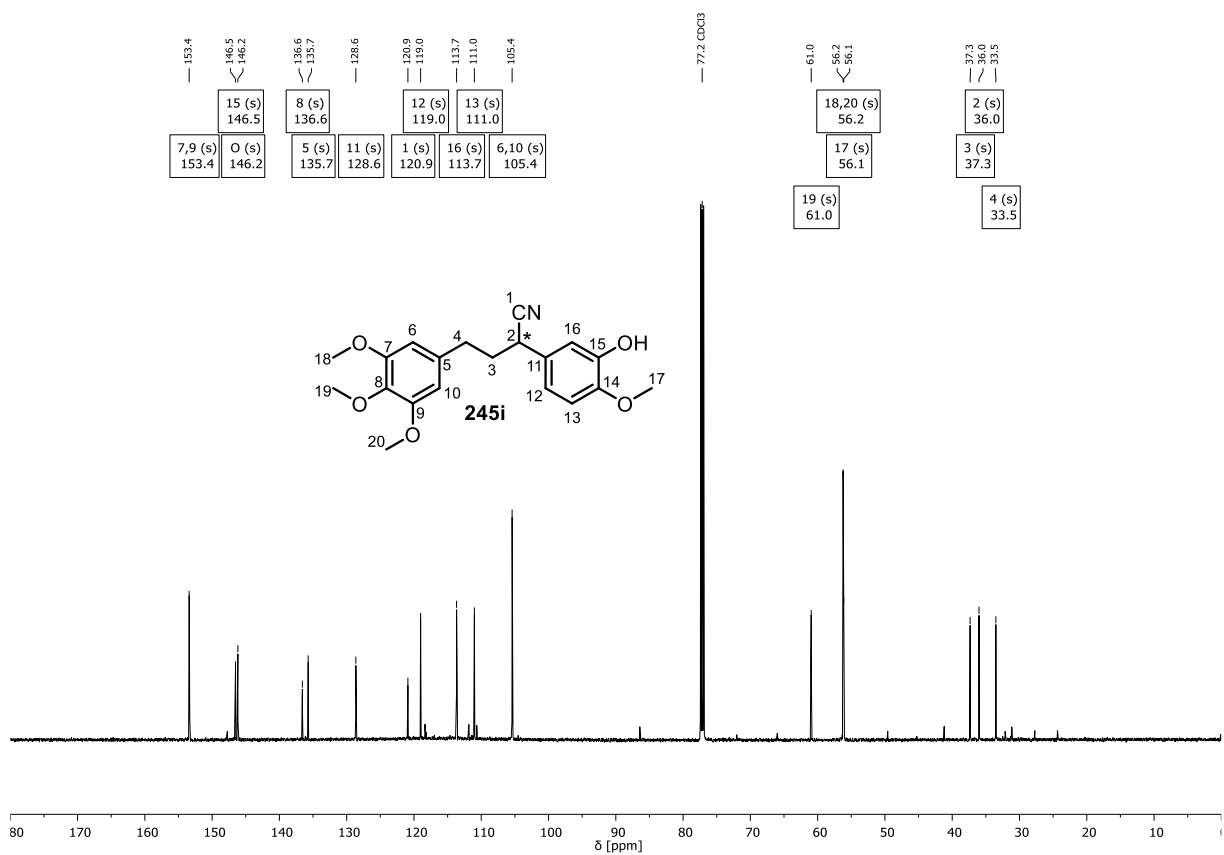
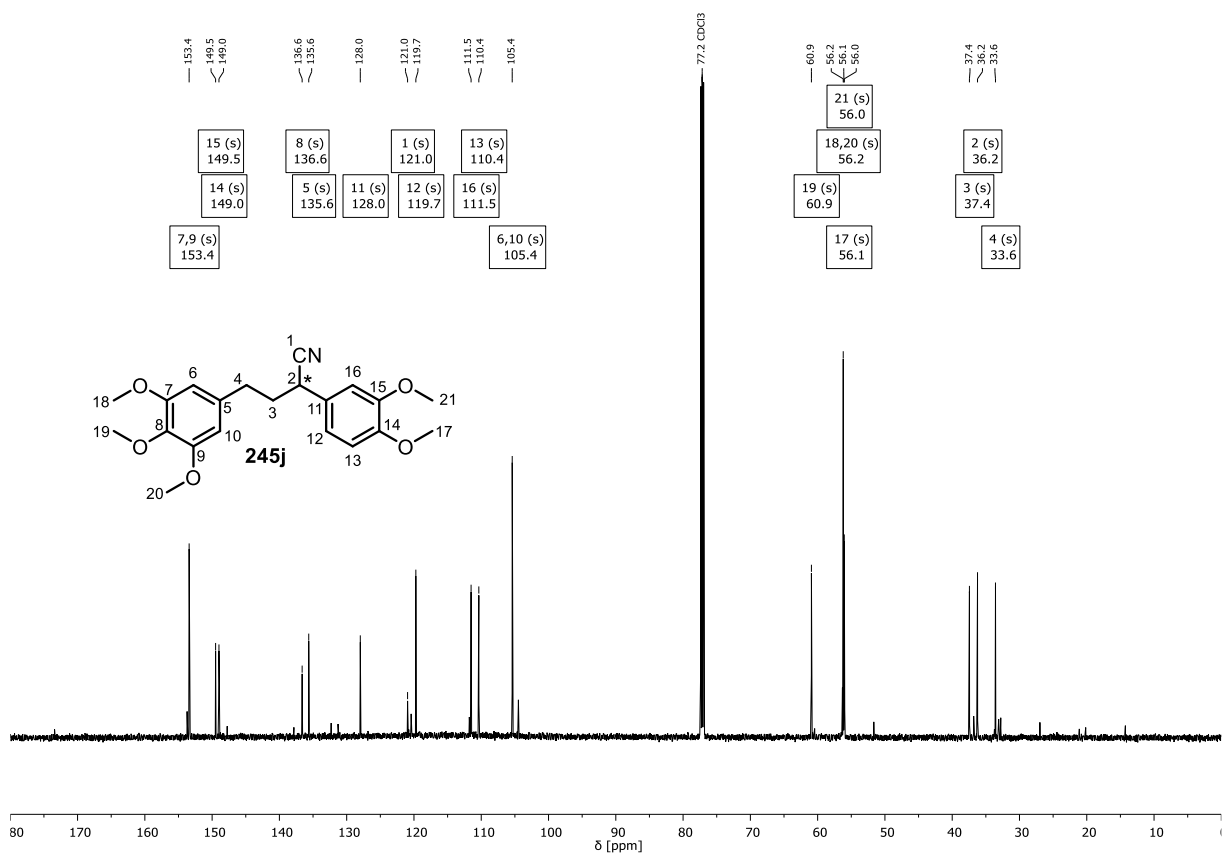
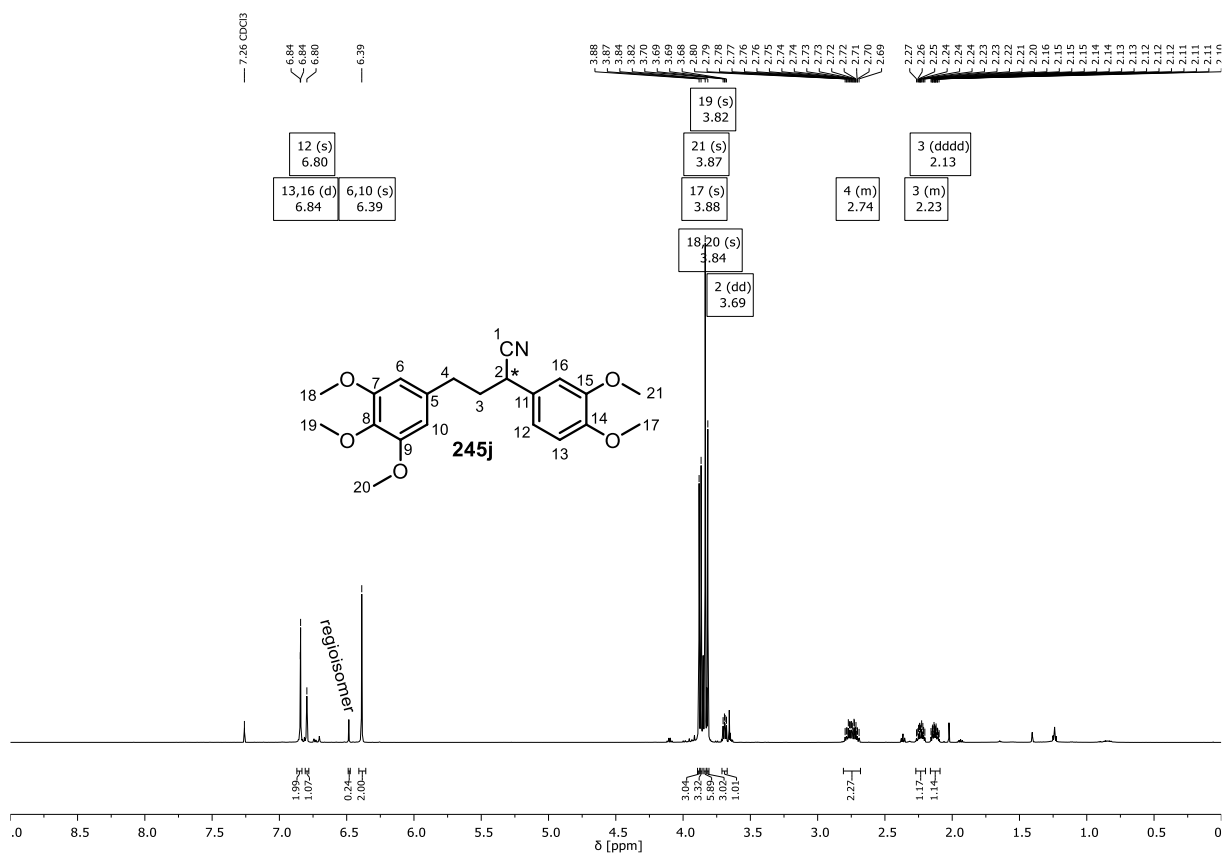


Figure 69: ^{13}C NMR (151 MHz, CDCl_3) spectrum of 2,4-diarylbutyronitrile **245i** (98:2 *r*).



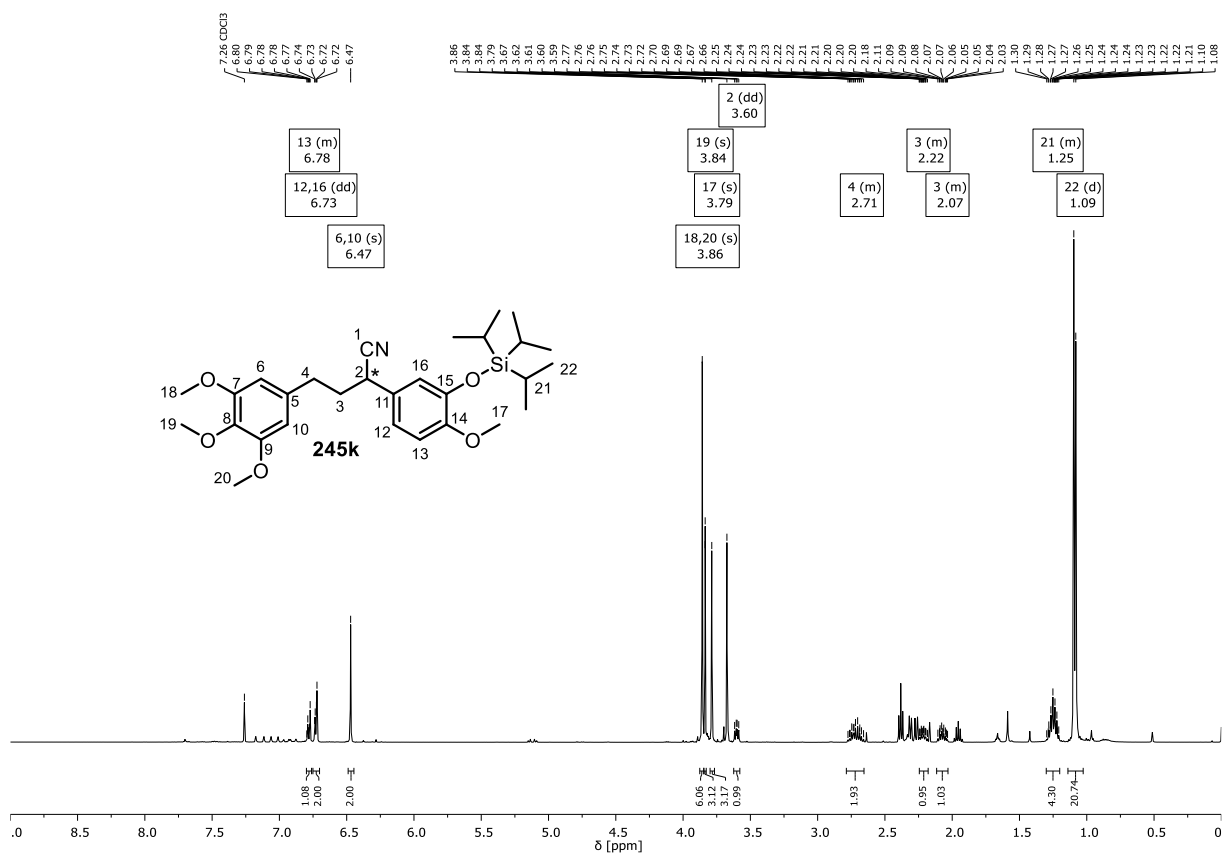


Figure 72: ^1H NMR (500 MHz, CDCl_3) spectrum of 2,4-diarylbutyronitrile **245k**.

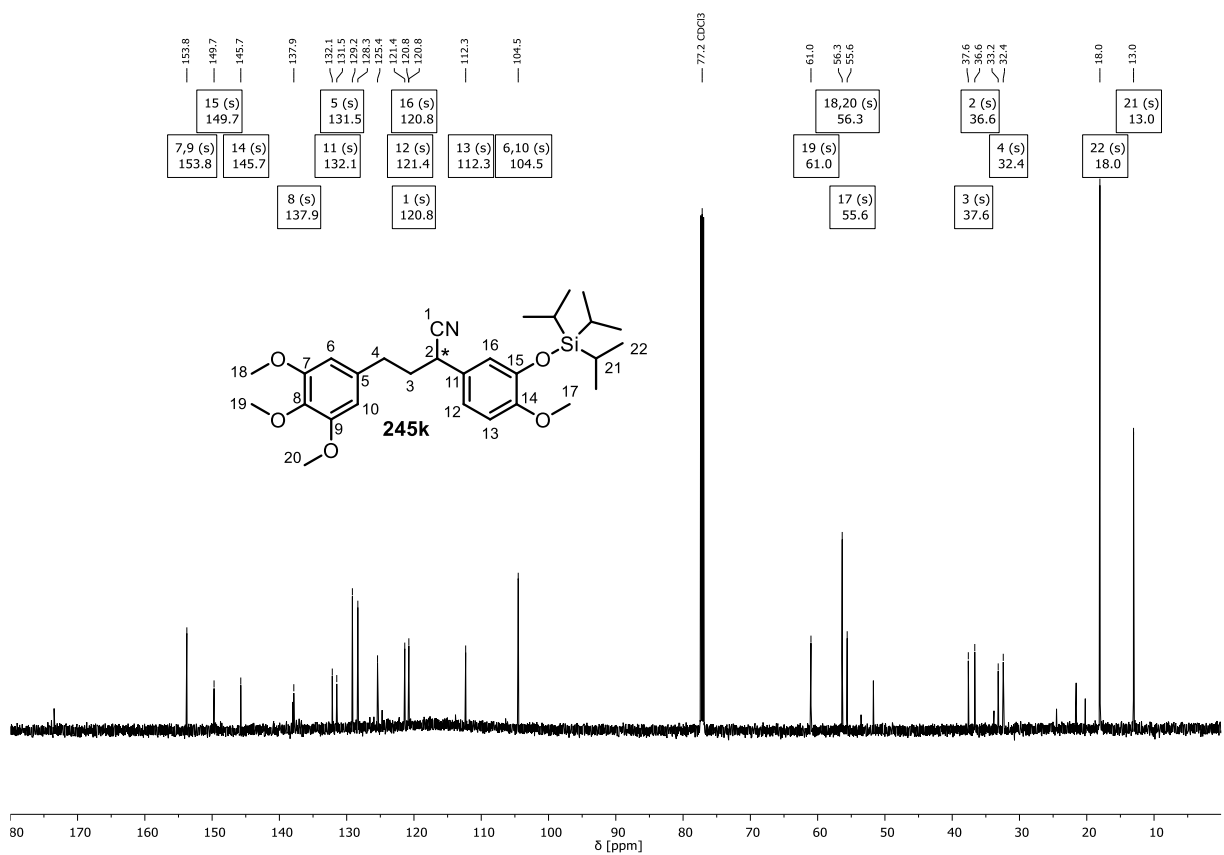
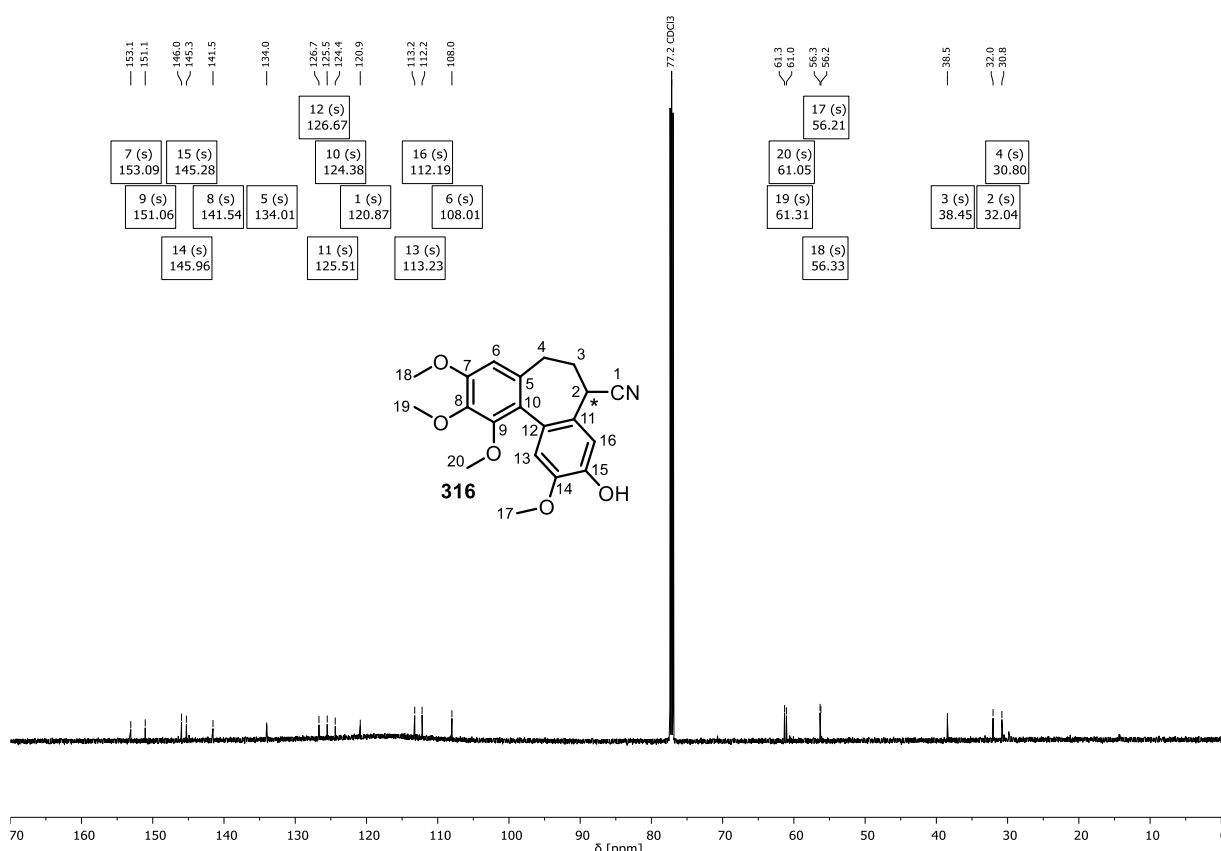
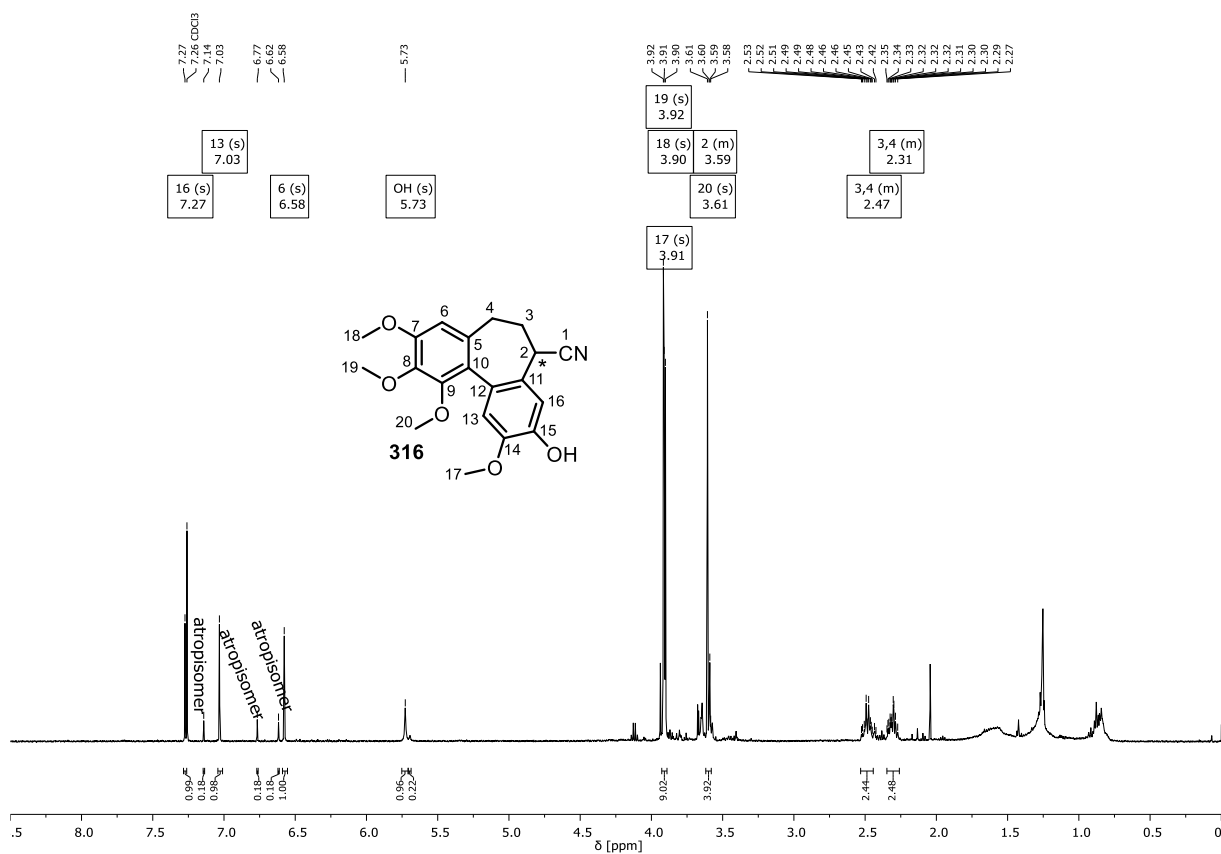
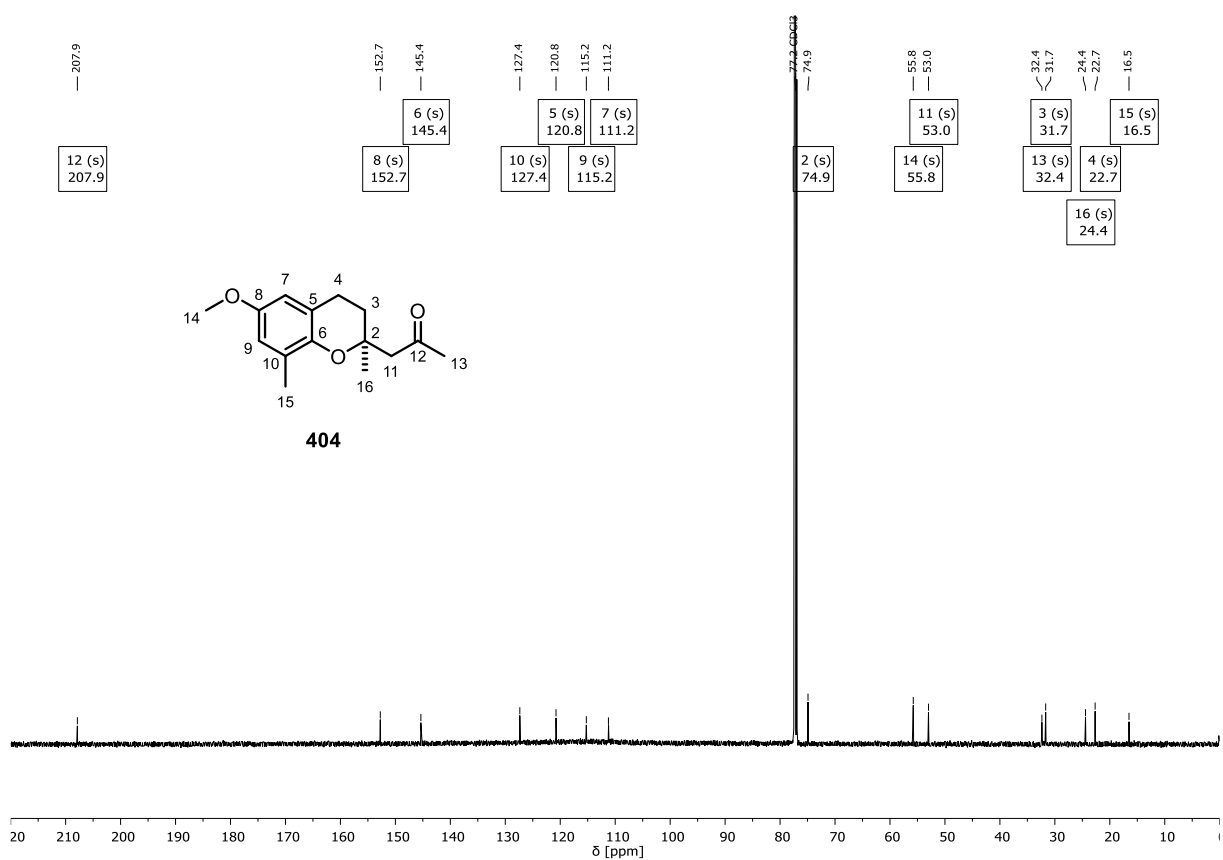
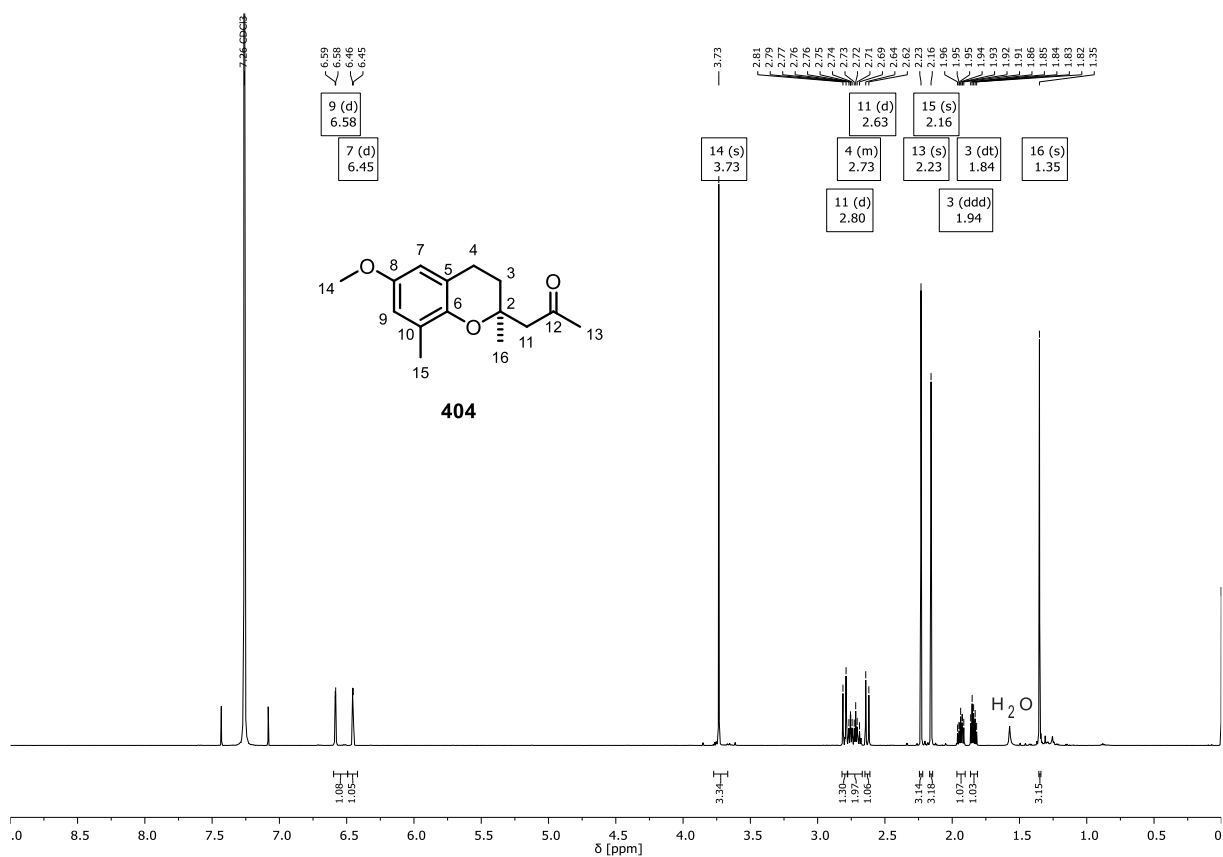
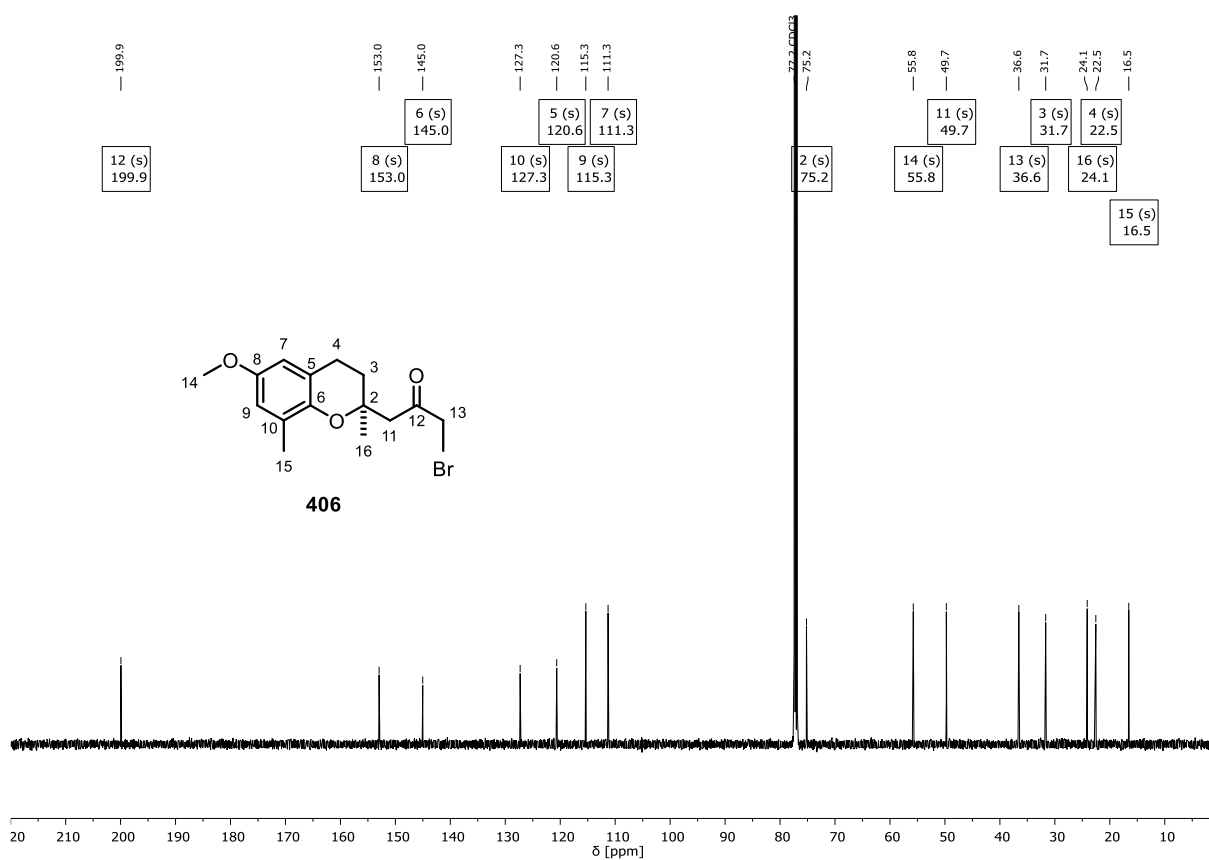
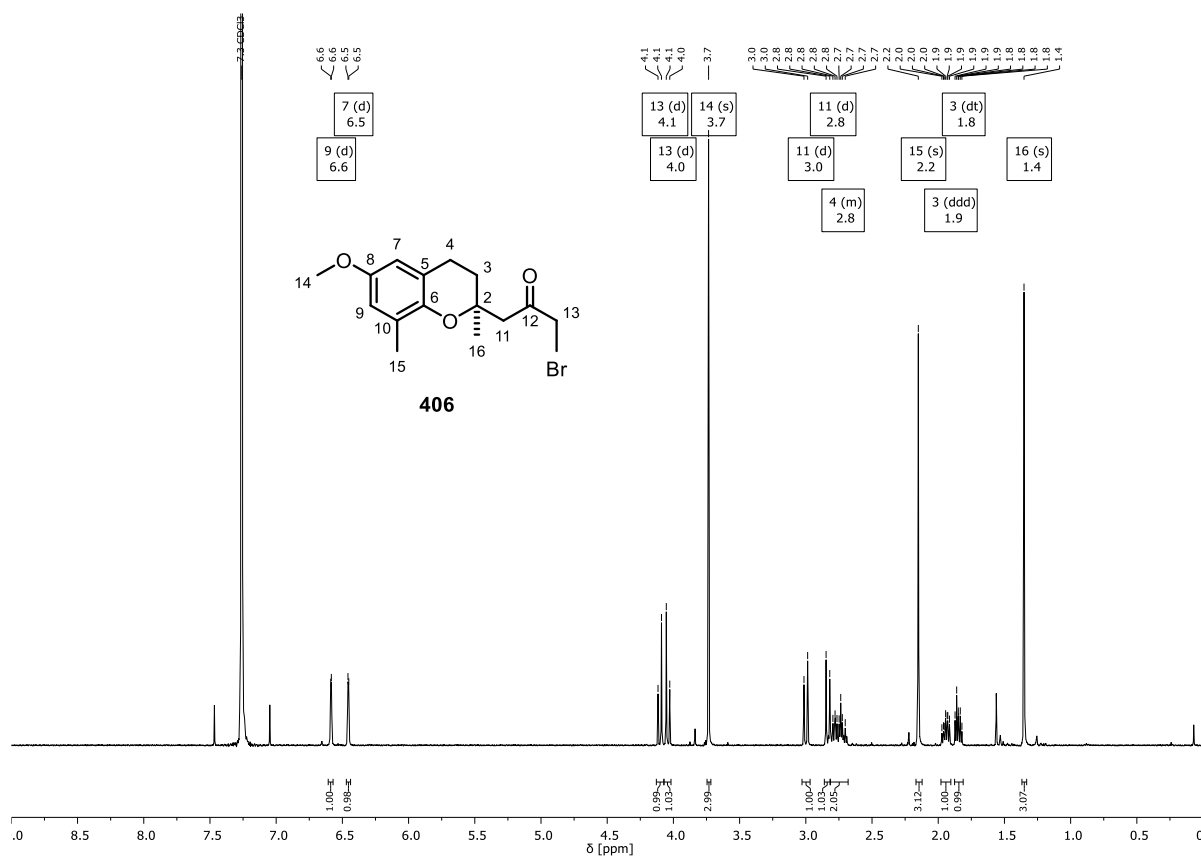


Figure 73: ^{13}C NMR (151 MHz, CDCl_3) spectrum of 2,4-diarylbutyronitrile **245k**.







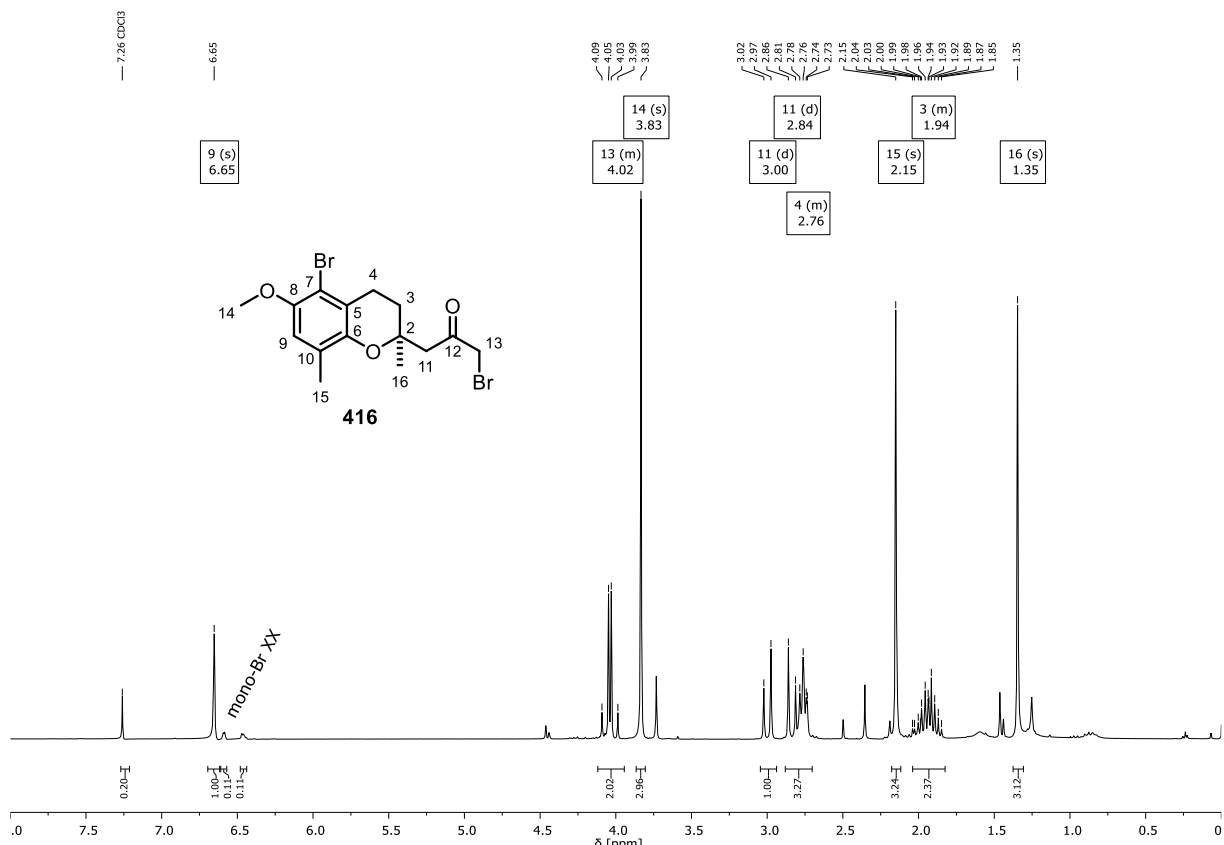


Figure 80: $^1\text{H NMR}$ (300 MHz, CDCl_3) spectrum of dibrominated chromane **416**. Monobrominated chromane **406** as ~10 mol% impurity.

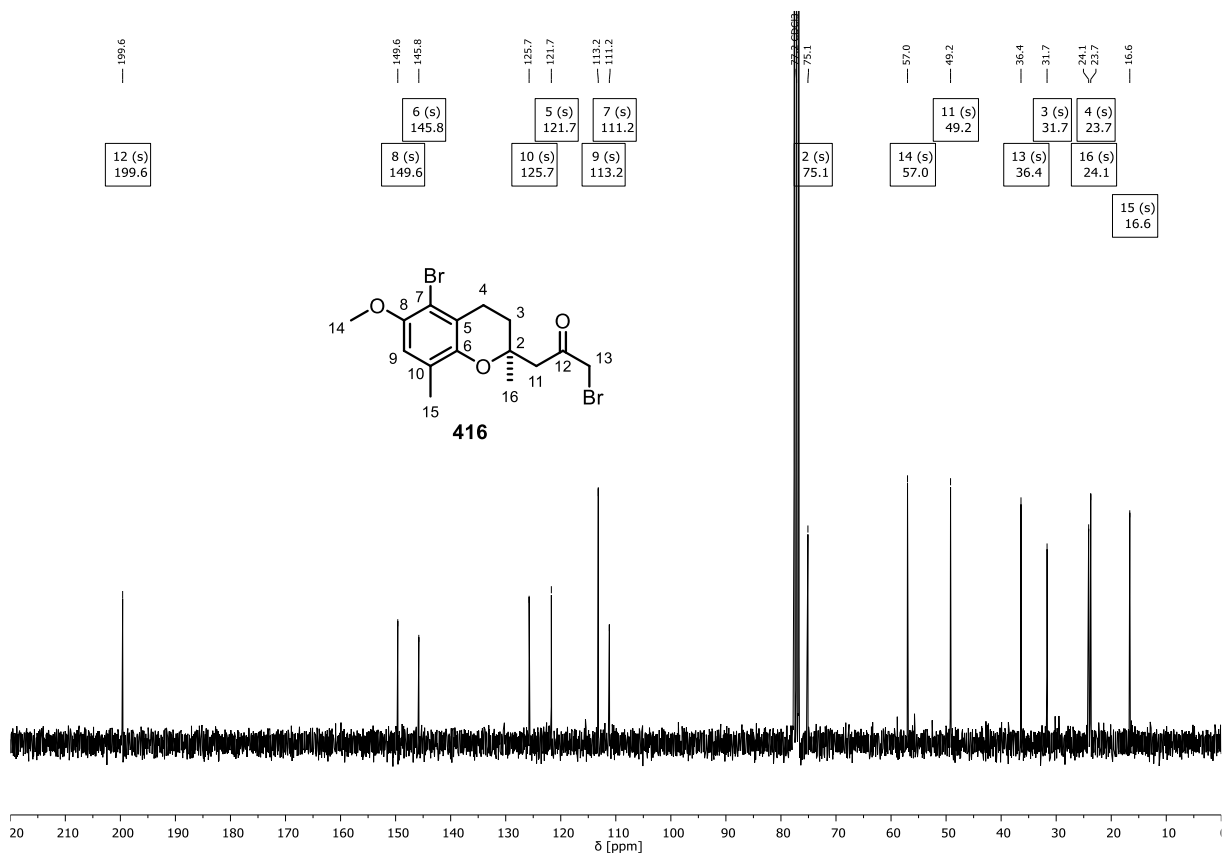
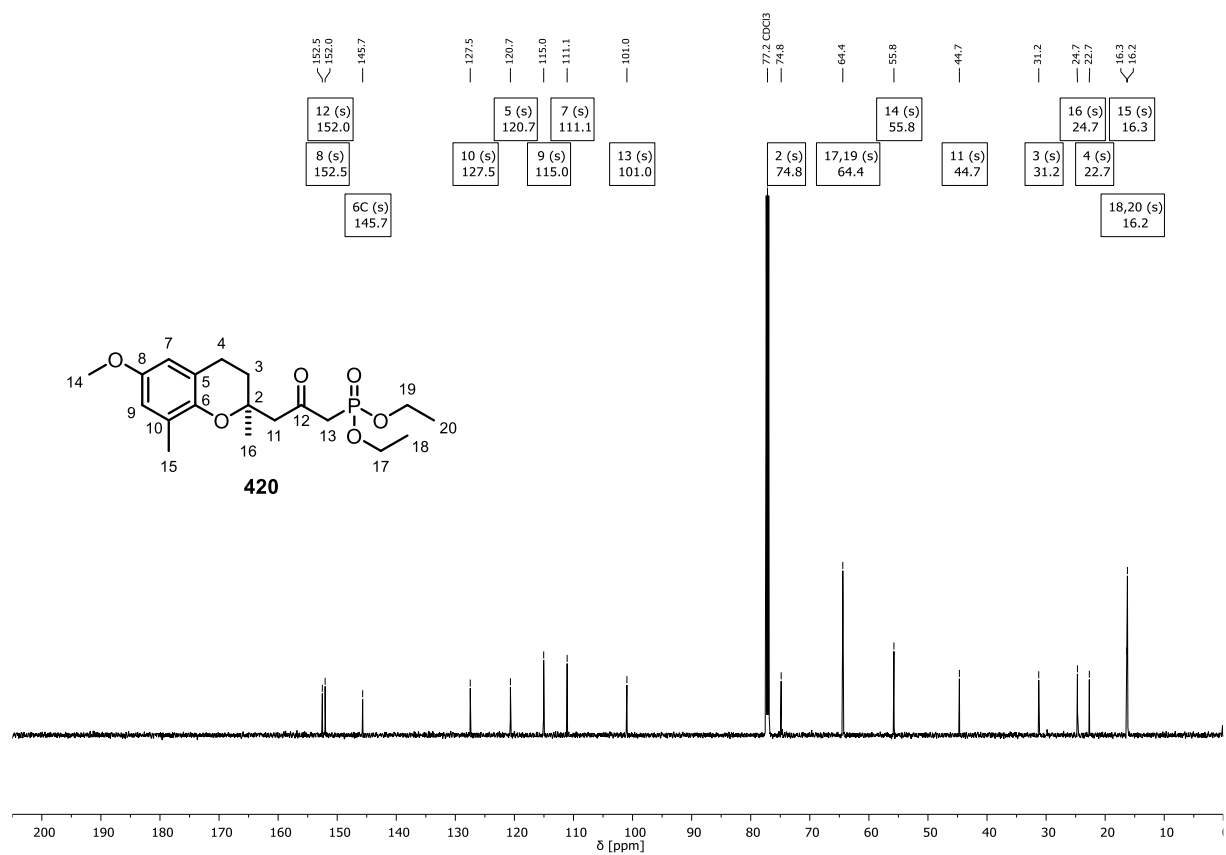
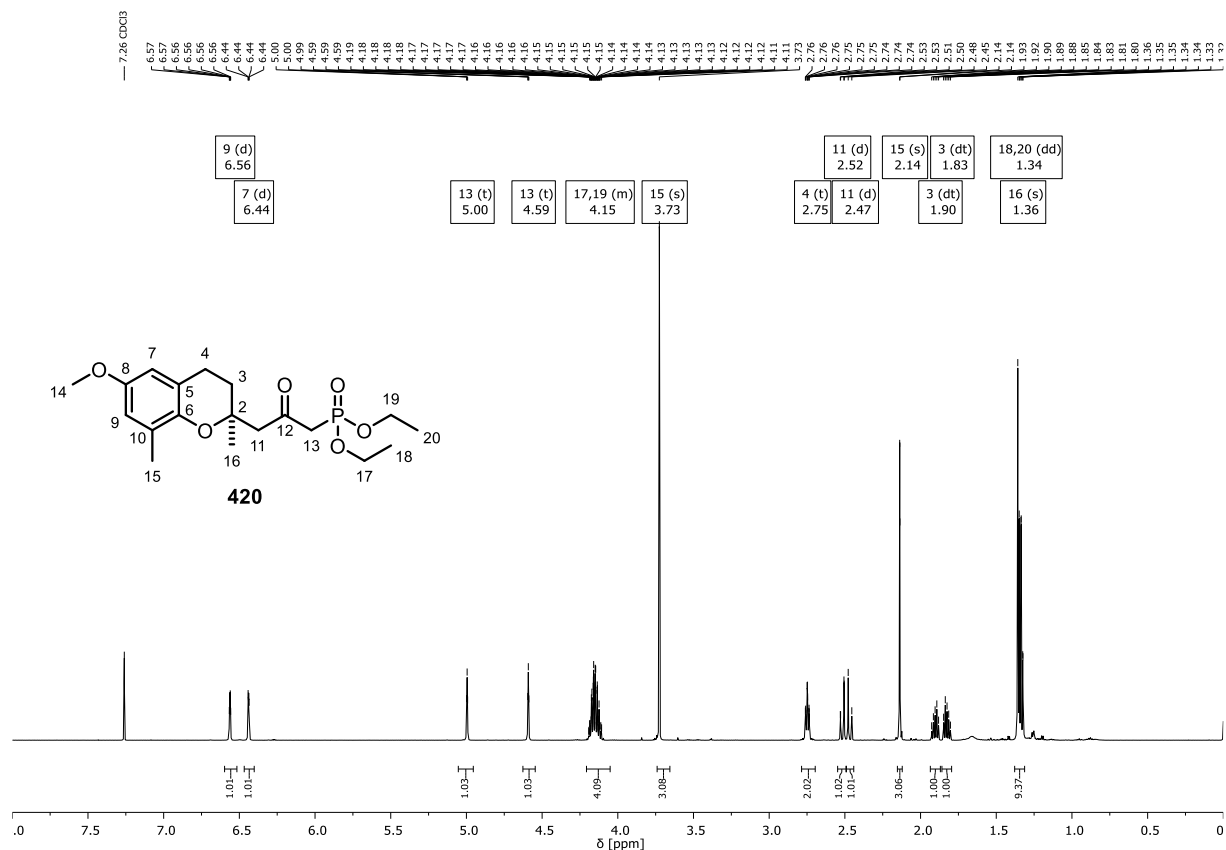
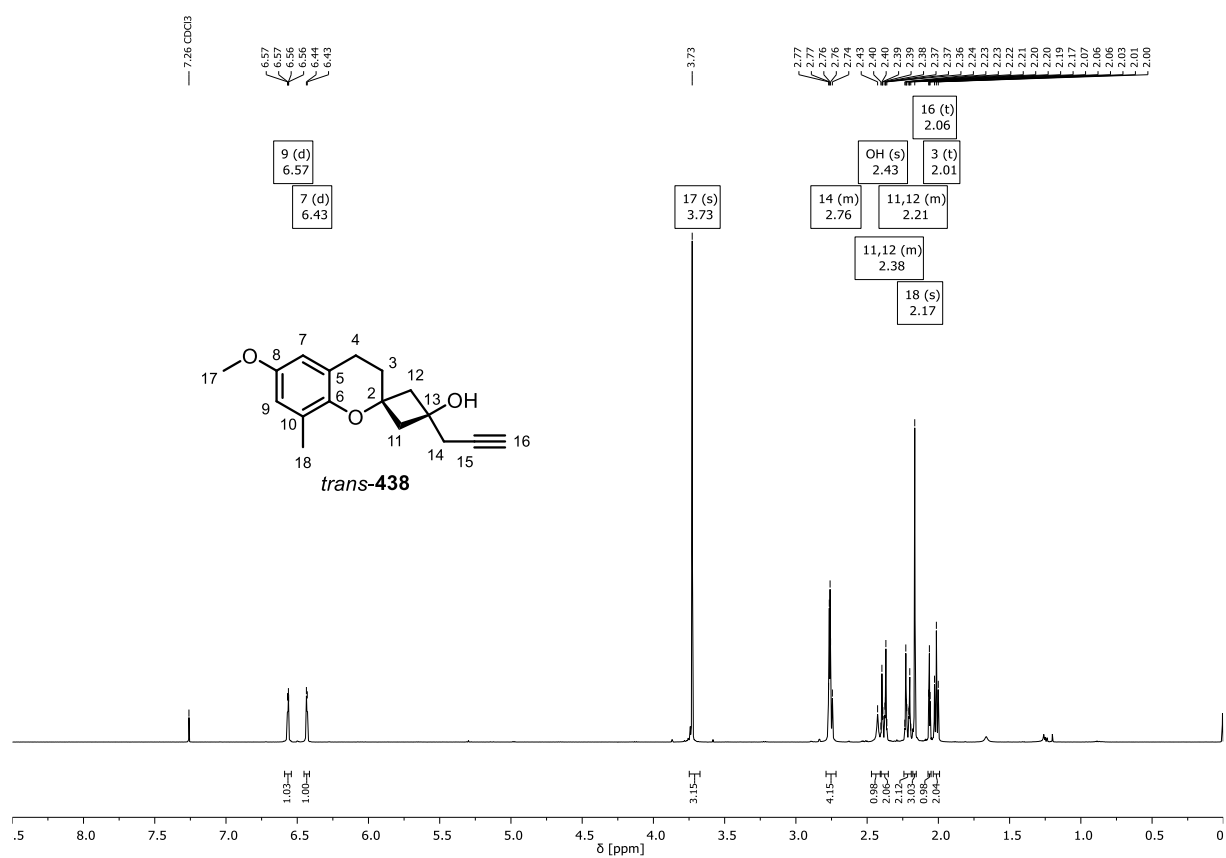
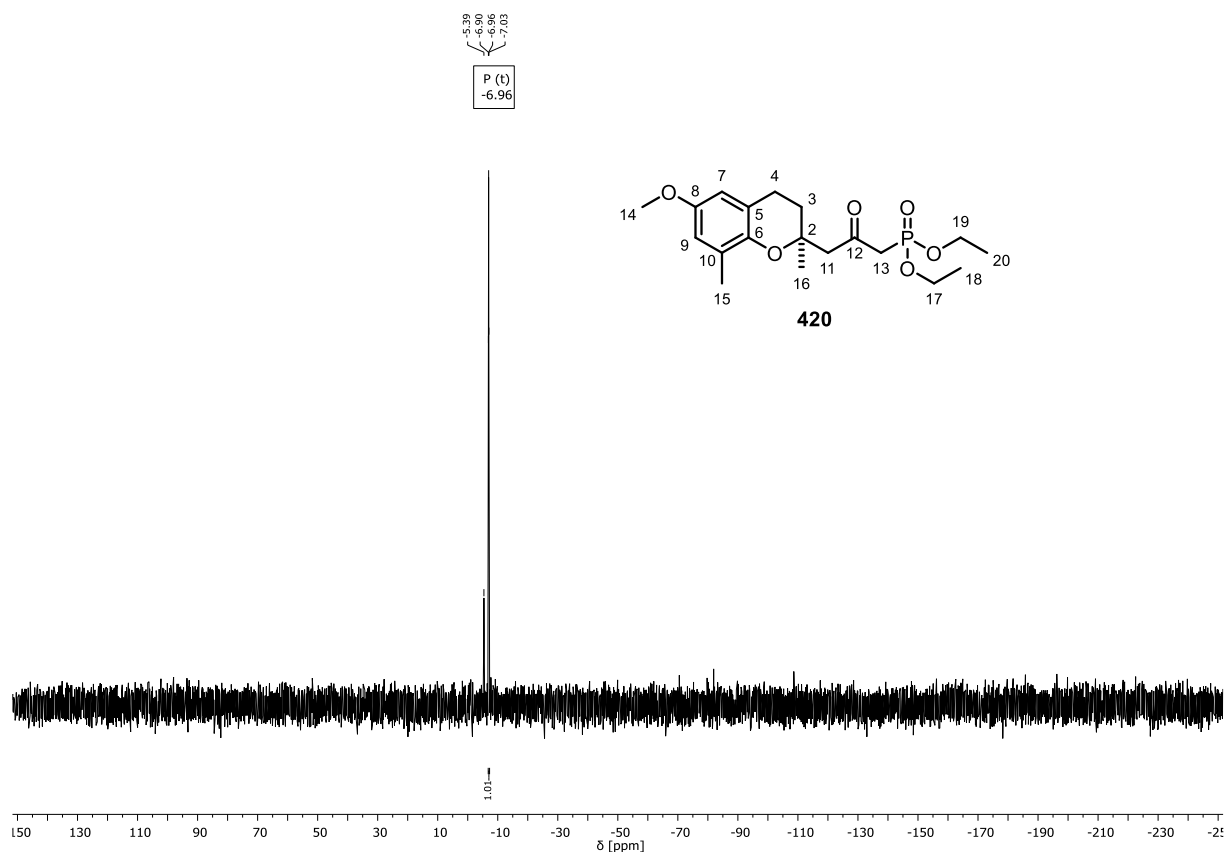


Figure 81: $^{13}\text{C NMR}$ (75 MHz, CDCl_3) spectrum of dibrominated chromane **416**. Monobrominated chromane **406** as ~10 mol% impurity.





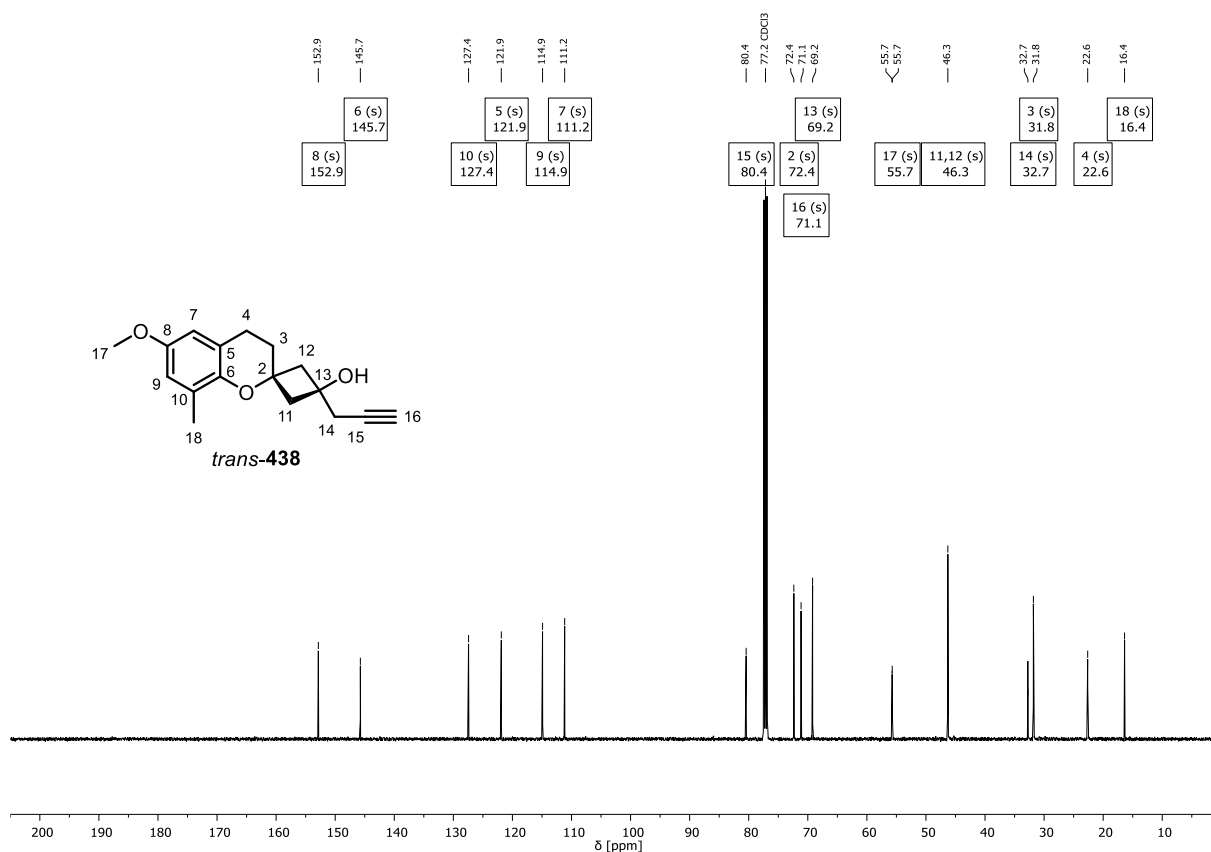


Figure 86: ^{13}C NMR (126 MHz, CDCl_3) spectrum of *spirochromanol trans-438*.

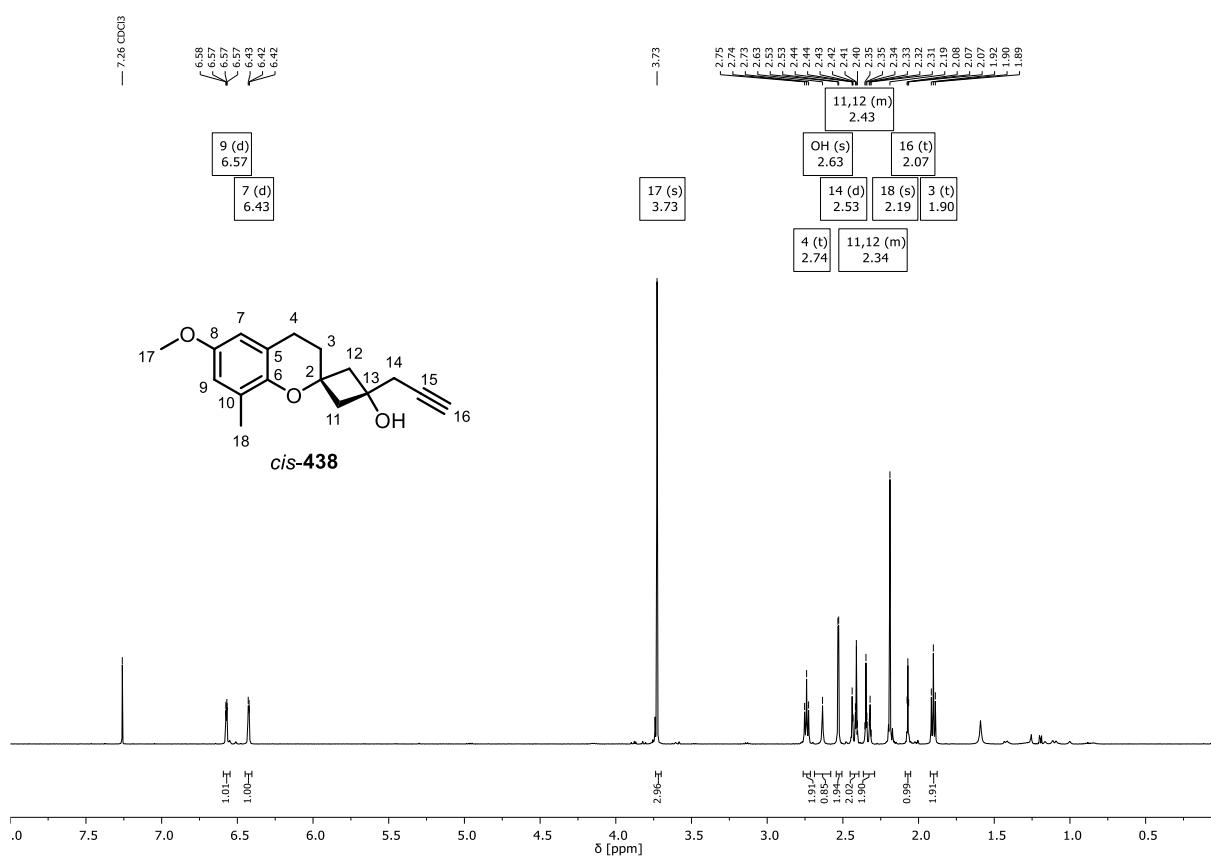
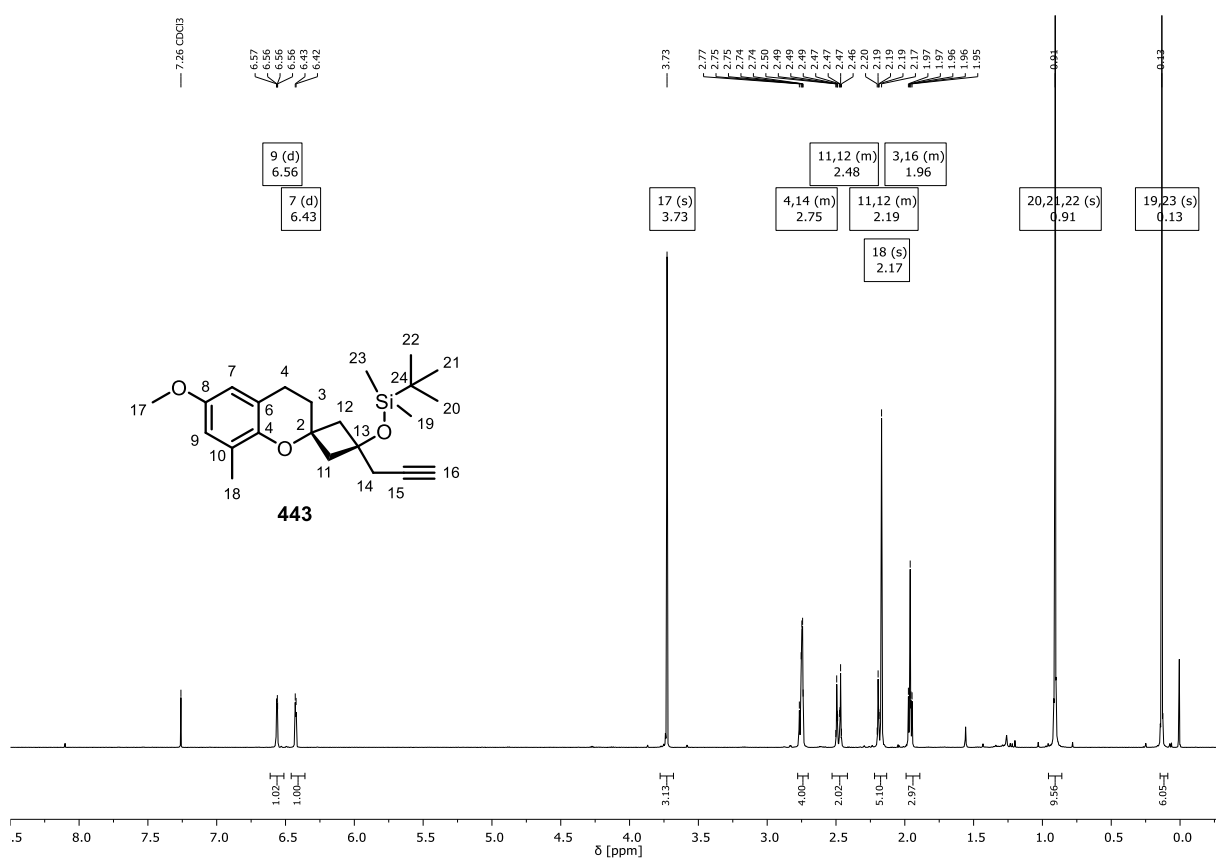
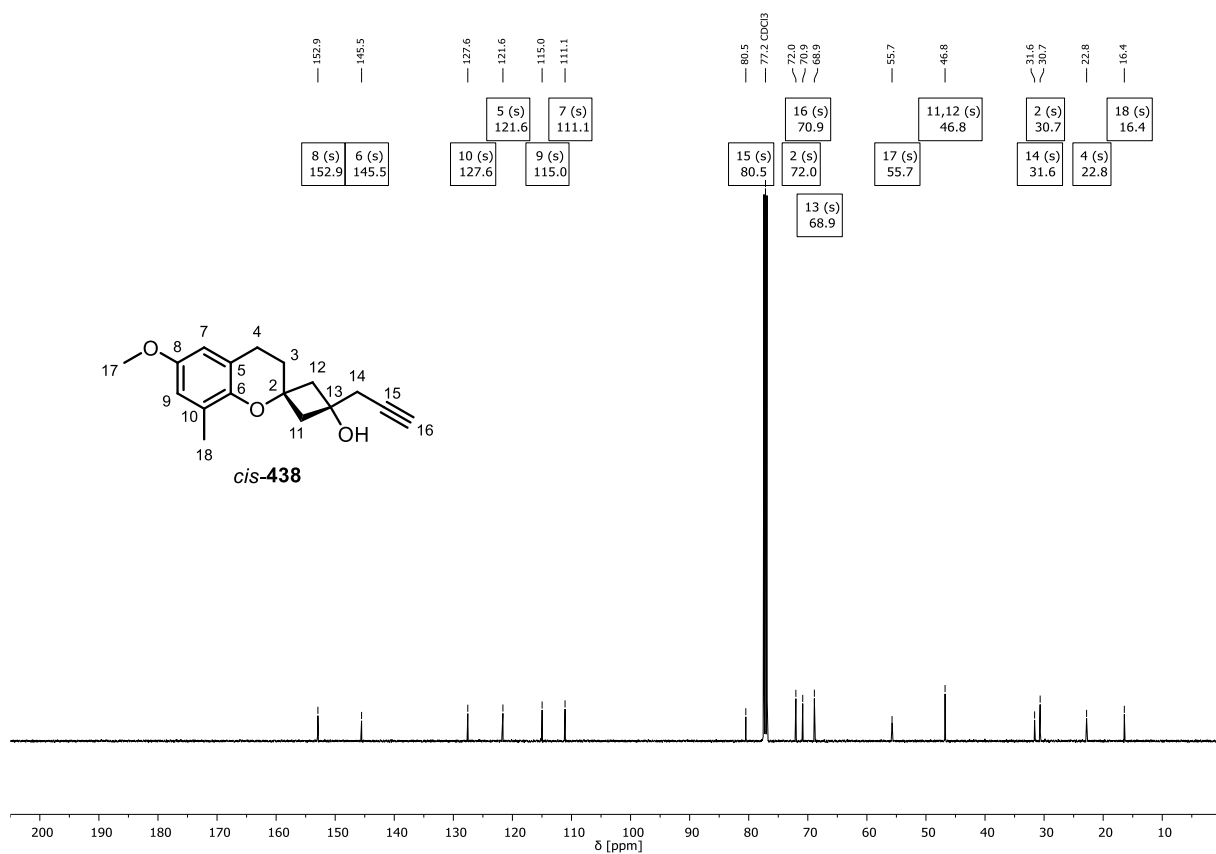
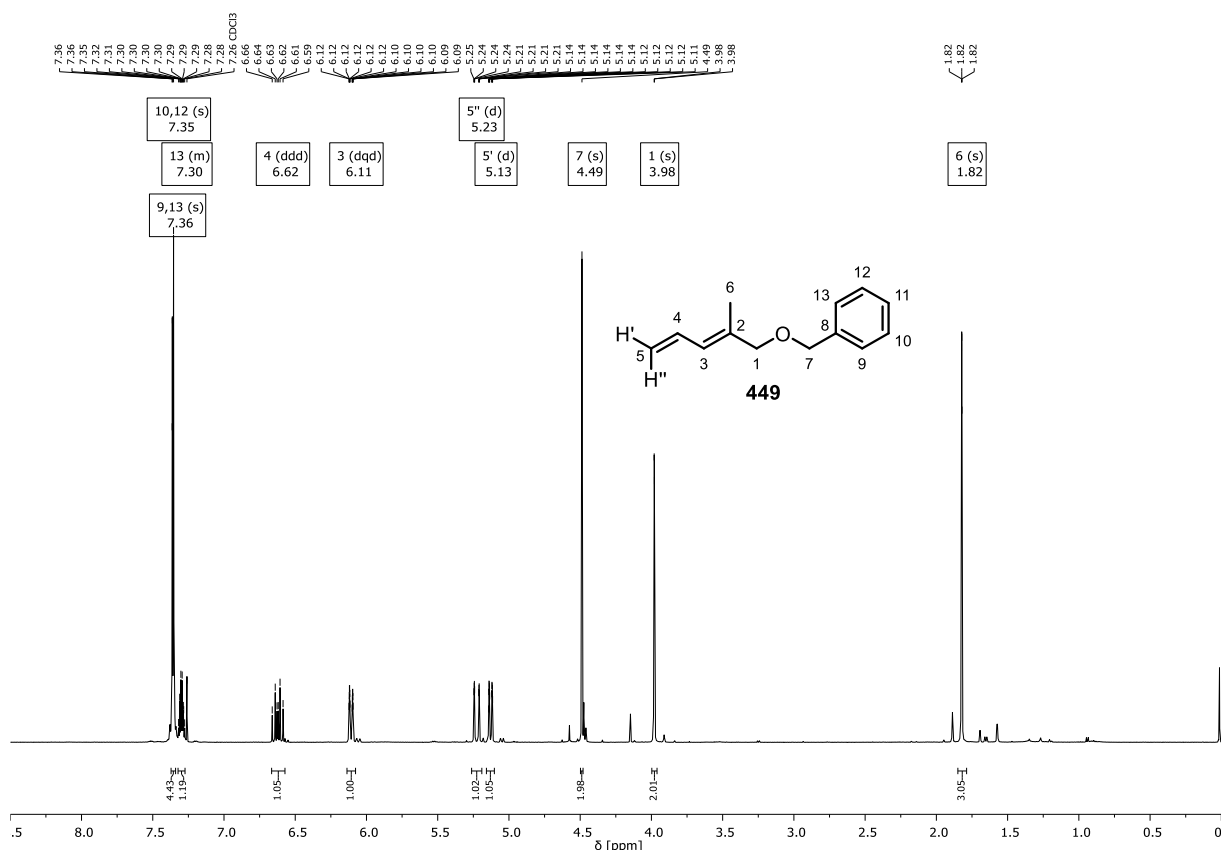
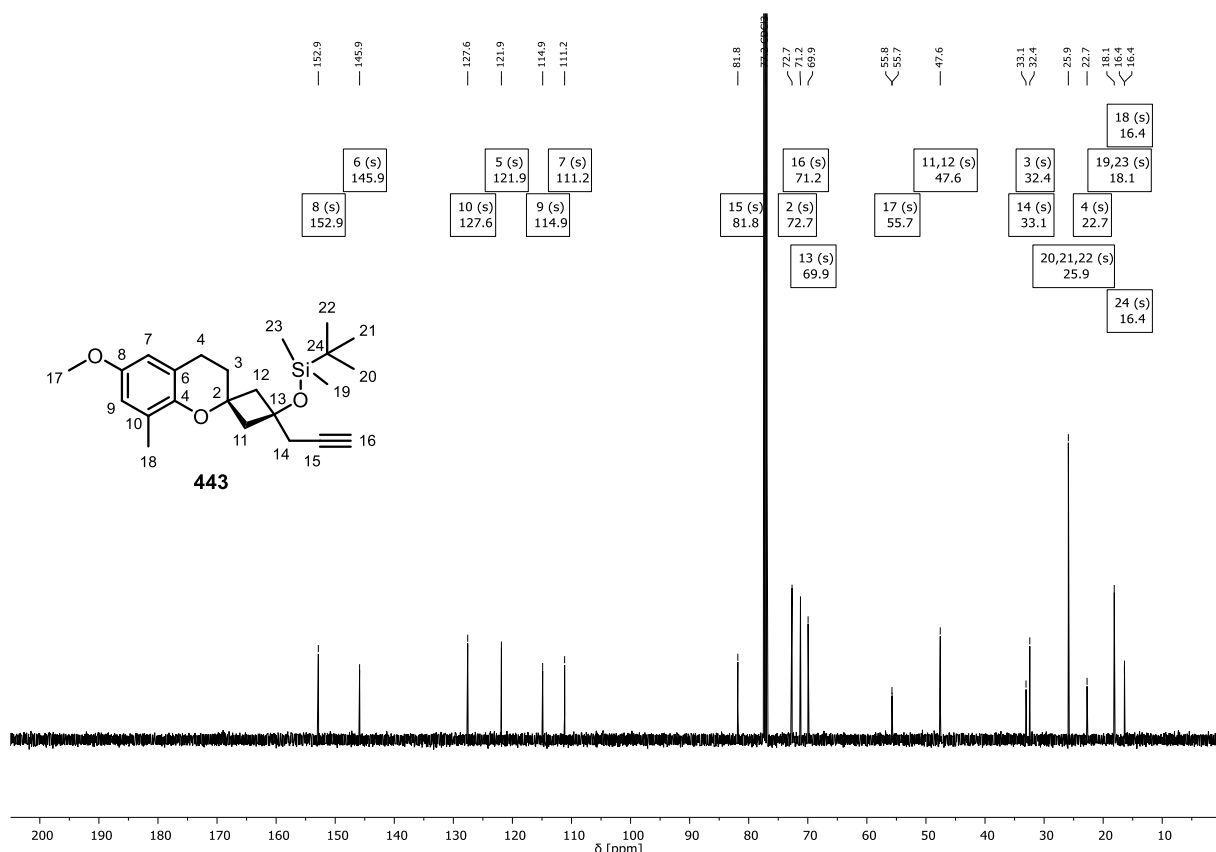
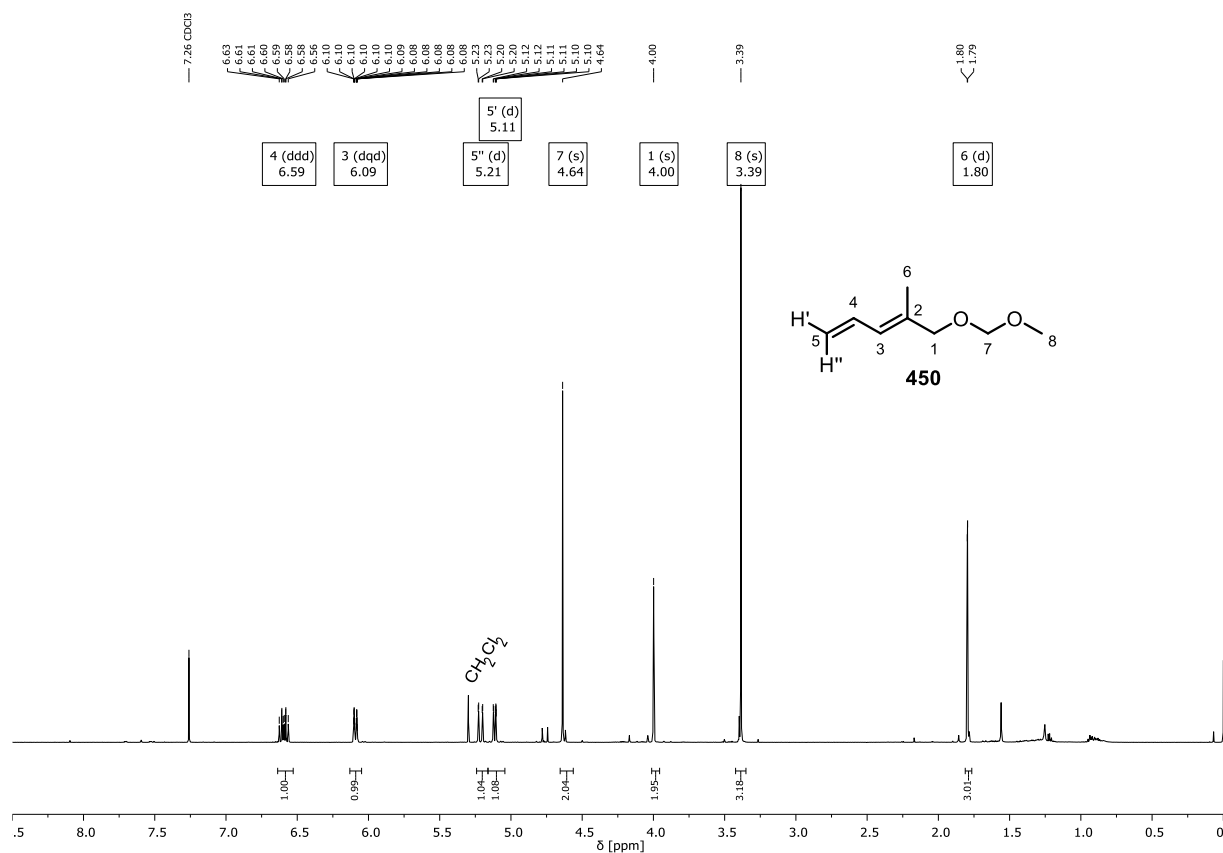
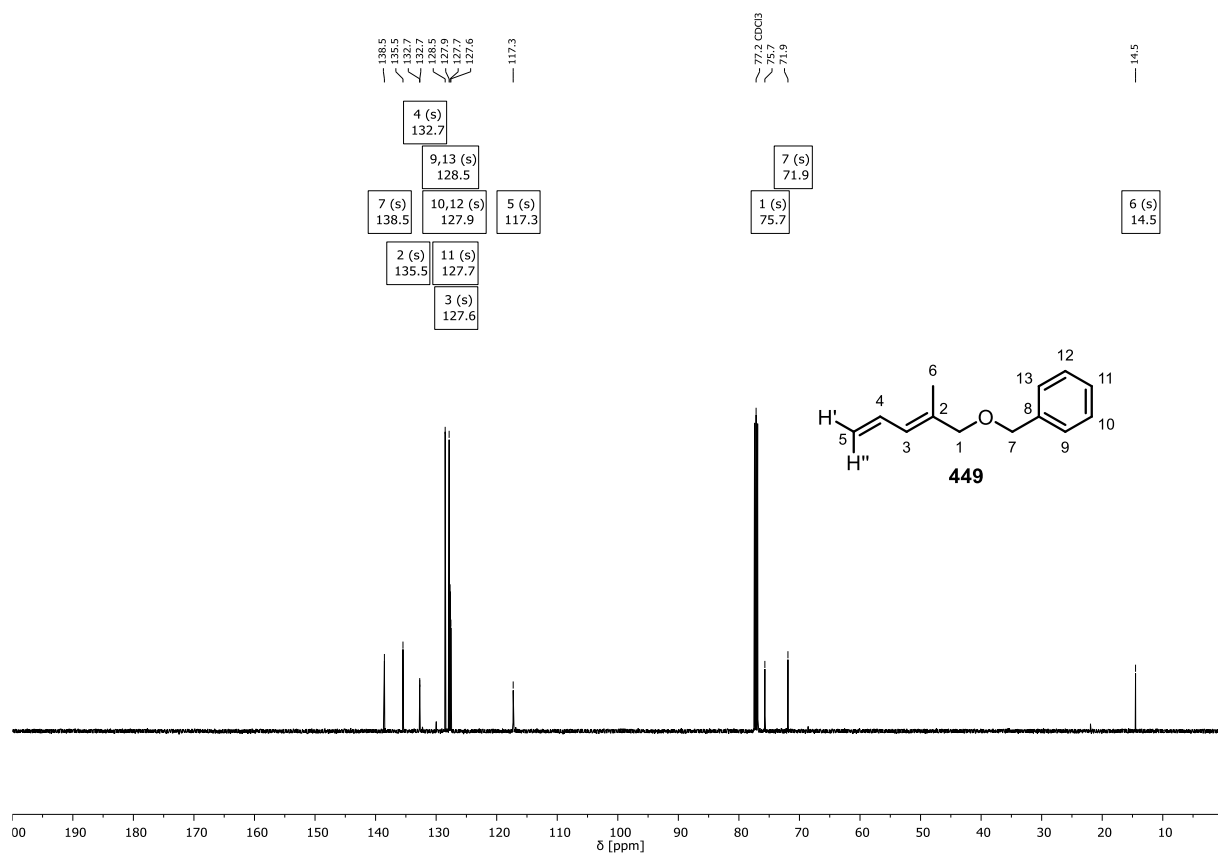


Figure 87: ^1H NMR (500 MHz, CDCl_3) spectrum of *spirochromanol cis-438*.







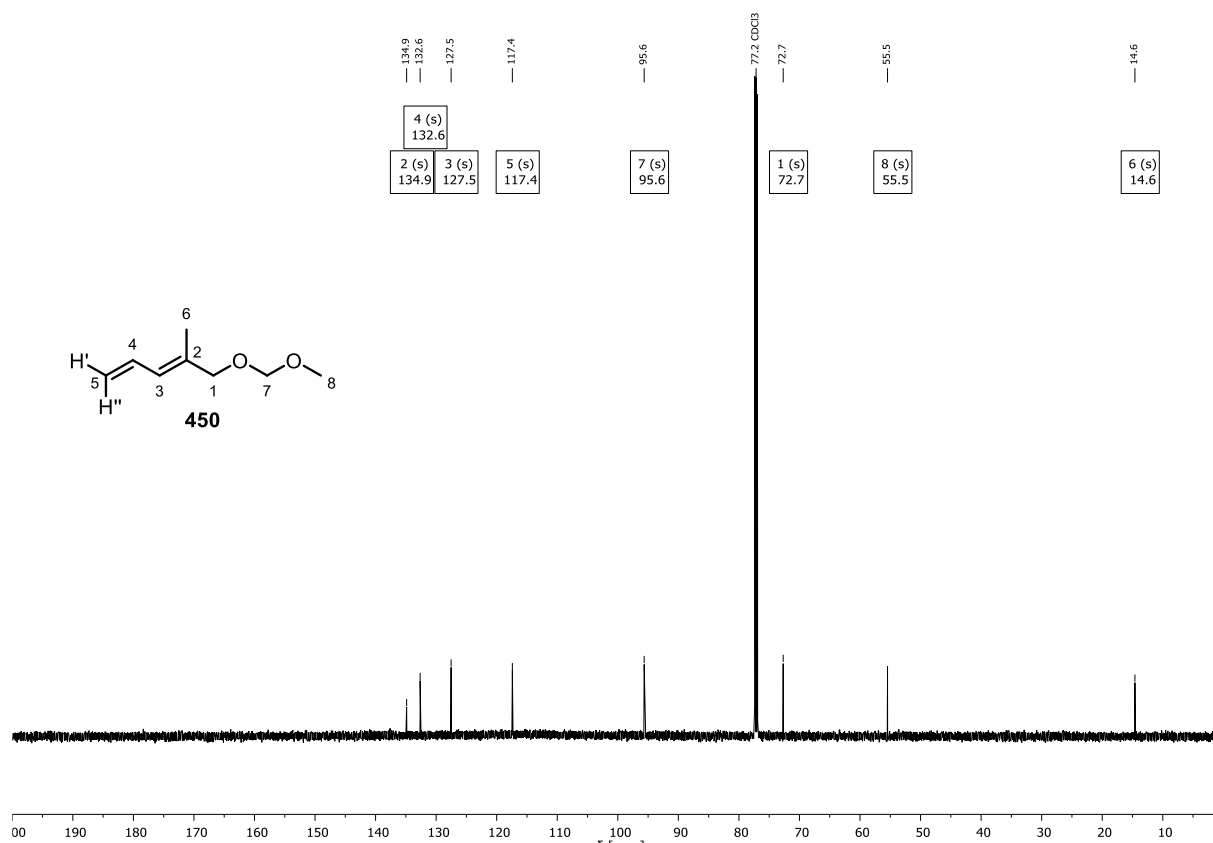


Figure 94: ^{13}C NMR (126 MHz, CDCl_3) spectrum of O-MOM-(2E)-2-methylpenta-2,4-dienol (**450**).

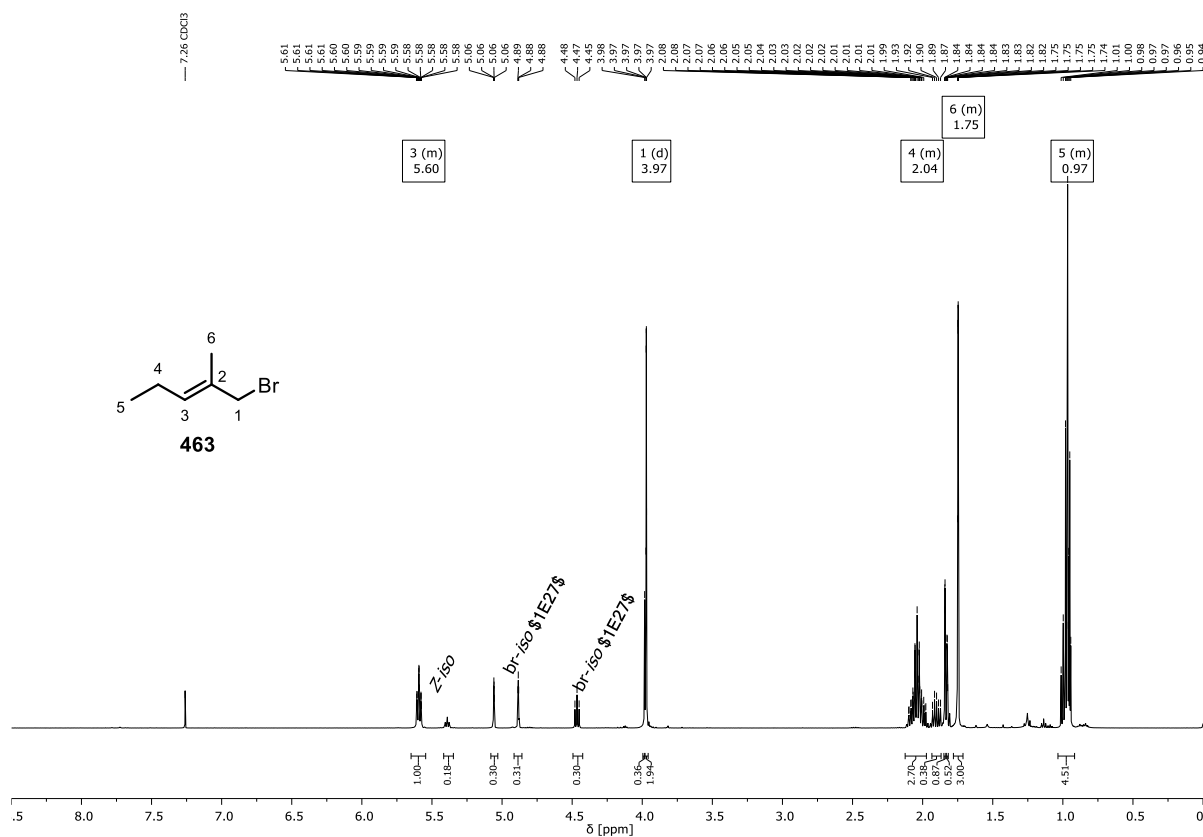
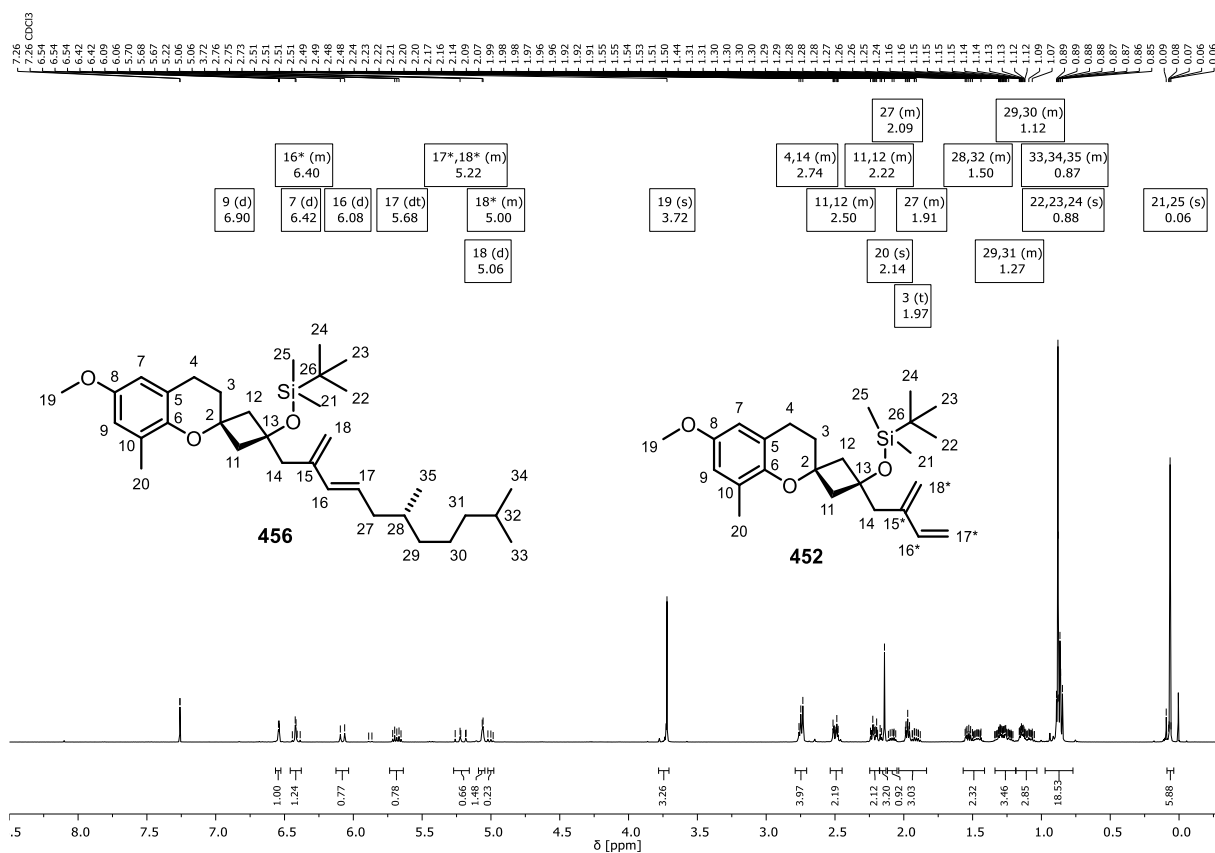
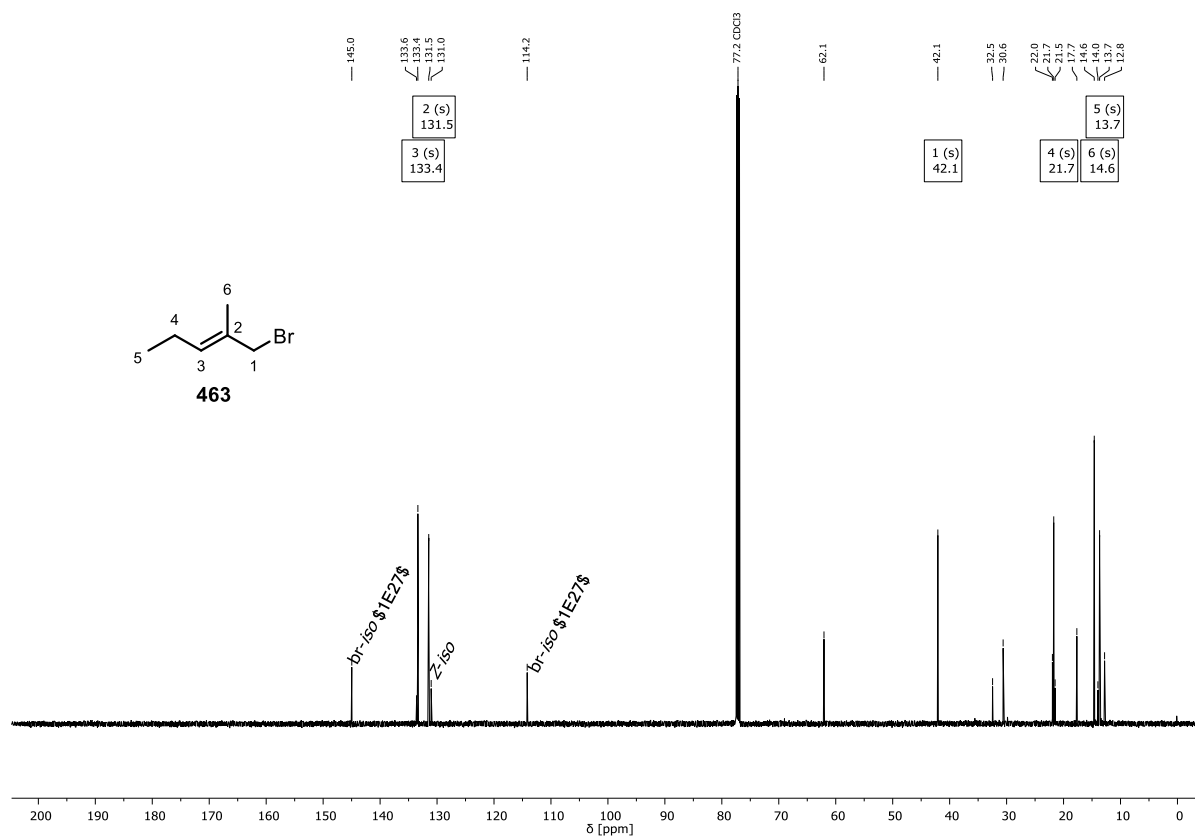


Figure 95: ^1H NMR (500 MHz, CDCl_3) spectrum of (E)-1-bromo-2-methyl-2-pentene (**463**). Equilibrium at r.t. of bromoallyl species led to isomer impurities (~20 mol% of branched isomer **464** and ~12 mol% of (Z)-isomer.



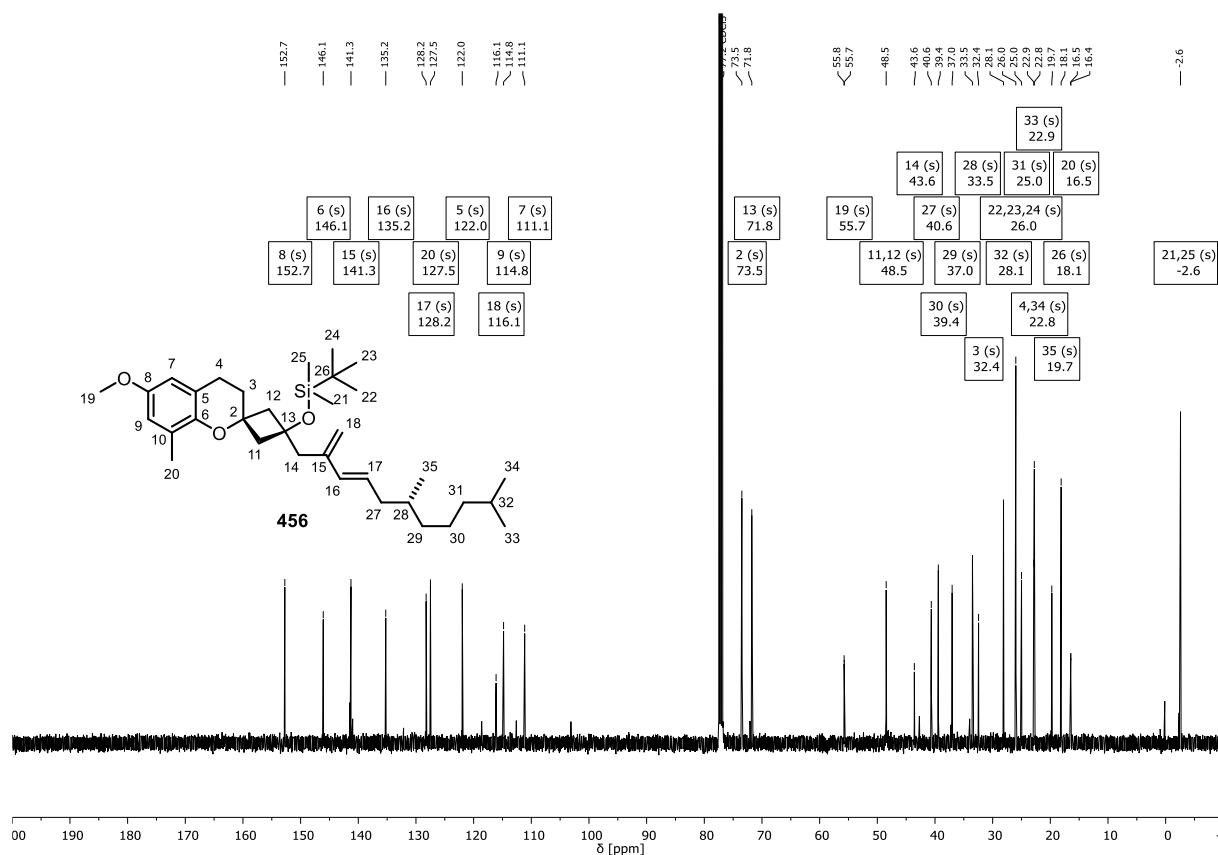


Figure 98: ^{13}C NMR (126 MHz, CDCl_3) spectrum of chromanyldiene **456** with byproduct **452** impurity (inseparable mixture; mol% ratio **456/452** ~70:30).

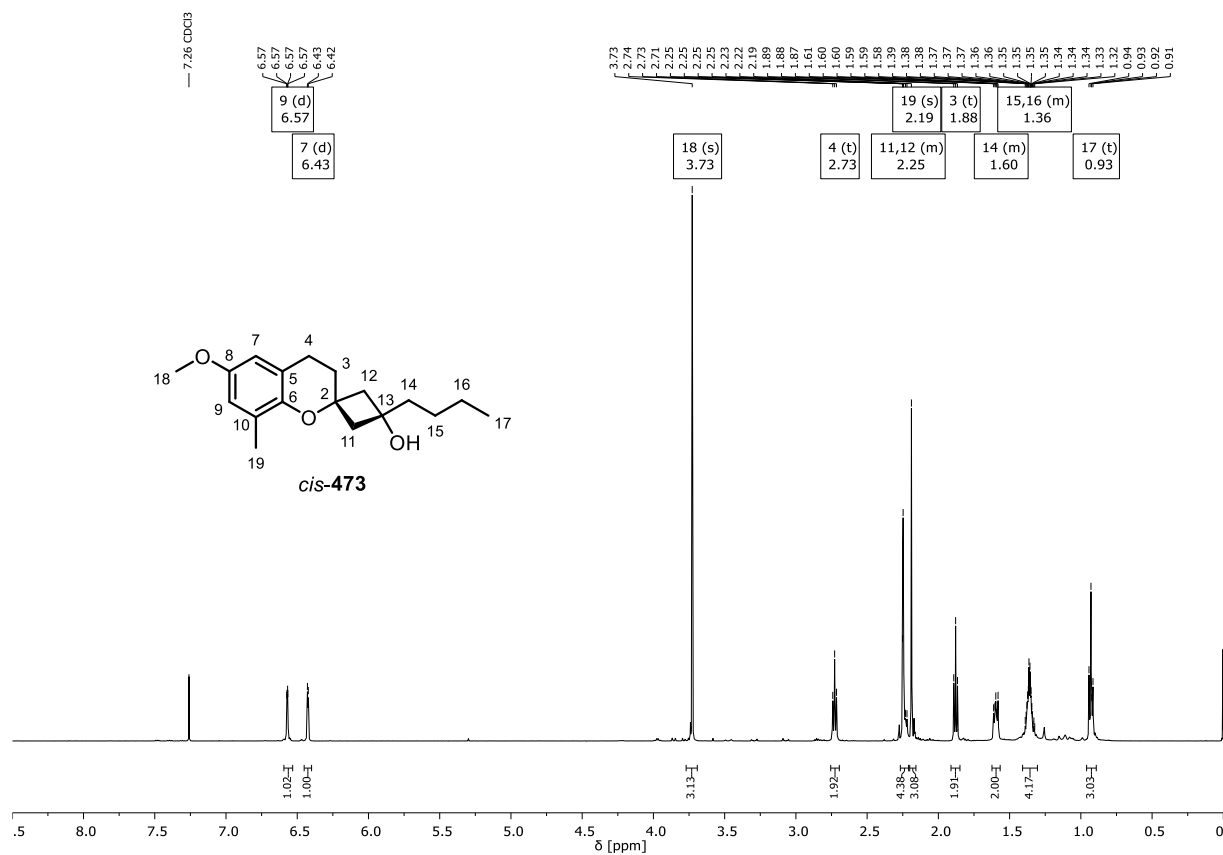
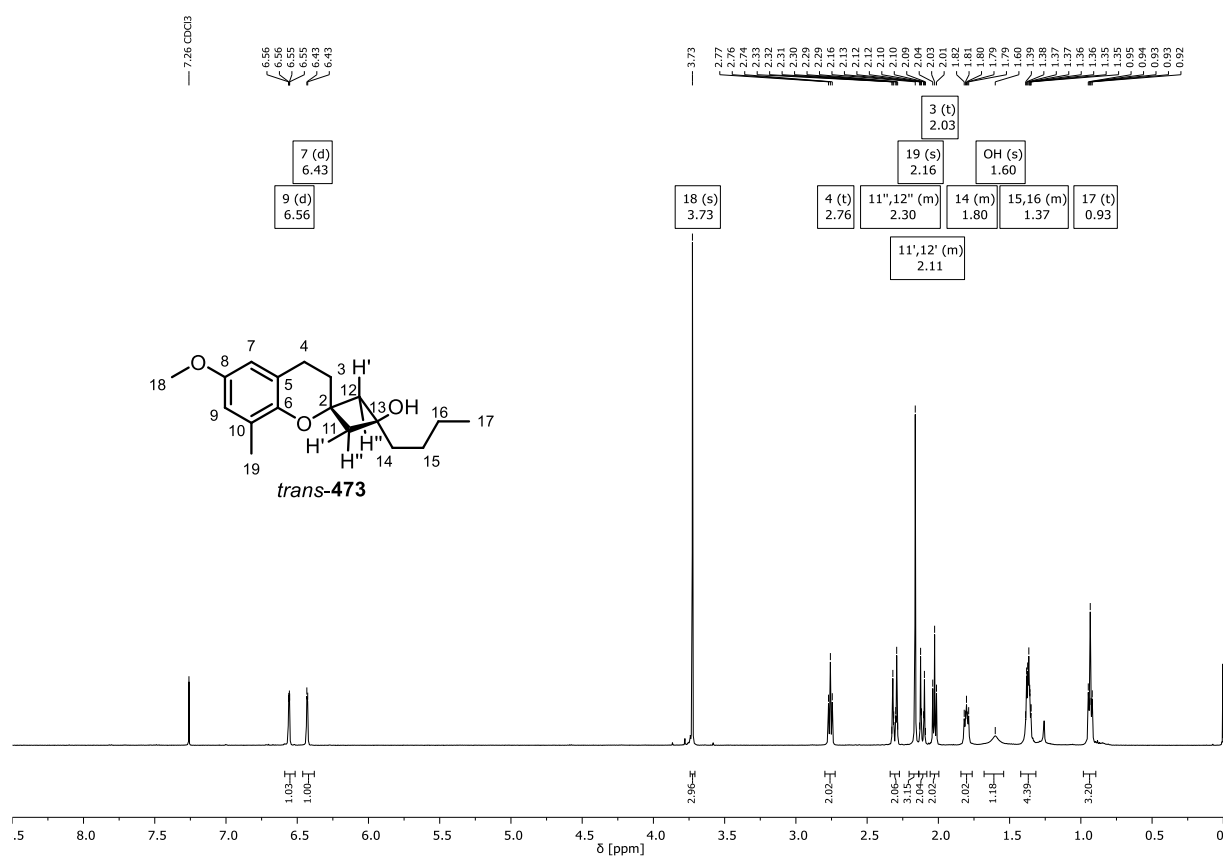
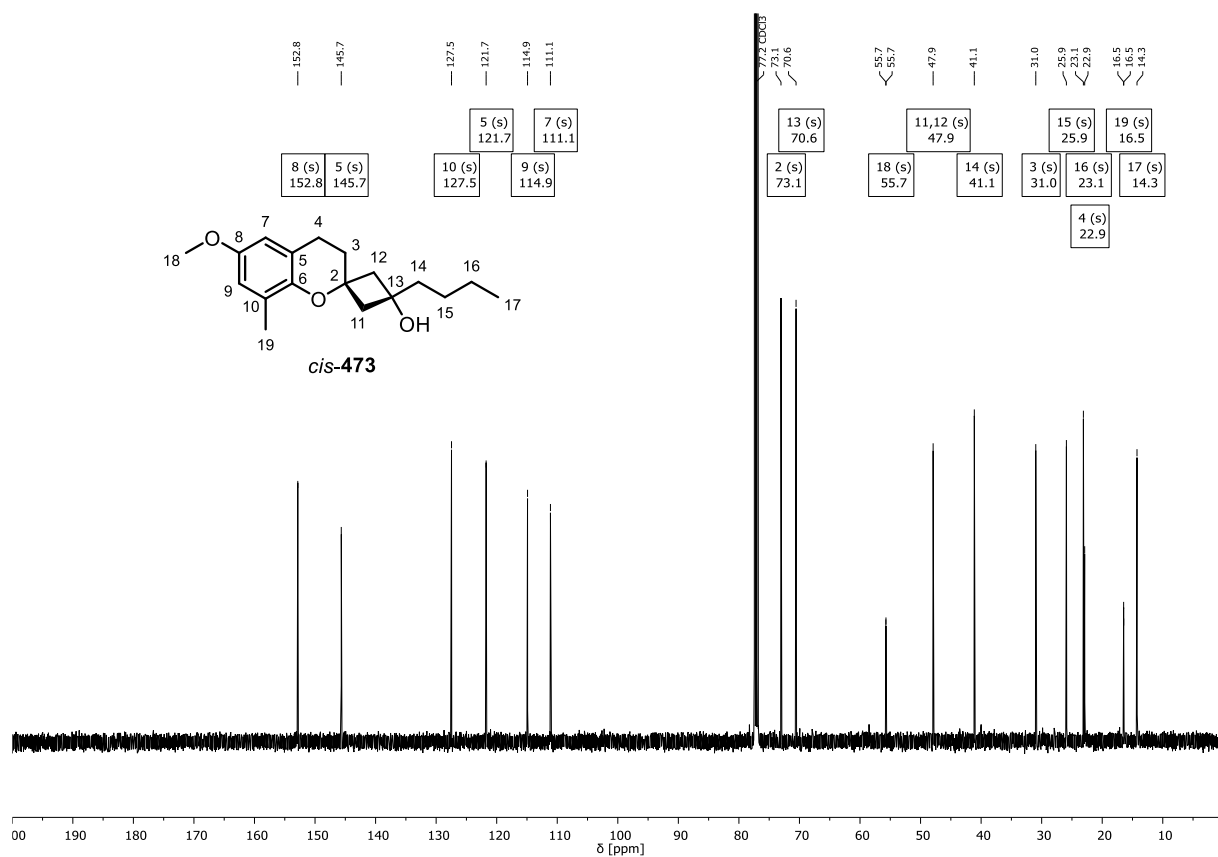
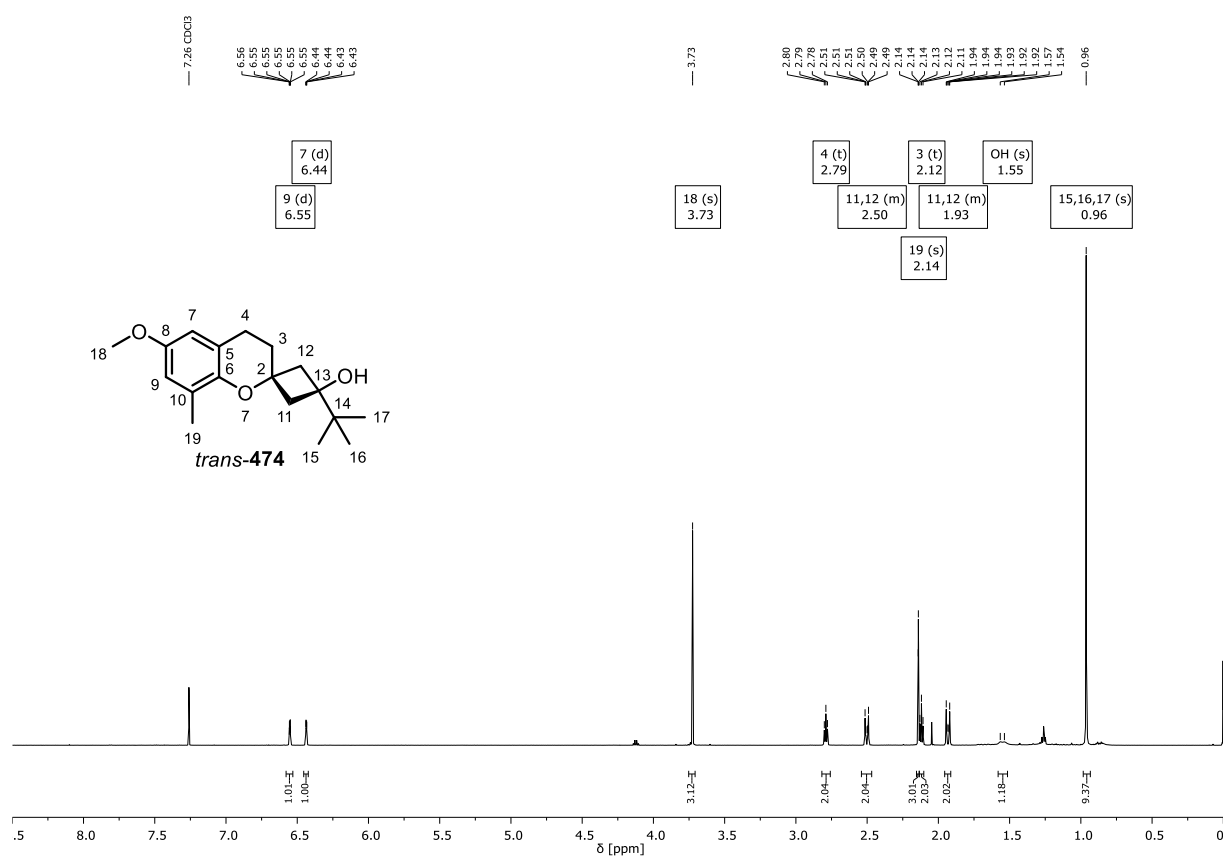
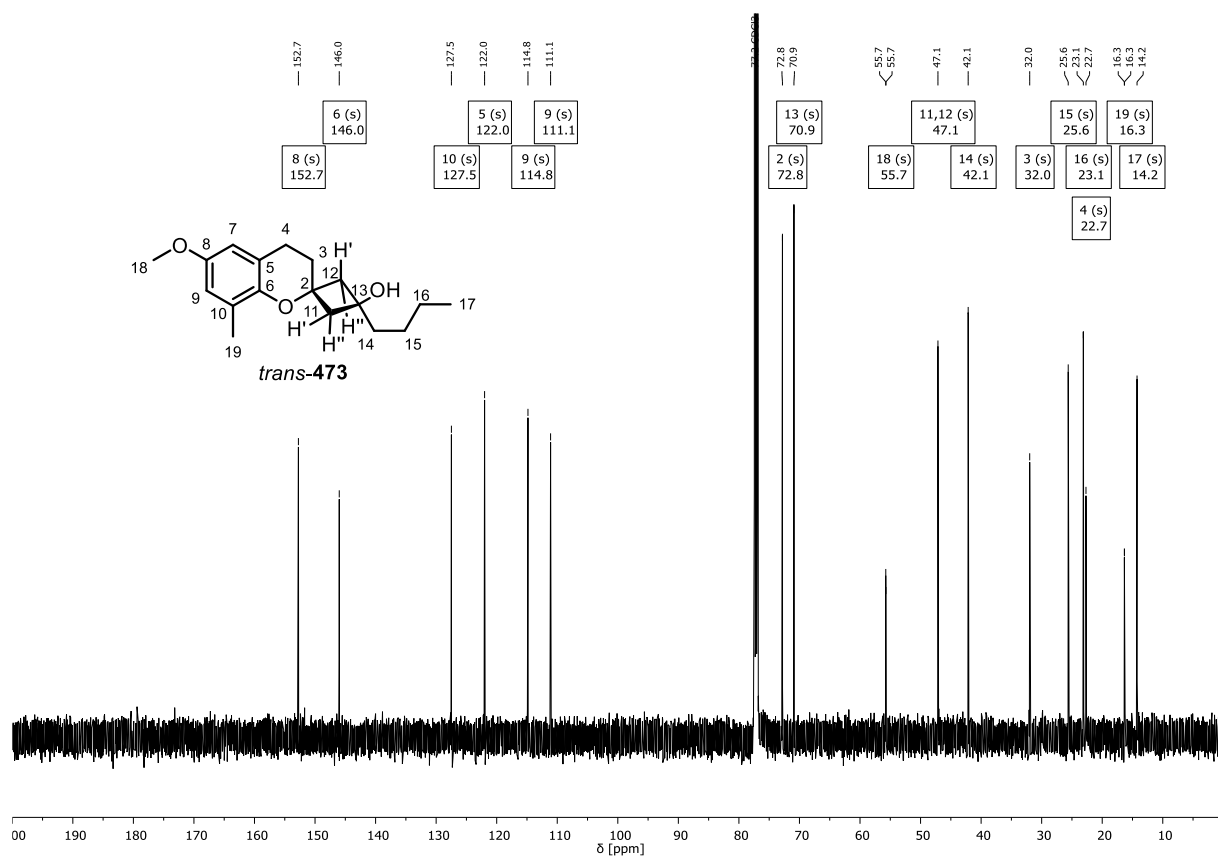


Figure 99: ^1H NMR (500 MHz, CDCl_3) spectrum of spirochromanol *cis*-**473**.





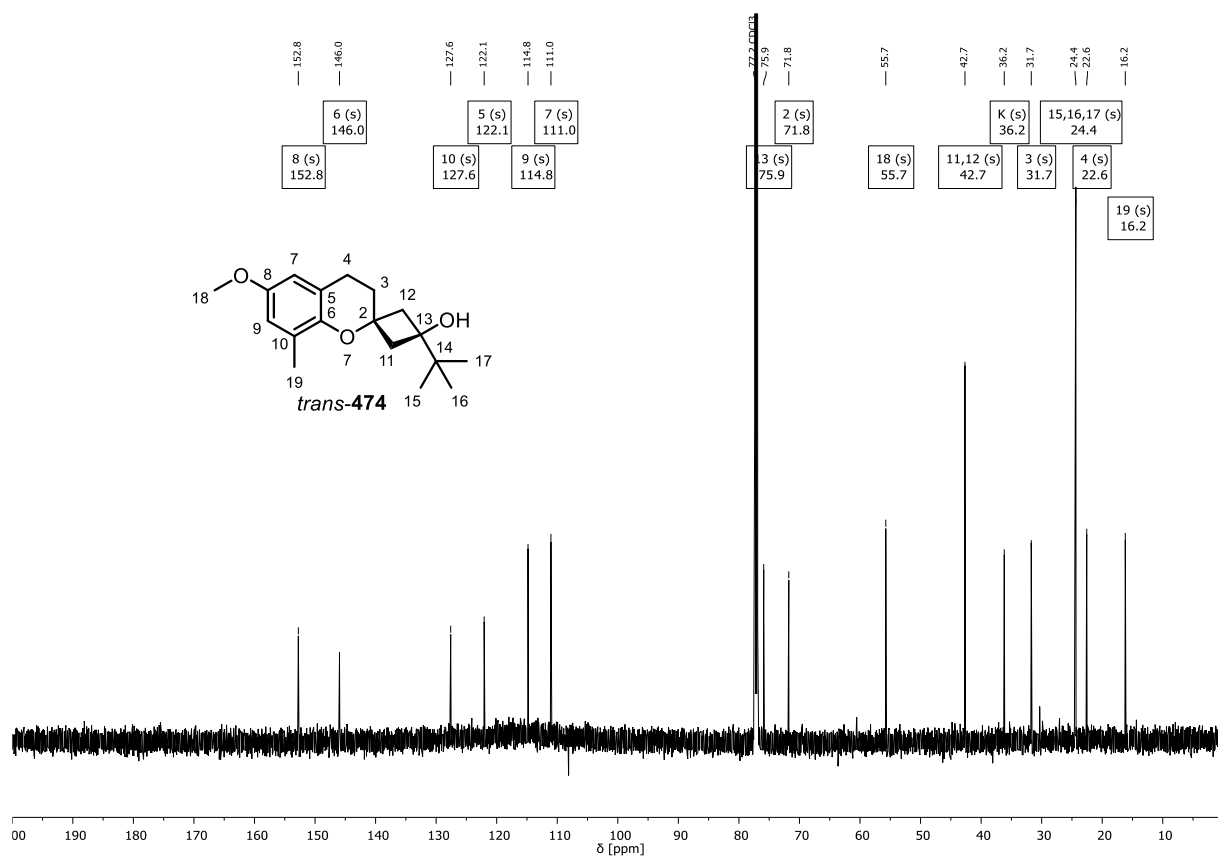


Figure 104: ^{13}C NMR (151 MHz, CDCl_3) spectrum of *spirochromanol trans-474*.

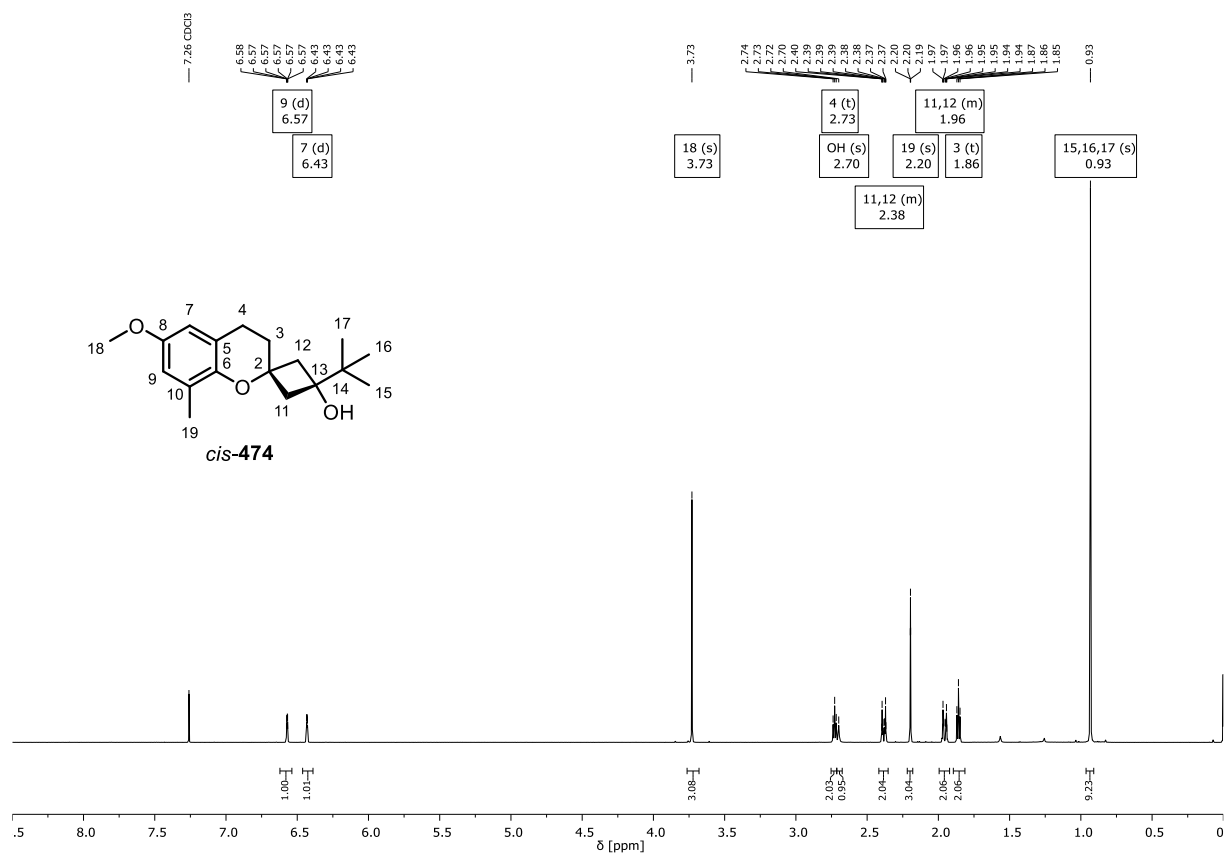


Figure 105: ^1H NMR (600 MHz, CDCl_3) spectrum of *spirochromanol cis-474*.

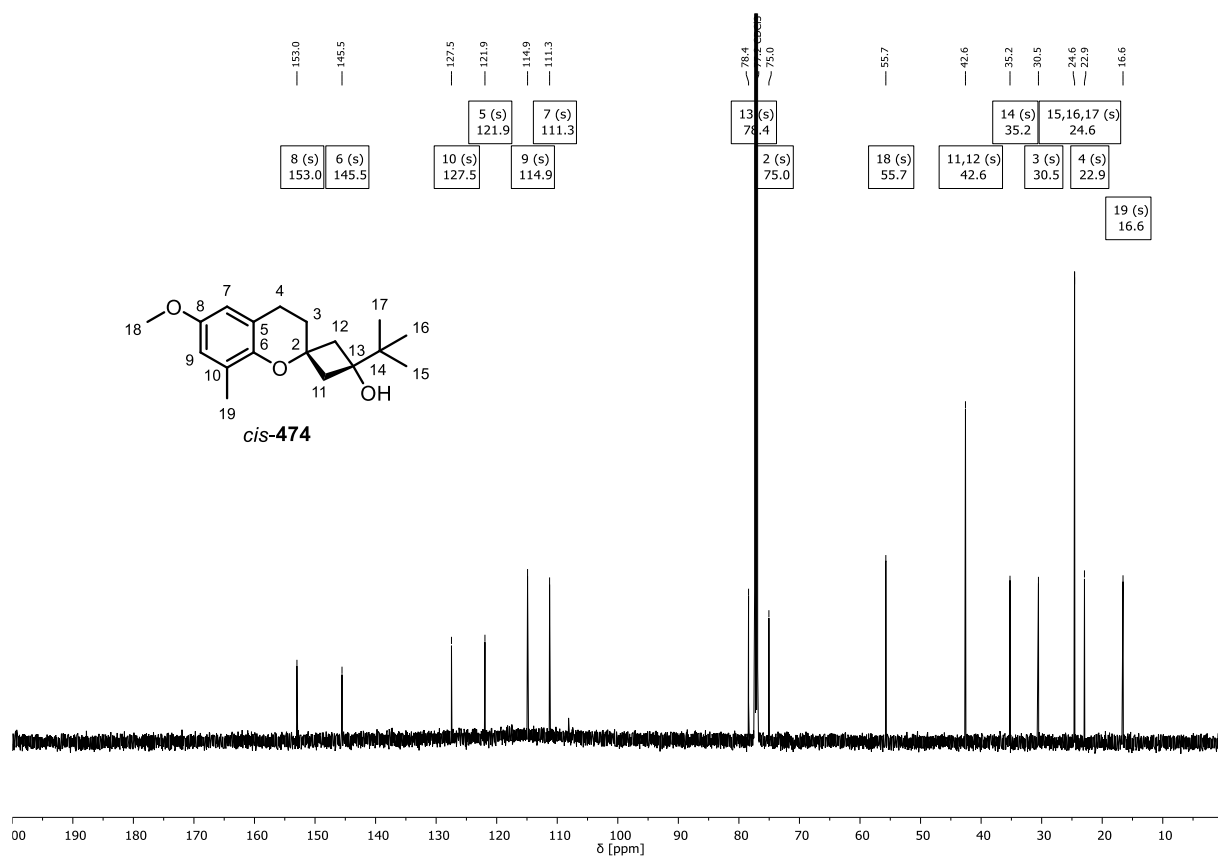
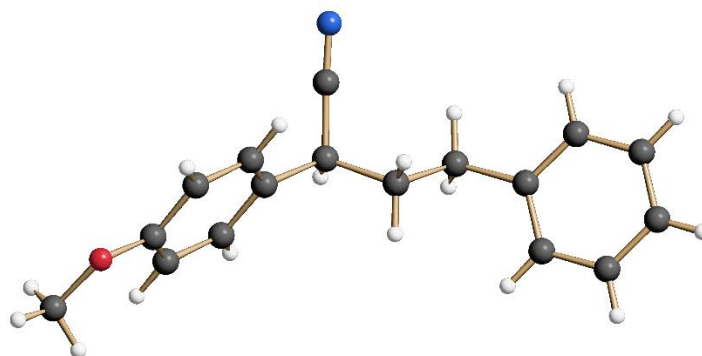


Figure 106: ¹³C NMR (151 MHz, CDCl₃) spectrum of *spirochromanol cis-474*.

12.3. X-ray crystallography

12.3.1. Crystal data of compound 245e

Table 10: Crystal data and structure refinement for *spirochromanol 245e*.

| | |
|-----------------------------------|----------------------------------------------------------------------------------------------|
| Identification code | jps314 |
| Empirical formula | C ₁₇ H ₁₇ NO |
| Moiety formula | C ₁₇ H ₁₇ NO |
| Molecular weight | 251.31 g/mol |
| Temperature | 100(2) K |
| Wavelength | 1.54178 Å |
| Crystal system | Monoclinic |
| Space group | P2 ₁ |
| Unit cell dimensions | a = 8.6090(3) Å, α = 90 ° b = 5.6470(2) Å, β = 105.424(2) ° c = 14.9535(6) Å, γ = 90 ° |
| Volume | 700.78(5) Å ³ |
| Z | 2 |
| Calculated density | 1.191 g/cm ³ |
| Absorption coefficient | 0.575 mm ⁻¹ |
| F(000) | 268 |
| Crystal size | 0.400 x 0.100 x 0.020 mm ³ |
| Θ-range for data collection | 3.066 ° to 72.477 °. |
| Index ranges | -10 ≤ h ≤ 10, -6 ≤ k ≤ 6, -18 ≤ l ≤ 18 |
| Reflections collected | 19663 |
| Independent reflections | 2730 [R(int) = 0.0443] |
| Completeness to Θ = 67.679° | 99.9% |
| Absorption correction | Semi-empirical from equivalents |
| Max. and min. transmission | 0.7536 and 0.5738 |
| Refinement method | Full-matrix least-squares on F ² |
| Data / restraints / parameters | 2730 / 1 / 173 |
| Goodness-of-fit on F ² | 1.043 |

| | |
|-----------------------------------|------------------------------------|
| Final R indices [$>2\sigma$ (1)] | R1 = 0.0299, wR2 = 0.0745 |
| R indices (all data) | R1 = 0.0312, wR2 = 0.0755 |
| Largest diff. peak and hole | 0.142 and -0.116 e.Å ⁻³ |

12.3.2. Crystal data of compound *cis*-438

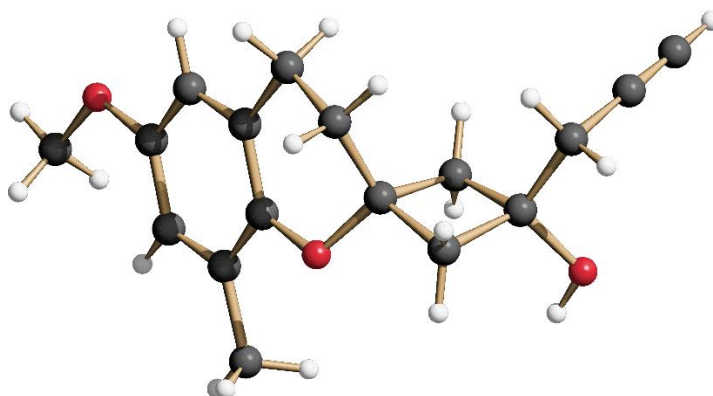


Table 11: Crystal data and structure refinement for *spirochromanol cis*-438.

| | |
|-----------------------------|----------------------------------------------------------------------------------------|
| Identification code | jps128 |
| Empirical formula | C ₁₇ H ₂₀ O ₃ |
| Moiety formula | C ₁₇ H ₂₀ O ₃ |
| Molecular weight | 272.33 g/mol |
| Temperature | 100(2) K |
| Wavelength | 1.54178 Å |
| Crystal system | Tetragonal |
| Space group | I4 ₁ /a |
| Unit cell dimensions | a = 23.0526(3) Å, α = 90 ° b = 23.0526(3) Å, β = 90 ° c = 11.4297(2) Å, γ = 90 ° |
| Volume | 6074.00(19) Å ³ |
| Z | 16 |
| Calculated density | 1.191 g/cm ³ |
| Absorption coefficient | 0.646 mm ⁻¹ |
| F(000) | 2336 |
| Crystal size | 0.100 x 0.060 x 0.020 mm ³ |
| Θ-range for data collection | 3.835 ° to 72.213 °. |
| Index ranges | -25 ≤ h ≤ 27, -28 ≤ k ≤ 28, -13 ≤ l ≤ 14 |
| Reflections collected | 39012 |
| Independent reflections | 2990 [R(int) = 0.0693] |
| Completeness to Θ = 67.679° | 99.7% |
| Absorption correction | Semi-empirical from equivalents |

| | |
|--------------------------------------|------------------------------------|
| Max. and min. transmission | 0.7536 and 0.6137 |
| Refinement method | Full-matrix least-squares on F^2 |
| Data / restraints / parameters | 2990 / 0 / 187 |
| Goodness-of-fit on F^2 | 1.054 |
| Final R indices [$I > 2\sigma$ (1)] | R1 = 0.0397, wR2 = 0.0971 |
| R indices (all data) | R1 = 0.0478, wR2 = 0.1015 |
| Largest diff. peak and hole | 0.326 and -0.173 e.Å ⁻³ |

12.3.3. Crystal data of compound *trans*-474

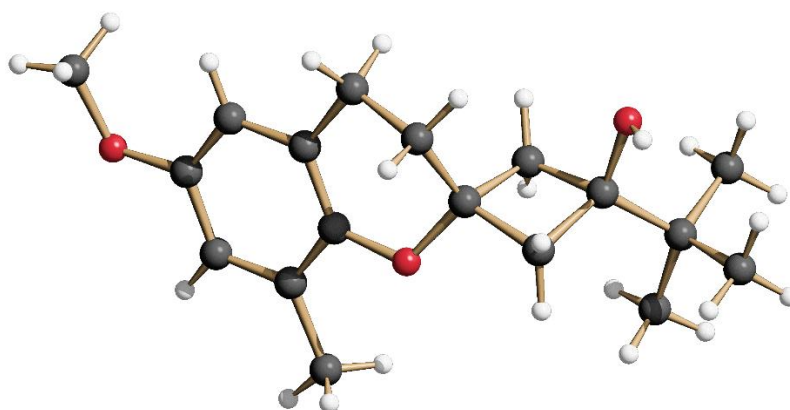


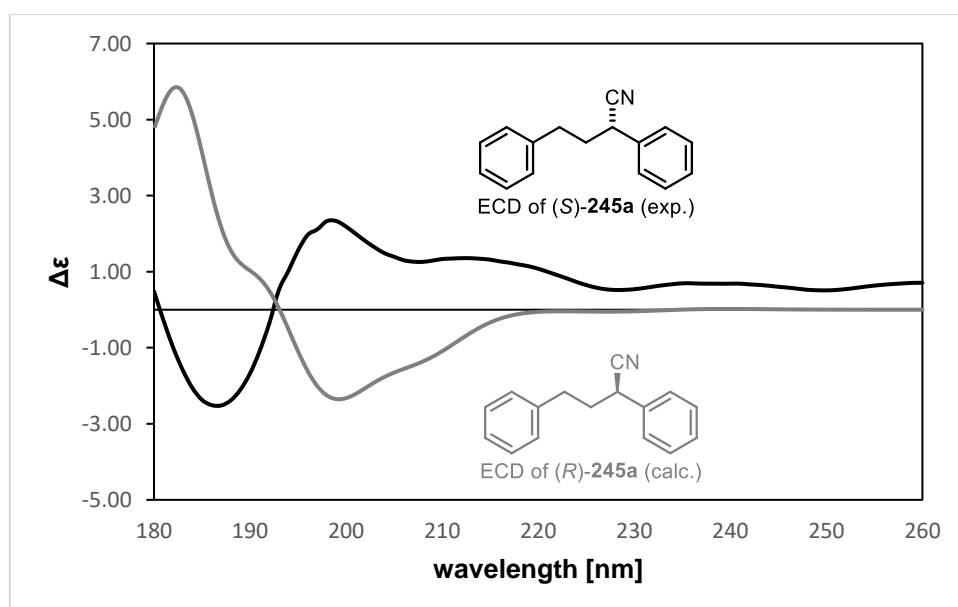
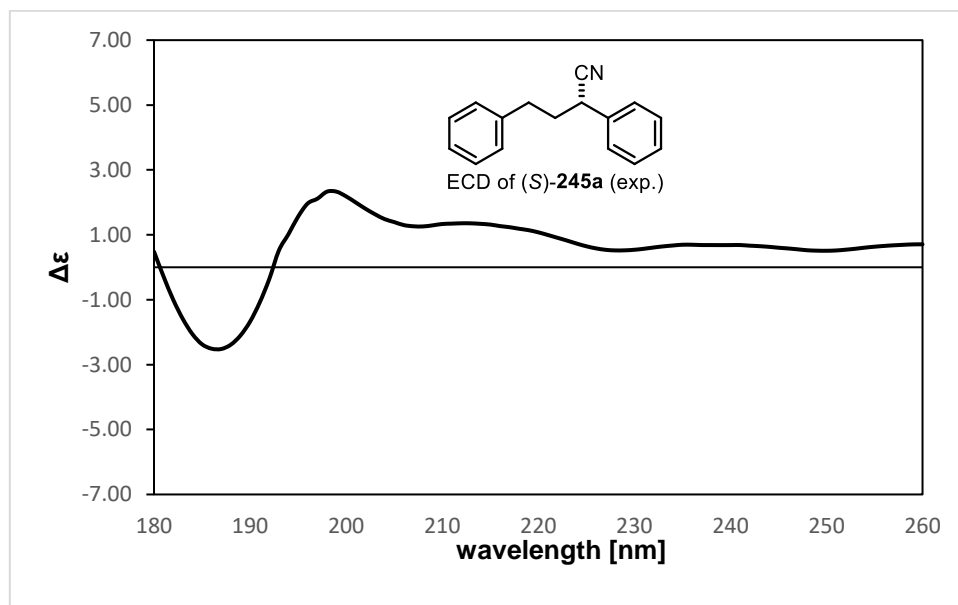
Table 12: Crystal data and structure refinement for *spirochromanol trans*-474.

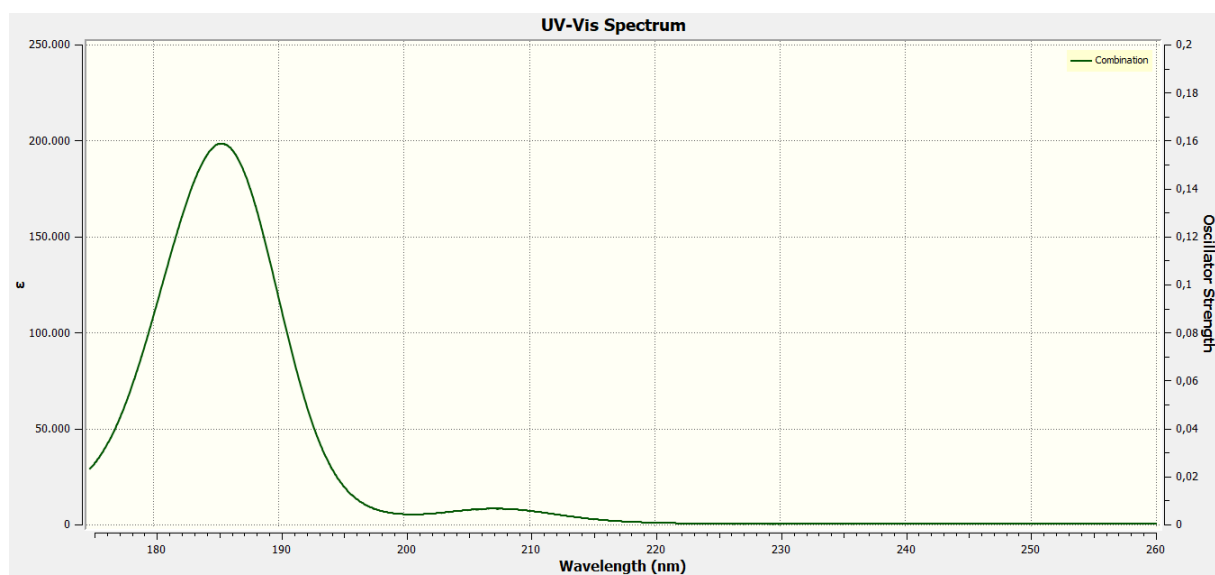
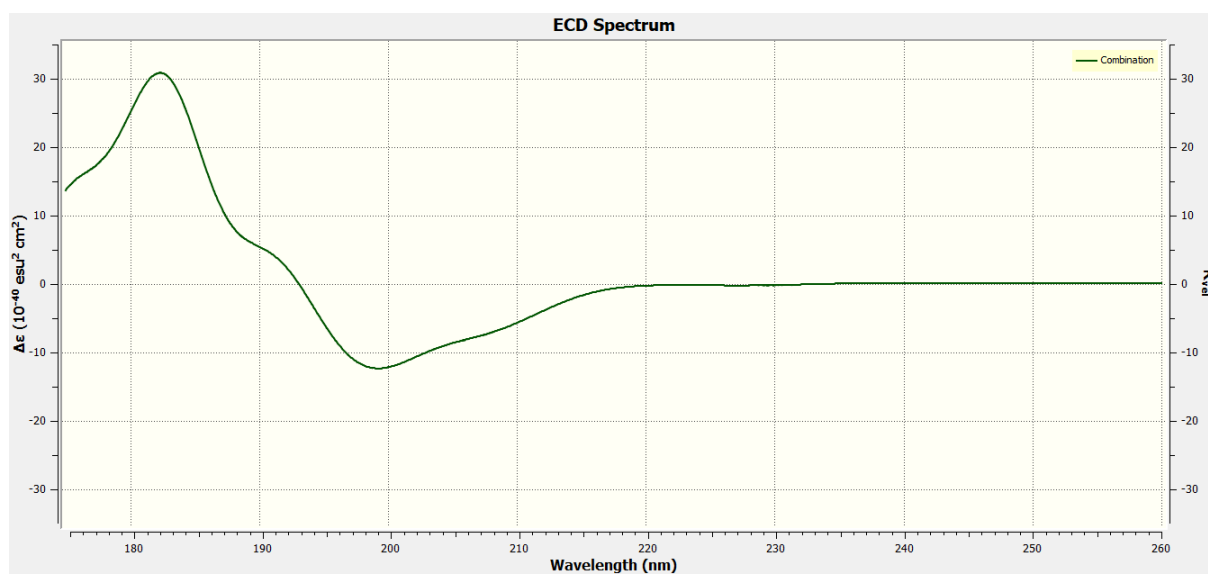
| | |
|-------------------------------------|----------------------------------------------------------------------------------------------------------------------------------------|
| Identification code | jps135 |
| Empirical formula | C ₁₈ H ₂₆ O ₃ |
| Moiety formula | C ₁₈ H ₂₆ O ₃ |
| Molecular weight | 290.40 g/mol |
| Temperature | 100(2) K |
| Wavelength | 1.54178 Å |
| Crystal system | Triclinic |
| Space group | P-1 |
| Unit cell dimensions | a = 5.97170(10) Å, α = 79.6030(10) ° b = 10.4362(2) Å, β = 85.1790(10) ° c = 13.5953(3) Å, γ = 75.2240(10) ° |
| Volume | 805.17(3) Å ³ |
| Z | 2 |
| Calculated density | 1.198 g/cm ³ |
| Absorption coefficient | 0.633 mm ⁻¹ |
| F(000) | 316 |
| Crystal size | 0.200 x 0.200 x 0.030 mm ³ |
| Θ -range for data collection | 3.308 ° to 72.200 °. |
| Index ranges | -7 ≤ h ≤ 7, -12 ≤ k ≤ 12, -16 ≤ l ≤ 16 |

| | |
|-----------------------------------------------------------|---------------------------------------|
| Reflections collected | 25620 |
| Independent reflections | 3142 [R(int) = 0.0551] |
| Completeness to $\Theta = 67.679^\circ$ | 99.1% |
| Absorption correction | Semi-empirical from equivalents |
| Max. and min. transmission | 0.7536 and 0.5909 |
| Refinement method | Full-matrix least-squares on F^2 |
| Data / restraints / parameters | 3142 / 0 / 199 |
| Goodness-of-fit on F^2 | 1.038 |
| Final R indices [$I > 2\sigma$ (1)] | R1 = 0.0407, wR2 = 0.1102 |
| R indices (all data) | R1 = 0.0430, wR2 = 0.1121 |
| Largest diff. peak and hole | 0.275 and -0.253 e. \AA^{-3} |

12.4. Stereochemical analysis by ECD

The ECD spectrum of (*S*)-2,4-diphenylbutyronitrile (**245a**) was measured on a Jasco j-715 CD spectropolarimeter in acetonitrile (0.030 mg/mL; 0.14×10^{-3} M solution). The calculated ECD and UV spectrum of (*R*)-2,4-diphenylbutyronitrile (*ent*-**245a**) was derived by DFT (CAM-B3LYP/Aug-CC-pVDZ, SCRF CPCM: Acetonitrile, Boltzmann-weighted on 15 conformers; peak half-width at half-height: 0.150 eV). Gaussian 16.0 Revision C.01 by Frisch *et al* was used.^[140]

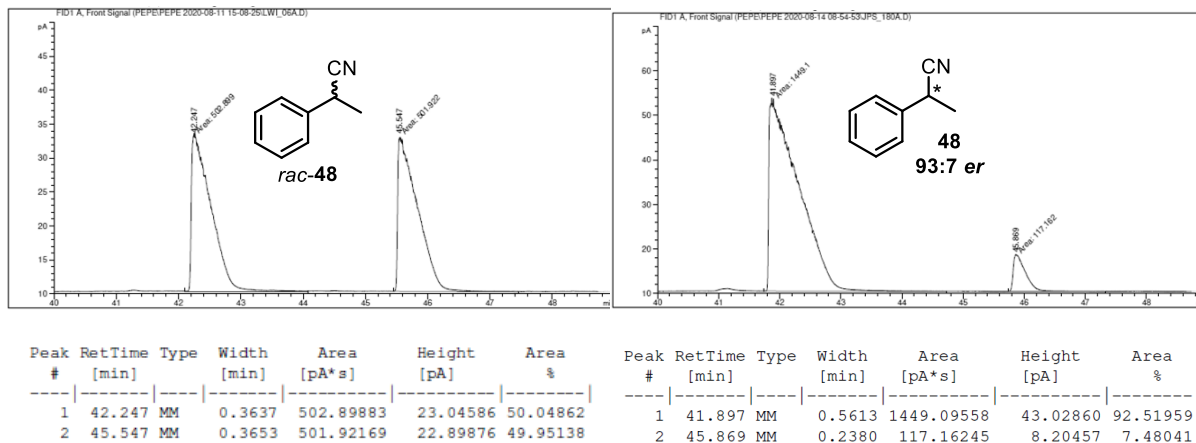




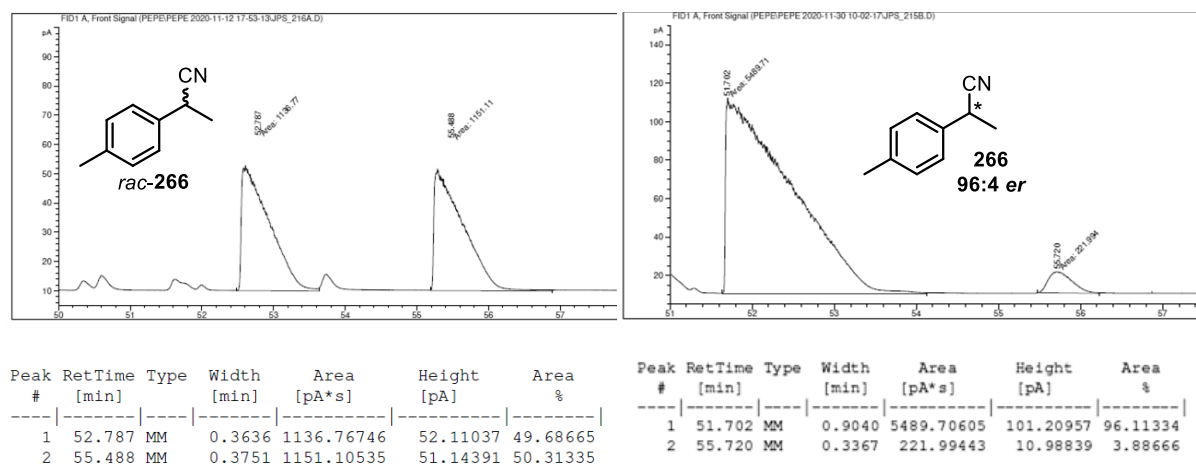
12.5. Stereochemical analysis by chromatography

12.5.1. Gas chromatography on chiral stationary phase

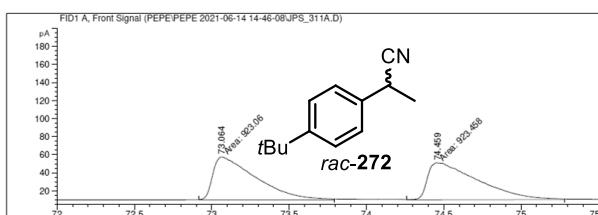
12.5.1.1. Enantiomeric resolution of compound 48



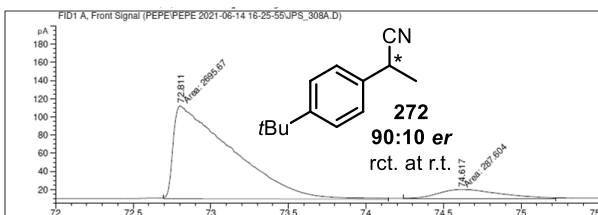
12.5.1.2. Enantiomeric resolution of compound 266



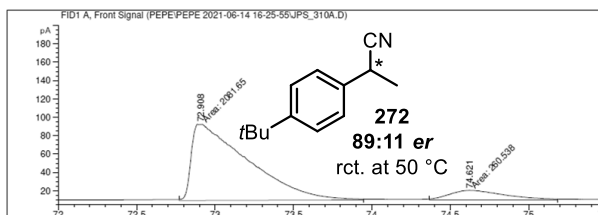
12.5.1.3. Enantiomeric resolution of compound 272



| Peak # | RetTime [min] | Type | Width [min] | Area [pA*s] | Height [pA] | Area % |
|--------|---------------|------|-------------|-------------|-------------|----------|
| 1 | 73.064 | MM | 0.3187 | 923.06042 | 48.27070 | 49.98924 |
| 2 | 74.459 | MM | 0.3738 | 923.45770 | 41.17212 | 50.01076 |

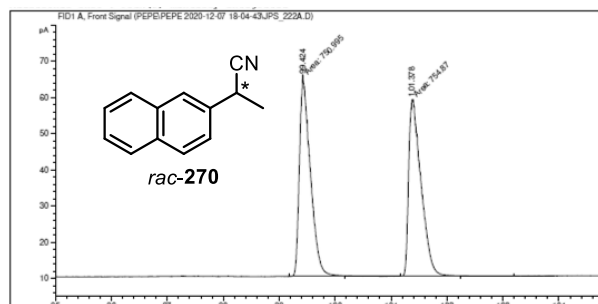


| Peak # | RetTime [min] | Type | Width [min] | Area [pA*s] | Height [pA] | Area % |
|--------|---------------|------|-------------|-------------|-------------|----------|
| 1 | 72.811 | MM | 0.4360 | 2695.67017 | 103.03954 | 90.35944 |
| 2 | 74.617 | MM | 0.4687 | 287.60440 | 10.22661 | 9.64056 |

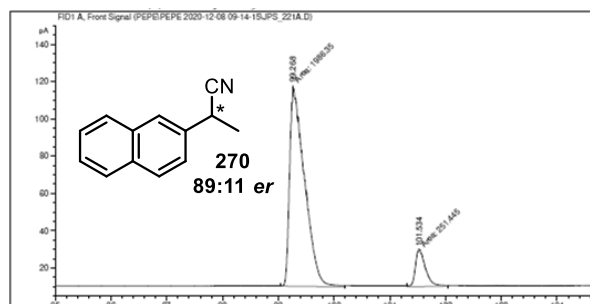


| Peak # | RetTime [min] | Type | Width [min] | Area [pA*s] | Height [pA] | Area % |
|--------|---------------|------|-------------|-------------|-------------|----------|
| 1 | 72.908 | MM | 0.4186 | 2081.65210 | 82.88372 | 88.87630 |
| 2 | 74.621 | MM | 0.4198 | 260.53815 | 10.34389 | 11.12370 |

12.5.1.4. Enantiomeric resolution of compound 270

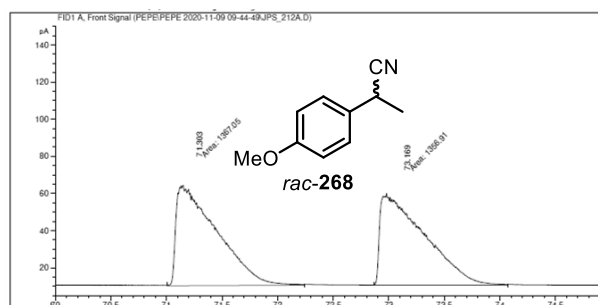


| Peak # | RetTime [min] | Type | Width [min] | Area [pA*s] | Height [pA] | Area % |
|--------|---------------|------|-------------|-------------|-------------|----------|
| 1 | 99.424 | MM | 0.2262 | 750.99457 | 55.33454 | 49.87132 |
| 2 | 101.378 | MM | 0.2564 | 754.87000 | 49.06187 | 50.12868 |

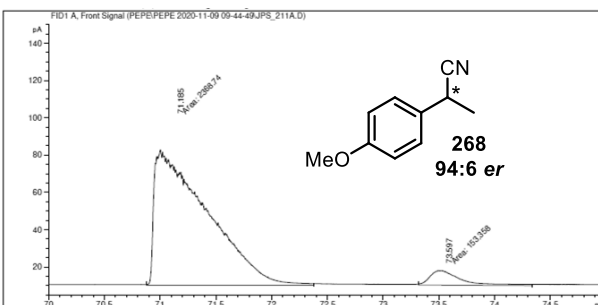


| Peak # | RetTime [min] | Type | Width [min] | Area [pA*s] | Height [pA] | Area % |
|--------|---------------|------|-------------|-------------|-------------|----------|
| 1 | 99.268 | MM | 0.3052 | 1986.35413 | 108.45785 | 88.76374 |
| 2 | 101.534 | MM | 0.2087 | 251.44493 | 20.07783 | 11.23626 |

12.5.1.5. Enantiomeric resolution of compound 268

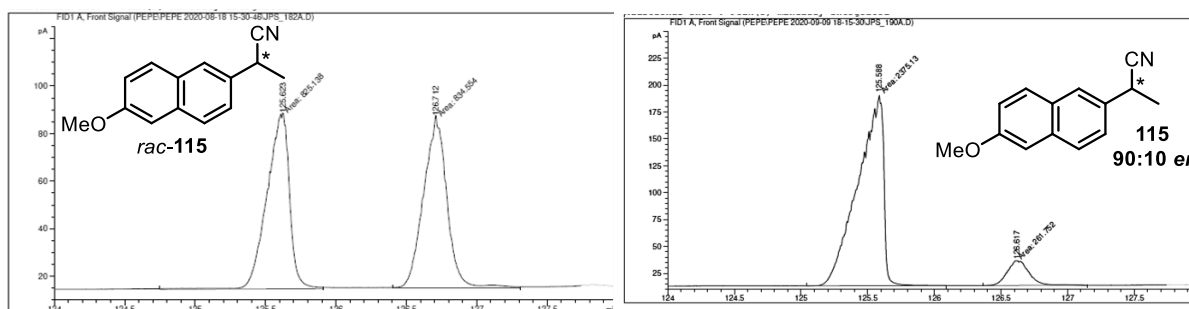


| Peak # | RetTime [min] | Type | Width [min] | Area [pA*s] | Height [pA] | Area % |
|--------|---------------|------|-------------|-------------|-------------|----------|
| 1 | 71.303 | MM | 0.3336 | 1367.04529 | 68.29559 | 50.18605 |
| 2 | 73.169 | MM | 0.3732 | 1356.90942 | 60.60064 | 49.81395 |



| Peak # | RetTime [min] | Type | Width [min] | Area [pA*s] | Height [pA] | Area % |
|--------|---------------|------|-------------|-------------|-------------|----------|
| 1 | 71.185 | MM | 0.4339 | 2368.74316 | 90.98766 | 93.91943 |
| 2 | 73.597 | MM | 0.2455 | 153.35811 | 10.41173 | 6.08057 |

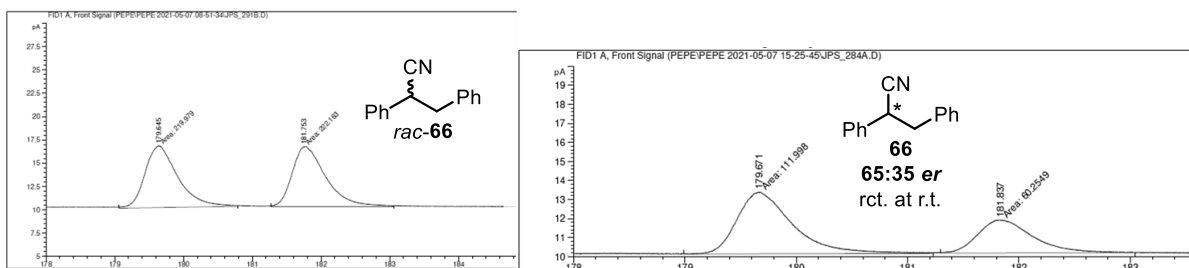
12.5.1.6. Enantiomeric resolution of compound 115



| Peak # | RetTime [min] | Type | Width [min] | Area [pA*s] | Height [pA] | Area % |
|--------|---------------|------|-------------|-------------|-------------|----------|
| 1 | 125.623 | MM | 0.1877 | 825.13849 | 73.26428 | 49.71636 |
| 2 | 126.712 | MM | 0.1951 | 834.55353 | 71.28531 | 50.28364 |

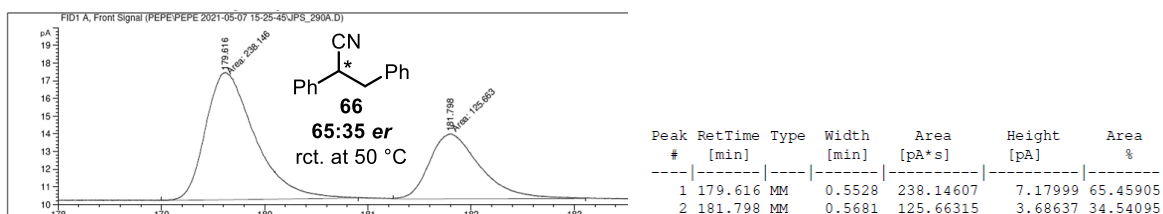
| Peak # | RetTime [min] | Type | Width [min] | Area [pA*s] | Height [pA] | Area % |
|--------|---------------|------|-------------|-------------|-------------|----------|
| 1 | 125.588 | MM | 0.2228 | 2375.12891 | 177.67867 | 90.07344 |
| 2 | 126.617 | MM | 0.1908 | 261.75156 | 22.86023 | 9.92656 |

12.5.1.7. Enantiomeric resolution of compound 66



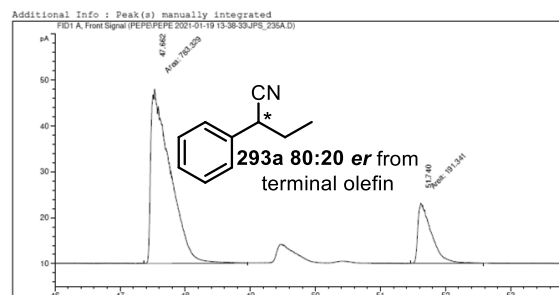
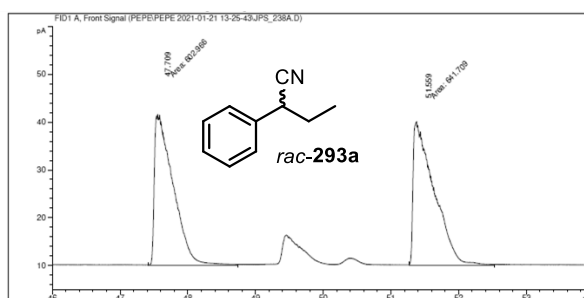
| Peak # | RetTime [min] | Type | Width [min] | Area [pA*s] | Height [pA] | Area % |
|--------|---------------|------|-------------|-------------|-------------|----------|
| 1 | 179.645 | MM | 0.5538 | 219.97852 | 6.62020 | 49.75300 |
| 2 | 181.753 | MM | 0.5712 | 222.16273 | 6.48269 | 50.24700 |

| Peak # | RetTime [min] | Type | Width [min] | Area [pA*s] | Height [pA] | Area % |
|--------|---------------|------|-------------|-------------|-------------|----------|
| 1 | 179.671 | MM | 0.5758 | 111.99785 | 3.24207 | 65.01950 |
| 2 | 181.837 | MM | 0.5811 | 60.25487 | 1.72830 | 34.98050 |



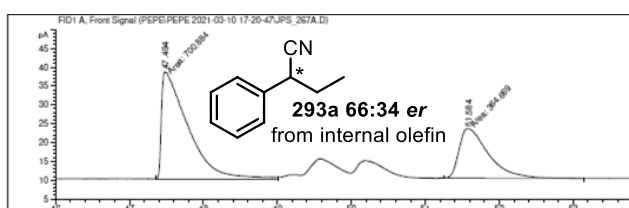
| Peak # | RetTime [min] | Type | Width [min] | Area [pA*s] | Height [pA] | Area % |
|--------|---------------|------|-------------|-------------|-------------|----------|
| 1 | 179.616 | MM | 0.5528 | 238.14607 | 7.17999 | 65.45905 |
| 2 | 181.798 | MM | 0.5681 | 125.66315 | 3.68637 | 34.54095 |

12.5.1.8. Enantiomeric resolution of compound 293a



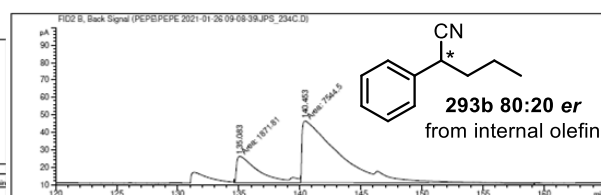
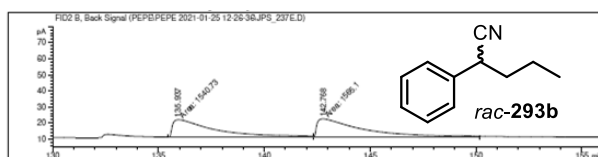
| Peak # | RetTime [min] | Type | Width [min] | Area [pA*s] | Height [pA] | Area % |
|--------|---------------|------|-------------|-------------|-------------|----------|
| 1 | 47.709 | MM | 0.2578 | 602.96564 | 38.98811 | 48.44362 |
| 2 | 51.559 | MM | 0.3098 | 641.70929 | 34.52360 | 51.55638 |

| Peak # | RetTime [min] | Type | Width [min] | Area [pA*s] | Height [pA] | Area % |
|--------|---------------|------|-------------|-------------|-------------|----------|
| 1 | 47.662 | MM | 0.2754 | 783.32855 | 47.39952 | 80.36861 |
| 2 | 51.740 | MM | 0.2009 | 191.34117 | 15.86982 | 19.63139 |



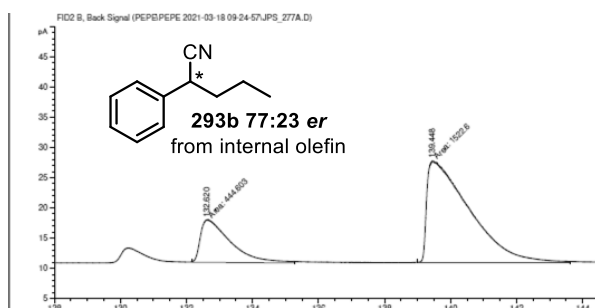
| Peak # | RetTime [min] | Type | Width [min] | Area [pA*s] | Height [pA] | Area % |
|--------|---------------|------|-------------|-------------|-------------|----------|
| 1 | 47.494 | MM | 0.4099 | 700.88373 | 28.49651 | 65.77655 |
| 2 | 51.584 | MM | 0.4623 | 364.66885 | 13.14759 | 34.22345 |

12.5.1.9. Enantiomeric resolution of compound 293b



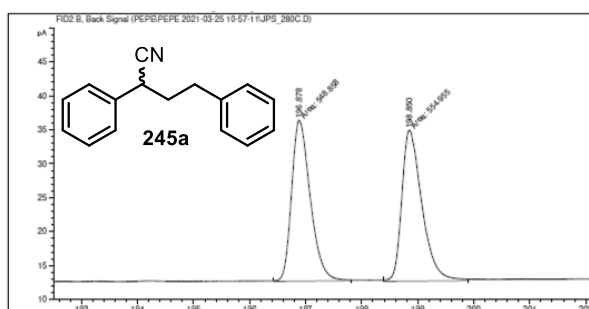
| Peak # | RetTime [min] | Type | Width [min] | Area [pA*s] | Height [pA] | Area % |
|--------|---------------|------|-------------|-------------|-------------|----------|
| 1 | 135.937 | MM | 2.3509 | 1540.72681 | 10.92307 | 49.60767 |
| 2 | 142.768 | MM | 2.3721 | 1565.09692 | 10.99644 | 50.39233 |

| Peak # | RetTime [min] | Type | Width [min] | Area [pA*s] | Height [pA] | Area % |
|--------|---------------|------|-------------|-------------|-------------|----------|
| 1 | 135.083 | MM | 2.0944 | 1871.80774 | 14.89539 | 19.87836 |
| 2 | 140.453 | MM | 3.5711 | 7544.50146 | 35.21056 | 80.12164 |

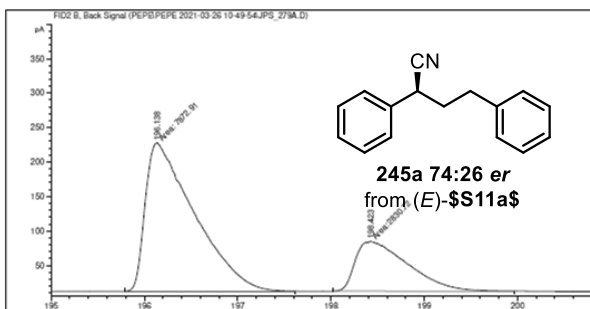


| Peak # | RetTime [min] | Type | Width [min] | Area [pA*s] | Height [pA] | Area % |
|--------|---------------|------|-------------|-------------|-------------|----------|
| 1 | 132.620 | MM | 1.0467 | 444.60333 | 7.07929 | 22.60083 |
| 2 | 139.448 | MM | 1.5022 | 1522.59607 | 16.89256 | 77.39917 |

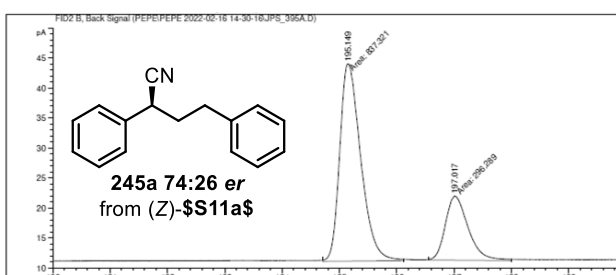
12.5.1.10. Enantiomeric resolution of compound 245a



| Peak # | RetTime [min] | Type | Width [min] | Area [pA*s] | Height [pA] | Area % |
|--------|---------------|------|-------------|-------------|-------------|----------|
| 1 | 196.878 | MM | 0.3856 | 548.85785 | 23.72592 | 49.72380 |
| 2 | 198.850 | MM | 0.4157 | 554.95526 | 22.25117 | 50.27620 |

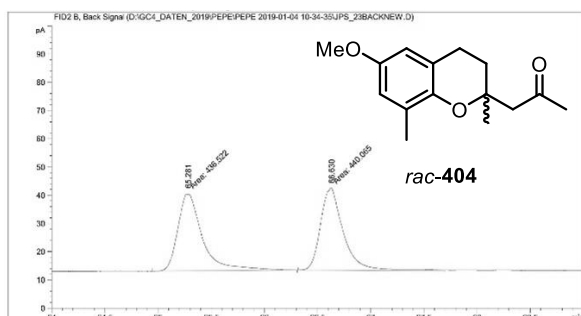


| Peak # | RetTime [min] | Type | Width [min] | Area [pA*s] | Height [pA] | Area % |
|--------|---------------|------|-------------|-------------|-------------|----------|
| 1 | 196.138 | MM | 0.6083 | 7872.90723 | 215.72379 | 73.55361 |
| 2 | 198.423 | MM | 0.6529 | 2830.72412 | 72.25616 | 26.44639 |

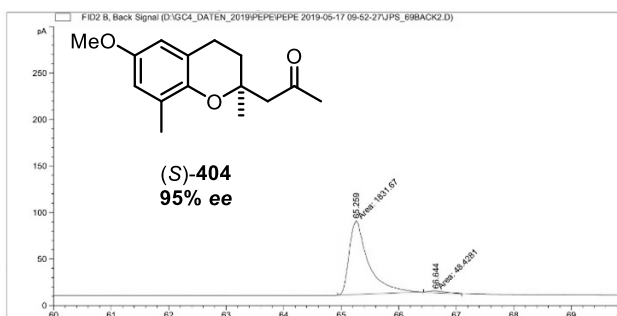


| Peak # | RetTime [min] | Type | Width [min] | Area [pA*s] | Height [pA] | Area % |
|--------|---------------|------|-------------|-------------|-------------|----------|
| 1 | 195.149 | MM | 0.4240 | 837.32129 | 32.91147 | 73.86321 |
| 2 | 197.017 | MM | 0.4599 | 296.28940 | 10.73773 | 26.13679 |

12.5.1.11. Enantiomeric resolution of compound 404



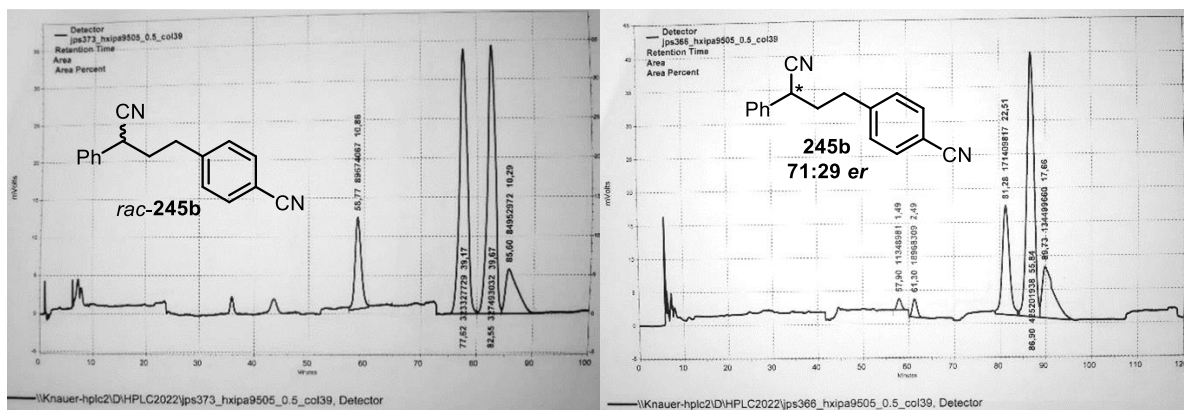
| Peak # | RetTime [min] | Type | Width [min] | Area [pA*s] | Height [pA] | Area % |
|--------|---------------|------|-------------|-------------|-------------|----------|
| 1 | 65.281 | MM | 0.2555 | 436.52219 | 28.47865 | 49.79790 |
| 2 | 66.630 | MM | 0.2439 | 440.06528 | 30.06711 | 50.20210 |



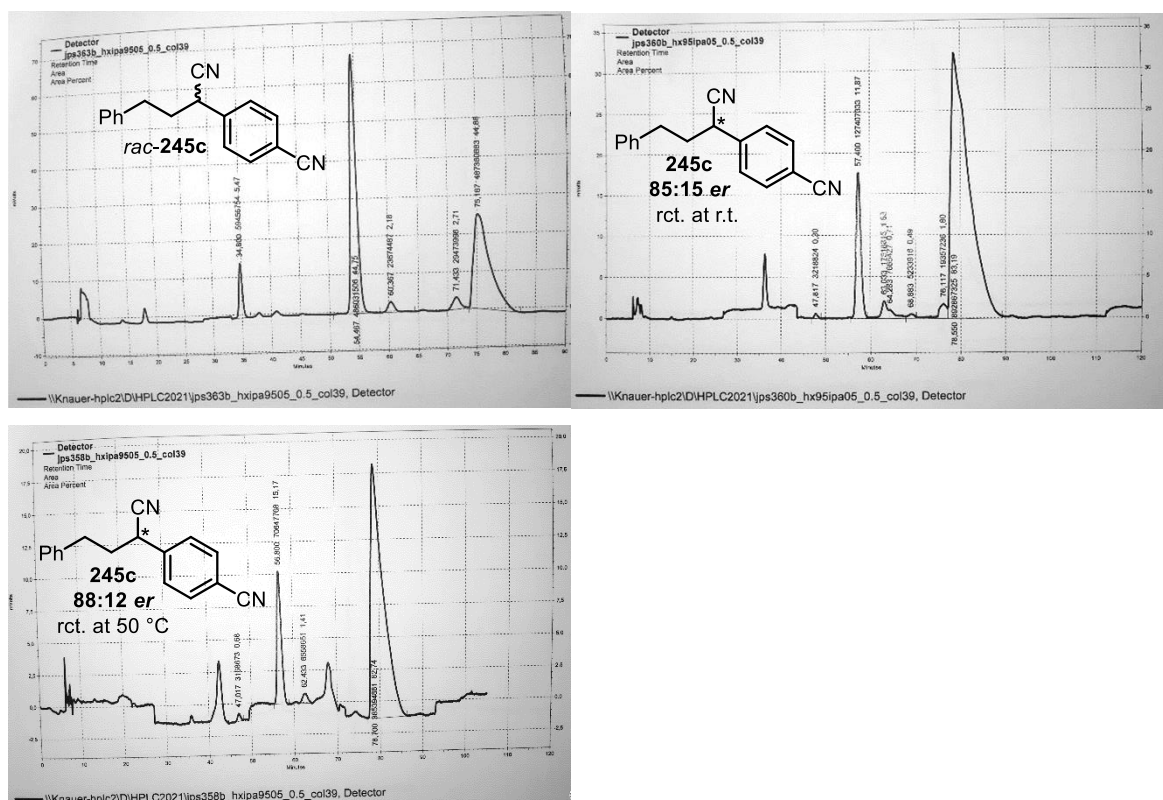
| Peak # | RetTime [min] | Type | Width [min] | Area [pA*s] | Height [pA] | Area % |
|--------|---------------|------|-------------|-------------|-------------|----------|
| 1 | 65.259 | MM | 0.3852 | 1831.67468 | 79.25670 | 97.42418 |
| 2 | 66.644 | MM | 0.3766 | 48.42808 | 2.14312 | 2.57582 |

12.5.2. High performance liquid chromatography on chiral stationary phase

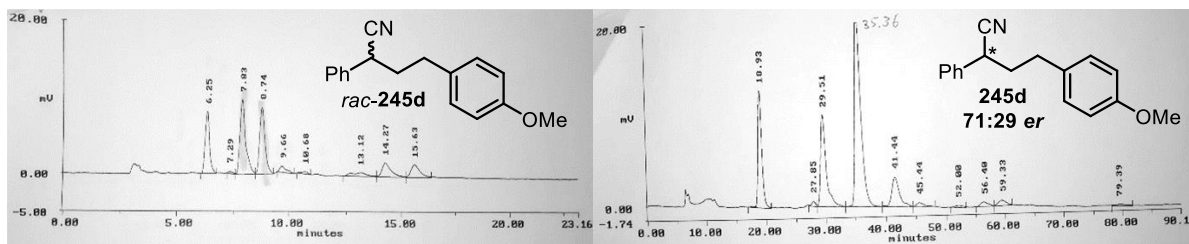
12.5.2.1. Enantiomeric resolution of compound 245b



12.5.2.2. Enantiomeric resolution of compound 245c

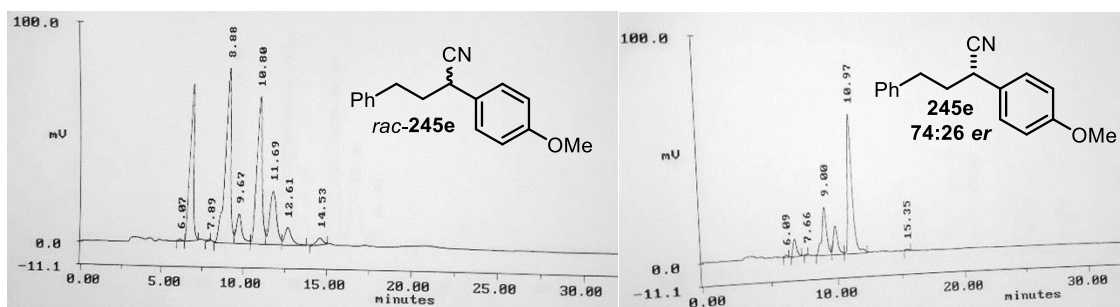


12.5.2.3. Enantiomeric resolution of compound 245d



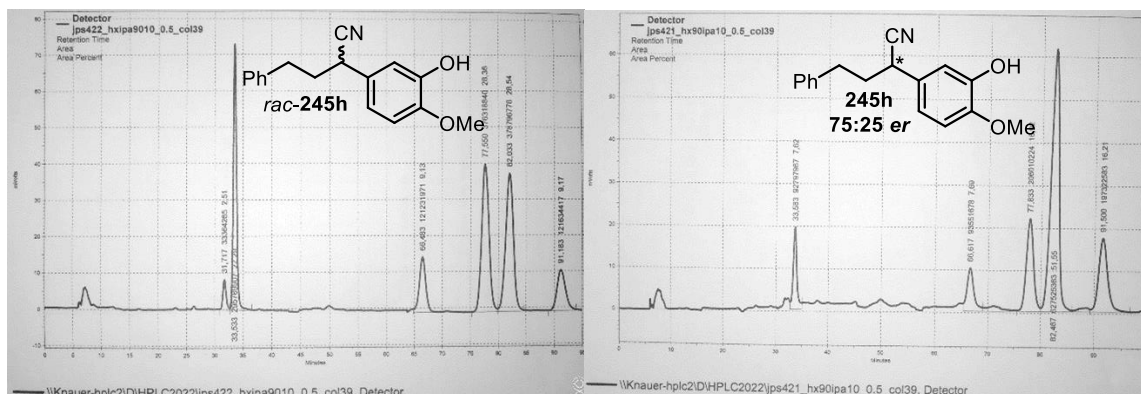
| NO | RT | AREA | BC | NO | RT | AREA | BC | | |
|-------|-------|--------|---------|----|----|-------|---------|--------|----|
| 1 | 6.25 | 107734 | 19.110 | BB | 1 | 18.93 | 560323 | 17.550 | BB |
| 2 | 7.29 | 1905 | 0.338 | BB | 2 | 27.85 | 16396 | 0.514 | BB |
| 3 | 7.83 | 173803 | 30.830 | BB | 3 | 29.51 | 629721 | 19.724 | BB |
| 4 | 8.74 | 147085 | 26.091 | BB | 4 | 35.36 | 1532102 | 47.987 | BB |
| 5 | 9.66 | 15739 | 2.792 | BB | 5 | 41.44 | 291433 | 9.128 | BB |
| 6 | 10.68 | 4918 | 0.872 | BB | 6 | 45.44 | 39219 | 1.228 | BB |
| 7 | 13.12 | 20841 | 3.697 | BB | 7 | 52.00 | 15275 | 0.478 | BB |
| 8 | 14.27 | 49088 | 8.707 | BB | 8 | 56.40 | 42182 | 1.321 | BB |
| 9 | 15.63 | 42635 | 7.563 | BB | 9 | 59.33 | 52031 | 1.630 | BB |
| TOTAL | | 563748 | 100.000 | | 10 | 79.39 | 14036 | 0.440 | BB |

12.5.2.4. Enantiomeric resolution of compound 245e

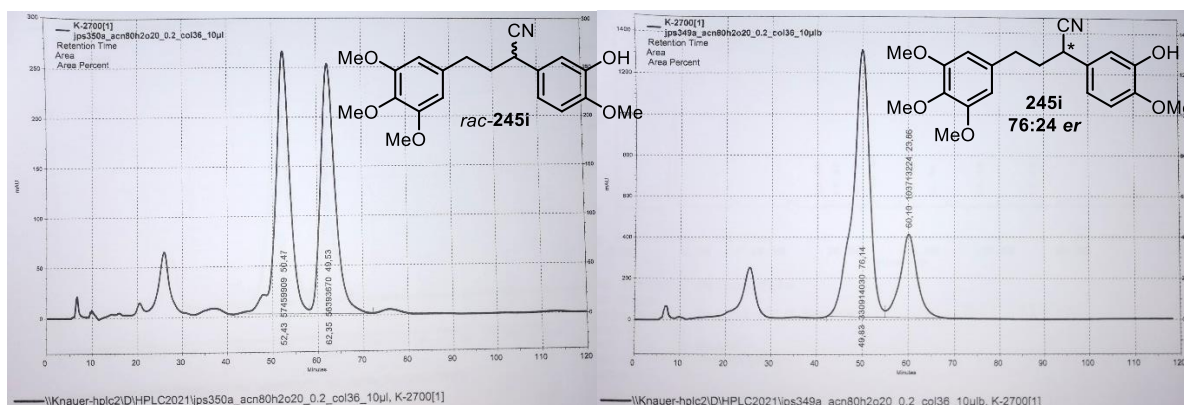


| NO | RT | AREA | BC | NO | RT | AREA | BC | | |
|-------|-------|---------|---------|----|-------|-------|---------|---------|----|
| 1 | 6.07 | 7259 | 0.127 | BB | 1 | 6.09 | 5373 | 0.221 | BB |
| 2 | 6.67 | 1163819 | 20.406 | BB | 2 | 6.73 | 135409 | 5.563 | BB |
| 3 | 7.89 | 4186 | 0.073 | BB | 3 | 7.66 | 3152 | 0.130 | BB |
| 4 | 8.88 | 1790111 | 31.387 | BV | 4 | 9.00 | 522190 | 21.452 | BV |
| 5 | 9.67 | 297968 | 5.224 | VV | 5 | 9.80 | 268938 | 11.048 | VB |
| 6 | 10.80 | 1487917 | 26.088 | VV | 6 | 10.97 | 1493453 | 61.353 | BB |
| 7 | 11.69 | 684589 | 12.003 | VV | 7 | 15.35 | 5684 | 0.234 | BB |
| 8 | 12.61 | 202173 | 3.545 | VB | | | | | |
| 9 | 14.53 | 65403 | 1.147 | BB | | | | | |
| TOTAL | | 5703425 | 100.000 | | TOTAL | | 2434199 | 100.000 | |

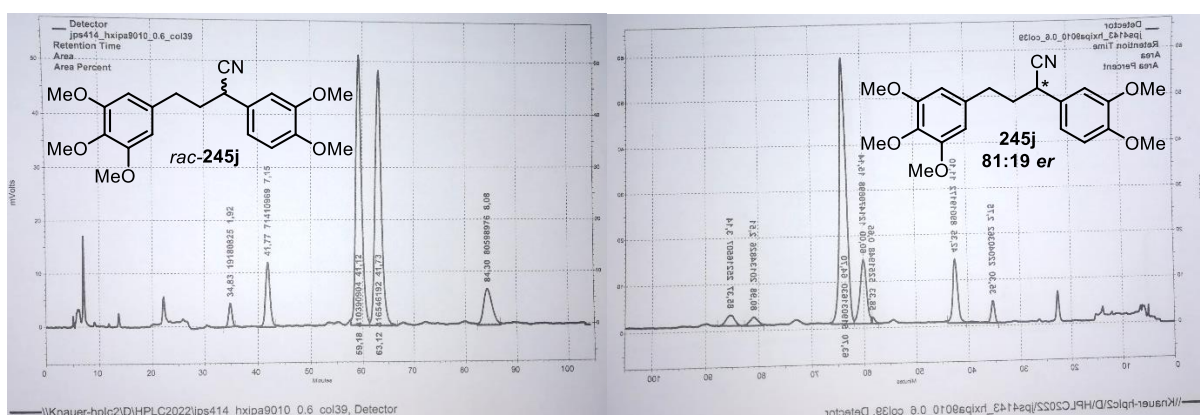
12.5.2.5. Enantiomeric resolution of compound 245h



12.5.2.6. Enantiomeric resolution of compound 245i



12.5.2.7. Enantiomeric resolution of compound 245j



12.6. Statutory Declaration

According to the doctoral degree regulations published 12th March 2020:

„Hiermit versichere ich an Eides statt, dass ich die vorliegende Dissertation selbstständig und ohne die Benutzung anderer als der angegebenen Hilfsmittel und Literatur angefertigt habe. Alle Stellen, die wörtlich oder sinngemäß aus veröffentlichten und nicht veröffentlichten Werken dem Wortlaut oder dem Sinn nach entnommen wurden, sind als solche kenntlich gemacht. Ich versichere an Eides statt, dass diese Dissertation noch keiner anderen Fakultät oder Universität zur Prüfung vorgelegen hat; dass sie - abgesehen von unten angegebenen Teilpublikationen und eingebundenen Artikeln und Manuskripten - noch nicht veröffentlicht worden ist sowie, dass ich eine Veröffentlichung der Dissertation vor Abschluss der Promotion nicht ohne Genehmigung des Promotionsausschusses vornehmen werde. Die Bestimmungen dieser Ordnung sind mir bekannt. Darüber hinaus erkläre ich hiermit, dass ich die Ordnung zur Sicherung guter wissenschaftlicher Praxis und zum Umgang mit wissenschaftlichem Fehlverhalten der Universität zu Köln gelesen und sie bei der Durchführung der Dissertation zugrundeliegenden Arbeiten und der schriftlich verfassten Dissertation beachtet habe und verpflichte mich hiermit, die dort genannten Vorgaben bei allen wissenschaftlichen Tätigkeiten zu beachten und umzusetzen. Ich versichere, dass die eingereichte elektronische Fassung der eingereichten Druckfassung vollständig entspricht.“

The following partial publications are available:

F. Ratsch, J. P. Strache, W. Schlundt, J.-M. Neudörfl, A. Adler, S. Aziz, B. Goldfuss, H.-G. Schmalz, „Enantioselective Cleavage of Cyclobutanols Through Ir-Catalyzed C–C Bond Activation: Mechanistic and Synthetic Aspects”, *Chem. Eur. J.* **2021**, 27, 4640-4652.

J. P. Strache, L. Münzer, A. Adler, D. Blunk, H.-G. Schmalz, „Enantioselective Nickel-Catalyzed Hydrocyanation of Homostilbenes“, *Eur. J. Org. Chem.* **2023**, e202300050.


Posters:

J. P. Strache, F. Ratsch, W. Schlundt, H.-G. Schmalz, „Enantioselective Synthesis of Chromane Natural Products *via* Iridium-Catalyzed C-C Bond Activation of Cyclobutanol Intermediates”, OMCOS July **2019**, Heidelberg.

J. P. Strache, A. Falk, H.-G. Schmalz, „Enantioselective Nickel-Catalyzed Hydrocyanation Employing TADDOL-derived Phosphine-Phosphite Ligands”, FJS 2021 March **2021**, Leipzig.

Cologne, February 08th

Joss Pepe Strache



(Place, Date)

(Name)

(Signature)